Los Angeles Department of Water & Power

BUILDING A STRONGER L.A.

May 6, 2024

Mr. Erik Ekdahl, Deputy Director
Division of Water Rights
California State Water Resources Control Board
1001 I Street, 14th Floor
Sacramento, California 95814

Dear Mr. Ekdahl:

Subject: Annual Monitoring Report for Runoff Year 2023-24

Pursuant to the Los Angeles Department of Water and Power Mono Basin Water Rights Amended License Nos. 10191 and 10192, please find the enclosed Annual Monitoring Report, which includes the following reports required by the Orders:

- Section I: Mono Basin Fisheries Monitoring Report Rush, Lee Vining, and Walker Creeks 2023
- Section II: Mono Basin Stream Monitoring Report, RY 2023
- Section III: Mono Lake Limnological Monitoring, 2023 Annual Report
- Section IV: Mono Basin Waterfowl Habitat Restoration Program, 2023 Monitoring Report

The submission of these reports fulfills the requirements of Section 20.g(2) and Section 22.c.

If you have any questions, please contact Mark Y. Ching at (213) 367-2132.

Sincerely,

Adam Perez
Aqueduct Manager

MYC:mt
Enclosures
c/enc: Eric B. Tillemans Mark Y. Ching Chad W. Lamacchia

Mono Basin
Annual Monitoring Reports

May 2024

Prepared for State Water Resources Control Board

In Accordance with the Terms and Conditions of Amended License Nos. 10191 and 10192

Contents

Section I. Mono Basin Fisheries Monitoring Report
Rush, Lee Vining, and Walker Creeks 2023

Prepared by Ross Taylor and Associates

Section II. Mono Basin Stream Monitoring Report, RY 2023
Prepared by William J. Trush

Section III. Mono Lake Limnological Monitoring
2023 Annual Report

Prepared by Robert Jellison, Caroline Vignardi, and John M. Melack

Section IV. Mono Basin Waterfowl Habitat Restoration
Program 2023 Monitoring Report

Prepared by Deborah House, Mono Basin Waterfowl Program Director
and Motoshi Honda, Watershed Resources Specialist

Section I. Mono Basin Fisheries Monitoring Report
Rush, Lee Vining, and Walker Creeks 2023

Prepared by Ross Taylor and Associates

Mono Basin Fisheries Monitoring Report
Rush, Lee Vining, and Walker Creeks
2023

Prepared by Ross Taylor and Associates for

The State Water Resources Control Board, the Los Angeles Department of Water and Power, and the Mono Basin Monitoring Administration Team

March 8, 2024

Table of Contents

Executive Summary 4
Odd-year Monitoring Metrics 4
PIT Tagging – New Tags and Recaptures 5
Summer Water Temperatures in Rush Creek 5
Proposed Fisheries Sampling for 2024 Season 5
Introduction 7
Study Area 7
Hydrology 7
Grant Lake Reservoir (GLR) 11
Methods 13
Channel Dimensions 15
Mortalities 15
Length-Weight Relationships 15
Relative Stock Density (RSD) Calculations 16
Water Temperature Monitoring 16
Results 18
Channel Lengths and Widths 18
Trout Capture Summaries 18
Relative Condition of Brown Trout 28
Relative Stock Density (RSD) for Rush and Lee Vining Creeks 33
PIT Tag Recaptures 37
PIT Tags Implanted between 2009 and 2023 37
Growth of Age-1 Brown Trout between 2022 and 2023 38
Growth of Age-2 Brown Trout between 2022 and 2023 39
Growth of Age-3 Brown Trout between 2022 and 2023 39
Growth of Age-4 Brown Trout between 2022 and 2023 40
Growth of Age-5 Brown Trout between 2022 and 2023 40
Growth of MGORD Brown Trout between 2022 and 2023 40
Movement of PIT Tagged Trout between Sections 41
PIT Tag Shed Rate of Trout Recaptured in 2023 41
Comparison of Length-at Age amongst Sample Sections 44
Summer Water Temperature 47
Discussion 55
Trout Population Metrics 55
Sampling in Beaver Modified Habitats 56
Methods Evaluation 59
Proposed Fisheries Sampling for 2024 Season 60
Recommended changes to SEF's based on 2023 Fisheries Monitoring 61
References Cited 63
Appendices for the 2023 Mono Basin Annual Fisheries Report 66
Appendix A: Aerial Photographs of Annual Sample Sites on Rush, Walker and Lee Vining Creeks 67

Appendix B: Tables of Numbers of Brown Trout and Rainbow Trout Implanted with PIT Tags (by sampling section) between 2009 and 2022 74
(Note: no tags implanted in 2013) 74
Appendix C: Table of PIT-tagged Fish Recaptured during October 2023 Sampling . 82

Executive Summary

The 2023 fisheries sampling was the second of ten years of biological monitoring of the Stream Ecosystem Flows (SEF), with oversight from the newly formed Mono Basin Monitoring Administration Team (MAT) as directed by the California State Water Resource Control Board's (SWRCB) amended Licenses 10191 and 10192. This monitoring continues a 25-year history of monitoring ordered by the SWRCB under Orders 98-05 and 98-07. Five of the reaches sampled in 2023 were similar in length to those sampled between 2009 and 2022. In 2023, three new sites were sampled, all within Rush Creek, and all associated with recent beaver activity. Sample site selection has evolved over time, with more sites annually sampled in 1999 through 2008 as the Fisheries Team was investigating potential differences in fish production based on proximity to the Grant Lake Reservoir (GLR) dam and varying channel slopes and confinement. For example, in Rush Creek, the Mono Gate One Return Ditch (MGORD) was selected because of its tailwater condition below the dam and its propensity to support older and larger Brown Trout. Upper Rush was selected for its moderately-sloped channel and its location just downstream of a confined, gorge-like section. Finally, the Bottomlands section was selected for its location in a low-gradient area that has more potential for the formation of meanders, deeply scoured pools, and side-channels.

The 2023 Runoff Year (RY) was 226% of normal and classified as an Extreme-wet RY type, as measured on April 1st. The range of runoff that defines an Extreme-wet RY is >160% exceedance. The preceding 11 years included a Dry RY of 60% in 2022, Dry RY of 58% in 2021, Dry-Normal-1 RY of 71% in 2020, a Wet RY of 140% in 2019, a Normal RY of 85% in 2018, a record Extreme-wet RY of 206% in RY 2017 and five consecutive below "Normal" RYs (RY 2016 was 74% of normal, RY 2015 was 25% of normal, RY 2014 was 48% of normal, RY 2013 was 66% of normal and RY 2012 was 55% of normal).

Based on the 2013 terms of settlement and the recently amended licenses, in odd years the fisheries' monitoring effort was reduced to single-pass electrofishing. Thus in 2023, single-pass electrofishing was conducted at the usual annually sampled sites: the MGORD, Upper Rush and the Bottomlands in Rush Creek, the Lee Vining Creek main channel, and in Walker Creek. In addition, single-pass electrofishing was conducted at three new locations in lower Rush Creek associated with recent beaver dam construction.

Odd-year Monitoring Metrics

For single-pass electrofishing in odd years, the monitoring metrics included condition factors, growth rates (in length and weight) from recaptures of previously PIT tagged trout, and relative stock densities (RSD) for three size classes of catchable trout (Table 1). Generating statistically valid population estimates, density estimates and standing crop estimates were infeasible with single-pass data and these metrics will only be generated in even-years.

Table 1 provides a concise view of comparisons of the 2023 monitoring metrics versus 2022 results. The Results section provides more detail regarding the percentages of the decreases and increases of all monitoring metrics (Table 1).

PIT Tagging – New Tags and Recaptures

In 2023, a total of 300 trout received PIT tags and adipose fin clips in Rush, Lee Vining, and Walker Creeks; the lowest number of tags deployed since PIT tagging started in 2009 due to very low numbers of trout <125 mm in length. In addition, two recaptured adipose fin-clipped fish had shed their original tags and were re-tagged, thus a total of 302 PIT tags were implanted during the 2023 fisheries sampling. Of the 302 trout tagged, 141 were age-0 Brown Trout and 139 were age-1 and older Brown Trout. For Rainbow Trout, 10 age-0 fish were tagged and 11 age-1 and older were tagged. Eight of the Brown Trout tagged in the MGORD section were up to 225 mm in total length and were presumed to be age-1 fish. In addition, 20 age-0 Brown Trout were tagged in the MGORD.

In October of 2023, a total of 61 previously tagged trout (that retained their tags) were recaptured in the Rush Creek watershed. Nine of the recaptures occurred in the Bottomlands section, followed by eight recaptures in the Upper Rush section (including two Rainbow Trout), 27 recaptures in Walker Creek, and five recaptures in the MGORD. In October of 2023, a total of 10 previously tagged Brown Trout and one Rainbow Trout (that retained their tags) were recaptured in the Lee Vining Creek main channel section. During the 2023 sampling, only three previously tagged Rainbow Trout were recaptured, thus very limited growth rate information was available for Rainbow Trout in Rush Creek and Lee Vining Creek. Growth rates of all PIT-tagged recaptured age-1 and age-2 Brown Trout increased from 2022 to 2023 (Table 1).

Summer Water Temperatures in Rush Creek

In 2023, a record Extreme-wet RY with an extended GLR spill resulted in favorable summer thermal conditions, with no peak water temperatures exceeding 70^{o}F at all Rush Creek monitoring locations. In 2023, daily mean temperatures and average daily maximum temperatures were the lowest or second-lowest recorded at all Rush Creek temperature monitoring locations since these data were collected. At most Rush Creek temperature monitoring locations, the maximum diurnal fluctuations were the lowest since the Extreme-wet RY of 2017.

Proposed Fisheries Sampling for 2024 Season

We intend to conduct population estimate sampling in the fall of 2024 at the following locations: MGORD Rush, Upper Rush, Bottomlands Rush, Lee Vining Creek main channel, and Walker Creek. In addition to conducting population estimate sampling at the annually sampled locations, the Fisheries Stream Scientist proposes to conduct single-pass sampling at the new Rush Creek sites sampled in 2023: the Caddis Channel, the Jeffrey Connector Channel, and the beaver dam pools of the Old Main Channel.

Table 1. Summary of Mono Basin Brown Trout annual monitoring metrics; changes between sampling years 2022 and 2023. N/A = not applicable or not available. For applicable metrics, the increases/decreases between 2022 and 2023 are provided in parentheses. For growth rates, increases/decreases between 2022 and 2023 are provided in millimeters or grams. Because single-pass electrofishing was conducted in 2023, no comparisons of population estimates, densities, standing crops and apparent survival rates were possible.

Annual Monitoring Metrics	Rush Creek - MGORD	Rush Creek - Upper	Rush Creek - Bottomlands	Walker Creek	Lee Vining Creek
Condition Factor	Increase	Increase	Decrease	Increase	Increase
Growth Rate (mm) of Age-1 Recaptures	Increase (39 mm)	Increase (39 mm)	Increase (24 mm)	Increase (14 mm)	Increase (2 mm)
Growth Rate (g) of Age-1 Recaptures	Increase (69 g)	Increase (57 g)	Increase (27 g)	Increase (12 g)	Increase (6 g)
Growth Rate (mm) of Age-2 Recaptures	Increase (94 mm)	N/A	N/A	Increase (15 mm)	Increase (2 mm)
Growth Rate (g) of Age-2 Recaptures	Increase (102 g)	N/A	N/A	Increase (19 g)	Increase (10 g)
RSD-225	Increase	Increase	Increase	N/A	Increase
RSD-300	Increase	Increase	Increase	N/A	Increase
RSD-375	increase	N/A	N/A	N/A	N/A

Introduction

Study Area

Between October 3rd and 10th 2023, Ross Taylor (the SWRCB's Fisheries Scientist) and a staff of five fisheries biologists conducted the annual fisheries monitoring surveys in reaches along Rush, Lee Vining, and Walker Creeks in the Mono Lake Basin. The 2023 fisheries sampling was the second of ten post-settlement years of biological monitoring of the Stream Ecosystem Flows (SEF), with oversight from the newly formed Mono Basin Monitoring Administration Team (MAT). The SEFs are an integral part of the amended water licenses in SWRCB's Order WR-2021-0086. The reaches sampled in 2023 included five of the annually sampled sites: MGORD Rush Creek, Upper Rush, Rush Creek Bottomlands, Lee Vining Creek main channel, and Walker Creek. In addition to these sites, three new sites were sampled in lower Rush Creek, associated with beaver dam activity, which created ponds and several side channels. These sites were named the Caddis Channel, the Jeffrey Connector Channel and the Old Main Channel. In October of 2023, the Caddis Channel carried most of the Rush Creek flow, followed by the Jeffrey Connector Channel. The Old Main Channel had minimal flow yet contained most of the beaver dams and associated pools/ponds. These new sites were located upstream of the Bottomlands section. Aerial photographs of the sampling reaches are provided in Appendix A.

Hydrology

The 2023 Runoff Year (RY) was 226% of normal and classified as an Extreme-wet RY type, as measured on April 1st. The range of runoff that defines an Extreme-wet RY is >160% exceedance. The preceding 11 years included a Dry RY of 60% in 2022, Dry RY of 58% in 2021, Dry-Normal-1 RY of 71% in 2020, a Wet RY of 140% in 2019, a Normal RY of 85% in 2018, an Extreme-wet RY of 206% in RY 2017 and five consecutive below "Normal" RY's (RY 2016 was 74% of normal, RY 2015 was 25% of normal, RY 2014 was 48% of normal, RY 2013 was 66% of normal and RY 2012 was 55% of normal).

Following the flow regimes developed for Los Angeles Department of Water and Power's (LADWP) State Water Board Order WR-2021-0086, in Extreme-wet runoff years, SEFs in Rush Creek were defined in Table 2-14 of the Synthesis Report (Table 2). For the actual 2023 Rush Creek hydrograph, the red line in Figure 1 depicts both snowmelt runoff and Southern Cal Edison (SCE) ramping in Rush Creek upstream of Grant Lake Reservoir (GLR). The purple line depicts the SEF releases by LADWP into the top end of the MGORD (Figure 1). The blue bars depict the 63-day spill over the dam spillway (Figure 1). The light-tan dotted line in Figure 1 depicts the combined flows below GLR of the SEF release plus the spill. The dashed blue line in Figure 1 depicts flows in lower Rush Creek with unregulated accretions from Parker and Walker Creeks. The brown dashed line depicts storage elevations in GLR (Figure 1). The daily average peak flow in Rush Creek below Parker and Walkers Creeks was 778 cfs on 7/4/23; lower Rush Creek experienced 22 days where the daily average discharge was >700 cfs and 43 days where

the daily average discharge was >600 cfs (Figure 1). The purple line of the 2023 Rush Creek Extreme-wet SEF release from the MGORD closely followed the benches, ascensions, snowmelt peak, and fast recession limb as prescribed in Table 2. The main deviation of the 2023 Rush Creek SEF release from the Synthesis Report's prescribed SEF release was a delay in the medium recession, where a bench of 183 cfs to 194 cfs was released for 40 days between 7/29/23 and 9/6/2023 (Figure 1). The purpose of this extended elevated bench was to move water out of GLR, to avoid the reservoir from filling and spilling later in the year, during the upcoming fall or winter months.

For RY 2023 in Lee Vining Creek, LADWP followed the diversion rate table (when diverting) and fall/winter baseflows consistent with the SEF regime defined in WR-2021-0086 (Figure 2). In 2023, multiple, large peaks occurred in Lee Vining Creek above the intake, with a peak of 522 cfs on 7/3/23 (Figure 2). Prior to the start of peak flows in mid-May, LADWP diverted flows from Lee Vining Creek to GLR when flows above the intake were >30 cfs and <250 cfs, consistent with the SEF diversion rate table (Figure 2). These early diversions ensured a maximum elevation in GLR to assist with Rush Creek's peak flows. As per LADWP's 2023 AOP, after the snowmelt peak, diversions to the Lee Vining conduit were curtailed, except for reducing flows to Lee Vining Creek in early October for the annual fisheries sampling (Figure 2).

Table 2. Rush Creek SEFs for Extreme-wet runoff year type as defined in the Synthesis Report.

Table 2-14. Rush Creek recommended SEFs for EXTREME-WET runoff year types.

EXTREME-WET RUNOFF YEAR					
Hydrograph Component	Start Date	End Date	Streamflow (cfs)	Duration (days)	Rate of Change
Spring Baseflow	April 1	April 30	40	30	
Spring Ascension	May 1	May 13	40-80	13	5%
Spring Bench	May 14	June 11	80	29	
Snowmelt Ascension	June 12	June 21	80-220	10	10%
Snowmelt Bench	June 22	August 10	220	36	
Snowmelt Flood	July 9	July 22	220-380-220	14	20%
Snowmelt Peak (release)	July 11	July 18	380	8	
Snowmelt Peak (spill)			750	5	20%
Fast Recession					10%
Medium Recession (Node)	August 11	August 24	220-90	14	6%
Slow Recession	August 25	September 30	90-27	37	3%
Summer Baseflow			0		
Fall Baseflow	October 1	November 30	27	61	
Winter Baseflow	December 1	March 31	27	121	

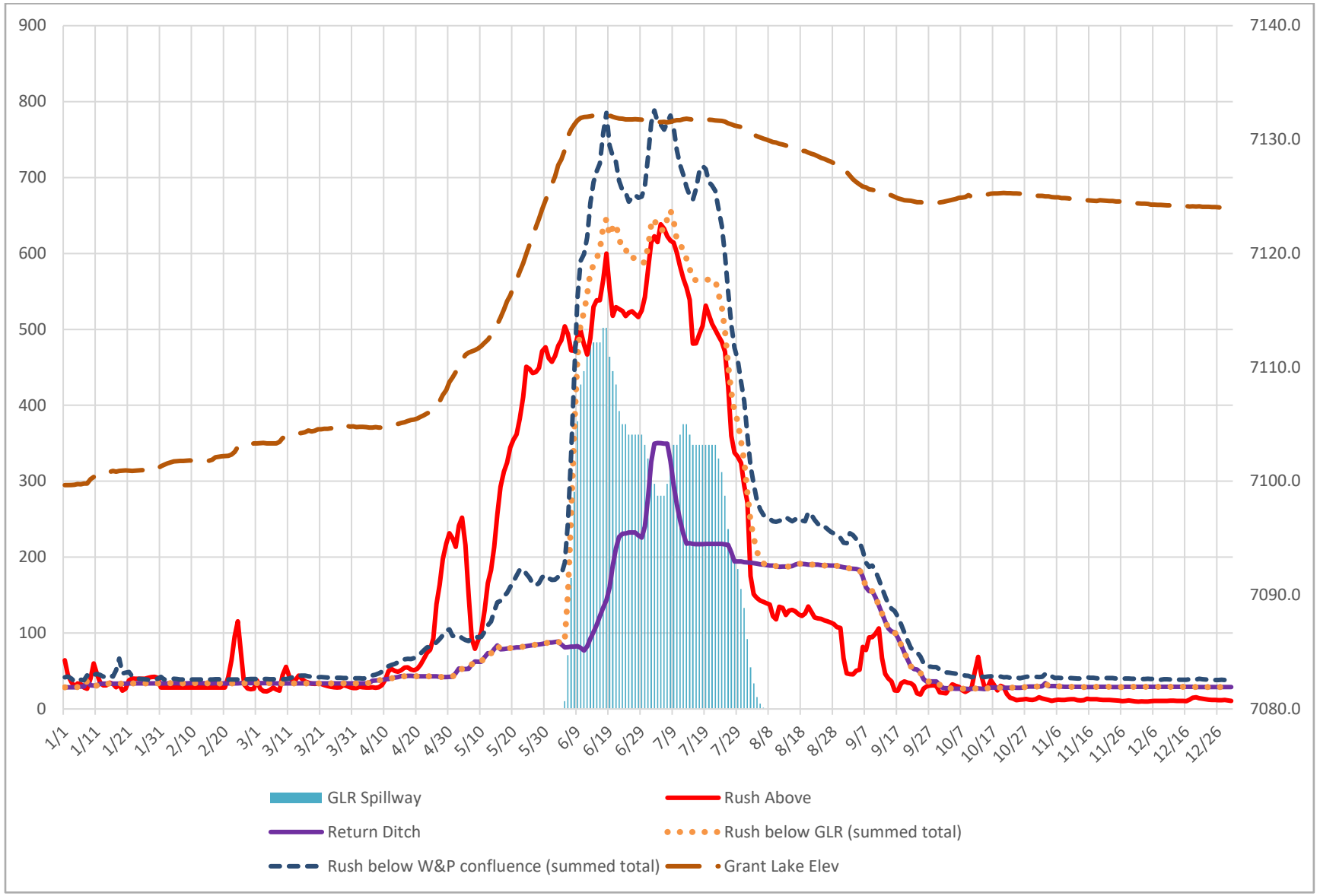

Figure 1. Rush Creek hydrographs between January 1st and December 31st of 2023.

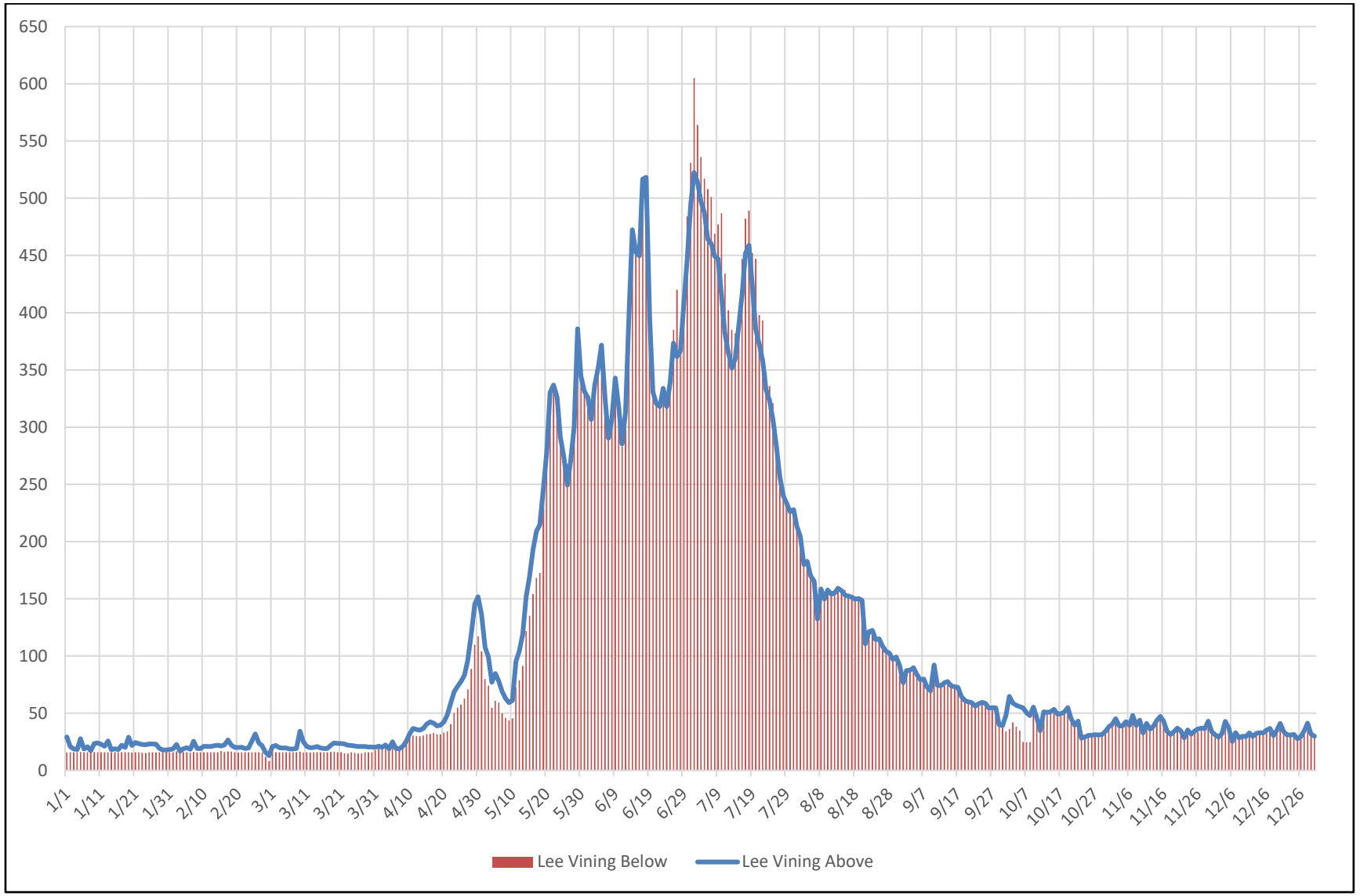

Figure 2. Lee Vining Creek hydrograph between January 1st and December 31st of 2023.

Grant Lake Reservoir (GLR)

In 2023, storage elevation levels in GLR fluctuated from a low of 7,099.7 ft on January 1st to a high of 7,132.2 ft on June 19th when the peak spill of 502 cfs was flowing over the dam's spillway (Figure 3). During the runoff from the Extreme-wet RY, GLR spilled for 63 days between June 6th and August 7th, including 41 days where the spill was >300 cfs (Figure 3). After the spill, GLR's elevation slowly dropped to an elevation of 7,124.5 ft on September 30th, then briefly rose between October 1st and 25th as flows into the MGORD were reduced for the annual fisheries sampling and for the fall into winter SEF baseflows (Figure 3). At the end of 2023, GLR's elevation was at 7,124.0 ft (Figure 3).

During the summer months of RY2023, GLR's elevation was well above the "low" GLR level as defined in the Synthesis Report by the Stream Scientists as a level where warm water temperatures should be a concern (<20,000 AF storage or approximately 7,100 ft elevation) (red horizontal line in Figure 3). From mid-August through mid-September, GLR was 25.1 ft to 29.3 ft above the 7,100 ft elevation. As would be expected, the 2023 summer water temperature monitoring documented cool water temperatures with relatively small diurnal fluctuations, leading to favorable thermal conditions for Brown Trout growth and survival, at all Rush Creek locations downstream of GLR for the entirety of the summer period, defined as July through September.

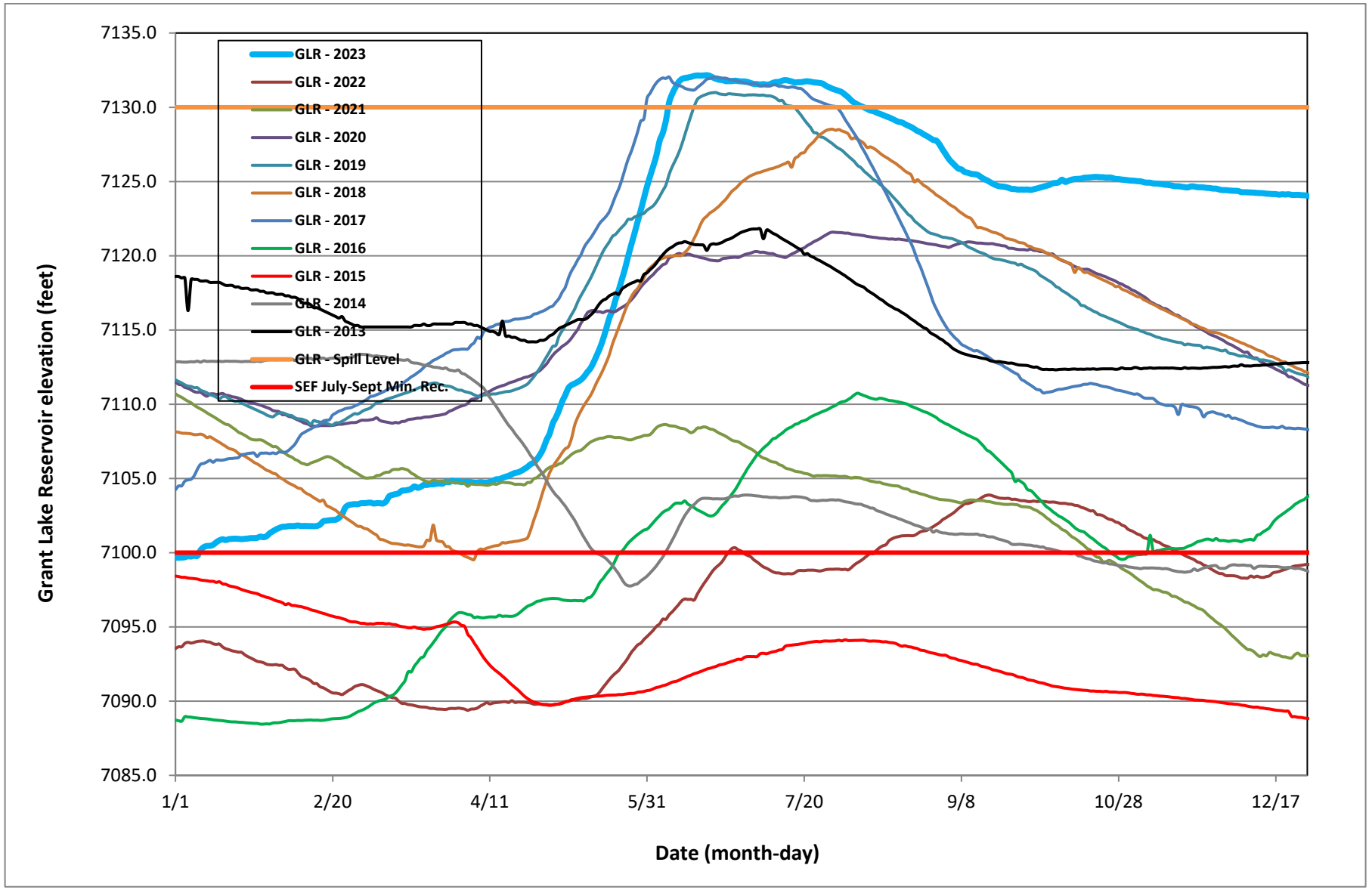

Figure 3. Grant Lake Reservoir's elevation between January 1st and December 31st 2013 - 2023.

Methods

The annual fisheries monitoring was conducted between October 3rd and 10th of 2023. The sampling was conducted by Ross Taylor of Ross Taylor and Associates (RTA), Lawrance Vernallis (RTA employee), Gavin Bandy (RTA employee), and three sub-consultants: Beth Chasnoff-Long, Tyler Rose and Olivia Vosburg. Single-pass electrofishing was used in 2023 to capture fish in the regularly sampled sections and three new Rush Creek sections. To avoid pushing fish out of sections, block fences or nets were installed at the lower end of each Rush Creek and Lee Vining section, except for the MGORD section. The block fences were 48 inches tall, constructed with ½-inch mesh hardware cloth, t-posts, and rope. Hardware cloth was stretched across the entire width of the creek and t-posts were then driven at roughly five-foot intervals through the hardware cloth on the upstream side approximately one foot from the edge. Rocks were placed on the upstream (lower) edge of the fence to prevent trout from swimming underneath the fence. Rope was secured across the tops of the t-posts and anchored to both banks upstream of the fence. The hardware cloth was then secured to the rope with sections of baling wire. A lower block fence was installed in the morning of sampling a particular section and was removed at the completion of sampling. To prevent failure, all fences were periodically cleaned of leaves and twigs during the day's sampling.

The bottom of the Walker Creek and the Rush Creek Jeffrey Connector Channel sections were blocked with a 1/4-inch-mesh nylon seine net. Rocks were placed on the lead line to prevent trout from swimming underneath the seine net. A long T-post was laid across the channel, on top of the banks, and then the cork line of the seine net was zip-tied to the T-post. Both ends of the seine net were weighted with rocks to hold it in place. As with the block fences, the seine net was periodically cleaned of leaves and twigs during the day's sampling.

Equipment used to conduct electrofishing on the MGORD, Upper, Bottomlands, and Caddis Channel sections of Rush Creek included a seven-foot plastic barge that contained the Smith-Root© 2.5 GPP electrofishing system, a generator, an insulated cooler, and battery powered aerators. The Smith-Root© 2.5 GPP electrofishing system included a 5.5 horsepower generator which powered the 2.5 GPP control box. Electricity from the 2.5 GPP control box was introduced into the water via two anodes. The electrical circuit was completed by the metal plate cathode attached to the bottom of the barge.

Sampling runs on the Upper, Bottomlands, and Caddis Channel sections of Rush Creek consisted of a single downstream pass starting at the upper end of the section and ending at the lower block fence. In 2023, the field crew consisted of a barge operator, two anode operators, and three netters: one for each anode and a "rover" netter. The barge operator's job consisted of carefully maneuvering the barge down the creek and ensuring the overall safety of the entire crew. The anode operators' job was to safely shock and hold trout until they were netted. The netters' job was to net and transfer fish to the insulated cooler and monitor trout for signs of stress. Once the cooler was full of fish, electrofishing was temporarily stopped to process the trout. The trout were then transferred from the cooler to live cars and placed back in the creek.

The trout were then processed in small batches and returned to a recovery net pen in the creek. Once all the trout were processed at a sub-stop, the crew resumed electrofishing until the cooler was once again full.

Because the Old Main Channel section of Rush Creek had minimal flow, the electrofishing was focused on the pools created by beaver dams. The sampling was conducted with two crew members operating Smith-Root© LR-20B and Model-12 POW backpack electrofishers, three netters, and one bucket carrier who transported the captured trout. In each pool, several electrofishing passes were made. Once a pool was sampled, the fish were processed and returned to their capture location.

The single-pass electrofishing on the Lee Vining Creek main channel consisted of an upstream pass starting at the lower block fence to the top of the section, a short 15–20-minute break, and then a downstream pass back down to the lower fence. The electrofishing crew consisted of two crew members operating Smith-Root© LR-20B and Model-12 POW backpack electrofishers, three netters, and one bucket carrier who transported the captured trout. As needed, the bucket carrier transferred fish into one of three net pens stationed along the channel when the bucket was full of trout.

Due to the depth of the MGORD, all electrofishing and netting was done from inside a drift boat. The drift boat was held perpendicular to the flow by two crew members who walked it down the channel. The electrofishing barge was secured to the upstream side of the drift boat and a single throw anode was used. A single netter used a 12-foot-long handle dipnet to net the stunned trout, which were then placed in an insulated cooler equipped with aerators. A safety officer sat at the stern of the drift boat whose job was to monitor the trout in the cooler, the electrofishing equipment, the electrofishing crew, and shut off the power should the need arise. Once the cooler was full, the trout were moved to a net pen and placed back in the creek for the shore-based crew to process before continuing the electrofishing effort. Any time the electrofishing crew unloaded fish into a net pen ahead of the processing crew, the net pen's location was marked with bright-colored survey flagging at the edge of the MGORD road.

For the Walker Creek and the Jeffrey Connector Channel sections, a single pass was considered an upstream pass from the lower seine net to the top of the section, followed by a downstream pass back to the lower seine net. One member of the electrofishing crew operated a Smith-Root© LR-20B electrofisher; another member was the primary netter, and a third member was the backup netter/bucket carrier. As needed, the bucket carrier transferred fish into a net pen when the bucket was full of trout.

To process trout, small batches of fish from the net pen were transferred to a five-gallon bucket equipped with aerators. Trout were then anesthetized, identified as either Brown Trout or Rainbow Trout, measured to the nearest millimeter (total length), and weighed to the nearest gram on an electronic balance. Before placing trout into the aerated recovery bucket, each fish was examined for a missing adipose fin. Trout missing their adipose fin were then scanned for their Passive Integrated Transponder (PIT) tag number. Any trout missing their adipose fin that

failed to produce a tag number when scanned were recorded as having "shed" the PIT tag; in most instances these fish were retagged. Partially regenerated adipose fins of fish with PIT tags were reclipped for ease of future identification. Once recovered, fish were then moved from the recovery bucket to a net pen to be held until the day's sampling effort was completed; this was done to prevent captured fish from potentially moving downstream into the actively sampled section. At the end of the electrofishing effort, fish were released from the net pens back into the sub-sections they had been captured in.

Between 2009 and 2012, PIT tags were implanted in most age-0 trout in Rush and Lee Vining Creeks and in all ages of trout in the MGORD. No PIT tags were deployed in 2013; however, the tagging program was resumed in 2014 and has continued annually through the 2023 field season. Starting in 2017, PIT tags implanted in trout caught in the MGORD were focused primarily on fish up to 225 mm in length, with the intent being to tag only age-0 and presumed age-1 trout.

All data collected in the field were written on hardcopy data sheets and also entered into Excel spreadsheets using an electronic tablet. Hardcopy data were used to provide a crucial back-up in case of in-field technical issues with the tablet. The hardcopy data sheets were also used to proof the Excel spreadsheets.

Channel Dimensions

To calculate the area of each sample section, channel lengths and wetted widths were measured within the sample reaches. Wetted widths were measured at approximately 10-meter intervals to 0.1-meter accuracy within each reach. Channel lengths were only measured if the start or end points differed, or if noticeable changes occurred to the channel reach, such as the cutting-off of a meander bend. Although no estimates of fish density or biomass were made in 2023, we still measured channel widths and lengths, primarily to capture any potential channel changes caused by the record runoff's high flows.

Mortalities

During single-pass electrofishing, we kept track of all fish mortalities for project permit purposes. PIT tags were removed from all mortalities with previously implanted tags. The PIT tag database was updated to confirm these mortalities and "tag pulled" was noted in the comments column because these tags were typically reused.

Length-Weight Relationships

Length-weight regressions (Cone 1989 as cited in Taylor and Knudson 2012) were calculated for all Brown Trout greater than 100 mm in all sections of Rush Creek. Regressions using Log10 transformed data were used to compare length-weight relationships by year and by section.

Fulton-type condition factors were computed in MicroFish 3.0 using methods previously reported (Taylor and Knudson 2012) for Brown Trout 150 to 250 mm. A trout condition factor

of 1.00 was considered the demarcation between poor and average condition (Reimers 1963; Barnham and Baxter 1998; Blackwell et al. 2000). The literature considers a trout condition factor of <1.00 as poor, a condition factor of 1.00-1.19 as average, and a condition factor ≥1.20 as good (Barnham and Baxter 1998).

Relative Stock Density (RSD) Calculations

Relative stock density (RSD) is a numerical descriptor of length frequency data (Hunter et al. 2007; Gabelhouse 1984). RSD values are the proportions (percentage x 100) of the total number of Brown Trout ≥150 mm in length that are also ≥225 mm or (RSD-225), ≥300 mm (RSD-300) and ≥375 mm or (RSD-375). A primary purpose of generating RSD values is to describe the structure of a fish population in terms of recreational fishing satisfaction. For Rush and Lee Vining Creeks this would be a descriptor of an eastern Sierra trout stream; as in, out of the estimated numbers of catchable trout (≥150 mm or ≈6 inches) what proportion are "stock" length (≥225 mm or ≈9 inches), "memorable" length (≥300 mm or ≈12 inches), or "trophy" length (≥375 mm or ≈15 inches). These three RSD values are calculated by the following equations:

RSD-225 = [(# of Brown Trout ≥225 mm) ÷ (# of Brown Trout ≥150 mm)] x 100
RSD-300 = [(# of Brown Trout ≥300 mm) ÷ (# of Brown Trout ≥150 mm)] x 100
RSD-375 = [(# of Brown Trout ≥375 mm) ÷ (# of Brown Trout ≥150 mm)] x 100

Water Temperature Monitoring

Water temperatures were recorded (in degrees Fahrenheit) at various locations within Rush and Lee Vining Creeks as part of the Fisheries Monitoring Program. Data loggers were deployed by Robbie Di Paolo of the Mono Lake Committee (MLC) in January and recorded data throughout the year in one-hour time intervals. Data loggers were downloaded at the end of the year and the data were summarized in spreadsheets. Water temperature data loggers utilized for this report were deployed at the following locations in 2023:

1. Rush Creek – upstream of GLR.
2. Rush Creek - top of MGORD.
3. Rush Creek - bottom of MGORD.
4. Rush Creek - at Upper Rush/Old Highway 395 Bridge.
5. Rush Creek - above Parker Creek.
6. Rush Creek - below Narrows.
7. Rush Creek - at County Road crossing.
8. Lee Vining Creek - at County Road crossing.

For the Fisheries Monitoring Program, the year-long data sets were edited to focus on the 2023 summer water temperature regimes (July – September) in Rush Creek. Analysis of summer water temperature included the following metrics:

1. Daily mean temperature.
2. Average daily minimum temperature.
3. Average daily maximum temperature.
4. Number of days with daily maximums exceeding 70^{o}F.
5. Number of hours with temperatures exceeding 66.2^{o}F.
6. Number of good/fair/poor potential growth days, based on daily average temperatures.
7. Number of bad thermal days based on daily average temperatures.
8. Maximum diurnal fluctuations.
9. Average maximum diurnal fluctuations for a consecutive 21-day period.

Results

Channel Lengths and Widths

Differences in wetted widths between years can be due to several factors such as magnitude of spring peak flows, stream flows at time of measurements, and locations of where the measurements were taken. Lengths, widths, and areas from 2022 were provided for comparisons (Table 3). The Upper Rush site experienced no change in average widths between 2022 and 2023. In contrast, the average widths in the Bottomlands section of Rush Creek, Walker Creek, and Lee Vining Creek were all wider in 2023 than in 2022 (Table 3). Within the Walker Creek section, several meanders were either cut-off or shortened by the record runoff in 2023, as depicted by the 24-meter decrease in reach length between 2022 and 2023 (Table 3).

The new Caddis Channel section was 407 meters in length and had an average wetted width of 5.0 meters. The new Jeffrey Connector Channel was 167 meters in length and had an average wetted width of 5.0 meters.

Table 3. Total length, average wetted width, and total surface area of sample sections in Rush, Lee Vining, and Walker Creeks sampled between October 3-10, 2023. Values from 2022 provided for comparisons.

Sample Section	Length (m) 2022	Width (m) 2022	Area (m^2) 2022	Length (m) 2023	Width (m) 2023	Area (m^2) 2023	Area (ha) 2023
Rush – Upper	381	7.2	2,743.2	381	7.2	2,743.2	0.2743
Rush - Bottomlands	437	6.6	2,884.2	437	7.6	3,321.2	0.3321
Rush – MGORD	2,230	8.5	18,955.0	2,230	8.5	18,955.0	1.8955
Lee Vining – Main	255	5.1	1,300.5	255	5.9	1,504.5	0.1505
Walker Creek	202	2.0	399.6	178	2.9	516.2	0.0516

Trout Capture Summaries

Upper - Rush Creek Section

In 2023, a total of 160 Brown Trout ranging in size from 75 mm to 488 mm were captured on a single electrofishing pass in the Upper Rush section (Figure 4). For comparison, in 2022 a total of 273 Brown Trout were caught on the mark-run. In 2023, age-0 Brown Trout comprised 35% of the total catch (compared to 53% in 2022 and 28% in 2021).

In 2023, the 10 Brown Trout captured in the 125-199 mm size class comprised 6% of the total catch in the Upper Rush section (compared to 29% in 2022 and 64% in 2021). The low numbers of Brown Trout captured in the 125-199 mm size class in 2023 was likely influenced by high growth rates of age-1 fish where most of these fish attained lengths greater than 200 mm.

The 95 Brown Trout ≥200 mm in length caught in 2023 comprised 59% of the Upper Rush total Brown Trout catch (compared to 18% in 2022 and 8% in 2021). In 2023, three Brown Trout >300 mm in length were captured in the Upper Rush section, including one fish >400 mm in total length.

A total of 29 Rainbow Trout were captured in the Upper Rush section comprising 15% of the section's total trout catch in 2023; Rainbow Trout comprised 12% of the total catch in 2022 and 11% of the total catch in 2021. The 29 Rainbow Trout ranged in length from 58 mm to 470 mm and six of these were age-0 fish (Figure 5). Several of the larger Rainbow Trout were likely of hatchery origin, based on observations of eroded fins. We suspect these fish came from GLR when the reservoir spilled during the record runoff.

Bottomlands - Rush Creek Section

In 2023, a total of 69 Brown Trout ranging in size from 90 mm to 483 mm were captured on a single electrofishing pass in the Bottomlands section of Rush Creek (Figure 6). For comparison, in 2022 a total of 154 Brown Trout were caught on the mark-run. Brown Trout <125 mm in length comprised 20% of the total catch in 2023 versus 60% of the total catch in 2022.

Brown Trout 125-199 mm in length comprised 30% of the total catch in the Bottomlands section in 2023 versus 31% of the total catch in 2022.

Brown Trout ≥200 mm in length comprised 50% of the total catch in the Bottomlands section in 2023 (versus 10% in 2022) with the largest trout 483 mm in total length (Figure 6). This large Brown Trout had an adipose fin clip, an indication that it was PIT tagged, unfortunately this fish had shed its tag when scanned with a tag reader.

MGORD - Rush Creek Section

Within the MGORD section of Rush Creek a total of 111 Brown Trout were captured on a single electrofishing pass in 2023 (Figure 7). In 2023, Brown Trout ranged in size from 81 mm to 533 mm in total length (Figure 7). A total of 19 Brown Trout <125 mm in length were captured in 2023, which comprised 18% of the total catch of Brown Trout (age-0 fish comprised 9% of the catch in 2022).

In 2023, one Brown Trout in the 125-199 mm size class was caught during the single electrofishing pass in the MGORD section; this fish was 125 mm in length and was an obvious age-0 fish. We suspect that no age-1 fish were caught in this size class due to high growth rates, as influenced by cooler summer water temperatures.

In 2023, the catch of 91 Brown Trout ≥200 mm in length comprised of 82% of the total Brown Trout catch in the MGORD section. Of these 91 Brown Trout ≥200 mm, 23 fish were ≥300 mm, compared to 28 fish ≥300 mm in 2022 and 47 fish ≥300 mm in 2021. Nine Brown Trout ≥375 mm in length were captured in 2023 (compared to six fish in 2022, 12 fish in 2021, six fish in 2020, four fish in 2019, 15 fish in 2018, 11 fish in 2017 and 20 fish in 2016). In 2023, seven of these Brown Trout were >400 mm in length (Figure 7).

In 2023, 24 Rainbow Trout were captured in the MGORD section (Figure 8), compared to 14 captured in 2022. Eight of the Rainbow Trout caught in 2023 were <125 mm in total length. In the previous 10 years, the Rainbow Trout catch in the MGORD has ranged from zero to 40 fish. Most of the Rainbow Trout captured in 2023 appeared to be of natural origin, with several larger fish exhibiting signs of hatchery origin, primarily eroded fins.

For the past 18 sampling years, electrofishing passes through the MGORD have produced the following total catch values (all size classes of Brown and Rainbow Trout):

- 2023 – Single pass = 135 trout.
- 2022 – Mark run = 100 trout. Recapture run = 148 trout. Two pass average = 124 fish.
- 2021 – Mark run = 273 trout. Recapture run = 387 trout. Two pass average = 330 fish.
- 2020 – Single pass = 457 trout.
- 2019 – Single pass = 361 trout.
- 2018 – Mark run = 233 trout. Recapture run = 188 trout. Two-pass average = 210.5 fish.
- 2017 – Single pass = 203 trout.
- 2016 – Mark run = 121 trout. Recapture run = 110 trout. Two-pass average = 115.5 fish.
- 2015 – Single pass = 176 trout.
- 2014 – Mark run = 206 trout. Recapture run = 268 trout. Two-pass average = 237 fish.
- 2013 – Single pass = 451 trout.
- 2012 – Mark run = 606 trout. Recapture run = 543 trout. Two-pass average = 574.5 fish.
- 2011 – Single pass = 244 trout.
- 2010 – Mark run = 458 trout. Recapture run = 440 trout. Two-pass average = 449 fish.
- 2009 – Single pass = 649 trout.
- 2008 – Mark run = 450 trout. Recapture run = 419 trout. Two-pass average = 434.5 fish.
- 2007 – Single pass = 685 trout.
- 2006 – Mark Run = 283 trout. Recapture run = 375 trout. Two-pass average = 329 fish.

Caddis Channel - Rush Creek Section

In 2023, a total of 106 Brown Trout ranging in size from 95 mm to 345 mm were captured on a single electrofishing pass in the Caddis Channel section of Rush Creek (Figure 9). A total of 17 Brown Trout <125 mm in length were caught; however, three other Brown Trout were 129 mm in total length, bringing the total number of age-0 fish to 20, based on the sharp break in size classes depicted on the length-frequency histogram (Figure 9). As with several other Rush Creek

sections in 2023, very few age-1 Brown Trout were in the 125-199 mm size class; including three fish caught in the Caddis Channel, which were 195, 196, and 199 mm in length (Figure 9). The remaining 83 Brown Trout were 200 mm to 345 mm in total length, including five fish >300 mm in total length (Figure 9).

Other trout species captured on 10/9/23 in the Caddis Channel included 11 Rainbow Trout, between 211 mm and 355 in length. Several of these fish appeared to be of hatchery origin due to eroded fins. We also caught one hybridized Lahontan Cutthroat Trout in the Caddis Channel. This fish was 294 mm in length and was the first hybridized Lahontan Cutthroat Trout sampled in Rush Creek over the past 27 years of annual sampling by the Stream Scientists (Figure 10). We suspect this fish washed over the GLR dam during the peak flows when GLR was spilling.

Jeffrey Connector Channel - Rush Creek Section

In 2023, a total of 43 Brown Trout ranging in size from 95 mm to 311 mm were captured on a single electrofishing pass in the Jeffrey Connector Channel section of Rush Creek (Figure 11). A total of 28 Brown Trout <125 mm in length were caught; however, six other Brown Trout were 125 to 133 mm in total length, bringing the total number of age-0 fish to 34, based on the sharp break in size classes depicted on the length-frequency histogram (Figure 11). As with several other Rush Creek sections in 2023, very few age-1 Brown Trout were within the 125-199 mm size class; including one fish caught in the Jeffrey Connector Channel, which was 197 mm in length (Figure 11). The remaining eight Brown Trout were 200 mm to 311 mm in total length (Figure 11).

One Rainbow Trout was captured in the Jeffrey Connector Channel and this fish was 233 mm in total length.

Old Main Channel - Rush Creek Section

In 2023, a total of 35 Brown Trout ranging in size from 98 mm to 335 mm were captured in the Old Main Channel section of Rush Creek (Figure 11). A total of seven Brown Trout <125 mm in length were caught (Figure 11). As with several other Rush Creek sections in 2023, very few age-1 Brown Trout were within the 125-199 mm size class; including three fish caught in the Old Main Channel, which were 158, 192, and 197 mm in length (Figure 11). The remaining 25 Brown Trout were 208 mm to 335 mm in total length, including six fish >300 mm in total length (Figure 11).

One Brook Trout was captured in the Jeffrey Connector Channel and this fish was 212 mm in total length. We suspect this fish washed over the GLR dam during the peak flows when GLR was spilling or washed out of Walker Lake during the peak flows.

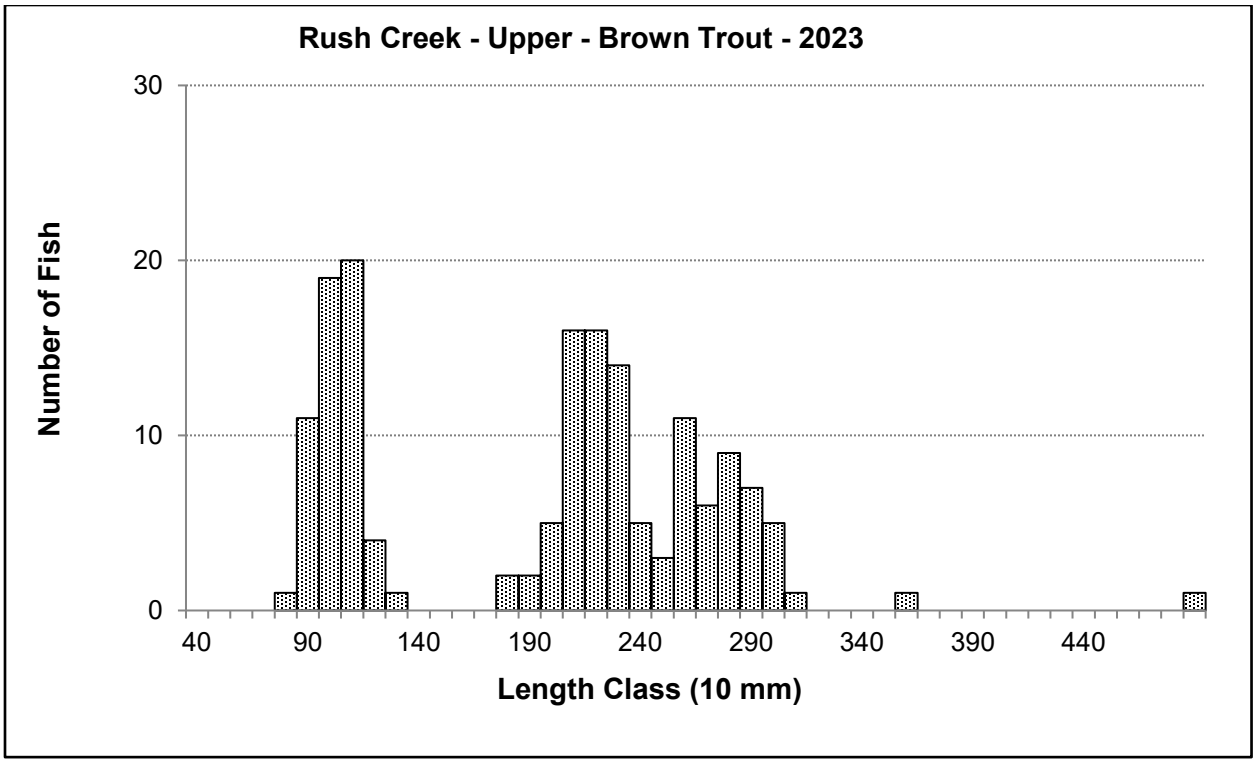

Figure 4. Length-frequency histogram of Brown Trout captured in Upper Rush on 10/3/2023.

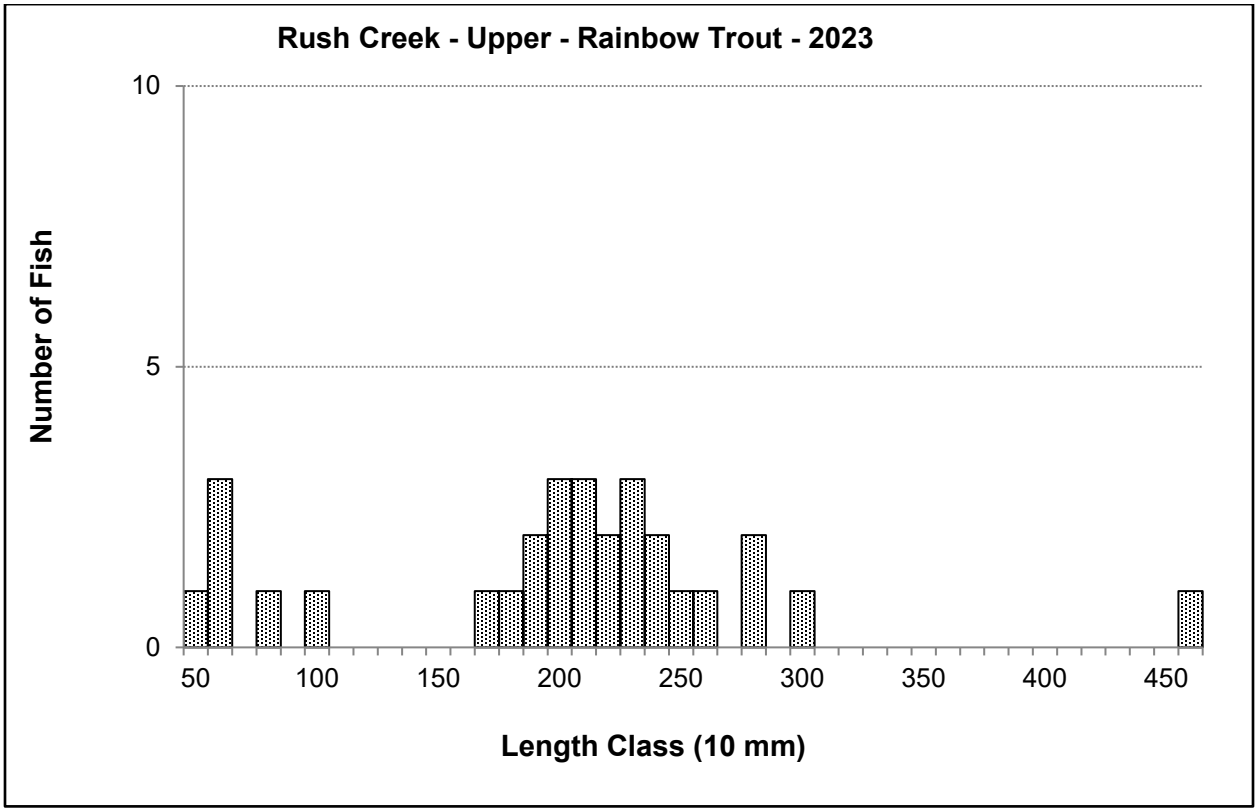

Figure 5. Length-frequency histogram of Rainbow Trout captured in Upper Rush on 10/3/2023.

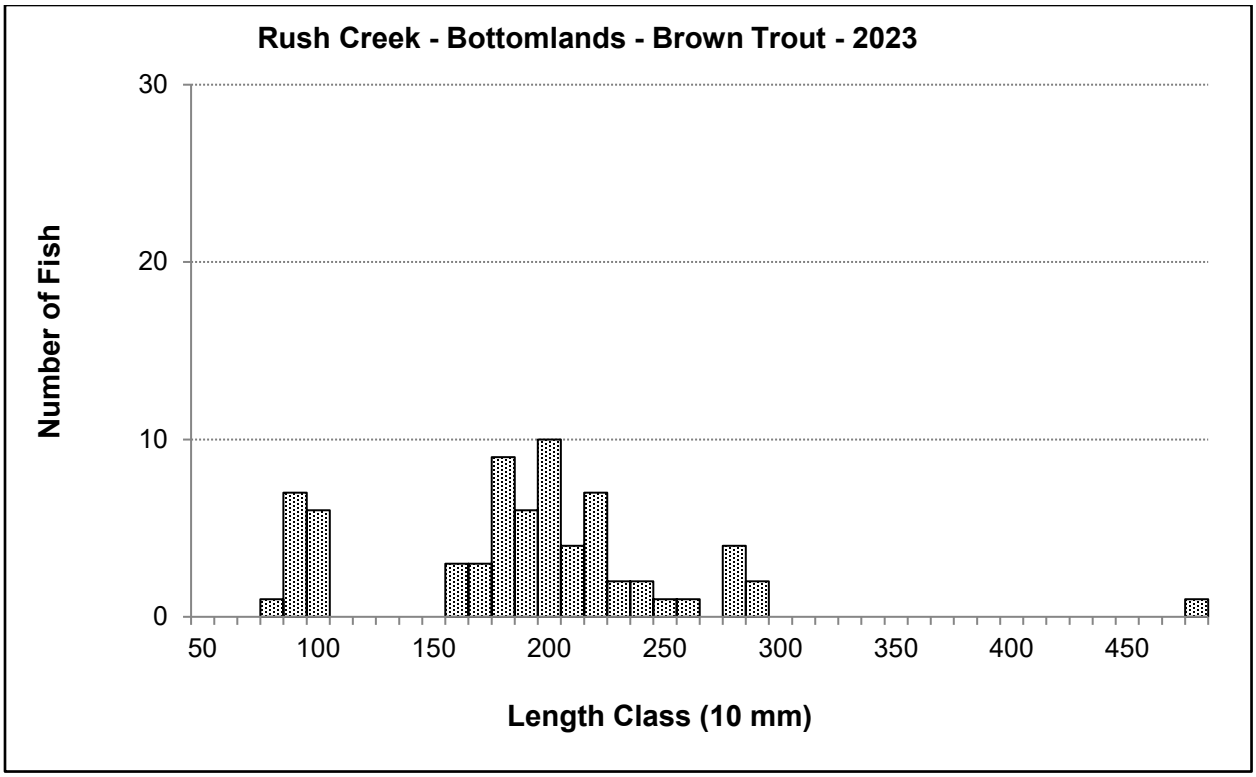

Figure 6. Length-frequency histogram of Brown Trout captured in the Bottomlands section of Rush Creek on 10/4/2023.

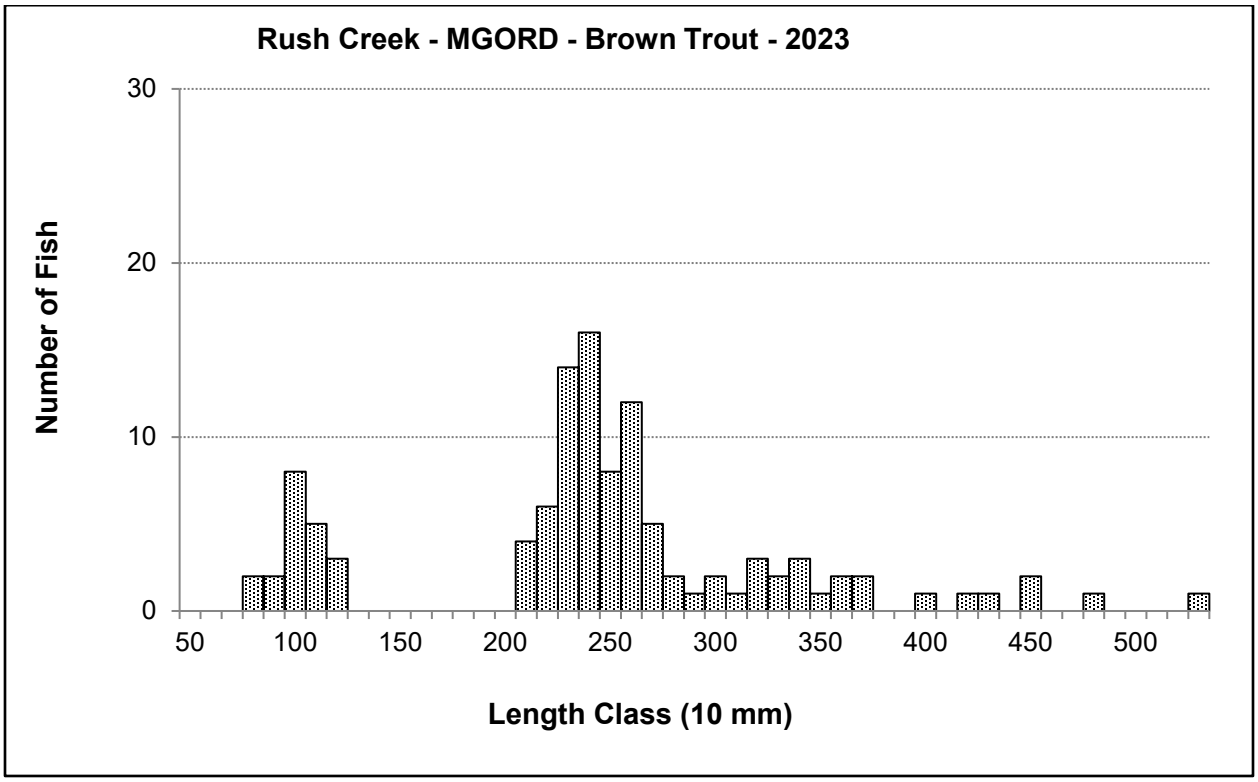

Figure 7. Length-frequency histogram of Brown Trout captured in the MGORD section of Rush Creek on 10/5/2023.

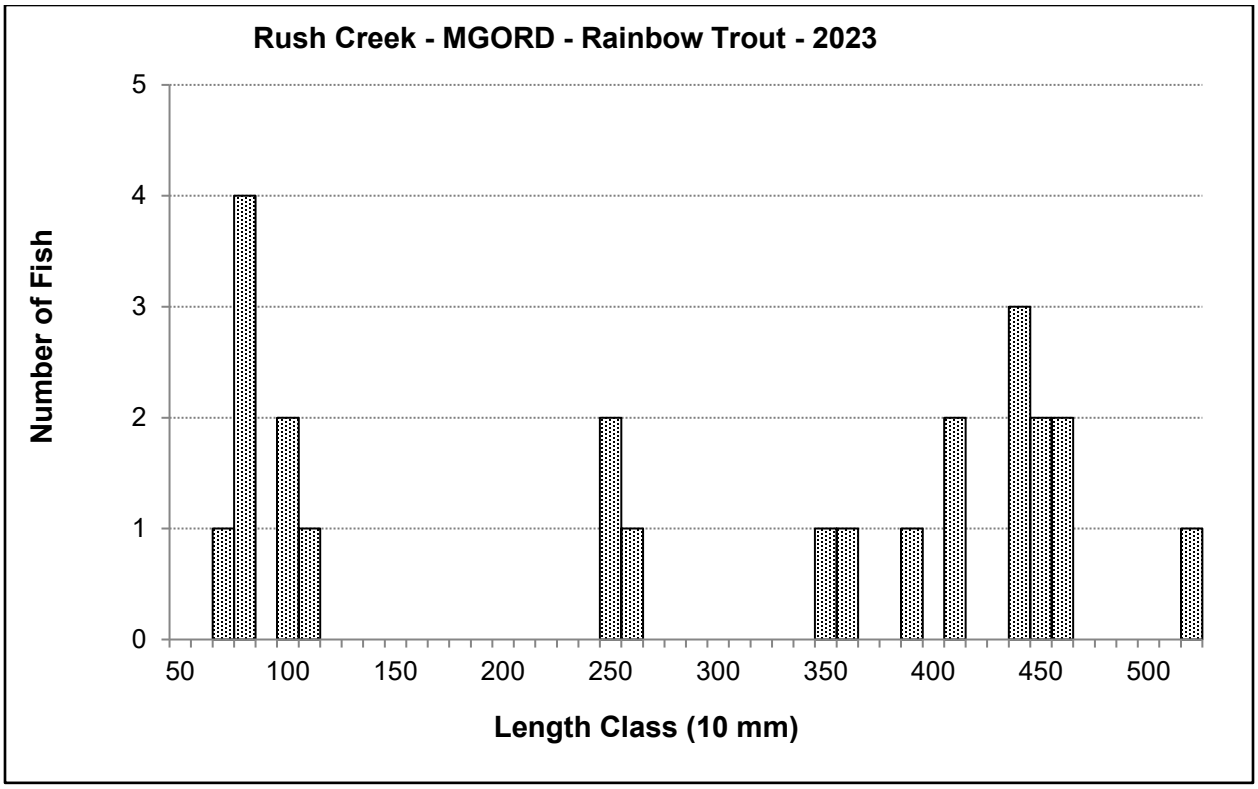

Figure 8. Length-frequency histogram of Rainbow Trout captured in the MGORD section of Rush Creek on 10/5/2023.

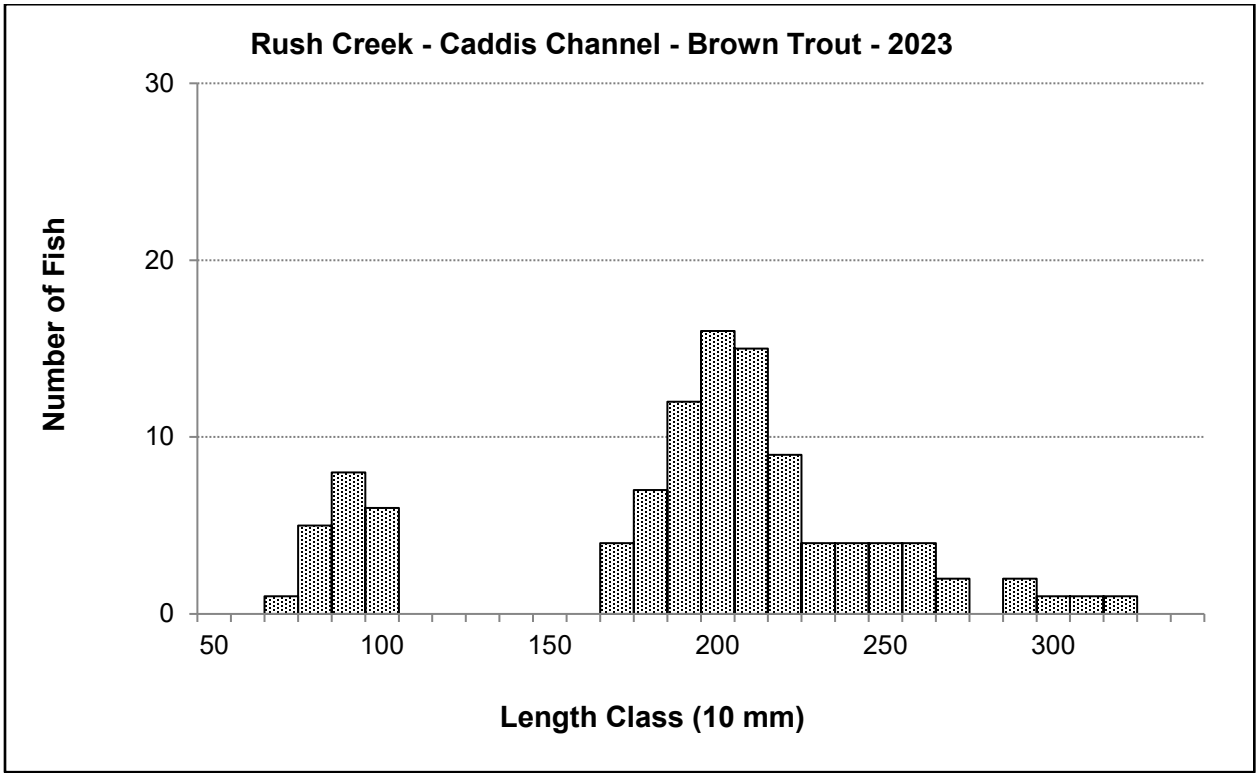

Figure 9. Length-frequency histogram of Brown Trout captured in the Caddis Channel section of Rush Creek on 10/9/2023.

Figure 10. Hybridized Lahontan Cutthroat Trout captured in the Caddis Channel section on 10/9/23.

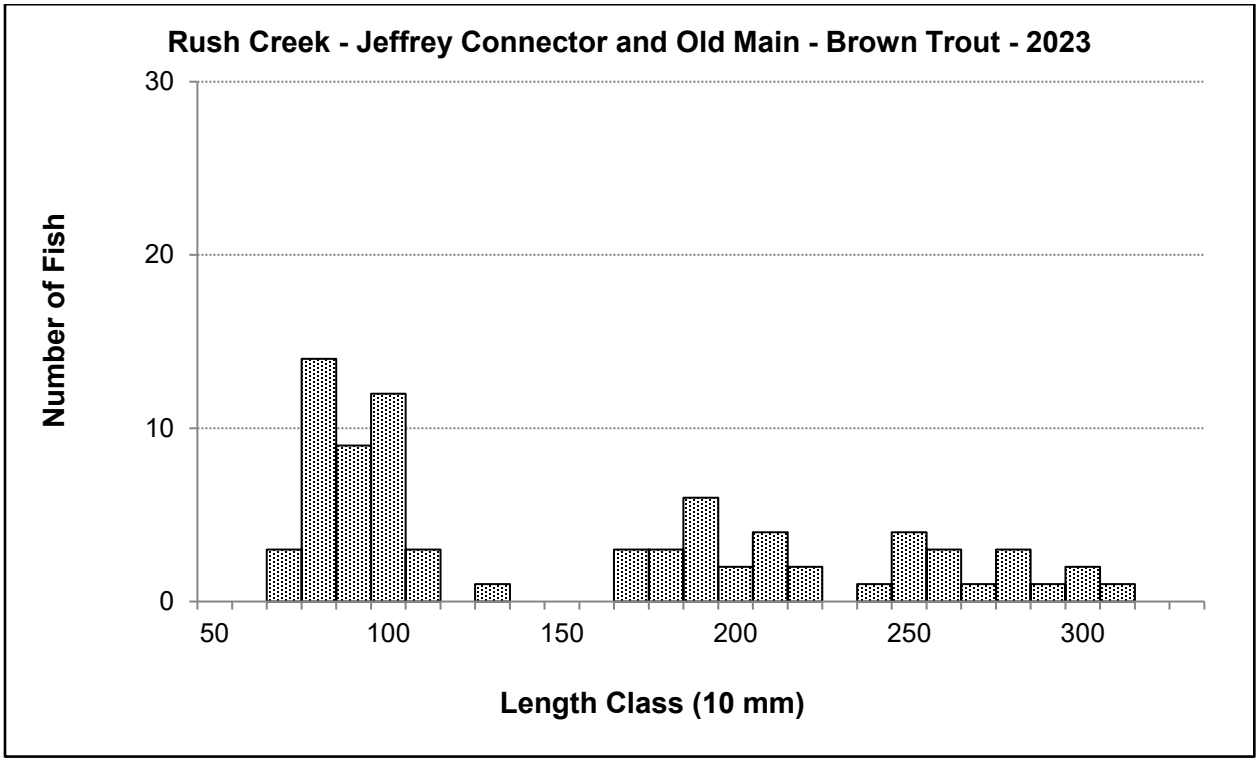

Figure 11. Length-frequency histogram of Brown Trout captured in the Jeffrey Connector and Old Main Channel sections of Rush Creek on 10/10/2023.

Lee Vining Creek

In 2023, a total of 81 trout were captured on the single electrofishing pass made in the Lee Vining Creek main channel section. Nearly all the trout captured in 2023 were Brown Trout (78 fish). In 2023, Brown Trout ranged in size from 144 mm to 322 mm in length (Figure 12). No Brown Trout <125 mm in length were captured in 2023, an age-class that has comprised 12% to 63% of the Lee Vining Creek Brown Trout catch between 2018 and 2022.

In 2023, Brown Trout 125-199 mm in length comprised 32% of the total Brown Trout catch in Lee Vining Creek's main channel section (versus 40% in 2022 and 76% in 2021).

In 2023, 53 Brown Trout ≥200 mm were captured in Lee Vining Creek's main channel (Figure 12). Three Brown Trout captured in 2023 were >300 mm in length (Figure 13).

The three Rainbow Trout caught in Lee Vining Creek in 2023 were 202, 264 and 305 mm in total length.

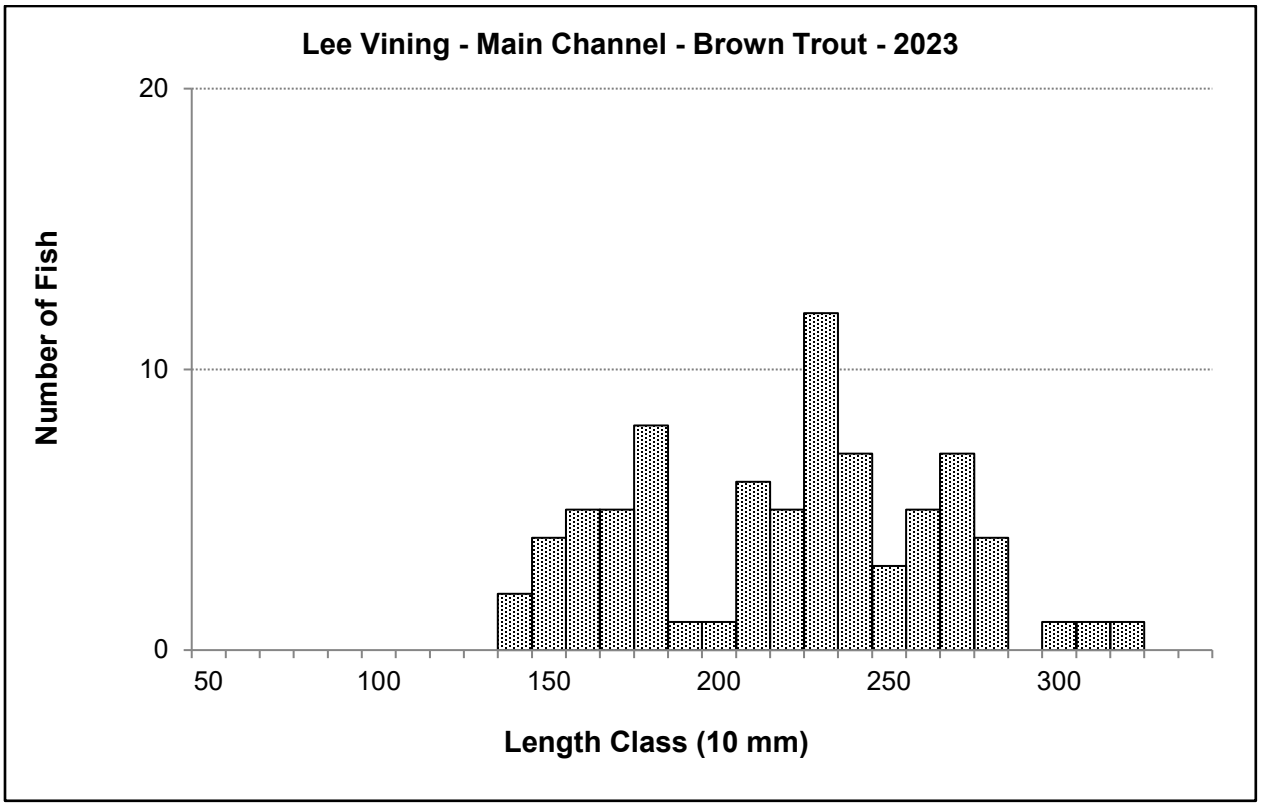

Figure 12. Length-frequency histogram of Brown Trout captured in the main channel section of Lee Vining Creek on 10/6/2023.

Walker Creek

In 2023, 93 Brown Trout were captured in one electrofishing pass in the Walker Creek section, versus 198 caught in the first depletion pass in 2022 and 317 in the first depletion pass in 2021. In 2023, only one Brown Trout <125 mm was caught versus 85 fish <125 mm caught on the first depletion pass in 2022 (Figure 13).

Brown Trout in the 125-199 mm size class (65 fish) accounted for 70% of Walker Creek's total catch in 2023 versus 48% of the catch in 2022.

Brown Trout ≥200 mm in length (27 fish caught) accounted for 29% of the total catch in 2023 versus 14 fish caught in 2022 that comprised 6% of the total catch. The largest Brown Trout captured in Walker Creek in 2023 was 299 mm in length (Figure 13).

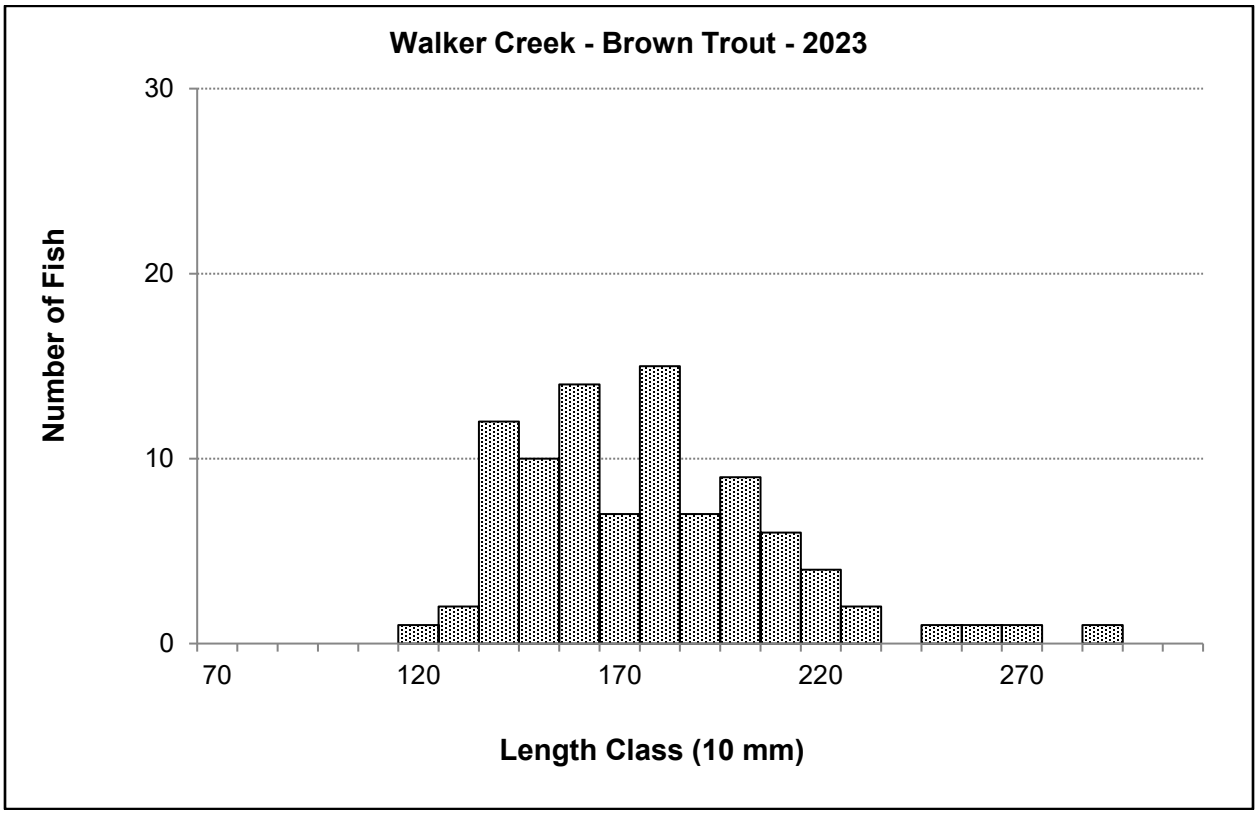

Figure 13. Length-frequency histogram of Brown Trout captured in Walker Creek on 10/7/2023.

Relative Condition of Brown Trout

Linear regressions of log-length to log-weight for captured Brown Trout ≥ 100 mm indicated strong correlations between length and weight (r^2 values 0.98 and greater) (Table 4). Slopes of these relationships were near 3.0 indicating isometric growth, which was assumed to compute fish condition factors, and were reasonable (Table 4).

Table 4. Regression statistics for log_{10} transformed length (L) to weight (WT) for Brown Trout 100 mm and longer captured in Rush Creek by sample section and year. The 2023 regression equations are in ***bold*** type.

Section	Year	N	Equation	r^2	P
Bottomlands	***2023***	***62***	***$Log_{10}(WT) = 3.1294*Log_{10}(L) – 5.3820$***	***0.98***	***<0.01***
	2022	253	$Log_{10}(WT) = 3.1013*Log_{10}(L) – 5.2251$	0.98	<0.01
	2021	205	$Log_{10}(WT) = 3.0091*Log_{10}(L) – 5.0526$	0.98	<0.01
	2020	223	$Log_{10}(WT) = 2.9792*Log_{10}(L) – 4.9754$	0.98	<0.01
	2019	310	$Log_{10}(WT) = 2.9631*Log_{10}(L) – 4.9409$	0.99	<0.01
	2018	226	$Log_{10}(WT) = 2.9019*Log_{10}(L) – 4.8059$	0.99	<0.01
	2017	160	$Log_{10}(WT) = 3.0398*Log_{10}(L) – 5.0998$	0.99	<0.01
	2016	132	$Log_{10}(WT) = 3.0831*Log_{10}(L) – 5.2137$	0.99	<0.01
	2015	301	$Log_{10}(WT) = 3.0748*Log_{10}(L) – 5.1916$	0.99	<0.01
	2014	238	$Log_{10}(WT) = 3.0072*Log_{10}(L) – 5.0334$	0.98	<0.01
	2013	247	$Log_{10}(WT) = 2.7997*Log_{10}(L) – 4.5910$	0.98	<0.01
	2012	495	$Log_{10}(WT) = 2.8149*Log_{10}(L) – 4.6206$	0.98	<0.01
	2011	361	$Log_{10}(WT) = 2.926*Log_{10}(L) – 4.8580$	0.99	<0.01
	2010	425	$Log_{10}(WT) = 2.999*Log_{10}(L) – 5.0050$	0.99	<0.01
	2009	511	$Log_{10}(WT) = 2.920*Log_{10}(L) – 4.8210$	0.99	<0.01
	2008	611	$Log_{10}(WT) = 2.773*Log_{10}(L) – 4.5240$	0.99	<0.01
Upper Rush	***2023***	***131***	***$Log_{10}(WT) = 3.044*Log_{10}(L) – 5.0950$***	***0.99***	***<0.01***
	2022	392	$Log_{10}(WT) = 2.9632*Log_{10}(L) – 4.9305$	0.99	<0.01
	2021	441	$Log_{10}(WT) = 2.9851*Log_{10}(L) – 4.9837$	0.98	<0.01
	2020	426	$Log_{10}(WT) = 2.9187*Log_{10}(L) – 4.8382$	0.99	<0.01
	2019	686	$Log_{10}(WT) = 2.9667*Log_{10}(L) – 4.9298$	0.99	<0.01
	2018	391	$Log_{10}(WT) = 2.9173*Log_{10}(L) – 4.8237$	0.99	<0.01
	2017	309	$Log_{10}(WT) = 3.0592*Log_{10}(L) – 5.1198$	0.99	<0.01
	2016	176	$Log_{10}(WT) = 3.0702*Log_{10}(L) – 5.1608$	0.99	<0.01
	2015	643	$Log_{10}(WT) = 2.9444*Log_{10}(L) – 4.8844$	0.99	<0.01

Table 4 (continued).

Section	Year	N	Equation	r^2	P
Upper Rush	2014	613	$Log_{10}(WT) = 2.9399*Log_{10}(L) - 4.8705$	0.99	<0.01
	2013	522	$Log_{10}(WT) = 2.9114*Log_{10}(L) - 4.8160$	0.99	<0.01
	2012	554	$Log_{10}(WT) = 2.8693*Log_{10}(L) - 4.7210$	0.99	<0.01
	2011	547	$Log_{10}(WT) = 3.006*Log_{10}(L) - 5.0140$	0.99	<0.01
	2010	420	$Log_{10}(WT) = 2.995*Log_{10}(L) - 4.9941$	0.99	<0.01
	2009	612	$Log_{10}(WT) = 2.941*Log_{10}(L) - 4.8550$	0.99	<0.01
	2008	594	$Log_{10}(WT) = 2.967*Log_{10}(L) - 4.9372$	0.99	<0.01
	2007	436	$Log_{10}(WT) = 2.867*Log_{10}(L) - 4.7150$	0.99	<0.01
	2006	485	$Log_{10}(WT) = 2.99*Log_{10}(L) - 4.9802$	0.99	<0.01
	2005	261	$Log_{10}(WT) = 3.02*Log_{10}(L) - 5.0203$	0.99	<0.01
	2004	400	$Log_{10}(WT) = 2.97*Log_{10}(L) - 4.9430$	0.99	<0.01
	2003	569	$Log_{10}(WT) = 2.96*Log_{10}(L) - 4.8920$	0.99	<0.01
	2002	373	$Log_{10}(WT) = 2.94*Log_{10}(L) - 4.8670$	0.99	< 0.01
	2001	335	$Log_{10}(WT) = 2.99*Log_{10}(L) - 4.9630$	0.99	< 0.01
	2000	309	$Log_{10}(WT) = 3.00*Log_{10}(L) - 4.9610$	0.98	< 0.01
	1999	317	$Log_{10}(WT) = 2.93*Log_{10}(L) - 4.8482$	0.98	< 0.01
MGORD	***2023***	***108***	$\boldsymbol{Log_{10}(WT) = 3.0180*Log_{10}(L) - 4.9965}$	***0.99***	***<0.01***
	2022	229	$Log_{10}(WT) = 3.1344*Log_{10}(L) - 5.3145$	0.99	<0.01
	2021	498	$Log_{10}(WT) = 2.9447*Log_{10}(L) - 4.8871$	0.99	<0.01
	2020	383	$Log_{10}(WT) = 3.0144*Log_{10}(L) - 5.0575$	0.98	<0.01
	2019	314	$Log_{10}(WT) = 2.9774*Log_{10}(L) - 4.9282$	0.98	<0.01
	2018	350	$Log_{10}(WT) = 3.0023*Log_{10}(L) - 5.0046$	0.98	<0.01
	2017	159	$Log_{10}(WT) = 3.0052*Log_{10}(L) - 5.0205$	0.99	<0.01
	2016	183	$Log_{10}(WT) = 3.0031*Log_{10}(L) - 5.3093$	0.99	<0.01
	2015	172	$Log_{10}(WT) = 3.131*Log_{10}(L) - 5.0115$	0.99	<0.01
	2014	399	$Log_{10}(WT) = 2.9805*Log_{10}(L) - 4.9827$	0.98	<0.01
	2013	431	$Log_{10}(WT) = 2.8567*Log_{10}(L) - 4.6920$	0.98	<0.01
	2012	795	$Log_{10}(WT) = 2.9048*Log_{10}(L) - 4.8081$	0.99	<0.01
	2011	218	$Log_{10}(WT) = 2.917*Log_{10}(L) - 4.8230$	0.98	<0.01
	2010	694	$Log_{10}(WT) = 2.892*Log_{10}(L) - 4.7563$	0.98	<0.01
	2009	689	$Log_{10}(WT) = 2.974*Log_{10}(L) - 4.9330$	0.99	<0.01
	2008	862	$Log_{10}(WT) = 2.827*Log_{10}(L) - 4.6020$	0.98	<0.01

Table 4 (continued).

Section	Year	N	Equation	r^2	P
MGORD	2007	643	$Log_{10}(WT) = 2.914*Log_{10}(L) - 4.8254$	0.98	<0.01
	2006	593	$Log_{10}(WT) = 2.956*Log_{10}(L) - 4.8722$	0.98	<0.01
	2004	449	$Log_{10}(WT) = 2.984*Log_{10}(L) - 4.9731$	0.99	<0.01
	2001	769	$Log_{10}(WT) = 2.873*Log_{10}(L) - 4.7190$	0.99	<0.01

Condition factors of Brown Trout ≥150 mm in length in 2023 increased from 2022 values in two of three Rush Creek sections and increased in the Lee Vining Creek main channel section, and in the Walker Creek section (Figures 14 and 15). In 2023, three sections had Brown Trout condition factors ≥1.00 (Figures 14 and 15).

Brown Trout in the Upper Rush section had a condition factor of 1.02 in 2023, the third consecutive increase since 2020, and the first year since 2017 with a value ≥1.00 (Figure 14). The Upper Rush section has had Brown Trout condition factors ≥1.00 in 12 of 24 sampling seasons (Figure 14).

Brown Trout in the Bottomlands section of Rush Creek had a condition factor of 0.94 in 2023, a decrease from 1.01 in 2022 (Figure 14). In 16 years of sampling the Bottomlands section, 2022 was the first year that the Brown Trout condition factor was ≥1.00 (Figure 14).

The MGORD's 2023 Brown Trout condition factor for fish ≥150 mm was 1.15, an increase from 1.01 in 2022 (Figure 14). The 2023 value of 1.15 was the highest condition factor recorded in the MGORD since the first year the section was sampled in 2000 (Figure 14). In 2023, condition factors for larger Brown Trout in the MGORD were computed: fish ≥300 mm had a condition factor of 1.10 (1.09 in 2022) and fish ≥375 mm had a condition factor of 0.99 (1.28 in 2022).

In 2023, the condition factor for Brown Trout in Lee Vining Creek's main channel was 1.05, an increase from 0.98 in 2022, and the first value ≥1.00 since 2018 (Figure 15). In 2023, a Rainbow Trout condition factor was not computed for the Lee Vining Creek main channel because of the extremely small sample size (three fish ≥150 mm in length).

In Walker Creek, Brown Trout had a condition factor of 0.94 in 2023, an increase from 0.88 in 2022 (Figure 14). Brown Trout condition factors in Walker Creek have been ≥1.00 in 12 of the 24 sampling years; however, in the past nine years, only the 2018 sampling year had a condition factor ≥1.00 (Figure 14).

Condition factors were also computed for the new Rush Creek sections sampled in 2023. Brown Trout in the Caddis Channel had a condition factor of 0.98 and Brown Trout in the beaver ponds of the Old Main Channel section had a condition factor of 1.00. Both sections had slightly higher condition factors than the closest regularly sampled section; the Bottomlands, located downstream, had a condition factor of 0.94 in 2023.

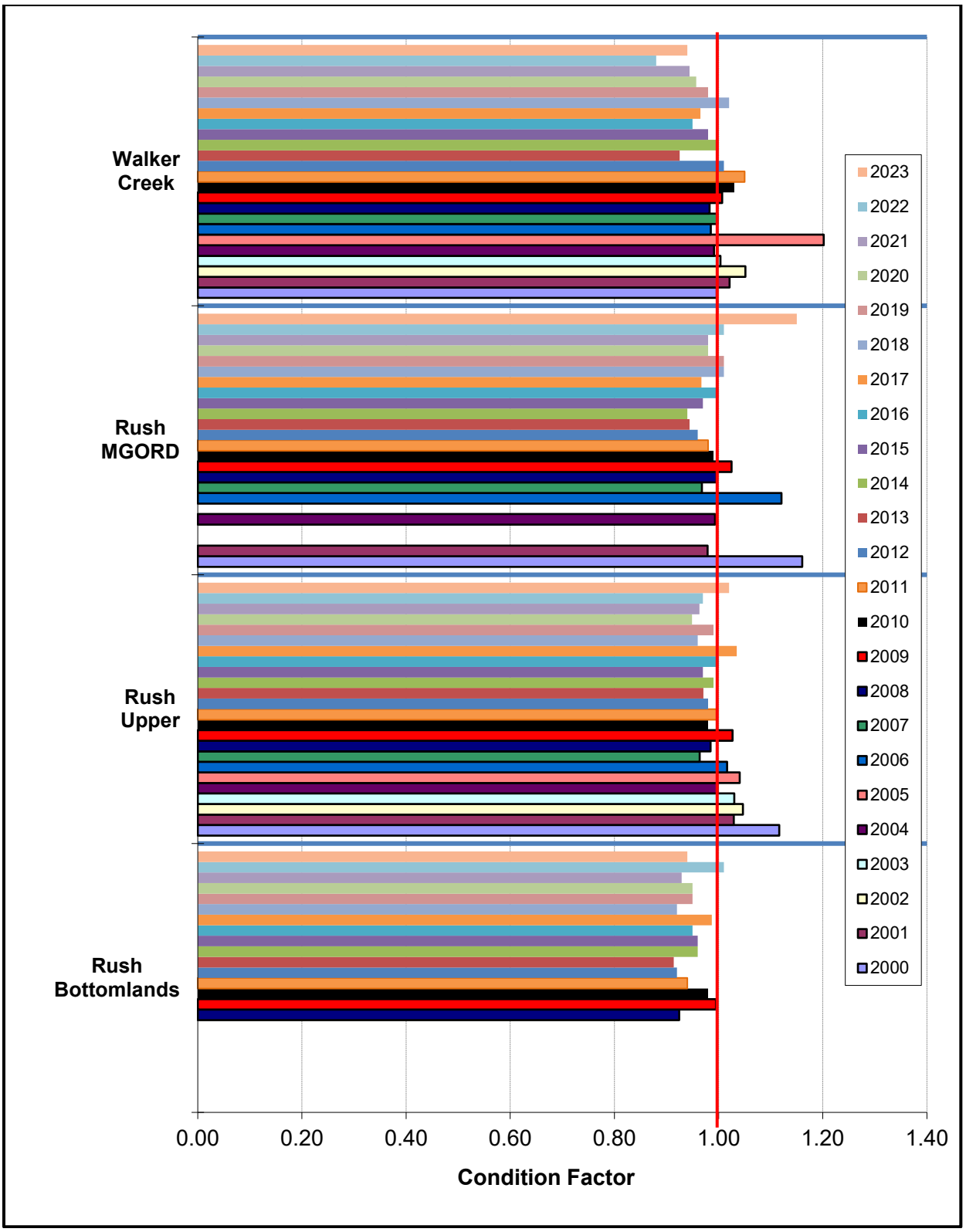

Figure 14. Condition factors for Brown Trout ≥150 mm in length from sample sections of Rush Creek and Walker Creeks from 2000 to 2023.

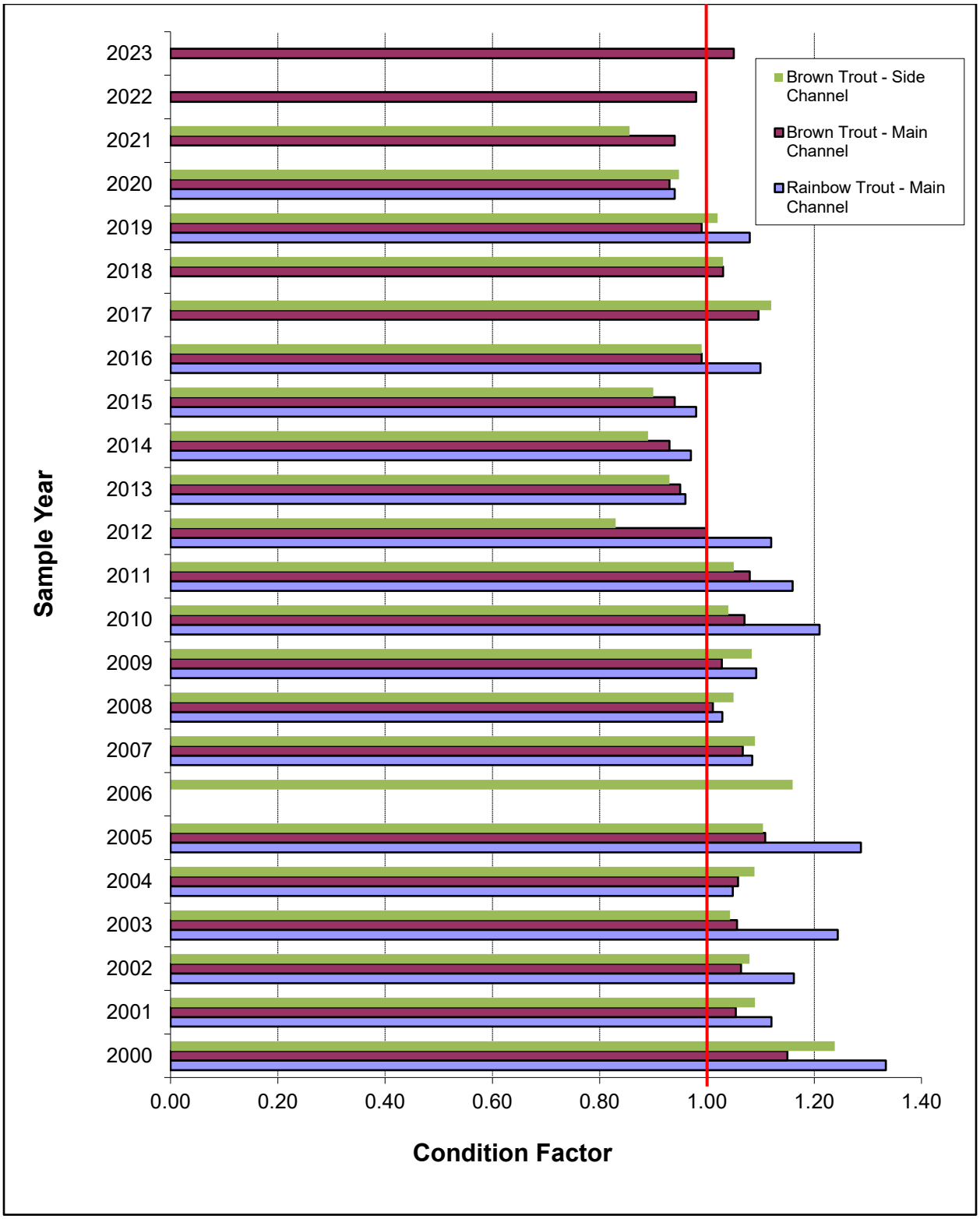

Figure 15. Condition factors for Rainbow Trout and Brown Trout 150 to 250 mm in length from the main channel and side channel sections of Lee Vining Creek from 2000 to 2023. Main channel was not sampled in 2006 due to high flows. The side channel was dropped from the annual sampling in 2022.

Relative Stock Density (RSD) for Rush and Lee Vining Creeks

In the Upper Rush section, the RSD-225 equaled 58 for 2023, the largest RSD-225 value for this section since the record RSD-225 value of 78 in 2017 (Table 5). The 2023 RSD-225 value was influenced by greater numbers of fish ≥225 mm than the numbers of fish in the 150 to 224 mm size class (Table 5). The RSD-300 value was 3 in 2023, the highest RSD-300 value over the past five sampling seasons (Table 5). Over 24 sampling years, a total of 158 Brown Trout ≥300 mm were captured in the Upper Rush Creek section, an average of 6.6 fish ≥300 mm per year (Table 5).

In the Bottomlands section of Rush Creek, the RSD-225 for 2023 equaled 29, the second consecutive substantial increase since 2018 (Table 5). As in the Upper Rush section, the Bottomlands 2023 RSD-225 value was most likely influenced by an increase in the numbers of fish ≥225 mm. The RSD-300 value was 2 in 2023, because one Brown Trout ≥300 mm was captured in the Bottomlands section (Table 5). Over the 16 sampling years, a total of 28 Brown Trout ≥300 mm were captured in the Bottomlands section, an average of 1.8 fish ≥300 mm per year (Table 5).

In the MGORD, the RSD-225 value has increased over the past five consecutive years, from 47 in 2019 to a record value of 93 in 2023 (Table 5). In 2023, the RSD-300 value was 25, the highest RSD-300 value since 2017 (Table 5). The RSD-375 value equaled 10 in 2023, the highest RSD-375 value since 2017 (Table 5). The one-pass catch of Brown Trout ≥150 mm in the MGORD during the 2023 season was 91 fish, which included 23 fish ≥300 mm in length and nine of these fish were ≥375 mm in length (Table 5). For sampling conducted between 2001 and 2012, the annual average catch of Brown Trout ≥300 mm equaled 180 fish/year; then for the past 11 sampling years the annual average catch of Brown Trout ≥300 mm equaled 38 fish/year (Table 5). This 79% decline in larger Brown Trout coincided with the five years of drier RY's and poor summer thermal regimes within the MGORD in 2012-2016. However, in the seven seasons following the five-year drought, the recruitment of larger, older fish appears to be a relatively slow process, possibly because for the three years of 2020-2022 summer water temperatures were generally unfavorable for Brown Trout growth and survival in the MGORD (Table 5).

RSD values were computed for the Caddis Channel and the Old Main Channel, the new sites associated with beaver activities in lower Rush Creek. For the Caddis Channel, the RSD-225 equaled 66 and the RSD-300 was 6. For the Old Main Channel, the RSD-225 was 64 and the RSD-300 equaled 21. These two sites had higher RSD-225 and RSD-300 values than Upper Rush and the Bottomlands.

RSD values in Lee Vining Creek were generated for the main channel only (Table 6). The RSD-225 value for main channel increased substantially from 3 in 2021 to 58 in 2023, the largest RSD-225 value for section for the 24 years of available data (Table 6). In 2023, three Brown Trout greater than 300 mm in length were captured in Lee Vining Creek main channel, thus the RSD-300 value was 4, the highest value since the 2017 and 2018 seasons (Table 6).

Table 5. RSD values for Brown Trout in Rush Creek sections from 2000 to 2023.

Sampling Location on Rush Creek	Sample Year	Number of Trout ≥150 mm	Number of Trout 150-224 mm	Number of Trout 225-299 mm	Number of Trout 300-374 mm	Number of Trout ≥375 mm	RSD-225	RSD-300	RSD-375
Upper Rush	**2023**	**104**	**44**	**57**	**2**	**1**	**58**	**3**	**1**
Upper Rush	2022	235	196	37	2	0	17	1	0
Upper Rush	2021	274	257	13	4	0	6	1	0
Upper Rush	2020	148	129	18	1	0	13	1	0
Upper Rush	2019	503	406	85	11	1	19	2	0
Upper Rush	2018	254	155	75	24	0	39	9	0
Upper Rush	2017	130	28	82	19	1	78	15	1
Upper Rush	2016	103	74	26	1	2	28	3	2
Upper Rush	2015	289	246	41	0	2	15	1	1
Upper Rush	2014	366	331	31	4	0	10	1	0
Upper Rush	2013	336	288	45	3	0	14	1	0
Upper Rush	2012	354	284	66	3	1	20	1	0
Upper Rush	2011	498	381	110	6	1	23	1	0
Upper Rush	2010	308	202	97	7	2	34	3	1
Upper Rush	2009	372	322	43	5	2	13	2	1
Upper Rush	2008	227	189	31	6	1	17	3	0
Upper Rush	2007	282	210	61	9	2	26	4	1
Upper Rush	2006	233	154	69	10	0	34	4	0
Upper Rush	2005	202	139	56	5	2	31	3	1
Upper Rush	2004	179	112	64	2	1	37	2	1
Upper Rush	2003	264	216	45	2	1	18	1	0
Upper Rush	2002	220	181	35	1	2	18	2	1
Upper Rush	2001	223	190	27	6	0	15	3	0
Upper Rush	2000	182	158	22	2	0	13	1	0
Bottomlands	**2023**	**55**	**39**	**15**	**0**	**1**	**29**	**2**	**2**
Bottomlands	2022	145	123	22	0	0	15	0	0
Bottomlands	2021	121	110	10	1	0	9	1	0
Bottomlands	2020	128	117	11	0	0	9	0	0
Bottomlands	2019	220	202	17	1	0	8	0	0
Bottomlands	2018	140	90	41	9	0	36	6	0
Bottomlands	2017	82	29	49	4	0	65	5	0
Bottomlands	2016	66	52	11	1	2	21	5	3
Bottomlands	2015	115	88	26	0	1	23	1	1
Bottomlands	2014	154	152	1	0	1	1	1	1
Bottomlands	2013	128	123	5	0	0	4	0	0
Bottomlands	2012	325	290	34	1	0	11	0	0
Bottomlands	2011	267	218	46	3	0	18	1	0
Bottomlands	2010	307	225	81	1	0	27	0	0

Table 5 (continued).

Sampling Location Rush Creek	Sample Year	Number of Trout ≥150 mm	Number of Trout 150-224 mm	Number of Trout 225-299 mm	Number of Trout 300-374 mm	Number of Trout ≥375 mm	RSD-225	RSD-300	RSD-375
Bottomlands	2009	379	321	56	1	1	15	1	0
Bottomlands	2008	160	141	19	0	0	12	0	0
MGORD	**2023**	**91**	**6**	**62**	**14**	**9**	**93**	**25**	**10**
MGORD	2022	198	56	114	22	6	72	14	3
MGORD	2021	431	204	180	35	12	53	11	3
MGORD	2020	322	167	112	37	6	48	13	2
MGORD	2019	275	145	102	24	4	47	10	1
MGORD	2018	326	98	162	51	15	70	20	5
MGORD	2017	104	12	64	17	11	88	27	11
MGORD	2016	179	46	95	18	20	74	21	11
MGORD	2015	116	33	54	20	9	72	25	8
MGORD	2014	388	184	175	19	10	53	7	3
MGORD	2013	411	237	118	41	15	42	14	4
MGORD	2012	694	176	319	173	26	75	29	4
MGORD	2011	216	36	117	55	8	83	29	4
MGORD	2010	694	252	292	115	35	64	22	5
MGORD	2009	643	156	338	123	26	76	23	4
MGORD	2008	856	415	301	118	22	52	16	3
MGORD	2007	621	144	191	259	27	77	46	4
MGORD	2006	567	60	200	280	27	89	54	5
MGORD	2004	424	130	197	64	33	69	23	8
MGORD	2001	774	330	217	119	108	57	29	14
Caddis Ch.	**2023**	**86**	**29**	**52**	**5**	**0**	**66**	**6**	**0**
Old Main Ch.	**2023**	**28**	**10**	**12**	**6**	**0**	**64**	**21**	**0**

Table 6. RSD values for Brown Trout in the Lee Vining Creek main channel section from 2000-2023.

Sampling Location	Sample Year	Number of Trout ≥150 mm	Number of Trout 150-224 mm	Number of Trout 225-299 mm	Number of Trout 300-374 mm	Number of Trout ≥375 mm	RSD-225	RSD-300
LV Main	**2023**	**76**	**32**	**41**	**3**	**0**	**58**	**4**
LV Main	2022	129	105	24	0	0	19	0
LV Main	2021	175	169	6	0	0	3	0
LV Main	2020	80	69	11	0	0	14	0
LV Main	2019	131	107	22	2	0	18	2
LV Main	2018	51	39	10	2	0	24	4
LV Main	2017	23	17	5	1	0	26	4
LV Main	2016	169	145	24	0	0	14	0
LV Main	2015	210	192	18	0	0	9	0
LV Main	2014	200	173	27	0	0	14	0
LV Main	2013	325	308	16	1	0	5	0
LV Main	2012	111	72	37	2	0	35	2
LV Main	2011	60	31	23	5	1	48	10
LV Main	2010	62	28	32	2	0	55	3
LV Main	2009	137	106	30	1	0	23	1
LV Main	2008	149	138	11	0	0	7	0
LV Main	2007	29	24	5	0	0	17	0
LV Main	2006	Not sampled in 2006 due to unsafe high flows						
LV Main	2005	60	37	20	2	1	38	5
LV Main	2004	70	60	8	2	0	14	3
LV Main	2003	52	27	23	2	0	48	4
LV Main	2002	100	74	23	3	0	26	3
LV Main	2001	90	71	16	3	0	21	3
LV Main	2000	51	32	18	1	0	37	2

PIT Tag Recaptures

PIT Tags Implanted between 2009 and 2023

Between 2009 and 2023, a total of 11,484 PIT tags were implanted in Brown Trout and Rainbow Trout within the annually sampled sections of Rush, Lee Vining and Walker Creeks. All PIT tagged fish received adipose fin clips. The numbers of PIT tags implanted each year varied according to fish availability and inventory of PIT tags, with year-specific information for 2009 through 2022 tabulated in Appendix B.

In 2023, a total of 300 trout received PIT tags and adipose fin clips in Rush, Lee Vining, and Walker Creeks; the lowest number of tags deployed since PIT tagging started in 2009 due to very low numbers of trout <125 mm in length (Table 7). In addition, two recaptured adipose fin-clipped fish had shed their original tags and were re-tagged, thus a total of 302 PIT tags were implanted during the 2023 fisheries sampling (Table 7). Of the 302 trout tagged, 141 were age-0 Brown Trout and 139 were age-1 and older Brown Trout (Table 7). For Rainbow Trout, 10 age-0 fish were tagged and 11 age-1 and older were tagged (Table 7). Eight of the age-1+ Brown Trout tagged in the MGORD section were up to 225 mm in total length and were presumed to be age-1 fish (Table 7). In addition, 20 age-0 Brown Trout were tagged in the MGORD (Table 7). Tagged and recaptured fish provided empirical information to estimate annual fish growth, tag retention, fish movements, and apparent survival rates.

Table 7. Total numbers of trout implanted with PIT tags during the 2023 sampling season, by stream, sample section, age-class and species.

Stream	Sample Section	Number of Age-0 Brown Trout (<125 mm)	Number of Age-1 and older Brown Trout	Number of Age-0 Rainbow Trout (<125 mm)	Number of Age-1 and older Rainbow Trout	Section Totals
Rush Creek	Upper Rush	53	2*	2	0	**57 Trout**
	Bottomlands	14	0	0	0	**14 Trout**
	MGORD	20	6**	8	0	**34 Trout**
Rush Creek – new sites	Caddis Channel	17	89***	0	11***	**117 Trout**
	Jeffrey Connector	29	14***	0	1***	**44 Trout**
	Old Main Ch.	7	28***	0	0	**35 Trout**
Lee Vining Creek	Main Channel	0	0	0	0	**0 Trout**
	Side Channel	0	0	0	0	**0 Trout**
Walker Creek	Above old 395	1	0	0	0	**1 Trout**
Species/Age Class Sub-totals:		**141**	**139**	**10**	**12**	**Total Trout: 302**

*shed tag/new tag implanted **up to 225 mm in total length ***all fish tagged in new sample sections

In October of 2023, a total of 61 previously tagged trout (that retained their tags) were recaptured in the Rush Creek watershed (Appendix C). Nine of the recaptures occurred in the Bottomlands section, followed by eight recaptures in the Upper Rush section (including two Rainbow Trout), 27 recaptures in Walker Creek, and five recaptures in the MGORD (Appendix C). In October of 2023, a total of 10 previously tagged Brown Trout and one Rainbow Trout (that retained their tags) were recaptured in the Lee Vining Creek main channel section (Appendix C). During the 2023 sampling, only three previously tagged Rainbow Trout were recaptured, thus very limited growth rate information was available for Rainbow Trout in Rush Creek and Lee Vining Creek.

In the following text, growth between 2022 and 2023 will be referred to as 2023 growth rates. A 2023 trout refers to a fish recaptured in October of 2023. The age of a PIT tagged trout reflects its age during the sampling year. For instance, an age-1 trout in 2023 indicates a trout that was tagged in September 2022 at age-0 and its length and weight were remeasured in October 2023 when it was recaptured.

Also note there's a separate results section for reporting growth rates of recaptures from the MGORD section of Rush Creek, primarily because most of these fish were tagged at presumed age-1 (based on lengths up to 225 mm), instead of at a known age-0. When captured in the MGORD, age-0 trout were also implanted with PIT tags.

Growth of Age-1 Brown Trout between 2022 and 2023

In 2023, a total of 30 known age-1 Brown Trout were recaptured that were tagged as age-0 fish in 2022, for an overall recapture rate of 5.1% (30 recaps/584 age-0 fish tagged in 2022). Of the 30 age-1 recaptures; 16 of these fish were from Rush Creek sections, 11 fish were from Walker Creek and five fish were from the Lee Vining Creek main channel section. Thus, by creek, the age-1 recapture rates for 2023 were 17% in Lee Vining Creek (15% in 2022, 22% in 2021, 14% in 2020, 23% in 2019, 29% in 2018 and 2% in 2017), 3% in Rush Creek (11% in 2022, 7% in 2021, 6% in 2020, 7% in 2019, 14% in 2018, 19% in 2017 and 5% in 2016), and 11% in Walker Creek (25% in 2022, 28% in 2021, 45% in 2020 and 19% in 2019). These recapture rates suggest survival between age-0 and age-1 in Rush and Walker Creeks in 2023 decreased from the previous year, and that survival rates in Lee Vining Creek in 2023 remained somewhat comparable to the previous year.

In the Upper Rush section, four age-1 Brown Trout were recaptured in 2023 and the average growth rates of these trout were 120 mm and 98 g, the second highest growth rates recorded for the 14 years of available data (Table 8). Compared to 2022 rates, the average growth rates of the four age-1 Brown Trout were higher by 39 mm and 57 g (Table 8). Growth rates of age-1 Brown Trout in the Upper Rush section had generally declined annually from 2010 to 2014, but the 2015-2017 growth rates increased each year, with the 2017 growth rates being the largest recorded for this section (Table 8). After the 2017 season, growth rates of age-1 Brown Trout in Upper Rush remained relatively low, with the 2020 and 2021 average growth rates the two lowest rates recorded for the 14 years of available data (Table 8). However, since 2020, growth

rates of age-1 Brown Trout in the Upper Rush section have increased for three consecutive years (Table 8).

In the Bottomlands section of Rush Creek, nine age-1 Brown Trout were recaptured in 2023 and the average growth rates of these trout were 104 mm and 68 g (Table 8). Compared to 2022 rates, the growth rates of the nine age-1 Brown Trout were higher by 24 mm and by 27 g (Table 8). In terms of weight, the average growth rates for age-1 Brown Trout in the Bottomlands had dropped for four consecutive years, 2018-2021, before the 15 g increase in 2022 and the 27 g increase in 2023 (Table 8). The 2023 growth rates of age-1 Brown Trout were the second highest rates for the 14 years of available data (Table 8).

In Walker Creek, 11 age-1 Brown Trout were recaptured in 2023 and the average growth rates of these 11 trout were 67 mm and 30 g (Table 8). Compared to 2022 rates, the growth rates of the 11 age-1 Brown Trout were higher by 14 mm and by 12 g (Table 8). The growth rates of age-1 Brown Trout in Walker Creek have typically been lower than the age-1 growth rates documented in Rush and Lee Vining Creeks (Table 8).

In Lee Vining Creek, five age-1 Brown Trout were recaptured in 2023 and the average growth rates of these trout were 71 mm and 39 g (Table 8). Compared to 2022 rates, the growth rates of the five age-1 Brown Trout were lower by 2 mm in length and higher by 6 g in weight (Table 8).

Growth of Age-2 Brown Trout between 2022 and 2023

In 2023, a total of nine known age-2 Brown Trout were recaptured that were tagged as age-0 fish in 2021, for a recapture rate of 2.0% (9 recaps/446 age-0 fish tagged in 2021). Eight of these fish were recaptured in Walker Creek and one fish was recaptured in Lee Vining Creek.

In Walker Creek, eight age-2 fish were recaptured in 2023 that had been tagged as age-0 fish in 2021 (Table 8). Between age-1 and age-2, the average growth rates of these eight Brown Trout were 52 mm and 42 g; increases of 15 mm and 19 g from the 2022 age-2 growth rates (Table 8).

In the Lee Vining Creek main channel section, one age-2 Brown Trout was recaptured in 2023 that was tagged at age-0 fish in 2021. Between age-1 and age-2, the growth rates of this Brown Trout were 57 mm and 64 g, a 2 mm and 10 g increase in growth rates from the previous year (Table 8).

Growth of Age-3 Brown Trout between 2022 and 2023

In 2023, five known age-3 Brown Trout were recaptured in Walker Creek that were tagged as age-0 fish in 2020; four of these fish were also recaptured each year since their initial tagging. Between age-2 and age-3, the average growth rates of these five Brown Trout were 39 mm and 51 g, versus average growth rates of 22 mm and 18 g of age-3 fish in 2022 (Table 8).

Growth of Age-4 Brown Trout between 2022 and 2023

In 2023, one known age-4 Brown Trout was recaptured in Walker Creek that was tagged as an age-0 fish in 2019. Between age-3 and age-4, the growth rates of this Brown Trout were 103 mm and 212 g, by far the largest growth rates ever documented for an individual Brown Trout in Walker Creek. This fish has been recaptured every year since being tagged in 2019, and between 2021 and 2022 its growth rates were 29 mm and 27 g (Table 8).

Growth of Age-5 Brown Trout between 2022 and 2023

In 2023, one known age-5 Brown Trout was recaptured in Walker Creek that was tagged as age-0 fish in 2018 (Table 8). Between 2022 and 2023, this age-5 Brown Trout grew by 22 mm in length and 36 g in weight (Table 8). This fish was also recaptured at age-2, age-3, and age-4. Between age-3 and age-4, this fish grew by grew by only 4 mm in length and by 0 g in weight. This was the first PIT-tagged age-5 fish recaptured in Walker Creek since 2014 (Table 8).

Growth of MGORD Brown Trout between 2022 and 2023

Starting in September of 2017, PIT tagging of Brown Trout in the MGORD section of Rush Creek was focused on known age-0 fish and presumed age-1 fish. Based on past years' length-frequency histograms and growth rates of know age-1 fish (from recaptures of previously tagged age-0 fish), a conservative cut-off of 225 mm in total length was used to define the probable upper limit for age-1 Brown Trout in the MGORD. Thus, moving forward, most re-captures of previously tagged fish within the MGORD will allow us to compute annual growth rates of fish in which their ages are known or accurately presumed.

In 2023, one age-1 Brown Trout was captured in the MGORD that was tagged at age-0 in the MGORD. Between 2022 and 2023, the growth rates of this fish were 162 mm and 169 g, compared to average growth rates of 123 mm and 100 g in 2022. At age-1, this Brown Trout had a total length of 254 mm (was 92 mm in 2022).

In 2023, one Brown Trout was recaptured that was tagged as presumed age-1 fish in 2022 and this presumed age-2 fish had growth rates of 86 mm and 167 g. The two presumed age-2 fish recaptured in 2023 had total lengths of 324 mm and 340 mm (the 324 mm fish was a non-sequential recapture – tagged at age-0 and recaptured at age-2).

In 2023, one Brown Trout was recaptured in the MGORD that had been PIT tagged in the MGORD as presumed age-1 fish in 2021 and was also recaptured as presumed age-2 fish in the MGORD in 2022. Between age-2 and age-3, the growth rates of this fish were 69 mm and 252 g.

In 2023, two previously tagged Brown Trout were recaptured in the MGORD as non-sequential recaptures. One fish was tagged in 2020 as a presumed age-1 fish (at 183 mm) and was recaptured in 2023 as a presumed age-4 fish at a total length of 375 mm. The other non-sequential recapture was a Brown Trout tagged at age-0 (at 85 mm) in the Upper Rush section in 2021 and was recaptured as an age-2 fish in 2023 in the MGORD at a total length of 324 mm.

Movement of PIT Tagged Trout between Sections

Previous annual fisheries reports have summarized documented movements of PIT tagged fish between the sample sections, with most movements occurring from the Upper Rush section upstream into the MGORD (Taylor 2021). These movements between the Upper Rush section and MGORD were initially documented during the radio telemetry study when approximately 50% of the radio-tagged fish left the MGORD during the fall/early winter spawning period (Taylor et al. 2009). As described in the previous paragraph, in 2023, one of the PIT tagged Brown Trout recaptured in the MGORD had moved from upstream from the Upper Rush section, sometime between age-0 and age-2.

PIT Tag Shed Rate of Trout Recaptured in 2023

In 2023, a total of 64 trout with adipose fin clips were recaptured and three of these fish failed to produce a PIT tag number when scanned with the tag reader (two from Upper Rush and one from Walker Creek). Assuming that all these fish were previously PIT tagged, the 2023 calculated shed rate was 4.7% (3 shed tags/64 clipped fish recaptured) versus shed rates of 3.8% in 2022, 2.3% in 2021 and 6.8% in 2020. Retention rates tend to be higher in juvenile fish because adult salmonids are known to shed tags during spawning (Bateman et al. 2009). Also, tag retention rates have also been linked to tagger's experience and crew turnover rates, with less experienced taggers resulting in higher shed rates (Dare 2003). For the past nine years, our crew members implanting tags have remained relatively stable, however in 2022 the fisheries crew was comprised of mostly new individuals and some with little or no tagging experience, which may explain the slightly higher shed rate.

Table 8a. Average growth (length and weight) of Brown Trout recaptured from 2009 through 2015 by age. Note: *denotes only one PIT tagged fish recaptured.

Stream and Reach	Cohort	Average Annual Growth in Length and Weight (mm/g)						
		2008 -2009	2009 -2010	2010 -2011	2011 -2012	2012 -2013	2013 -2014	2014 -2015
Upper Rush Creek	Age 1	89/51	81/50	83/48	72/33	67/35		90/55
	Age 2		58/70	54/73	43/42	41/42		64/69
	Age 3				14/29		24/41	
	Age 4					12/-22		
	Age-5							
Rush Creek Bottom-lands	Age 1	84/43	77/40	71/35	58/25	56/24		84/41
	Age 2		50/54	35/32	30/28	27/22	32/29*	62/62
	Age 3			13/14	17/16	11/9	35/31	
	Age 4				4/-11		18/20	
	Age-5							
LV Main Channel Brown Trout	Age 1		80/42	72/37	99/52	61/27		73/33
	Age 2		66/95		77/110	33/34	35/29	47/40
	Age 3			34/92		23/48*	16/20*	27/32
	Age 4				21/41*			
	Age-5							
LV Main Channel RB Trout	Age 1					78/47		80/35
	Age 2						40/48*	52/50
	Age 3							
	Age 4							
	Age-5							
Walker Creek Above Old 395	Age 1	68/27	51/20	71/34	68/36	59/23		58/24
	Age 2		31/26	60/56	40/33	27/21	39/35	
	Age 3			28/44	18/12	9/2	20/36	27/29
	Age 4				7/2	2/-16*		28/45*
	Age-5						0/-10*	

Table 8b. Average growth (length and weight) of Brown Trout recaptured from 2016 through 2023 by age. Note: *denotes only one PIT tagged fish recaptured. •denotes one fish that moved from Upper Rush to the MGORD.

Stream and Reach	Cohort	Average Annual Growth in Length and Weight (mm/g)							
		2015 -2016	2016 -2017	2017 -2018	2018 -2019	2019 -2020	2020 -2021	2021 -2022	2022 -2023
Upper Rush Creek	Age 1	105/77	132/129	83/56	77/43	55/21	66/27	81/41	120/98
	Age 2	99/176•	108/239	39/66	48/71	44/55	54/42	68/67*	
	Age 3			11/40*	15/27*	41/49*			
	Age 4						38/144*		
	Age-5							15/-49*	
Rush Creek Bottom-lands	Age 1	94/62	118/96	72/42	74/38	64/29	67/26	80/41	104/68
	Age 2			39/55	36/44*		35/33*	81/84*	
	Age 3					21/20*			
	Age 4								
	Age-5								
LV Main Channel Brown Trout	Age 1	74/40	110/92*	103/77	71/41	72/29	63/27	73/33	71/39
	Age 2	47/49	77/128*		60/91*	70/81	46/47	55/54	57/64*
	Age 3	42/75					30/48		
	Age 4	25/47*						31/67*	
	Age-5								
LV Main Channel RB Trout	Age 1				80/43*				105/71*
	Age 2	62/74*							
	Age 3	38/82*							
	Age 4								
	Age-5								
Walker Creek Above Old 395	Age 1	72/36	66/33		55/28	54/24	47/18	53/18	67/30
	Age 2	47/44	37/37	42/52		36/30	25/19	37/23	52/42
	Age 3		42/59*	25/37	25/37		12/19	22/18	39/51
	Age 4			27/37*		8/-5		13/-5	103/212*
	Age-5								22/36*

Comparison of Length-at Age amongst Sample Sections

During the October 2023 sampling, five age-classes of PIT tagged Brown Trout were recaptured within four fisheries monitoring sections of Rush, Walker, and Lee Vining Creeks (Tables 9 and 10). Along with providing age-specific length information for each section, these data allowed comparisons of length-at-age between sample sections and between the years 2013-2023 (Tables 9 and 10).

In Upper Rush, the average length-at-age-1 in 2023 was 222 mm, 53 mm greater than the average length-at-age-1 in 2022 and 68 mm greater than the average length-at-age-1 in 2021 (Table 9). In 2023, age-1 Brown Trout in Upper Rush were, on average, 20 mm longer than age-1 fish in the Bottomlands section (Table 9). In the Bottomlands section, the average length-at-age-1 in 2023 was 202 mm, 36 mm longer than the 2022 average length-at-age-1, and the second highest average value for the past nine years of available data (Table 9).

In Upper Rush, the average length-at-age-2 in 2023 was 276 mm, 48 mm longer than the average length-at-age-2 in 2022 and 78 mm longer than the average length-at-age-2 in 2021 (Table 9). For Upper Rush, this was the second increase in average length after four consecutive years of decreasing average length-at-age-2 (Table 9). In the Bottomlands section, no PIT-tagged age-2 Brown Trout were recaptured (Table 9).

In 2023, no PIT-tagged age-3 Brown Trout were recaptured in either the Upper Rush section or the Bottomlands section of Rush Creek (Table 9). Also, no PIT-tagged age-4 or age-5 Brown Trout were recaptured in these sections (Table 9).

For Walker Creek in 2023, 11 age-1 Brown Trout were recaptured, and the average length-at-age-1 was 159 mm, 19 mm longer than the average length-at-age-1 in 2022 (Table 9). In 2023, eight PIT tagged age-2 Brown Trout were recaptured in Walker Creek and the average length-at-age-2 equaled 191 mm, 16 mm longer than the average length-at-age-2 in 2022 (Table 9). In 2023, five PIT tagged age-3 Brown Trout were recaptured in Walker Creek and the average length-at-age-3 equaled 214 mm, 15 mm longer than the 2022 average (Table 9). In 2023, two PIT tagged age-4 Brown Trout were recaptured in Walker Creek and the average length-at-age-4 was 270 mm, 57 mm longer than the age-4 fish recaptured in 2022 (Table 9). In 2023, one age-5 Brown Trout was recaptured, and this fish was 227 in length; this was the first age-5 recapture in Walker Creek since 2014 (Table 9).

For the Lee Vining Creek main channel in 2023, five age-1 Brown Trout were recaptured and the average length-at-age-1 for these Brown Trout was 170 mm, 9 mm longer than in 2022 and 16 mm longer than in 2021 (Table 10). In 2023, four previously tagged age-2 Brown Trout were recaptured, and the average length-at-age-2 equaled 225 mm, 17 mm longer than in 2022 (Table 10). In 2023, one age-3 Brown Trout was recaptured, and this fish was 266 mm, 30 mm longer than the average length-at-age-3 in 2022 (Table 10).

These findings of average lengths by age-class continue to support previous conclusions by the Stream Scientist that very few Brown Trout reach age-4 or older in Rush Creek or Lee Vining Creek (Taylor 2022). Outside of the MGORD, we have never recaptured a PIT tagged Brown Trout older than age-5. However, the growth rates that Brown Trout exhibited in 2017 and 2018 confirmed that some age-2 and age-3 fish were near or just above lengths of 300 mm, the size class approaching the metrics of the pre-1941 fishery. These growth rates appeared to have been a function of relatively low fish densities and mostly favorable summer water temperature conditions in 2017 and 2018. The increased growth rates of age-1 and age-2 Brown Trout in 2023 in Rush Creek also appeared to be influenced by cooler water temperatures and lower densities. The MGORD section continues to be the only section where Brown Trout consistently approach or exceed 300 mm in total length by age-2 or age-3. In 2023, two age-2 MGORD recaptures had total lengths of 324 mm and 340 mm. In 2023, one age-3 MGORD recapture had a total length of 345 mm (≈13.5 inches).

Table 9. Size range of PIT tagged recaptures in 2013-2023 by age class for Brown Trout at three electrofishing sections on Rush and Walker Creeks. NOTE: years omitted if no tagged fish were recaptured.

Section	Cohort	Size Range (mm)	Average Length (mm)
Upper Rush	Age-1	**2023** = 193-258 **2022** = 151-189 **2021** = 126-185 **2020** = 124-167 **2019** = 128-202 **2018** = 158-232 **2017** = 224-264 **2016** = 192-237 **2015** = 169-203	**2023** = 222 **2022** = 169 **2021** = 154 **2020** = 145 **2019** = 173 **2018** = 193 **2017** = 243 **2016** = 208 **2015** = 187
	Age-2	**2023** = 267-285 **2022** = 217-237 **2021** = 174-233 **2020** = 209-235 **2019** =203-251 **2018** = 236-305 **2017** = 284-337 **2016** = 289* **2015** = 205-242	**2023** = 276 **2022** = 228 **2021** = 198 **2020** = 221 **2019** = 237 **2018** = 274 **2017** = 313 **2016** = 289* **2015** = 217
	Age-3	**2021** = 220 **2020** = 287 **2019** = 251 **2018** = 295 **2014** = 226-236 **2013** = 227-263	**2021** = 220 **2020** = 287 **2019** = 251 **2018** = 295 **2014** = 231 **2013** = 245
	Age-4	**2021** = 325 **2014** = 288 **2013** = 252-255	**2021** = 325 **2014** = 288 **2013** = 254
	Age-5	**2022** = 340 **2014** = 298	**2022** = 340 **2014** = 298
Bottomlands	Age-1	**2023** = 177-222 **2022** = 142-204 **2021** = 155 **2020** = 141-187 **2019** = 133-196 **2018** = 166-199 **2017** = 189-246 **2016** = 172-217 **2015** = 150-181	**2023** = 202 **2022** = 166 **2021** = 155 **2020** = 155 **2019** = 168 **2018** = 181 **2017** = 221 **2016** = 197 **2015** = 169
	Age-2	**2022** = 202-236 **2021** = 186 **2019** = 219 **2018** = 251-287 **2015** = 197-239 **2014** = 192 **2013** = 156-196	**2022** = 219 **2021** = 186 **2019** = 219 **2018** = 267 **2015** = 219 **2014** = 192 **2013** = 178
	Age-3	**2021** = 214-248 **2020** = 240 **2014** = 194 **2013** = 194-227	**2021** = 231 **2020** = 240 **2014** = 194 **2013** = 204
	Age-4	**2014** = 215-219	**2014** = 216
	Age-5	**2016** = 318	**2016** = 318

*Fish was tagged in Upper Rush but moved to MGORD between age-1 and age-2.

Table 9 (continued).

Section	Cohort	Size Range (mm)	Average Length (mm)
Walker Creek	Age-1	**2023** = 131-187 **2022** = 114-169 **2021** = 121-154 **2020** = 132-170 **2019** = 141-168 **2017** = 151-179 **2016** = 145-187 **2015** = 133-177	**2023** = 159 **2022** = 140 **2021** = 138 **2020** = 151 **2019** = 159 **2017** = 166 **2016** = 167 **2015** = 154
	Age-2	**2023** = 167-220 **2022** = 151-205 **2021** = 155-187 **2020** = 190-196 **2018** = 191-221 **2017** = 180-224 **2016** = 180-226 **2014** = 168-200 **2013** = 181-208	**2023** = 191 **2022** = 175 **2021** = 175 **2020** = 194 **2018** = 210 **2017** = 202 **2016** = 201 **2014** = 186 **2013** = 197
	Age-3	**2023** = 209-221 **2022** = 180-215 **2021** = 200-212 **2019** = 215-235 **2018** = 204-245 **2017** = 238 **2015** = 211-231 **2014** = 207-222 **2013** = 219-221	**2023** = 214 **2022** = 199 **2021** = 205 **2019** = 220 **2018** = 228 **2017** = 238 **2015** = 219 **2014** = 217 **2013** = 220
	Age-4	**2023** = 240-299 **2022** =205-221 **2020** = 224-243 **2018** = 265 **2015** = 249 **2014** = 211 **2013** = 219	**2023** = 270 **2022** = 213 **2020** = 234 **2018** = 265 **2015** = 249 **2014** = 211 **2013** = 219
	Age-5	**2023** = 227 **2014** = 220	**2023** = 227 **2014** = 220

Table 10. Size range of PIT tagged fish recaptured in 2013-2023 by age class for Brown Trout and Rainbow Trout on Lee Vining Creek. NOTE: years omitted if no tagged fish were recaptured.

Section	Cohort	Size Range (mm)	Average Length (mm)
Brown Trout in Lee Vining Main Channel	Age-1	**2023** = 154 - 181 **2022** = 145-169 **2021** = 126-182 **2020** = 125-185 **2019** = 142-209 **2018** = 170-194 **2017** = 210 **2016** = 147-186 **2015** = 149-190	**2023** = 170 **2022** = 161 **2021** = 154 **2020** = 155 **2019** = 174 **2018** = 183 **2017** = 210 **2016** = 171 **2015** = 166
	Age-2	**2023** = 212-250 **2022** = 183-230 **2021** = 163-225 **2020** = 212-270 **2019** = 222-274 **2017** = 247 **2016** = 205-217 **2015** = 176-214 **2014** = 174-195 **2013** = 206-225	**2023** = 225 **2022** = 208 **2021** = 195 **2020** = 232 **2019** = 247 **2017** = 247 **2016** = 211 **2015** = 197 **2014** = 188 **2013** = 215
	Age-3	**2023** = 266 **2022** =226-246 **2021** = 246 **2017** = 280-305 **2016** = 210-256 **2015** = 188-228 **2014** = 234-241 **2013** = 238-271	**2022** = 236 **2021** = 246 **2017** = 293 **2016** = 240 **2015** = 215 **2014** = 238 **2013** = 253
	Age-4	**2022** = 277 **2016** = 237	**2022** = 277 **2016** = 237
	Age-5	None captured in past nine years	
Rainbow Trout in Lee Vining Main Channel	Age-1	**2023** = 202 **2019** = 165 **2015** = 140-177	**2023** = 202 **2019** = 165 **2015** = 157
	Age-2	**2016** = 232 **2015** = 195-216 **2014** = 201-229	**2016** = 232 **2015** = 204 **2014** = 215
	Age-3	**2016** = 242	**2016** = 242
	Age-4	None captured in past nine years	
	Age-5	None captured in past nine years	

Summer Water Temperature

During the past 12 years, the Mono Basin has experienced a five-year drought (2012-2016), an Extreme-wet RY (2017), a Normal RY with a full GLR (2018), a Wet RY (2019), a Dry-normal-1 RY (2020), a Dry RY (2021), a Dry RY (2022), and a record Extreme-wet RY in 2023. These RY types have resulted in a range of summer water temperatures in Rush Creek, from moderate-to-severely stressful conditions in drier RYs to thermal regimes mostly conducive to fair-to-good growth conditions in wetter RYs.

In 2023, the water temperature monitoring was conducted by the MLC. The extended elevated flows of the record runoff resulted in the loss of the data logger at the Rush Creek/Bottom of MGORD location. Also at several locations, the data loggers became exposed to air when flow levels dropped, causing an interruption of water temperature data collection at Old 395 Bridge/Upper Rush on 9/26/23, at Below Narrows on 9/21/23, and at Rush/County Road on 8/5/23. Thus, during the 92-day period of July-September when summer water temperatures were examined, the Old 395 Bridge site was missing four days of data, the Below Narrows site was missing nine days of data, and the County Road site was missing 57 days of data (most of August and all of September).

In 2023, a record Extreme-wet RY with an extended GLR spill resulted in favorable summer thermal conditions, with no peak water temperatures exceeding 70^{o}F at all Rush Creek monitoring locations (Table 11). In 2023, daily mean temperatures and average daily maximum temperatures were the lowest or second-lowest recorded at all Rush Creek temperature monitoring locations since these data were collected (Table 11). At most Rush Creek temperature monitoring locations, the maximum diurnal fluctuations were the lowest since the Extreme-wet RY of 2017 (Table 11).

Similar to the 2013-2022 annual reports, 2023 Rush Creek summer average daily water temperature data were classified based on its predicted influence on growth of Brown Trout as either: 1) good potential growth days, 2) fair potential growth days, 3) poor potential growth days (daily averages within one degree or less of a “bad thermal day”), or 4) bad thermal days (Table 12). Development of these thermal-based growth criteria were fully described in previous annual reports (Taylor 2013 and 2014). Using these growth prediction metrics, good potential growth days in 2023 varied from 69% to 100% of days in Rush Creek where data were available within the period from July 1 to September 30 (Table 12). For all Rush Creek monitoring locations, the number of days classified as “fair” potential growth days in 2023 ranged from 0% to 31% of the summer days where data were available (Table 12). In 2023, none of the water temperature monitoring locations experienced poor potential growth days or bad thermal days (Table 12).

As was done with the 2013-2022 data, the diurnal temperature fluctuations for July, August and September 2023 were characterized by the one-day maximum fluctuation that occurred each month and by monthly averages (Table 13). Also, for each temperature monitoring location, the highest average diurnal fluctuations over consecutive 21-day durations were determined (Table 13). The diurnal fluctuations throughout the summer of 2023 were relatively low, especially

when compared to the two previous Dry-RY years (2021 and 2022) (Table 13). Over the 21-day durations, no diurnal fluctuations were above or close to the threshold of 12.6°F considered detrimental to trout growth (Werley et al. 2007) during the summer of 2023 (Table 13). In contrast, the Above Parker, Below Narrows and County Road temperature monitoring locations had 21-day durations with diurnal fluctuations exceeding 12.6°F during the previous summer of 2022 (Table 13).

The thermal window bounded by 66.2-71.6°F where Brown Trout may be physiologically stressed and living at the edge of their survival tolerance as defined by Bell (2006) was quantified for each Rush Creek temperature monitoring location in 2013 through 2023. The hourly temperature data for the 92-day (or 2,208-hour) summer period were sorted from low to high and the number of hours where temperatures exceeded 66.2°F were summed by month and entire summer period (Table 14). The values from 2013 - 2022 were also included to better illustrate the variability that occurred at all the temperature monitoring locations (Table 14). The 2023 data show that five of the six Rush Creek temperature monitoring locations experienced no hours where water temperatures exceeded 66.2°F (Table 14). At the County Road location, hourly water temperatures exceeded 66.2°F for two hours on the afternoon when the data logger stopped recording water temperatures (Table 14).

In 2023, the extended high flows of cooler water travelling down Rush Creek obscured any temperature effects of cooler water accretions from Parker and Walker Creeks on Rush Creek's summer thermal regime. In drier years, slight improvements to Rush Creek's thermal regime are noticeable when examining the temperature metrics from the Above Parker and Below Narrows temperature monitoring locations. However, previous annual reports have determined these slight improvements to water temperature from Parker and Walker accretions were localized and unnoticeable downstream at the County Road temperature monitoring location (Taylor 2023).

Summer water temperatures in Lee Vining Creek were all within the range of fair-to-good growth potential during 2023. Regardless of water-year type, excessively warm water has not been an issue in Lee Vining Creek, thus detailed analyses were not performed with the 2023 data.

Table 11. Summary of water temperature data during the summer of RY 2023 (July to September). Averages were calculated for daily mean, daily minimum, and daily maximum temperatures between July 1st and September 30th. All temperature data are presented in °F. When available, values for 2013-2022 are provided for comparison.

Temperature Monitoring Location	Daily Mean (°F)	Ave Daily Minimum (°F)	Ave Daily Maximum (°F)	No. Days > 70°F	Max Diurnal Fluctuation (°F)	Date of Max. Fluctuation
Rush Ck. – At Damsite	**2023 = 55.2**	**2023 = 53.0**	**2023 = 58.3**	**2023 = 0**	**2023 = 10.0**	**9/18/23**
Rush Ck. – Top of MGORD	2013 = 63.1	2013 = 62.7	2013 = 63.7	2013 = 0	2013 = 3.4	7/09/13
	2014 = 64.8	2014 = 64.6	2014 = 65.0	2014 = 0	2014 = 3.9	8/13/14
	2015 = 64.4	2015 = 64.1	2015 = 64.8	2015 = 0	2015 = 2.1	7/03/15
	2016 = 63.8	2016 = 63.0	2016 = 64.7	2016 = 0	2016 = 6.5	7/07/16
	2017 = 57.0	2017 = 56.5	2017 = 58.1	2017 = 0	2017 = 5.4	9/07/17
	2018 = 60.7	2018 = 59.6	2018 = 61.9	2018 = 0	2018 = 6.7	8/20/18
	2019 = 58.5	2019 = 57.2	2019 = 59.9	2019 = 0	2019 = 8.2	8/10/19
	2020 = 63.2	2020 = 62.1	2020 = 64.4	2020 = 0	2020 = 6.4	7/02/20
	2021 = 65.9	2021 = 65.2	2021 = 66.8	2021 = 5	2021 = 6.5	7/13/21
	2022 = 65.9	2022 = 65.0	2022 = 67.0	2022 = 3	2022 = 6.6	7/12/22
	2023 = 54.0	**2023 = 53.3**	**2023 = 55.0**	**2023 = 0**	**2023 = 8.2**	**8/31/23**
Rush Ck. – Bottom of MGORD	2013 = 63.2	2013 = 60.9	2013 = 67.1	2013 = 1	2013 = 9.0	7/09/13
	2014 = 64.8	2014 = 62.9	2014 = 68.5	2014 = 20	2014 = 8.3	7/13/14
	2015 = 64.4	2015 = 62.3	2015 = 68.0	2015 = 20	2015 = 8.4	7/06/15
	2016 = 63.8	2016 = 61.8	2016 = 66.9	2016 = 1	2016 = 8.0	7/04/16
	2017 = 57.1	2017 = 56.5	2017 = 58.5	2017 = 0	2017 = 6.4	9/07/17
	2018 = 61.0	2018 =58.9	2018 = 63.9	2018 = 0	2018 = 8.7	7/05/18
	2019 = 58.7	2019 = 56.6	2019 = 61.3	2019 = 0	2019 = 8.1	8/10/19
	2020 = 63.2	2020 = 60.5	2020 = 67.5	2020 = 17	2020 = 10.0	8/03/20
	2021 = 65.8	2021 = 63.4	2021 = 69.8	2021 = 44	2021 = 8.5	7/24/21
	2022 = 65.9	2022 = 63.7	2022 = 69.5	2022 = 50	2022 = 8.7	7/29/22
	2023 = N/A	**2023 = N/A**	**2023 = N/A**	**2023 = N/A**	**2023 = N/A**	**2023 = N/A**
Rush Ck. – Old Highway 395 Bridge/Upper Rush section	2013 = 62.6	2013 = 58.8	2013 = 68.7	2013 = 40	2013 = 13.5	7/09/13
	2014 = 64.0	2014 = 60.5	2014 = 69.8	2014 = 51	2014 = 13.3	7/13/14
	2015 = N/A	2015 = N/A	2015 = N/A	2015 = N/A	2015 = N/A	N/A
	2016 = 63.5	2016 = 60.1	2016 = 68.8	2016 = 47	2016 = 12.5	7/11/16
	2017 = 59.0	2017 = 57.5	2017 = 61.0	2017 = 0	2017 = 7.6	9/07/17
	2018 = 60.9	2018 = 58.0	2018 = 65.3	2018 = 0	2018 = 10.9	7/10/18
	2019 = 58.7	2019 = 56.1	2019 = 62.3	2019 = 0	2019 = 10.7	9/14/19
	2020 = 62.6	2020 = 58.5	2020 = 68.4	2020 = 30	2020 = 14.0	8/03/20
	2021 = 65.0	2021 = 61.2	2021 = 70.8	2021 = 63	2021 = 12.8	8/02/21
	2022 = 64.7	2022 = 60.4	2022 = 70.6	2022 = 55	2022 = 15.2	8/07/22
	2023 = 57.4	**2023 = 55.8**	**2023 = 59.6**	**2023 = 0**	**2023 = 9.6**	**8/31/23**

Table 11 (continued).

Temperature Monitoring Location	Daily Mean (°F)	Ave Daily Minimum (°F)	Ave Daily Maximum (°F)	No. Days > 70°F	Max Diurnal Fluctuation (°F)	Date of Max. Fluctuation
Rush Ck. – Above Parker	2016 = 63.2	2016 = 58.8	2016 = 69.4	2016 = 55	2016 = 13.7	7/11/16
	2017 = 59.0	2017 = 57.2	2017 = 61.9	2017 = 0	2017 = 8.6	9/08/17
	2018 = 60.9	2018 = 57.2	2018 = 66.3	2018 = 0	2018 = 13.4	7/10/18
	2019 = 58.4	2019 = 55.5	2019 = 62.3	2019 = 0	2019 = 11.8	9/14/19
	2020 = 62.2	2020 = 57.1	2020 = 68.6	2020 = 40	2020 = 16.1	8/03/20
	2021 = 64.4	2021 = 59.6	2021 = 70.8	2021 = 61	2021 = 14.4	8/02/21
	2022 = 64.5	2022 = 59.4	2022 = 70.7	2022 = 59	2022 = 15.7	8/07/22
	2023 = 57.5	**2023 = 55.6**	**2023 = 60.4**	**2023 = 0**	**2023 = 10.7**	**9/27/23**
Rush Ck. – below Narrows	2013 = 61.2	2013 = 56.2	2013 = 67.6	2013 = 24	2013 = 16.3	7/19/13
	2014 = 63.2	2014 = 57.1	2014 = 69.4	2014 = 46	2014 = 17.3	7/26/14
	2015 = 62.3	2015 = 58.8	2015 = 66.1	2015 = 0	2015 = 11.5	9/23/15
	2016 = 61.7	2016 = 56.9	2016 = 68.3	2016 = 34	2016 = 14.3	7/13/16
	2017 = 58.4	2017 = 56.3	2017 = 61.3	2017 = 0	2017 = 8.2	9/07/17
	2018 = 60.0	2018 = 56.0	2018 = 65.4	2018 =0	2018 = 12.4	7/10/18
	2019 = 57.8	2019 = 54.4	2019 = 62.2	2019 = 0	2019 = 12.7	9/22/19
	2020 = 61.0	2020 = 55.5	2020 = 67.5	2020 = 16	2020 = 15.7	8/03/20
	2021 = 63.2	2021 = 58.0	2021 = 69.7	2021 = 49	2021 = 14.9	8/12/21
	2022 = 63.2	2022 = 58.0	2022 = 69.5	2022 = 52	2022 = 14.7	7/29/22
	2023 = 57.3	**2023 = 55.2**	**2023 = 60.3**	**2023 = 0**	**2023 = 8.9**	**8/31/23**
Rush Ck. – County Road*	2013 = 61.4	2013 = 56.5	2013 = 66.6	2013 = 7	2013 = 14.7	8/02/13
	2014 = 62.0	2014 = 56.7	2014 = 67.8	2014 = 24	2014 = 17.6	7/26/14
	2015 = 62.1	2015 = 59.1	2015 = 65.5	2015 = 2	2015 = 9.2	7/28/15
	2016 = 61.6	2016 = 56.0	2016 = 68.3	2016 = 32	2016 = 16.1	7/11/16
	2017 = N/A	2017 = N/A	2017 = N/A	2017 = N/A	2017 = N/A	N/A
	2018 = N/A	2018 = N/A	2018 = N/A	2018 = N/A	2018 = N/A	N/A
	2019 = 58.2	2019 = 54.0	2019 = 63.6	2019 = 0	2019 = 13.5	9/13/19
	2020 = 61.0	2020 = 54.5	2020 = 68.5	2020 = 42	2020 = 18.2	8/03/20
	2021 = 63.1	2021 = 56.6	2021 = 70.7	2021 = 57	2021 = 17.4	9/02/21
	2022 = 63.3	2022 = 57.5	2022 = 70.2	2022 = 55	2022 = 16.8	7/29/22
	2023 = 61.4	**2023 = 56.8**	**2023 = 63.6**	**2023 = 0**	**2023 = 12.6**	**8/04/23**

*logger stopped working on 8/5/23.

Table 12. Classification of 2013-2023 summer water temperature data into good growth days, fair growth days, poor growth days and bad thermal days based on daily average temperatures (92-day period from July 1 to September 30). The percentage (%) designates each thermal day-type's occurrence for the 92-day summer period.

Temperature Monitoring Location	No. of Days for Good Growth Potential – Daily Ave. ≤60.5°F	No. of Days for Fair Growth Potential – Daily Ave. 60.6° – 63.9°F	No. of Days of Poor Growth Potential – Daily Ave. 64.0° - 64.9°F	No. of Bad Thermal Days - Daily Ave. ≥65°F
Rush Ck. – At Damsite	**2023 = 92 (100%)**	**2023 = 0**	**2023 = 0**	**2023 = 0**
Rush Ck. – Top of MGORD	2013 = 14 (15%) 2014 = 5 (6%) 2015 = 7 (8%) 2016 = 10 (11%) 2017 = 66 (71%) 2018 = 47 (51%) 2019 = 65 (71%) 2020 = 6 (6%) 2021 = 0 2022 = 12 (13%) **2023 = 90 (98%)**	2013 = 43 (47%) 2014 = 14 (15%) 2015 = 20 (22%) 2016 = 32 (35%) 2017 = 26 (29%) 2018 = 42 (46%) 2019 = 23 (25%) 2020 = 50 (54%) 2021 = 30 (33%) 2022 = 21 (23%) **2023 = 2 (2%)**	2013 = 17 (18%) 2014 = 25 (27%) 2015 = 5 (5%) 2016 = 17 (18%) 2017 = 0 2018 = 3 (3%) 2019 = 4 (4%) 2020 = 12 (13%) 2021 = 8 (9%) 2022 = 5 (6%) **2023 = 0**	2013 = 18 (20%) 2014 = 48 (52%) 2015 = 60 (65%) 2016 = 33 (36%) 2017 = 0 2018 = 0 2019 = 0 2020 = 24 (26%) 2021 = 54 (59%) 2022 = 54 (59%) **2023 = 0**
Rush Ck. – Bottom MGORD	2013 = 11 (12%) 2014 = 6 (6%) 2015 = 8 (9%) 2016 = 9 (10%) 2017 = 67 (73%) 2018 = 48 (52%) 2019 = 62 (68%) 2020 = 4 (4%) 2021 = 14 (15%) 2022 = 23 (25%) **2023 = N/A**	2013 = 38 (41%) 2014 = 11 (12%) 2015 = 20 (22%) 2016 = 31 (34%) 2017 = 25 (27%) 2018 = 42 (46%) 2019 = 28 (30%) 2020 = 50 (54%) 2021 = 30 (33%) 2022 = 14 (15%) **2023 = N/A**	2013 = 20 (22%) 2014 = 21 (23%) 2015 = 5 (6%) 2016 = 16 (17%) 2017 = 0 2018 = 2 (2%) 2019 = 2 (2%) 2020 = 18 (20%) 2021 = 13 (14%) 2022 = 7 (8%) **2023 = N/A**	2013 = 23 (25%) 2014 = 54 (59%) 2015 = 59 (64%) 2016 = 36 (39%) 2017 = 0 2018 = 0 2019 = 0 2020 = 20 (22%) 2021 = 35 (38%) 2022 = 48 (52%) **2023 = N/A**
Rush Ck. – Old Highway 395 Bridge/Upper Rush section	2013 = 14 (15%) 2014 = 7 (8%) 2015 = N/A 2016 = 16 (17%) 2017 = 75 (82%) 2018 = 36 (39%) 2019 = 64 (70%) 2020 = 17 (18%) 2021 = 24 (26%) 2022 = 29 (32%) **2023 = 77 (89%)**	2013 = 41 (45%) 2014 = 25 (27%) 2015 = N/A 2016 = 24 (26%) 2017 = 17 (18%) 2018 = 56 (61%) 2019 = 28 (30%) 2020 = 48 (52%) 2021 = 30 (33%) 2022 = 17 (18%) **2023 = 10 (11%)**	2013 = 33 (36%) 2014 = 27 (29%) 2015 = N/A 2016 = 19 (21%) 2017 = 0 2018 = 0 2019 = 0 2020 = 17 (18%) 2021 = 11 (12%) 2022 = 7 (8%) **2023 = 0**	2013 = 4 (4%) 2014 = 33 (36%) 2015 = N/A 2016 = 33 (36%) 2017 = 0 2018 = 0 2019 = 0 2020 = 10 (11%) 2021 = 27 (29%) 2022 = 39 (42%) **2023 = 0**
Rush Ck. – Above Parker Ck.	2016 = 17 (18%) 2017 = 65 (71%) 2018 = 28 (30%) 2019 = 67 (73%) 2020 = 24 (26%) 2021 = 30 (33%) 2022 = 31 (34%) **2023 = 81 (88%)**	2016 = 26 (28%) 2017 = 27 (29%) 2018 = 64 (70%) 2019 = 25 (27%) 2020 = 41 (45%) 2021 = 34 (37%) 2022 = 16 (17%) **2023 = 11 (12%)**	2016 = 24 (26%) 2017 = 0 2018 = 0 2019 = 0 2020 = 21 (23%) 2021 = 10 (11%) 2022 = 7 (8%) **2023 = 0**	2016 = 25 (27%) 2017 = 0 2018 = 0 2019 = 0 2020 = 10 (11%) 2021 = 18 (20%) 2022 = 38 (41%) **2023 = 0**

Table 12 (continued).

Temperature Monitoring Location	No. of Days for Good Growth Potential – Daily Ave. ≤60.5°F	No. of Days for Fair Growth Potential – Daily Ave. 60.6°– 63.9°F	No. of Days of Poor Growth Potential – Daily Ave. 64.0° - 64.9°F	No. of Bad Thermal Days - Daily Ave. ≥65°F
Rush Ck. – Below Narrows	2013 = 17 (18%) 2014 = 13 (14%) 2015 = 24 (26%) 2016 = 22 (24%) 2017 = 75 (82%) 2018 = 46 (50%) 2019 = 74 (80%) 2020 = 36 (39%) 2021 = 26 (28%) 2022 = 33 (36%) **2023 = 75 (90%)**	2013 = 69 (75%) 2014 = 58 (63%) 2015 = 44 (48%) 2016 = 52 (57%) 2017 = 17 (18%) 2018 = 46 (50%) 2019 = 18 (20%) 2020 = 53 (58%) 2021 = 39 (42%) 2022 = 22 (24%) **2023 = 8 (10%)**	2013 = 6 (7%) 2014 = 18 (20%) 2015 = 22 (24%) 2016 = 16 (17%) 2017 = 0 2018 = 0 2019 = 0 2020 = 2 (2%) 2021 = 10 (11%) 2022 = 27 (29%) **2023 = 0**	2013 = 0 2014 = 3 (3%) 2015 =2 (2%) 2016 = 2 (2%) 2017 = 0 2018 = 0 2019 = 0 2020 = 1 (1%) 2021 = 17 (18%) 2022 = 8 (9%) **2023 = 0**
Rush Ck. – County Road*	2013 = 17 (18%) 2014 = 17 (18%) 2015 = 25 (27%) 2016 = 24 (26%) 2017 = N/A 2018 = N/A 2019 = 71 (77%) 2020 = 31 (34%) 2021 = 26 (28%) 2022 = 33 (36%) **2023 = 24 (69%)**	2013 = 64 (70%) 2014 = 59 (65%) 2015 = 39 (42%) 2016 = 50 (54%) 2017 = N/A 2018 = N/A 2019 = 21 (23%) 2020 = 50 (54%) 2021 = 31 (34%) 2022 = 15 (16%) **2023 = 11 (31%)**	2013 = 8 (9%) 2014 = 14 (15%) 2015 =23 (25%) 2016 = 13 (14%) 2017 = N/A 2018 = N/A 2019 = 0 2020 = 10 (11%) 2021 = 9 (10%) 2022 = 8 (9%) **2023 = 0**	2013 = 3 (3%) 2014 = 2 (2%) 2015 = 5 (6%) 2016 = 5 (6%) 2017 = N/A 2018 = N/A 2019 = 0 2020 = 1 (1%) 2021 = 26 (28%) 2022 = 36 (39%) **2023 = 0**

*data logger stopped working on 8/5/23.

Table 13. Diurnal temperature fluctuations in Rush Creek for 2023: maximum daily for month, daily average for month, and highest average for consecutive 21-day duration (92-day period from July 1 to September 30). NOTE: 2022 values in ( ) for comparison.

Temperature Monitoring Location	Maximum and Average Daily Diurnal Fluctuation for July	Maximum and Average Daily Diurnal Fluctuation for August	Maximum and Average Daily Diurnal Fluctuation for September	Highest Average Diurnal Fluctuation for a Consecutive 21-Day Duration
Rush Ck. – At Damsite	Max = 5.7°F Ave = 4.3°F	Max = 7.3°F Ave = 4.7°F	Max = 10.0 °F Ave = 7.2°F	7.5°F Sept 11 – 30
Rush Ck. – Top of MGORD	Max = 3.6°F (6.6) Ave = 1.3°F (3.0)	Max = 8.2°F (3.3) Ave = 2.5°F (1.7)	Max = 3.2°F (2.9) Ave = 1.1°F (1.1)	2.4°F (3.4) Aug 20 – Sept 9
Rush Ck. – Old Hwy 395 Bridge	Max = 4.3°F (13.2) Ave = 3.0°F (9.5)	Max = 9.6°F (15.2) Ave = 4.0°F (10.4)	Max = 7.8°F (12.8) Ave = 4.6°F (10.6)	4.7°F (11.8) Sept 5 - 25
Rush Ck. – Above Parker Ck.	Max = 4.6°F (14.6) Ave = 3.4°F (11.0)	Max = 9.7°F (15.7) Ave = 4.8°F (11.5)	Max = 10.7°F (14.1) Ave = 6.3°F (11.3)	7.2°F (12.8) Sept 10 - 30
Rush Ck. – below Narrows	Max = 5.6°F (14.7) Ave = 4.5°F (11.4)	Max = 8.9°F (14.2) Ave = 5.2°F (11.5)	Max = 7.8°F (14.7) Ave = 5.8°F (11.7)	6.0°F (13.2) Aug 31 – Sept 20
Rush Ck. – County Road*	Max = 7.8°F (16.8) Ave = 6.6°F (12.8)	Max = N/A (15.6) Ave = N/A (15.5)	Max = N/A (14.7) Ave = N/A (12.1)	7.0°F (14.5) July 15 - Aug 4

*data logger stopped working on 8/5/23.

Table 14. Number of hours (percent of hours in parentheses) that temperature exceeded 66.2°F in Rush Creek: by month and for 92-day period from July 1 to September 30, 2013 - 2023. The total number of hours within each month is in parentheses in the column headings.

Temperature Monitoring Location	Number of Hours Temperature exceeded 66.2°F in July (744 hours)	Number of Hours Temperature exceeded 66.2°F in August (744 hours)	Number of Hours Temperature exceeded 66.2°F in Sept. (720 hours)	Number of Hours Temperature exceeded 66.2°F in 92-day period
Rush Ck. – At Damsite	**2023 = 0 hrs**	**2023 = 0 hrs**	**2023 = 0 hrs**	**2023 = 0 hrs**
Rush Ck. – Top of MGORD	2013 = 4 hrs (0.5%) 2014 = 315 hrs (42%) 2015 = 140 hrs (19%) 2016 = 42 hrs (6%) 2017 = 0 hrs 2018 = 0 hrs 2019 = 0 hrs 2020 = 0 hrs 2021 = 488 hrs (66%) 2022 = 246 hrs (33%) **2023 = 0 hrs**	2013 = 4 hrs (0.5%) 2014 = 96 hrs (13%) 2015 = 205 hrs (28%) 2016 = 127 hrs (17%) 2017 = 0 hrs 2018 = 6 hrs 2019 = 0 hrs 2020 = 71 hours (10%) 2021 = 588 hrs (79%) 2022 = 728 hrs (98%) **2023 = 0 hrs**	2013 = 0 hrs 2014 = 0 hrs 2015 = 0 hrs 2016 = 0 hrs 2017 = 0 hrs 2018 = 0 hrs 2019 = 13 hrs 2020 = 47 hrs (7%) 2021 = 35 hrs (5%) 2022 = 343 hrs (48%) **2023 = 0 hrs**	2013 = 8 hrs (0.4%) 2014 = 411 hrs (19%) 2015 = 345 hrs (16%) 2016 = 169 hrs (8%) 2017 = 0 hrs 2018 = 6 hrs (0.3%) 2019 = 13 hrs (0.6%) 2020 = 118 hrs (5%) 2021 = 1,111 hrs (50%) 2022 = 1,317 hrs (60%) **2023 = 0 hrs**
Rush Ck. – Old 395 Bridge/Upper Rush	2013 = 181 hrs (24%) 2014 = 287 hrs (39%) 2016 = 216 hrs (29%) 2017 = 0 hrs 2018 = 17 hrs (2%) 2019 = 0 hrs 2020 = 113 hrs (15%) 2021 = 351 hrs (47%) 2022 = 252 hrs (34%) **2023 = 0 hrs**	2013 = 228 hrs (31%) 2014 = 248 hrs (33%) 2016 = 263 hrs (35%) 2017 = 0 hrs 2018 = 32 hrs (4%) 2019 = 4 hrs (0.5%) 2020 = 241 hrs (32%) 2021 = 328 hrs (44%) 2022 = 350 hrs (47%) **2023 = 0 hrs**	2013 = 73 hrs (10%) 2014 = 117 hrs (16%) 2016 = 53 hrs (7%) 2017 = 3 hrs (0.4%) 2018 = 33 hrs (5%) 2019 = 41 hrs (6%) 2020 = 87 hrs (12%) 2021 = 127 hrs (18%) 2022 = 162 hrs (23%) **2023 = 0 hrs**	2013 = 482 hrs (22%) 2014 = 639 hrs (29%) 2016 = 532 hrs (24%) 2017 = 3 hrs = (0.1%) 2018 = 82 hrs (4%) 2019 = 45 hrs (2%) 2020 = 441 hrs (20%) 2021 = 806 hrs (37%) 2022 = 764 hrs (35%) **2023 = 0 hrs**
Rush Ck. – Above Parker Creek	2016 = 240 hrs (32%) 2017 = 0 hrs 2018 = 70 hrs (9%) 2019 = 0 hrs 2020 = 146 hrs (20%) 2021 = 342 hrs (46%) 2022 = 276 hrs (37%) **2023 = 0 hrs**	2016 = 269 hrs (36%) 2017 = 0 hrs 2018 = 68 hrs (9%) 2019 = 11 hrs (2%) 2020 = 257 hrs (35%) 2021 = 316 hrs (42%) 2022 = 348 hrs (47%) **2023 = 0 hrs**	2016 = 65 hrs (9%) 2017 = 14 hrs (2%) 2018 = 44 hrs (6%) 2019 = 27 hrs (4%) 2020 = 73 hrs (10%) 2021 = 122 hrs (17%) 2022 = 157 hrs (22%) **2023 = 0 hrs**	2016 = 574 hrs (26%) 2017 = 14 hrs (0.6%) 2018 = 182 hrs (8%) 2019 = 38 hrs (2%) 2020 = 476 hrs (22%) 2021 = 780 hrs (35%) 2022 = 781 hrs (35%) **2023 = 0 hrs**
Rush Ck. – below Narrows	2013 = 158 hrs (21%) 2014 = 244 hrs (33%) 2015 = 129 hrs (17%) 2016 = 167 hrs (22%) 2017 = 0 hrs 2018 = 36 hrs (5%) 2019 = 0 hrs 2020 = 109 (15%) 2021 = 273 hrs (37%) 2022 = 243 hrs (33%) **2023 = 0 hrs**	2013 = 192 hrs (26%) 2014 = 193 hrs (26%) 2015 = 189 hrs (25%) 2016 = 222 hrs (30%) 2017 = 0 hrs 2018 = 42 hrs (6%) 2019 = 13 hrs (2%) 2020 = 204 hrs (27%) 2021 = 267 hrs (36%) 2022 = 265 hrs (36%) **2023 = 0 hrs**	2013 = 55 hrs (7%) 2014 = 105 hrs (15%) 2015 = 0 hrs (0%) 2016 = 49 hrs (7%) 2017 = 0 hrs 2018 = 36 hrs (5%) 2019 = 8 hrs (1%) 2020 = 43 hrs (6%) 2021 = 104 hrs (14%) 2022 = 109 hrs (15%) **2023 = 0 hrs**	2013 = 405 hrs (18%) 2014 = 542 hrs (25%) 2015 = 318 hrs (14%) 2016 = 438 hrs (20%) 2017 = 0 hrs 2018 = 114 hrs (5%) 2019 = 21 hrs (1%) 2020 = 356 hrs (16%) 2021 = 644 hrs (29%) 2022 = 617 hrs (28%) **2023 = 0 hrs**

Table 14 (continued).

Temperature Monitoring Location	Number of Hours Temperature exceeded 66.2°F in July (744 hours)	Number of Hours Temperature exceeded 66.2°F in August (744 hours)	Number of Hours Temperature exceeded 66.2°F in Sept. (720 hours)	Number of Hours Temperature exceeded 66.2°F in 92-day period
Rush Ck. – County Road	2013 = 197 hrs (27%) 2014 = 222 hrs (30%) 2015 = 174 hrs (23%) 2016 = 212 hrs (28%) 2017 = N/A 2018 = N/A 2019 = 0 hrs 2020 = 195 hrs (26%) 2021 = 301 hrs (40%) 2022 = 290 hrs (39%) **2023 = 0 hrs**	2013 = 172 hrs (23%) 2014 = 195 hrs (26%) 2015 = 119 hrs (16%) 2016 = 233 hrs (31%) 2017 = N/A 2018 = N/A 2019 = 76 hrs (10%) 2020 = 241 hrs (32%) 2021 = 278 hrs (37%) 2022 = 282 hrs (38%) **2023 = 2 hrs***	2013 = 42 hrs (6%) 2014 = 79 hrs (11%) 2015 = 0 hrs (0%) 2016 = 42 hrs (6%) 2017 = N/A 2018 = N/A 2019 = 10 hrs (1%) 2020 = 41 hrs (6%) 2021 = 99 hrs (14%) 2022 = 107 hrs (15%) **2023 = N/A***	2013 = 411 hrs (19%) 2014 = 496 hrs (23%) 2015 = 293 hrs (13%) 2016 = 487 hrs (22%) 2017 = N/A 2018 = N/A 2019 = 86 hrs (4%) 2020 = 477 hrs (22%) 2021 = 678 hrs (31%) 2022 = 679 hrs (31%) **2023 = N/A***

*data logger stopped working on 8/5/23. On 8/4/23 the daily max temperature was 67.2°F.

Discussion

The 2023 sampling was marked by being the second year of fisheries monitoring under the newly issued WR-2021-0086, which amended LADWP's license and signaled the start of the 10-year post-settlement monitoring period. During this 10-year period, all watershed monitoring activities (fisheries, geomorphic/riparian, and Mono Lake limnology) will be conducted by consultants, with oversight from the MAT. The purpose of the post-settlement monitoring is to evaluate the effectiveness of the SEF flow regimes and as needed, make recommended changes to these flows (timing and magnitude), as long as the overall quantity of water released by LADWP is not increased from those defined in WR-2021-0086.

The 2023 sampling year was also highlighted by extended high flows in all study creeks due to the record snowpack and Extreme-wet RY. These high flows resulted in good summer water temperatures in Rush Creek; however, these extended high flows may have impacted the survival and recruitment of age-0 trout in Rush, Walker, and Lee Vining Creeks.

In 2023, new sections of Rush Creek were electrofished, the first time in 16 years that new sections were sampled by the fisheries team since the Bottomlands Rush section was added in 2008. These new sections were a product of beaver activity in lower Rush Creek that created a multi-channel network of side channels and beaver dam pools and ponds. In the past several decades, the importance of beaver modified in-channel habitats has gained recognition and is the focus of both research and habitat enhancement/restoration efforts (Bouwes et al. 2016).

Thus, this report's Discussion is focused on the long-term trout population metrics and the sampling of beaver modified habitats. The Discussion section concludes with a methods evaluation and proposed fisheries monitoring activities for 2024.

Trout Population Metrics

Annual fisheries sampling in Rush and Lee Vining Creeks since 1999 has provided an unusually long-term data set of trout population metrics. The overarching theme of these data is that trout populations respond better to wetter runoff years than to average-to-drier runoff years. The best example of this trend was the five-year drought of 2012-2016 in which the recruitment of age-0 Brown Trout decreased by 95% in the Upper Rush section and by 89% in the Bottomlands section. Numbers and condition factors of older trout also decreased during this five-year drought. Then, two good runoff years in 2017 and 2018 with a full GLR, saw trout populations rebound quickly with age-0 recruitment increasing nearly two-fold (200%) in Upper Rush and more than 12-fold (1,200%) in the Bottomlands section. Growth rates and condition factors also improved in the two years post-drought. In fact, growth rates measured in October of 2017 were the highest ever recorded, with elevated streamflows all summer long. PIT tag recaptures in 2023 also confirmed excellent growth rates of Brown Trout during another Extreme-wet RY with relatively cool summer water temperatures. The high growth rates in 2023 were also exhibited by the relatively low numbers of Brown Trout captured in the 125-199 mm size class because most age-1 fish had grown to lengths >200 mm. Thus, trout numbers,

growth rates and conditions factors in Rush and Lee Vining Creeks can oscillate widely depending on runoff year type. Changing climate and variable snowpack conditions in the eastern Sierra will most likely dictate the long-term fate and viability of Rush Creek's Brown Trout fishery. However, continued SEF releases, maturation of the riparian canopy, eight more years of annual monitoring, and adaptive management may push the restoration of the creeks and the trout fisheries in a positive direction.

The October 2023 fisheries sampling resulted in extremely low numbers of age-0 trout and the fewest number of PIT tags deployed in age-0 trout since the tagging program was started in 2009. No age-0 Brown Trout were captured in the Walker Creek section and in the Lee Vining Creek section. This low recruitment may have been a combination of two factors. First, poor spawning success in the fall of 2022 after a second consecutive summer of poor and stressful water temperatures. Several studies have shown that the condition of female Brown Trout at the time of spawning is critical to fecundity and egg viability (Bell 2006). Stressful water temperatures, available food base and water quality during the summer and early fall can affect female condition, leading to low fecundity, smaller egg size, and decreased egg viability (Bell 2006 and Pender and Kwak 2002). In turn, juvenile trout fitness and survival has been positively related to egg size (Ojanguren et al. 1996). Second, the peak flows during the Extreme-wet runoff, including steep rising limbs of the Rush and Lee Vining Creeks' hydrographs may have resulted in high displacement and low survival of newly emerged Brown Trout fry. Wagner (2015) conducted a literature review of flow effects on Brown Trout, including peak flood flows. Jensen and Johnsen (1999) documented the highest mortality rates of Brown Trout occurred during spring peak flood flows as fry were emerging or newly emerged. Ottaway and Clarke (1981) determined that displacement of Brown Trout fry was correlated with surface velocities.

Sampling in Beaver Modified Habitats

The three new Rush Creek sections sampled in October of 2023 were associated with habitats influenced by a series of beaver dams. The Caddis Channel section was previously named the 8-Channel, and prior to beaver activity, the 8-Channel carried a minor portion of Rush Creek's flow. When sampled by the fisheries crew on 10/9/23, the Caddis Channel carried approximately 80-90% of the flow and was characterized by pool/riffle sequences with relatively fast-flowing water. The Jeffrey Connector Channel section was a small side channel off the Caddis Channel that flowed through a beaver-dam pond at its upper end, then downstream of the pond most of this channel consisted of low-gradient riffles with several shallow pools. The Jeffrey Connector Channel also appeared to have numerous areas with suitable sized substrate for trout spawning. The Jeffrey Connector Channel re-connected with the Caddis Channel within the reach of the Caddis Channel sampled by the fisheries crew. The Old Main Channel section carried very little flow when sampled on 10/10/23, probably less than 10% of Rush Creek's total flow. The Old Main Channel supported seven beaver dams and associated ponds/pools that were sampled by the fisheries crew.

Beaver dams, associated ponds/pools, and other channel modifications are generally seen as beneficial to trout in many regions globally, including the western United States (Naiman et al. 1988), Europe (Bouwes et al. 2016), and South America (Arismendi et al. 2020). Beavers are

often called ecosystem engineers for their ability to alter watershed dynamics through their dam construction and riparian foraging; the processes they influence are varied with numerous benefits to trout and other aquatic organisms (Figure 16) (Figure 1 in Bouwes et al. 2016). The following text was associated with Figure 1 in Bouwes et al. 2016:

Beaver-made dams and beaver dam analogs (BDAs) slow and increase the surface height of water upstream of the dam. Beaver dams above and plunge pools below dams change the plane bed channel to a reach of complex geomorphic units providing resting and efficient foraging opportunities for juvenile trout. Deep pools allow for temperature stratification and greater hydraulic pressures forcing downwellings to displace cooler groundwater to upwell downstream, increasing thermal heterogeneity and refugia. Dams and associated overflow channels produce highly variable hydraulic conditions resulting in a greater diversity of sorted sediment deposits. Gravel bars form near the tail of the pond and just downstream from the scour below the dam, increasing spawning habitat and concealment substrate for juveniles. Complex depositional and erosional patterns cause an increase in channel aggradation, widening, and sinuosity and a decrease in overall gradient, also increasing habitat complexity. Frequent inundation of inset floodplains creates side channels, high flow refugia and rearing habitat for age-0 juveniles and increasing recruitment of riparian vegetation. Flows onto the floodplain during high discharge dissipates stream power, and the likelihood of dam failure. The increase in pond complexes and riparian vegetation increases refugia for beavers, their food supply and caching locations, resulting in higher survival, and more persistent beaver colonies. Beavers will maintain dams and associated geomorphic and hydraulic processes that create complex fish habitat.

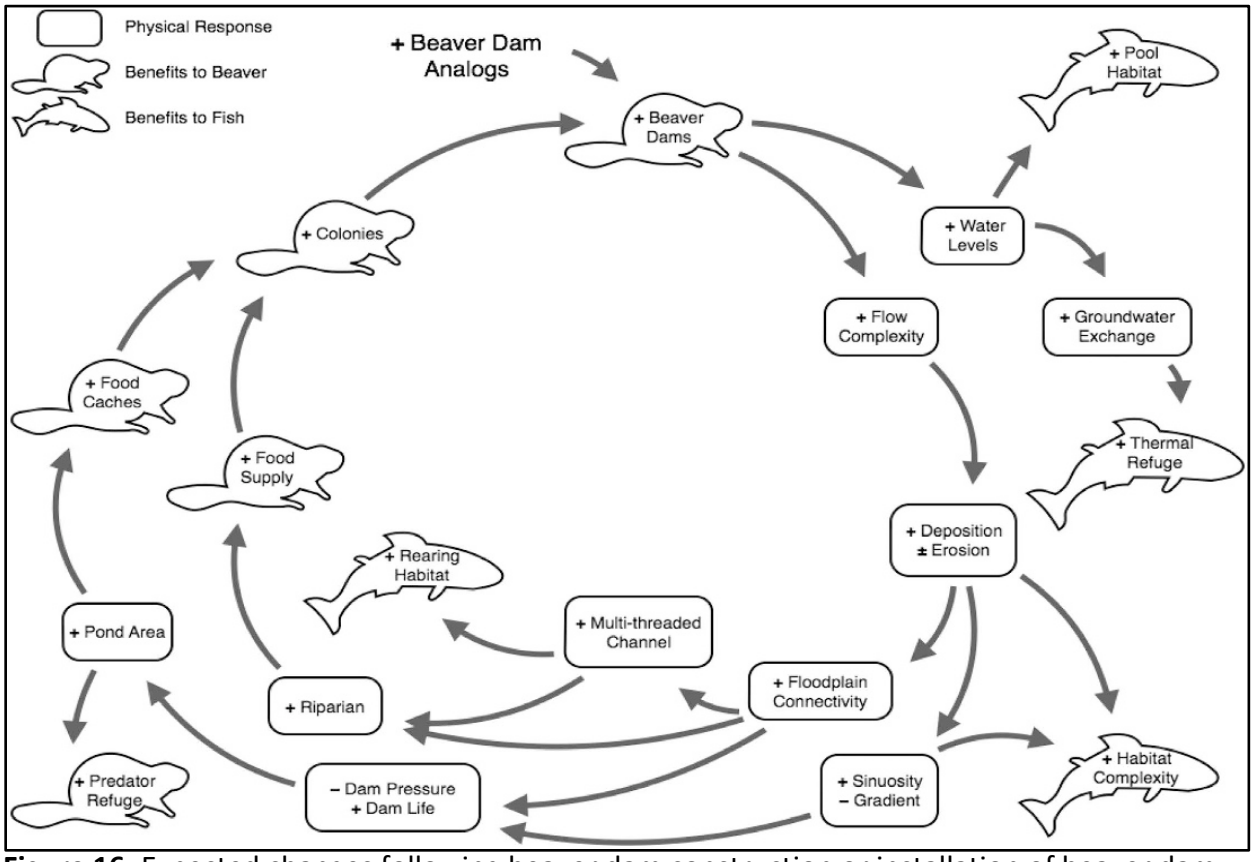

Figure 16. Expected changes following beaver dam construction or installation of beaver dam analogs (BDAs).

The heterogeneity described by Bouwes et al. (2016) was apparent in the beaver influenced reach of Rush Creek sampled in October of 2023. A main flow channel that was at one time a relatively minor side channel (the Caddis Channel), a reach of extensive dams and associated

ponds/pools (the Old Main Channel), and a shallow side channel providing high-flow refugia and abundant age-0 habitat (the Jeffrey Connector Channel). These systems were mostly intact after experiencing a period of sustained high flows (22 days where the discharge was >700 cfs and 43 days where the discharge was >600 cfs). Although we observed some flow-related damage to several of the beaver dams, we also observed beaver activity (and a beaver) in the dam/pond located in the upper section of the Jeffrey Connector Channel.

Two research groups (Bouwes et al. 2016 and Needham et al. 2021) conducted paired watershed studies to examine the physical and biological responses of beavers, beaver dams and/or BDAs. Bouwes et al. 2016 installed BDAs in treatment reaches of an incised tributary of the John Day River in Oregon that were then used by beavers as stable platforms to construct multi-dam complexes. Compared to untreated reference reaches, the BDA reaches experienced significant increases in the densities, survival, and production of juvenile steelhead without impacting upstream and downstream migration of fish (Bouwes et al. 2016). Needham et al. 2021 studied the effects of reintroducing Eurasian beavers to an enclosed 40-hectare (≈100 acre) reach of a first-order stream feeding into Loch Grant in Scotland, with an adjacent first-order stream as their control. The enclosed area contained approximately 1.2 km of channel and within two years, the beavers had constructed five dams. Electrofishing and PIT tagging of Brown Trout occurred in both streams. By the second year, Brown Trout in the beaver manipulated stream were more abundant with a more diverse age-class structure and higher growth rates than fish in the adjacent untreated stream (Needham et al. 2021). This study also observed PIT tagged fish moving from the untreated stream to the treated stream, but no movement was detected in the other direction (Needham et al. 2021).

While we only have a single season of electrofishing data from the beaver influenced reach of Rush Creek, our data suggests that age-0 Brown Trout fared better in this reach than the predominantly single-thread channel of the Bottomlands section (the closest annually sampled section). The age-0 proportion of the total Brown Trout catch in the Bottomlands was 20% versus 30% in the beaver-influenced reach (65% in the Jeffrey Connector, 20% in the Old Main, and 19% in the Caddis Channel). A box and whisker plot of the weights of age-0 Brown Trout shows median and average weights were greater in the beaver-influenced reach than all other Rush Creek sample sections (Figure 17). The Jeffrey Connector had the greatest age-0 average weight of 14.9 g, followed by 14.0 g in the Old Main, 13.9 g in the Caddis Channel, 13.4 g in the MGORD, 10.0 g in Upper Rush, and 9.0 g in the Bottomlands (Figure 17). The Bottomlands' box plot and median value has no overlap with the box plots and median values of the three sites within the beaver-influenced reach, indicating a clear difference in the weights of age-0 Brown Trout (Figure 17). The Upper Rush box plot has some overlap with the box plots of the three sites within the beaver-influenced reach, yet Upper Rush's median value falls outside the boxes of the three sites within the beaver-influenced reach, suggesting there's likely a difference in the weights of age-0 Brown Trout (Figure 17). Condition factors of age-1 and older Brown Trout in the beaver influenced reach were higher than the Bottomlands section: 0.98 in the Caddis Channel and 1.00 in the Old Main Channel versus 0.94 in the Bottomlands section. Finally, the RSD-225 values in the Caddis Channel (64) and Old Main Channel (66) were more than twice the Bottomlands' valve (29) and the RSD-300 values were also much greater in the Caddis Channel (6) and the Old Main Channel (21), versus a value of 2 in the Bottomlands.

We intend to sample the beaver influenced reach of Rush Creek in 2024 to continue tracking how Brown Trout fare in these habitats. Because we PIT tagged all the trout caught in 2023, recaptures in 2024 will allow us to compare growth rates between the beaver influenced reach and our annually sampled Rush Creek sections.

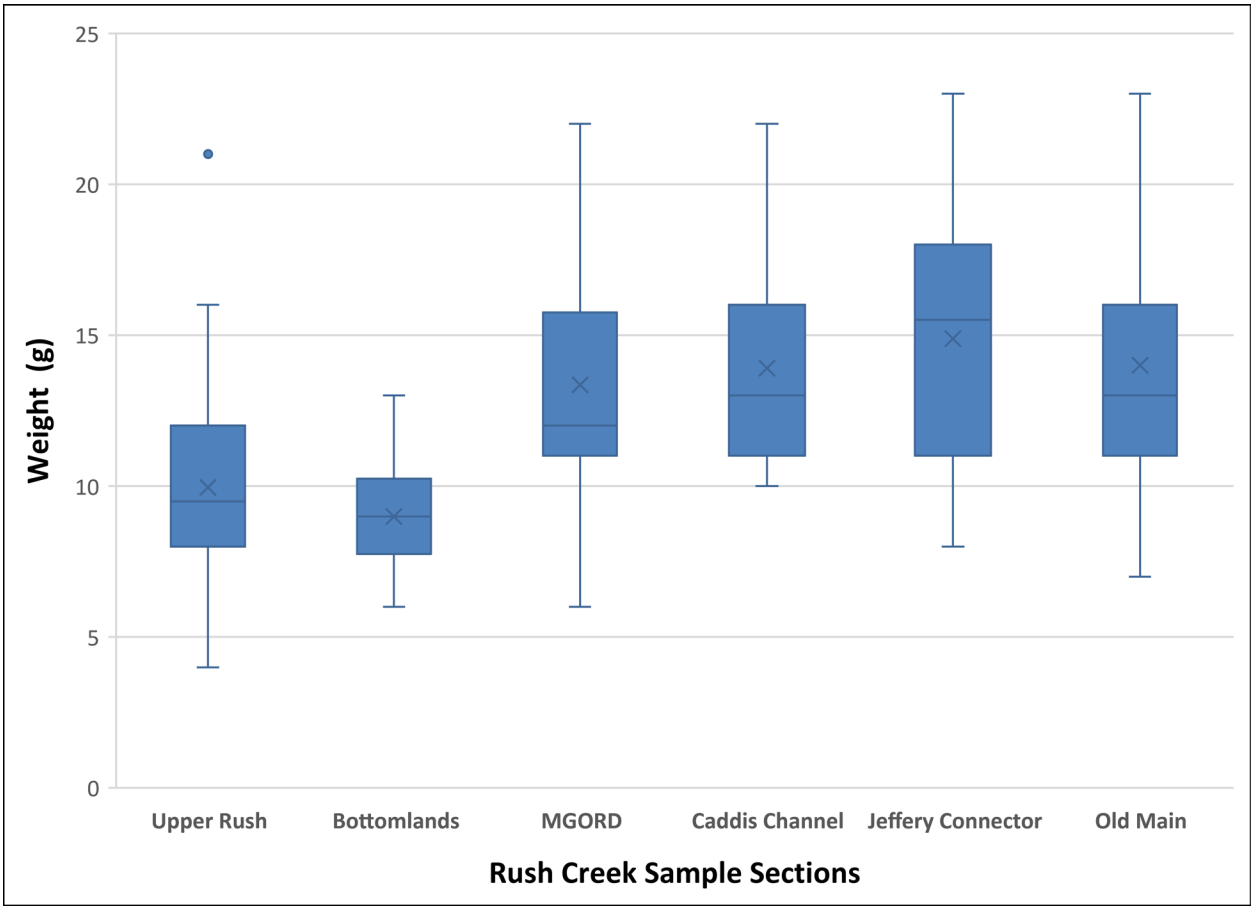

Figure 17. Box and whisker plots of age-0 Brown Trout weights from Rush Creek sections sampled in October of 2023.

Methods Evaluation

As in previous years, small variations in wetted channel widths were measured, which resulted in changes to sample section areas. Thus, we recommend that channel lengths and widths are re-measured annually.

In 2022 the MLC assumed sole responsibility of the water temperature monitoring in Mono Basin streams. As described in the Results section, the extended high flows in 2023 resulted in the loss of one data logger (Bottom of MGORD) and incomplete summer water temperature data sets at three additional Rush Creek locations. Starting in 2024, it is recommended that the MLC either place redundant data loggers at all Rush Creek water temperature monitoring locations or conduct periodic visits to the data loggers to ensure that complete data sets are collected during the months of July, August, and September to preserve the integrity of the summer water temperature monitoring program. In the past, LADWP placed redundant data

loggers at all sites and on several occasions the back-up loggers were relied on to provide complete data sets.

The PIT tagging program was continued during the September 2023 sampling; tags were implanted in age-0 fish in all sections, in presumed age-1 fish in the MGORD, and in all fish captured in the new Rush Creek sections. The PIT tagging program allowed us to continue to document annual growth rates of trout, calculate apparent survival rates, and assess the ability of fish to reach or exceed lengths of 300 mm. Continuation of the PIT tagging program is recommended during the post-settlement Fisheries Monitoring Program.

Trout size classes (<125, 125-199, and ≥200 mm) developed and discussed during the 2008 annual report should continue to be used for calculations of population estimates (Hunter et al. 2008). Using these size classes provides for long-term consistency as well as year to year consistency with the annual fisheries data sets. However, we acknowledge that in Walker Creek, some age-1 Brown Trout are occasionally less than 125 mm in total length and in MGORD are bigger than 199 mm. We also acknowledge that in the MGORD and occasionally in other Rush Creek sections age-0 fish may exceed 125 mm in total length, especially in high runoff years when cooler summer water temperatures result in higher growth rates.

To ensure that electrofishing sampling can be conducted safely and efficiently, flow in Rush Creek should not exceed **35 cfs** and flow in Lee Vining Creek should not exceed **30 cfs** during the annual sampling period. Allowances for flow variances to allow for safe wading conditions and effective sampling were included in the new SWRCB WR-2021-0086.

The first two seasons of the post-settlement fisheries monitoring were conducted with a six-person field crew. In previous years when the annual monitoring was conducted with the SWRCB fisheries scientist and LADWP personnel, a seven-person field crew was employed. This allowed us to use four netters when using the electrofishing barge and allowed us to have four people processing fish when sampling the MGORD. The past two seasons have felt short-staffed, and our capture efficiencies most likely dropped from pre-settlement sampling due to using one less netter. Thus, if the annual MAT budget allows, the Fisheries Stream Scientist recommends the fisheries field crew be increased to seven people.

As of early March of 2024, the Mono Basin was experiencing close to an average snowpack, and on 2/29/24, the snowpack in the Mono Basin was measured at 75% of normal. Another substantial snowstorm hit the basin during the first week of March. Depending on GLR storage levels going into May and June, released flows from GLR may translate into cool summer temperatures with a full reservoir or possibly warmer water temperatures in Rush Creek with a moderate to low reservoir level.

Proposed Fisheries Sampling for 2024 Season

We intend to conduct population estimate sampling in the fall of 2024 at the following locations: MGORD Rush, Upper Rush, Bottomlands Rush, Lee Vining Creek main channel, and Walker Creek. In addition to conducting population estimate sampling at the annually sampled

locations, the Fisheries Stream Scientist proposes to conduct single-pass sampling at the new Rush Creek sites sampled in 2023: the Caddis Channel, the Jeffrey Connector Channel, and the beaver dam pools of the Old Main Channel. Summer water temperatures would also be collected within these specific habitats.

In 2009, the fisheries crew collected benthic macroinvertebrates (BMI) from Rush and Lee Vining Creeks following methods developed for determining a BMI index of biological integrity (IBI) for stream assessments in the eastern Sierra Nevada of California (Herbst and Silldorff 2009). Our 2009 collections from Rush Creek showed improved IBI scores over samples collected in 2000 and reported by Herbst and Silldorff (2009). The Fisheries Stream Scientist proposes that a discussion occur with the MAT to repeat these BMI collections and IBI analyses in 2024 or 2025, 15-16 years since the past effort was made to determine if the creeks are still trending towards recovery of their BMI populations. If implemented, the responsibilities of this task could be shared with the Geomorphic/Riparian Stream Scientist (Bill Trush) and/or MLC staff.

The Fisheries Stream Scientist continues to recommend that a bathymetric survey of GLR is conducted to assess the amount of sediment infill and to determine the actual storage capacity of GLR. Reduced storage may negate assumptions about minimum storage levels for suitable summer water temperatures in Rush Creek, as well as affect water availability for future exports. Bathymetric surveys are commonly used to assess rates of sedimentation in reservoirs and the loss of storage capacity can depend on several factors (Iradukunda and Bwanbale 2021). Globally the overall loss of reservoir storage capacity is estimated at 1 to 2% of total storage capacity per year (Iradukunda and Bwanbale 2021). In 1991, the GLR thermal characteristics study by Cullen and Railsback (1993) determined that their reservoir thermal model underpredicted water surface elevations, which corresponded to a storage volume error of approximately 1,000 acre-feet and that sedimentation may have caused this discrepancy in their depth-to-volume regression.

Recommended changes to SEF's based on 2023 Fisheries Monitoring

The Fisheries Stream Scientist's primary recommendation heading into a runoff-year close to a Normal RY is to enter the spring and summer of 2024 with GLR as full as feasibly possible. A fuller GLR will provide better summer water temperatures in Rush Creek, thus promoting higher trout growth rates and condition factors.

In February of 2024, LADWP communicated to the Stream Scientists and Mono Basin stakeholders that during the 2023 peak releases from GLR to the MGORD, the roto-valve that moderates flows, started to vibrate unusually at flows greater than 200 cfs. A subsequent inspection by the Division of Safety of Dams (DSOD) confirmed that the nearly 90-year-old roto-valve was comprised and must be replaced prior to LADWP commencing on the GLR spillway modification project. As of early March 2024, LADWP was unsure if the 80-foot-deep shaft housing the roto-valve is also in need of replacement. Depending on the scope of the project, LADWP's initial replacement time estimate is two to five years. During this timeframe, the maximum flow releases into the top of the MGORD will be 175 cfs, meaning that in RYs of a

Dry-Normal II and wetter, LADWP will fail to meet SEF peak flow requirements. Several meetings and calls have occurred to start considering how to manage Rush Creek flows for RY2024, especially if the RY is a Normal or Wet-Normal year type and LADWP is unable to release the SEF peak flows. Decisions include where in the annual hydrograph to release the extra water not released as a SEF peak flow, and determining the timing and magnitude of GLR spills during periods when spills aren't necessarily wanted or beneficial.

The Fisheries Stream Scientist will work with the Geomorphic/Riparian Stream Scientist in reviewing LADWP's draft AOP for 2024 and provide comments, as needed. This year's AOP includes addressing Rush Creek flow releases via the compromised roto-valve and LADWP's export allowance based on Mono Lake's level when measured on 4/1/24.

References Cited

Arismendi, I., B.E. Penaluna, and C.G. Jara. 2020. Introduced beaver improve growth of non-native trout in Tierra del Fuego, South America. Ecology and Evolution, 10: 9454-9465.

Armour, C.L. 1997. Evaluating temperature regimes for the protection of Brown Trout. U.S. Department of the Interior, National Biological Survey, Resource Publication #201. 26 p.

Barnham, C. and A. Baxter. 1998. Condition factor, K, in salmonid fish. Fisheries Notes #FN0005 State of Victoria, Australia. 3 p.

Bateman, D.S., R.E. Gresswell and A.M. Berger. 2009. Passive integrated tag retention rates in headwater populations of coastal cutthroat trout. North American Journal of Fisheries Management 29: 653-657.

Bell, J.M. 2006. The assessment of thermal impacts on habitat selection, growth, reproduction, and mortality in Brown Trout (*Salmo trutta*): a review of the literature. Vermillion River EPA Grant #WS 97512701-1. 23p.

Blackwell, B.G., M.L. Brown and D.W. Willis. 2000. Relative weight (W_r) status and current use in fisheries assessment and management. Reviews in Fisheries Science, 8(1): 1-44.

Bouwes, N., N. Weber, C.E. Jordan, W.C. Saunders, and I.A. Tattam. 2016. Ecosystem experiment reveals benefits of natural and simulated beaver dams to a threatened population of steelhead (*Oncorhynchus mykiss*). Nature, Science Report #28581.

Cone, R.S. 1989. The need to reconsider the use of condition indices in fishery science. Transactions of the American Fisheries Society 118: 510-514.

Cullen, R.T. and S.F. Railsback. 1993. Summer thermal characteristics of Grant Lake, Mono County, California. Feasibility Study #2, Trihey and Associates, Concord, CA. 118 p.

Dare, M.R. 2003. Mortality and long-term retention of passive integrated tags by spring Chinook salmon. North American Journal of Fisheries Management 23: 1015-1019.

Gabelhouse, D. W., Jr. 1984. A length-categorization system to assess fish stocks. North American Journal of Fisheries Management 4:273-285.

Herbst, D.B. and E.L. Silldorff. 2009. Development of a benthic macroinvertebrate index of biological integrity (IBI) for stream assessments in the eastern Sierra Nevada of California. Final technical report for the Surface Water Ambient Monitoring Program (SWAMP). 90 p.

Hunter, C., B. Shepard, K. Knudson, R. Taylor and M. Sloat. 2004. Fisheries Monitoring Report for Rush, Lee Vining, Parker and Walker Creeks 2003. Los Angeles Department of Water and Power. 45 p.

Hunter, C., R. Taylor, K. Knudson, B. Shepard, and M. Sloat. 2005. Fisheries Monitoring Report for Rush, Lee Vining, Parker and Walker Creeks 2004. Los Angeles Department of Water and Power. 51 p.

Hunter, C., R. Taylor, K. Knudson and B. Shepard. 2006. Fisheries Monitoring Report for Rush, Lee Vining, Parker and Walker Creeks 2005. Los Angeles Department of Water and Power. 61 p.

Hunter, C., R. Taylor, K. Knudson and B. Shepard. 2007. Fisheries Monitoring Report for Rush, Lee Vining, Parker and Walker Creeks 2006. Los Angeles Department of Water and Power. 74 p.

Hunter, C., R. Taylor, K. Knudson and B. Shepard. 2008. Fisheries Monitoring Report for Rush, Lee Vining, Parker and Walker Creeks 2007. Los Angeles Department of Water and Power. 49 p.

Iradukunda, P. and E. Bwambale. 2021. Reservoir sedimentation and its effect on storage capacity – a case study of Murera Reservoir, Kenya. Cogent Engineering 8: 14 p.

McB&T and RTA. 2010. Synthesis of instream flow recommendations to the State Water Resources Control Board and the Los Angeles Department of Water and Power. 159 p.

Naiman, R.J., C.A. Johnson, and J.C. Kelley. 1988. Alteration of North American streams by beaver. BioScience, Vol. 38(11): 753-762.

Needham, R.J., M. Gaywood, A. Tree, N. Sotheron, D. Roberts, C.W. Bean, and P.S. Kemp. 2021. The response of a brown trout (*Salmo trutta*) population to reintroduced Eurasian beaver (*Castor fiber*) habitat modification. Canadian Journal of Fisheries and Aquatic Sciences, 78 (11): 1650-1660.

Ojanguren, A.F., F.G. Reyes-Gavilan, and F. Brana. 1996. Effects of egg size on offspring development and fitness in brown trout *Salmo Trutta*. Aquaculture 147: 9-20.

Pender, D.R. and T.J. Kwak. 2002. Factors influencing brown trout reproductive success in Ozark tailwater rivers. Transactions of the American Fisheries Society 131: 698-717.

Reimers, N. 1963. Body condition and over-winter survival of hatchery-reared trout in Convict Creek, California. Transactions of the American Fisheries Society 92 (1): 39-46.

Shepard, B., R. Taylor, K. Knudson and C. Hunter. 2009. Effects of flow, reservoir storage and water temperature on trout in Rush and Lee Vining Creeks, Mono County, California. Prepared for LADWP. 117 p.

Taylor, R. and K. Knudson. 2012. Fisheries Monitoring Report for Rush, Lee Vining, Parker and Walker Creeks 2011. Los Angeles Department of Water and Power. 90 p.

Taylor, R. 2013. Fisheries Monitoring Report for Rush, Lee Vining, Parker and Walker Creeks 2012. Los Angeles Department of Water and Power. 100 p.

Taylor, R. 2014. Fisheries Monitoring Report for Rush, Lee Vining, Parker and Walker Creeks 2013. Los Angeles Department of Water and Power. 89 p.

Taylor, R. 2019. Fisheries Monitoring Report for Rush, Lee Vining, Parker and Walker Creeks 2018. Los Angeles Department of Water and Power. 89 p.

Taylor, R. 2020. Fisheries Monitoring Report for Rush, Lee Vining, Parker and Walker Creeks 2019. Los Angeles Department of Water and Power. 96 p.

Taylor, R. 2021. Fisheries Monitoring Report for Rush, Lee Vining, Parker and Walker Creeks 2020. Los Angeles Department of Water and Power. 97 p.

Taylor, R. 2022. Fisheries Monitoring Report for Rush, Lee Vining, Parker and Walker Creeks 2021. Los Angeles Department of Water and Power. 97 p.

Trush, W.J. 2006. Technical Memorandum: status and recommended revisions to the SWRCB Orders 98-05 and 98-07 riparian vegetation and geomorphic termination criteria. Prepared for the SWRCB and LADWP.

Wagner, E.J. 2015. A review of the effects of flow on brown trout. Utah Division of Wildlife Resources, Fisheries Experiment Station, Logan, Utah. 9 p.

Appendices for the 2023 Mono Basin Annual Fisheries Report

Appendix A: Aerial Photographs of Annual Sample Sites on Rush, Walker and Lee Vining Creeks

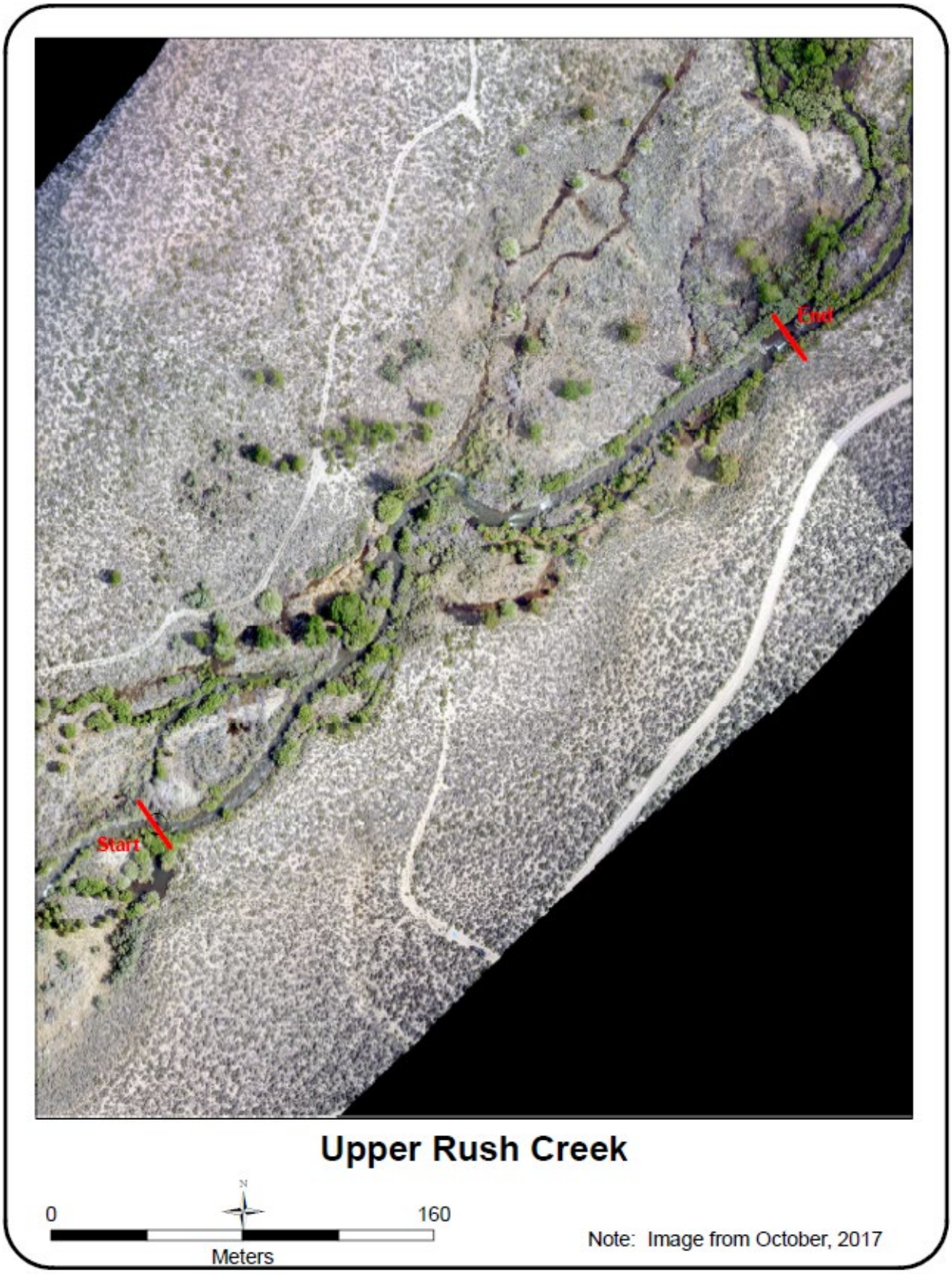
End
Start
Upper Rush Creek
N
0
160
Meters
Note: Image from October, 2017

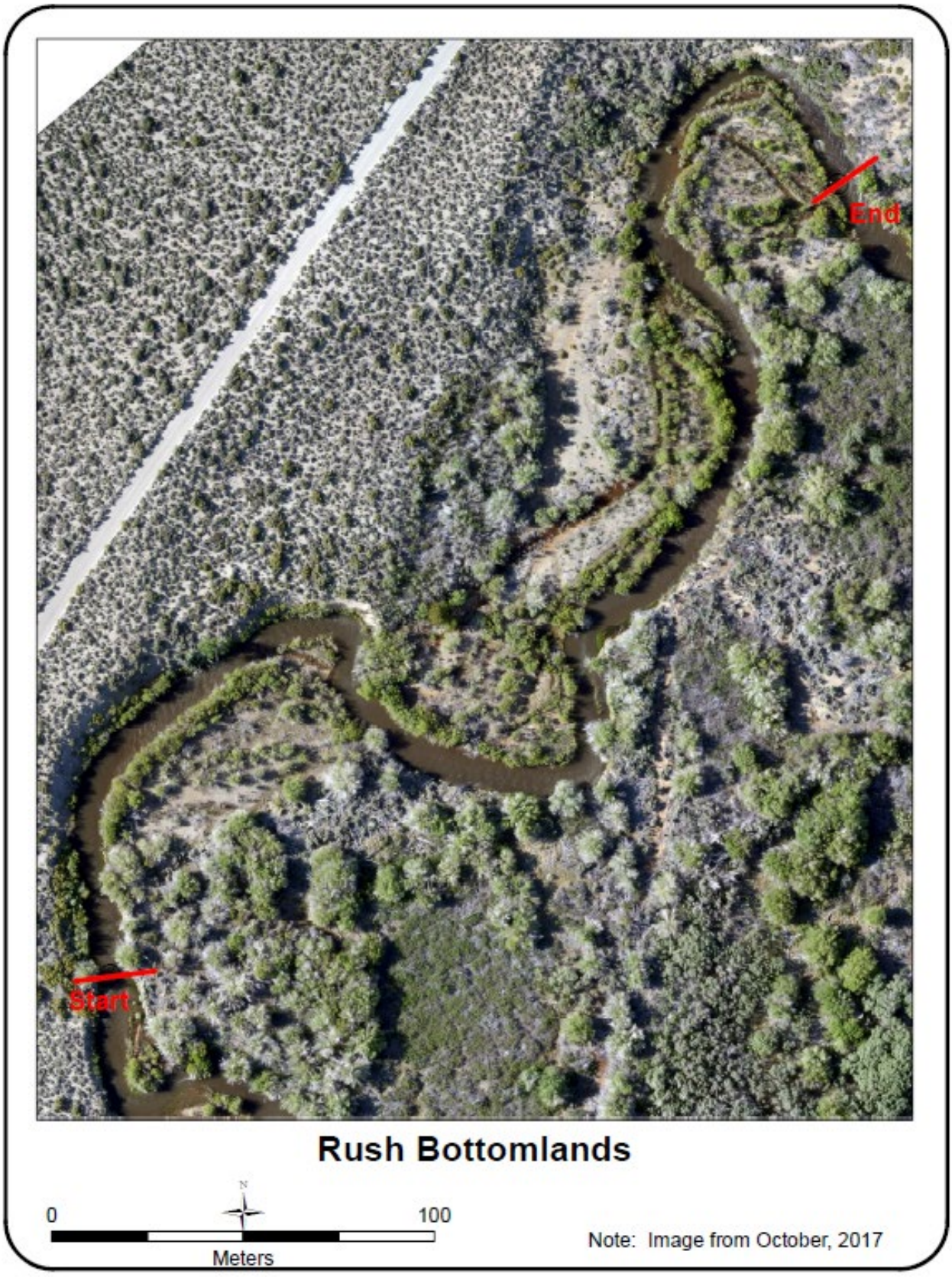
End
Start
Rush Bottomlands
N
0
100
Meters
Note: Image from October, 2017

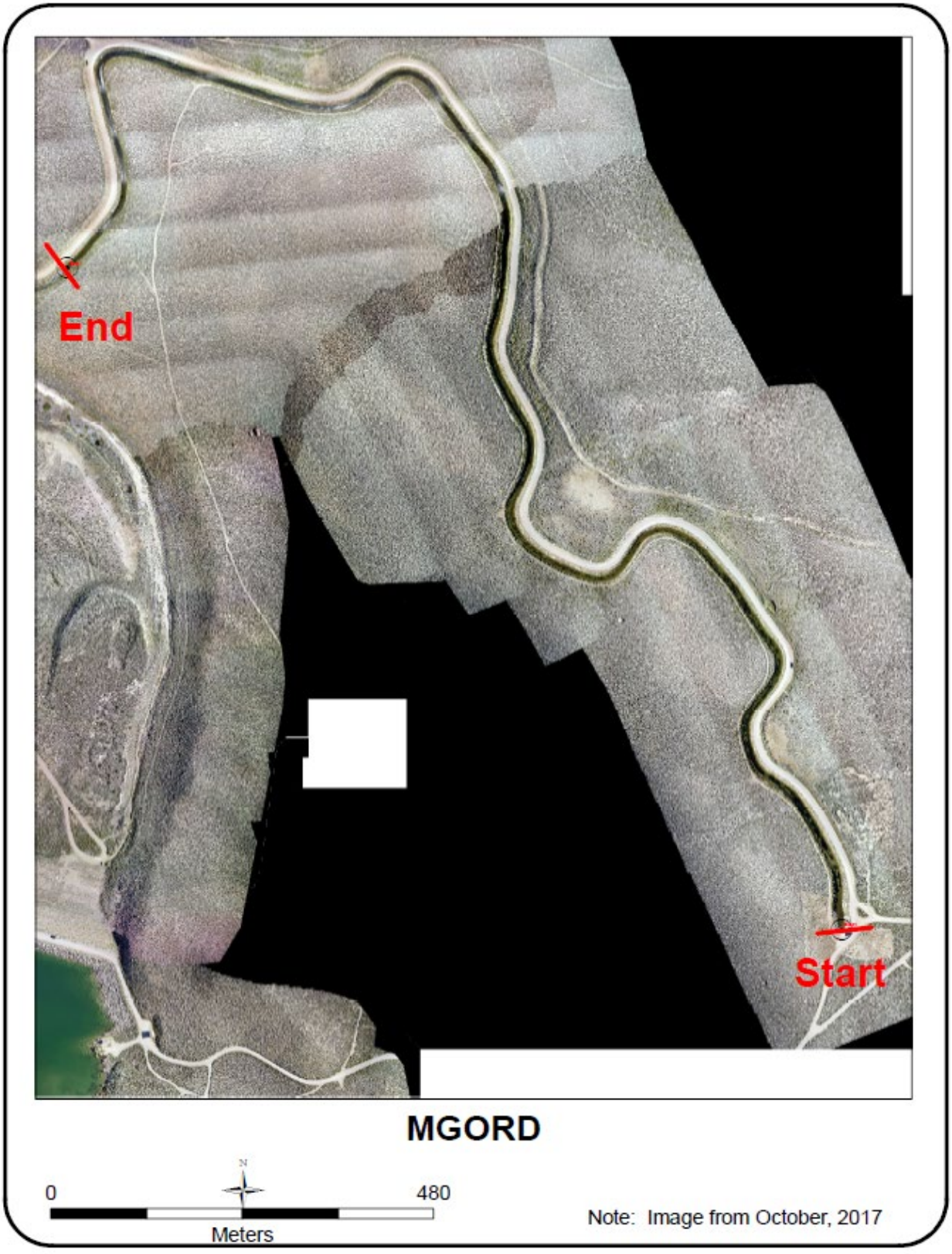
End
Start
MGORD
0
480
Meters
Note: Image from October, 2017


End
Start
Walker Creek
N
0
100
Meters
Note: Image from October, 2017


End
End
Lee Vining side channel
Lee Vining main channel
Start
Start
Lee Vining Creek Main and B-1 Side Channels
N
0
80
Meters
Note: Image from October, 2017

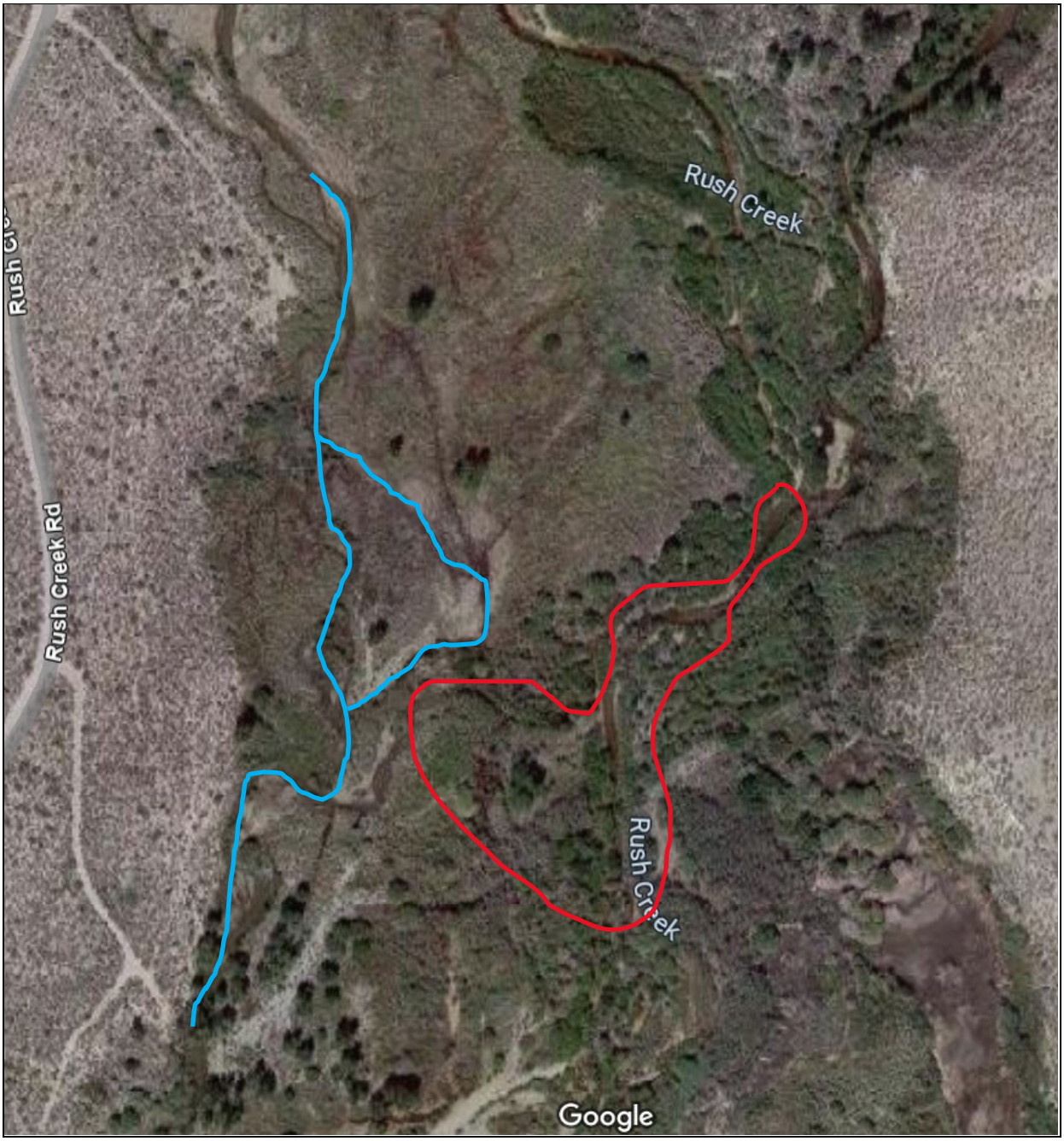

New Rush Creek sections sampled in 2023 – Caddis Channel (longer blue line), Jeffrey Connector Channel (shorter blue line), and Old Main Channel (beaver ponds within area circled in red).

Appendix B: Tables of Numbers of Brown Trout and Rainbow Trout Implanted with PIT Tags (by sampling section) between 2009 and 2022 (Note: no tags implanted in 2013)

Table B-1. Total numbers of trout implanted with PIT tags during the 2009 sampling season, by stream, sample section, age-class and species.

Stream	Sample Section	Number of Age-0 Brown Trout	Number of Age-1 Brown Trout	Number of Age-0 Rainbow Trout	Number of Age-1 Rainbow Trout	Reach Totals
Rush Creek	Upper Rush	256	26	15	1	**298 Trout**
	Bottomlands	164	68	0	0	**232 Trout**
	County Road	108	29	0	0	**137 Trout**
	MGORD	54	642*	0	0	**696 Trout**
Lee Vining Creek	Main Channel	10	45	4	3	**62 Trout**
	Side Channel	5	0	0	1	**6 Trout**
Walker Creek	Above old 395	114	51	0	0	**165 Trout**
Totals:		**711**	**861**	**19**	**5**	**Total Trout: 1,596**

*Many of these MGORD trout were >age-1.

Table B-2. Total numbers of trout implanted with PIT tags during the 2010 sampling season, by stream, sample section, age-class and species.

Stream	Sample Section	Number of Age-0 Brown Trout (<125 mm)	Number of Age-1 and older Brown Trout	Number of Age-0 Rainbow Trout (<125 mm)	Number of Age-1 and older Rainbow Trout	Reach Totals
Rush Creek	Upper Rush	242	11	4	0	**257 Trout**
	Bottomlands	284	3	0	0	**287 Trout**
	County Road	210	7	0	0	**217 Trout**
	MGORD	1	359*	0	12	**372 Trout**
Lee Vining Creek	Main Channel	24	8	0	1	**33 Trout**
	Side Channel	13	0	0	0	**13 Trout**
Walker Creek	Above old 395	81	14	0	0	**95 Trout**
Totals:		**855**	**402**	**4**	**13**	**Total Trout: 1,274**

*Many of these MGORD trout were >age-1.

Table B-3. Total numbers of trout implanted with PIT tags during the 2011 sampling season, by stream, sample section, age-class and species.

Stream	Sample Section	Number of Age-0 Brown Trout (<125 mm)	Number of Age-1 and older Brown Trout	Number of Age-0 Rainbow Trout (<125 mm)	Number of Age-1 and older Rainbow Trout	Reach Totals
Rush Creek	Upper Rush	393	3	30	0	**426 Trout**
	Bottomlands	178	1	11	0	**190 Trout**
	County Road	196	1	6	0	**203 Trout**
	MGORD	8	142*	3	3	**156 Trout**
Lee Vining Creek	Main Channel	24	0	0	0	**24 Trout**
	Side Channel	11	14	0	0	**25 Trout**
Walker Creek	Above old 395	41	0	0	0	**41 Trout**
Totals:		**851**	**161**	**50**	**3**	**Total Trout: 1,065**

*Many of these MGORD trout were >age-1.

Table B-4. Total numbers of trout implanted with PIT tags during the 2012 sampling season, by stream, sample section, age-class and species.

Stream	Sample Section	Number of Age-0 Brown Trout (<125 mm)	Number of Age-1 and older Brown Trout	Number of Age-0 Rainbow Trout (<125 mm)	Number of Age-1 and older Rainbow Trout	Reach Totals
Rush Creek	Upper Rush	117	1	2	0	**120 Trout**
	Bottomlands	110	1	6	0	**117 Trout**
	County Road	0	2	0	0	**2 Trout**
	MGORD	0	0	0	0	**0 Trout**
Lee Vining Creek	Main Channel	125	0	72	0	**197 Trout**
	Side Channel	0	0	0	0	**0 Trout**
Walker Creek	Above old 395	60	0	0	0	**60 Trout**
Age Class Sub-totals:		**412**	**4**	**80**	**0**	**Total Trout: 496**

Table B-5 Total numbers of trout implanted with PIT tags during the 2014 sampling season, by stream, sample section, age-class and species.

Stream	Sample Section	Number of Age-0 Brown Trout (<125 mm)	Number of Age-1 Brown Trout (125-170 mm)	Number of Age-0 Rainbow Trout (<125 mm)	Number of Age-1 Rainbow Trout (125-170 mm)	Section Totals
Rush Creek	Upper Rush	243	86	1	0	**330 Trout**
	Bottomlands	34	43	0	0	**77 Trout**
	MGORD	13	125-199 mm = 60 Brown Trout ≥200 mm = 185 Brown Trout			**258 Trout**
Lee Vining Creek	Main Channel	127	103	5	22	**257 Trout**
	Side Channel	0	0	0	0	**0 Trout**
Walker Creek	Above old 395	42	0	0	0	**42 Trout**
Age Class Sub-totals:		**459**	**232***	**6**	**22**	**Total Trout: 964**

*this sub-total excludes age-1 and older MGORD fish

Table B-6. Total numbers of trout implanted with PIT tags during the 2015 sampling season, by stream, sample section, age-class and species.

Stream	Sample Section	Number of Age-0 Brown Trout (<125 mm)	Number of Age-1 and older Brown Trout	Number of Age-0 Rainbow Trout (<125 mm)	Number of Age-1 and older Rainbow Trout	Section Totals
Rush Creek	Upper Rush	234	2*	7	0	**243 Trout**
	Bottomlands	167	3*	0	0	**170 Trout**
	MGORD	29	125-199 mm = 37 Brown Trout ≥200 mm = 83 Brown Trout (2 shed/new)			**149 Trout**
Lee Vining Creek	Main Channel	195	1*	0	0	**196 Trout**
	Side Channel	0	0	0	0	**0 Trout**
Walker Creek	Above old 395	113	0	0	0	**113 Trout**
Age Class Sub-totals:		**738**	**6****	**7**	**0**	**Total Trout: 871**

*shed tag/new tag implanted **this sub-total excludes age-1 and older MGORD fish

Table B-7. Total numbers of trout implanted with PIT tags during the 2016 sampling season, by stream, sample section, age-class and species.

Stream	Sample Section	Number of Age-0 Brown Trout (<125 mm)	Number of Age-1 and older Brown Trout	Number of Age-0 Rainbow Trout (<125 mm)	Number of Age-1 and older Rainbow Trout	Section Totals
Rush Creek	Upper Rush	36	0	1	0	**37 Trout**
	Bottomlands	79	1*	0	0	**80 Trout**
	MGORD	4 BNT 1 RBT	125-199 mm = 9 BNT ≥200 mm = 154** BNT and 7 RBT			**175 Trout**
Lee Vining Creek	Main Channel	46	1*	0	0	**47 Trout**
	Side Channel	1	0	0	0	**1 Trout**
Walker Creek	Above old 395	228	1*	0	0	**229 Trout**
Age Class Sub-totals:		**394**	**166**	**2**	**7**	**Total Trout: 569**

*shed tag/new tag implanted **two of these BNT = shed tag/new tag implanted

Table B-8. Total numbers of trout implanted with PIT tags during the 2017 sampling season, by stream, sample section, age-class and species.

Stream	Sample Section	Number of Age-0 Brown Trout (<125 mm)	Number of Age-1 and older Brown Trout	Number of Age-0 Rainbow Trout (<125 mm)	Number of Age-1 and older Rainbow Trout	Section Totals
Rush Creek	Upper Rush	192	2*	14	0	**208 Trout**
	Bottomlands	34	0	0	0	**34 Trout**
	MGORD	38	0	2	0	**40 Trout**
Lee Vining Creek	Main Channel	31	0	0	0	**31 Trout**
	Side Channel	5	0	0	0	**5 Trout**
Walker Creek	Above old 395	0	0	0	0	**0 Trout**
Age Class Sub-totals:		**300**	**2**	**16**	**0**	**Total Trout: 318**

*shed tag/new tag implanted

Table B-9. Total numbers of trout implanted with PIT tags during the 2018 sampling season, by stream, sample section, age-class and species.

Stream	Sample Section	Number of Age-0 Brown Trout (<125 mm)	Number of Age-1 and older Brown Trout	Number of Age-0 Rainbow Trout (<125 mm)	Number of Age-1 and older Rainbow Trout	Section Totals
Rush Creek	Upper Rush	314	3*	72	1*	**390 Trout**
	Bottomlands	288	0	0	0	**288 Trout**
	MGORD	25	148**	1	7	**181 Trout**
Lee Vining Creek	Main Channel	87	0	8	0	**95 Trout**
	Side Channel	0	0	0	0	**0 Trout**
Walker Creek	Above old 395	43	2*	0	0	**45 Trout**
Age Class Sub-totals:		**757**	**153**	**81**	**8**	**Total Trout: 999**

*shed tag/new tag implanted **≤250 mm in total length

Table B-10. Total numbers of trout implanted with PIT tags during the 2019 sampling season, by stream, sample section, age-class and species.

Stream	Sample Section	Number of Age-0 Brown Trout (<125 mm)	Number of Age-1 and older Brown Trout	Number of Age-0 Rainbow Trout (<125 mm)	Number of Age-1 and older Rainbow Trout	Section Totals
Rush Creek	Upper Rush	257	3*	28	0	**288 Trout**
	Bottomlands	152	3*	0	0	**155 Trout**
	MGORD	64	167** 8*	1	5	**245 Trout**
Lee Vining Creek	Main Channel	174	0	0	0	**174 Trout**
	Side Channel	0	0	0	0	**0 Trout**
Walker Creek	Above old 395	137	1*	0	0	**138 Trout**
Age Class Sub-totals:		**784**	**182**	**29**	**5**	**Total Trout: 1,000**

*shed tag/new tag implanted **≤250 mm in total length

Table B-11. Total numbers of trout implanted with PIT tags during the 2020 sampling season, by stream, sample section, age-class and species.

Stream	Sample Section	Number of Age-0 Brown Trout (<125 mm)	Number of Age-1 and older Brown Trout	Number of Age-0 Rainbow Trout (<125 mm)	Number of Age-1 and older Rainbow Trout	Section Totals
Rush Creek	Upper Rush	242	1*	27	0	**270 Trout**
	Bottomlands	65	0	0	0	**65 Trout**
	MGORD	80	132** 1*	2	7	**222 Trout**
Lee Vining Creek	Main Channel	102	1*	0	0	**103 Trout**
	Side Channel	0	0	0	0	**0 Trout**
Walker Creek	Above old 395	92	4*	0	0	**96 Trout**
Age Class Sub-totals:		**581**	**139**	**29**	**7**	**Total Trout: 756**

*shed tag/new tag implanted **≤250 mm in total length

Table B-12. Total numbers of trout implanted with PIT tags during the 2021 sampling season, by stream, sample section, age-class and species.

Stream	Sample Section	Number of Age-0 Brown Trout (<125 mm)	Number of Age-1 and older Brown Trout	Number of Age-0 Rainbow Trout (<125 mm)	Number of Age-1 and older Rainbow Trout	Section Totals
Rush Creek	Upper Rush	148	1*	36	0	**185 Trout**
	Bottomlands	106	0	0	0	**106 Trout**
	MGORD	115	259** 1*	0	9	**384 Trout**
Lee Vining Creek	Main Channel	53	0	0	0	**53 Trout**
	Side Channel	17	0	0	0	**17 Trout**
Walker Creek	Above old 395	122	1*	0	0	**123 Trout**
Age Class Sub-totals:		**561**	**262**	**36**	**9**	**Total Trout: 868**

*shed tag/new tag implanted **≤250 mm in total length

Table B-13. Total numbers of trout implanted with PIT tags during the 2022 sampling season, by stream, sample section, age-class and species.

Stream	Sample Section	Number of Age-0 Brown Trout (<125 mm)	Number of Age-1 and older Brown Trout	Number of Age-0 Rainbow Trout (<125 mm)	Number of Age-1 and older Rainbow Trout	Section Totals
Rush Creek	Upper Rush	225	4*	35	0	**264 Trout**
	Bottomlands	225	0	0	0	**225 Trout**
	MGORD	26	49**	1	1	**77 Trout**
Lee Vining Creek	Main Channel	30	1*	1	0	**32 Trout**
	Side Channel	0	0	0	0	**0 Trout**
Walker Creek	Above old 395	104	0	0	0	**104 Trout**
Age Class Sub-totals:		**610**	**54**	**37**	**1**	**Total Trout: 702**

*shed tag/new tag implanted **up to 225 mm in total length

Appendix C: Table of PIT-tagged Fish Recaptured during October 2023 Sampling

Date of Recapture	Species	Length (mm)	Weight (g)	PIT Tag Number	Location of 2023 Recapture	Location of Initial Capture and Tagging	Comments
10/3/2023	BNT	285	236	989001038116884	Upper Rush	Upper Rush	
10/3/2023	BNT	267	196	989001039661023	Upper Rush	Upper Rush	
10/3/2023	BNT	193	72	989001039661729	Upper Rush	Upper Rush	
10/3/2023	**RBT**	247	182	989001039661773	Upper Rush	Upper Rush	
10/3/2023	BNT	231	123	989001039661806	Upper Rush	Upper Rush	
10/3/2023	**RBT**	204	92	989001042091139	Upper Rush	Upper Rush	
10/3/2023	BNT	258	164	989001042091223	Upper Rush	Upper Rush	
10/3/2023	BNT	207	80	989001042091268	Upper Rush	Upper Rush	
10/3/2023	BNT	250	155	989001045526433	Upper Rush	Upper Rush	Shed tag, new tag implanted
10/3/2023	BNT	179	52	989001045526490	Upper Rush	Upper Rush	Shed tag, new tag implanted
10/4/2023	BNT	222	113	989001039661862	Bottomlands	Bottomlands	
10/4/2023	BNT	202	76	989001039661870	Bottomlands	Bottomlands	
10/4/2023	BNT	205	76	989001039661901	Bottomlands	Bottomlands	
10/4/2023	BNT	217	86	989001039661938	Bottomlands	Bottomlands	
10/4/2023	BNT	177	52	989001039661949	Bottomlands	Bottomlands	
10/4/2023	BNT	193	68	989001042091332	Bottomlands	Bottomlands	
10/4/2023	BNT	201	74	989001042091334	Bottomlands	Bottomlands	
10/4/2023	BNT	184	61	989001042091338	Bottomlands	Bottomlands	
10/4/2023	BNT	221	90	989001042091360	Bottomlands	Bottomlands	
10/5/2023	BNT	375	601	989001038116762	MGORD	MGORD	
10/5/2023	BNT	324	433	989001039661040	MGORD	**Upper Rush**	
10/5/2023	BNT	345	472	989001039661599	MGORD	MGORD	
10/5/2023	BNT	254	177	989001039661767	MGORD	MGORD	
10/5/2023	BNT	340	396	989001042091109	MGORD	MGORD	

Date of Recapture	Species	Length (mm)	Weight (g)	PIT Tag Number	Location of 2023 Recapture	Location of Initial Capture and Tagging	Comments
10/6/2023	BNT	250	152	989001038117078	LV Main	LV Main	
10/6/2023	BNT	212	94	989001038117100	LV Main	LV Main	
10/6/2023	BNT	266	199	989001038117204	LV Main	LV Main	
10/6/2023	BNT	169	45	989001039661690	LV Main	LV Main	
10/6/2023	BNT	223	110	989001039661730	LV Main	LV Main	
10/6/2023	BNT	215	106	989001039661747	LV Main	LV Main	
10/6/2023	BNT	181	56	989001042091045	LV Main	LV Main	
10/6/2023	BNT	166	50	989001042091055	LV Main	LV Main	
10/6/2023	BNT	178	54	989001042091077	LV Main	LV Main	
10/6/2023	**RBT**	202	79	989001042091081	LV Main	LV Main	
10/6/2023	BNT	154	35	989001042091084	LV Main	LV Main	
10/7/2023	BNT	227	111	989001028114224	Walker Creek	Walker Creek	
10/7/2023	BNT	240	131	989001031371725	Walker Creek	Walker Creek	
10/7/2023	BNT	299	283	989001031372378	Walker Creek	Walker Creek	
10/7/2023	BNT	209	77	989001038117290	Walker Creek	Walker Creek	
10/7/2023	BNT	212	87	989001038117301	Walker Creek	Walker Creek	
10/7/2023	BNT	219	104	989001038117314	Walker Creek	Walker Creek	
10/7/2023	BNT	221	107	989001038117355	Walker Creek	Walker Creek	
10/7/2023	BNT	209	103	989001038117357	Walker Creek	Walker Creek	
10/7/2023	BNT	187	59	989001039661169	Walker Creek	Walker Creek	
10/7/2023	BNT	182	62	989001039661179	Walker Creek	Walker Creek	
10/7/2023	BNT	167	44	989001039661189	Walker Creek	Walker Creek	
10/7/2023	BNT	200	85	989001039661192	Walker Creek	Walker Creek	
10/7/2023	BNT	220	88	989001039661201	Walker Creek	Walker Creek	

Date of Recapture	Species	Length (mm)	Weight (g)	PIT Tag Number	Location of 2023 Recapture	Location of Initial Capture and Tagging	Comments
10/7/2023	BNT	192	62	989001039661217	Walker Creek	Walker Creek	
10/7/2023	BNT	182	59	989001039661322	Walker Creek	Walker Creek	
10/7/2023	BNT	201	81	989001039661333	Walker Creek	Walker Creek	
10/7/2023	BNT	151	34	989001039661684	Walker Creek	Walker Creek	
10/7/2023	BNT	166	41	989001039661687	Walker Creek	Walker Creek	
10/7/2023	BNT	153	27	989001039661706	Walker Creek	Walker Creek	
10/7/2023	BNT	187	56	989001039661728	Walker Creek	Walker Creek	
10/7/2023	BNT	131	23	989001039661760	Walker Creek	Walker Creek	
10/7/2023	BNT	154	33	989001042091433	Walker Creek	Walker Creek	
10/7/2023	BNT	161	40	989001042091434	Walker Creek	Walker Creek	
10/7/2023	BNT	173	46	989001042091450	Walker Creek	Walker Creek	
10/7/2023	BNT	155	34	989001042091451	Walker Creek	Walker Creek	
10/7/2023	BNT	147	30	989001042091470	Walker Creek	Walker Creek	
10/7/2023	BNT	169	47	989001042091484	Walker Creek	Walker Creek	
10/7/2023	BNT	261	179	989001045526558	Walker Creek	Walker Creek	

Section II. Mono Basin Stream Monitoring Report, RY 2023

Prepared by William J. Trush

Mono Basin Stream Monitoring Report RY2023

May 5, 2024

RY2023
Mono Basin Stream Monitoring Report

William J. Trush

Dept. Environmental Science and Management
Cal Poly Humboldt River Institute
Arcata, California 95521

May 8, 2023

Introduction

RY2023 Stream Monitoring Project Objectives and Scheduling

The Mono Basin Stream Monitoring Project for RY2023 had similar monitoring objectives consistent with previous annual runoff years (RYs): (1) continue channel morphology and riparian floodplain monitoring and (2) evaluate/recommend monitoring techniques that objectively measure cause-effect outcomes as unambiguously and efficiently (w/r to effort, cost, and information) as possible. Overall, our monitoring has been, and will continue to be, guided by Aldo Leopold's definition for ecosystem health called 'The Capacity for Self-Renewal':

Conservation is a state of health in the land. The land consists of soil, water, plants, and animals, but health is more than a sufficiency of these components. It is a state of vigorous self-renewal in each of them, and in all collectively. Such collective functioning of interdependent parts for the maintenance of the whole is characteristic of an organism. In this sense land is an organism, and conservation deals with its functional integrity, or health. From: Aldo Leopold's 1944 essay titled Conservation: In Whole or in Part?

Project approval for RY2023 fieldwork was not verified until May 18, 2023 upon receiving the ‘Mono Fully Executed Funding Agreement.’ We could not advertise student work positions until certain of project approval. Students finishing Spring’23 semester were already committed to summer jobs advertised months earlier. However, many folks had been involved in the project approval process, and there was still much that could be accomplished. Also, RY2023 was promising to be a record runoff year with an extremely large snowpack producing a record maximum peak snowmelt runoff. The greatest uncertainty in allocating streamflow releases via Desired Ecological Outcomes Table 3.1 of the Synthesis Report was the larger recommended peak flood hydrograph magnitudes and durations. Opportunities to observe large floods are relatively rare. Expected outcomes could have been more specific if there had been more large flood events observed. Since Synthesis Report functional completion, roughly 2010, monitoring has focused on Lower Rush Creek with its dynamic mainstem channel and complex side-channel floodplain network. An important objective in RY2023 was to focus more fieldwork on mainstem Lee Vining Creek. We will do the same for the RY2024 field season.

We want to especially thank Robbie Di Paolo, of the Mono Lake Committee, for his participation during the RY2023 field season. Robbie not only assisted in the labor of fieldwork, but also in relentlessly discussing and critiquing the science of the fieldwork, especially as we tried to piece-together the chain of events culminating in the RY2023 flood hydrograph’s impact to Lower Rush Creek 8-Floodplain and 4-Floodplain.

Technical Note: Utilizing LADWP Stream Gaging Data

In utilizing LADWP's 15-min gaging data, we relied on the daily average (AV) of LADWP 15-min data at The Narrows (i.e., including streamflows from Parker Creek and Walker Creek). The July 17, 2023 daily average streamflow (Q_{AV}) of 685 cfs observed our first week of RY2023 fieldwork is presented as 17July2023 Q_{AV} = 685 cfs. Some 15-min streamflows on July 17 exceed 685 cfs while other 15-min streamflows on July 17 were lower than 685 cfs.

The date in RY2023 with the highest (peak) recorded daily average streamflow (QPK) for Lower Rush Creek (i.e., below The Narrows) occurred July 04, 2023 with a Q_{AV} of 788 cfs. The date in RY2023 with the highest (peak) recorded daily average streamflow (QPK_{AV}) for Lee Vining Creek (i.e., below The Narrows) occurred July 03, 2023 with a Q_{AV} of 605 cfs.

These Q_{AV} data are presented as hydrographs. Figure 1 is RY2023 Below Narrows Hydrograph April 01 through October 31 and Figure 2 is RY2023 Upper Lee Vining Creek Hydrograph April 01 through October 31.

In words:
QPK_{AV} RY2023 = 'The Peak Daily Average Streamflow for RY 2023'

Q_{AV} 17July2023 = 'The Daily Average Streamflow for 17July2023.'

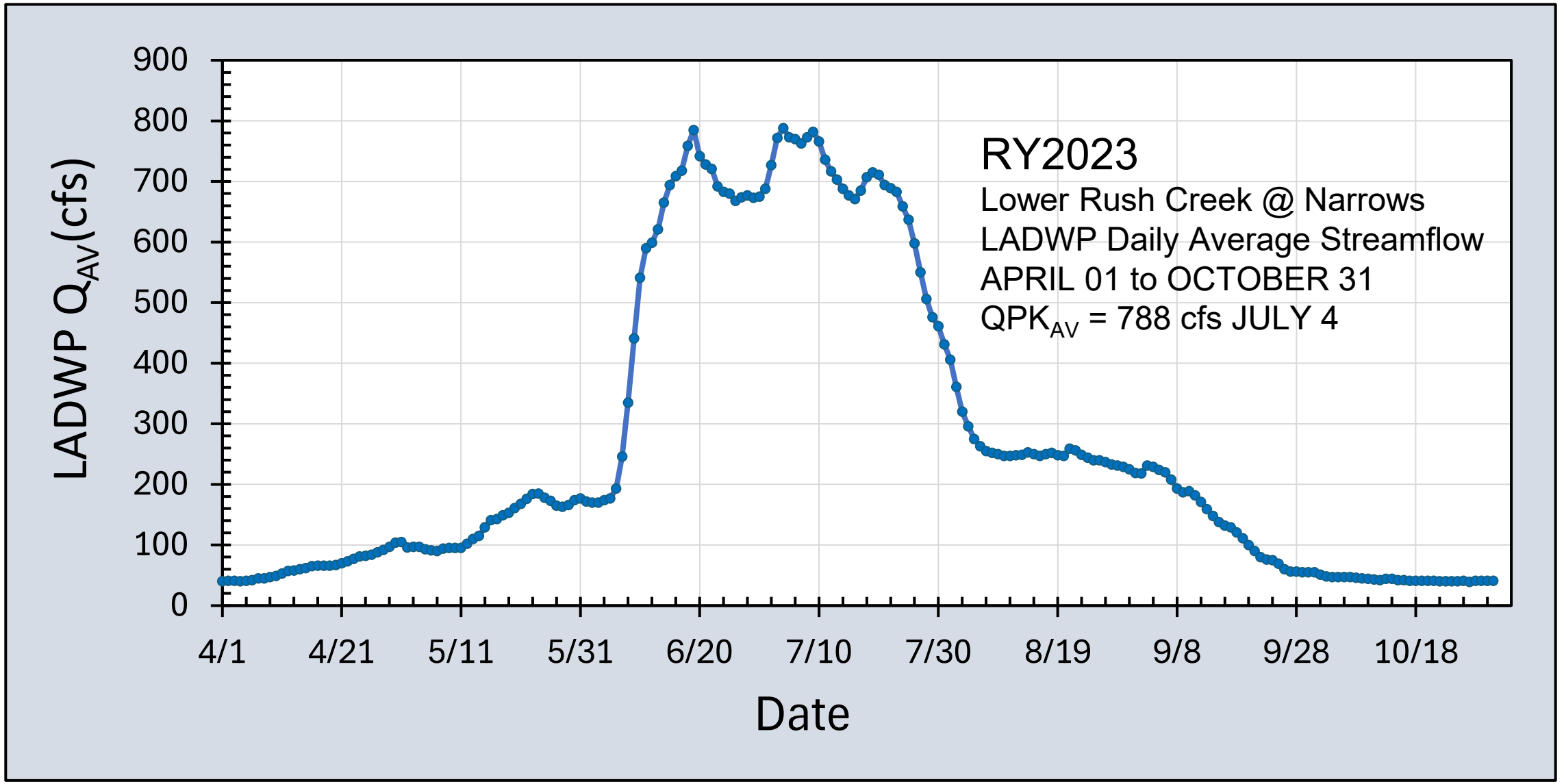

Figure 1. Lower Rush Creek RY2023 Hydrograph April 1 through October 31 (Q_{AV}).

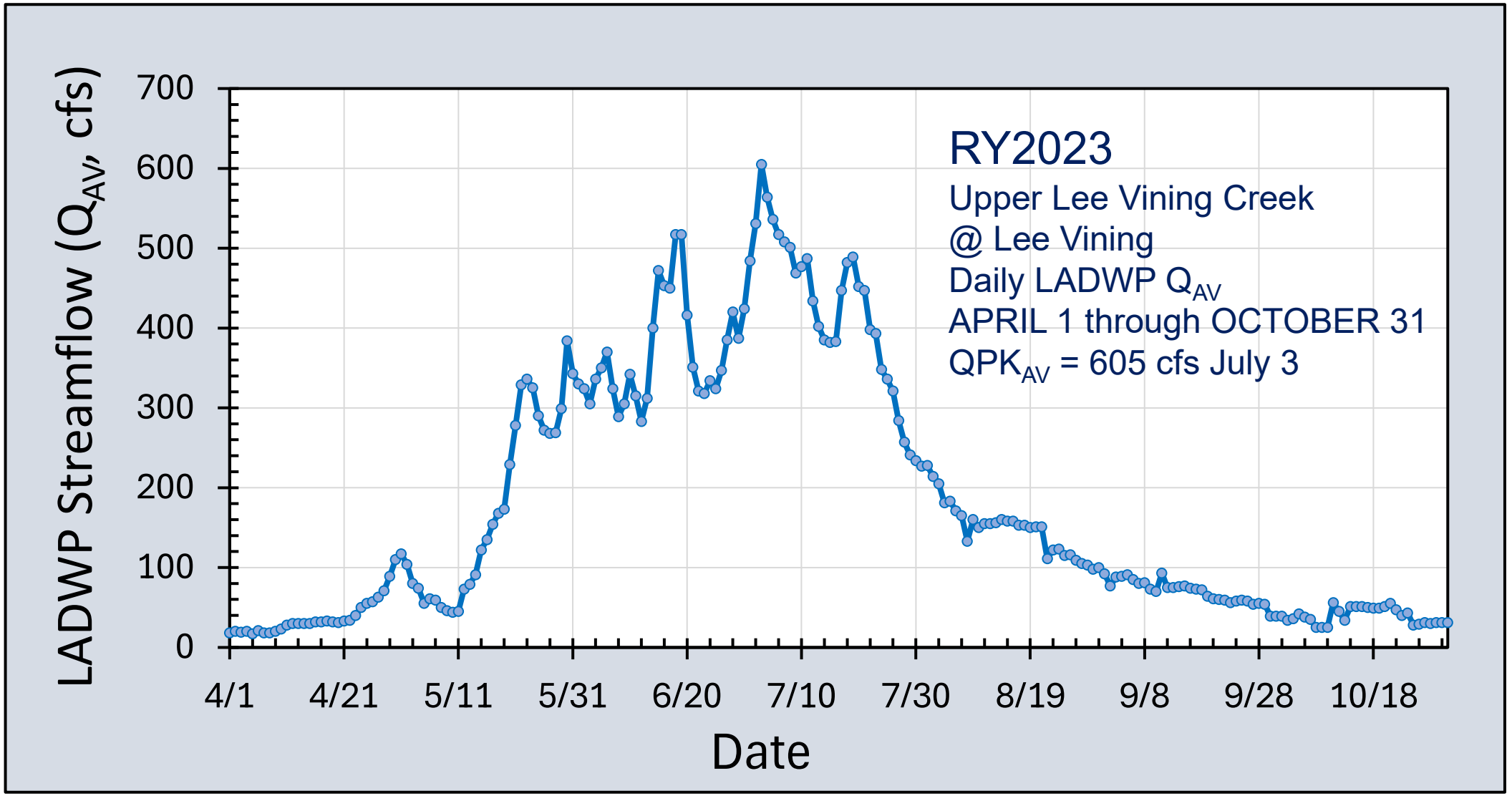

Figure 2. Lee Vining Creek nr Lee Vining RY2023 Hydrograph April 1 through October 31 (Q_{AV}).

Stream access was extremely restrictive through early-August by high streamflows (> 300 cfs) preventing safe channel wading. Unable to wade in many locations, we walked along both mainstem channels given this was the highest streamflow personally observed since becoming a stream scientist in 1993. I wanted to walk both channels soon after they had peaked to observe geomorphic effects, then compare these observations to desired ecological outcomes stated in the Synthesis Report. We got lucky scheduling three one-week-long field visits, with each targeting a distinctive feature of the RY2023 hydrograph (Figure 3). The first fieldtrip week, beginning 17 July and ending 22 July (with an additional travel day on each end), occurred near the end of peak flows. The second fieldtrip week, beginning 10 September and ending 16September, was intended to target a high flow bench following peak flows. It just barely did. Ideally, the second fieldtrip should have begun 23 August when streamflow was just at the active channel bench of 240 cfs on Lower Rush Creek. The third fieldtrip week, beginning 09 October and ending 14 October, successfully targeted early-autumn baseflow. Our UAV surveys were scheduled 02 August for Lee Vining Creek and 03 August for Lower Rush Creek.

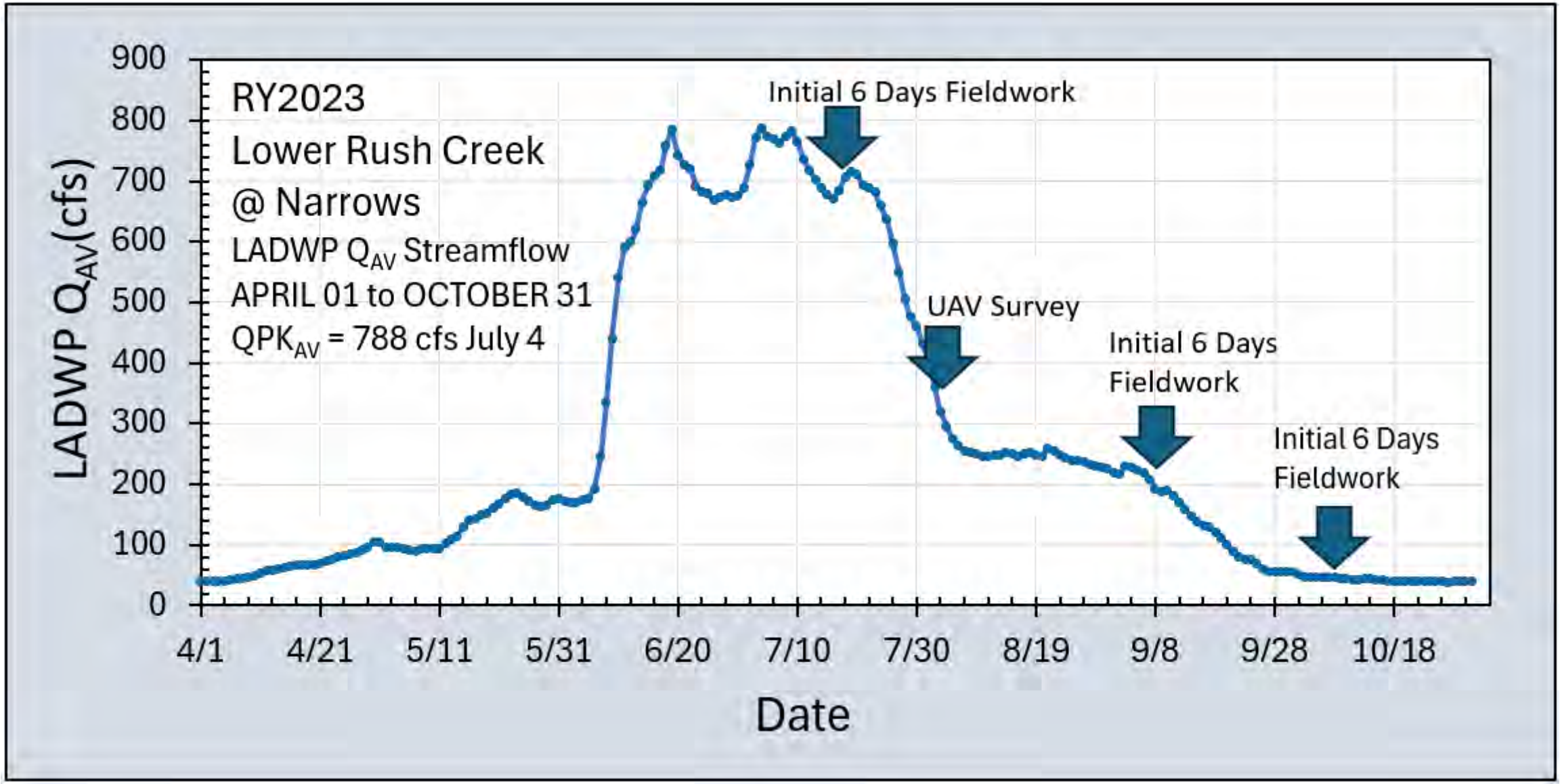

Figure 3. Scheduled RY2023 fieldwork targeting different segments of the RY2023 Below Narrows hydrograph. The arrows mark three scheduled fieldwork time periods and a UAV survey early-August.

RY2023 Fieldwork Tasks

RY2023 Mono Basin Stream Monitoring Report is organized and presented by these 15 tasks. Each begins either with an active voice verb or posed as a question.

Task No.1. Measure and Assess Stream Gaging Restrictions at the Former10-Falls Gage Site.
Task No.2. Conduct Unoccupied Aerial Vehicle (UAV) Surveys of Lee Vining Creek and Lower Rush Creek Floodplains.
Task No.3. Construct a Boulder Rib Thalweg (BRT) Rating Curve for Upper Lee Vining Creek.
Task No.4. Synoptically Measure RY2023 Baseflows in Lower Rush Creek 8-Floodplain.
Task No.5. Investigate Paintbrush Side-Channel Capacity Self-Renewal.
Task No.6. Investigate Hydraulic Performance of the 8 Side-Channel Inlet.
Task No.7. How Did Hydraulic Performance of the 8 Side-Channel Inlet Affect the 8-Floodplain?
Task No.8. How Did Hydraulic Performance of the 8 Side-Channel Inlet Affect the 4-Floodplain?
Task No.9. What is a Rush Creek Mainstem River Willow Forest?
Task No.10. Track Restoring Capacity for Self-Renewal in the Mainstem River Willow Forest.
Task No.11. Will Beavers Adapt to Life in a River Willow Forest?
Task No.12. Reconstruct RY2023 QPK Flood/Seepage Access to a Grove of Yellow Willows in the Central 4-Floodplain and Gauge a Yellow Willow's Vigor Response.
Task No.13. Resurvey Grand Old Cottonwood Cross-Section and RCT Channelbed Elevation.
Task No.14. Inventory Cattail and Narrowleaf Willow Expansion Throughout the 8-Floodplain.
Task No.15. Reserve One Morning for Reconnaissance of Lower Cottonwood Creek.

Task No.1.
Measure and Assess Stream Gaging Restrictions at the Former 10-Falls Gage Site.

The 10-Falls mainstem reach is located immediately downstream of the Left Bank (LB) 8-Floodplain, and Right Bank (RB) 10-Floodplain (Figure 4). The RB 4-Floodplain is upstream of the 10-Floodplain. This is one of the narrowest locations within the entire Lower Rush Creek floodplain corridor from the Narrows downstream to the Rush Creek Road ford. It is strategically located for measuring/evaluating potential streamflow losses attributable to floodplain evapotranspiration and rapid shallow groundwater storage upstream. Concerning future streamflow monitoring and recommending construction of a new gaging station, we are not certain whether the present gage location can entirely contain all flow in a big flood event. A gage that requires cableways for estimating high streamflows is considerably more expensive to operate. The RB 10-Falls mainstem reach is a classic bankfull floodplain that extends approximately 50 ft back-from the active channel bank. That would not pose a problem. But the LB mainstem surface is a considerably higher (in elevation) terrace. Can a big flood event, such as the one that just occurred in RY2023, overtop and spill onto this LB terrace? If so, this would pose a gaging limitation. Our first objective was to estimate the cfs of a QPK_{AV} depth that could overtop the LB terrace and therefore bypass the stream gage.

Figure 4. Lower Rush Creek 10-Falls Mainstem Reach and former stream gage.

Four wooden stake benchmarks were installed along the 10-Falls mainstream left bank (LB) to document Q_{AV} stage on July 17 and the RY2023 floodpeak (QPK_{AV}) on July 4. Peak flood stage (QPK_{AV}) estimation should be accurate given the fresh flood debris lines (Figure 5). Collectively, the four benchmarks also allow surveying an accurate water slope estimate with an engineers' level. Reserved for RY2024 fieldwork, a Mannings equation can be used to back-calculate a channel roughness coefficient, relying on LADWP's gaging data for the necessary estimate of peak flood discharge for RY2023.

Figure 5. Peak QPK stage on 04July2023 identified by undisturbed fine debris line under a Jeffrey Pine at LB Benchmark No.1.

An RCT-Q Rating Curve was constructed (Figure 6) for the lowermost LB Benchmark Stake No.1 (closest to the Riffle Crest Thalweg at the bottom of the 10-Falls gaging reach) using four stage measurements and LADWP Q_{AV}'s.

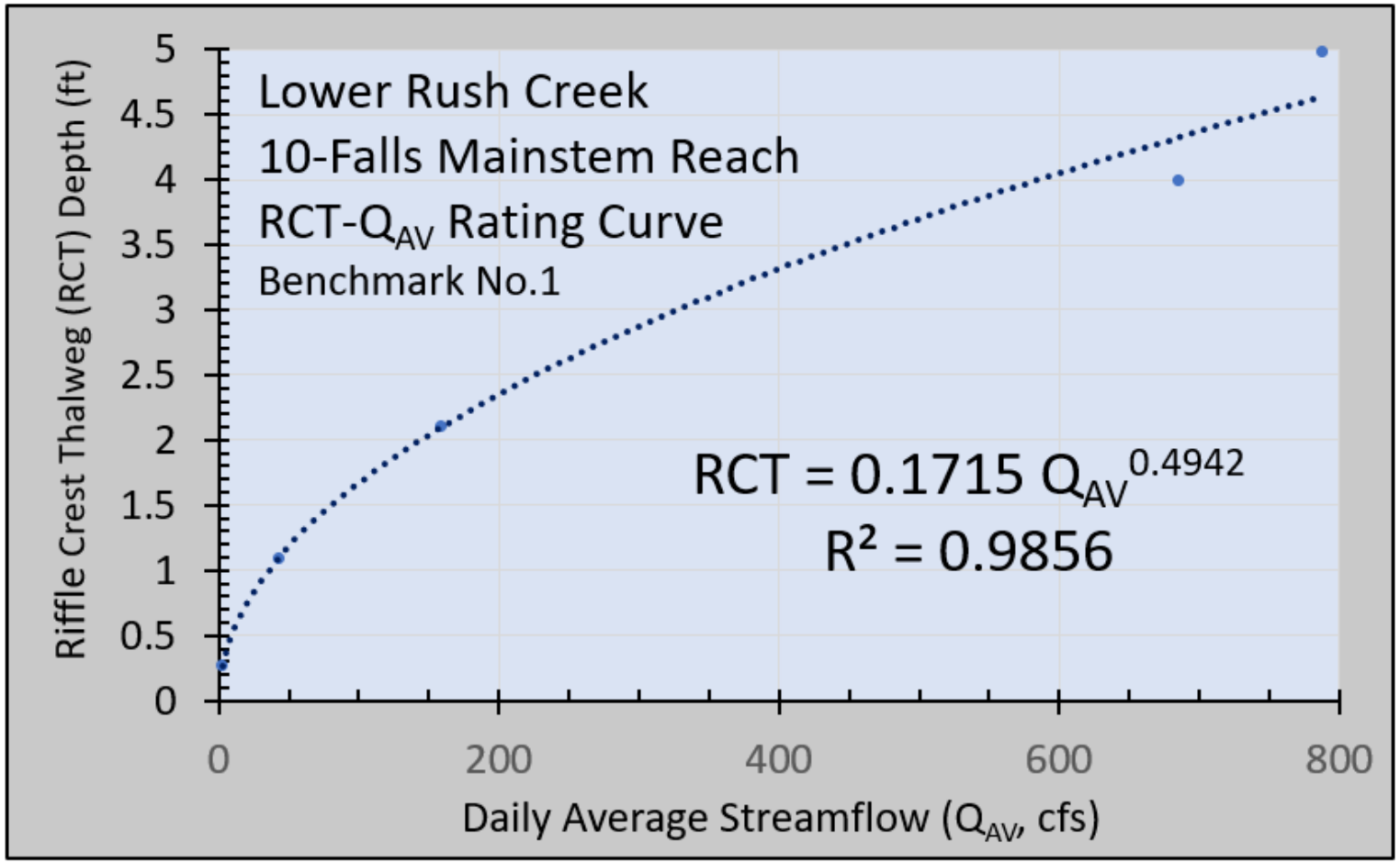

Figure 6. Preliminary RCT-Q Rating Curve @ LB Benchmark Sta. No.1 in 10-Falls Mainstem Reach, Lower Rush Creek RY2023.

The RCT-Q Rating Curve (Figure 6) was necessary to estimate a QPK_{AV} capable of overtopping the LB terrace. Placing a stadia rod on top of the QPK_{AV} flood line at Benchmark No.1 (Figure 5), then estimated with a hand-held level (shooting only 6 ft away) the added stage necessary to overtop the LB Terrace. The RCT-Q Rating Curve was then used to compute an over-topping QPK_{AV} streamflow:

Flood Debris Line @ QPK_{AV} = 788 cfs w/ RCT Depth = 5.30 ft
RCT = 5.30 ft + 1.0 ft abv 788 cfs overtops LB terrace = 6.30 ft
RCT = 5.30 ft + 0.8 ft abv 788 cfs overtops LB terrace = 6.10 ft
Q = 1300 cfs RCT = 5.93 ft
Q = 1400 cfs RCT = 6.15 ft
Q = 1500 cfs RCT = 6.37 ft

Estimate: QPK_{AV} = 1400 cfs overtops LB Terrace at Benchmark No.1.

Another key factor in evaluating the 10-Falls location as a future gage site was whether some streamflows could bypass the gage undetected. A levee effect, where the LB floodplain slightly dips down and away-from the mainstem channel, could capture a small percentage of the total flood flows bypassing the present LB gage location. In Figure 4, this backwater environment is labeled ‘Dense LB Backwater Willows.’ Rough bypass streamflow estimates were made by criss-crossing the dense backwater willows for active surface flows on 17July2023 and for clear evidence of higher peak surface flow earlier. One flowing channel 6.5 ft wide was located that also provided clear depositional evidence of greater peak runoff a few weeks prior. Using a velocity of 2.5 ft/sec, a mean depth of 0.5 ft, and width of 8 ft, estimated streamflow on July 17 was 10 cfs. An estimated bypass streamflow at peak runoff (2.5 ft/sec, 8 ft wide, 1.3 ft deep) was 26 cfs. During our second week’s fieldwork (beginning 12Sept2023), this bypass channel was only ‘moist.’

Having an RCT-Q rating curve at Benchmark No.1 (Figure 6) offered the opportunity to examine how RCT depth changes with streamflow. The next three figures are photographs of the same location at three streamflows (Q_{AV}): 685 cfs (Figure 7), 159 cfs (Figure 8), and 43 cfs (Figure 9). Using the RCT-Q Rating Curve, estimated RCT depths for the three streamflows were: 4.32 ft, 2.10 ft, and 1.10 ft respectively. Estimated RCT depth for QPK_{AV} = 788 cfs was 4.63 ft. I expected greater depths for what was considered a very high flood peak. There are several clear debris lines in all three figures, however, that corroborate RCT depths of 4.6 to 5.0 ft for the QPK_{AV}. In Lower Rush Creek locations significantly wider (e.g., 8-Floodplain), RCT depths should be even smaller. The overall change in RCT depth between baseflow (44 cfs) and the QPK_{AV}2023 was 3.53 ft.

Figure 7. Bottom of 10-Falls Mainstem Looking Downstream 17July2023 1:16PM.
Q_{AV} = 685 cfs QPK_{AV} = 788 cfs. Blue X is RCT location.

Figure 8. Bottom of 10-Falls Mainstem Looking Downstream 13Sept2023 1:16PM Q_{AV} = 159 cfs. Blue X is RCT location.

Figure 9. Bottom of 10-Falls Mainstem Looking Downstream 11October2023 1:16PM Q_{AV} = 43 cfs. Blue X is RCT location.

Active channel streamflow was estimated at 240 cfs in Mono Basin Stream Monitoring Report RY2021. One important trait of the active channel streamflow is losing a visual distinction between pool and riffle, i.e., when riffles are ‘drowned out.’ Figure 10 has a streamflow (Q_{AV}) of 159 cfs with the short riffle remaining discernable.

Figure 10. Downstream riffle crest with enlarged right bank and projected flood peak line at QPK_{AV} = 788 cfs.

Task No. 2. Conduct Unoccupied Aerial Vehicle (UAV) Surveys of Lee Vining Creek and Lower Rush Creek Floodplains.

On August 2nd and 3rd, Dr. Jim Graham, at Cal Poly Humboldt, and Julie Avina, an undergraduate at Cal Poly Humboldt, conducted a series of aerial surveys over the mainstem channels and riparian areas in: (1) Lee Vining Creek from the town of Lee Vining downstream to the county road/ford and (2) Lower Rush Creek from the top of the 4-Floodplain downstream to the Rush Creek Road ford (Figure 11).

These surveys were completed with a DJI Mavic Pro 2 Unoccupied Aerial Vehicle (UAV) or drone. The UAV was flown at a height between 300 and 400 meters and resulted in images with a resolution of approximately 3 centimeters per pixel. Images were converted into orthomosaics using the Agisoft Metashape software. There was one orthomosaic for each survey totaling eight orthomosaics for Lee Vining Creek and five for Rush Creek.

Figure 11. Locator map for Lower Rush Creek 03August2023 UAV Survey.

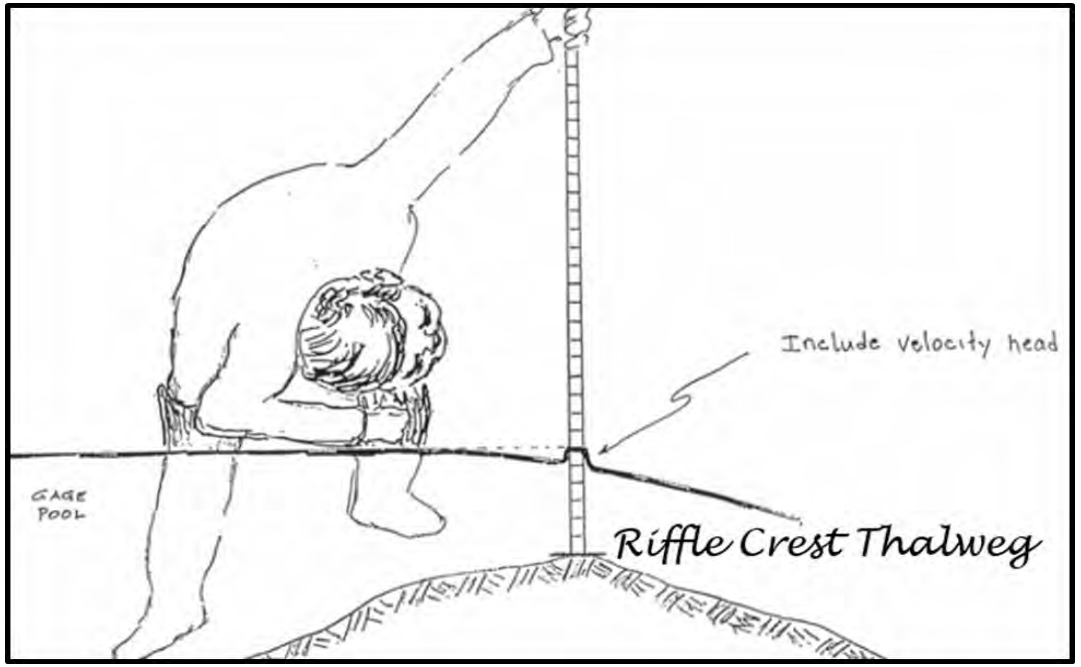

Task No. 3. Construct a Boulder Rib Thalweg (BRT) Rating Curve for Upper Lee Vining Creek.

Constructing an RCT-Q Rating Curve requires: (1) locating the thalweg of the riffle crest, (2) documenting changes in riffle crest thalweg (RCT) depth over a wide range of streamflows, then (3) fitting a power function to the RCT depth-streamflow relationship. Refer to Mono Basin Stream Monitoring Report RY2021 for an in-depth description of RCT-Q Curve construction. If the MAT would desire an in-depth presentation, that could be arranged at/near the end of the RY2024 field season. The RY2024 field season is slated for more BRT-Q Rating curves accompanied by significantly more photographs.

The Upper Lee Vining Creek channel morphology is boulder-dominated where boulders assemble as ‘ribs’ spanning the active channel (Figure 12). Upstream of each boulder rib will be a pool or run visible at lower streamflows. Locating the greatest thalweg depth across the entire boulder rib (BRT) is the same as locating the greatest RCT depth across an entire riffle crest cross-section in an alluvial channel (Figure 13).

Figure 12. Boulder rib pool morphology of Upper Lee Vining Creek.

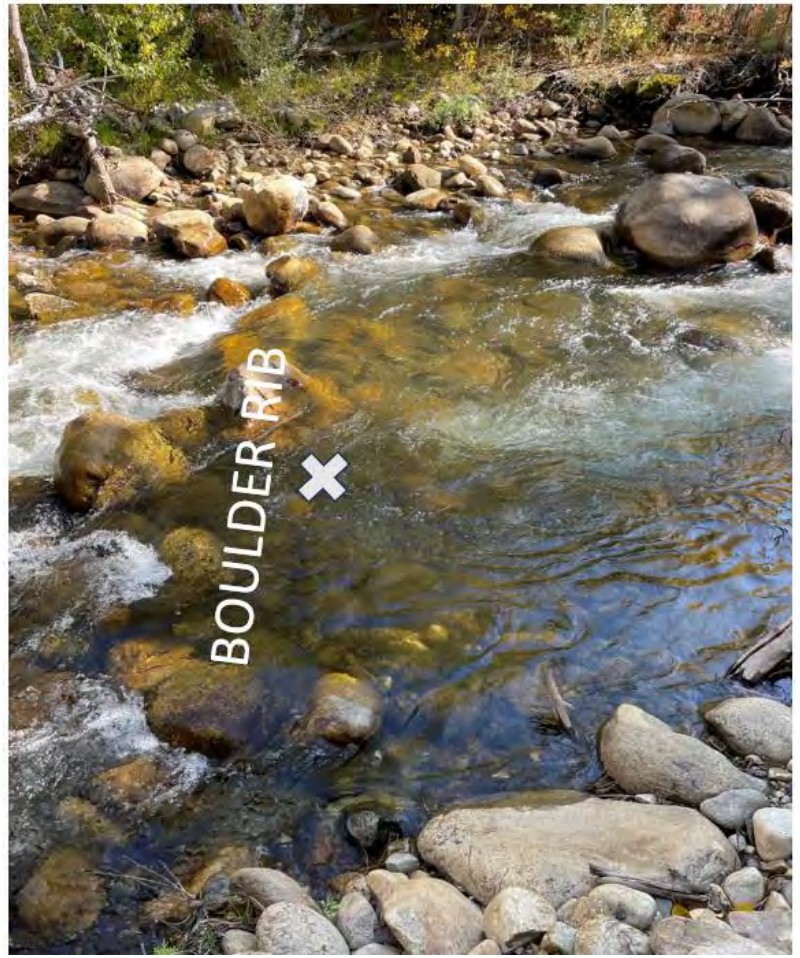

Figure 13. Upper Lee Vining Creek boulder rib and its thalweg 13October2023 2:14PM Q_{AV} = 34 cfs.

The purpose for constructing this BRT-Q Rating Curve is to provide an objective procedure for estimating streamflow depth (Figure 14) for a given flow release. LADWP has been concerned over increasingly erratic SCE streamflows in Lee Vining Creek making daily diversion adjustments challenging. Streamflow changes are difficult to envision. Changes in streamflow depth are much easier to envision.

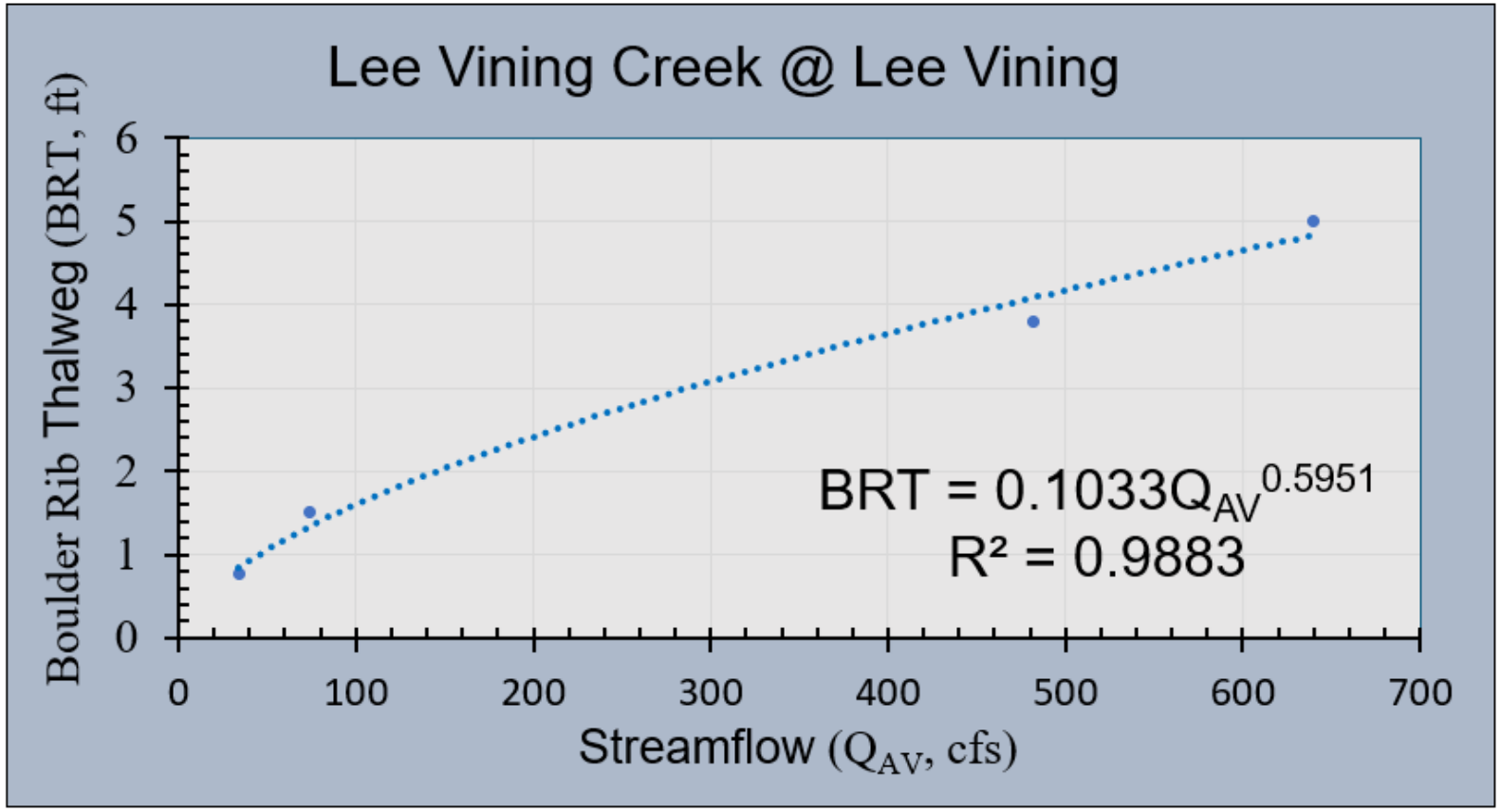

Figure 14. Boulder Rib Thalweg (BRT) Rating Curve constructed for an Upper Lee Vining Creek boulder pool in RY2023.

RCT or BRT Rating Curves require the same effort. Once a boulder pool or riffle crest has been selected on either Lee Vining Creek or Rush Creek, the first step is installing a benchmark. Generally, a half-inch diameter rebar, 3-to-4 ft long, is hammered into the channelbank. Two foot long wooden stakes were also used where there is a desire to keep data collection temporary. The top of the rebar or stake is assigned a reference elevation such as 100.00 ft. All water stage measurements are then surveyed relative to this rebar/stake top. In RY2023, Robbie Di Paolo and Bill Trush first visited on the week beginning 17July when snowmelt runoff was still high and spilling out of Lee Vining Creek's banks. Sometimes, a temporary stake was used first as a benchmark, when high flows precluded getting sufficiently close to drive-in a permanent rebar benchmark. Such was the 'high flow' situation on Upper Lee Vining Creek.

A major portion of the work had already been completed: estimated streamflows were being provided by LADWPs gage just several hundred feet upstream. Two stage heights with identifiable streamflows were measured. One was the present high streamflow, where the recorded time provided access to LADWP's gaging record. The other stage, of the flood peak, was readily identified by a fresh debris line left in early-July. Stage was surveyed relative to the stake top using string and a line level (distance from debris line to the stake did not exceed approximately 10 ft). The other two points on the BRT-Q Rating Curve (Figure 14) are streamflow stages measured during two other site visits … beginning the weeks of 11September and 09October2023.

One final measurement was critical. Higher flows lasting into August made locating and accurately measuring BRT depth impossible. Instead, we waited until the October site visit to measure the thalweg bed elevation relative to the top of our benchmark. Without this referenced elevation there would be no way to calculate BRT depths for any of the four streamflows surveyed. Although the R^2 value of the power function fit to the BRT-Q data (Figure 15A and 15B) seems impressive ($R^2 = 0.9883$), there remains some uncertainty. At least two, and better three, additional measurements should be surveyed between 150 cfs and 400 cfs during RY2024.

Figure 15A. Bill Trush locating the thalweg along a boulder rib in Upper Lee Vining Creek 12SEPT2023 2:13PM.

Figure 15B. Close-up of Bill Trush locating the thalweg along a boulder rib in Upper Lee Vining Creek 12SEPT2023 2:13PM.

What if a streamflow of 35 cfs is reduced to 30 cfs (i.e., if 5 cfs diverted)? This would amount to a 14.3% flow reduction. Boulder Rib Thalweg depth at 35 cfs is 0.86 ft using the BRT Rating Curve in Figure 14. BRT depth at 30 cfs would be 0.78 ft. This diversion would amount to an 8.7% overall BRT depth reduction. The actual reduction in BRT depth equals 0.85 ft – 0.78 ft = 0.06 ft. While the 8.7% BRT reduction may be generally informative, the actual BRT depth reduction of 0.06 ft is ecologically informative.

What if a streamflow of 150 cfs is reduced to 100 cfs? This would amount to a 33.3% streamflow reduction. Boulder Rib Thalweg (BRT) depth at 150 cfs is 2.04 ft using the BRT Rating Curve in Figure _. BRT depth at 100 cfs would be 0.78 ft., culminating in a 21.6% BRT depth loss. Reduction in BRT depth would be 0.44 ft.

There is this one big difference between the 35 cfs diversion scenario and the 150 cfs diversion scenario explored: we have a photograph of the boulder pool at 35 cfs but not at 150 cfs. Figure 16 is simply a magnification of the boulder pool's right bank at 35 cfs. Inspecting Figure 16, a 0.06 ft decrease in BRT depth, going from 35 cfs to 30 cfs, would not likely pose a significant impact. But if asked whether a 14.3% streamflow reduction would not, we might be uncertain. Streamflow percentage changes are too abstract to envision; streamflow depth changes are much easier to envision.

Figure 16. Magnified right bank of monitored Upper Lee Vining Creek boulder pool 13Oct2023 2:16 PM Q_{AV} = 35 cfs.

The leading edge of two velocity cores with highly turbulent flow (the core of bubbles) extends farther downstream into the pool as streamflows increase (Figure 17). Each boulder rib hydraulically dominates upstream pool turbulence at the present Q_{AV} = 34 cfs. But as streamflows increase, Lee Vining Creek's boulder ribs will become more and more inundated, eventually loosing most of their individual hydraulic dominance.

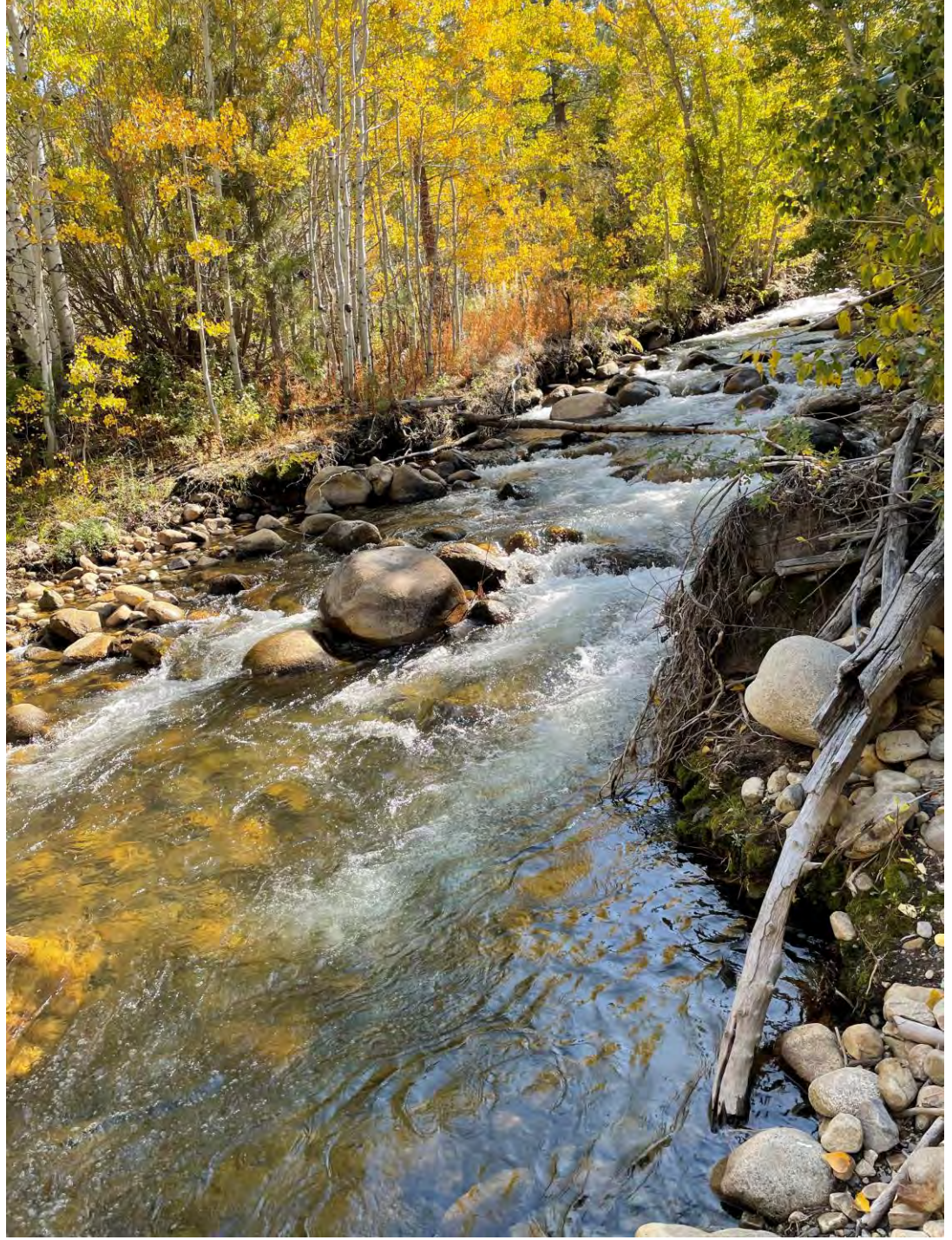

Figure 17. Upper Lee Vining Creek pool with two distinct velocity cores. 13October2023 3:13PM.

Task No. 4. Synoptically Measure RY2023 Baseflows in Lower Rush Creek 8-Floodplain and at the 10-Falls Mainstem.

A synoptic streamflow measurement strategy can offer significant ecological insight that only continuous streamflow gaging at multiple locations traditionally provide. The term “synoptic” literally means “seen together.” Synoptic requires taking more than a single stream measurement at the same time at other strategic locations. Therefore, the informational value (or insight) derived from any single streamflow measurement relies (i.e., ‘is seen together’) on all other measurements taken at essentially the same time.

Our intent was to track stream baseflow loss below the Narrows for an Extreme Wet RY2023. LADWP provides a good starting point: 15 minute collective estimates of streamflow (from several upstream gages) exiting the Narrows throughout each day. We chose October 11, 2023 (Figure 18). At the entrance of the 8-Channel, was the new reality that almost all stream baseflow was going down the 8-Channel rather than down the mainstem. This had partially begun in the RY2017 flood. Mainstem baseflow was so low below the 8-Channel entrance that we could not measure it with a current meter. A rough estimate was 1.5 cfs. Early in the day we walked the right-bank mainstem channel upstream to be sure no surface streamflow was finding its way into the 4-Floodplain. None was evident.

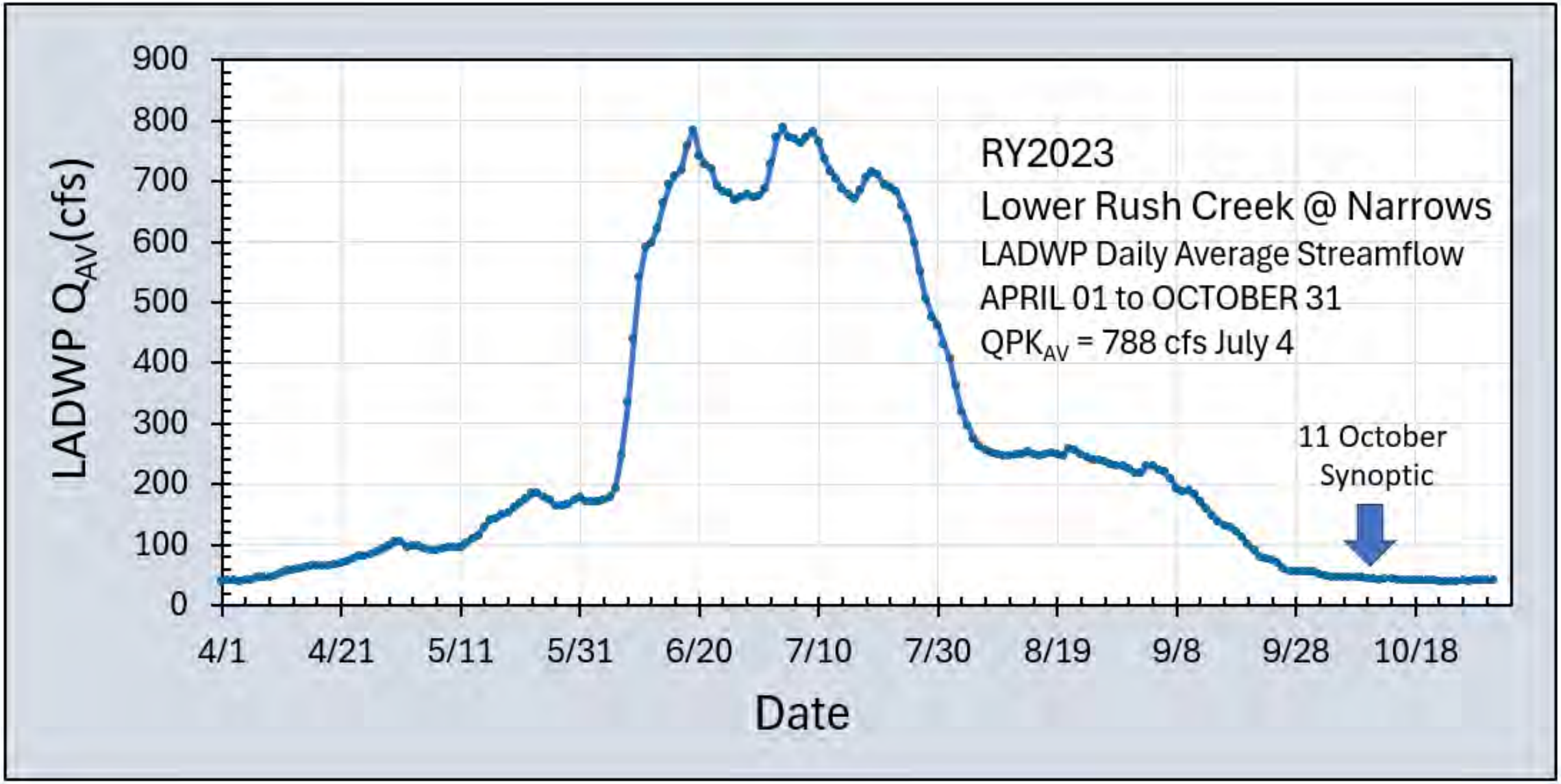

Figure 18. LADWP Daily Average Streamflows (Q_{AV}) 01April through 30September.

Our plan was to measure streamflow at three primary locations: (1) in the 8-Channel just downstream from its entrance, (2) along the far-left side of the middle 8-Flooplain in the Caddis Channel, and (3) at the former gage site immediately below the old 10-Falls, where all floodplain surface streamflows would have spilled back-into the mainstem. We estimated the three locations could all be measured within 2.5 hours.

Our findings on 11October2023 (Q_{AV} = 41.9 cfs) were as follows:

(1) 8-Channel Entrance @ Boulder Parking Area (Figure 19)

11:55 AM Robbie/Bill Q = 32.2 cfs,

(2) Caddis Channel on Left Edge of Mid 8-Floodplain (Figure 20)

1:50 PM Robbie/Bill Q = 34.2 cfs,

(3) Old 10-Falls Gaging Station Blw 8-Floodplain (Figure 21)

12:50 PM Robbie/Bill Q = 34.3 cfs.

The results were what we hoped. We expected some streamflow loss below the Narrows at all three locations. Unusually long duration of high RY2023 streamflows at the Narrows was sustained at greater than 600 cfs from 16June through 26July (Figure 18). The shallow groundwater table should have fully recharged by early-October, explaining the standing water observed throughout the 8-Floodplain. Robbie and I also expected, but could not predict, streamflow loss due to evapotranspiration. However, the consistency of the differences in streamflow between the Narrows and the three downstream locations measured gave this effort some credibility. In RY2024, we plan to do more synoptic streamflow monitoring.

Figure 19. Site of streamflow measurement on the 8-Channel Right Dog Leg 11Oct2023 12:24 PM.

Note dense Narrowleaf Willows now occupying both banks. Also note how straight this channel is. As willows mature, will Caddis Channel begin to resemble a typical alluvial stream with a meandering RCT?

Figure 20. Robbie Di Paolo taking baseflow notes on Caddis Channel 8-Floodplain 11OCT2023 1:39 PM.

Figure 21. Robbie Di Paolo @ 10-Falls channel reach Q measurement 11Oct2023 12:39PM.

Task No. 5.
Evaluate Lee Vining Creek's Paintbrush Side-Channel Capacity for Self-Renewal.

Robbie Di Paolo and I hiked from upper Lee Vining Creek down to middle Lee Vining Creek on July 19 in the first fieldwork week. We wanted to observe Lee Vining Creek at high streamflows shortly following the peak flood occurring July 03 (QPK_{AV}) = 605 cfs (Figure 22).The intent was to find physical evidence of significant geomorphic change, or as stated in the Synthesis Report, 'desired ecological outcomes' attributable to these higher flood flows.

One of the largest side-channels (S-C) in Lee Vining Creek is located near the USFS Visitor Center. Yet this prominent side-channel, which we have named Paintbrush Side-Channel, received no attention in the Synthesis Report. Instead, fieldwork focused on a tight network of interconnected mainstem channels farther downstream near the Lee Vining Creek County Road ford. But there might be a more compelling reason for its omission.

Figure 22. Lee Vining Creek RY2023 Hydrograph from April 01 through October 31.

Photographs taken from the hilltop on July 19, 2023, immediately below the USFS Visitor Center, captured a vigorous Paintbrush Side-Channel with abundant pools and long, hydraulically complex riffles both serving as ideal fish habitat and productive benthic invertebrate habitat (Figures 23 and 24). Climbing down to the side-channel revealed physical features typical of a healthy alluvial stream channel (Figure 25). Its floodplain is covered in sagebrush and scattered black cottonwoods.

Figure 23. Lower Lee Vining Creek Paintbrush Side-Channel July 19, 2023 8:17 AM. Lee Vining Q_{AV} = 489 cfs.

Figure 24. Upper Lee Vining Creek Paintbrush Side-Channel July 19, 2023 8:16 AM LV Q_{AV} = 489 cfs.

Figure 25. Paintbrush Side-Channel point bar on 19July2023 8:16 AM (Lee Vining Creek Q_{AV} = 489 cfs) with a pronounced capillary fringe (i.e., areas of saturated sand/silt) but without seedlings. Ellery McQuilkin assisting in the fieldwork.

The arrow identifies (Figure 26) the likely highest scour line attributable to the QPK_{AV} in mainstem Lee Vining Creek on 03July2023 (QPK_{AV} = 605 cfs) along the outside bend of the point bar in Figure 25. In the mainstem channel on19July2023, Q_{AV} was 489 cfs. The difference in stage between the flood peak scour line and the present water surface was 0.42 ft.

Figure 26.Close-up of outside bend in Paintbrush Side-Channel with a likely flood peak scour line around 03July2023.

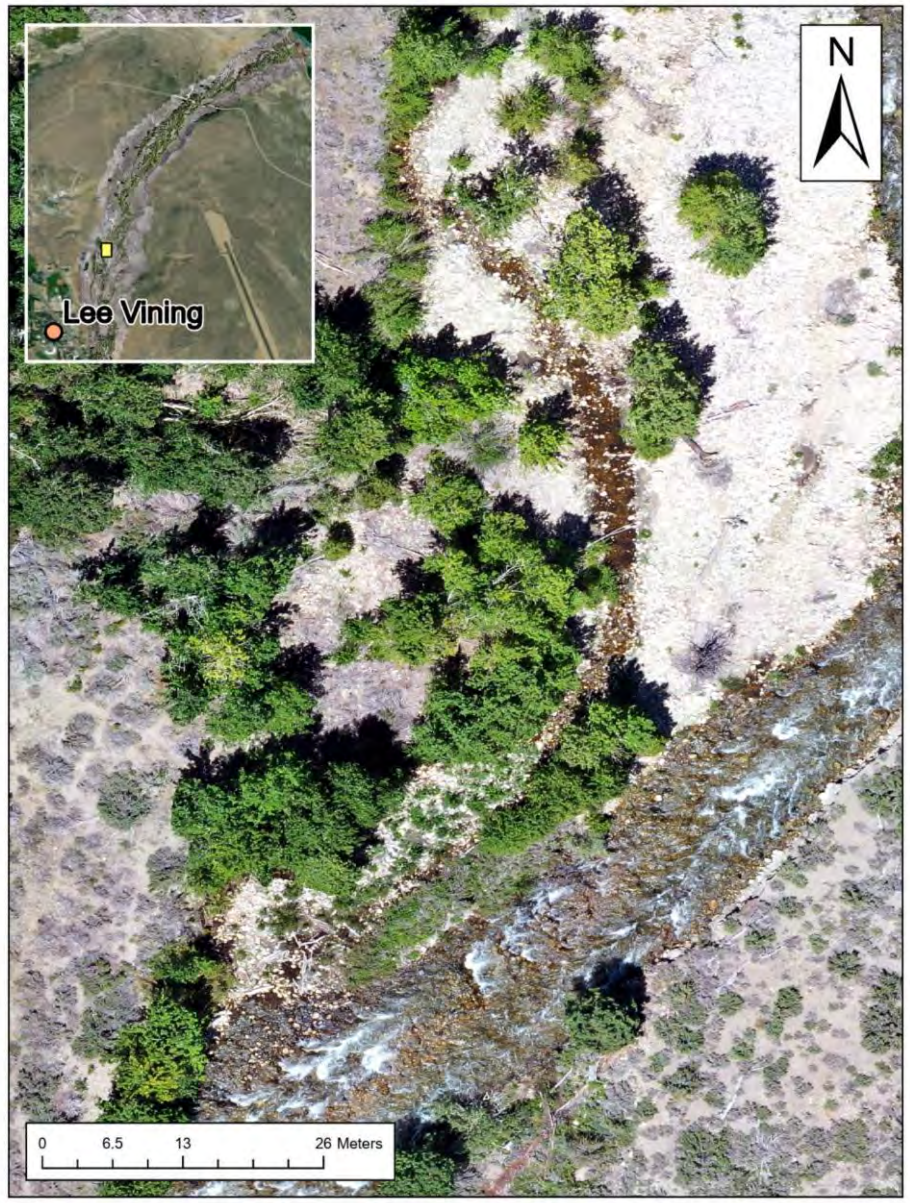

Figure 27. Entrance to Paintbrush S-C, Humboldt CalPoly UAV Survey. 02August2023 Lee Vining Creek Q_{AV} = 214 cfs.

The entrance to Paintbrush Side-Channel is complex (Figure 27) with no succinct point of streamflow entry obvious. Daily streamflows entering Paintbrush Side-Channel (S-C) are regulated by a large debris jam and a dense LB riparian bench. Locating the Paintbrush S-C's invert (def. channel floor of the S-C entrance) would be challenging. For Lee Vining Creek (LV) streamflows entering Paintbrush S-C, mainstem streamflow must exceed the S-C invert's baseline elevation.

As flood runoff dissipates, receding Lee Vining Creek streamflows will eventually drop below the invert elevation, thus cutting-off Lee Vining Creek's surface streamflow entirely to Paintbrush Side-Channel. Our UAV survey of Lee Vining Creek was flown on 02August2023, 16 days following our initial hiking encounter on 19July2023.

Paintbrush Side-Channel's ecological importance, and contribution to Lee Vining Creek's capacity-for-self-renewal, will depend on the window of opportunity streamflows would be required to trigger and sustain productive side-channel habitat. And if not productive fish habitat, then replenishment of the Paintbrush Side-Channel floodplain's shallow groundwater table.

The Synthesis Report presents an essential tool required to adopt/implement a ‘capacity for self renewal’ recovery strategy. Only three data have been addressed: QPK on 02July QPK_{AV} = 605 cfs, a photograph on 19July Q_{AV} = 489 cfs, and a UAV Survey on 02AugustQ_{AV} = 214 cfs. These numbers carry little intuitive meaning unless put into some context. Figure 28 provides complete unimpaired RY hydrographs from RY1990 through RY2008 as context.

The first step is to place horizontal lines at 214 cfs, 489 cfs, and 605 cfs. Now the context. When we were standing on the hillside 19July, we were witnessing an infrequent event in Paintbrush S-C having been exceeded only in 3 RY’s between RY1990 and RY2008. But the most revealing might be Q_{AV} = 214 cfs on 02August with only a very small portion of the S-C flowing (Figure 28). As a first proxy, rounding 214 cfs to 200 cfs offers a reasonable threshold for a functionally wet side-channel.

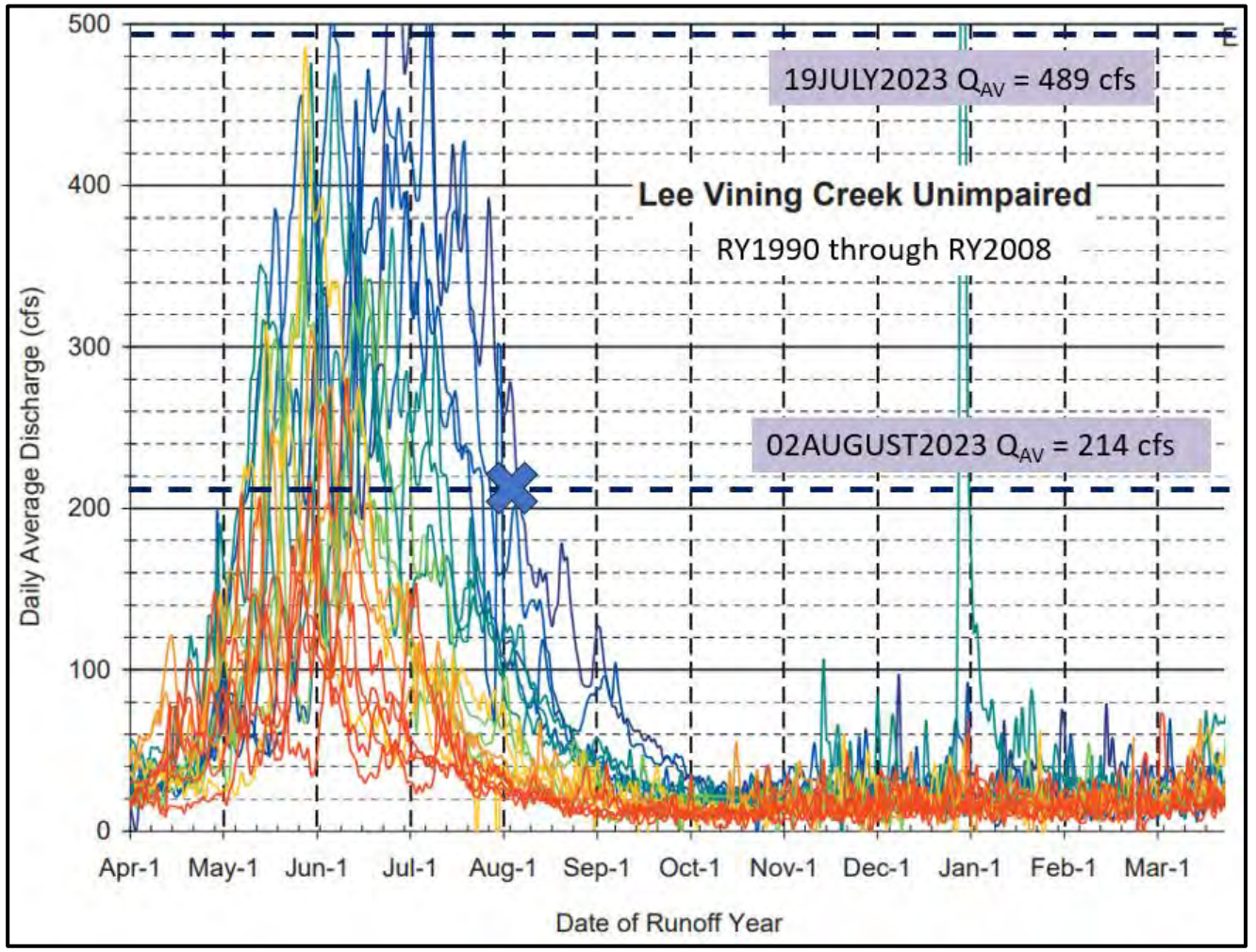

Figure 28. Magnitude, duration, frequency, and timing of daily streamflows all help ensure a stream ecosystem’s capacity for self-renewal. This is how it looks graphically for RY1990 through RY2008 (copied from Synthesis Report Figure 4-1, p.74).

Having the unimpaired daily streamflows RY1999 through RY2008 (Figure 28) permits an analysis regarding the role of Paintbrush Side-Channel supplying surface flows to recharge the shallow groundwater table of its floodplain. The key threshold, a minimum Lee Vining Creek flowing into Paintbrush Side-Channel, was fortuitously supplied by our UAV Survey. A threshold Q_{AV} of 200 cfs. Referring again to Figure 28, a flat line can be drawn at 200 cfs. Then for each RY, count the total number of days Lee Vining Creek Q_{AV} exceeds 200 cfs. Just as shown for describing the distribution of RCT depths by QPK Lee Vining Creek flowing into Paintbrush Side Channel, an exceedence curve can also be readily constructed for Paintbrush Side-Channel 'water delivery' over all the RYs. There may be other Q_{AV} thresholds. The complex network of side-channels within the floodplain may require a higher Lee Vining Creek threshold Q_{AV} to replenish the shallow groundwater throughout the entire floodplain.

After hiking down to the side-channel on July19, we surveyed several hundred feet of Paintbrush Side Channel by measuring: (1) Riffle Crest thalweg (RCT) depths and Boulder Rib thalweg (BRT) depths at the present streamflow and (2) by measuring Flood Peak RCT depths and BRT depths by referencing recent flood peak deposits made on July 3rd. The procedure at each riffle crest or boulder rib was straightforward. First, measure maximum flow depth along the riffle crest or boulder rib at the present streamflow. This is the RCT or BRT depth. Next, locate a fresh debris line on the channel bank deposited by the peak flood. Stretch a level chalk line (using a hand-held line leveler) from the top of the bank deposit over to the present water surface. Take a ruler and measure the distance from the leveled chalk line down to the present water surface. And last, take this distance and add it to the RCT or BRT depth already accomplished for the present streamflow. This sum equals the RCT or BRT depth of the peak flood on July 2nd. A total of 21 RCTs and BRTs was measured.

These twenty-one data points are presented as two exceedence probability curves (also called ‘cumulative frequency curves’), one for the present Lee Vining Creek Q_{AV} = 489 cfs streamflow and one for the QPK_{AV} (both in Figure 29).

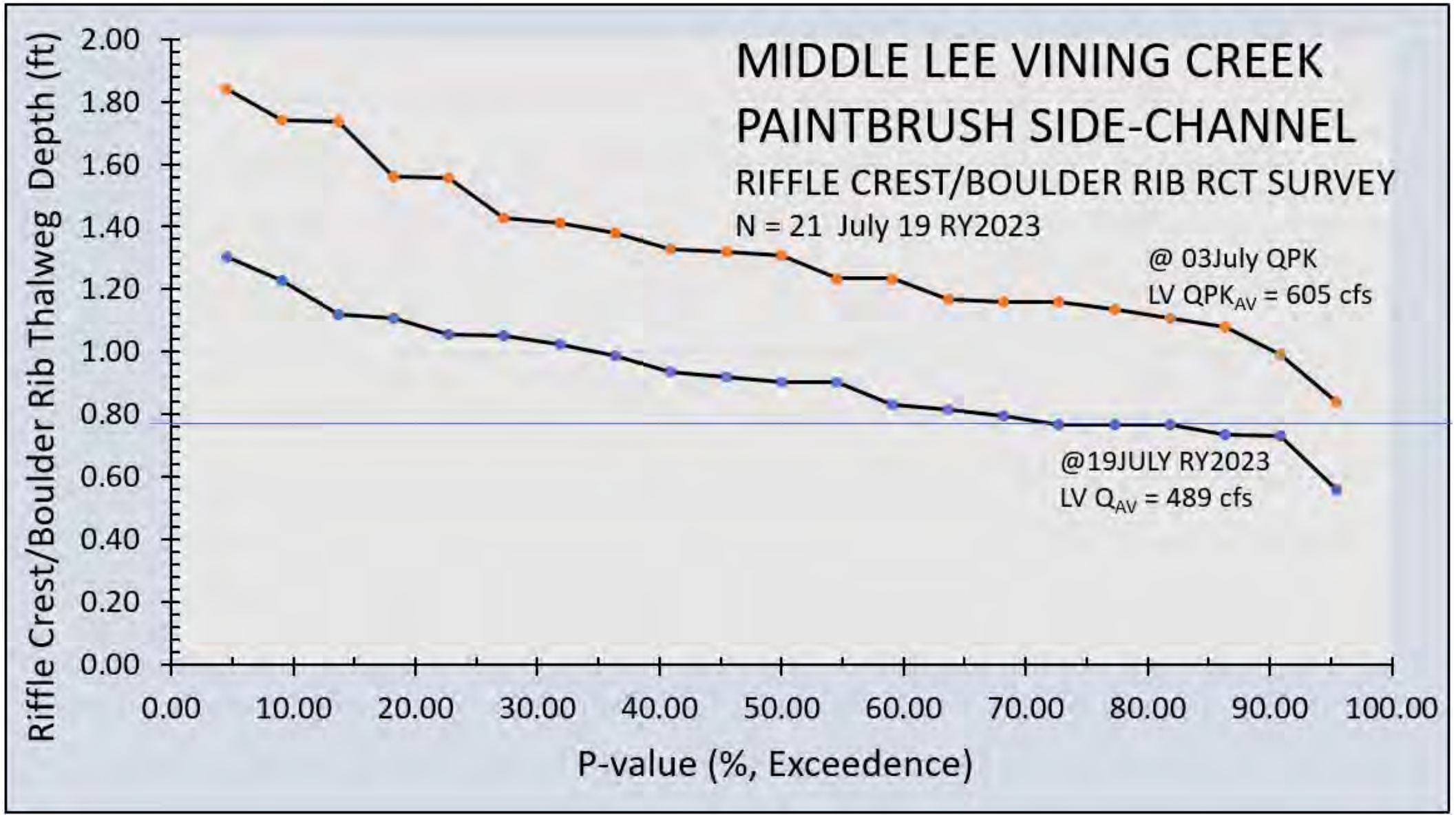

Figure 29. Exceedence Curves for RCT/BRT Depths in Paintbrush Side-Channel for Q_{AV} 19July and QPK_{AV} Streamflow.

Constructing and utilizing exceedence curves as in Figure 29 can require all or some of the following seven steps:

Step No.1. Rank RCT/BRT depths from greatest to least depth … assigning the greatest depth a rank = 1 and the least depth a rank of 21. Good to have an odd sample size (i.e., to have a point on the graph cleanly representing the 50th percentile). A minimum sample size is 10 thalweg depths.

Step No.2. Compute exceedence for each RCT/BRT depth measured using the following equation: P-value = Rank/(N+1)*100 with N = sample size). From Figure 29 an RCT/BRT depth of 0.90 ft measured on July 19 at Q_{AV} = 489 cfs has a P-value of 50%. In words, fifty percent (i.e., the median P-value = 50%) of the RCT/BRT depths measured in Paintbrush Side Channel on July 19th had depths equal to OR GREATER THAN 0.90 ft. For the July 2nd Lee Vining QPK_{AV} of 605 cfs, the median RCT/BRT measured depth was 1.31 ft (i.e., on July 2nd, 50% of the RCT/BRT depth measurements were GREATER THAN 1.31 ft).

Step No.3. Begin plotting a rating curve relating Lee Vining Creek Q_{AV} (cfs) on the X-axis (independent variable) for other given percentile RCT/BRT depth on the Y-axis (dependent variable). Select the median (50% P-value) to start. Oftentimes, cumulative frequency curves for RCT/BRT exhibit a distinctive change in slope above an exceedence of 20% and below an exceedence of 80%. Therefore, three rating curves can be constructed, each targeting a specific exceedence (in this example: P-values of 20%, 50%, and 80%). Each rating curve generated has only two data points (i.e., only two streamflows measured). A task in RY2024 is to measure RCT and BRT depths at additional Lee Vining Creek streamflows.

Step No.4. To reasonably fit rating curves, RCT/BRT's measured at 5 to 6 streamflows (LV Q_{AV}'s) will be required for each rating curve. Proposed RY2024 fieldwork on Paintbrush Side-Channel includes measuring RCT/BRT depths for additional Lee Vining Creek Q_{AV}'s.

Step No.5. This is where some magic happens when applying completed rating curves to investigating Lee Vining Creek's capacity for self-renewal. It begins with the duration, magnitude, frequency, and timing of daily streamflows comprising each unregulated annual hydrograph. Figure 4.1 p.74 in the Synthesis Report, and reproduced in Figure 28, provides individually plotted annual hydrographs for RY1990 through RY2008, all on one graph, for unimpaired Lee Vining Creek streamflows. RY2023 was an unusually high and late runoff RY compared to those of RY1990 through RY2008 (Figure 28).

Step No.6. Our UAV Survey on 02August2023 revealed Paintbrush Side-Channel flowing at its entry point to mainstem Lee Vining Creek, but also that surface streamflows rapidly dry-up a short distance downstream. This single UAV image, therefore, provides a provisional threshold mainstem streamflow, i.e., the Q_{AV} on the day of the survey of fish access/habitat in Paintbrush Side-Channel. Fish habitat access can be readily quantified. Take each unregulated RY in Figure 28 and count the number of days mainstem Lee Vining Q_{AV}'s remain above 214 cfs. To appraise aquatic habitat quality, take the RCT/BRT analysis just discussed and count the number of days in each RY when RCT/BRT depth remains deeper than the median particle size of side-channel riffles (roughly large cobbles) as an initial proxy for productive benthic macroinvertebrate habitat.

Step No.7. Perhaps the most consequential process is shallow groundwater re-charge. UAV surveys can document patterns of surface water inundation/drying-up within the Paintbrush Side-Channel network. The 2Aug2023 UAV survey shows streaks of green with cottonwoods, in an otherwise grey-brown sagebrush surface. Given how important small changes in channelbed elevation can be, this side-channel network may have once been more closely plumbed into the floodplain/terrace. Riparian vegetation vigor (addressed in several annual reports) can be measured, as well as inventorying annual increases/decreases in cottonwood runners.

Topic No.6. Investigate Hydraulic Performance of the 8 Side-Channel Inlet.

Mainstem streamflow passing through the Narrows was reallocated in RY2023. The left bank (LB) 8 Side-Channel located at the very top of the 8-Floodplain now diverts a much greater percentage of total mainstem streamflow into the 8-Floodplain rather than allowing it to pass farther down the mainstem channel to the 4-Floodplain. This reallocation generated significant outcomes for the LB 8-Floodplain and RB 4-Floodplain in RY2023. And will in RY2024.

The cause of this streamflow reallocation originates in the RY2017 hydrograph. During the RY2017 flood peak, approximately 1500 ft of the mainstem Rush Creek channel backwatered causing large-scale cobble aggradation upstream (Figure 30). A long, deep mainstem left bank run was entirely buried. Our hypothesis, a plausible explanation for an observed phenomenon, is that dense willow encroachment of the mainstem channel between the two floodplains sharply increased hydraulic roughness. During major peak runoff events, encroachment could generate a backwater capable of inducing major cobble deposition upstream. Beaver dams also likely contributed to the backwater as well.

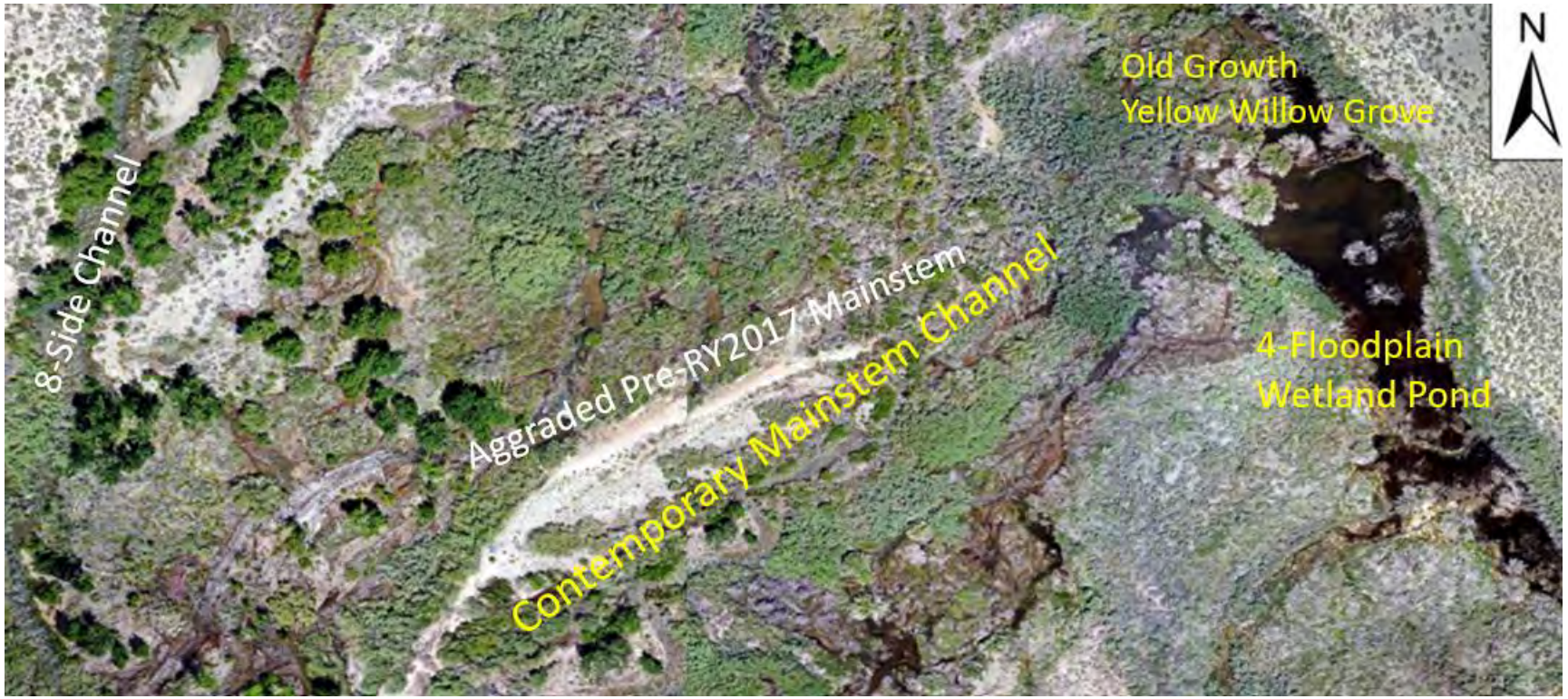

Figure 30. Contemporary UAV image of 4-Floodplain and mainstem Rush Creek channel on 03August2023.

Aggradation forced the mainstem channel to shift to its right, re-occupying remnants of an older mainstem channel and essentially butting-into the RB 4-Floodplain (Figure 30). Encountering the aggraded channel, mainstream surface flows now turn to the right approximately 200 ft downstream of the 8 Side-Channel Inlet and either enter the ‘new’ mainstem channel as surface streamflow, or/and as seepage flow later in summer and autumn. If mainstem channel avulsion was the sole impact of the RY2023 Flood Peak, there would not be too much cause for concern coming RY2024. But mainstem aggradation triggered something more troubling at the 8 Side-Channel Inlet.

Significant change in the 8 Side-Channel Inlet began when LADWP placed a large boulder in front of the entrance and notched the LB willow bench in RY2014-15. Both actions encouraged the 8 Side-Channel Inlet to capture more of the mainstem streamflow. Figure 31 duplicates Figure 13 in the RY2017 Mono Basin Stream Monitoring Report, showing what the 8 Side-Channel Inlet looked like in RY2015. However, the added dashed line on the boulder provides additional valuable insight. Only the very top of the boulder (last few inches) remained visible in RY2017 following significant aggradation caused by the major flood of RY2017. Modest mainstem aggradation continued, and the boulder eventually disappeared in RY2018-19.

Figure 31. The 8 Side-Channel Inlet on 05August2015 with large boulder and aggraded channelbed elevation surveyed following the RY2017 flood on 07October2017.

This simple exercise was a cause for concern. The photographer on October 14, 2023 is standing on the left bank just upstream of the 8 Side-Channel Inlet and shooting downstream (Figure 32). You can see mainstem streamflow spilling from the pool (our photographer has his back to the upstream pool entrance) and flowing into the 8 Side-Channel Inlet instead of continuing downstream.

Figure 32. LB 8 Side-Channel Inlet and downstream mainstem channel.

The riffle crest at the bottom of the pool is 25 ft farther downstream from the Inlet. Figure 33 provides a close-up view of this downstream riffle crest. The riffle crest is so shallow that measuring streamflow was difficult. Excavating a little ditch and using a float, an approximate streamflow was an optimistic 1.5 cfs.

Figure 33. Riffle Crest Below 8 Side-Channel Inlet 13OCTOBER2023 10:03AM Q_{AV} = 44.0 cfs. Estimated mainstem streamflow @ Riffle Crest ~ 1.5 cfs.

Do the math. Approximately Q_{AV} = 44 cfs passes through the Narrows. Considering a 5 cfs loss down to the 8 Side-Channel, a likely streamflow entering the mainstem pool would have been 39 cfs. Subtract the 1.5 cfs exiting the pool leaves 37.5 cfs diverted down the 8 Side-Channel Inlet. Figure 34 is the 8 Side-Channel approximately 250 ft downstream from the Inlet providing an additional view of the diverted mainstem streamflow. Almost all this streamflow will find its way into the 8-Floodplain.

Figure 34. The 8 Side-Channel Dogleg Bend near boulder parking area approximately 300 ft downstream from the Inlet.14OCT2023 2:34PM.

If the riffle crest thalweg's elevation exceeds that of the invert of the 8 Side-Channel Inlet's invert, the hydraulic environment favors mainstem streamflow diversion down the Inlet. If the riffle crest thalweg elevation is lower than the invert's elevation, mainstem streamflows would continue downstream. At a Q_{AV} streamflow entering the pool at 39 cfs, the efficiency of streamflow diverted into the Inlet is at an extremely high 'efficiency' of roughly 96%. As streamflow entering the pool increases, Inlet diversion efficiency should ultimately decrease. Other hydraulic factors must be considered. For example, an irregular geometry and hydraulic roughness from dense willows at the Inlet would decrease efficiency. Fieldwork in RY2024 will include surveying the riffle crest thalweg and 8 Side-Channel Invert (i.e., the floor of the Inlet) elevations.

Another simple exercise troubled us more. We pieced together this exercise in the off-season using notes and saved photographs. In Figure 35, there are these three photographs of the Rush Creek mainstem all taken the morning of 14Sept2023 between 9:30AM to 11:30AM: (1) ~150 ft downstream of the 8 Side-Channel Inlet, (2) ~250 ft upstream of the 8 Side-Channel Inlet, and (3) an additional ~250 ft upstream. Q_{AV} for 14Sept2023 was 148 cfs. In Photograph No.1, there is only ponded seepage water. However in Photographs No.2 and No.3 there is significant streamflow available in the mainstem channel.

Again, where did the mainstem streamflow go approaching the 8 Side-Channel Inlet? The one simple explanation is the one already presented for the observed 13October2023 mainstem streamflow (with a much lower Q_{AV} of 44.0 cfs). The efficiency of the Inlet attracting mainstem streamflow on 14Sept2023 may not have been 96% but likely remained very high, possibly 50% to 65% efficient.

Lower Mainstem Rush Creek

September 14, 2023

Q_{AV} = 148 cfs

9:51 AM

10:30 AM

11:33 AM

Figure 35. Three mainstem photographs taken on 14September2023 revealing the potential impact of the 8 Side-Channel Inlet's high efficiency in directing increased mainstem streamflow into the 8-Floodplain.

In Summary:

The 8-Channel has a history. Following completion of the Synthesis report (roughly 2010), the 8-Channel drew additional attention for providing more streamflow watering of the large Black Cottonwood stand at the top of the 8-Floodplain.

There will be a lot riding on how we deal with (manage?) the future 8-Channel. Presently, the 8-Floodplain is enjoying more streamflow than ever experienced in recent memory. It can be heralded as a star example of Lower Rush Creek's considerable capacity-for-self-renewal. This major increase in streamflow plumbing through the 8-Floodplain, via the 8-Channel, requires somewhere else receive much less. That would be the 4-Floodplain on the opposite side of the mainstem channel.

Task No. 7.
How Did Hydraulic Performance of the 8 Side-Channel Inlet Affect the 8-Floodplain in RY2023?

On 14September2023, we had to cross Caddis Channel which flows along the extreme left boundary of the 8-Floodplain (Figure 36). It became immediately clear, standing on the LB bank of Caddis Channel, that a very large percentage of the total Q_{AV} of 148 cfs passing through the Narrows was now flowing down the Caddis Channel via the 8 Side-Channel. Since three runoff seasons ago, Narrowleaf Willow has grown into a tall, dense wall along both banks of the Caddis Channel (Figure 36). Providing a sizable streamflow in the future will require the 8 Side-Channel Inlet remain highly efficient at depleting mainstream channel streamflow.

Figure 36. Robbie Di Paolo crossing upper Caddis Channel in the 8-Floodplain. 14Sept2023 8:42AM. QAV = 148 cfs.

This impressive RB cobble bar within the 8 Side-Channel (Figure 37) (just downstream from the dogleg right and close to the parking area boulders) did not exist prior to RY2023. There is no cobble bar of its size anywhere within the 8 Side-Channel. Most streamflow broke right, rather than left before RY2023.

Given a sizable streamflow would have been necessary to supply and then construct this prominent cobble bar, should the 8 Side-Channel Inlet remain highly efficient at depleting mainstem channel streamflow?

Figure 37. RB Cobble Bar within the 8 Side-Channel did not exist prior to RY2023. 09Oct2023 10:15AM Q_{AV} = 45 cfs.

Our UAV Survey on 03August2023 captured an image of the ‘new’ broad RB cobble bar in the lower left. Streamflow was initially redirected toward the LB of the 8-Floodplain (Blue arrows). But just past the top of the cobble bar, the 8 Side-Channel splits into two branches (Figure 38): (1) one heading north becoming the Caddis Channel and (2) the other heading northeast. The 8 Side-Channel heading northeast continues in Figure 39.

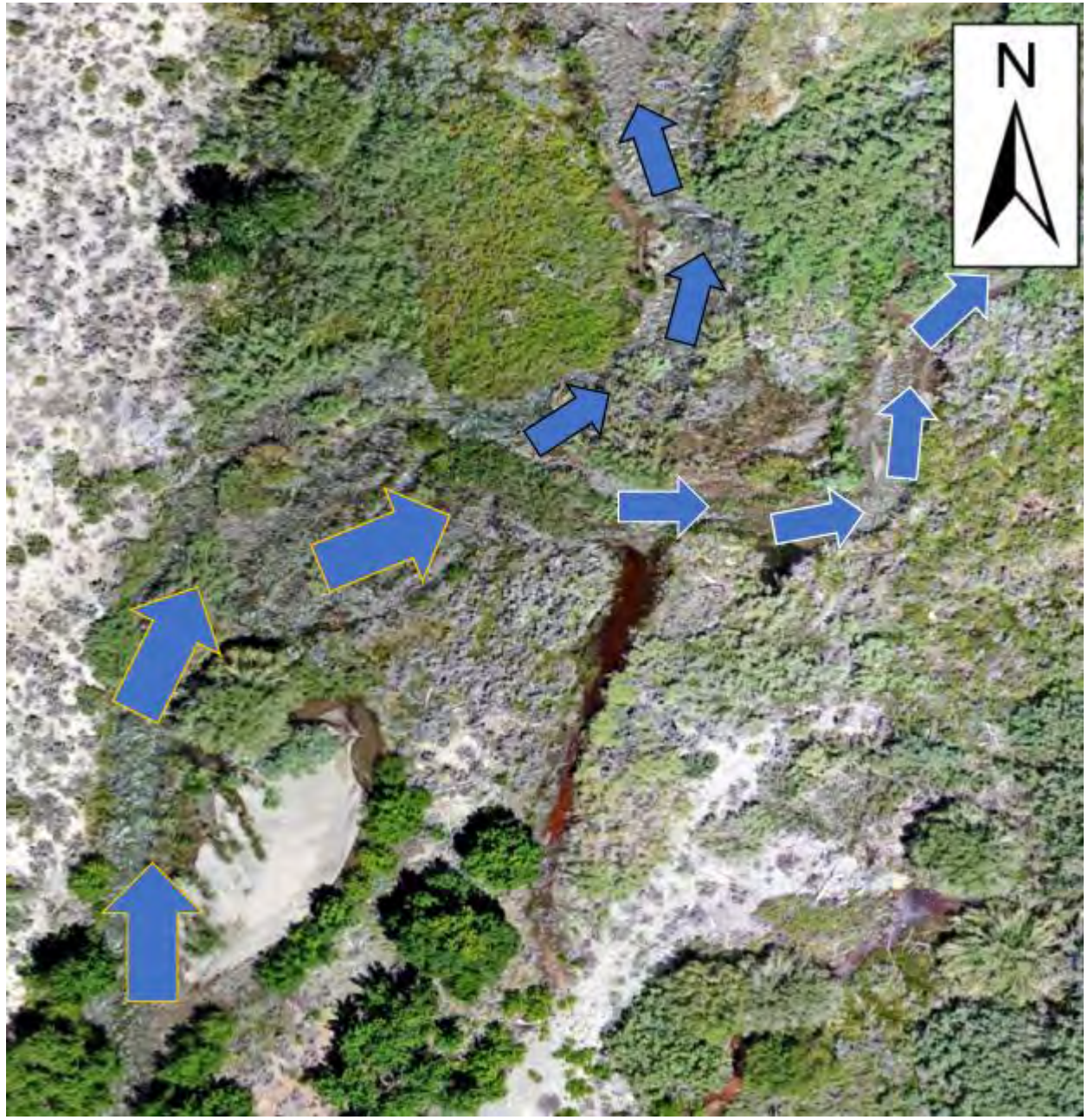

Figure 38.The 8 Side-Channel with split streamflows. O3August2023 UAV Survey, Q_{AV} = 320 cfs.

WETLANDIA

Jim Graham's UAV Survey on 3August2023 Q_{AV} = 320 cfs captured a complete image of Wetlandia (Figure 39). The 8 Side-Channel heading northeast eventually encounters backwater conditions created by beaver dams. Beavers have been earning their title 'busy as beavers." This has been the only location I have regularly seen Rush Creek beavers, totally engaged in building and caring for their wetland utopia. It just seemed appropriate to call their utopian wetland home *Wetlandia*.

Beaver Wetlandia is being sustained by an unknown portion of the 8-Channel streamflows.

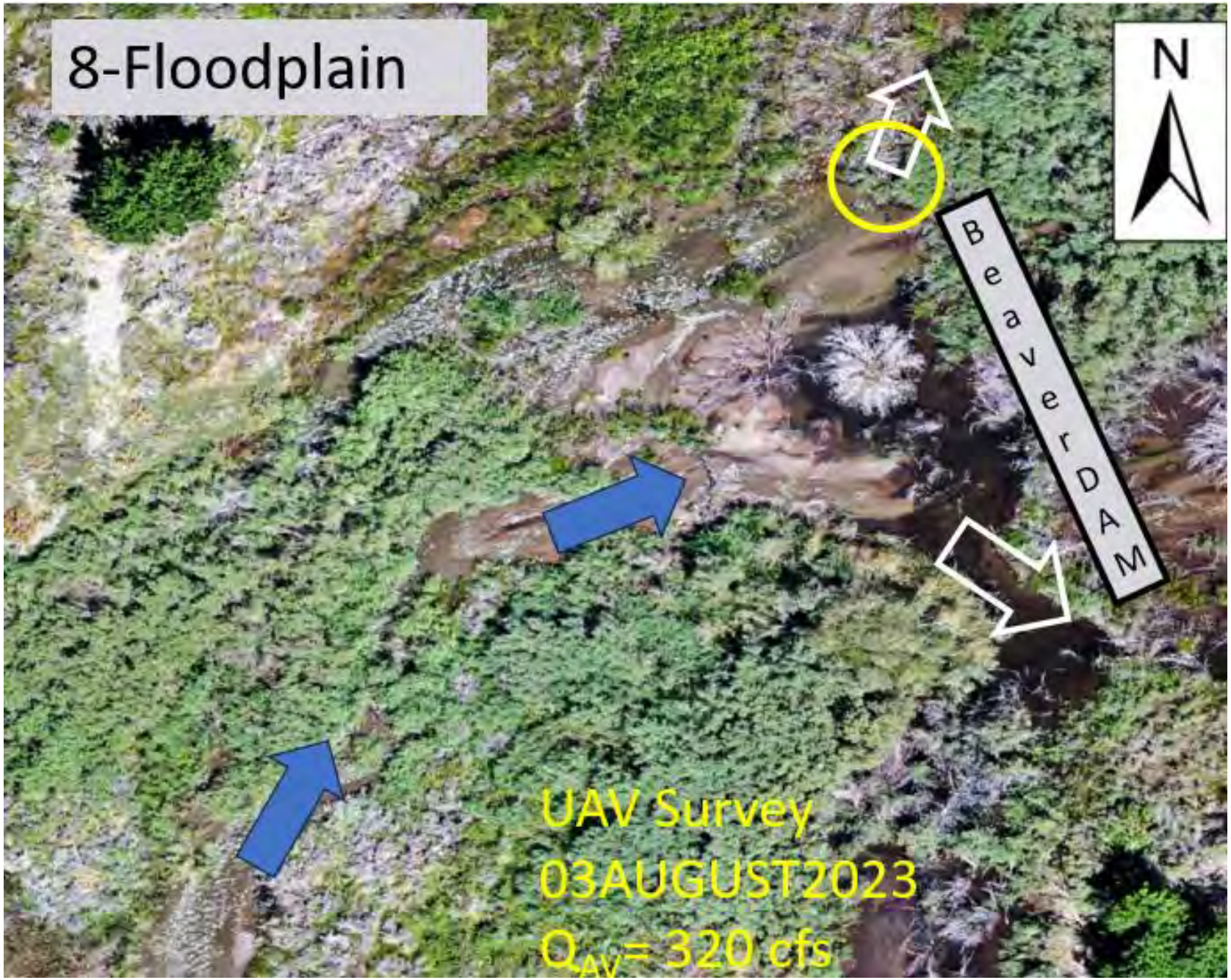

Figure 39. Beavers backwater 8 Side-Channel streamflows to create Wetlandia.

Few environments are better at expressing an ecosystem's capacity for self-renewal than are newly-evolving wetlands. We are not sure when this beaver-induced wetland began taking shape. Figure 7 in the RY2016 Mono Stream Monitoring Report identifies beaver dam activity at the 8-Channel's terminus, with the caption stating 8-Channel streamflows eventually return to the mainstem channel.

There are two exit locations for 8 Side-Channel streamflows (Figure 39): (1) the yellow circle in the upper right is a sill over which 8 Side-Channel streamflows exit Wetlandia, then flow across the interior of the 8-Flooplain, and eventually join Caddis Channel and (2) streamflows can pass through the beaver dams and rejoin the mainstem channel (the white arrow in Figure 39).

Although we did not know how much mainstem streamflow was being captured by the 8-Channel Entrance, the streamflow was considerably greater than what we had experienced in the past. The black water of the beaver pond in Figure 39 was being contained by a disorganized collection of damaged beaver dams. Wetlandia only exists by being built in the lee of the 8-Floodplain's Cottonwood Grove, thus keeping partially sheltered from the direct force of the early-July RY2023 QPK.

This sill already stood-out in RY2021 (Figure 40); the photograph was taken in RY2021 at the exact same location (a wooden stake and again at the blue ‘X’ on a RY2021 photograph) on 14September2023 (Figure 41) to document extremely rapid growth of Narrowleaf Willow since RY2021.

The white arrow in Figure 40 points to one exposed beaver dam at the far end of the pond. There is leakage past these dams that re-enters the mainstem channel downstream. Approaching the dams from below reveals several large pools with coarse woody debris near their base.

Figure 40. Looking upstream into Wetlandia on 27AugustRY2021 12:09PM Q_{AV} = 237 cfs.

The sill allows 8-Channel streamflows to exit Wetlandia, cross the 8-Floodplain and eventually spill into Caddis Channel. Situated on the far-left edge of the 8-Floodplain, Caddis Channel continues downstream until spilling back into the mainstem close to the old 10-Falls.

Figure 41 is looking downstream and across the 8-Floodplain. The Blue ‘X’ was monumented with a wooden stake.

Figure 41. Sill with 8-Channel streamflow exiting Beaver Wetlandia on 27August2021 12:10PM.

Bill Trush is standing on the Wetlandian sill that allows streamflows to exit the wetland (Figure 42). He is standing on the exact location photographed in RY2021 (Figure 41). Note the rapid growth of Narrowleaf willows since RY2021.

Figure 42. Wetlandia outgoing streamflow at the sill. 14Sept2023 9:25 AM.

Backwater created by beaver activities in early stage of wetland formation with extensive deposition of sand and silt (Figure 43). Note no evidence of woody debris jams among the willows because the huge backwater effect of the beaver dams.

Figure 43. A young Wetlandia. 14September2023 Q_{AV} = 148 cfs. Robbie Di Paolo photograph.

Figure 44. Wetlandia depositional features deposited by beaver dam backwater at higher 8-Channel streamflows. September 14, 2023. Robbie Di Paolo photograph.

Even though Q_{AV} dropped from 148 cfs on 14Sept to 45 cfs on 09October, spawning habitat for Brown Trout was abundant on both dates (Figure 45).

Figure 45. Good brown trout spawning habitat in the 8-Floodplain interior formed by multiple small converging channels on 09Oct and 14Sept.

Task No. 8.
How Did Hydraulic Performance of the 8 Side-Channel Inlet Affect the 4-Floodplain in 2023?

The Lower 4-Floodplain Wetland Pond is approximately 2000 ft downstream of the 8 Side-Channel Inlet (Figure 46). The 4-Floodplain is vulnerable to low late-summer through mid-autumn mainstem baseflows depending on the RY type.

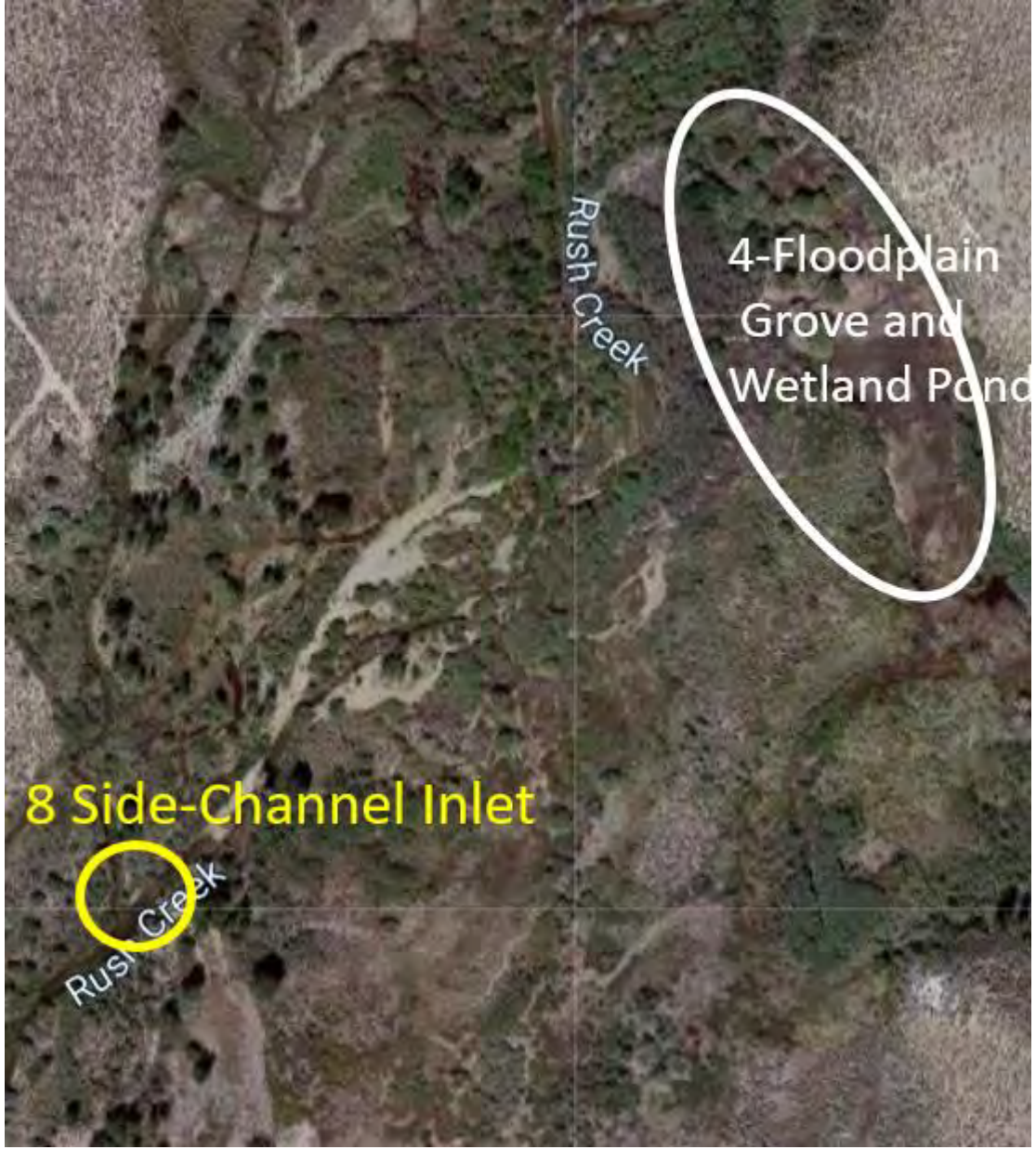

Figure 46. Location of the 8 Side-Channel Inlet relative to Lower 4-Floodplain's Old Growth Yellow Willow Grove and Wetland Pond.

Given flood flows were too great to wade late-June 2023, Robbie hiked to the ridgetop to take a photograph on June 22, 2023 (Figure 47) to capture the RY2023 flood peak (Figure 48). This is the entire 4-Floodplain; you are looking upstream. Farther to the right, is mainstem Lower Rush Creek (just a sliver is visible), and farther still, is the opposing 8-Floodplain. The wetland pond, at the base of the ridgetop, is full. Past the pond's outlet to the right, is a grove of old-growth Yellow Willow trees. Both wetland pond and willow grove are special. Their capacities for self-renewal will depend on how well mainstem streamflows access the 4-Floodplain.

Figure 47. The 4-Floodplain in Lower Rush Creek during peak snowmelt runoff on June 22, 2023. Q_{AV} = 721 cfs. Robbie Di Paolo photograph.

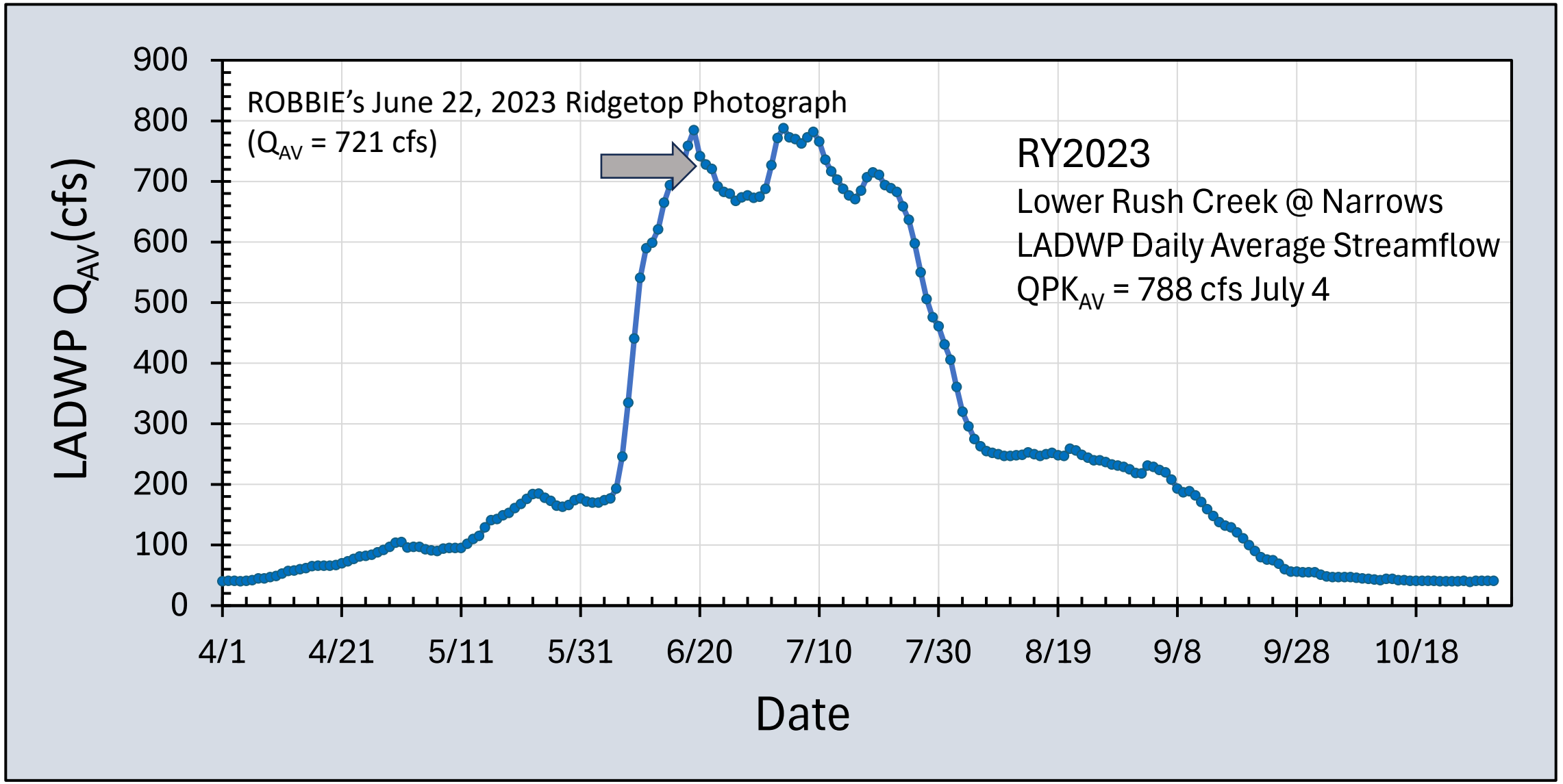

Figure 48. Robbie Di Paolo's ridgetop photograph of Lower Rush Creek's 4-Floodplain taken June 22, 2023.

The 4-Floodplain is divided into three parts. Upper 4-Floodplain is identified by its large black cottonwood groves (Figure 49). A relatively small 4Bii side-channel, located at the very tip of the 4-Floodplain, can transport limited flood flows but not mainstem baseflows. Central 4-Floodplain has the snaking streamflow running down its centerline (Figure 49). These streamflows originate from mainstem overflow into the riparian zones during peak flows (as on June 22, 2023), and later during the receding hydrograph as greatly reduced surface flow and then as seepage flow. Central 4-Floodplain spills into Lower 4-Floodplain with its Wetland Pond and Yellow Willow Grove. In Figure 49, there are two primary streamflow sources: (1) streamflow entering the Upper 4-Floodplain at its very tip via the 4Bii Side-Channel and (2) lateral surface streamflows and seepage flows, from right-to-left (in this photograph), of the ‘new’ (Post RY2017 Flood) mainstem channel in Central and Lower 4-Floodplain.

Figure 49. The 4-Floodplain primary streamflow sources. June 22, 2023. Q_{AV} = 721 cfs. Robbie Di Paolo photograph

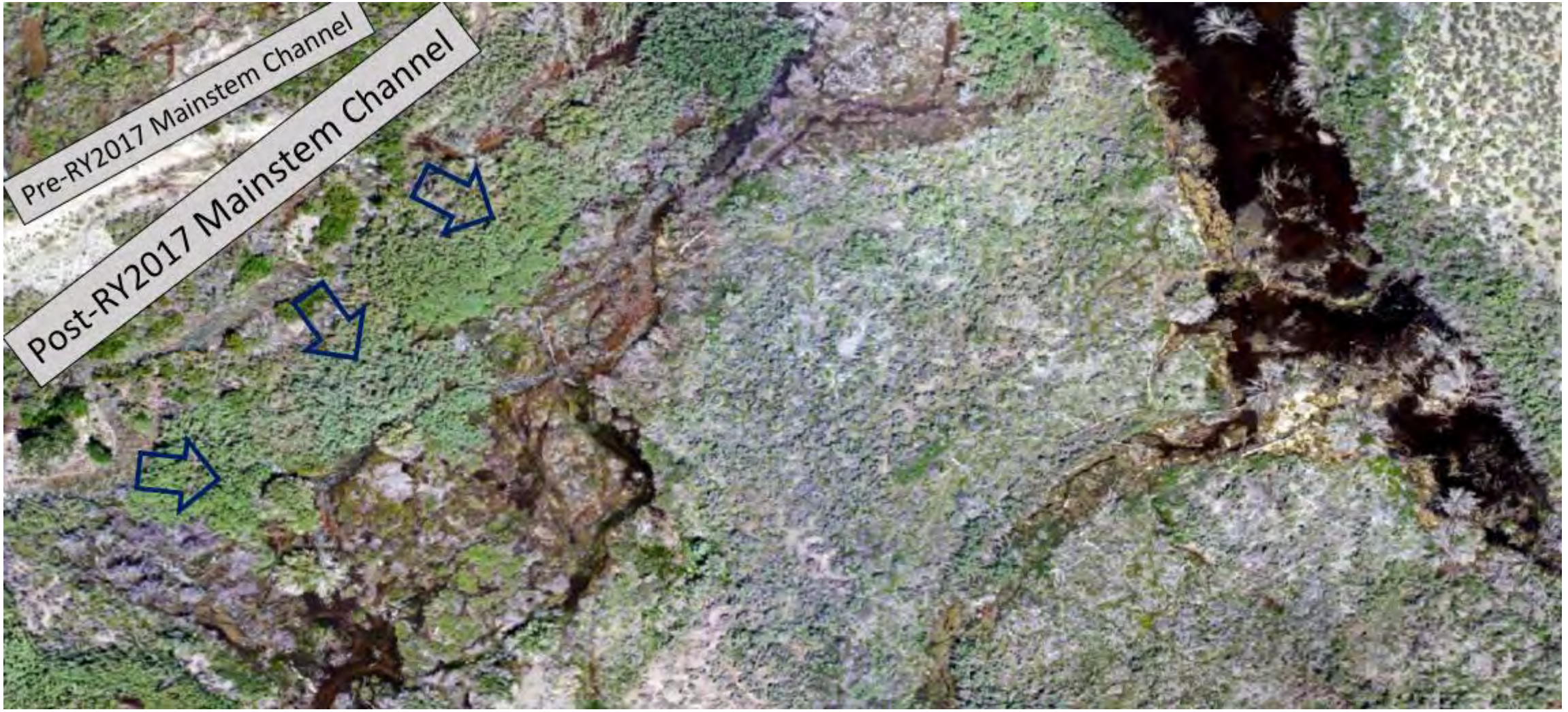

Figure 50. Lower and Central 4-Floodplain with mainstem streamflow access left-to-right. Directional Blue Outlined Arrows for mainstem surface streamflows and late-summer/autumn seepage. CalPoly Humboldt UAV Survey on August 3, 2023.Q_{AV} = 320 cfs.

Basically, the bright green to the left of surface 'black' streamflow (Figure 50) heading toward the Wetland Pond and Yellow Willow Grove, is the riparian zone for the 4-Floodplain. To the right of the surface streamflow, is a slightly higher surface supporting Great Basin sagebrush and a few Yellow Willows.

If you were standing on one of the three blue arrows in Figure 50, it would look just like Figure 51. Mainstem streamflow and seepage entry into Central 4-Floodplain Riparian Zone. However, there was no flowing water on 14September2023, but instead significant seepage (Figure 51). Note abundant maturing Black Cottonwood runners mixed with dead/dying sagebrush against a backdrop of dense 8 ft to 10 ft high Narrowleaf willows and tall Black Cottonwoods in this Riparian Zone of Lower 8-Floodplain.

Figure 51. The post-2017 Flood 4-Floodplain Riparian Zone. 14Sept2023 Q_{AV} = 148 cfs.(Robbie Di Paolo Photograph).

During RY2024 Field Season: We will shoot, with an engineer's level, a QPK elevation estimated from this debris jam (Figure 52), then determine how far into Central 4-Floodplain the QPK extended. Note the silt lines on the Narrowleaf Willow stems correspond favorably with the top of the debris jam. This may offer another way to estimate flood extension into Central 4-Floodplain. The QAV for 13 Oct2023 is 159 cfs. The dry surface in the bottom left indicates seepage had ceased for some time.

Figure 52. QPK Flood Debris Line in Central 4-Floodplain Riparian Zone. 13 Oct2023 10:42AM. Q_{AV} = 159 cfs.

This photograph (Figure 53) ‘lies within’ the yellow-circle featured in Figure 49. Where does QPK stage intersect this side-channel spilling into the Lower 4-Floodplain? Looking at the algal matting, there never was a backwater during RY2023 inundating it. Where this steep channel spills into Lower 4-Floodplain would be of ecological interest.

Figure 53. Side-channel of Central 4-Floodplain before spilling into Lower 4-Floodplain. 13Oct2023 11:28AM.

Very different outcomes for Yellow Willow Old Growth Grove and Wetland Pond in Lower 4-Floodplain with relatively small differences in October Q_{AV}'s between two RY's with similar peak floods (Figure 54). A plausible explanation can be made: the distance from the 8 Side-Channel Inlet to the Old Growth Yellow Willows is approximately 2000 ft. At a Q_{AV} = 44 cfs on 14OCT2023 the 8 Side-Channel Inlet diverted ~96% of the mainstem flow into the 8 Side-Channel, leaving only 1.5 cfs in the mainstem channel. A 1.5 cfs streamflow cannot sustain ample flow to Wetland Pond or the Old Growth Yellow Willow Grove in Lower 4-Floodplain (Figure 55 and 56). In RY2017, the Side-Channel Inlet was not diverting mainstream flows. A Q_{AV} = 63.5 cfs in RY2017 without excessive diversion could sustain the Wetland Pond and Old Growth Yellow Willow Grove.

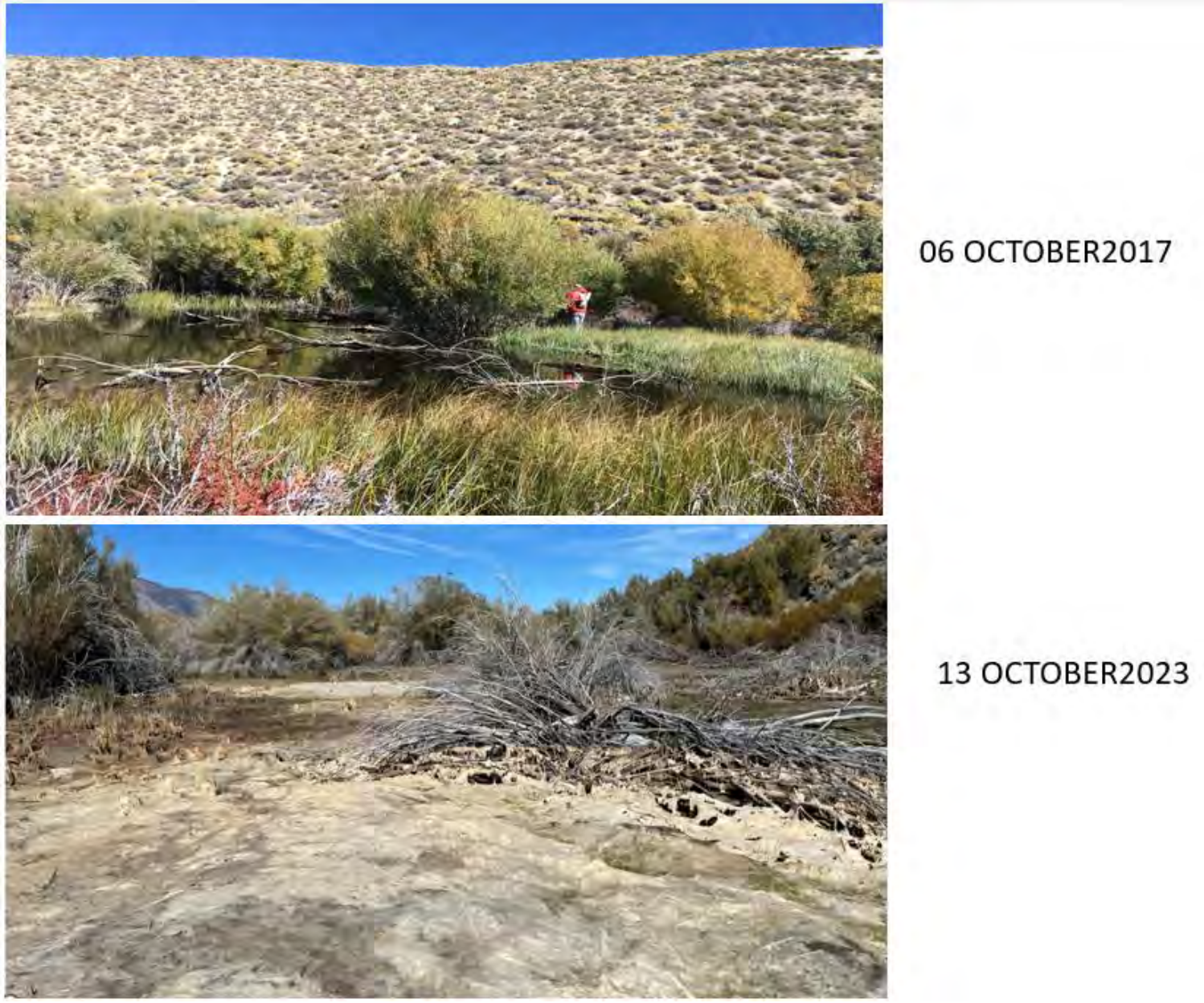

Figure 54. Yellow Willow Grove in Lower 4-Floodplain: 06OCTOBER2017 Q_{AV} = 63.5 cfs and 13OCTOBER2023 Q_{AV} = 44.0 cfs.

Figure 55.
Wetland Pond
13OCTOBER2023
10:50AM
Q_{AV}@NARROWS = 44 cfs

Figure 56. June 22, 2023 filling 4-Floodplain Wetland Pond with Q_{AV} = 721 cfs and on October 13, 2023 desiccated Wetland Pond with Q_{AV} = 44.0 cfs.

Task No.9. What is a Rush Creek Mainstem River Willow Forest?

What is a River Willow Forest? This is an important question given the beavers call the River Willow Forest home. Extensive willow forests occupy segments of the Lower Rush Creek mainstem channel. Willows are typically considered riparian. A riparian area in the mainstem channel is the transition from an aquatic area to an upland area. There is a dense willow forest now occupying the mainstem channel within the banks of the 8-Floodplain and banks of the 4-Floodplain. These willow forests are not in the mainstem's riparian areas … but rather in the mainstem's aquatic areas. Dense willow forests occupy these aquatic areas, so we are labeling them 'River Willow Forests.' Narrowleaf Willow and Yellow Willow are the dominant species. There are no black cottonwood groves; only a few solitary, older Black Cottonwoods.

Save the descriptor 'riparian' for mainstem channel banks bordering the 8-Floodplain and 4-Floodplain. It's an alluvial world of silts, sands, gravel, and cobbles trapped on their way to Mono Lake. Yet the mainstem channel exhibits very few alluvial features common in most alluvial rivers. One conspicuous feature is the abundance of straight, long, rectangular, and narrow channel reaches that simply do not meander and remain almost perfectly straight. These could almost be labeled 'trenches.'

I realized how unique this River Willow Forest was while bushwacking through dense willows in RY2023 to locate beaver dams old and new. On 15 September 2023, Robbie and I stumbled upon this relict M&T gage plate as a reminder of ever-present change (Figure 57). In the late-1990's this gage plate was estimating baseflows. Now, it is perched 3.5 feet above baseflow. The gage plate is not located on the outside of a meander bend being cut-off, but rather on a very long, very straight, and very narrow mainstem channel. Yet long, straight, and narrow is atypical for most 'healthy' alluvial stream channels.

Figure 57. M&T Gage Plate. Upstream of Big Beaver Pond 15 September 2023.

The origin of River Willow Forests may be the direct outcome of Rush Creek's historic flow management legacy only going back to 1994 (Figure 58):

MONO LAKE BASIN
WATER RIGHT DECISION 1631

Decision and Order Amending Water Right Licenses to Establish Fishery Protection Flows in Streams Tributary to Mono Lake and to Protect Public Trust Resources at Mono Lake and in the Mono Lake Basin

(Water Right Licenses 10191 and 10192, Applications 8042 and 8043, City of Los Angeles, Licensee)

September 28,1994

STATE OF CALIFORNIA
WATER RESOURCES CONTROL BOARD

We grew a dense river willow forest spanning the mainstem's aquatic area between the banks of opposing 4-Floodplain and 8-Floodplain.

TABLE 13: INSTREAM FLOW REQUIREMENTS FOR RUSH CREEK

DRY HYDROLOGIC CONDITIONS -RUSH CREEK	
APRIL 1 THROUGH SEPTEMBER 30	31 CFS[1]
OCTOBER 1 THROUGH MARCH 31	36 CFS[1]
NORMAL HYDROLOGIC CONDITIONS -RUSH CREEK	
APRIL 1 THROUGH SEPTEMBER 30	47 CFS[2]
OCTOBER 1 THROUGH MARCH 31	44 CFS[2]
WET HYDROLOGIC CONDITIONS -RUSH CREEK	
APRIL 1 THROUGH SEPTEMBER 30	68 CFS[2]
OCTOBER 1 THROUGH MARCH 31	52 CFS[2]

TABLE 14: CHANNEL MAINTENANCE & FLUSHING FLOW REQUIREMENTS RUSH CREEK

HYDROLOGIC CONDITION	REQUIREMENT
DRY YEAR	NO REQUIREMENT
DRY-NORMAL YEAR	NO REQUIREMENT
NORMAL YEAR	200 CFS FOR 5 DAYS
WET-NORMAL YEAR	300 CFS FOR 2 DAYS RAMP DOWN TO 200 CFS, MAINTAIN 200 CFS FOR 10 DAYS
WET YEAR	300 CFS FOR 2 DAYS RAMP DOWN TO 200 CFS, MAINTAIN 200 CFS FOR 10 DAYS
RAMPING RATE - NOT TO EXCEED A 10% CHANGE IN STREAMFLOW PER 24 HOURS	

Figure 59. Mono Lake Basin Water Right Decision 1631. September 28, 1994.

Mr. Trihey suggested that with a range of streamflows from 30 to 100 cfs (DFG's recommendation) the treatments that are in place will work well. Channel flushing and maintenance flows of 350 cfs would result in minimal erosion of streambed and banks. He also indicated that opening up the historic channels would lessen the erosive effects, and that the reemergence of riparian vegetation would solidify the channel and provide good refuge habitat for fish during overbank flows, thus allowing even higher flows without injury to the fishery. (NAS&MLC 1X, p. 12.)

Figure 60. Trihey comments. Copied from Mono Lake Basin Water Right Decision 1631. September 28, 1994, page 61.

Woody Trihey, as did most fish biologists, supported streamflow recommendations in Mono Lake Basin Water Right Decision 1631 (Figure 60) that provided good fish refuge habitat. But in doing so, was denying the stream's ability to sustain its capacity for self-renewal.

In Table 14 of Figure 59, Decision 1631 recommended QPK releases of 300 cfs for 3 days in Wet RY's. Walking Lower Rush Creek while streamflows remained high in July RY2023 was instructive. In the unimpaired annual hydrographs of Figure 61, a 300 cfs peak event for 3 days would not have been capable of effective channel maintenance in wetter RYs. In doing so, Rush Creek's capacity for self-renewal was diminished.

In Figure 59 Table 13, recommended instreamflows were basically for providing fish habitat. But they were also ideally capable of germinating and growing Narrowleaf Willows and Yellow Willows.

Consequently, we grew a dense river willow forest spanning the mainstem's aquatic area between the riparian banks of opposing 4-Floodplain and 8-Floodplain. The current SEFs is an attempt at recovering capacity for self-renewal.

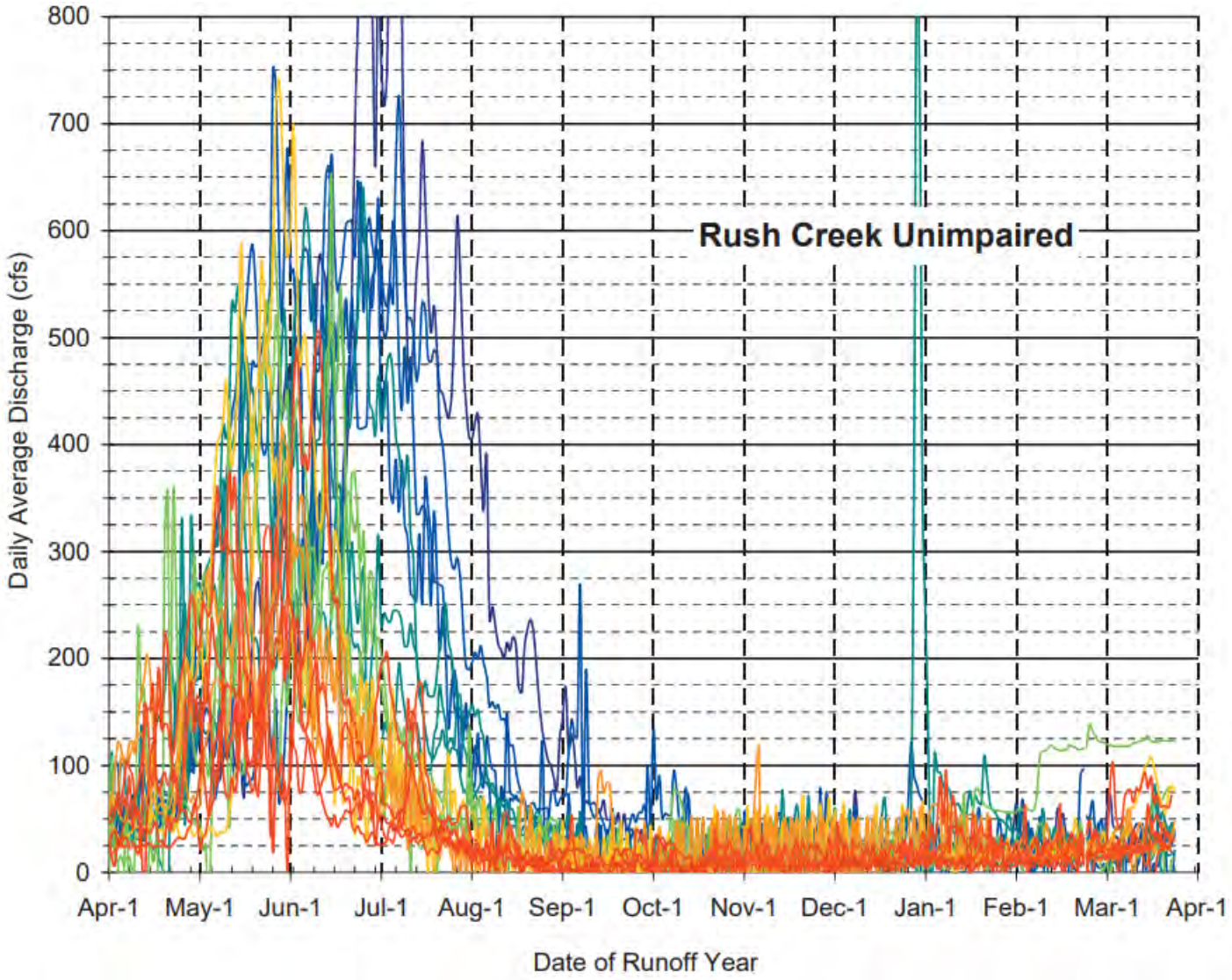

Figure 61. Copied from Synthesis Report, Figure 5-1 p.90 RY's 1990 to 2008. Estimated Rush Creek Unimpaired Annual Hydrographs RY's 1990 through 2008..

Task No.10. Track Restoring Capacity for Self-Renewal in the Mainstem River Willow Forest.

Narrow channels with near vertical opposing banks does describe a ‘trench.’ Clearly this stream bank eroded in RY2023 (Figure 62). Was the channelbed downcut? Were both banks eroded? What was once a horizonal root is now dangling in space, indicating a 1.0 to 1.5 ft bank retreat. To think and see ‘capacity for self-renewal’ requires a different mindset than prescribing physical restoration measures (e.g., opening a plugged side-channel). The very small debris jam enclosed within the yellow rectangle in Figure 62 tells us: (1) that the RY2023 flood flow was from right to left based on stick arrangement in the willows (though you can simply look down at your feet to conclude the same!) and more importantly (2) that the maximum QPK depth in RY2023 (peak flood flow) was 3.0 to 3.5 ft to slightly more (always carry a pocket portable stadia rod). Small clusters of twigs suspended up in the willow limbs, but close to the bed surface, confirms that the peak flood in RY2023 did barely overtop the floodplain surface of dense willow roots by approximately 0.5 ft.

Restoring capacity for self-renewal can simply mean becoming alluvial again. To accomplish ‘becoming alluvial again’ requires removal of the existing trenches and the dense mats of willow roots armoring alluvial deposits underneath that prevent their mobilization. With implementation of the SEF’s, we are witnessing Rush Creek tearing-down its legacy River Willow Forest. Rush Creek will not be renewing/preserving it. This is good news for the beavers. Becoming more alluvial encourages greater species diversity with each species contributing uniquely, and in doing so, strengthening the entire stream ecosystem.

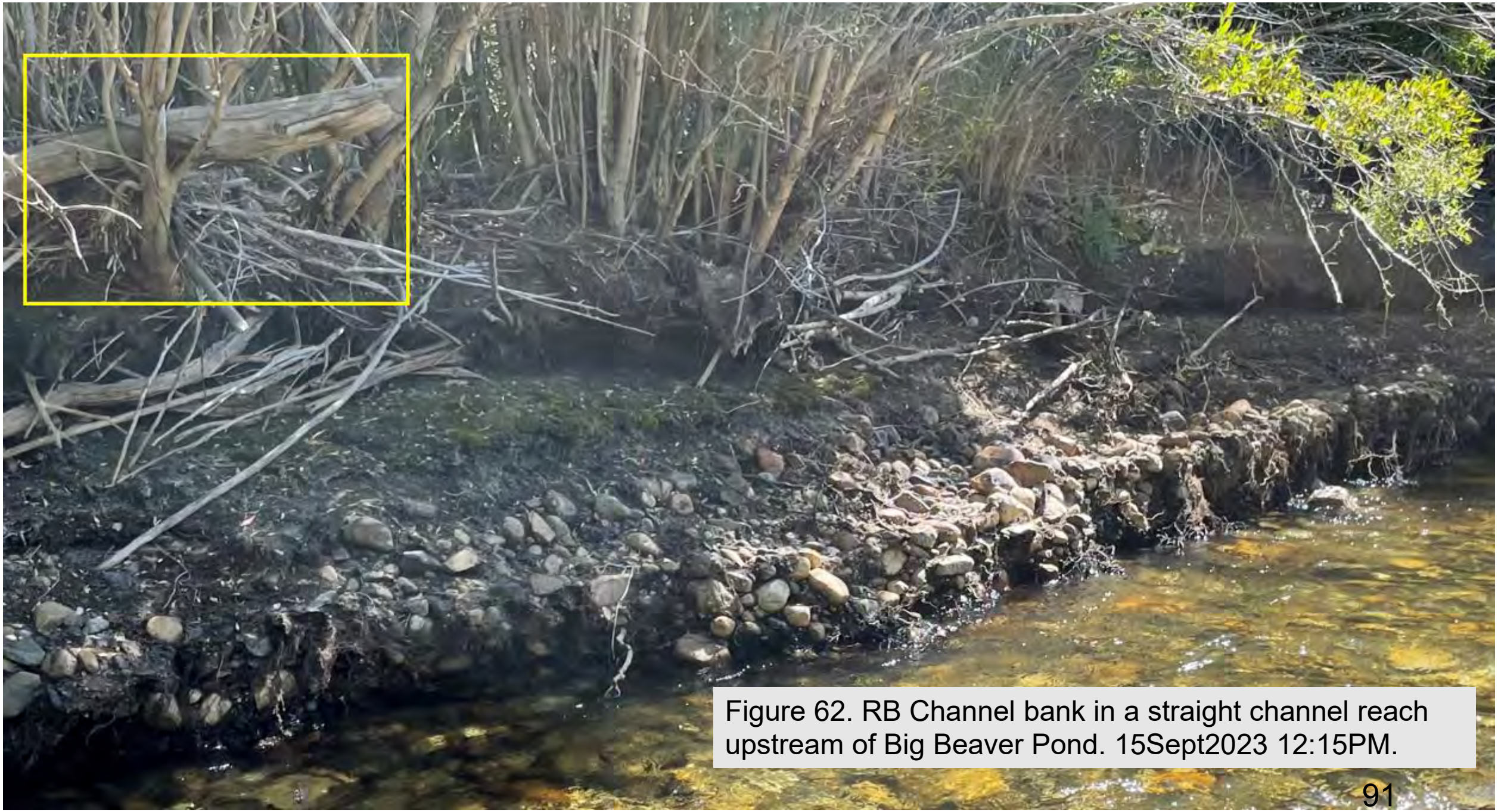

Figure 62. RB Channel bank in a straight channel reach upstream of Big Beaver Pond. 15Sept2023 12:15PM.

Figure 63. A scour hole in River Willow Forest interior. 28AUGUST2023 10:38AM

Figure 64. Deep within the River Willow Forest, an active mainstem headcut. 15SEPT2023 12:15PM.

Scattered throughout the River Willow Forest are scours (Figure 63) and mini-headcuts (Figure 64) that are breaking-up the near impenetrable surface layer of dense willow roots. A long-term inventory of headcuts and scour holes could be one measure of mainstem channel becoming more alluvial increasing alluvialness.

Mainstem Rush Creek channel upstream of Big Beaver Pond barely beginning to function as an alluvial river. In walking the channel, there was no discernable thalweg meander. Eroded banks are depositing cobbles that might become precursors to dynamic cobble bars.

Figure 65. Wider, and not quite so straight mainstem channel upstream of Big Beaver Pond. 10OCTOBER2023 1:41PM

Figure 66. Just upstream from Big Beaver Pond. With widened active channel and alluvial features beginning to appear. Within the River Willow Forest, Rush Creek is reasserting its capacity for self-renewal. Nothing glamorous. Simple.

Figure 67. Close-up RB bank looks very similar to smaller ‘Trench’ channels within the Ruver Willow Forest, 10OCT2023 1:41PM.

Figure 68. Above Big Beaver Pond
10 OCT2023 1:40PM.
This may be site of a blown-out beaver dam.
Only one big log. Big Beaver Pond just around the bend.

Task No. 11. How Will Beavers Adapt to Life in a River Willow Forest?

Our beavers' world is not a riparian forest or riparian wetland, but a dense river willow forest. Save the descriptor 'riparian' for the mainstem channel banks that abruptly transition into the 8-Floodplain and 4-Floodplain. It's an alluvial world of silts, sands, gravel, and cobbles trapped on their way to Mono Lake. Yet the mainstem channel exhibits very few alluvial features common in most alluvial rivers. One conspicuous feature is the abundance of straight, long, uniform, and narrow channel reaches that simply do not meander and remain almost perfectly straight. These could be labeled 'trenches' rather than stream channels.

Big Beaver Pond is located along the right valley wall just downstream of the 4-Floodplain Yellow Willow Grove (Figure 69. It is impressive. Not just for its relative size to other beaver ponds in Lower Rush Creek, but for withstanding a norm of constant change. In RY2017, Big Beaver Pond was drained (Figure 70; In RY2021, Big Beaver Pond was full (Figures 71 and 72; In RY2023, Big Beaver Pond was drained again (Figure 73). Did beavers create this impressive physical setting, or are they opportunists taking advantage of a unique physical setting as best they can? I suspect the latter. If so, then the future may not include more big dams with big ponds.

Figure 69. Big Beaver Pond is located close to the right valley wall and just downstream from the Lower 4-Floodplain's Yellow Willow Grove. The white arrow is an exit location. If you stood on its tip and looked across the 8-Floodplain …you would see the above view.

In the lee of the 8-Floodplain cottonwood grove, the frontal beaver dam remained mostly intact after the RY2017 flood. Can't conclude that the RY2017 Flood did/did not 'fill-in' a much bigger Beaver Pond. Very low slope to the cobble bars' surface, indicating freshly deposited gravel/cobble did encounter a big pond capable of generating a prominent backwater inducing deposition.

Figure 70. Big Beaver Pond 06October2017 1:29PM.

Figure 71. Streamflow entering a full Big Beaver Pond on 28August2021 10:45AM.

Figure 72. Largest Beaver Pond in Mainstem Rush Creek.
August 28, 2021 10:45 AM
Looking Upstream from Dam.

The QPK RY2023 blew-out both plugs in Big Beaver Dam. With annual monitoring, we can estimate the magnitude of the peak flood (QPK) causing or not causing plug blow-out to Big Beaver Pond's dam. However, this particular plug is not ordinary. First, it is the biggest plug. And second, the plug comes in segments because there is a mature Yellow Willow in the plug's center (i.e., separate plugs must be built by beavers on both sides of this centerpiece mature Yellow Willow).

Figure 73. Drained Big Beaver Pond with Robbie inspecting the dual plug blow-out. Photo Taken: 15Sept2023 1:21PM.

Dam Plugs

The plug is a critical component of any beaver dam even though it often comprises a small percentage of total dam length. When a peak snowmelt event shoots down the active channel, there is nothing behind the plug offering support or resistance. Floods oftentimes will blow-out the plug. While the remainder of the beaver dam, built with branches inter-twined among tall supple willows, remains generally intact. Therefore in most RYs, repair/replace the damaged/missing plugs once the flood subsides, and beavers are soon ‘back-in-business.’ Plug failure might even be considered ‘planned failure’ minimizing widespread damage.

One reason Big Beaver Pond exists might be due to the presence of a large, mature Yellow Willow occupying the center of the dam’s plug area. Two small plugs as opposed to one long plug would have a better chance surviving a big flood. With annual monitoring, we can estimate the magnitude of the peak flood (QPK) causing or not causing plug blow-out to Big Beaver Pond’s dam.

Dual plugs are required at damsite for Big Beaver Pond. A mature Yellow Willow requires a plug on each side (Figures 74 - 76). Note the small size of construction branches. Without larger materials (e.g., logs), the dam is vulnerable to big floods. And likely, not so big floods. However, the end result in RY2021 was impressive. I do not know what happened in RY2022.

In RY2023, both plugs were blown-out by a peak flood similar to the RY2017 flood peak.

Figure 74. Robbie Di Paolo measuring height in Big Beaver Pond plug on 28August2021 10:45AM. Typical branch sizes used to replace most plugs.

Figure 75. Big Beaver Pond in Lower Rush Creek
Looking Downstream
September 15, 2023 1:21 PM
Q_{AV}@Narrows = 138 cfs

Figure 76. Close-up of Robbie Di Paolo inspecting dual plug blow-out on Big Beaver Pond. Good view of a dense River Willow Forest. 15 SEPT2023 1:21PM.

A beaver dam ‘plug’ is approximately the width of the active channel. In Lower Rush Creek, the streamflow associated with the active channel stage is ~240 cfs (i.e., a streamflow completely filling the active channel). Most of the dams are small (Figure 77) because most of the channels are narrow. There are many smaller dams that have ‘plug blow-out’ with lesser QPK’s. Oftentimes, these smaller dams generate backwaters in linear mainstem channel reaches, rather than creating more recognizable ‘ponds.’ Note background against RB valley wall with the tall black cottonwoods in the true riparian zone (RB bank of the Lower 4-Floodplain), not in the aquatic area of the mainstem channel occupied by the River Willow Forest.

Figure 77. Small beaver dam below Big Beaver Pond … just pure plug. 28APRIL2021 11:58AM.

Oftentimes it's easy to walk past a former beaver dam site without realizing there was a dam the previous RY (Figure 78). The plug is only slightly wider than the active channel width. The steep downstream face of this RB cobble bar is a reliable indicator, i.e., something (the former dam plug) provided the necessary backwater to cause cobble deposition.

Figure 78. Former small beaver dam with plug pulled in RY2023 15Sept2023 12:04PM.

In RY's when the plug has been swept away, the best remaining trout habitats are debris jams along the channel banks of the drained pond (Figure 79) Usually an older Red Willow or Yellow Willow (and occasionally Black Cottonwood) retains woody debris to induce a scour hole (pool). Warm water temperatures may be an issue. For RY2024, we are considering installing HOBO Waterproof Temperature Data Loggers.

Figure 79. Debris pool within Big Beaver Pond with blown-out plug. 15Sept2023 1:21 PM.

Mature cottonwoods are relatively rare within the River Willow Forest bracketed on both sides by the 4-Floodplain and 8-Floodplain. This may have significant bearing on how beavers strategize dam construction. Big Beaver Pond could use a few big cottonwood logs like this one (Figure 80) located not far from the dam plug. This cottonwood is not in the dense river willow forest, but in a narrow riparian zone along the 8-Floodplain border.

Moving segments of this cottonwood through the dense Narrowleaf Willow Forest to Big Beaver Pond would be an accomplishment. To learn from the beavers, we plan field site visits to places such as this downed, riparian cottonwood to better understand the beavers' future intentions and needs.

Figure 80. Mature cottonwood cut down close to Big Beaver Pond. 15Sept2023 1:32 PM.

This River Willow Forest channel (Figure 81) likely too wide for a single plug beaver dam. During QPK2023, the maximum flood peak barely over-topped the banks. While wading, there was a very slight thalweg meander.

Figure 81. Straight, narrow trench-like channel upstream of Big Beaver Pond 15SEPT2023 12:15PM.

Both channels (Figures 82 and 83) seem well-suited to accommodate a one plug beaver dam.

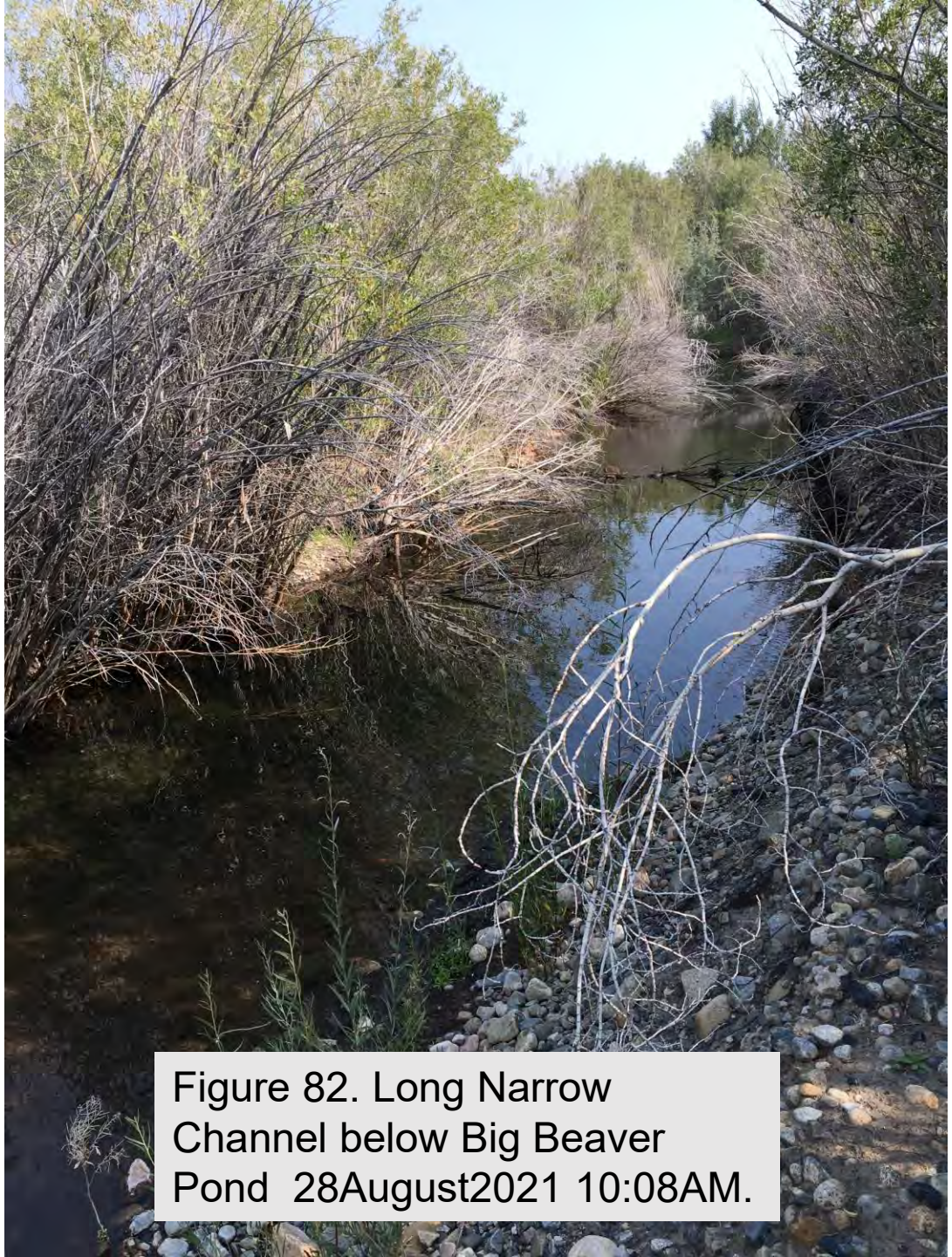

Figure 82. Long Narrow Channel below Big Beaver Pond 28August2021 10:08AM.

Figure 83. Straight channel 15Sept2023 12:16 PM. Another straight channel with no discernable thalweg meander.

Monitoring Not Just About Beaver Dams

Keeping watch over Lower Rush Creek should include on-the-ground periodic surveillance for beaver presence/absence, nibbled stems, and coarser construction activities from the Narrows downstream to Test Station Road culvert. Such a survey would require two full fieldwork days (and possibly three days for at least two crew members. If possible, this survey would be followed-up with a UAV survey. It would not reveal beaver-chewed willow stems but would locate recently-downed trees (especially if the on-the-ground crew provided co-ordinates of downed trees observed in the ground survey. Suspect UAV locations could be field-checked.

An interim (supplemental approach might prove useful. Two prominent pools upstream from the Rush Creek road crossing offers desirable beaver habitat: Jim Smith Pool (Figure 84 and Turnabout Pool (Figure 85. Access from Rush Creek Road to either pool would require maybe a two-minute walk from the car. When I drove down from Humboldt County for my second week of fieldwork, I stopped-off at Turnaround Pool and discovered very recent beaver cuttings (Figure 86).

Figure 84.
Gary Smith Pool
SEPT 13, 2023 2:19 PM
LADWP Q_{AV} = 159 cfs

Figure 85. Turnaround Pool 11OCT2023 3:58PM.

Presence and arrangement of beaver chewings (Figure 86) indicated they were here well after peak streamflows, and likely came by as recently as two weeks prior to taking the photograph. Reference yellow circle in Figure 85 for location of cuttings in Turnaround Pool.

Figure 86. Fresh beaver cuttings at Turnabout Pool. 11SEPT2023 10:31AM.

Figure 86b. Yellow Willow Grove in Central 4-Floodplain.

Task No.11. Reconstruct RY2023 QPK Flood/Seepage Access to a Grove of Yellow Willows in the Central 4-Floodplain and Gauge a Yellow Willow's Vigor Response.

An important RY2023 monitoring objective was to retrace how/where streamflows entered Central and Lower 4-Floodplains. Although not in the field when RY2023 QPK peaked on July 4th, we searched for recent high flow depositional features cleanly identifying maximum flood stage (i.e., maximum water surface stage). Two primary streamflow pathways were investigated to determine whether the base of Yellow Willow R5_26 was inundated during the QPK RY2023.

The second pathway required mainstem flood flows entering the 4Bii Side-Channel (Figure 87) at the very top of the 4-Floodplain, and then flowing down into the interior of the Central 4-Floodplain via smaller branching sub-channels. The 4Bii Entrance has been encountering extended mainstem channel downcutting. In the 1990s and early-2000s, QPKs as low as 250 cfs to 300 cfs inundated the 4Bii Side-Channel invert (i.e., the floor of the side channel's entrance), then continued flowing downstream into the Central 4-Floodplain interior. But now, the 4Bii Entrance requires considerably greater flood peaks just to inundate the 4Bii invert. The RY2023 QPK_{AV} (788 cfs at its peak) inundated the 4Bii invert by only 1.21 ft. This streamflow depth was estimated by carefully surveying organic debris lines left by the QPK in multiple locations surrounding the 4Bii invert. Knowing flow depth at the invert, however, is not an estimate for streamflow.

Figure 87. The 4Bii Side-Channel Inlet at top of the 4-Floodplain. 27SEPT2018 10:19AM.

Two measurements of surface water elevation in this scour hole pool in the 4Bii Side-Channel (relative to top of a wooden stake benchmark) were taken mid-September and early-October.

This scour hole is located within the Yellow Willow Grove (Figure 88). A high priority task for the 2024 Field Season will be to survey the water surface in this scour hole (and top of the wood stake) with an engineer's level to a streamflow stage benchmark at the 8 Side-Channel Inlet on the mainstem channel.

Figure 88. Nature's scour hole 'piezometer' (in the 4Bii Side-Channel) in Central 4-Floodplain inside the Yellow Willow Grove 14 Sept2023 11:07AM.

Eventually, both pathways team-up downstream to supply surface water to the Lower 4-Floodplain Wetland Pond. We expected, given the magnitude and duration of the RY2023 QPK, that Yellow Willow R5_26 would have had its base temporarily inundated by surface flow.

Each water pathway could have wetted the base of Yellow Willow No. R5_26 (Figure 89). The Mono Basin Stream Monitoring Report RY2017 concluded the following: *After observing riparian floodplain responses in many RYs, this one 'given' seems solid: groundwater recharge from the top-down (i.e., by flowing side-channels) is much faster than lateral groundwater recharge from mainstem streamflows. This is particularly important in RYs with modest/poor snowmelt runoff of relatively short duration.*

Figure 89. Yellow Willow R5_26 in Central 4-Floodplain 13October2023 10:30AM.

Farther downstream, perched algal mats are indicative of sustained 4Bii Side-Channel streamflows near the Yellow Willow grove in Central 4-Floodplain (Figures 90 and 91). Sustained 4Bii Side-Channel streamflow may have lasted almost two continuous months.

Figure 90. Perched algal mats in Central 4-Floodplain 13OCTOBER2023 10:27AM.

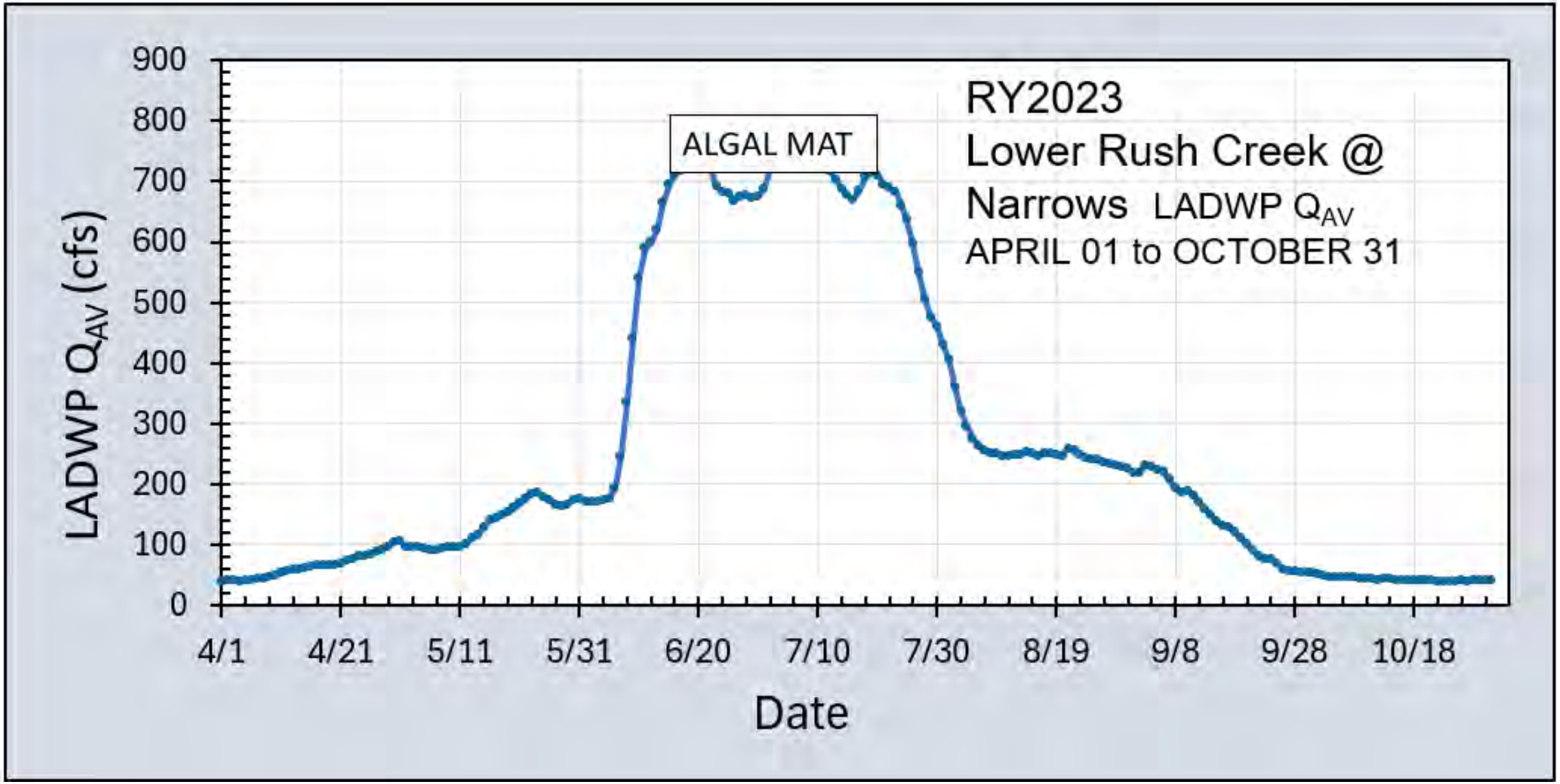

Figure 91. Lower Rush Creek RY2023 Hydrograph, with prolonged high streamflow lasting approximately two months forming distinctive algal mats in Central 4-Floodplain.

The grove is situated at an elevation higher than the standing water. As we walked across the ponded water (while admiring all the mountain lion tracks) and toward the grove, stranded stringers of algal mats indicated once-flowing water had turned downhill … toward the left. Walking even closer to the grove, there was evidence of another flowing water source emerging from the right. This would have been from the 4Bii Side-Channel that takes-in water from the very upstream tip of the 4-Foodplain, then ‘delivers’ the water down the spine of the 4-Floodplain as it breaks into several smaller distributary channels.

On October 14, 2023, we located a cleanly identifiable maximum algal mat elevation for QPK maximum stage. It did not reach the Yellow Willow Grove. Another 1.3 ft to 1.6 ft stage increase would be necessary to inundate the base of R5_26. Surface streamflow from the 4-Bii Side-Channel also did not inundate the base of R5_26; another 0.70 ft to 0.90 ft increase in stage would have been necessary.

We also wanted to track the fall in QPK stage going into mid-September through mid-October in the Riparian Zone of the 4-Floodplain (in the last two scheduled fieldtrips). While the base was not inundated, close proximity to receding streamflows and seepage water could still benefit Yellow Willow R5_26 vigor.

The photograph in Figure 92 was taken 14October2023, the day we went searching for QPK2023 flood lines. Note the dry ground surface everywhere. Another photograph on 14Sept2023 was taken near the 14October2023 photograph (Figure 93) that captured significant seepage throughout the riparian landscape. To help orient yourself, the label ‘LOG’ (in white) identifies the same log in Figures 92 and 93. The contribution of seepage to the shallow groundwater underlying the Yellow Willow Grove very likely is benefitting the willows.

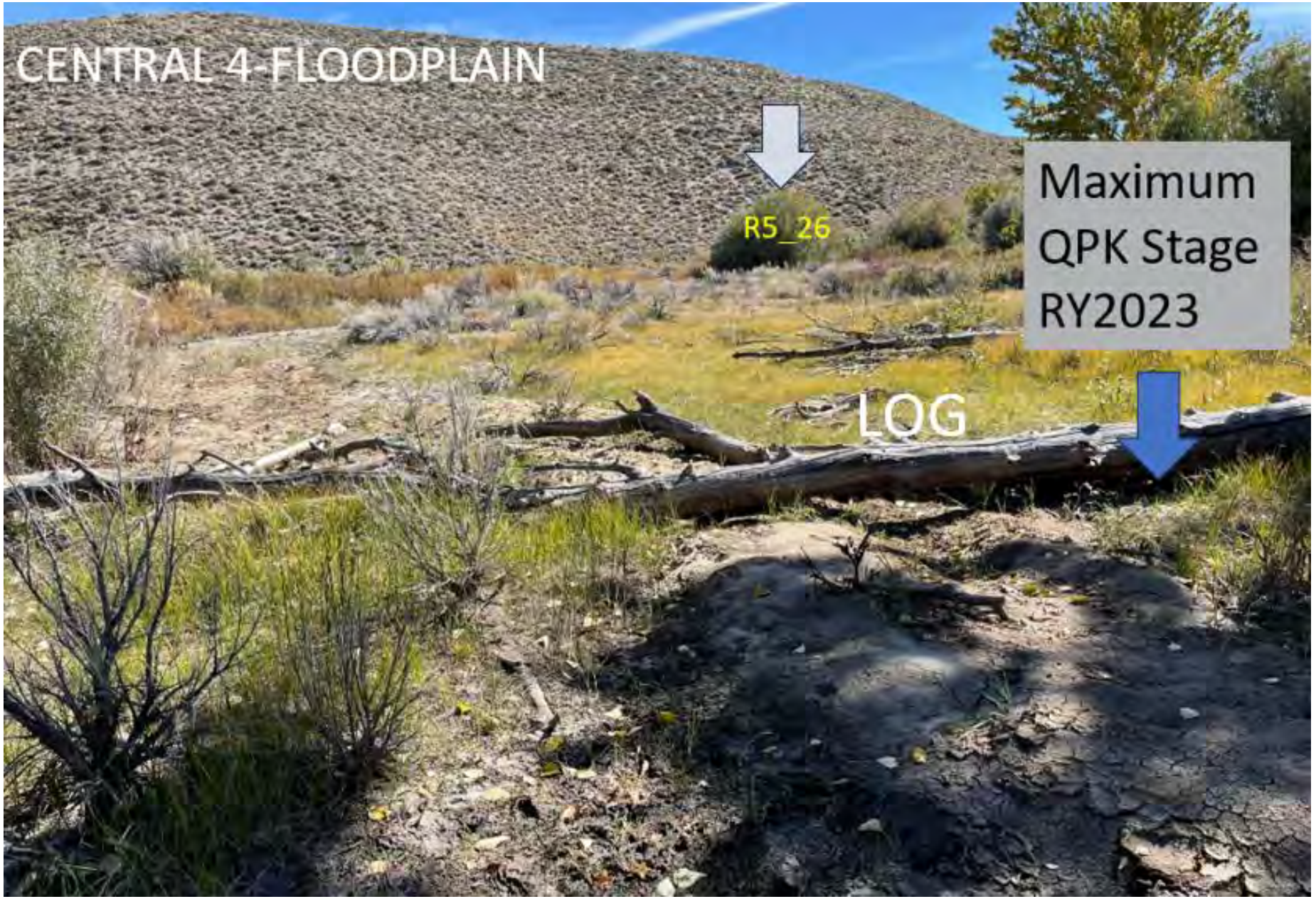

Figure 92. Yellow Willow R5_26 in Central 4-Floodplain 14October2023 1:57 PM.

The Q_{AV} on 14SEPT2023 was 148 cfs. If the 8 Side-Channel Inlet, was diverting a large proportion of the total mainstem streamflow, this Central 4-Floodplain Riparian Zone seems to be receiving adequate water (Figure 93). Going back to the 14OCT2023 photograph in Figure 92, the dry ground surface indicates inadequate water exposure. Q_{AV} was 44 cfs. But in our investigation, only an inadequate ~1.5 cfs of the 44 cfs was getting past the 8 Side-Channel Inlet. This could easily be impacting the Yellow Willow Grove.

Figure 93. LB of Central 4-Floodplain Riparian Zone on 14SEPT2023 9:26AM. Q_{AV} = 148 cfs. All seepage, no current.

Evaluate Yellow Willow R5_26 Vigor in RY2023 relative to previous RYs in the Central 4-Floodplain.

Only one yellow willow tree was measured in RY2023 to use as an example. However, R5_26 has been measured for vigor in four previous RYs under varying RY types. RY2023, with its abundant streamflow capable of thoroughly replenishing the shallow groundwater table, should encourage relatively high vigor (i.e., stem growth). Vigor was assessed using Annual Branch Increment (ABI): total branch length (mm) since last year's terminal bud scar. Refer to previous Mono Basin Stream Monitoring Reports RY2016,RY2017, and RY2018 for background information on ABI. The cumulative frequency distribution of R5_26's thirty ABI measurements (Figure 94) serves as its own baseline.

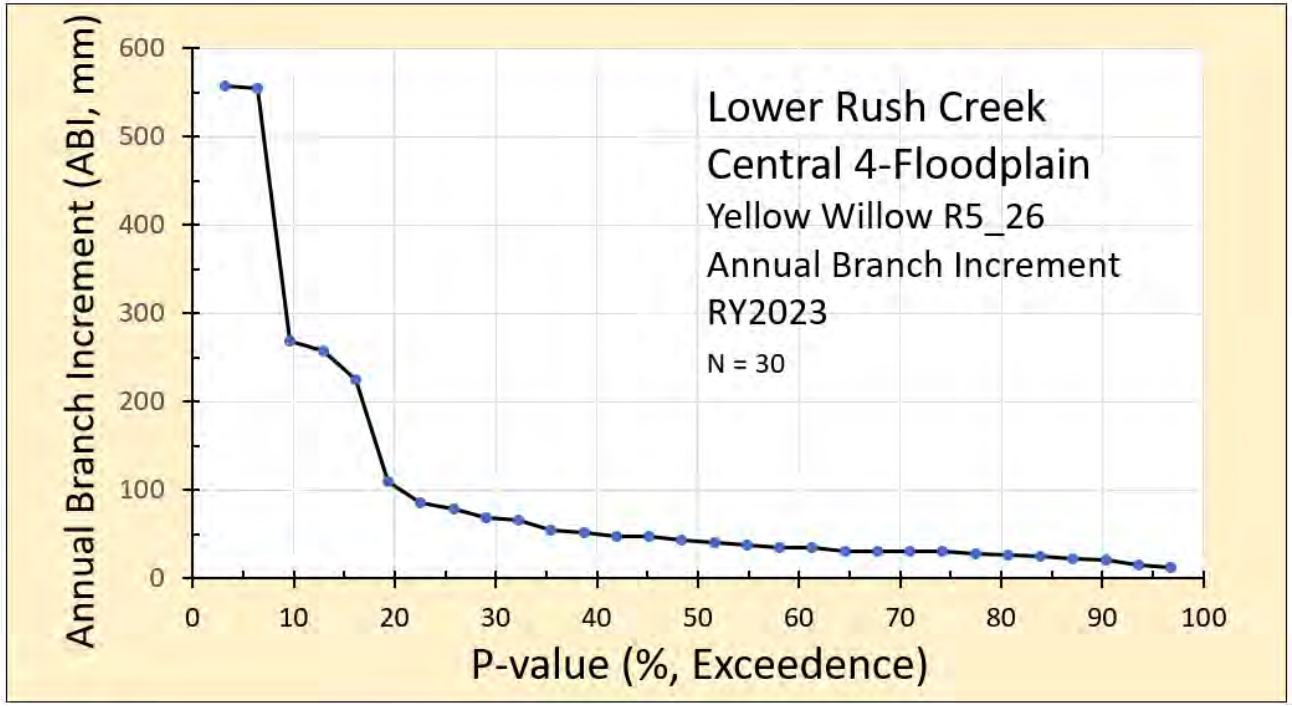

Figure 94. Annual branch Increment (ABI) exceedence curve for Yellow Willow R5_26 Central 4-Floodplain measured on 14October2023.

An exceedence curve is a simple analytical tool. At an exceedence of 20%, ABI equals 100 mm. This means: 20% of the ABIs measured had lengths of 100 mm or greater. The shape of this exceedence curve is very typical for Yellow Willows in Lower Rush Creek. There almost always are a few stems with very large ABI's. Generally, selecting these exceedence probabilities of 10%, 20%, 50%, 80%, and 90% for comparison among other years' ABIs seems to be a good strategy.

Yellow Willow R5_26 received special attention in RY2021, and that is why we focused on it in RY2023 (Figure 95). Text taken from RY2021 Mono Basin Stream Monitoring Report (with some minor editing): *The four ABI exceedence curves for Yellow Willow R5_26 were segregated into two general responses. RY2016 and RY2021 resulted in poor vigor and RY2017 and RY2018 resulted in considerably better vigor. Why the differences between RY2017/2018 and RY2016/2021? RY2016 was a dry-normal water year with a peak snowmelt release of 260+ cfs; in RY2021 peak release was 240+ cfs. Streamflow did not enter the 4-Side Channel in RY2021 and only barely entered in RY2016. R5_26 is located along the pathway of the 4-Side Channel as it passes through the center of the 4-Floodplain. In contrast, a peak flood of 900+ cfs in RY2017 provided ample, sustained flow in the side-channel. RY2018 had a peak flood release 450+ cfs providing significant side-channel flow.*

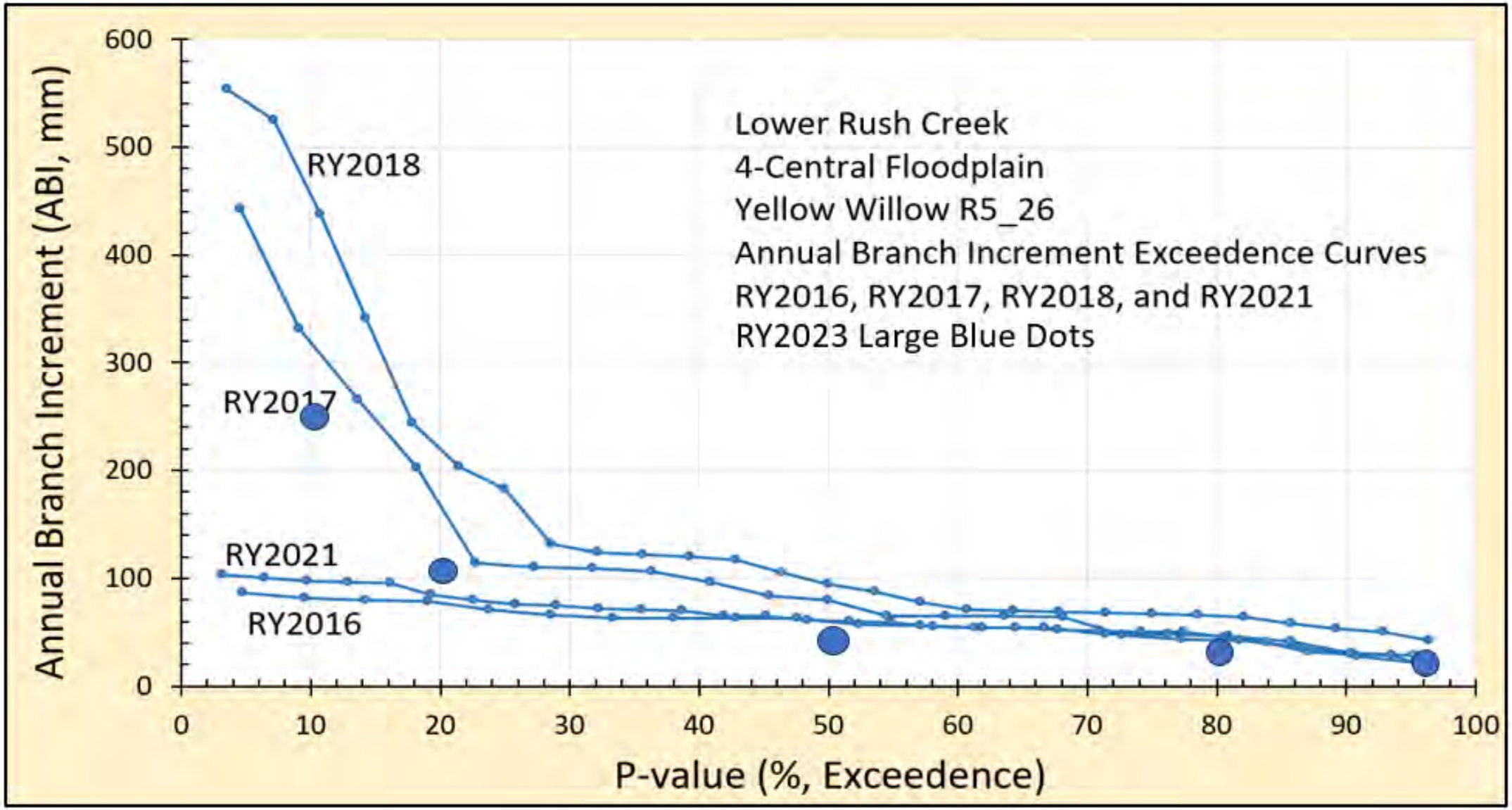

Figure 95. Annual branch Increment (ABI) exceedence curve for Yellow Willow R5_26 Central 4-Floodplain measured on 14October2023 and compared to previous ABI measurements in RY2016, RY2017, RY2018, and RY2021.

In summary, we determined that surface streamflows originating from the 4Bii Side-Channel and the mainstem channel did not inundate the base of Yellow Willow R5_26 in RY2023. Surface seepage water within the riparian zone was close to the Yellow Willow Grove September through mid-October. We expected vigor in RY2023 to exceed vigor in wet RY2017 and RY2018 (Figure 95). Vigor was better than the two drier RYs but did not outperform either wetter RY. But remember this was only one tree.

In previous RYs, ABI data were collected from many Black Cottonwood and Yellow Willow trees canvassing swaths of terraces and floodplains. Scientifically, this is a reasonable sampling strategy. But a sampling strategy that generates a story, around discrete groups of trees (i.e., groves), might achieve more awareness and improve our understanding. We plan on identifying several groves each with a unique story. The Yellow Willow Grove sampled in RY2023, and discussed here, is located on a higher Central 4-Floodplain surface. If excessive surface streamflow is being lost to the 8-Floodplain, this grove might become the ‘mine canary’ sending us a warning.

TASK No. 13. Resurvey Grand Old Cottonwood Cross-Section in RY2023 and Compare to the RY2021 Survey.

Grand Old Cottonwood Cross-Section represents the pre-1940's channel morphology of Lower Rush Creek. During fieldwork in RY2018, a hydraulic unit (HU) approximately 600 ft upstream of the 4Bii Side Channel Inlet to the 4-Floodplain was found to have maintained its pre-1941 channel morphology. A large, old growth cottonwood on the left bank (LB) was rooted at the historic bankfull channel elevation (Figure 96), with the trunk buried 0.8 ft deep in fine silty flood deposits. This cottonwood was just downstream of a dense, old-growth red willow stand also rooted on the same surface. Since 2018, the right trunk has broken off.

Figure 96. Grand Old Cottonwood cross-section August 25, 2021.

Figure 97. Standing on the Riffle Crest Thalweg and looking upstream at survey tape stretched between bank benchmarks.

Field Measurement Technique Note

When assessing downcutting, do not go to your cross-sections. Instead, measure channelbed elevations at the Riffle Crest Thalweg (RCT). Pools can scour or fill year-to-year, but this does not mean the channel is downcutting. Grand Old Cottonwood cross-section was placed near the downstream end of a deep pool, close to where the pool tail begins ramping upwards toward the pool's end (which is where the riffle crest is)(Figure 97).

Once finished surveying the cross-section, one of us wades down to the riffle crest to locate the RCT. The perpendicular distance from the cross-section tape (noting the tape station number) down to the RCT is measured. And last, we shoot-in, with the engineer's level, the channelbed elevation at the RCT. This allows us to return and measure the same spot whenever we choose.

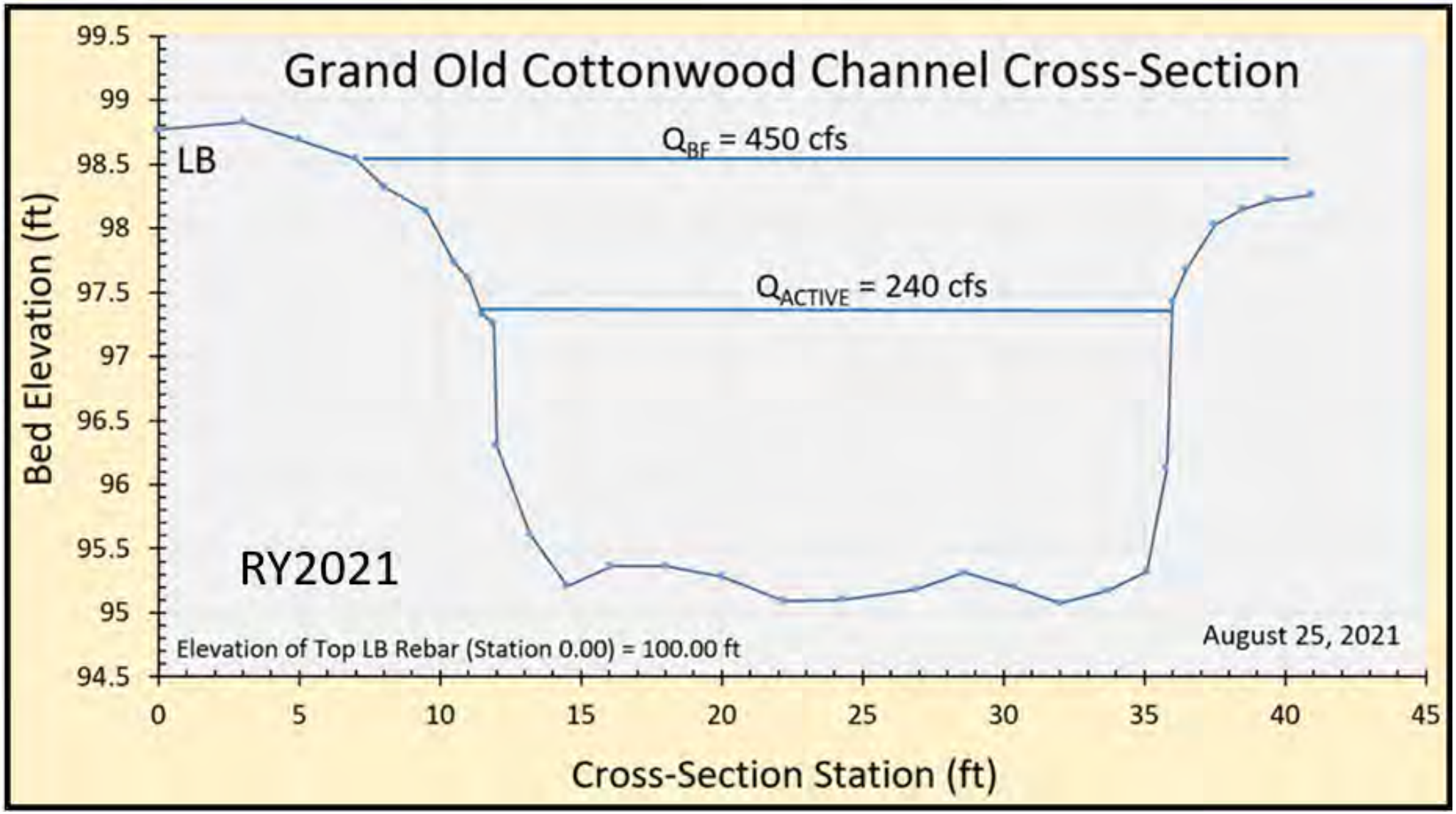

Figure 98. RY2021 Grand Old Cottonwood Cross-Section Survey 25August2021. Copied from Mono Basin Stream Monitoring Report RY2021.

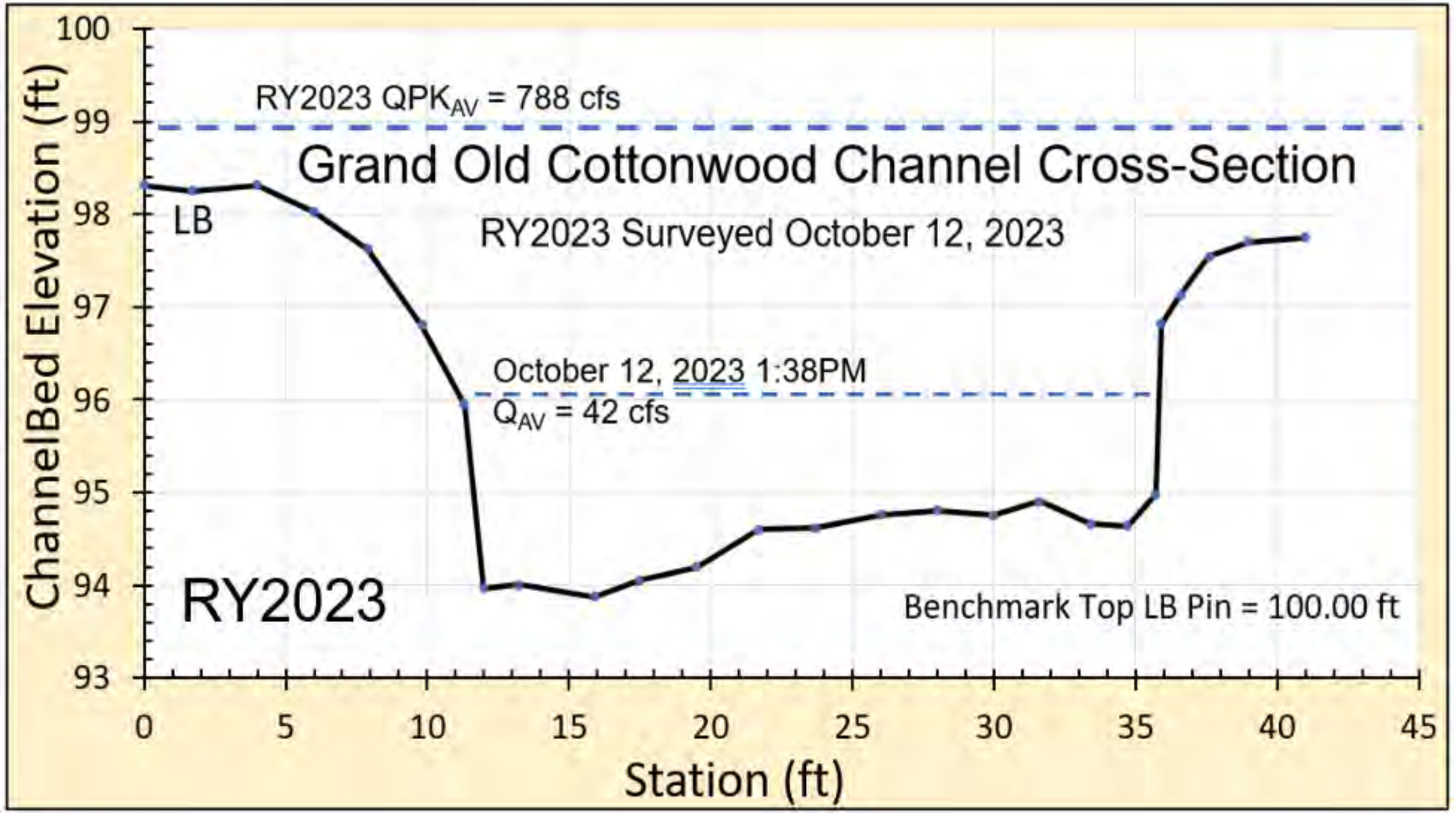

Figure 99. RY2023 Grand Old Cottonwood Channel Cross-Section surveyed October 12, 2023.

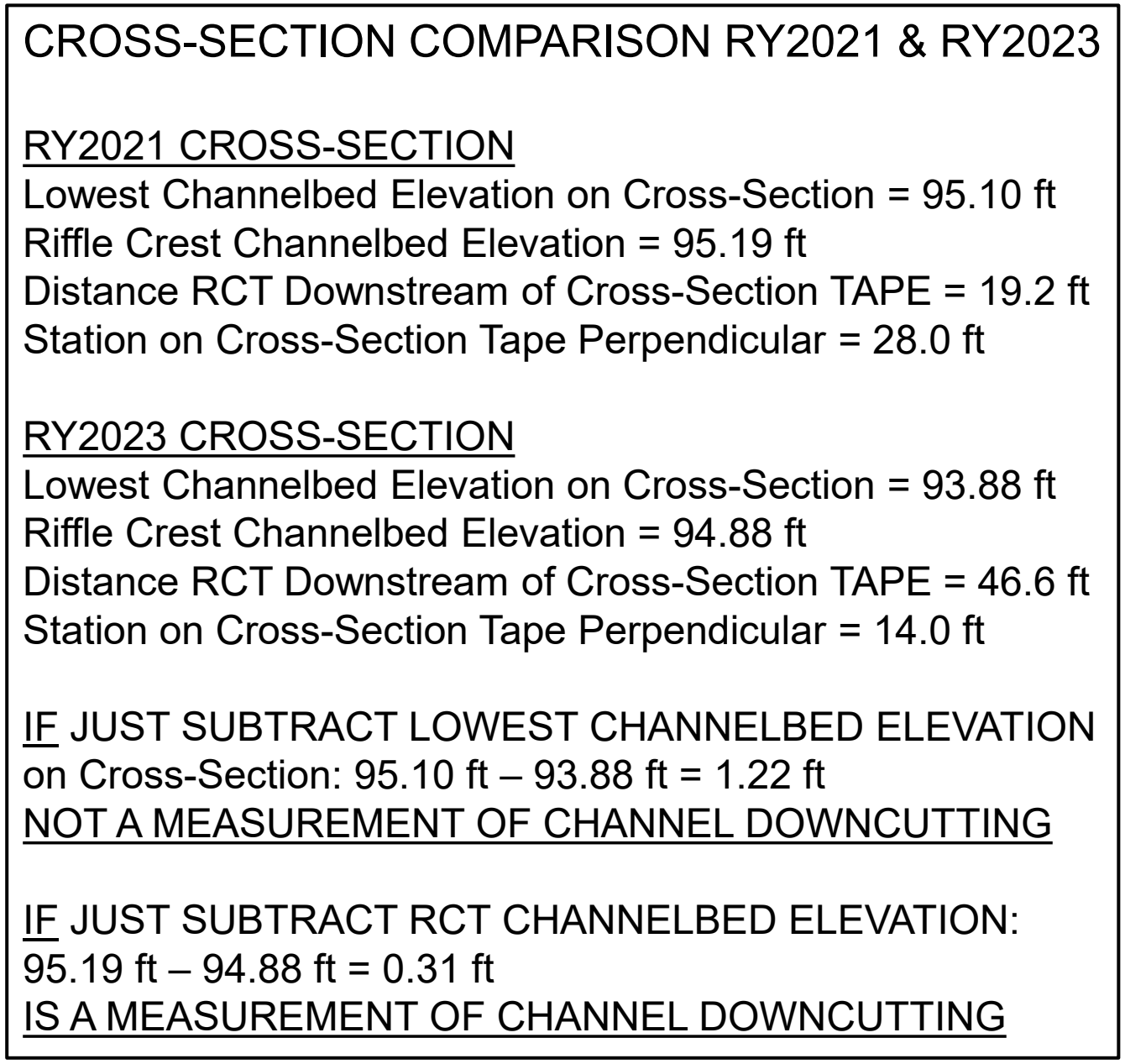

Figure 100. Comparison between RY2021 and RY2023 surveyed Grand Old Cottonwood Channel Cross-Sections.

Grand Old Cottonwood Channel Cross-Section RY2021 (Figure 98) had a minimum channelbed elevation of 95.10 ft and an RCT channelbed elevation of 95.19 ft that was 19.2 ft downstream of the cross-section. Grand Old Cottonwood Channel Cross-Section RY2023 (Figure 99) had a minimum channelbed elevation of 93.88 ft and an RCT channelbed elevation of 94.88 ft that was 46.6 ft downstream of the cross-section. Given the magnitude of the RY2023 QPK, there was only a minor difference in RCT channelbed elevation (95.19 ft RY2021 and 94.88 ft RY2023) of 0.31 ft. While this could be a real difference, and therefore evidence of mainstem channel downcutting, the measurement error involved in locating and measuring RCT channelbed elevation could easily be 0.15 ft. However, if we had relied on assessing mainstem downcutting using the minimum channelbed elevation on each cross section, we would be reporting downcutting of 1.22 ft (which would be false). We will be exploring how to use UAVs for monitoring accurate longitudinal stream profiles based on riffle crest bed elevations.

And last, note that the change in stage (Figure 101) between the baseflow on October 12 (Q_{AV} = 42 cfs on October 12, the date of surveying) and stage of RY2023 July 04 QPK was only 2.80 ft. Small changes in stage can have major consequences.

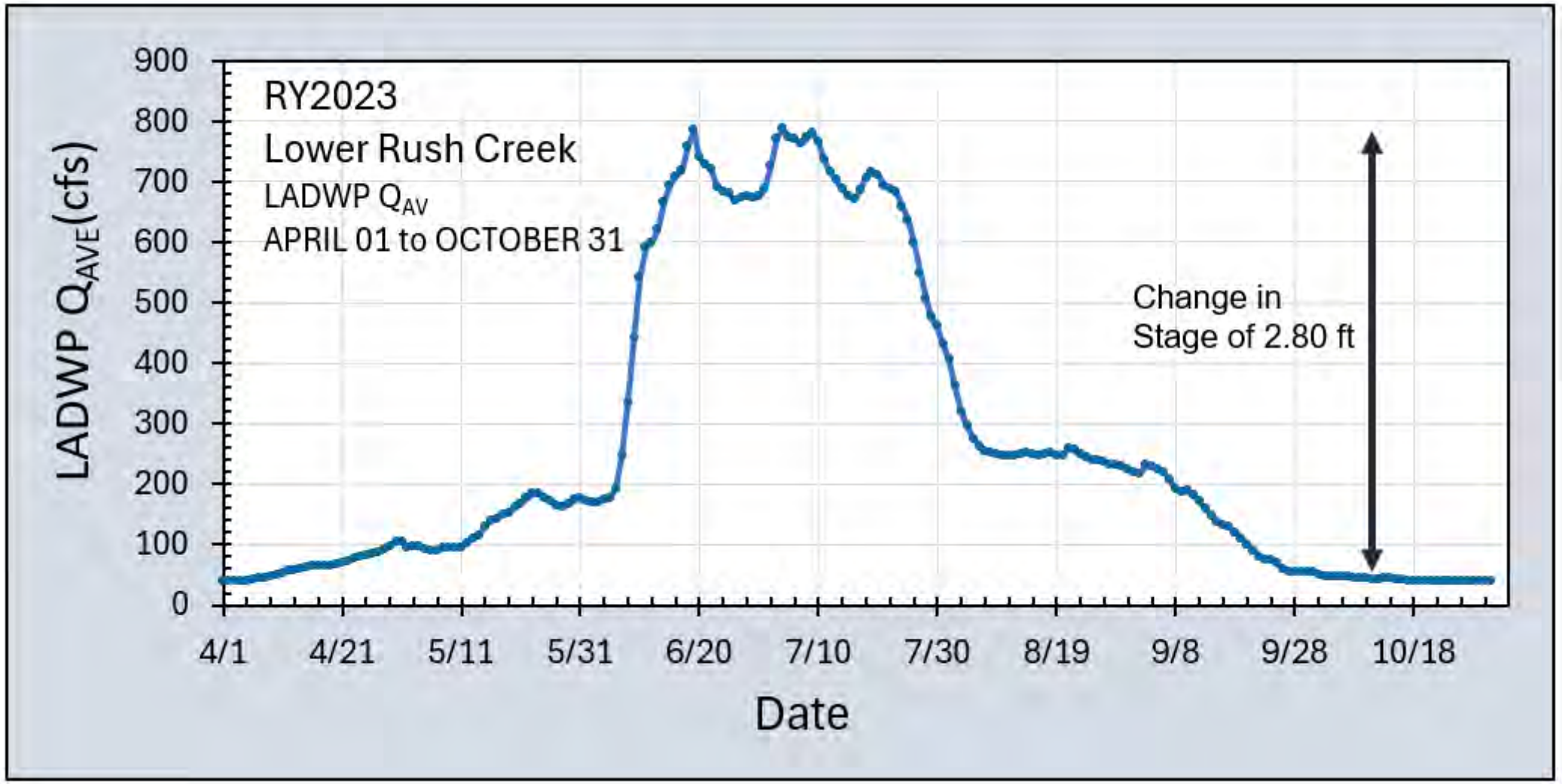

Figure 101. Change in overall stage on the RY2023 Grand Old Cottonwood Cross-Section over the full range of streamflows between 01April and October 31.

Knickpoint Cross-Section (Figure 102) was intentionally located within a very dynamic channel morphology we believed was actively downcutting. Mainstem Rush Creek is transitioning from a much narrower and steeper channel upstream to a much lower slope and wider channel downstream. However, even after one of the biggest QPK experienced, there was no change in Knickpoint Cross-Section (Figure 103). Again, the change in overall stage (from baseflow to QPK) was only 2.30 ft.

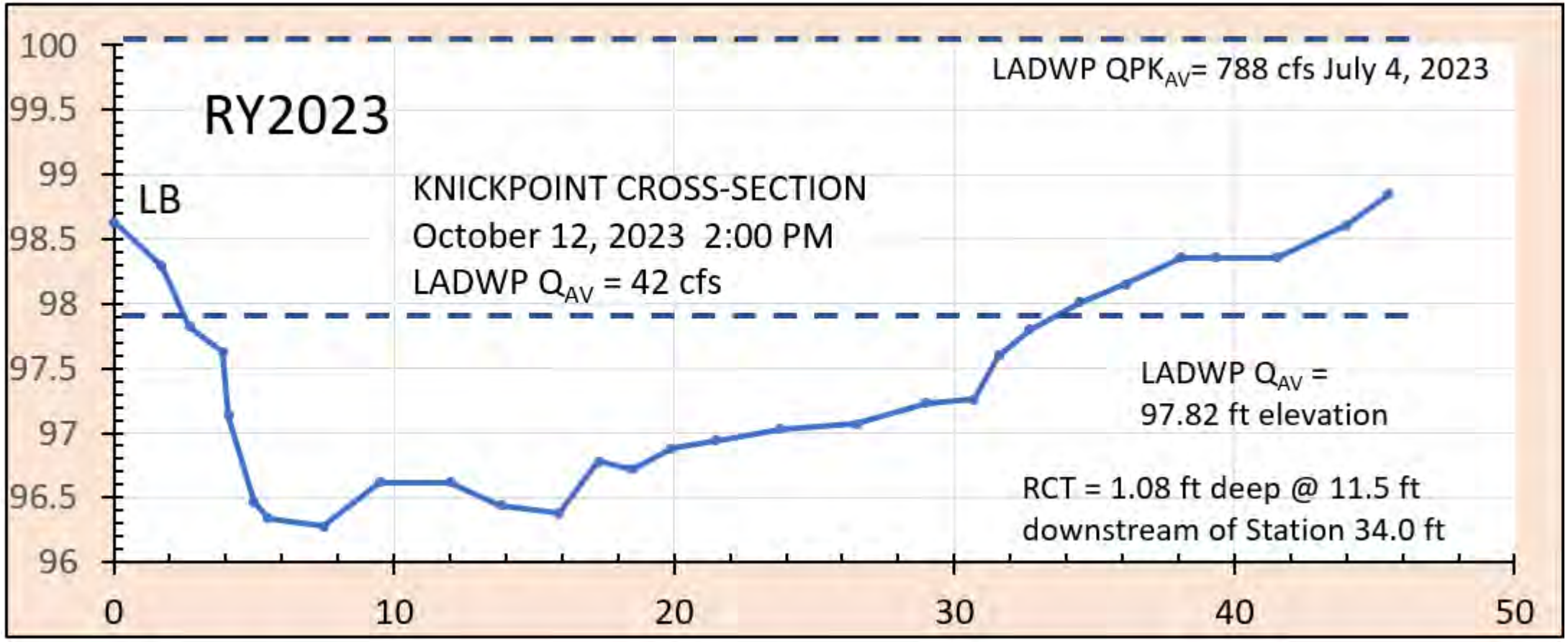

Figure 102. Knickpoint Cross-Section at Top of 4-Floodplain Surveyed 12October2023.

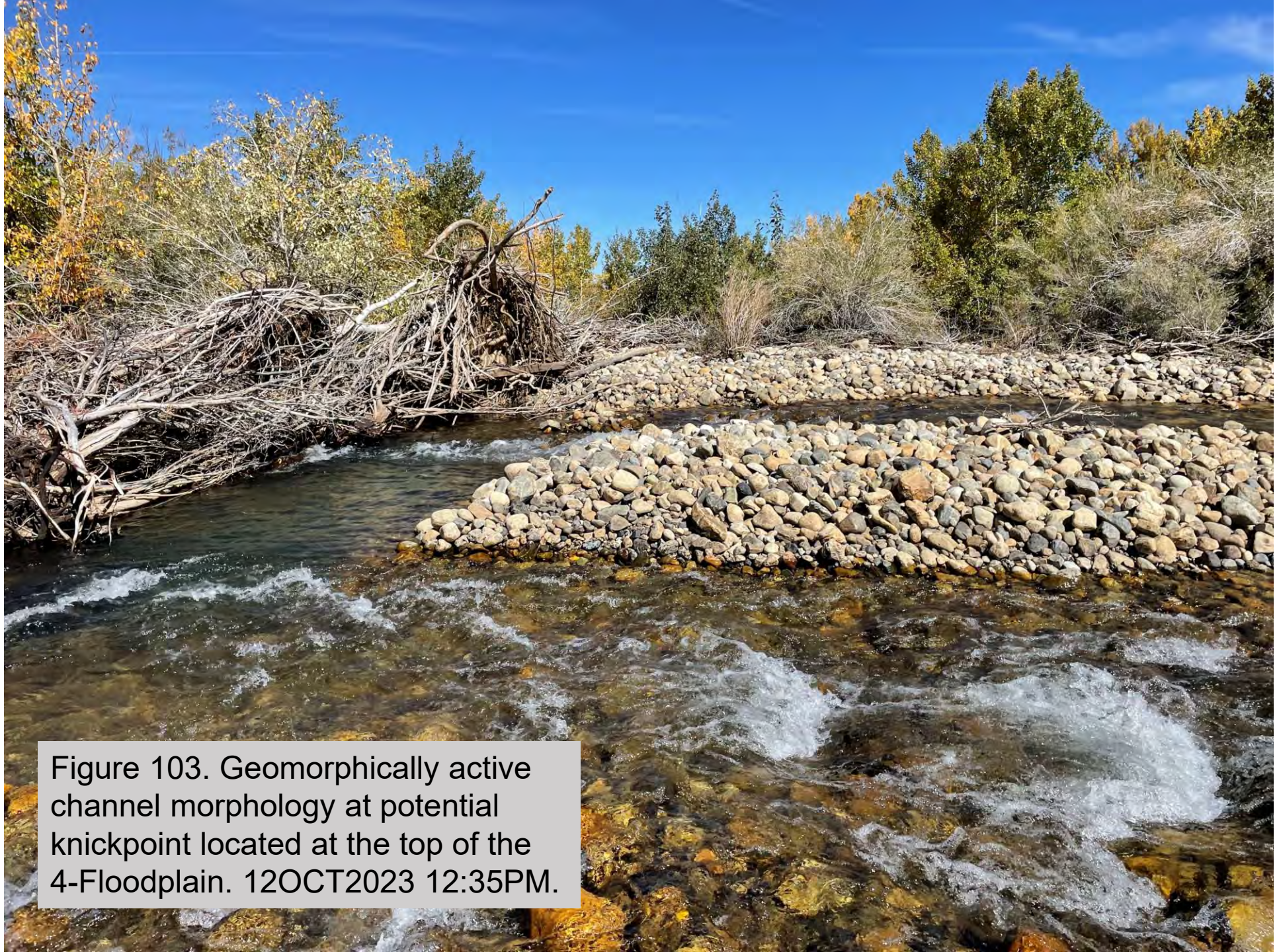

Figure 103. Geomorphically active channel morphology at potential knickpoint located at the top of the 4-Floodplain. 12OCT2023 12:35PM.

Task No.14. Inventory Cattail and Narrowleaf Willow Expansion Throughout the 8-Floodplain.

Conversion from Great Basin sagebrush (*Artemisia tridentata*) to wetland in the 8-Floodplain of Lower Rush Creek has been rapid. Recent events of mainstem snowmelt streamflows flowing into the 8-Floodplain in RY2017, and once again in RY2023, have created distinctive winners and losers. Primary losers have been Great Basin sagebrush and Jeffrey Pine. One primary winner has been the cattail (*Typha latifolia)*. Another has been Narrowleaf Willow (*Salix exigua*). Other biological interactions, triggered as a response to cattail expansion, may be underway. For example, red winged blackbirds are attracted to large cattail stands.

Figure 104. Distinctive winner (cattail) and loser (the dead Jeffrey Pine) within 8-Floodplain's rapidly evolving wetland since RY2017 (Photograph taken 27August2021).

Cattail is an obligate wetland species. Small cattail stands were first noted in RY2018, though there has been no systematic inventory. The RY2017 flood was the stimulus, when a relatively large percentage of extended mainstem flood flows was re-directed into the 8-Channel. Standing water, a clear nemesis to sagebrush, was highly favored by cattails throughout summer and early-fall of RY2017 (Figure 105). A story many would appreciate is a chronology of cattail stand expansion in the 8-Floodplain as one defining indicator of sagebrush displacement. Other biological interactions, triggered as a response to cattail expansion, may be underway. For example, red winged blackbirds are attracted to large cattail stands.

Figure 105. Expanding cattail stand in the 8-Floodplain near the solitary Jeffrey Pine on 15Sept2023 11:40AM.

Although cattail stands attract our attention, Narrowleaf willows are the fastest responding riparian species since RY2017. Almost every stream channel large and small throughout the 8-Floodplain now has dense Narrowleaf willows occupying both banks (Figure 106).

Figure 106. Small channels in the 8-Floodplain interior. 14SEPT2023 9:39AM with small debris jam. Q_{AV} = 148 cfs. Note flood peak of woody debris deposit on left bank.

Yellow Willow has been monitored for ABI (Annual Branch Increment) as an indicator of plant vigor since RY2016. Photographs were not always taken whenever ABI was measured. However, searching through stored photographs over the winter sometimes uncovers a reward. In Figure 107, there is a single cattail runner approximately 20 ft in front of Yellow Willow R4_05 in RY2021. We can readily locate this willow in the upcoming field season and hopefully find the cattail runner alive (and spreading!).

Figure 107. Yellow Willow R4_05 with a single cattail runner on 27August2021 11:27AM.

Black Cottonwoods had winners and losers as well. Cobble aggradation downstream of Rush Creek below the 8-Channel Entrance, caused by QPK 2017, shifted the mainstem channel toward the Central 4-Floodplain. This left many individual cottonwoods abruptly stranded in unfavorable micro-habitats. In Figure 108, Emily Cooper-Hertel is collecting ABI data (Annual Branch Increment) from a healthy, mature cottonwood now trapped in standing water following QPK 2017. Black Cottonwoods prefer their roots on top the water and not in prolonged standing water. To the left of Emily several cottonwood runners seem to be doing fine in RY2018. But by RY2021 this tree was clearly stressed, and in RY2023 was dead. In the RB bank foreground is the ever-present, recent outburst of Narrowleaf willows.

Figure 108. Emily Cooper-Hertel measuring Black Cottonwood ABI on mainstem Rush Creek downstream of 8 Side-Channel Inlet. 26SEPT2018.

Questions such as what is the minimum quantifiable cattail stand size in our UAV surveys will require investigating. Can cattail stand area be utilized as an indirect measure of standing/saturated water surface area? A systematic UAV survey in RY2024 would be timely. A UAV can be taken down to about 20 feet above a stand without the prop wash moving the plants around too much. Cattail images should be amazing. We will need to determine if there is a specific spectral signature for cattails. If they are the only thing that is as bright as the photographs show, finding a signature should be easy. This may apply to other obligate wetland plant species as well.

But here is the rub. Most of the streamflow entering the 8-Floodplain was not planned. The 8 Side-Channel, located at the very tip of the 8-Floodpain, was supposed to circulate some mainstem streamflow around the Black Cottonwood stand, also at the top of the 8-Floodplain, and then return the ‘borrowed’ streamflow back to the mainstem channel. There was no stated intention of re-watering the entire 8-Floodplain down to the 10-Falls as happened in RY2023.

With recent, greatly elevated mainstem streamflows entering Upper 8-Floodplain via the 8-Side-Channel, Narrowleaf Willow growth has physically dominated the transition from sagebrush to wetland (Figure 109).

Figure 109. Upper Caddis Channel in 8-Flooplain 14Sept2023 8:40AM. Q_{AV} = 148 cfs. Robbie Di Paolo Photograph.

Figure 110. Upper 8-Floodplain electrofishing crew in very recent Narrowleaf Willow canopy. 09October2023 11:41AM.

In Summary:

A story many would appreciate is a quantitative chronology of ongoing cattail stand and Narrowleaf Willow expansion in the 8-Floodplain as defining indicators of Great Basin sagebrush displacement (Figure 110). The RY2017 flood was the initial stimulus, when a relatively large percentage of extended mainstem flood flows was re-directed into the 8-Channel. Standing water, a clear nemesis to sagebrush, was highly favored by cattails throughout summer and early-fall beginning in RY2017. While our metric for cattail expansion will be stand number and area, we have not settled-on a metric for Narrowleaf Willow expansion.

We are considering UAV Surveys the best tool for tracking cattail and Narrowleaf willow expansion, as well for Riparian Zones in the 4-Floodplain. But we must remember that supplying the 8-Floodplain with considerably more mainstem streamflow was unplanned. This will challenge how we manage capacity for self-renewal in the near future.

Task No.15. Reserve One Morning for Reconnaissance of Lower Cottonwood Creek.

Robbie Di Paolo and I hiked lower Cottonwood Creek on the morning of October 14, 2023 as our final day of RY2023 fieldwork. Its mainstem channel, dominated by Black Cottonwood groves, is undergoing significant adjustment based on the abundance of small, active 0.5 to 1.5 ft headcuts everywhere along the mainstem channel and side-channels (Figure 111). One however was 2.5 ft to 3.0 ft high approximately 800 yds upstream from the road crossing (Figure112). We began by taking individual headcut coordinates, but soon conceded a different strategy was warranted. We will schedule a UAV survey of Lower Cottonwood Creek for the RY2024 field season, focusing on its developing floodplains (Figure 113).

Figure 111. Downcutting in a Mill Creek Side-Channel 14October2023 9:40AM.

Figure 112. Primary Cottonwood Creek head-cut 14OCT2023 10:22AM.

Figure 113. Lower Cottonwood Creek alluvial, highly mobile, gravel/cobble floodplain. 14Oct2023 10:07AM.

Task Priority for RY2024

The most pressing issue will be significantly improving our understanding of how the 8 Side-Channel Inlet diverts mainstem streamflow. This will require a better understanding of the hydraulics involved. Wetland Pond and the Old Growth Yellow Willow Grove in Lower 4-Floodplain will likely be stressed again in RY2024 given the poor outcome in October2023. Managing the 8 Side-Channel to prevent excessive diversion (down the 8 Side-Channel) will be manipulating capacity-for-self-renewal. The 8-Floodplain can tolerate reduced mainstem streamflows, but the question will be by how much. This will also mean that we should better connect the hydrograph to the 4-Floodplain Riparian Zone surface streamflows and seepage flows. The big positive response of brown trout occupying the Caddis Channel's mainstem and smaller channels in the 8-Floodplain will not make any decision-making simple.

Section III. Mono Lake Limnological Monitoring 2023 Annual Report

Prepared by Robert Jellison, Caroline Vignardi, and John M. Melack

2023 Annual Report

Mono Lake Limnological Monitoring

Robert Jellison, Caroline Vignardi, and John M. Melack

Earth Research Institute

University of California

Santa Barbara, CA 93106

Submitted to:

Los Angeles Department of Water and Power

31 March 2024

TABLE OF CONTENTS

LIST OF TABLES iii

LIST OF FIGURES v

CHAPTER 1 INTRODUCTION 1
Overview 1
Background 2
Acknowledgments 3

CHAPTER 2 METHODS 4
Meteorology 4
Sampling Regime 4
Field Procedures 5
In Situ Profiles *5*
Water Samples *7*
Artemia Samples *7*
Laboratory Procedures 8
Water Samples *8*
Artemia Samples *9*

CHAPTER 3 RESULTS AND DISCUSSION 10
Surface Elevation 10
Meteorological Data 10
Wind Speed and Direction *11*
Air Temperature *12*
Incident Photosynthetically Available Radiation (PAR) *14*
Relative Humidity and Precipitation *14*
Lake Temperatures 16
Seasonal Water Temperatures at Station 6 23
Specific Conductance 28
Density Stratification: Thermal and Chemical 37
Transparency and Light Attenuation 38
Dissolved Oxygen 39
Fluorescence 42
Nutrients (ammonium) 47
Phytoplankton 49
Artemia Population Dynamics 52
Hatching of Over-wintering Cysts and Maturation of the 1st Generation *52*
Ovoviviparous Reproduction and the Second Generation *60*
Artemia Biomass *67*

CHAPTER 4 EVALUATION OF MONITORING METHODS, 2012–2022 68
Conductivity, Temperature, and Depth Data 68
Ammonium 68
Chlorophyll 72

CHAPTER 5 SEASONAL, ANNUAL, AND LONG-TERM TRENDS 77
Introduction 77
Density Stratification and Meromictic Episodes 77

Long-term Trends in *Artemia* 81
Artemia Mean Annual Abundance, 1979–2023 ..... *81*
Effects of Meromixis on Seasonal Mean Adult Artemia Abundance *90*
Naupliar and Cyst Production *93*
Transparency *100*
Summary 102

REFERENCES **105**

LIST OF TABLES

Table 1. Temperature (°C) at Station 6, April–December 2023. 27
Table 2. Specific conductance (mS cm^{-1} at 25ºC) at Station 6, April–December 2023.....36
Table 3. Secchi depths (m), April–December 2023.....38
Table 4. Dissolved oxygen (mg L^{-1}) at Station 6, April–December 2023. 42
Table 5. Ammonium (µM) profiles at Station 6, May–December 2023.....47
Table 6. Ammonium (µM) lakewide at 7 stations in upper 9 m of water column, April–December 2023. 48
Table 7. Chlorophyll *a* (µg L^{-1}) at Station 6, May–December 2023.....50
Table 8. Chlorophyll *a* (µg L^{-1}) at 7 stations in upper 9 m of water column, April–December 2023. 51
Table 9. Mean *Artemia* lakewide and sector abundances (m^{-2}), April–December 2023. ..53
Table 10. Standard errors of *Artemia* lakewide and sector means (Table 9), April–December 2023. 54
Table 11. Percentage in different classes for *Artemia* lakewide and sector means (Table 9), April–December 2023. 55
Table 12. Mean *Artemia* lakewide and sector instar analysis, April–December 2023. 57
Table 13. Standard errors of *Artemia* lakewide and sector instar analysis (Table 12), April–December 2023.....58
Table 14. Lakewide and sector percentage (given as percentage of total shrimp) in different classes for *Artemia* instar analysis (Table 12), April–December 2023...59
Table 15. Mean *Artemia* lakewide and sector reproductive summary, April–December 2023.....62
Table 16. Standard errors of *Artemia* lakewide and sector reproductive summary (Table 15), April–December 2023. 63
Table 17. *Artemia* lakewide and sector reproductive summary percentages (Table 15), April–December 2023.....64
Table 18. *Artemia* fecundity summary, June–December 2023.....66
Table 19. *Artemia* biomass (g dry weight m^{-2}) summary, July–December 2023. 67

Table 20. Comparison of ammonium (µM) profiles at Station 6, July–November 2023, University of California Davis Analytical Lab versus University of California Santa Barbara. 70
Table 21. Comparison of chlorophyll *a* (µg L^{-1}) at Station 6 in upper 9 m of water column, May– November 2023. University of Maryland Center for Environmental Science versus University of California Santa Barbara. 74
Table 22. Meromictic episodes. 79
Table 23. Mean annual adult *Artemia* abundance (1 May–30 November) and centroid of distribution, 1979–2023. 82
Table 24. Seasonal mean abundance of *Artemia* versus mixing status....91
Table 25. Annual nauplii and cyst production, 1983–2023. 94

LIST OF FIGURES

Fig. 1. Sampling stations on Mono Lake. 5
Fig. 2. Mono Lake surface elevation (ft asl, USGS datum).....10
Fig. 3. Hourly mean wind speed (m s^{-1}).....11
Fig. 4. Wind rose (hourly mean direction and speed), 30 May–31 December 2023. 12
Fig. 5. Paoha Island versus Lee Vining air temperatures (°C). 13
Fig. 6. Hourly mean air temperatures (°C) at Lee Vining and Paoha Island. 13
Fig. 7. Daily photosynthetically available radiation, 2023. 14
Fig. 8. Mean daily relative humidity (%), 2023.....15
Fig. 9. Daily precipitation (mm). 16
Fig. 10. Lake temperatures (ºC), 30 April 2023.....17
Fig. 11. Lake temperatures (ºC), 19 May 2023.....18
Fig. 12. Lake temperatures (ºC), 13 June 2023.....19
Fig. 13. Lake temperatures (ºC), 12 July 2023. 19
Fig. 14. Lake temperatures (ºC), 17 August 2023. 20
Fig. 15. Lake temperatures (ºC), 18 September 2023.....21
Fig. 16. Lake temperatures (ºC), 12 October 2023. 21
Fig. 17. Lake temperatures (ºC), 14 November 2023. 22
Fig. 18. Lake temperatures (ºC), 12 December 2023.....22
Fig. 19. Seasonal water temperatures at Station 6. 25
Fig. 20. Temperature (ºC) at Station 6, 2023. 25
Fig. 21. Time-depth plot of isotherms (°C) at Station 6 from 1 June 2023 to 14 October 2023.....26
Fig. 22. Specific conductance (mS cm^{-1}), 30 April 2023.....28
Fig. 23. Specific conductance (mS cm^{-1}), 19 May 2023.....29
Fig. 24. Specific conductance (mS cm^{-1}), 13 June 2023.....30
Fig. 25. Specific conductance (mS cm^{-1}), 12 July 2023. 31
Fig. 26. Specific conductance (mS cm^{-1}), 17 August 2023. 32
Fig. 27. Specific conductance (mS cm^{-1}), 18 September 2023.....32
Fig. 28. Specific conductance (mS cm^{-1}), 12 October 2023. 33

Fig. 29. Specific conductance (mS cm^{-1}), 14 November 2023. 34
Fig. 30. Specific conductance (mS cm^{-1}), 12 December 2023.....34
Fig. 31. Seasonal specific conductance at Station 6. 35
Fig. 32. Specific conductance (mS cm^{-1} at 25 ºC) at Station 6, 2023. 35
Fig. 33. Density stratification between 2 and 32 m, 2023. 37
Fig. 34. PAR light attenuation (fraction of surface) at Station 6, 2023. 39
Fig. 35. Seasonal dissolved oxygen at Station 6, 2023. 40
Fig. 36. Dissolved oxygen (mg L^{-1}) at Station 6, 2023. 41
Fig. 37. Seasonal fluorescence profiles at Station 6, 2023. 43
Fig. 38. Temperature, specific conductance, dissolved oxygen, and fluorescence at Station 6, 12 July 2023.....44
Fig. 39. Temperature, specific conductance, dissolved oxygen, and fluorescence at Station 6, 17 August 2023.....44
Fig. 40. Temperature, specific conductance, dissolved oxygen, and fluorescence at Station 6, 18 September 2023. 45
Fig. 41. Temperature, specific conductance, dissolved oxygen, and fluorescence at Station 6, 12 October 2023. 45
Fig. 42. Temperature, specific conductance, dissolved oxygen, and fluorescence at Station 6, 14 November 2023. 46
Fig. 43. Temperature, specific conductance, dissolved oxygen, and fluorescence at Station 6,12 December 2023. 46
Fig. 44. Ammonium at Station 6, 2023. 48
Fig. 45. Ammonium (µM) in upper 9 m of the water column at 7 stations, 2023. 49
Fig. 46. Chlorophyll *a* (µg L^{-1}) at Station 6, May–December, 2023. 50
Fig. 47. Chlorophyll *a* (µg L^{-1}) in upper 9 m of the water column at 7 stations, 2023. 51
Fig. 48. Lakewide *Artemia* abundance during 2023: nauplii (instars 1-7), juveniles (instars 8-11), and adults (instars 12+). 60
Fig. 49. Reproductive characteristics of *Artemia* during 2023. 65
Fig. 50. Regression analysis of ammonium concentrations measured by UCSB on day of collection and UCDAL after storage. 71

Fig. 51. Residual analysis (in µM) depicting the temporal variation in ammonium concentrations (µM) for UCDAL and UCSB. 71
Fig. 52. Stability trends over time: Bland-Altman comparison of samples analyzed on the day of collection vs. stored ammonium samples. 72
Fig. 53. Regression analysis of chlorophyll *a* concentrations (µg L^{-1}) measured by UCSB within 10 days of collection and by UMCES after long-term storage. 74
Fig. 54. Residual analysis (in µg L^{-1}) depicting the temporal variation in chlorophyll *a* concentration (µg L^{-1}) for UMCES and UCSB. 75
Fig. 55. Relationship between chlorophyll *a* and transparency (Secchi depth) for all 9-meter integrated samples....76
Fig. 56. Relationship between chlorophyll *a* and transparency (Secchi depth) for LADWP data sampled from January to June and from July to December. 76
Fig. 57. Density stratification between 2 and 32 m at Station 6, 1983–2023. 78
Fig. 58. Surface elevation and meromictic episodes at Mono Lake. 80
Fig. 59. Yearly change in surface elevation (ft asl). 80
Fig. 60. Historic (1912–present) surface elevations of Mono Lake (ft asl). 81
Fig. 61. Summary statistics of the seasonal (1 May through 30 November) lakewide abundance of adult *Artemia*, 1979–2023. 83
Fig. 62. Long-term trend in mean seasonal adult *Artemia* abundance, 1979–2023....84
Fig. 63. STL decomposition of adult *Artemia* abundance, 1983–2023. 85
Fig. 64. Long-term trend of adult *Artemia* with seasonal component removed. 86
Fig. 65. STL decomposition of *Artemia* biomass, 2000–2023. 87
Fig. 66. Long-term trend of *Artemia* biomass with seasonal component removed. 88
Fig. 67. Adult *Artemia* abundance, 1982–2023. 89
Fig. 68. Abundance-weighted centroid of adult *Artemia*, 1979–2023. 90
Fig. 69. Mean spring (April–May) lakewide abundance of adult *Artemia* during different mixing regimes....92
Fig. 70. Long-term variation in annual cyst and nauplii production, 1983–2023. 93
Fig. 71. Trend line of lakewide temperature at 2 m with seasonal component removed, 1983–2023....96
Fig. 72. Long-term variation in abundance-weighted fecundity, 1983–2023....97

Fig. 73. Long-term variation in abundance-weighted adult female length, 1983–2023....98
Fig. 74. Mean adult female weighted fecundity versus summer (1 June– 30 September) mean lakewide conductivity at 2 m depth.....99
Fig. 75. Mean adult female weighted length versus summer (1 June– 30 September) mean lakewide conductivity at 2 m depth. 99
Fig. 76. Long-term changes in transparency (Secchi depth) and surface elevation. 101
Fig. 77. Long-term changes in transparency and adult *Artemia* abundance. 102

CHAPTER 1
INTRODUCTION

Overview

Saline lakes are widely recognized as productive aquatic habitats, that harbor distinctive assemblages of species, and often support large populations of resident or migratory birds. Saline lakes throughout the world are threatened by decreasing size and increasing salinity due to climate changes and diversions of freshwater inflows for irrigation and other human uses. At Mono Lake, California, diversions of freshwater streams out of the basin beginning in 1941 has led to a decline in surface elevation and an approximate doubling of the lake's salinity. In 1994, the State Water Resources Control Board (SWRCB) of California issued a decision to amend Los Angeles' water rights (Decision 1631) by restricting water diversions until the surface elevation of the lake reached 1,948 m (6392 ft).

Long-term monitoring of the plankton and their physical, chemical, and biological environment is essential to understanding the effects of changing lake levels and salinities and has been mandated by the SWRCB. Measurements of the vertical distribution of temperature, dissolved oxygen, conductivity, and nutrients are requisite for interpreting how variations in these variables affect the plankton populations. The limnological monitoring program at Mono Lake includes the collection and interpretation of limnological data.

This report fulfills the requirements for limnological monitoring of Mono Lake set forth in State Water Resources Control Board Order Nos. 98-05 and 98-07. The limnological monitoring program consists of four components: meteorological, physical and chemical, phytoplankton, and brine shrimp populations. Meteorological data are collected with sensors on Paoha Island, while the other three components are assessed during monthly surveys (except when the lake is inaccessible in winter). The methodology employed is detailed in Chapter 2, results and discussion of the data obtained during 2023 are presented in Chapter 3, methodological comparisons with

monitoring conducted from 2012 to 2022 by LADWP are provided in Chapter 4, and long-term integrative trends and variation are presented in Chapter 5.

Background

Limnological and related environmental conditions in Mono Lake are reviewed in Melack et al. (2017) and summarized here.

Mono Lake (38°N, 119°W) lies in a hydrologically closed basin on the western edge of the North American Great Basin below the eastern slope of the Sierra Nevada. Most precipitation falls as snow on the western side of the basin and during snowmelt flows into the lake. Groundwater enters the lake via springs and seepage. Annual evaporation from the lake is estimated to be equivalent to about 1 m of water. Daily air temperatures range from around -11°C in winter to a maximum of around 24°C in summer.

Mono Lake is hypersaline, and, as the lake level declined from 1940 to 1980, the lake's salinity increased from 48 g kg^{-1} to 87 g kg^{-1}. During the period from 1991 through 2023 mean salinity at 2 m ranged from 69 to 91 g kg^{-1}. Sodium is the major cation and carbonate, chloride, and sulphate are the major anions. The high salinity and particular chemical composition result in distinct physical properties of the lake water, e.g., density increases as a monotonic function of temperature decrease to below 0°C.

Vertical stratification and mixing alternate between periods with stratification continuing for several years (meromictic conditions) and periods when the lake mixes thoroughly during winter (monomictic conditions). The quantity of freshwater introduced during snowmelt from the Sierra Nevada and the proportion diverted to the City of Los Angeles determine the occurrence and persistence of these two states. Concentrations of soluble reactive phosphorus are high, and inorganic nitrogen can limit algal growth. Two major sources of recycled ammonium are brine shrimp excretion and vertical mixing of ammonium-rich deep water. Mixing in winter is, therefore, a key factor in controlling nutrient supply to the upper water column.

Few species of phytoplankton occur in the lake, and the unicellular green alga, *Picocystis* sp. accounts for most of the algal biomass, as indicated by chlorophyll

concentrations. Cyanobacteria and bacillarophytes also occur. Strong redox gradients associated with vertical stratification result in stratified microbial communities, aerobic and anaerobic methane oxidation, and dissimilatory sulphate reduction.

The phytoplankton usually have large seasonal variations in abundance with maxima in early spring, low values from late spring to late summer as a result of grazing by *Artemia monica,* and increased abundances in autumn and winter as *Artemia* grazing declines. The brine shrimp (*Artemia monica*) is the dominant and often sole species of zooplankton in the pelagic waters. *Artemia* hatch in late winter and spring from cysts; a second, summer generation is produced ovoviviparously. In autumn, the *Artemia* population declines, because of predation by migratory grebes, decreasing water temperature and senescence. In near-shore habitats, the alkali fly (*Ephydra hians*) is abundant seasonally.

The brine shrimp and alkali fly larvae provide food for large numbers of birds including a breeding colony of the California gull (*Larus Californicus*) and migratory eared grebes (*Podiceps nigricollis*), Wilson's phalaropes (*Phalaropus tricolor)* and red-necked phalaropes (*Phalaropus lobatus*). No fish occur in the lake. The grebes depend on the abundant *Artemia* during autumn when they molt and increase their body weight before continuing their southward migration late in the year.

Acknowledgments

This work was supported by a contract from the National Fish and Wildlife Foundation with funds from the Los Angeles Department of Water and Power (LADWP) to J. M. Melack at the Earth Research Institute, University of California, Santa Barbara. Laboratory work was performed at the Sierra Nevada Aquatic Research Laboratory, University of California. To facilitate analysis of long-term trends, LADWP provided the limnological monitoring data documented and discussed in their annual compliance reports to the State Water Resources Control Board (LADWP 2014–2023).

CHAPTER 2
METHODS

Meteorology

Meteorological measurements are recorded at a station located on the southwestern shore of Paoha Island at 1948 m elevation (Fig. 1), approximately 2 meters above the current elevation of the lake. The data were logged as 5-minute readings and stored on an Onset RX3004 logger; data are uploaded to HOBOlink web-based software at cellular connection intervals of 1 hour. The meteorological station was installed on 30 May 2023; the air temperature/relative humidity sensor malfunctioned for a portion of the summer.

Wind speed and direction are measured at a height of 3 m above the surface of the island with an R.M. Young wind monitor (model 5103 with threshold of 1 m s^{-1} for propeller and 1.1 m s^{-1} for vane and accuracy of ±0.3 m s^{-1} or 1% of reading, and ±3° for wind direction). Mean wind speed and direction and maximum wind speed during each five-minute interval are recorded. Additional measurements include photosynthetically available radiation (PAR, spectral range 400 to 700 nm, Onset sensor S-LIA-M003 with a resolution of 2.5 μmol m^{-2} s^{-1} and accuracy of ±5 μmol m^{-2} s^{-1}), solar radiation (spectral range 300 to 1100 nm, Onset sensor S-LIB-M003 with resolution of 1.25 W m^{-2} and accuracy of ±10 W m^{-2} or ±5%, if greater), barometric pressure (Onset sensor S-BPM-CM50 with resolution of 0.01 mbar and accuracy of ±3.0 mbar), and relative humidity (RH) and air temperature (Onset sensor S-THC with a resolution of 0.02°C and of 0.01% for RH, and accuracy of ±0.25°C and ±2.5% from 10% to 90% RH or ±5% below 10% and above 90% RH). Rainfall rates and cumulative amounts are obtained with an unheated tipping bucket gauge (Onset sensor S-RGB-M002 with a resolution of 0.2 mm, and 1% accuracy for rainfall rates up to 12.7 cm h^{-1}).

Sampling Regime

The limnological monitoring program in 2023 included monthly surveys from April through December. Exceptional snowfall delayed access to the lake until April. Surveys include sampling at 12 stations (Fig. 1) over one or two days depending on the

weather conditions. When conducted over two days, lakewide surveys and Station 6 profiles are conducted on consecutive days, when possible.

Fig. 1. Sampling stations on Mono Lake. Red points and numbers indicate permanently moored buoys, + sign indicates location of Paoha Island meteorological Station. Depth contours are in meters.

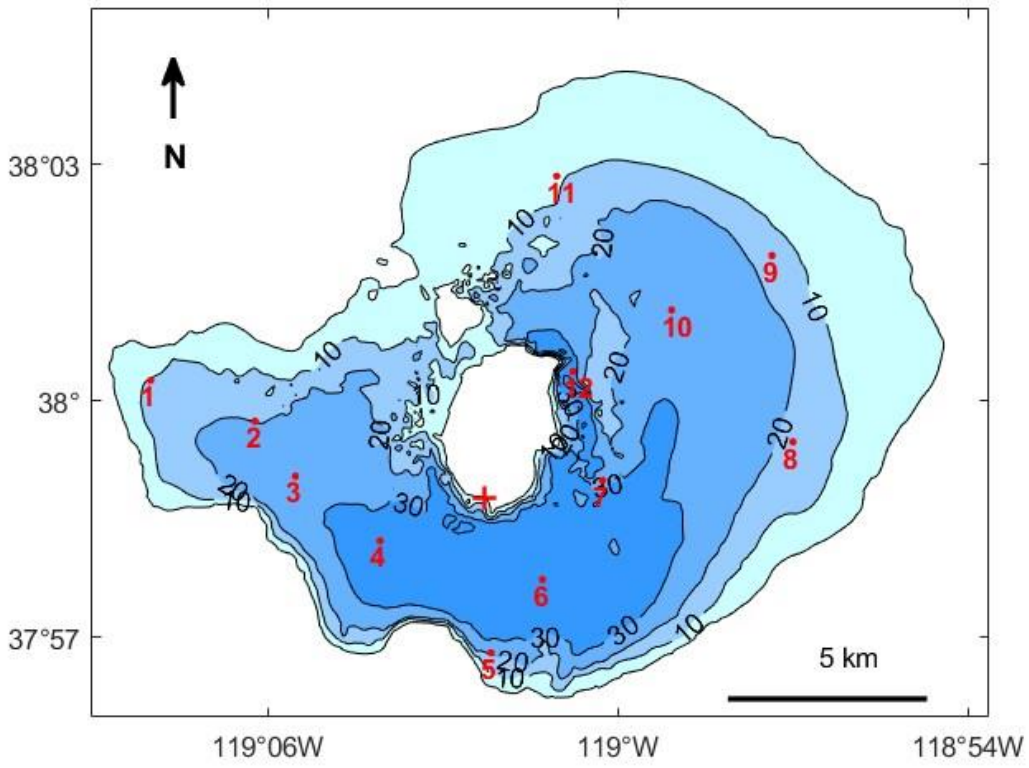

Field Procedures

In Situ Profiles

Depth, water temperature, conductivity, dissolved oxygen, fluorescence and turbidity are measured at twelve buoyed stations with a free-falling profiler (Rinko profiler model ASTD 102 with extended conductivity range): depth, resolution 0.02 m and accuracy ±0.3%; temperature, resolution 0.001°C and accuracy ±0.01°C; conductivity, resolution 0.001 mS cm^{-1} and accuracy ±0.01 mS cm^{-1}; dissolved oxygen, resolution 0.01 mg L^{-1} and accuracy ±2%. The Rinko oxygen probe was calibrated against Miller titrations (Walker et al. 1970) of Mono Lake water at a range of salinities.

Fluorescence and turbidity outputs require calibration for conditions in Mono Lake to convert readings to chlorophyll and total suspended solids, respectively.

The profiler is lowered at a rate of ~0.2 m s^{-1} and sampled at 100-ms intervals or approximately every 2 cm. Pressure readings are converted to depth using ambient air pressure at the time of readings and the density profile based on in-situ temperature and salinity. Relationships between conductivity, temperature, salinity, and density for the chemical composition of Mono Lake are given by Jellison et al. (1999a, b). Conductivity readings at in-situ temperatures (C_t) are converted to specific conductance at 25°C (C_{25}) using:

$$C_{25} = \frac{C_t}{1 + 0.02124(t-25) + 9.16\times10^{-5}(t-25)^2}$$

where t is the in-situ temperature. The density of Mono Lake water is given by:

$$\rho(t, C_{25}) = 1.0034 + 1.335\times10^{-5}t - 6.20\times10^{-6}t^2 + 4.897\times10^{-4}C_{25} + 4.23\times10^{-6}C_{25}^2 - 1.35\times10^{-6}tC_{25}$$

Total dissolved solids derived from conductivity for Mono Lake water is given by:

$$TDS(g\ kg^{-1}) = 3.386 + 0.564\times C_{25} + 0.00427\times C_{25}^2.$$

To obtain TDS in grams per liter, the above expression was multiplied by the density at 25°C for a given standardized conductivity given by:

$$\rho_{25}(C) = 0.99986 + 5.2345\times10^{-4}C + 4.23\times10^{-6}C^2$$

Mono Lake often has strong vertical temperature and salinity gradients. A mismatch in sensor time constants or water parcel sampled by the thermistor and conductivity electrode will result in spiking. While the time constants for the Rinko thermistor and conductivity electrodes are both listed by the manufacturer as 0.2 s, laboratory experiments indicated thermistor and conductivity electrode time constants of 0.14 s and 0.05 s, respectively. Conductivity spiking was examined after shifting the temperature readings by 0, 0.1, 0.2, 0.3, 0.4, and 0.5 s relative to conductivity in profiles over the course of the year, with a 0.2 s shift providing the least amount of spiking. Therefore, temperature readings were shifted by 0.2 s when calculating standardized (25°C) conductivity. Depending on the details of each profile spiking may still occur

after accounting for the difference in sensor response times; spikes were removed by visually inspecting each profile and then conductivity readings were further smoothed by a 6-point (~0.12 m) moving average.

Time-series measurements of water temperature were obtained with RBR Solo® thermistors (accuracy 0.002°C) sampling every ten seconds and deployed on a mooring at Station 6. Uppermost thermistors were suspended below and shaded by a surface float, and deeper ones were on a taut-line mooring suspended from a float ~0.5 m below the water surface.

Transparency is estimated as the depth a white Secchi disc, 20 cm in diameter, is visible, viewed on the shaded side of the boat to avoid glare, and, under calm conditions, if possible.

Vertical profiles of photosynthetically active radiation (400 to 700 nm, PAR) were obtained using a Licor LI-192 SB underwater sensor, and the attenuation coefficient of PAR was computed from the profiles.

Water Samples

Samples for chlorophyll and ammonium analyses are collected from eight to nine discrete depths at Station 6, and with a 0 to 9 m integrating tube sampler at seven Stations (1, 2, 5, 6, 7, 8, and 11). Samples for ammonium analyses are filtered immediately upon collection through Gelman A/E glass-fiber filters and kept chilled and dark until returned to the laboratory. Water samples used for analysis of chlorophyll are filtered through a 120-µm sieve to remove all stages of *Artemia* and kept chilled and dark until filtered in the laboratory.

Artemia Samples

Artemia are sampled by one net tow at each of the twelve, buoyed stations. Samples are taken with a plankton net (1 m x 0.30 m diameter, 120-µm Nitex mesh) towed vertically through the water column. Samples are preserved with 5% formalin in lake water. When adults are present, an additional net tow is taken from Stations 1, 2, 5, 6, 7, 8 and 11 to collect adult females for brood size and length analysis. A net efficiency factor of 70% was used (Lenz 1984).

Laboratory Procedures

Water Samples

Samples are returned to the laboratory and within 7 hours of collection are analyzed for ammonium and filtered for subsequent chlorophyll determinations. Chlorophyll samples are filtered onto 47 mm Whatman GF/F filters and kept frozen until the pigments are analyzed within one to two weeks.

Filters for chlorophyll *a* analyses are homogenized in 90% acetone and extracted at room temperature in the dark. Following clarification by centrifugation, absorption is measured at 750 and 663 nm on a spectrophotometer (Abbott Corporation, model SV1100D spectrophotometer). The sample is then acidified in the cuvette, and absorption again determined at the same wavelengths to correct for phaeopigments. Absorptions were converted to phaeophytin-corrected chlorophyll *a* concentrations with the formula (Golterman & Clymo, 1969):

$$Chl_s = 27.46[(A663_0 - A750_0) - 1.054(A663_a - A750_a)]1000v/V$$

where:

Chl_S = chlorophyll *a* concentration of sample I (µg L^{-1})
$A663_0$ = absorption at 663 nm before acidification
$A750_0$ = absorption at 750 nm before acidification
$A663_a$ = absorption at 663 nm after acidification
$A750_a$ = absorption at 750 nm after acidification
v = Volume of extract (mL)
V = Volume of filtered water (mL)
1.054 = volume correction after addition of 200 µL acid

During periods of low phytoplankton concentrations (<5 µg chl *a* L^{-1}), fluorescence of extracted pigments is measured on a fluorometer (Turner Designs, model TD-700) calibrated using dilutions of samples measured spectrophotometrically. Fluorometric determination of chlorophyll *a* is obtained with the formula:

$$Chl_s = [(\tau/\tau - 1)(R_0 - R_a)]/(v/V)$$

where:

Chls = Chlorophyll a concentration of the sample, in µg L^{-1}
τ = ratio of standard Rb/Ra
R0 = before acid fluorometer reading (µg L^{-1})
Ra = after acid fluorometer reading of sample (µg L^{-1})
v = volume extracted (mL)
V = volume filtered (mL)

Ammonium concentrations are measured using the indophenol blue method (Strickland & Parsons 1972). Internal standards are used because the molar extinction coefficient is less in Mono Lake water than in distilled water. For samples with sub - micromolar ammonium concentrations, the OPA method is used (Holmes et al. 1999, Protocol A, and Taylor et al. 2000).

Artemia Samples

Artemia are counted under a stereomicroscope (6x or 12x power). Depending on the number of shrimp, counts were made of the entire sample or of subsamples made with a Folsom plankton splitter. Samples are split such that a count of >100 animals are obtained. Shrimp are classified into adults (instars > 12), juveniles (instars 8–11), and nauplii (instars 1–7) according to Heath's classification (Heath 1924). Adults are sexed and adult females divided into ovigerous and non-ovigerous. Adult ovigerous females are further classified according to their reproductive mode, ovoviviparous or oviparous. A small percentage of ovigerous females are unclassifiable if eggs are in an early developmental stage. Nauplii at seven stations (Stations 1, 2, 5, 6, 7, 8, and 11) are further classified into distinct instars 1–7.

Live females collected for brood size and length analysis are kept cool and in low densities during transport to the laboratory. Immediately on return to the laboratory, females are randomly selected, isolated in individual vials, and preserved. Brood size is determined by counting the number of eggs in the ovisac including those dropped in the vial, and egg type and shape are noted. Female length (mm) is measured from the tip of the head to the end of the caudal furca (setae not included).

Artemia biomass (dry weight) is obtained from the whole sample or first split of counted samples by drying at 60°C for 48 h.

CHAPTER 3
RESULTS AND DISCUSSION

Surface Elevation

In 2023, above average snowmelt runoff reduced the salinity in the upper water column and led to a large difference in salinity with depth that affects many aspects of the physical and biological conditions in the lake. On 1 January 2023, the surface elevation of Mono Lake was 6378.6 ft (1944.2 m) (Mono Lake Committee, pers. comm.). Above average snowmelt runoff resulted in a 4.6 ft (1.4 m) rise in surface elevation to 6383.3 ft (1945.6 m) by September. This was followed by a slight decrease to 6383.15 ft by the end of the year (Fig. 2).

Fig. 2. Mono Lake surface elevation (ft asl, USGS datum).

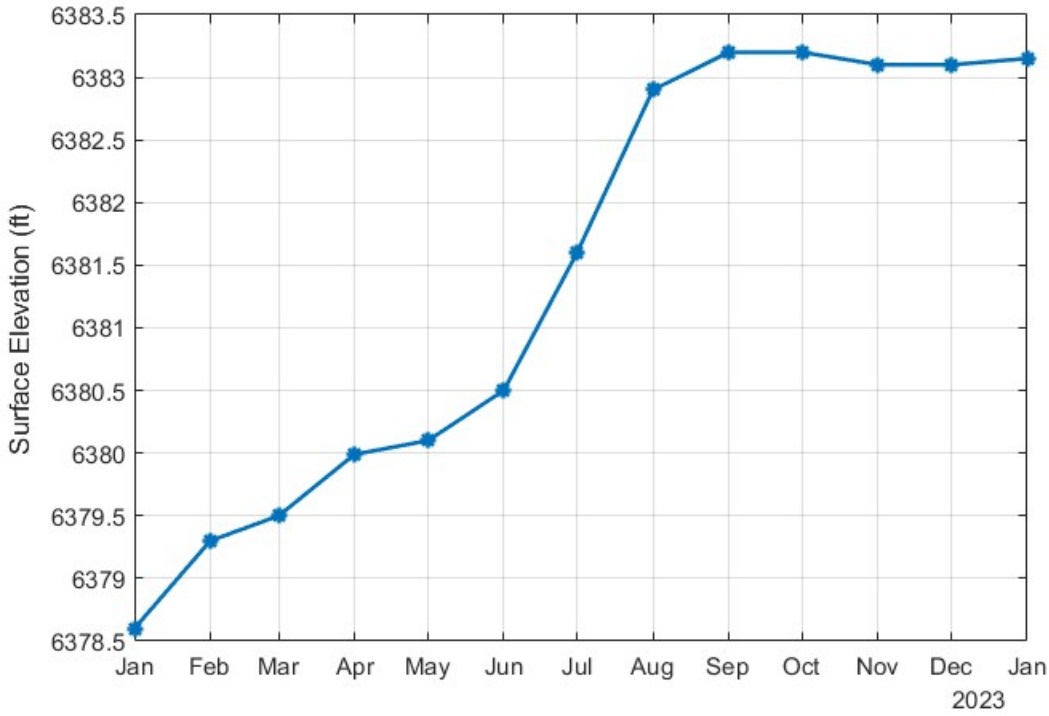

Meteorological Data

The Mono Lake limnological monitoring program collects meteorological data at a site located on the southwest shore of Paoha Island. The meteorological station was installed and began recording data on 30 May 2023. Complementary meteorological data

are also collected by the Great Basin Air Pollution Control District at Lee Vining and on the northeast shore of Mono Lake.

Wind Speed and Direction

Hourly mean wind speeds varied from 0.1 to 13.2 m s^{-1} from 31 May to 31 December (Fig. 3). The maximum gust was 22.6 m s^{-1} observed on 19 November at 00:15. There were several periods of sustained high winds, most notably 17–20 June and 31 August–3 September, and others in late November and December. These likely caused enhanced mixing. Winds were predominately from the west southwest (Fig. 4).

Fig. 3. Hourly mean wind speed (m s^{-1}).

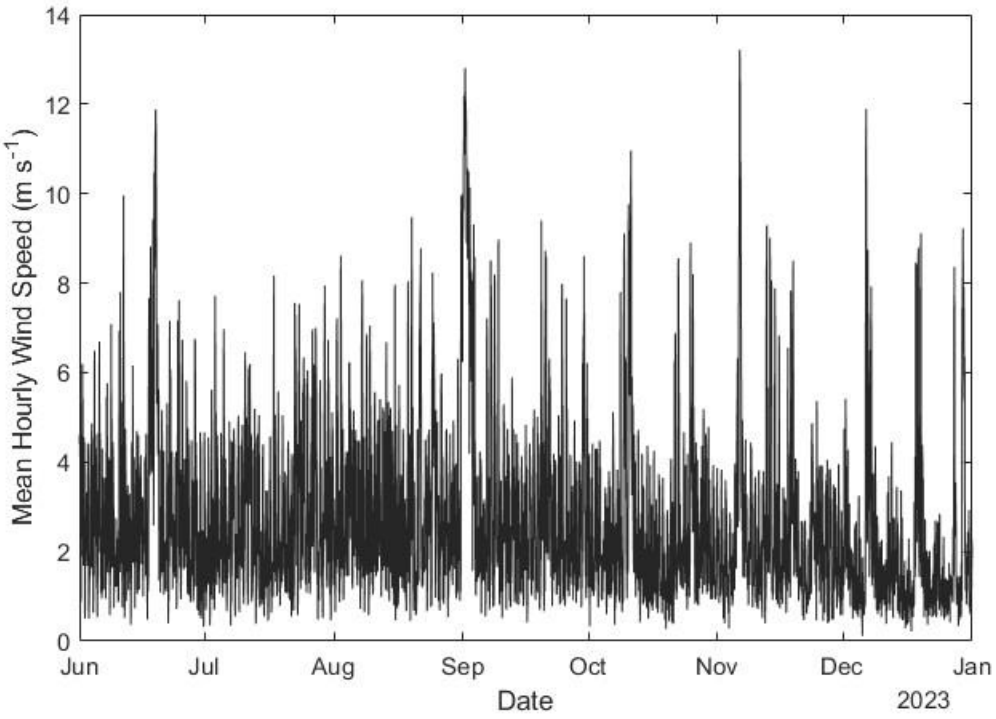

Fig. 4. Wind rose (hourly mean direction and speed), 30 May–31 December 2023. u_w denotes wind speed, and numbers with color bars are wind speeds in m s^{-1}. Percentages refer to the proportion of time spent in each 10-degree wind direction sector.

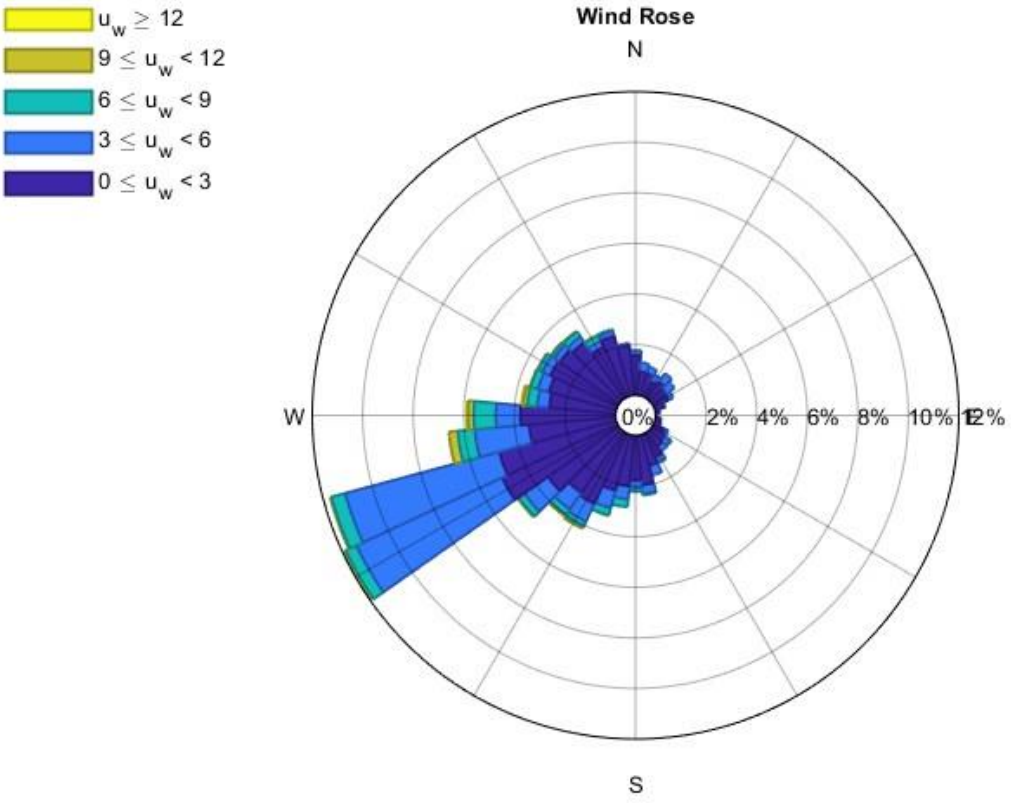

Air Temperature

Hourly mean air temperatures generally ranged from ~10 to 30°C in summer and from ~-5 to 10°C in winter (Fig. 6), although temperatures as high as 35°C and as low as -10°C occurred several times. Due to a probe failure, air temperatures (and relative humidity and dew point) were absent from 9 September through 18 October. Air temperature is also collected at a station in Lee Vining. Although a comparison indicated hourly differences can be 6°C, a highly significant linear regression (r^2=0.97) yielded a slope near one (0.997) and an intercept of 0.52°C (Fig. 5). This relation was used to fill the gap in the data.

Fig. 5. Paoha Island versus Lee Vining air temperatures (°C).

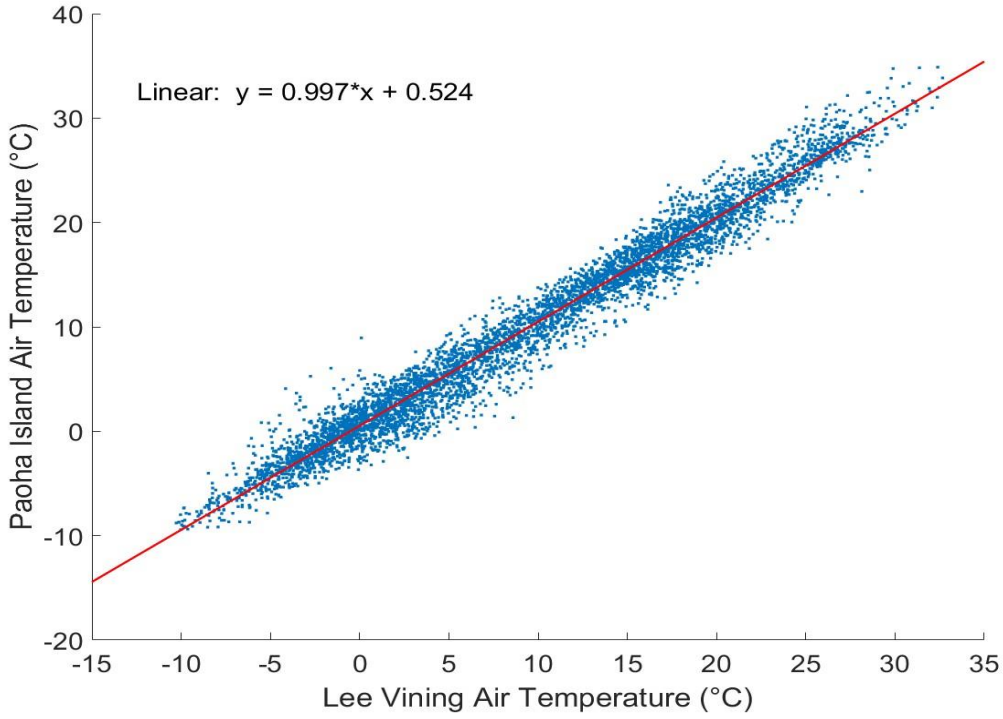

Fig. 6. Hourly mean air temperatures (°C) at Lee Vining and Paoha Island

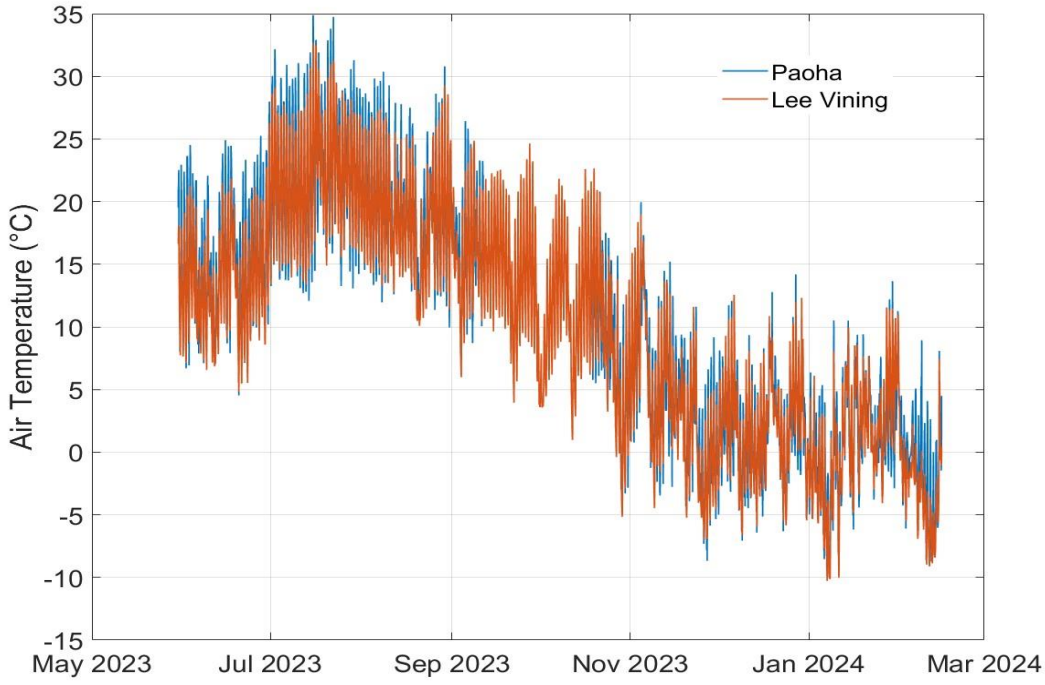

Incident Photosynthetically Available Radiation (PAR)

Maximum daily values of photosynthetically available radiation (400-700 nm) typically ranged from about ~19 Einsteins m^{-2} day^{-1} at the winter solstice to ~64 Einsteins m^{-2} day^{-1} in mid-June (Fig. 7). During 2023, the June–December mean was 37.9 Einsteins m^{-2} day^{-1}, with daily values ranging from 8.7 Einsteins m^{-2} day^{-1} on 21 December to 64.2 Einsteins m^{-2} day^{-1} on 20 June.

Fig. 7. Daily photosynthetically available radiation, 2023.

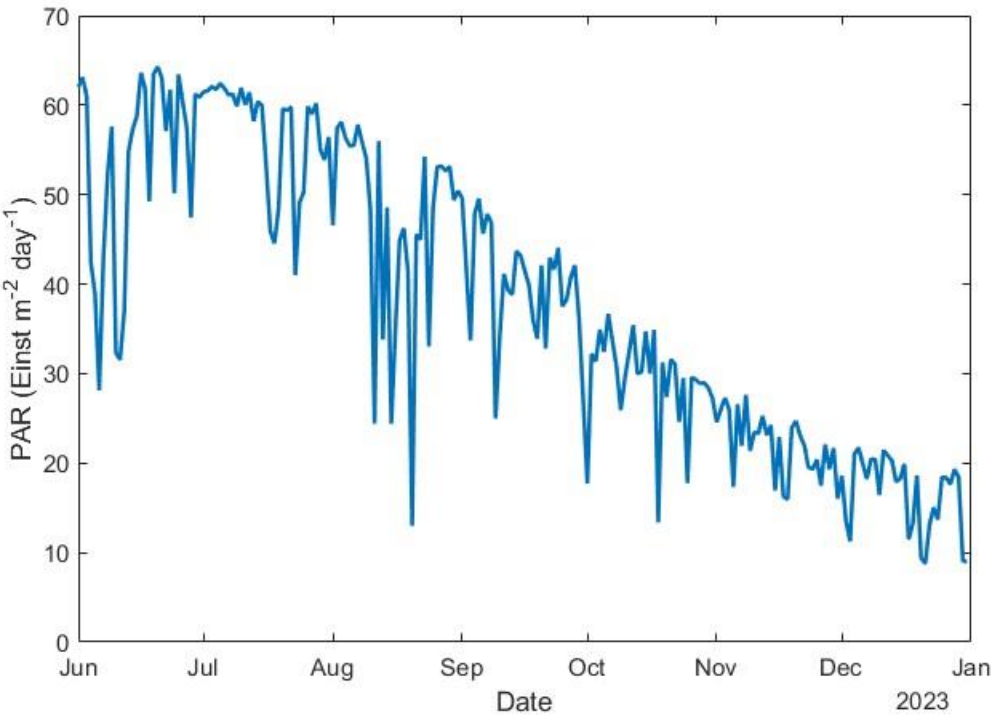

Relative Humidity and Precipitation

Mean daily relative humidity values were variable ranging from 30 to 92% from 1 June to 31 December. A general pattern of lower values (mostly 30–60%) in midsummer was followed by increased values (mostly 60–80%) in November and December (Fig. 8).

Fig. 8. Mean daily relative humidity (%), 2023.

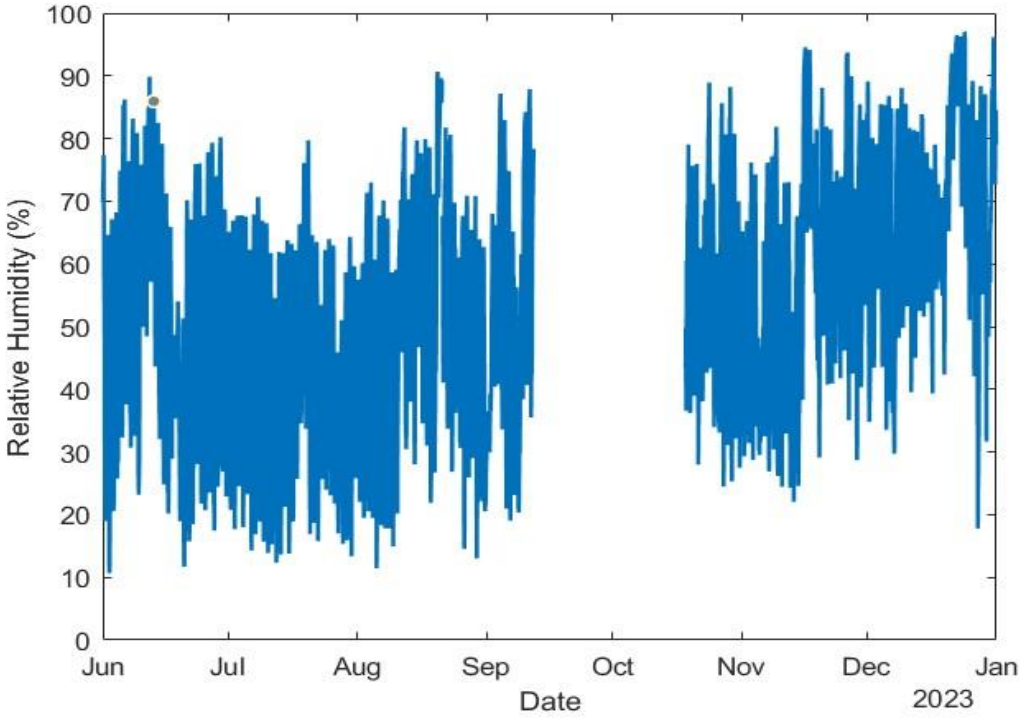

Precipitation from June through December 2023 measured at Paoha Island was 72.4 mm (2.9 inches) (Fig. 9) with the largest amount (12.2 mm) occurring on 6 June 2023.

Fig. 9. Daily precipitation (mm).

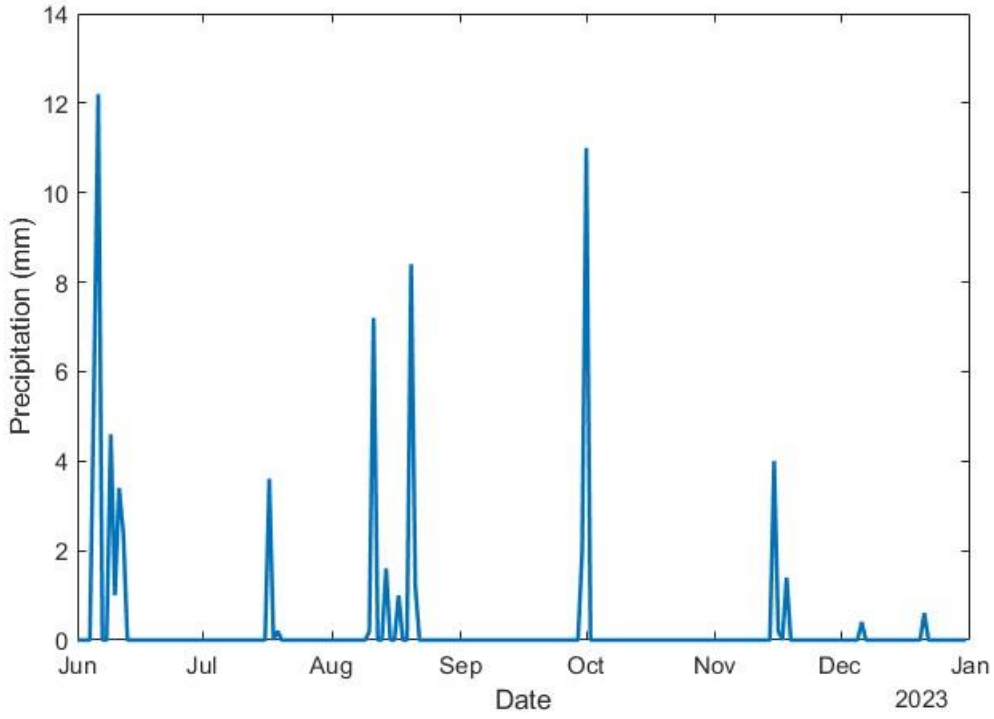

Lake Temperatures

The complex morphometry of Mono Lake (steep-sided western basins, shallow sloping eastern basin, two large islands and several small islets in the center), southwesterly prevailing winds, and freshwater inflows predominantly into the western basins result in spatial heterogeneity of physical, chemical, and biological features in the lake. Here, we examine the spatial and temporal variation in temperature before discussing the overall seasonal trend of stratification. Detailed temperature profiles are collected at all 12 stations and facilitate understanding of seasonal patterns of warming and stratification.

Exceptionally large winter snowfall precluded access to the lake until the first lakewide survey conducted on 30 April 2023. By then the lake was strongly stratified with near-surface temperatures of 12–18ºC while those below 15 m were 1.5–2.0ºC (Fig. 10). Water temperatures were generally cooler at western stations (Stations 1 to 6) than at eastern stations (Stations 7 to 12). During May (Fig. 11), the upper 2 m water

temperatures ranged from 12 to 15ºC at western stations, and from 16 to 18ºC at eastern stations.

Fig. 10. Lake temperatures (ºC), 30 April 2023.

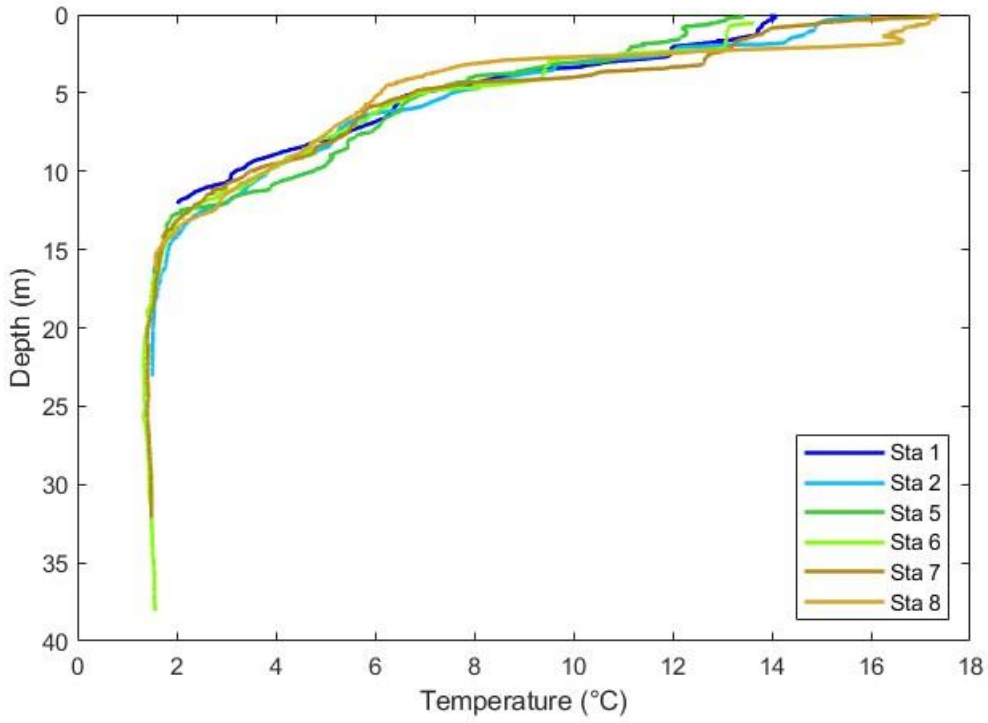

Fig. 11. Lake temperatures (ºC), 19 May 2023

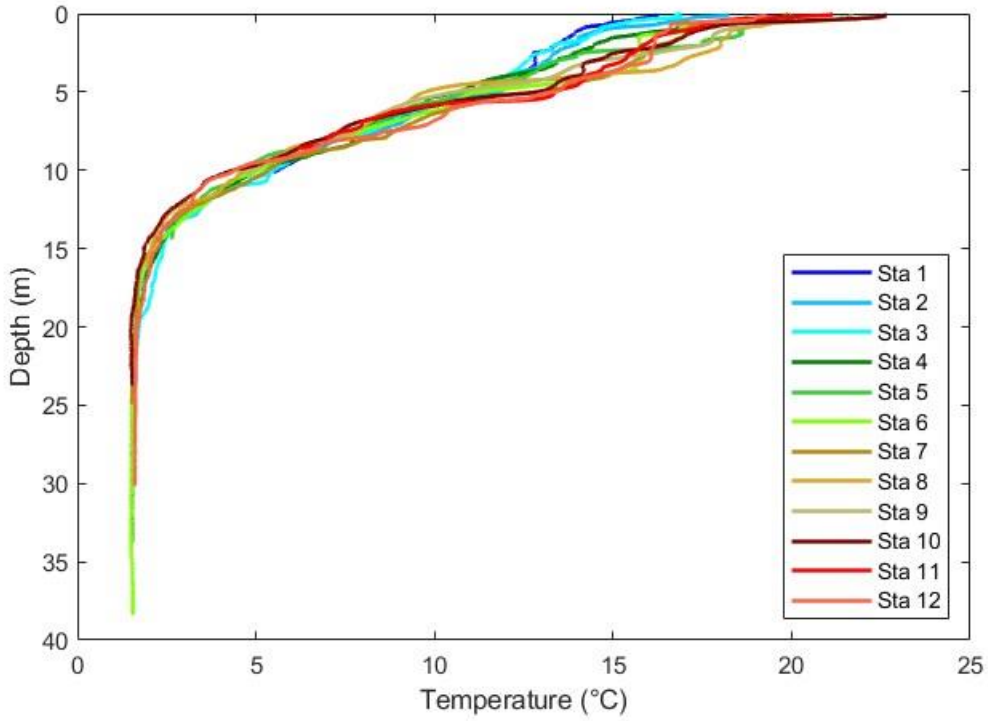

The epilimnion warmed during the spring with water temperatures near the surface (1 m) increasing to 16–17°C at western stations and to 17.5–20.5°C at eastern stations on 13 June (Fig. 12). Station 1 is the shallowest Station in the western sector (10.4 m), and from June onwards its near-surface temperatures (2 m) were generally ~1°C warmer compared to the other western stations.

During the July survey (Fig. 13), near-surface (2 m) water temperatures at western stations ranged from 20 to 25°C, and from 22 to 24.5°C at eastern stations. From 3 m to 15 m, water temperatures decreased to 2.3–3.3°C at 15 m. Strong thermal gradients persisted in August (Fig. 14), with water temperatures at western stations ranging from 22°C at 4 m to 25°C at 5 m, while at eastern stations, water temperatures were 21.5°C at 4.5 m and 24.5°C at 5.5 m. Below 6 m, water temperatures decreased to 2.8–3.5°C at 15 m.

Fig. 12. Lake temperatures (ºC), 13 June 2023.

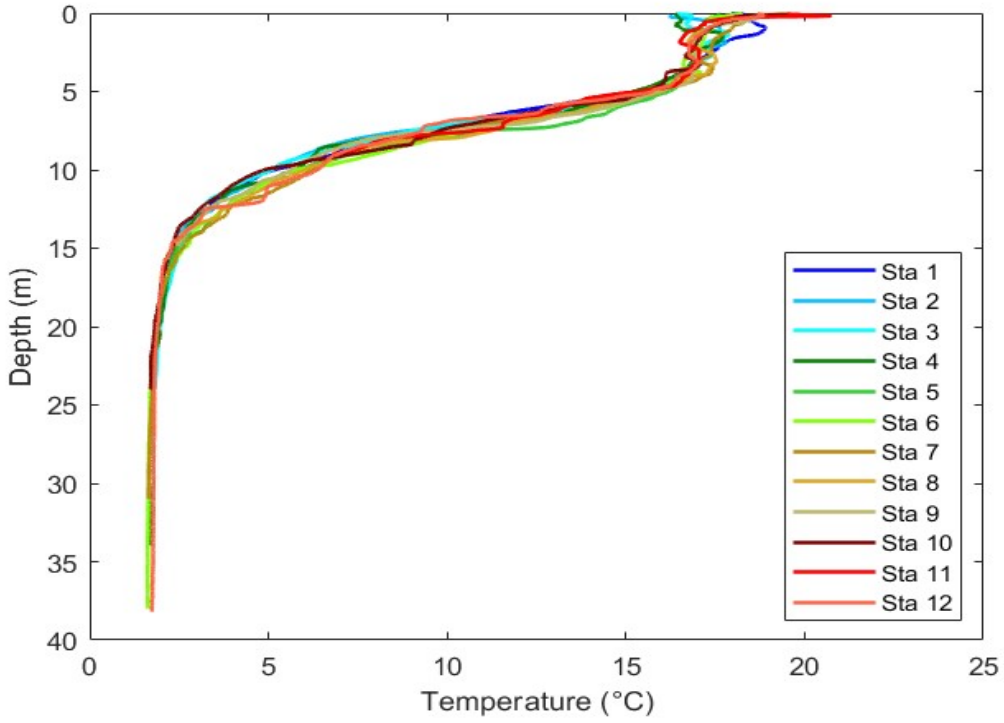

Fig. 13. Lake temperatures (ºC), 12 July 2023.

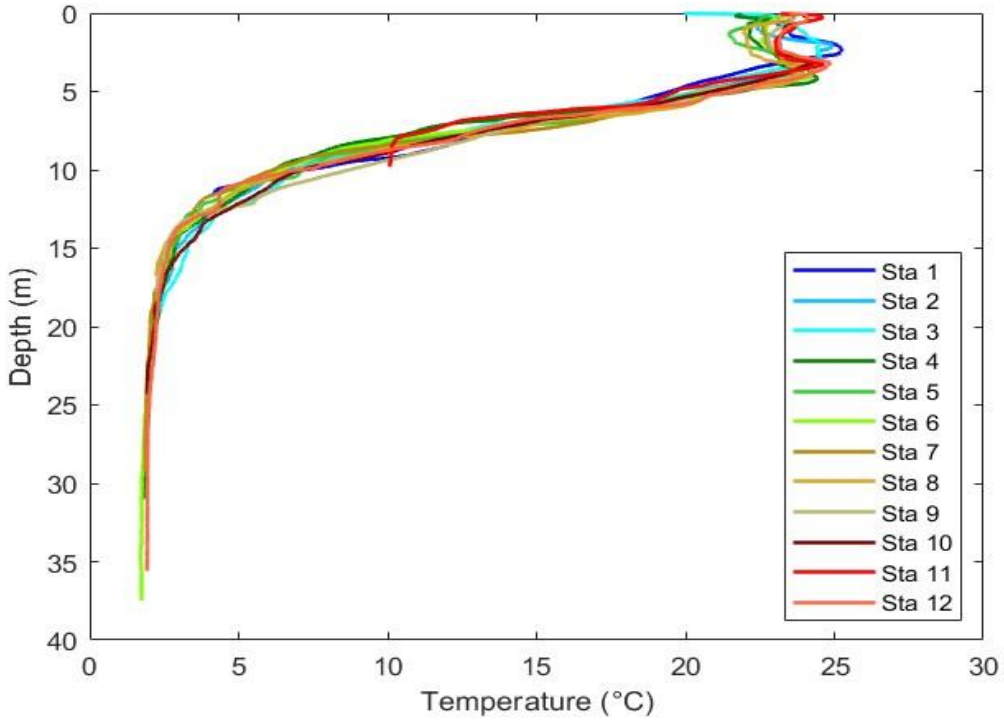

Fig. 14. Lake temperatures (ºC), 17 August 2023.

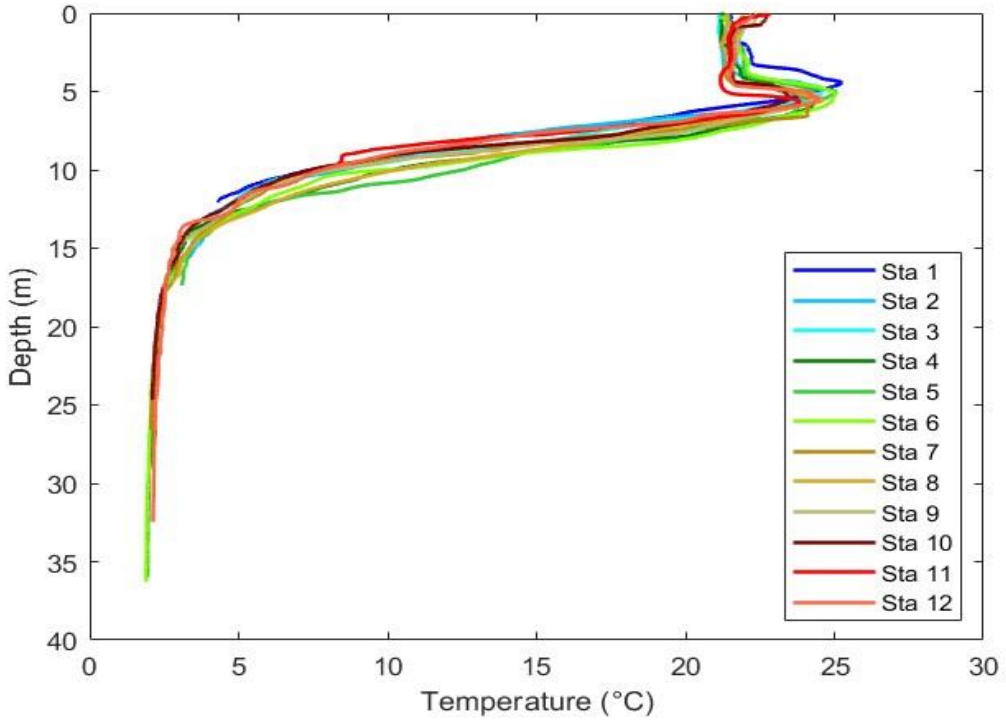

Water temperatures near the surface (2 m) at the western stations remained colder than at the eastern stations in September (Fig. 15) until December, except for Stations 1 and 2 which were warmer than the other western stations in November (Fig. 17). The subsurface temperature maximum in October (Fig. 16), November (Fig. 17) and December (Fig. 18) resulted because the upper water cooled faster than the water in the pycnocline associated with the salinity gradient (see below). Between 6 and 15 m, thermal stratification persisted through December (Fig. 18) with gradual deepening in western and eastern stations. Below 15 m the water remained near 2ºC.

Fig. 15. Lake temperatures (ºC), 18 September 2023.

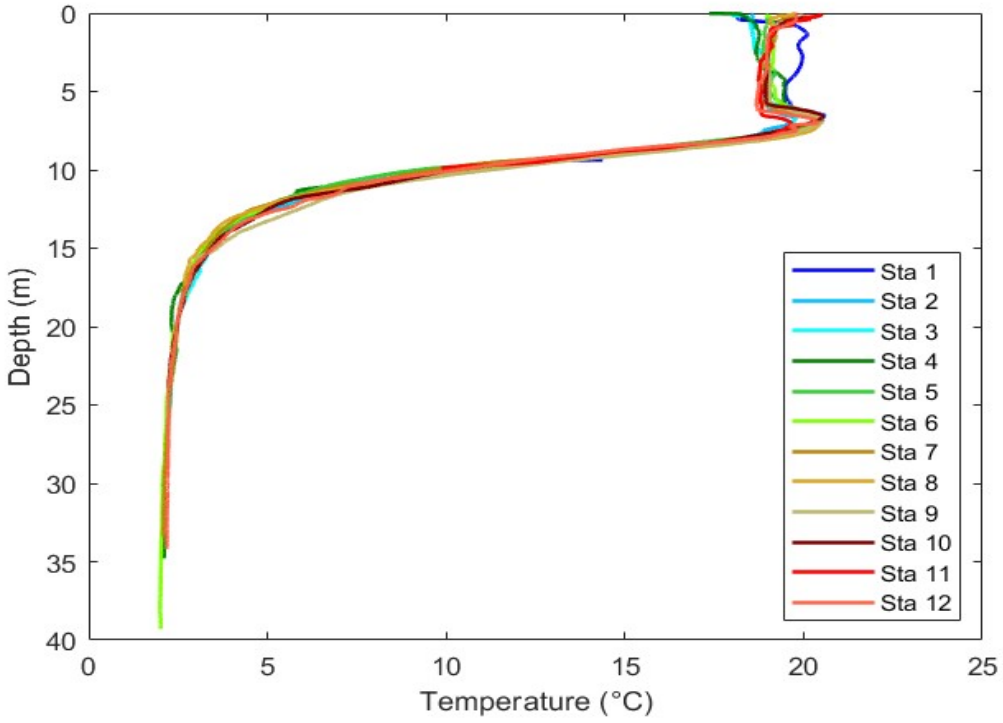

Fig. 16. Lake temperatures (ºC), 12 October 2023.

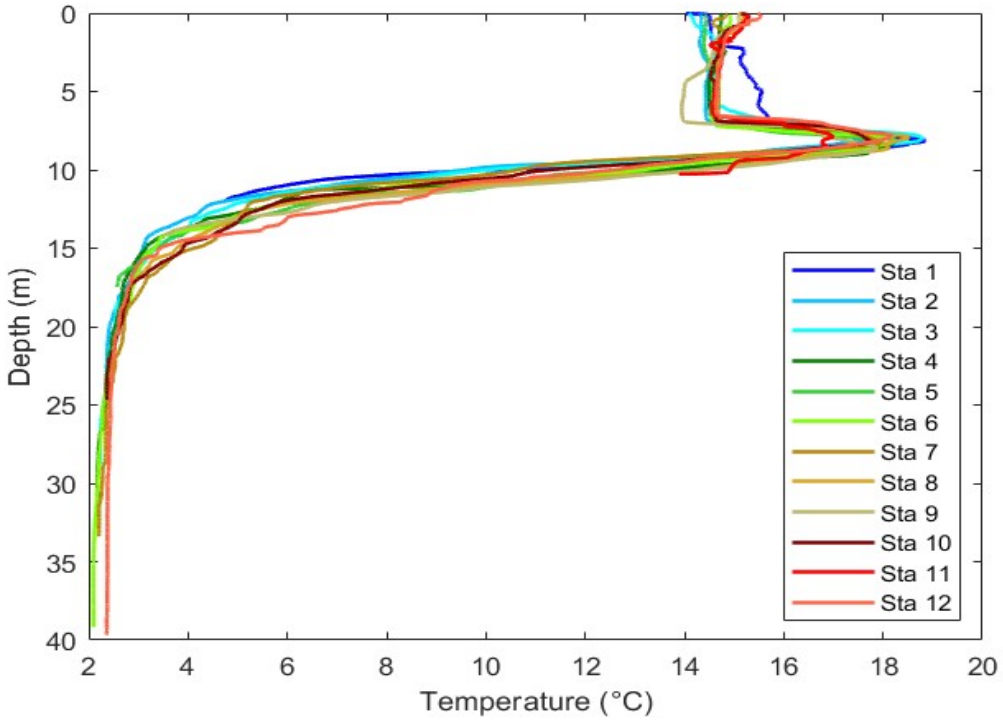

Fig. 17. Lake temperatures (ºC), 14 November 2023.

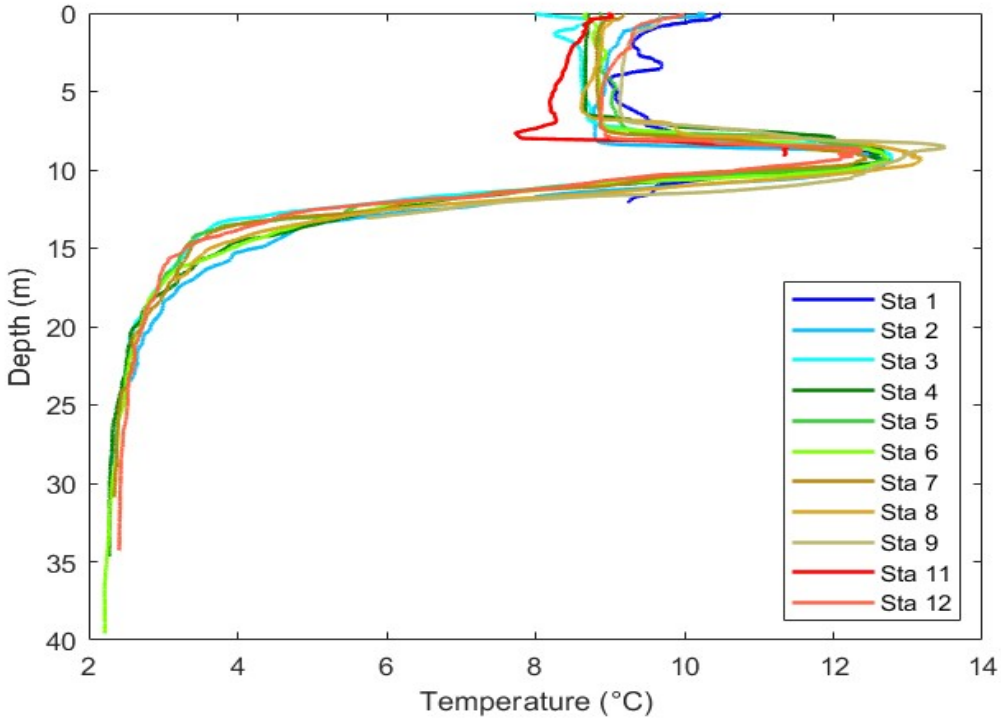

Fig. 18. Lake temperatures (ºC), 12 December 2023.

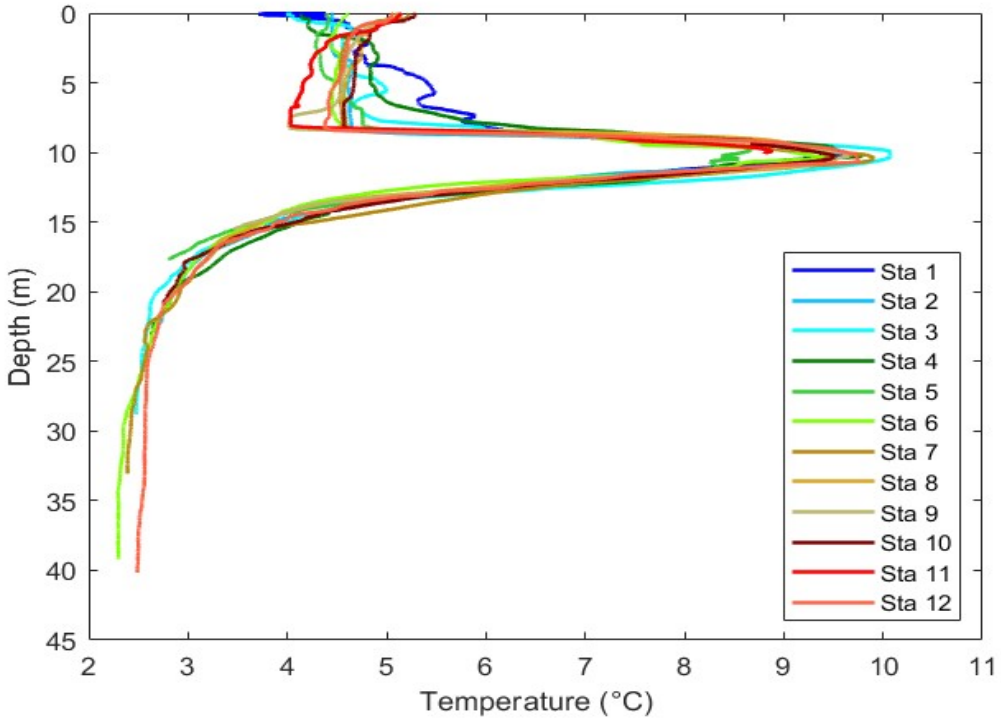

Seasonal Water Temperatures at Station 6

The annual pattern of thermal stratification in Mono Lake results from seasonal variations in climatic factors (e.g., air temperature, solar radiation, wind speed, humidity) and their interaction with density stratification arising from the timing and magnitude of freshwater inputs. The typical annual pattern observed for large temperate lakes differs from that in hypersaline Mono Lake due to the absence of ice cover and unique temperature-density properties, resulting in an extended period of winter holomixis. In Mono Lake, the annual winter period of holomixis typically extends from late November to early February after which seasonal thermal and salinity stratification are initiated due to warming air temperatures, increased insolation, and increased inflows. This pattern has been altered by five episodes of meromixis (1983–1988, 1994–2003, 2005–2007, 2010–2012, 2017–2020) during which vertical salinity gradients accompanying increased freshwater inflows prevented winter holomixis. During 2021 through 2022 winter holomixis and monomictic conditions prevailed. In late 2022, partial mixing of upper waters into the hypolimnion occurred between November and December but a period of complete mixing (i.e., holomixis) did not occur and thus a 6th episode of meromixis has been initiated.

January represents a period of low biological activity due to cold water temperatures, low light levels, and the absence of *Artemia*. January surveys are only conducted when unusual circumstances warrant it and weather permitting. While monthly surveys are usually initiated in February, there are years, as in 2023, when the launching site cannot be reached due to snow on the access road.

Measurements at Station 6, a central deep station, include vertical profiles of ammonium and chlorophyll as well as profiles of temperature, conductivity, fluorescence, and dissolved oxygen; also, the station has one of longest records. Therefore, seasonal patterns at Station 6 are described in more detail first for temperature and below for other variables.

The first survey of the year was conducted on 30 April 2023 when water temperatures were 13°C at 2 m and decreased in steps to 1.7°C at 15 m. From 15 m to the bottom, water temperatures were 1.3–1.7°C (Fig. 19, Fig. 20, Table 1).

The epilimnion warmed during the spring with water temperatures at 2 m increasing to 15.7°C on 19 May and 17.1°C on 13 June. Strong thermal gradients were present in the upper 7 m on July 12, when water temperatures decreased from 22.8°C at 2 m to 14.3°C at 7 m, with the presence of a warmer intermediate layer with temperature up to 24.2 °C at 4 m. Strong thermal gradients persisted in mid-August, when water temperatures decreased from 21.8°C at 2 m to 14.2°C at 9 m. A warmer intermediate layer with a temperature of 24.9°C at 5 m was present.

In mid-September, a well-defined epilimnion was present at 5 m with water temperatures of 19 to 19.2°C. The warmer intermediate layer persisted until mid-December and became approximately 1 m deeper with each survey. In mid-September, the warmer layer was at 7 m with a temperature of 20.4°C and was 18.6°C at 8 m. Water temperatures decreased 13°C across the thermocline from 8 m to 12 m. Below the September thermocline temperatures decreased slowly to 2°C to 39 m.

Annual maximum water temperatures were observed during mid-August, when temperatures in the warmer intermediate layer at 5 and 6 m were 24.9–24.6°C, respectively. During early autumn the epilimnion gradually cooled, the persistent thermocline deepened, and the deeper water remained warmer. By 12 October 2023 the epilimnion extended to 7 m with water temperatures ranging from 14.6°C to 14.8°C in the upper 7 m. Right beneath the epilimnion, water temperatures were 18.2°C at 8 m and 16.7°C at 9 m. Temperatures then decreased across the thermocline to 3.1°C at 16 m and then more slowly to 2.1°C at 39 m.

The lake continued to cool and on 14 November 2023, water temperatures were 8.8–8.9°C in the epilimnion (0–7 m), followed by the warmer intermediate layer with temperatures of 10.5°C at 8 m, 12.7°C at 9 m, and 12.2°C at 10 m. Temperatures then dropped rapidly across the metalimnion to 2.7°C at 20 m and then more slowly to 2.2°C near the bottom. On 12 December, the epilimnion extended to 8 m with water temperatures ranging from 4.4–4.5°C in the upper 8 m. Beneath the epilimnion, temperatures in the warmer intermediate layer were 7.1°C at 9 m, 9.1°C at 10 m, 8.5°C at 11 m, and 6.4°C at 12 m. Temperatures then decreased across the metalimnion to 2.9°C at 20 m and then more slowly to 2.3°C at 39 m.

Fig. 19. Seasonal water temperatures at Station 6.

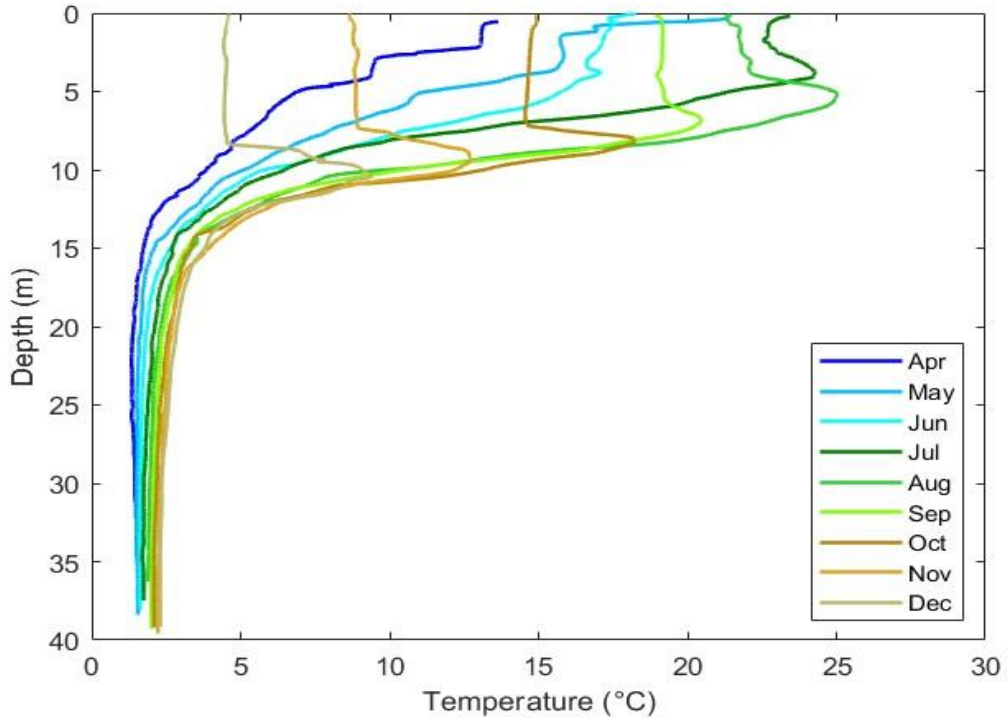

Fig. 20. Temperatures (ºC) at Station 6, 2023 (red triangles indicate sampling dates).

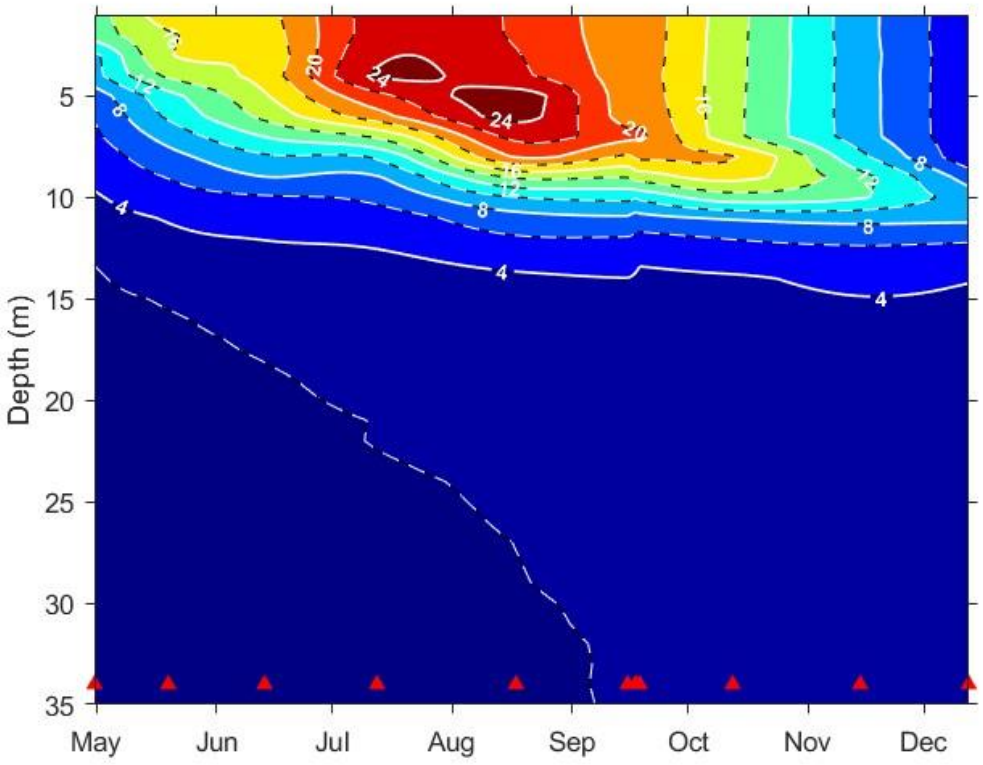

The continuous temperature measurements at a series of depths on moored thermistors (Fig. 21) add temporal resolution to the monthly data illustrated in Fig. 20 and by the profiles at the 12 stations (Fig. 10 to Fig. 18). During the month of June (Day of Year (DOY) 152-181), the upper 5 m comprised the upper mixed layer, and intermittently stratified and mixed for several hours to days. From DOY 180 to 220 (29 June to 8 August) the upper 6 m warmed and a strong thermal gradient formed between 4 and 6 m. Episodes of diel heating and cooling in the upper 4 m continued through the record. From DOY 200 to 220 (19 July to 8 August) or so, warmer water occurred from 3 to 6 m. As warm water is less dense than cooler water, this pattern can occur because freshwater inflows slightly diluted the upper water and warmer, more saline water was under the less saline layer. The upper 7 m gradually cooled and lost stratification from DOY 220 (8 August) to mid-October. Warmer, more saline water persisted at the base of the upper mixed layer through the period of record. Between 5 and 12 m, thermal stratification was pronounced and persisted through our study with gradual deepening and weakening at its base. Below 15 m the water remained near 2°C.

Fig. 21. Time-depth plot of isotherms (°C) at Station 6 from 1 June 2023 to 14 October 2023. Two-hour averages of 10 second readings. Red dots indicate depths of thermistors (see Chapter 2 for details on sensors and deployment).

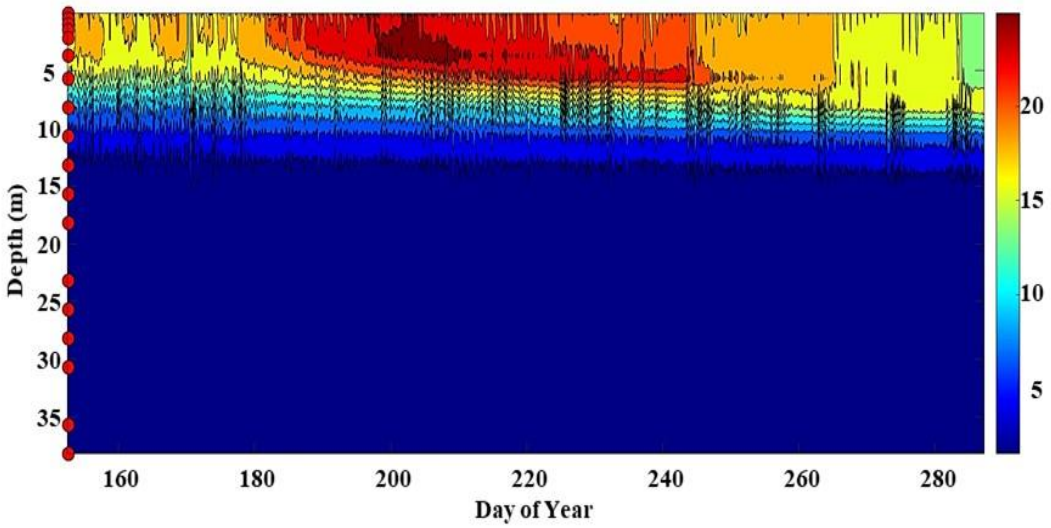

Table 1. Temperature (°C) at Station 6, April–December, 2023.

Depth (m)	4/30	5/19	6/13	7/12	8/17	9/18	10/12	11/14	12/12
1	13.1	16.9	17.4	22.7	21.8	19.2	14.8	8.8	4.5
2	13.1	15.7	17.1	22.8	21.8	19.2	14.7	8.8	4.4
3	9.5	15.8	16.6	23.7	22.1	19.1	14.7	8.9	4.5
4	9.4	14.3	16.9	24.2	22.4	19.0	14.7	8.8	4.5
5	6.9	11.3	15.8	21.4	24.9	19.2	14.6	8.9	4.5
6	6.1	10.3	14.5	19.2	24.6	19.6	14.6	8.9	4.5
7	5.6	8.7	12.0	14.3	22.6	20.4	14.6	8.9	4.4
8	4.9	7.3	9.7	10.3	20.1	18.6	18.2	10.5	4.5
9	4.4	6.1	8.0	7.9	14.2	15.0	16.7	12.7	7.1
10	3.8	5.1	5.8	6.5	9.9	10.5	13.2	12.2	9.1
11	3.3	4.1	4.8	5.1	7.2	7.4	8.2	8.7	8.5
12	2.5	3.7	4.1	4.4	5.8	5.4	6.1	6.4	6.4
13	2.1	3.0	3.5	3.7	4.7	4.3	4.9	5.3	4.8
14	1.9	2.5	2.9	3.0	3.6	3.6	3.7	4.5	4.1
15	1.7	2.1	2.6	2.7	3.4	3.2	3.3	3.9	3.8
16	1.7	1.9	2.4	2.5	3.0	2.9	3.1	3.4	3.4
17	1.5	1.8	2.1	2.4	2.7	2.8	2.9	3.0	3.2
18	1.5	1.7	2.0	2.3	2.5	2.7	2.9	2.9	3.0
19	1.4	1.7	1.9	2.2	2.4	2.5	2.8	2.8	2.9
20	1.4	1.7	1.9	2.1	2.3	2.4	2.6	2.7	2.9
21	1.4	1.6	1.8	2.0	2.3	2.3	2.5	2.6	2.8
22	1.3	1.6	1.8	2.0	2.2	2.3	2.5	2.6	2.7
23	1.4	1.5	1.7	2.0	2.1	2.3	2.4	2.5	2.6
24	1.4	1.5	1.7	1.9	2.1	2.2	2.4	2.5	2.6
25	1.4	1.5	1.7	1.9	2.1	2.2	2.3	2.5	2.6
26	1.4	1.5	1.7	1.8	2.0	2.2	2.3	2.4	2.5
27	1.4	1.5	1.7	1.8	2.0	2.1	2.2	2.4	2.5
28	1.4	1.5	1.7	1.8	2.0	2.1	2.2	2.4	2.4
29	1.4	1.5	1.6	1.8	2.0	2.1	2.2	2.3	2.4
30	1.4	1.5	1.7	1.7	2.0	2.1	2.2	2.3	2.3
31	1.5	1.5	1.6	1.7	1.9	2.1	2.2	2.3	2.3
32	1.5	1.5	1.6	1.7	1.9	2.1	2.1	2.3	2.3
33	1.5	1.5	1.6	1.7	1.9	2.0	2.1	2.3	2.3
34	1.5	1.5	1.6	1.7	1.9	2.0	2.1	2.3	2.3
35	1.5	1.5	1.6	1.7	1.9	2.0	2.1	2.2	2.3
36	1.6	1.5	1.6	1.7	1.9	2.0	2.1	2.2	2.3
37	1.6	1.6	1.6	1.7		2.0	2.1	2.2	2.3
38	1.6	1.6				2.0	2.1	2.2	2.3
39						2.0	2.1	2.2	2.3

Specific Conductance

The large volume of freshwater inflows beginning in 2023 created strong vertical chemical gradients, with lake specific conductance generally lower at western stations (Stations 1 to 6) than at eastern stations (Stations 7 to 12) near the surface (2 m). In the first lakewide survey (Fig. 22), specific conductance in the upper 2 m was 80.6–83.5 mS cm^{-1} at the western stations and 82.5–83.9 mS cm^{-1} at the eastern stations. In May (Fig. 23), the upper 2 m specific conductance at the western stations had decreased, varying from 63 to 82.5 mS cm^{-1} and from 82 to 83 mS cm^{-1} at the eastern stations. The low conductance of 63 mS cm^{-1} in the western sector occurred at Station 3, located near inflow from Lee Vining Creek.

Fig. 22. Specific conductance (mS cm^{-1}), 30 April 2023.

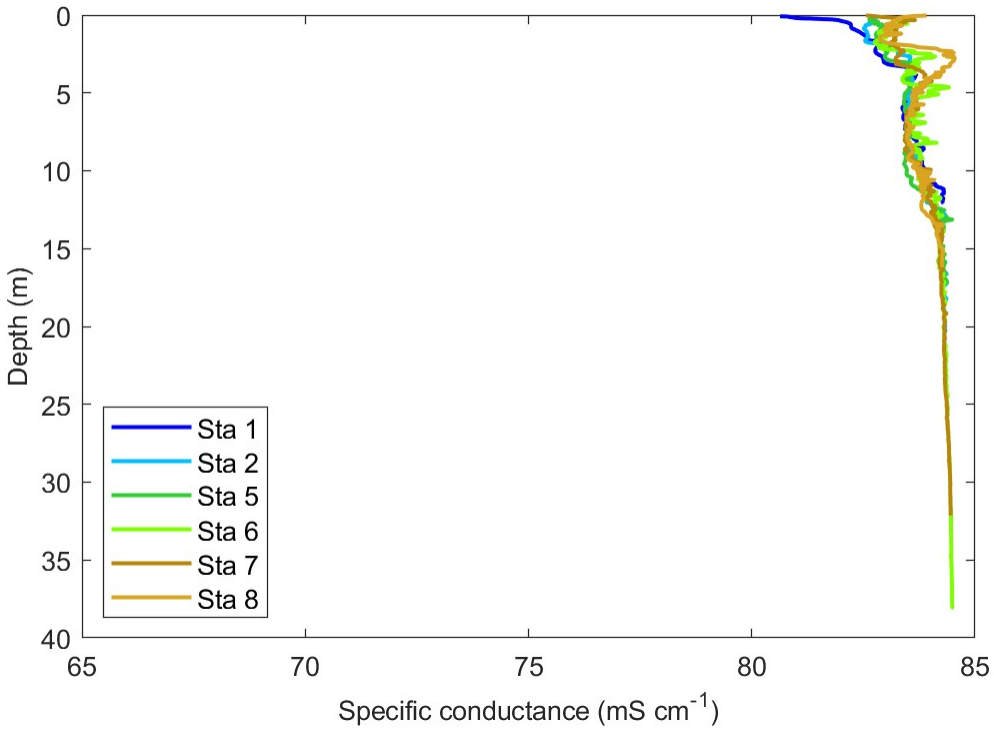

Fig. 23. Specific conductance (mS cm^{-1}), 19 May 2023.

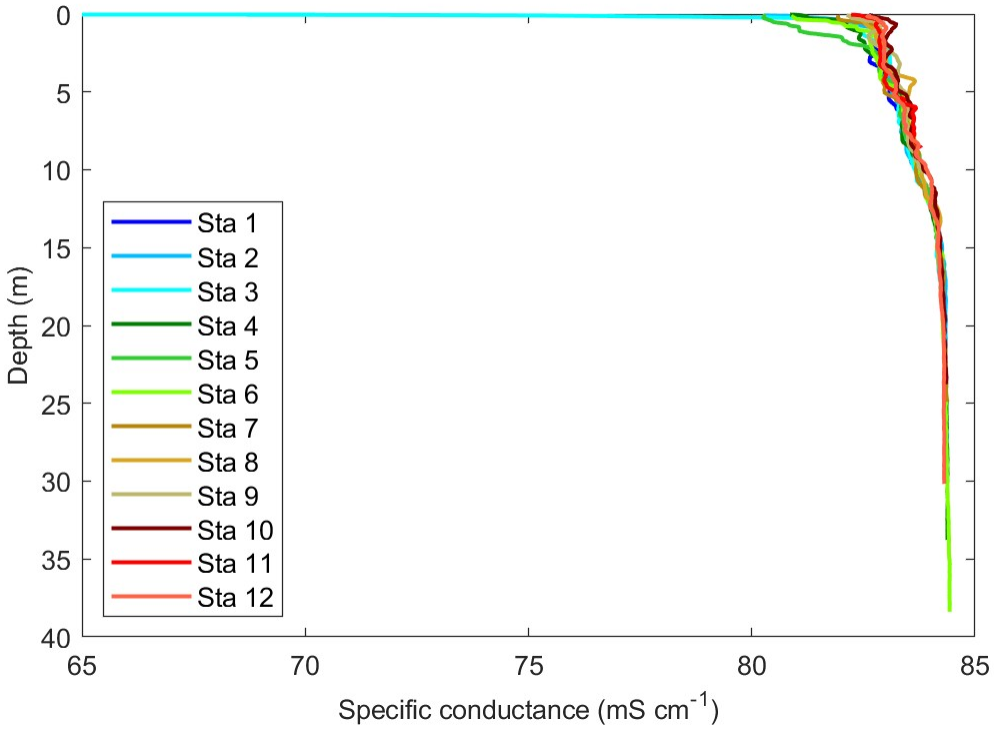

Freshwater inflow continued during the spring and by 13 June (Fig. 24), the lake was chemically stratified with specific conductance near the surface (1 m) ranging from 59.4 to 79 mS cm^{-1} at western stations and from 75.7 to 80.4 mS cm^{-1} at eastern stations. In June, Station 5 had the lowest conductance of the year (59.4 mS cm^{-1}) as it received a large volume of freshwater coming mainly from Rush Creek, which peaked in June and July. Below 2 m, specific conductances at western stations were similar to eastern stations, ranging from 79.5 to 80.5 mS cm^{-1} at 2 m, and from 83.5 to 83.9 mS cm^{-1} at 9 m. Below 10 m specific conductance remained near 84.3 mS cm^{-1}.

Fig. 24. Specific conductance (mS cm^{-1}), 13 June 2023.

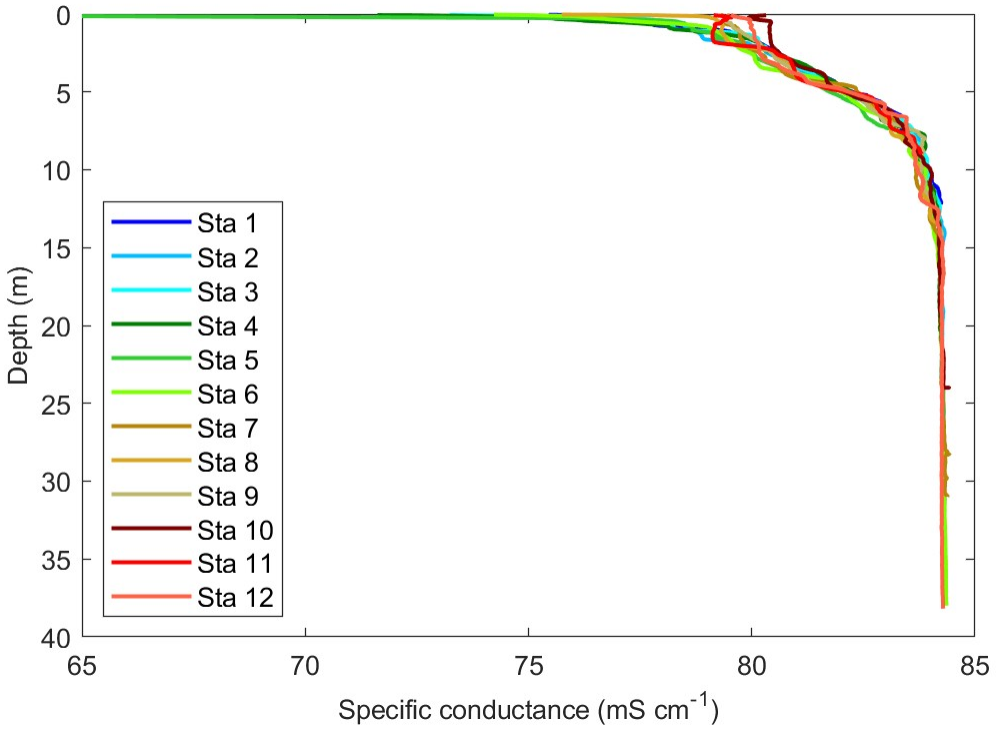

Strong chemical gradients were present in July as freshwater inflows continued, with near-surface (2 m) specific conductances at western stations ranging from 61.7 to 72.5 mS cm^{-1} and from 72.3 to 74.1 mS cm^{-1} at eastern stations. The low conductance of 61.7 mS cm^{-1} occurred at Stations 3 and 4 located near inflow from Lee Vining Creek which peaked in July. The mixolimnion ranged similarly between western and eastern stations, and the monimolimnion specific conductance remained near 84.3 mS cm^{-1} until the end of the year.

Fig. 25. Specific conductance (mS cm^{-1}), 12 July 2023.

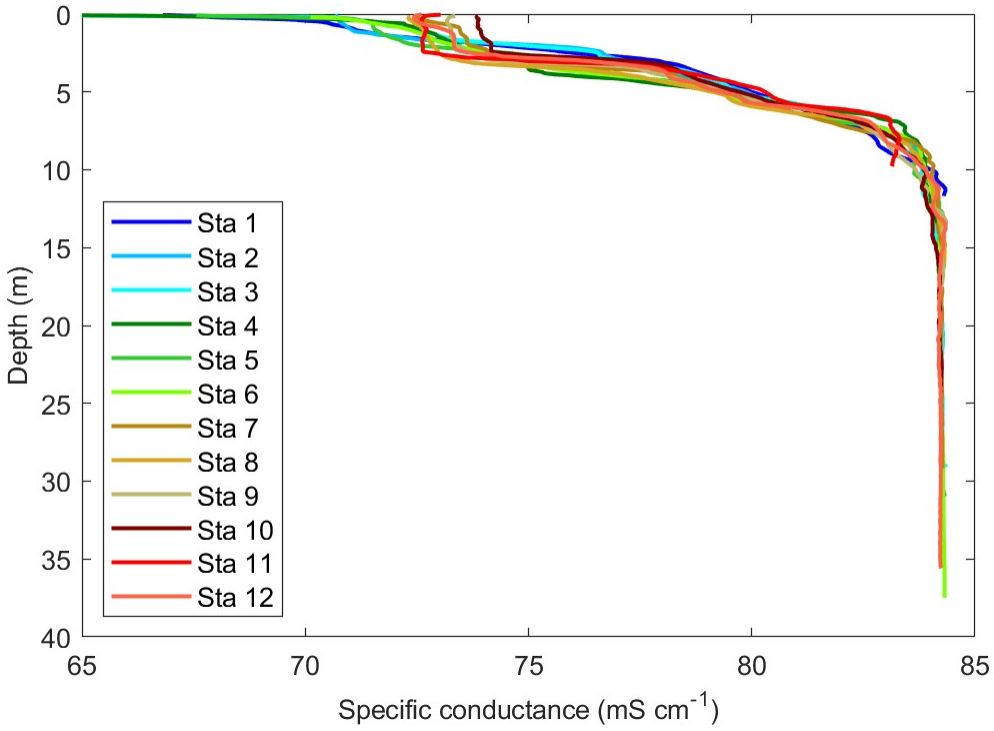

Specific conductance near-surface (2 m) at western stations ranged from 63.9 to 70.7 mS cm^{-1} in August (Fig. 26), and from 66.8 to 72.8 mS cm^{-1} in September (Fig. 27). Specific conductance near-surface (2 m) at eastern stations ranged only from 70 – 71.5 mS cm^{-1} in August, and from 72.6 to 73.1 mS cm^{-1} in September. The mixolimnion deepened to 6 m by September, and specific conductance remained similar among western and eastern stations.

Fig. 26. Specific conductance (mS cm^{-1}), 17 August 2023.

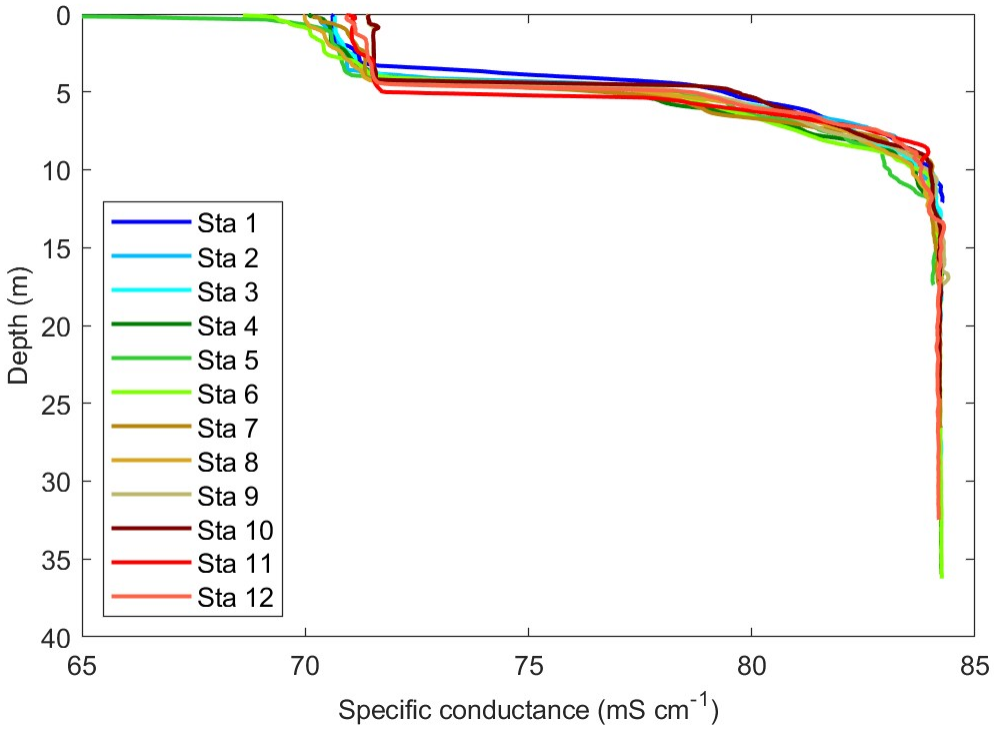

Fig. 27. Specific conductance (mS cm^{-1}), 18 September 2023.

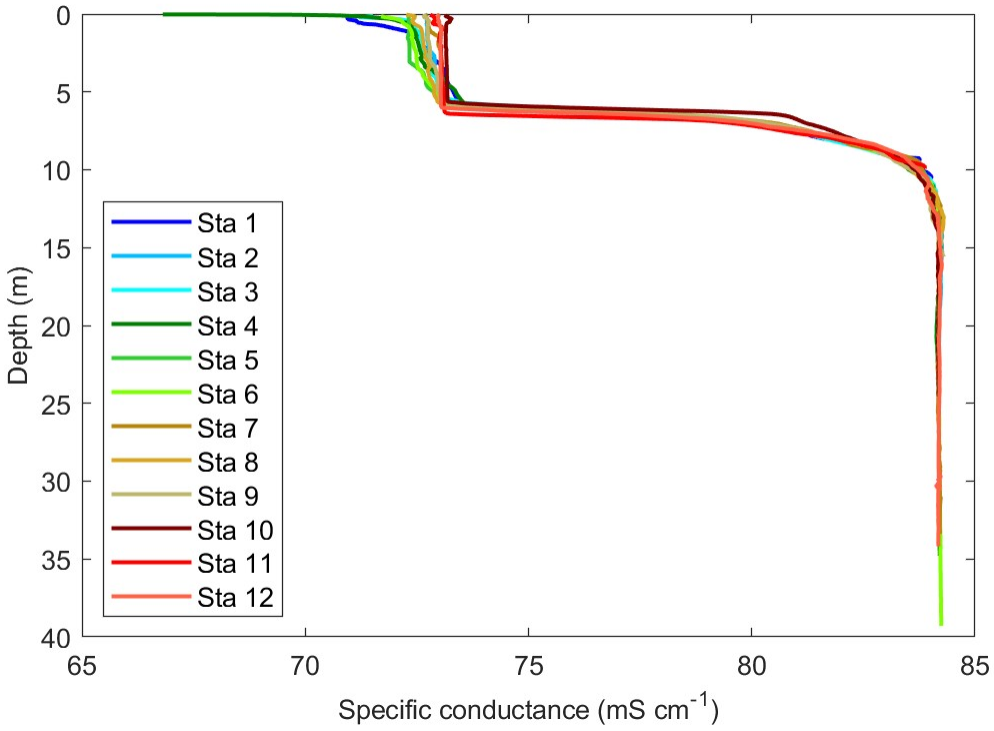

As inflows reduced during the autumn (October, November and December), specific conductances increased slightly in the upper water (2 m) to 71.7–73.1 mS cm^{-1} in October (Fig. 28), 74.4–75.6 mS cm^{-1} in November (Fig. 29), and 73.7–76.1 mS cm^{-1} in December (Fig. 30).

Fig. 28. Specific conductance (mS cm^{-1}), 12 October 2023.

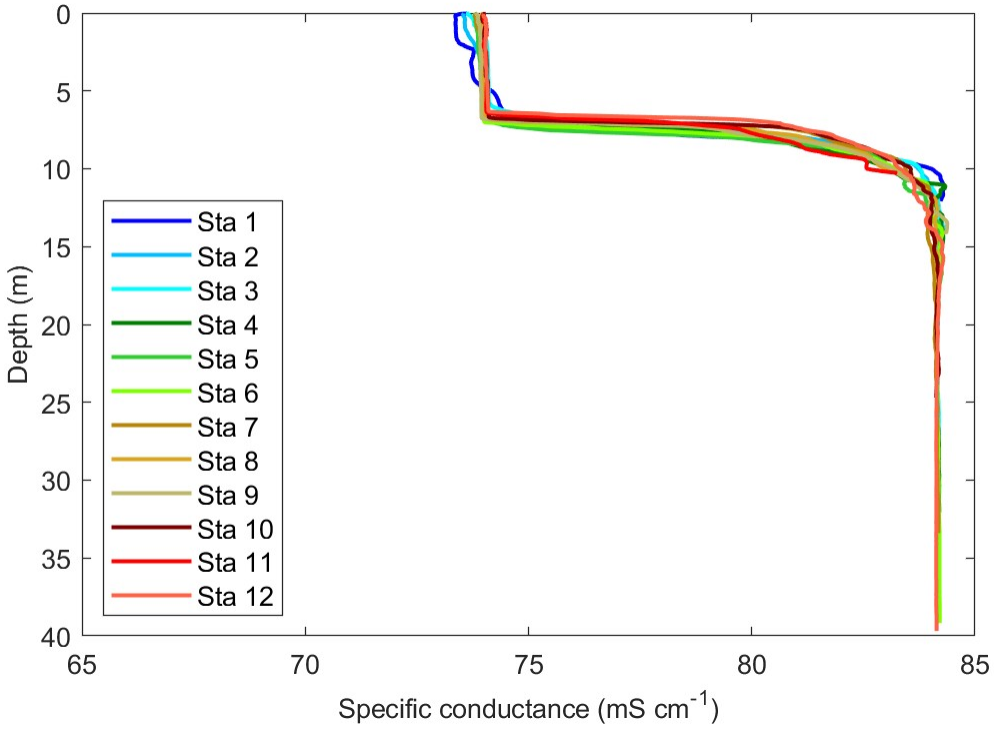

Fig. 29. Specific conductance (mS cm^{-1}), 14 November 2023.

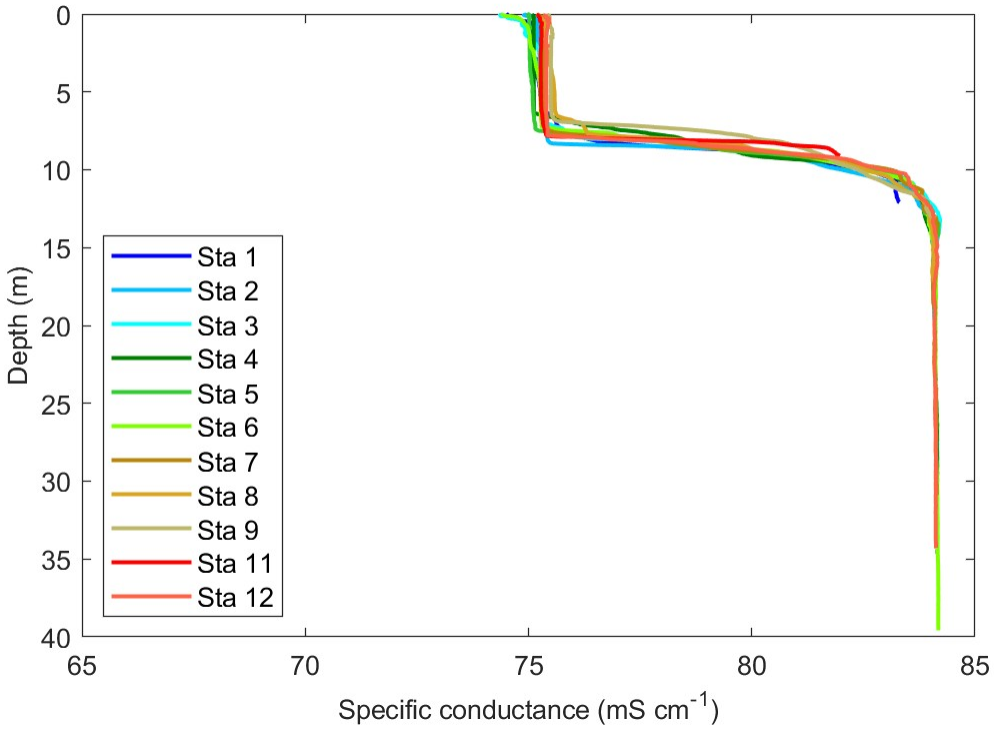

Fig. 30. Specific conductance (mS cm^{-1}), 12 December 2023.

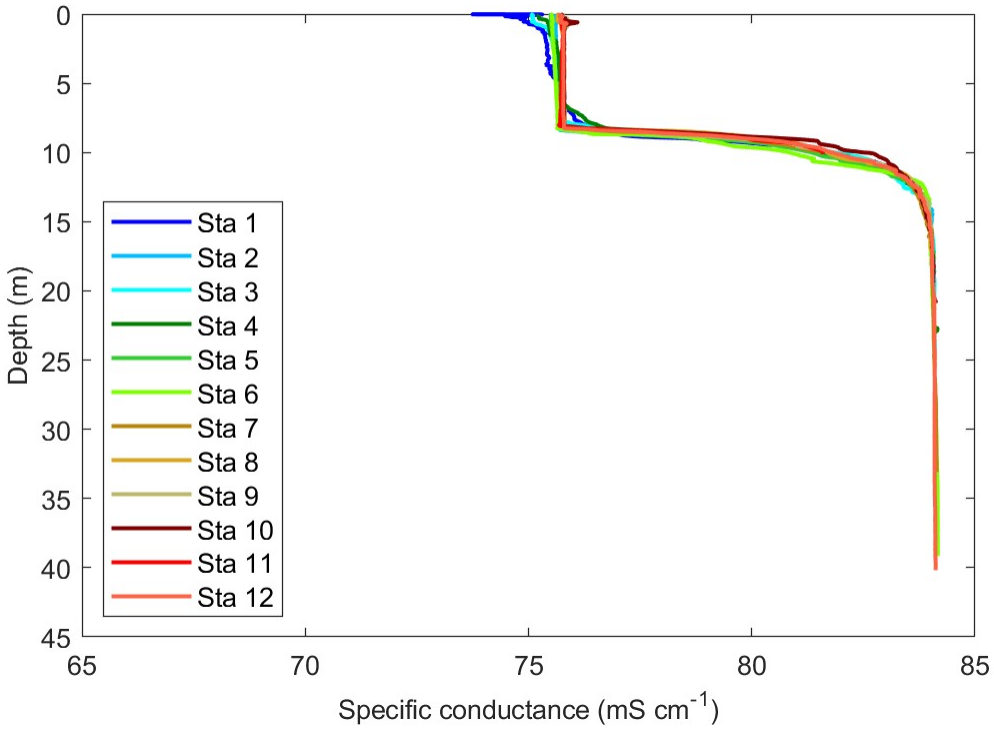

Fig. 31. Seasonal specific conductance at Station 6.

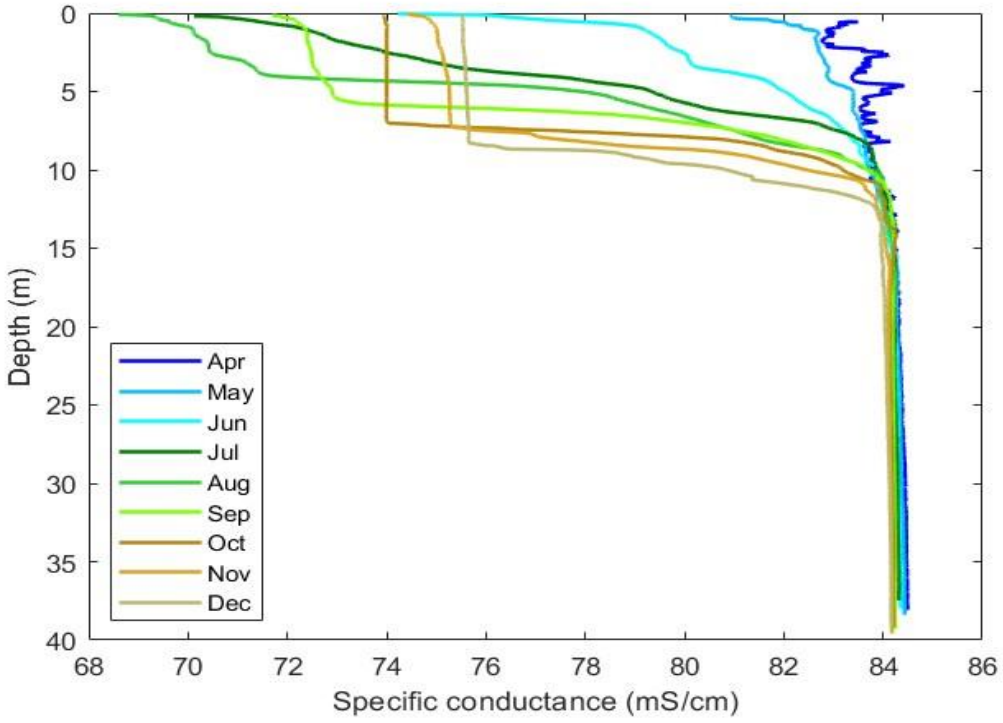

Fig. 32. Specific conductance (mS cm^{-1} at 25 ºC) at Station 6, 2023 (red triangles indicate sampling dates).

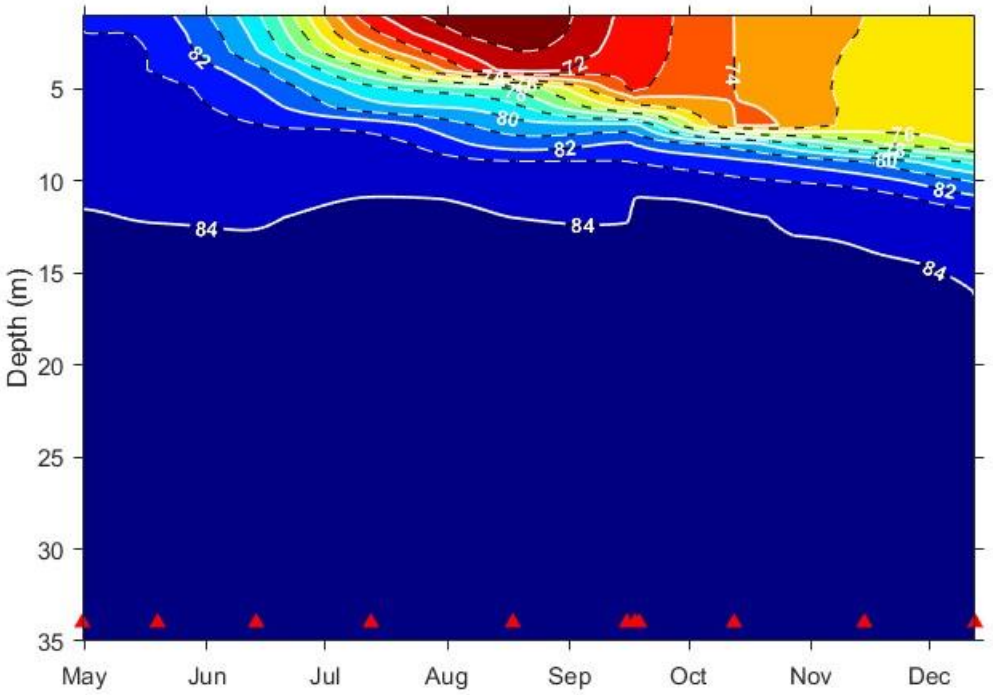

Table 2. Specific conductance (mS cm^{-1} at 25ºC) at Station 6, April–December, 2023.

Depth (m)	4/30	5/19	6/13	7/12	8/17	9/18	10/12	11/14	12/12
1	82.9	82.4	79.2	72.3	70.1	72.4	74.0	75.0	75.5
2	83.0	82.7	79.6	73.3	70.4	72.4	74.0	75.0	75.5
3	83.7	82.8	80.1	74.8	71.1	72.5	74.0	75.2	75.6
4	83.4	82.9	81.3	77.1	71.7	72.6	74.0	75.2	75.6
5	83.9	83.4	82.0	79.3	77.9	72.9	74.0	75.3	75.6
6	83.5	83.4	82.5	80.3	79.2	75.2	74.0	75.3	75.6
7	83.7	83.5	83.0	82.6	80.5	80.0	74.0	75.3	75.6
8	83.9	83.6	83.4	83.5	81.5	81.9	80.5	77.3	75.6
9	83.8	83.7	83.6	83.8	83.1	83.0	82.3	81.0	78.7
10	83.8	83.7	83.9	83.9	83.7	83.7	83.2	82.5	80.8
11	83.9	83.9	83.9	84.0	84.0	84.0	83.9	83.6	82.3
12	84.1	84.0	84.0	84.1	84.0	84.2	84.0	83.9	83.6
13	84.1	84.1	84.0	84.2	84.1	84.2	84.0	84.0	83.9
14	84.2	84.2	84.1	84.2	84.1	84.2	84.3	84.0	84.0
15	84.3	84.2	84.2	84.2	84.2	84.2	84.2	84.1	84.0
16	84.2	84.3	84.2	84.2	84.2	84.2	84.2	84.1	84.0
17	84.2	84.3	84.2	84.2	84.2	84.2	84.2	84.1	84.0
18	84.3	84.3	84.2	84.2	84.2	84.2	84.1	84.1	84.0
19	84.3	84.3	84.2	84.2	84.2	84.2	84.1	84.1	84.0
20	84.3	84.3	84.2	84.2	84.2	84.2	84.1	84.1	84.0
21	84.3	84.3	84.3	84.2	84.2	84.2	84.1	84.1	84.1
22	84.3	84.3	84.3	84.2	84.2	84.2	84.1	84.1	84.1
23	84.3	84.3	84.3	84.2	84.2	84.2	84.2	84.1	84.1
24	84.4	84.3	84.3	84.2	84.2	84.2	84.2	84.1	84.1
25	84.4	84.4	84.3	84.2	84.2	84.2	84.2	84.1	84.1
26	84.4	84.4	84.3	84.3	84.2	84.2	84.2	84.1	84.1
27	84.4	84.4	84.3	84.3	84.2	84.2	84.2	84.1	84.1
28	84.4	84.4	84.3	84.3	84.2	84.2	84.2	84.1	84.1
29	84.4	84.4	84.3	84.3	84.2	84.2	84.2	84.1	84.1
30	84.4	84.4	84.3	84.3	84.2	84.2	84.2	84.2	84.1
31	84.5	84.4	84.3	84.3	84.2	84.2	84.2	84.2	84.1
32	84.5	84.4	84.3	84.3	84.3	84.2	84.2	84.2	84.1
33	84.5	84.4	84.3	84.3	84.2	84.2	84.2	84.2	84.2
34	84.5	84.4	84.3	84.3	84.2	84.2	84.2	84.2	84.2
35	84.5	84.4	84.3	84.3	84.3	84.2	84.2	84.2	84.2
36	84.5	84.4	84.4	84.3	84.3	84.2	84.2	84.2	84.2
37	84.5	84.4	84.4	84.3		84.2	84.2	84.2	84.2
38	84.5	84.4				84.2	84.2	84.2	84.2
39						84.2	84.2	84.2	84.2

Density Stratification: Thermal and Chemical

The large seasonal variation in freshwater inflows observed in the eastern Sierra Nevada and year-to-year climatic variation has led to complex patterns of seasonal density stratification over the last 40 years. Much of the year-to-year variation in the plankton dynamics observed at Mono Lake can be attributed to marked differences in chemical stratification resulting from variation in freshwater inflows and its effect on nutrient cycling. Density difference between 2 and 32 m varied from 3.9 to 20.3 kg m^{-3} over the course of the 2023 year (Fig. 33).

Seasonal density stratification reflects contributions from both thermal and salinity stratification (Fig. 33). Peak stratification during monomictic periods usually occurs during July due to the combined effect of spring runoff and warm epilimnetic temperatures. In 2023, peak stratification occurred in August when the difference in salinity between 2 and 32 m contributed 15.6 kg m^{-3} to vertical density stratification compared to 4.7 kg m^{-3} due to temperature stratification. The overall density stratification in August was as high as during the 1982–1988 meromictic episode (Jellison and Melack 1993).

Fig. 33. Density stratification between 2 and 32 m, 2023.

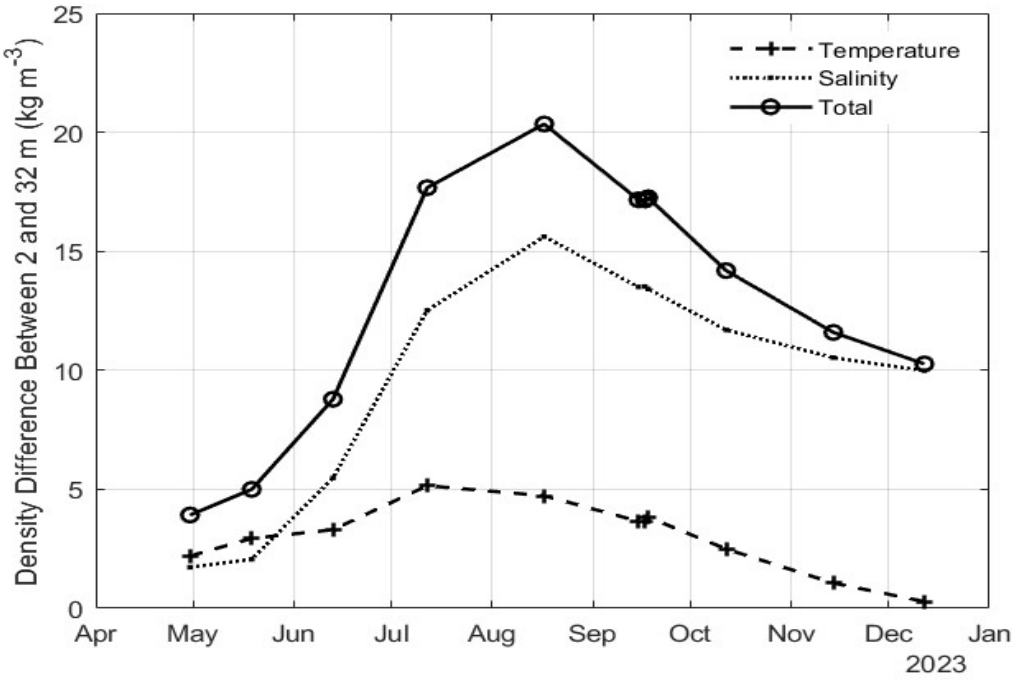

Transparency and Light Attenuation

In Mono Lake, variation in transparency is largely due to changes in algal biomass. Standing algal biomass reflects the balance between growth and loss processes (e.g., grazing). Thus, variation in transparency as measured by Secchi depth often reflects abundance of *Artemia* as well as changes in nutrient availability and primary productivity.

The lakewide mean Secchi transparency was 0.43±0.01 m in April and 0.42±0.02 m in May (Table 3). Transparency increased throughout the year to 7.1±0.13 m in mid-September before decreasing to 2.4±0.07 m by November and 2.3±0.03 m in December.

Table 3. Secchi depths (m), April–December, 2023. S.E. is standard error. 'n' in last rows refers to number of stations averaged.

	Dates								
Station	4/30	5/19	6/13	7/12	8/17	9/18	10/12	11/14	12/12
Western sector									
1	0.42	0.30	0.65	5.0	6.3	7.2	7.2	2.2	2.1
2	0.40	0.42	0.80	5.3	6.9	7.2	6.6	2.3	2.4
3	0.40	0.40	0.80	5.0	6.6	7.5	5.5	2.5	2.4
4	0.45	0.42	0.80	5.2	6.8	6.9	5.9	2.4	2.3
5	0.45	0.40	0.70	5.6	7.0	7.3	6.6	2.4	2.3
6	0.37	0.38	0.75	5.5	6.5	7.3	7.0	2.9	2.2
Mean	0.42	0.39	0.75	5.3	6.7	7.2	6.5	2.5	2.3
S.E.	0.01	0.02	0.03	0.1	0.1	0.1	0.3	0.1	0.0
n	6	6	6	6	6	6	6	6	6
Eastern sector									
7	0.45	0.42	0.90	5.0	6.1	7.4	6.2	2.6	2.3
8	0.45	0.45	0.80	5.9	5.7	7.5	5.8	2.3	2.3
9	0.50	0.50	0.78	4.6	6.4	7.1	5.6	2.5	2.1
10	0.48	0.52	0.78	4.9	6.4	7.0	6.0	2.7	2.1
11	0.31	0.38	0.85	4.3	5.6	6.0	5.5	2.1	2.3
12	0.45	0.50	0.90	4.6	5.9	6.5	5.7	2.1	2.2
Mean	0.44	0.46	0.84	4.9	6.0	6.9	5.8	2.4	2.2
SE	0.03	0.02	0.02	0.2	0.1	0.2	0.1	0.1	0.0
n	6	6	6	6	6	6	6	6	6
Lakewide									
Mean	0.43	0.42	0.79	5.1	6.4	7.1	6.1	2.4	2.3
S.E.	0.01	0.02	0.02	0.1	0.1	0.1	0.2	0.1	0.0
n	12	12	12	12	12	12	12	12	12

Attenuation of PAR within the water column varies seasonally, primarily as a function of changes in algal biomass (Fig. 34).

Fig. 34. PAR light attenuation (fraction of surface) at Station 6, 2023.

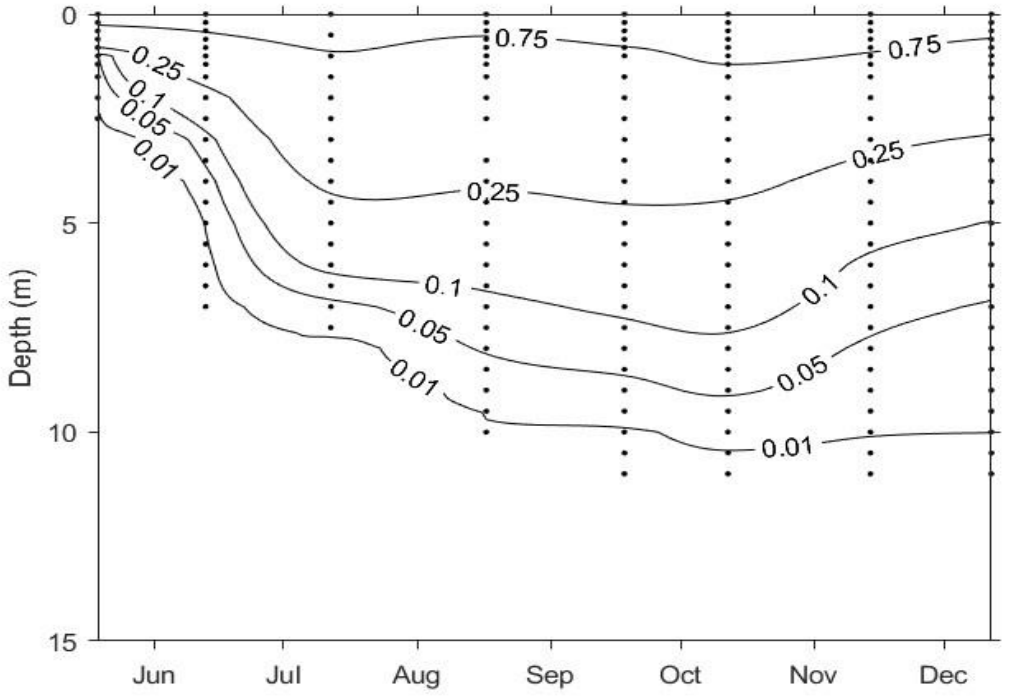

Dissolved Oxygen

Dissolved oxygen concentrations are a function of salinity, temperature, and the balance between photosynthesis and community respiration. In the euphotic zone of Mono Lake, dissolved oxygen concentrations are typically highest during the spring. As the water temperature and *Artemia* population increase through the spring, dissolved oxygen concentrations decrease. Beneath the euphotic zone, bacterial and chemical processes deplete the oxygen once the lake stratifies. During meromictic periods, the monimolimnion (the region beneath the persistent chemocline) remains anoxic throughout the year.

In 2023, dissolved oxygen concentrations in the upper mixed layer (≤10 m) ranged from 0.8 to 13.7 mg L^{-1} (Table 4, Fig. 35, Fig. 36) with the highest concentrations occurring in the upper 5 m during April and May and at a mid-depth algal peak during October. The lowest epilimnetic values occurred during July when dissolved oxygen was

2–2.8 mg L^{-1} in the upper 5 m of the water column. The lower hypolimnion below 20 m was suboxic during April and became anoxic (<0.5 mg L^{-1}) below 14 m by June. The absence of autumn holomixis resulted in anoxic conditions remaining below 14 m through the remainder of the year.

Fig. 35. Seasonal dissolved oxygen at Station 6.

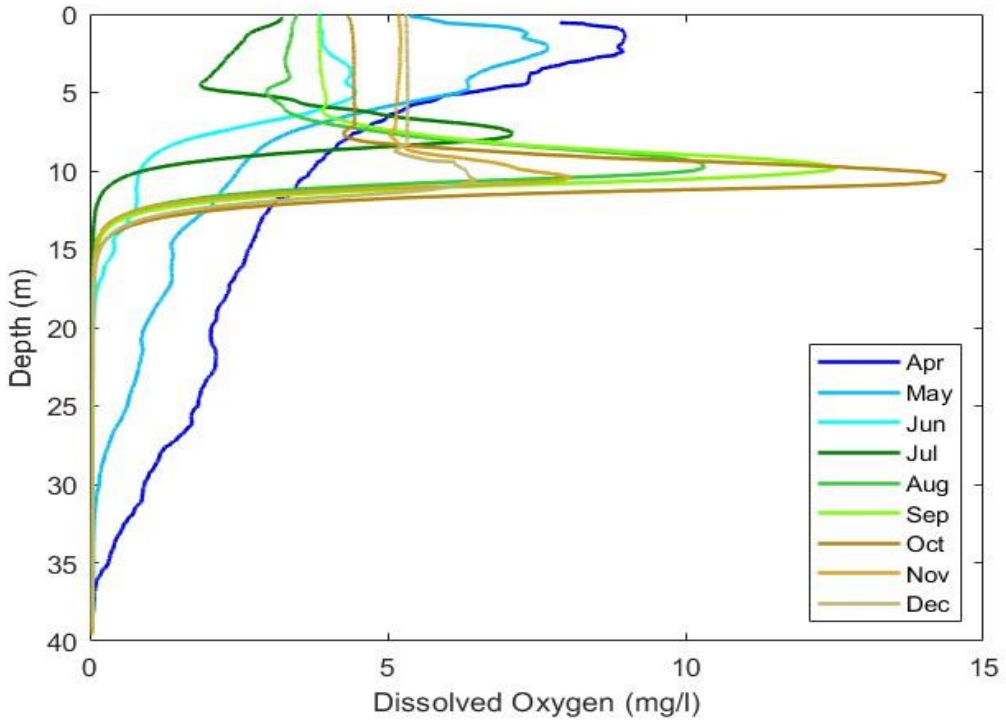

Fig. 36. Dissolved oxygen (mg L^{-1}) at Station 6, 2023.

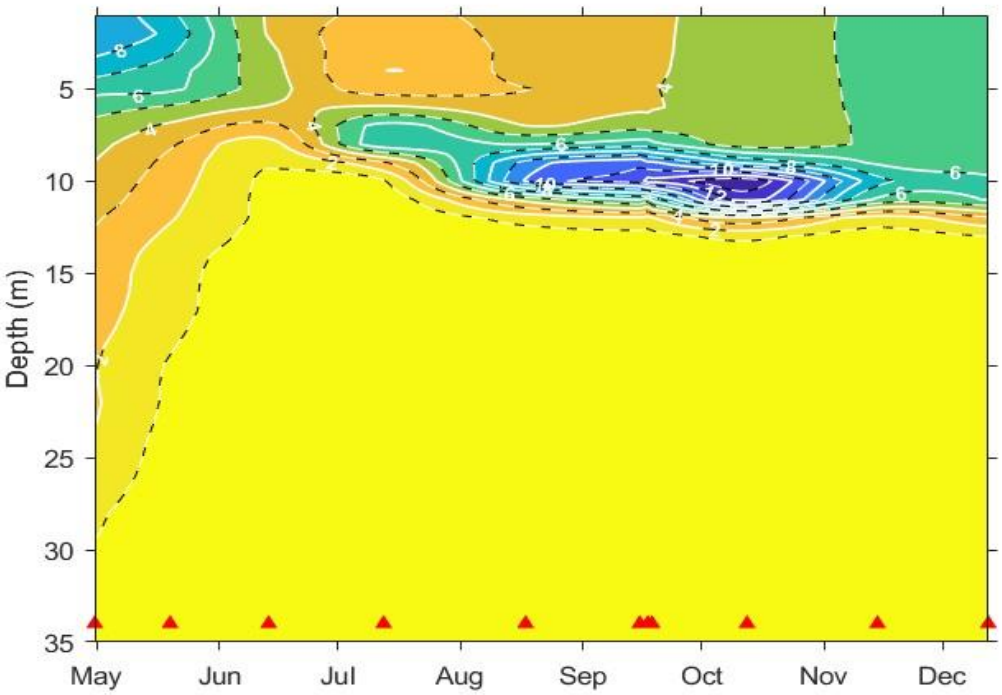

Table 4. Dissolved oxygen (mg L^{-1}) at Station 6, April–December, 2023.

Depth (m)	4/30	5/19	6/13	7/12	8/17	9/18	10/12	11/14	12/12
1	8.9	7.2	3.9	2.8	3.4	3.9	4.4	5.2	5.3
2	8.9	7.7	3.9	2.5	3.3	3.9	4.4	5.2	5.3
3	8.2	7.1	4.2	2.3	3.3	3.9	4.4	5.2	5.3
4	7.4	6.4	4.4	2.0	3.4	3.9	4.4	5.2	5.3
5	6.4	6.2	4.5	2.4	3.0	4.0	4.4	5.2	5.3
6	5.3	4.9	3.9	4.1	3.3	3.9	4.4	5.2	5.3
7	4.7	3.8	2.8	6.3	4.0	4.5	4.4	5.1	5.3
8	4.3	3.1	1.6	6.7	6.0	6.3	4.4	5.1	5.3
9	4.0	2.7	1.1	2.9	9.3	10.2	7.8	5.8	5.3
10	3.7	2.5	0.8	0.9	10.1	12.3	13.7	7.4	6.3
11	3.5	2.3	0.8	0.3	4.3	6.3	12.4	5.9	6.1
12	3.1	2.1	0.8	0.1	1.4	1.9	3.8	1.6	2.8
13	2.9	1.8	0.7	0.1	0.5	0.6	1.2	0.5	1.0
14	2.8	1.5	0.5	0.1	0.2	0.2	0.4	0.2	0.4
15	2.7	1.4	0.4	0.1	0.1	0.1	0.2	0.1	0.2
16	2.6	1.4	0.3	0.1	0.1	0.1	0.1	0.1	0.1
17	2.4	1.4	0.2	0.0	0.1	0.1	0.1	0.1	0.1
18	2.3	1.2	0.1	0.0	0.1	0.1	0.1	0.1	0.1
19	2.1	1.1	0.1	0.0	0.1	0.1	0.1	0.1	0.1
20	2.0	0.9	0.1	0.0	0.1	0.1	0.1	0.1	0.1
21	2.0	0.9	0.1	0.0	0.1	0.1	0.1	0.1	0.1
22	2.1	0.9	0.1	0.0	0.1	0.1	0.1	0.1	0.1
23	2.0	0.8	0.1	0.0	0.1	0.1	0.1	0.1	0.1
24	1.9	0.7	0.1	0.0	0.1	0.1	0.1	0.1	0.1
25	1.8	0.6	0.1	0.0	0.0	0.0	0.1	0.1	0.1
26	1.7	0.5	0.1	0.0	0.0	0.0	0.1	0.0	0.1
27	1.5	0.4	0.1	0.0	0.0	0.0	0.1	0.1	0.1
28	1.2	0.3	0.1	0.0	0.0	0.0	0.1	0.0	0.1
29	1.1	0.2	0.0	0.0	0.0	0.0	0.0	0.0	0.1
30	0.9	0.2	0.1	0.0	0.0	0.0	0.0	0.0	0.1
31	0.9	0.1	0.0	0.0	0.0	0.0	0.0	0.0	0.0
32	0.7	0.1	0.1	0.0	0.0	0.0	0.0	0.0	0.0
33	0.5	0.1	0.1	0.0	0.0	0.0	0.0	0.0	0.0
34	0.4	0.1	0.0	0.0	0.0	0.0	0.0	0.0	0.0
35	0.3	0.1	0.0	0.0	0.0	0.0	0.0	0.0	0.0
36	0.1	0.1	0.0	0.0	0.0	0.0	0.0	0.0	0.0
37	0.1	0.1	0.0	0.0		0.0	0.0	0.0	0.0
38	0.1	0.1				0.0	0.0	0.0	0.0
39						0.0	0.0	0.0	0.0

Fluorescence

Fluorescence intensity (as measured by the Rinko profiler) provides an indication of amount of chlorophyll, but is influenced by differences in the species and physiological condition of the phytoplankton.

In 2023, fluorescence at Station 6 (Fig. 37) in the upper water (2 m) in April, May, and June was higher than in July to December. From July onwards, high

fluorescence occurred between depths of 6 to 8 m, and deepened by December with high fluorescence found between 8 and 12 m. Below 15 m, vertical variations in fluorescence were muted, but shifted seasonally with lower values from October to December.

Fig. 37. Seasonal fluorescence profiles at Station 6.

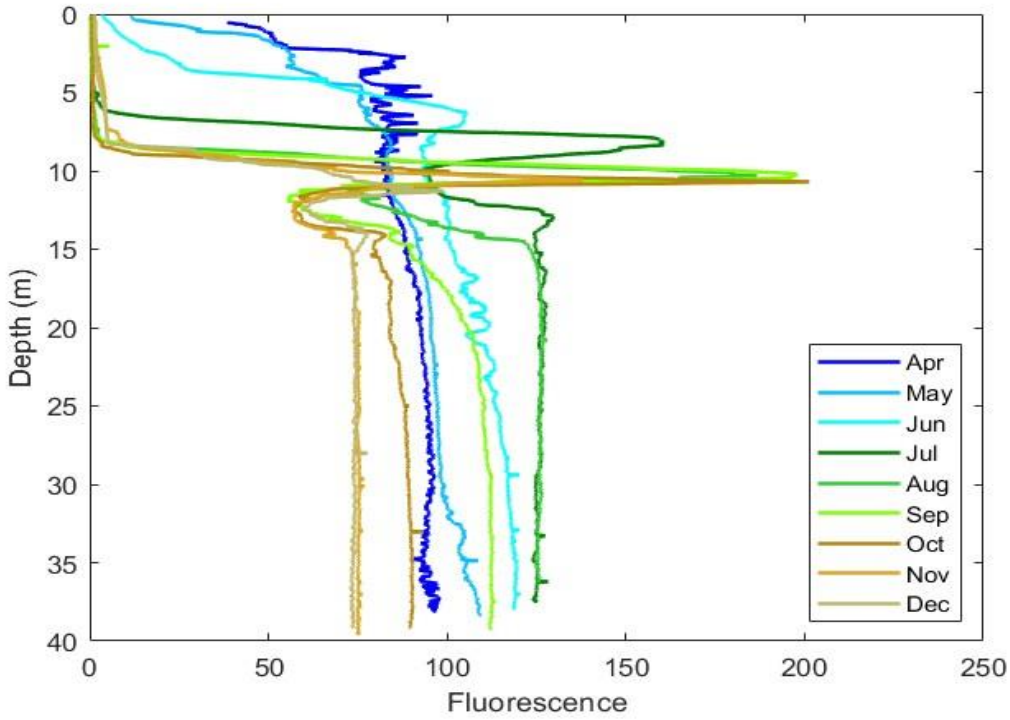

Vertical Distributions of Temperature, Specific Conductance, Dissolved Oxygen and Fluorescence (Station 6): Summer and Autumn

Beginning in July, a conspicuous peak in dissolved oxygen and fluorescence occurred in the pyncocline associated with gradients in temperature and specific conductance (Fig. 38 to Fig. 43). A likely reason for the elevated dissolved oxygen is photosynthetic oxygen production by abundant phytoplankton, as indicated by the peak in fluorescence intensity. Within the pynocline vertical mixing would be reduced and confine the oxygen production to this narrow zone. *Artemia* could preferentially graze this zone of elevated phytoplankton. Discrete-depth sampling of *Artemia* would be required to examine this possibility.

Fig. 38. Temperature, specific conductance, dissolved oxygen, and fluorescence at Station 6, 12 July 2023.

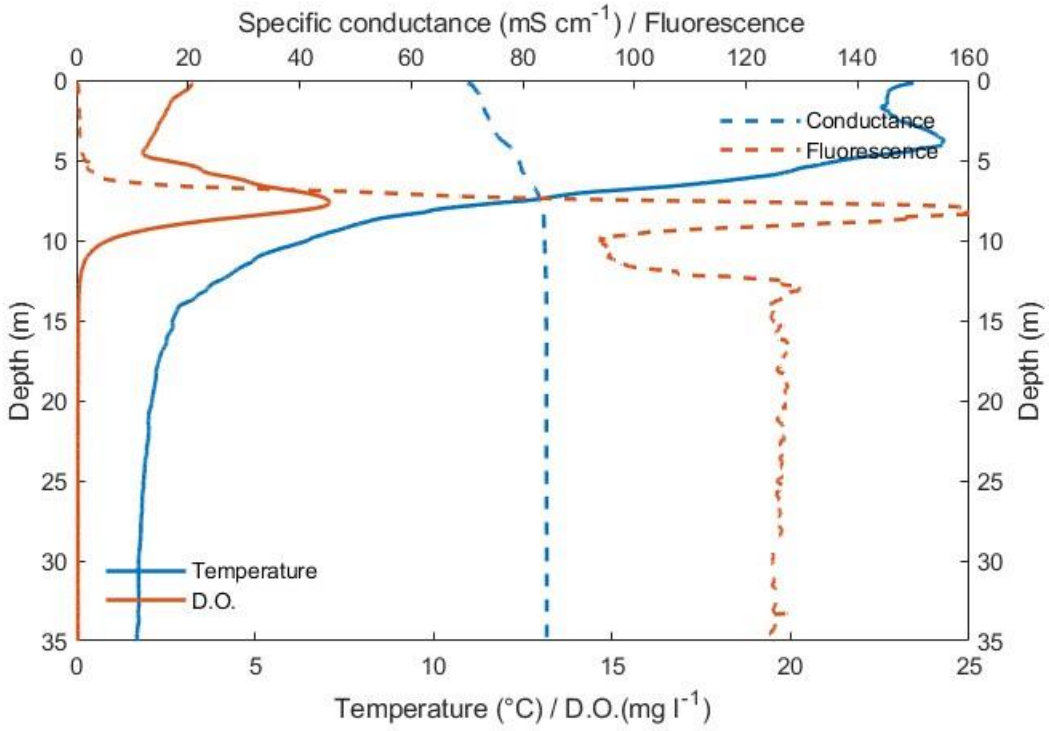

Fig. 39. Temperature, specific conductance, dissolved oxygen, and fluorescence at Station 6, 17 August 2023.

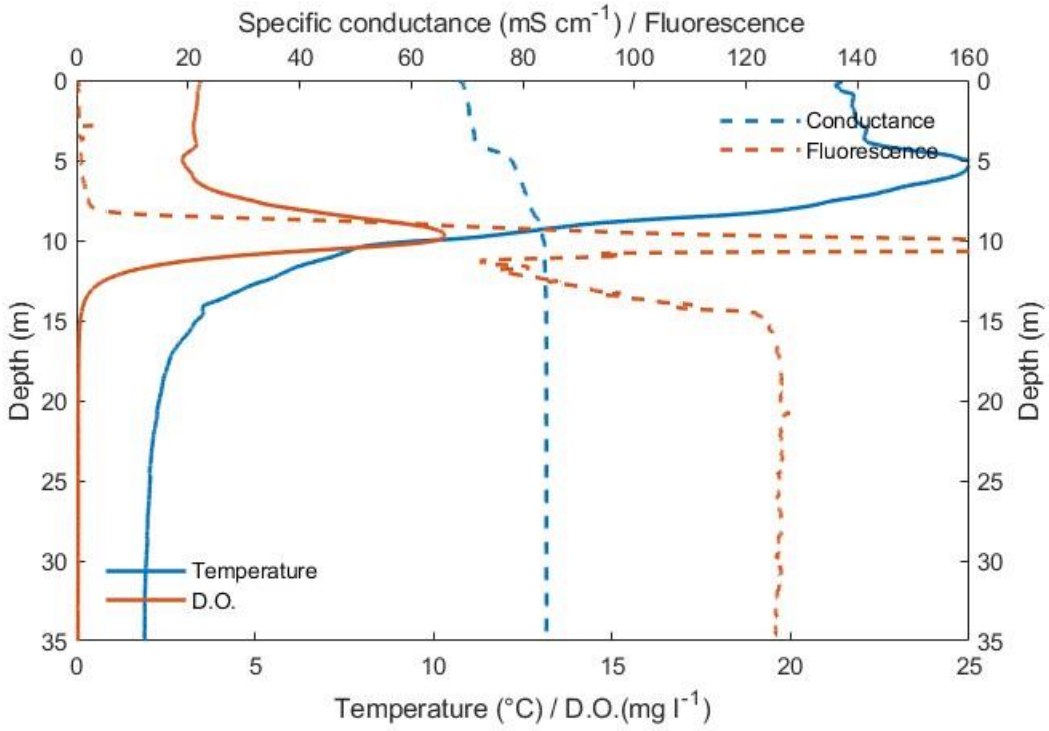

Fig. 40. Temperature, specific conductance, dissolved oxygen, and fluorescence at Station 6, 18 September 2023.

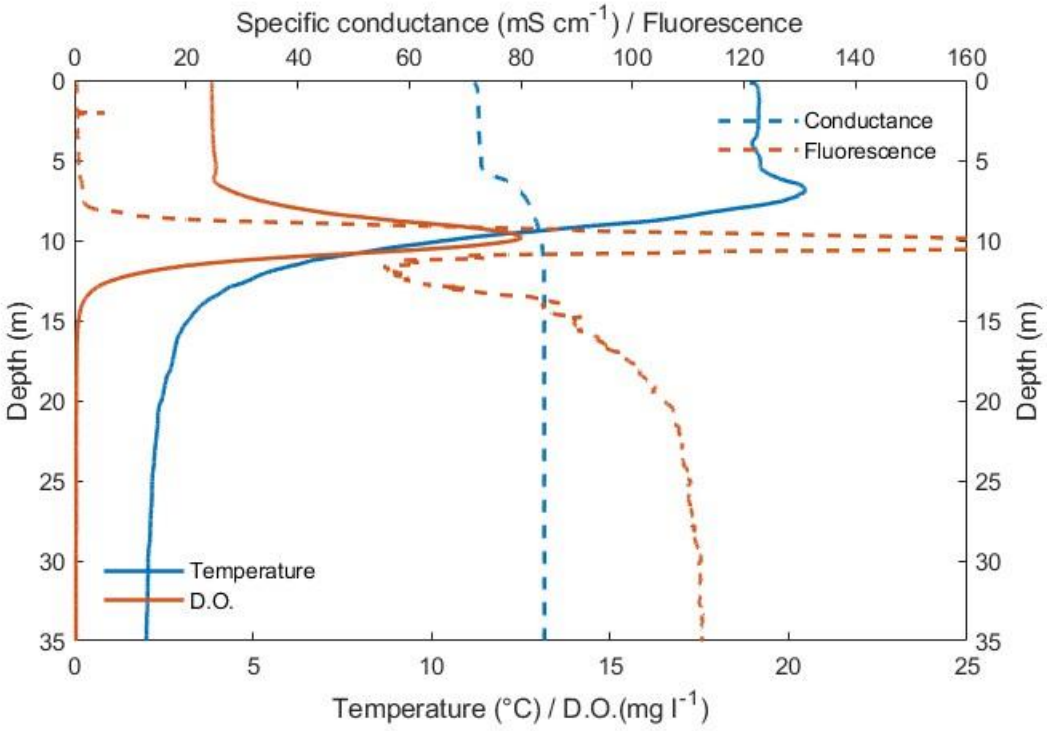

Fig. 41. Temperature, specific conductance, dissolved oxygen, and fluorescence at Station 6, 12 October 2023.

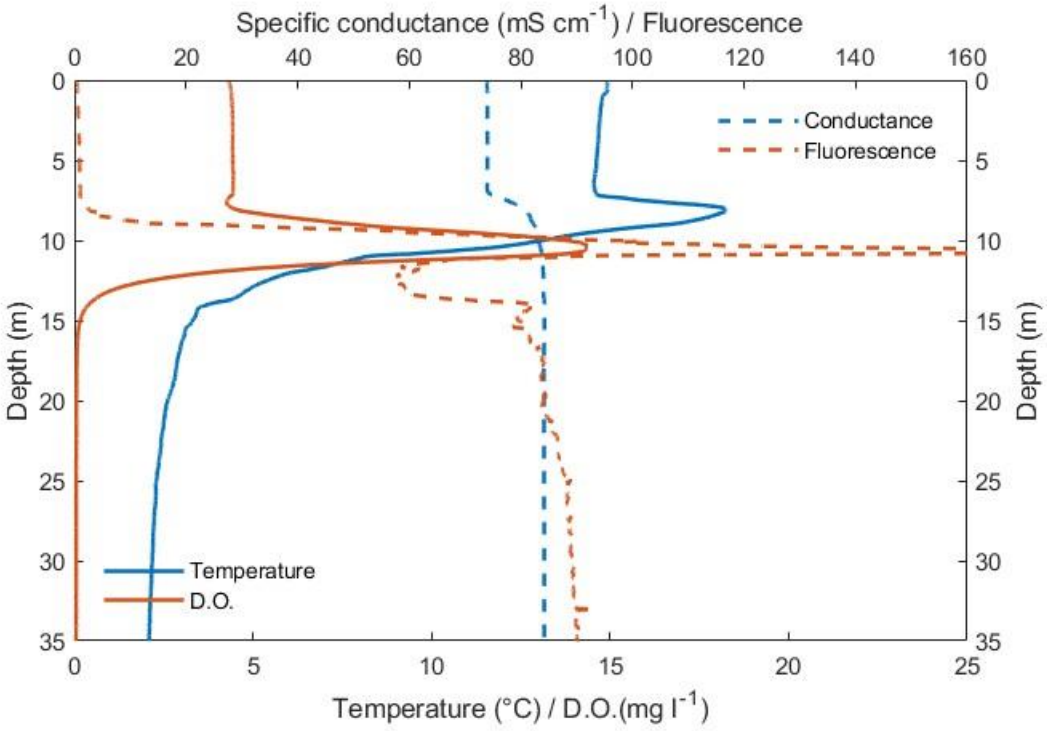

Fig. 42. Temperature, specific conductance, dissolved oxygen, and fluorescence at Station 6, 14 November 2023.

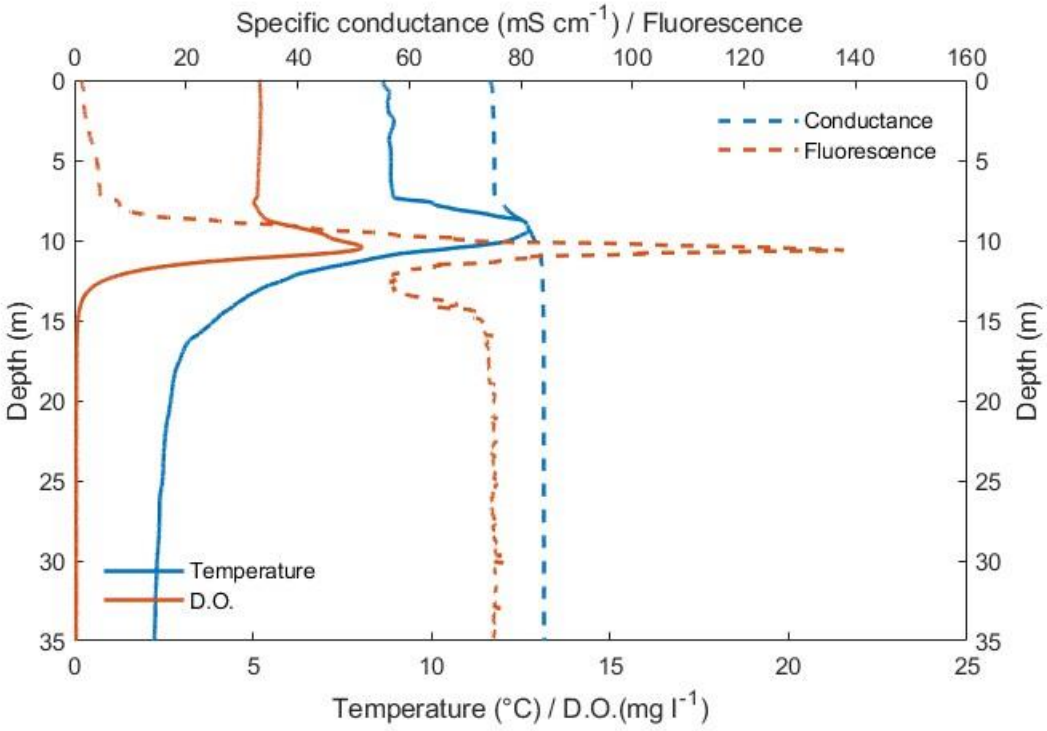

Fig. 43. Temperature, specific conductance, dissolved oxygen, and fluorescence at Station 6,12 December 2023.

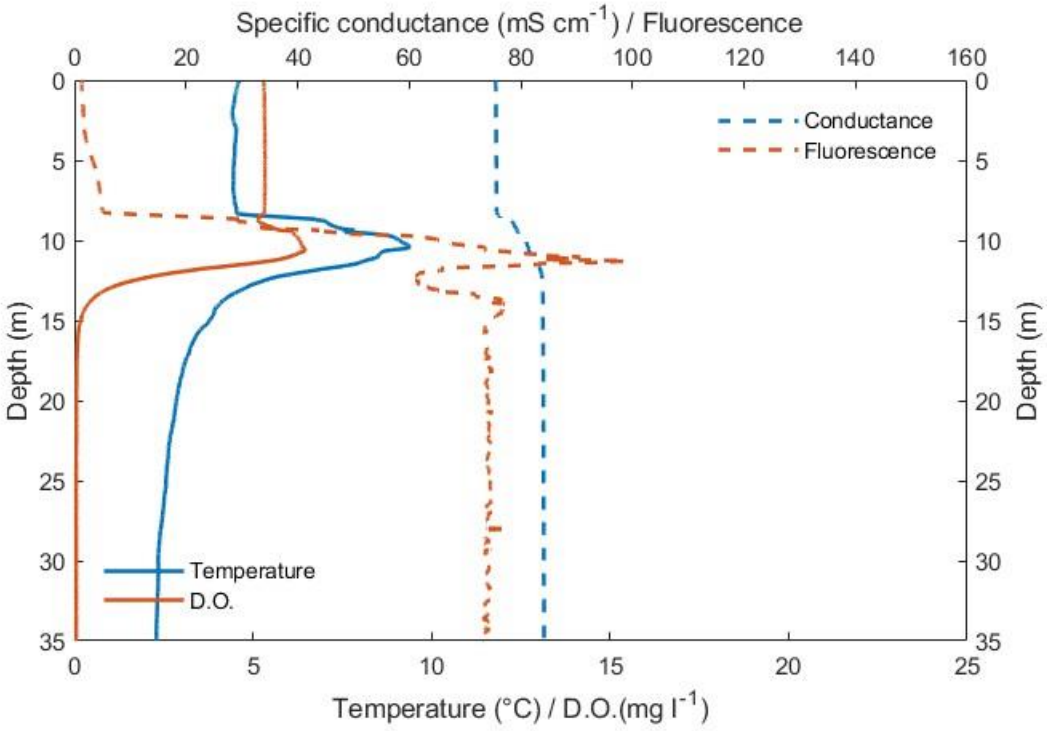

Nutrients (ammonium)

Nitrogen is the primary limiting macronutrient in Mono Lake as phosphate is abundant (350-450 µM) throughout the year (Jellison *et al.* 1994). External inputs of nitrogen are low relative to recycling fluxes within the lake (Jellison and Melack 1993a, b). Ammonium concentrations in the euphotic zone reflect the dynamic balance between excretion by shrimp, uptake by algae, upward vertical fluxes through thermocline and chemocline, release from sediments, ammonium volatilization, and small external inputs. Because a large portion of particulate nitrogen, in the form of algal debris and *Artemia* fecal pellets, sink to the bottom and are remineralized to ammonium in the hypolimnion (or monimolimnion during meromixis), vertical mixing controls much of the annual internal recycling of nitrogen.

During 2023 ammonium concentrations at the deep, central Station 6 exhibited the typical pattern of low concentrations in the epilimnion and a seasonal increase to >50 µM in the hypolimnion (Table 5, Fig. 44). On 19 May 2023, ammonium concentrations ranged from 4.2 to 5.2 µM at 12 m and above and reached 17.7 µM at 35 m. The seasonal increase in hypolimnetic ammonia led to concentrations near the bottom of 54–77 µM during October through December.

Table 5. Ammonium (µM) profiles at Station 6, May–December, 2023. Depth profile was not taken during the April survey due to weather conditions.

Depth	Dates							
(m)	5/19	6/13	7/12	8/17	9/18	10/12	11/14	12/12
0.2			4.8	1.7	0.9	1.3	0.8	0.7
2	5.2	1.2	2.7	1.2	0.6	1.1	0.9	0.8
8	4.3	2.9	2.1	1.3	0.5	1.3	1.1	0.8
12	4.2	2.8	5.3	5.9	14.3	16.8	24.3	13.9
16	10.2	7.6	13.2	16.2	31.9	45.9	53.7	58.1
20	12.3	9.0	18.2	18.9	37.7	59.1	55.8	63.1
24	13.5	14.6	17.8	20.6	36.0	57.3	62.1	71.2
28	15.8	17.9	16.0	22.8	38.9	55.1	67.8	73.8
35	17.7	22.7	26.9	32.3	35.1	58.1	73.3	76.7

Fig. 44. Ammonium at Station 6, 2023. Isopleths are ammonium concentrations (µM).

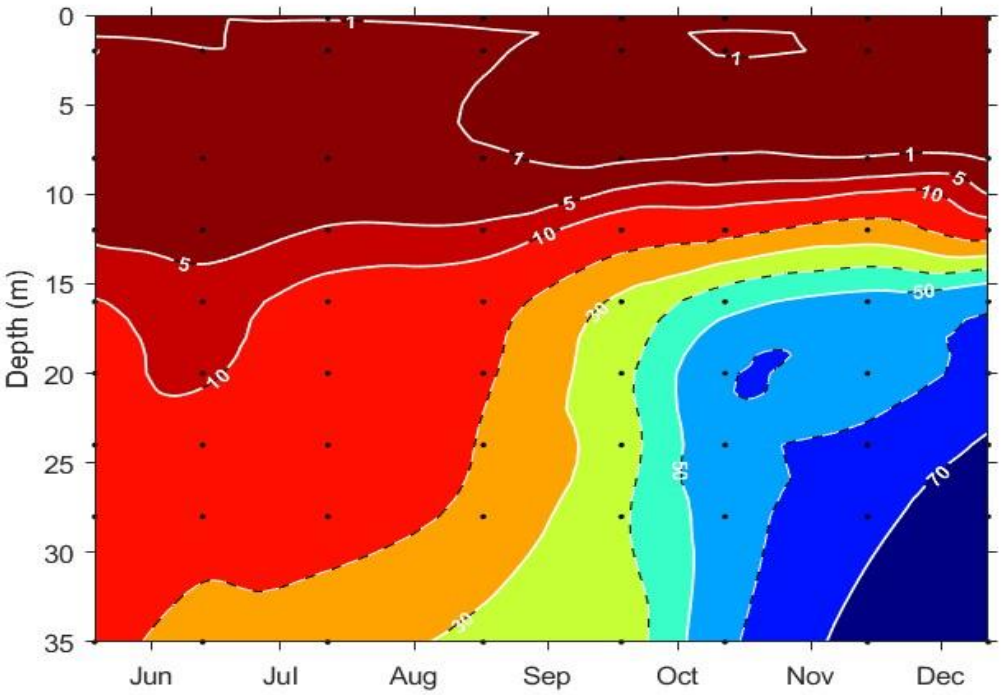

Epilimnetic concentrations as indicated by the upper 9-m integrated samples were generally less than 2 µM except during late spring (May) (Table 6, Fig. 45). During June, July, and August there was little ammonium variation from 1.2 to 2.2 µM, and during September, ammonium reached its lowest concentration (0.4 µM).

Table 6. Ammonium (µM) lakewide at 7 stations in upper 9 m of water column, April–December, 2023. S.E. is standard error.

	Dates								
Station	4/30	5/19	6/13	7/12	8/17	9/18	10/12	11/14	12/12
1	1.1	3.5	1.3	1.6	1.8	0.6	1.1	0.6	0.9
2	2.4	3.8	1.9	1.2	1.3	0.4	1.0	0.8	0.8
5	2.8	4.5	1.5	1.7	1.3	0.6	1.0	0.8	0.7
6	1.5	4.6	1.4	2.2	1.3	0.5	1.1	0.9	0.8
7	2.6	3.6	1.5	1.5	1.2	0.8	1.2	1.0	0.7
8	1.8	4.5	1.8	1.4	1.2	0.6	1.0	0.9	0.8
11	1.7	4.6	2.0	1.4	1.5	0.6	1.0	1.0	0.6
Mean	2.0	4.2	1.6	1.6	1.4	0.6	1.0	0.9	0.8
S.E.	0.2	0.2	0.1	0.1	0.1	0.0	0.0	0.0	0.0

Fig. 45. Ammonium (µM) in upper 9 m of the water column at 7 stations, 2023.

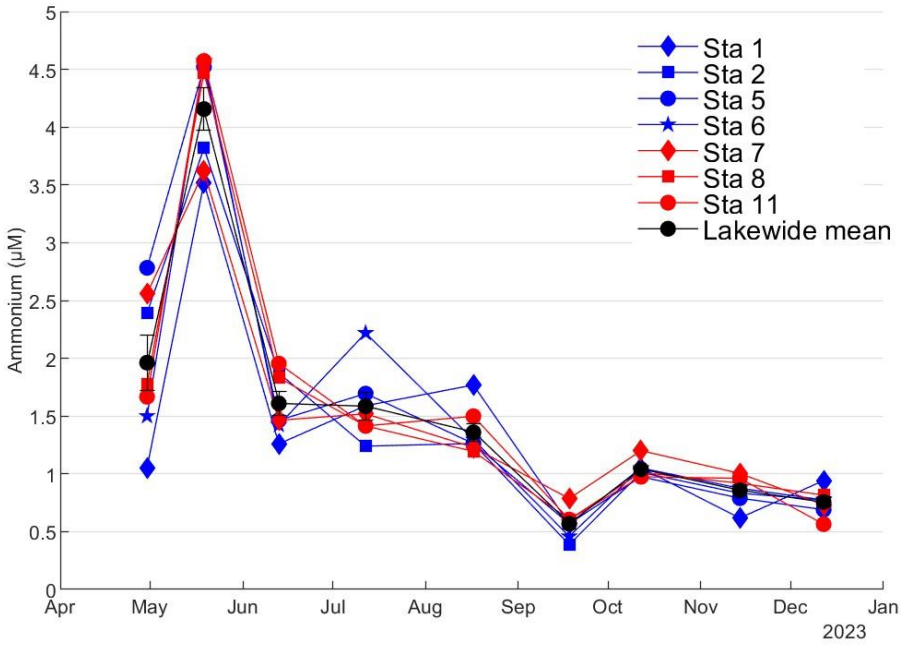

Phytoplankton

Phytoplankton abundance, as characterized by chlorophyll *a* concentration, shows pronounced seasonal variation. High phytoplankton abundance in spring is followed by low phytoplankton biomass during summer due to *Artemia* grazing.

On 19 May 2023 chlorophyll concentrations at Station 6 were high throughout the water column ranging from 90 to 145 µg chl L^{-1} (Table 7, Fig. 46. Chlorophyll *a* at Station 6, May–December, 2023. Isopleths of chlorophyll concentration (µg L^{-1}).Fig. 46), and remained high during June ranging from 21 to 157 µg chl L^{-1}. On 12 July near surface and 2 m concentrations had decreased to 0.6–1.7 µg chl L^{-1}. The lowest concentrations were found in late summer and autumn at 8 m and above, with small variations from 0.2 to 0.7 µg chl L^{-1} in August, 0.3 to 0.6 µg chl L^{-1} in September, and 0.2 to 0.4 µg chl L^{-1} in October. On November and December surveys, chlorophyll concentrations had increased slightly at 8 m and above, ranging from 0.8 to 1.2 µg chl L^{-1}. At 12 m and below, chlorophyll concentrations remained high, ranging from 97 to 150 µg chl L^{-1} in November and from 97 to 164 µg chl L^{-1} in December.

Table 7. Chlorophyll *a* (µg L^{-1}) at Station 6, May–December 2023. Depth profile was not taken during the April survey due to weather conditions.

Depth	Dates							
(m)	5/19	6/13	7/12	8/17	9/18	10/12	11/14	12/12
0.2			0.6	0.2	0.4	0.2	0.8	0.8
2	90.2	21.0	1.7	0.3	0.3	0.3	1.0	0.9
8	144.6	156.6	84.9	0.7	0.6	0.4	1.2	0.9
12	147.2	108.6	140.8	160.3	101.3	170.3	149.7	164.5
16	136.2	144.0	118.1	139.4	144.1	124.4	110.3	118.7
20	143.1	152.0	116.1	141.1	130.3	124.8	101.9	111.0
24	143.5	144.6	112.9	137.7	124.4	130.1	102.1	113.0
28	145.2	140.5	97.8	130.6	128.1	121.2	100.7	109.0
35	145.0	133.4	131.7	125.9	132.9	125.1	97.4	97.3

Fig. 46. Chlorophyll *a* at Station 6, May–December, 2023. Isopleths of chlorophyll concentration (µg L^{-1}).

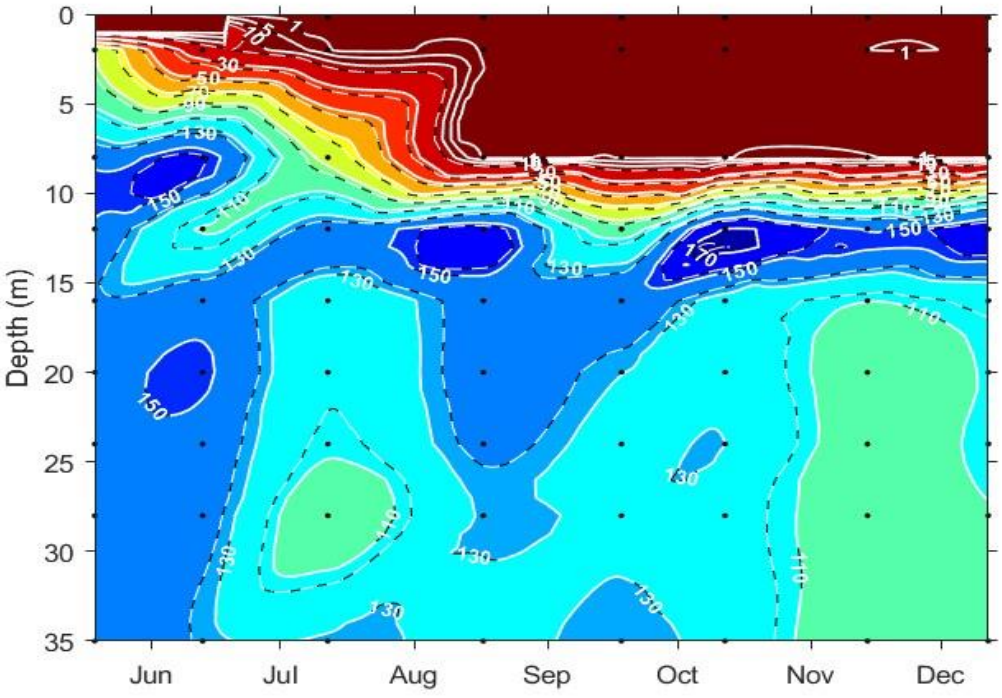

Chlorophyll *a* in upper 9-m integrated samples collected at 7 lakewide stations in April and May ranged from 108 to 136 µg chl L^{-1} with a mean of 122.8±2.0 µg chl L^{-1} in April and a mean of 115.7±2.8 µg chl L^{-1} in May (Table 8, Fig. 47). By June epilimnetic algal biomass in the upper 9 m decreased to 62 to 83 µg chl L^{-1} with a lakewide mean of

74.1±1.9 µg chl L^{-1}. Epilimnetic chlorophyll concentrations declined to 26.5 µg chl L^{-1} in July and further to <2.5 µg chl L^{-1} in August to October, reaching concentrations as low as 0.3 µg chl L^{-1}, before increasing to levels above 1 µg chl L^{-1} in late autumn.

Table 8. Chlorophyll *a* (µg L^{-1}) at 7 stations in upper 9 m of water column, April–December 2023. S.E. is standard error.

	Dates								
Station	4/30	5/19	6/13	7/12	8/17	9/18	10/12	11/14	12/12
1	131.6	108.1	81.8	19.7	2.2	0.6	0.3	1.1	1.0
2	128.0	135.9	62.0	34.3	2.3	0.6	0.4	0.9	0.9
5	127.9	110.7	77.6	19.4	0.5	0.3	0.4	0.9	0.9
6	122.6	112.6	68.5	27.1	0.8	0.4	0.3	0.9	0.9
7	120.0	113.5	76.4	16.2	0.8	0.4	0.4	0.9	0.8
8	117.5	108.9	82.8	29.8	0.5	0.4	0.4	0.9	0.8
11	111.6	121.4	72.6	38.5	1.5	0.7	0.3	0.8	0.8
Mean	122.8	115.7	74.1	26.5	1.2	0.5	0.3	0.9	0.9
S.E.	2.0	2.8	1.9	2.0	0.2	0.0	0.0	0.0	0.0

Fig. 47. Chlorophyll *a* (µg chl *a* L^{-1}) in upper 9 m of the water column at 7 stations, 2023.

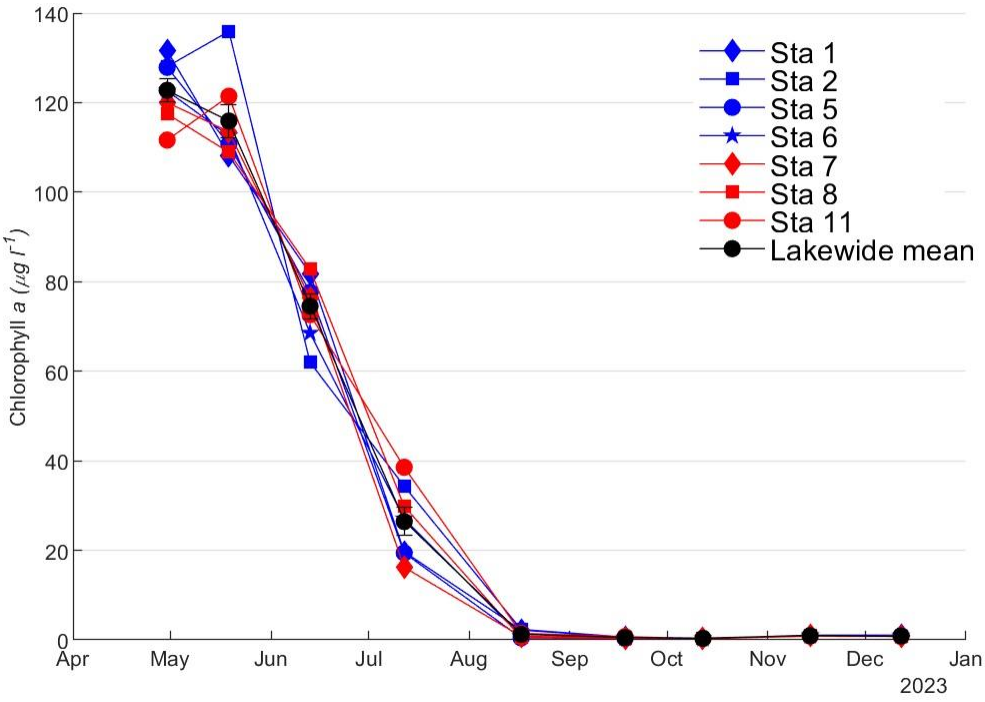

The large seasonal variation in epilimnetic (upper 9-m integrated) chlorophyll obscures the significant but less marked spatial differences observed during the year. Phytoplankton are generally less abundant in the eastern portion of the lake compared to western stations early in the year and more abundant during summer. This pattern is inversely related to *Artemia* abundance. In 2023, chlorophyll concentrations were generally more similar across the lake except that all three eastern stations (Stations 7, 8, and 11) were lower than western ones (Stations 1, 2, 5, and 6) in August (Table 8, Fig. 47).

Artemia Population Dynamics

Zooplankton populations in temperate lakes are highly variable across spatial and temporal scales. The Mono Lake monitoring program collects samples from 12 stations distributed across the lake and the relative standard errors of lakewide estimates are typically 10-20%. However, on any given sample date the standard error of a lakewide estimate may be smaller or larger depending on the spatial variability. Local convergences of water masses may concentrate shrimp to well above the overall mean. For these reasons, a single level of significant figures in presenting data (e.g., rounding to 10s, 100s, 1000s or even 10,000s) is inappropriate, and standard errors of each lakewide estimate are included using the ± notation. The reader is cautioned to consider the standard errors when making inferences from the data.

Hatching of Over-wintering Cysts and Maturation of the 1st Generation

Hatching of overwintering cysts is initiated by warming water temperatures and oxic sediment conditions. The peak of hatching usually occurs during March, but significant hatching may occur during February. A small amount of hatching may even occur during January in shallow nearshore regions during periods of above normal air temperatures. The 30 April survey indicated the spring hatch of overwintering cysts was well underway. *Artemia* lakewide abundance was 45,761±35,641 m^{-2}, and lakewide mean abundance of naupliar instars was 44,353±5,455 m^{-2} (Table 9, Table 10) with most of the instars (>80%) evenly distributed in the 2nd (10%), 3rd (22%), 4th (16%), and 5th (24%) developmental stage (Table 11, Table 12, Table 14). A small number of instars 7 and juveniles were present, but no adults were present.

Table 9. Mean *Artemia* lakewide and sector abundances (m^{-2}), April–December 2023. Adult females are separated depending on eggs present: und, undifferentiated egg mass; empty, empty ovisac; cyst, cysts in ovisac; nauplii, naupliar eggs in ovisac. Western sector refers to Stations 1-6, and eastern sector refers to Stations 7-12. Note: Before making inferences from this data, it is important to review the standard error associated with *Artemia* counts in Table 10.

	Instars		Adult	Adult female				Adult fem	Adult	
	1-7	8-11	male	und	empty	cyst	nauplii	total	total	total
Lakewide										
4/30	44,353	1,408	0	0	0	0	0	0	0	45,761
5/19	26,378	16,231	2,126	469	1,449	27	0	1,945	4,071	46,680
6/13	5,614	16,519	10,899	1,462	4,762	1,073	973	8,270	19,168	41,301
7/12	1,073	5,969	21,462	4,373	5,607	11,871	1,958	23,810	45,272	52,314
8/17	376	2,535	12,757	1,301	523	11,630	1,207	14,661	27,418	30,329
9/18	3,374	134	14,138	711	966	8,162	1,120	10,959	25,097	28,605
10/12	2,850	617	7,203	154	134	5,875	600	6,764	13,967	17,435
11/14	2,700	434	1,821	3	220	1,712	347	2,282	4,103	7,237
12/12	1,823	262	126	0	183	62	7	252	377	2,461
Western Sector										
4/30	31,214	1,100	0	0	0	0	0	0	0	32,314
5/19	12,502	11,133	2,307	429	993	54	0	1,476	3,783	27,418
6/13	4,681	14,608	13,803	1,180	4,641	939	765	7,525	21,328	40,617
7/12	1,180	8,156	29,510	4,775	7,565	14,970	2,414	29,725	59,235	68,571
8/17	107	3,192	16,794	1,583	483	13,924	1,422	17,411	34,205	37,505
9/18	4,373	134	20,630	939	1,288	10,704	1,663	14,594	35,225	39,732
10/12	2,656	443	7,002	188	121	6,036	597	6,942	13,944	17,042
11/14	2,508	644	2,039	0	221	1,911	443	2,575	4,614	7,767
12/12	1,717	245	151	0	198	84	7	288	439	2,401
Eastern Sector										
4/30	57,492	1,717	0	0	0	0	0	0	0	59,209
5/19	40,255	21,328	1,945	510	1,905	0	0	2,414	4,359	65,942
6/13	6,546	18,431	7,995	1,744	4,883	1,207	1,180	9,014	17,009	41,985
7/12	966	3,783	13,414	3,970	3,649	8,773	1,502	17,894	31,308	36,056
8/17	644	1,878	8,719	1,019	563	9,336	993	11,911	20,630	23,152
9/18	2,374	134	7,646	483	644	5,620	577	7,324	14,970	17,478
10/12	3,045	791	7,404	121	148	5,714	604	6,586	13,991	17,827
11/14	2,891	225	1,603	7	218	1,512	252	1,989	3,592	6,707
12/12	1,928	278	101	0	168	40	7	215	315	2,522

Table 10. Standard errors of *Artemia* lakewide and sector means (Table 9), April–December 2023. Adult females are separated depending on eggs present: und, undifferentiated egg mass; empty, empty ovisac; cyst, cysts in ovisac; nauplii, naupliar eggs in ovisac. Western sector refers to Stations 1-6, and eastern sector refers to Stations 7-12.

	Instars		Adult		Adult female			Adult fem	Adult	
	1-7	8-11	male	und	empty	cyst	nauplii	total	total	total
Lakewide										
4/30	5,455	498	0	0	0	0	0	0	0	5,641
5/19	8,035	3,947	479	201	476	27	0	507	940	12,588
6/13	837	2,765	1,557	410	509	212	229	925	2,043	4,925
7/12	313	1,459	3,300	803	858	2,098	356	3,449	6,623	7,825
8/17	149	419	1,439	222	140	1,087	152	1,367	2,669	2,801
9/18	445	53	2,842	112	192	1,710	236	2,159	4,934	5,231
10/12	206	88	983	46	60	1,426	96	1,602	2,550	2,501
11/14	232	137	241	3	49	265	90	356	574	606
12/12	135	34	13	0	34	13	3	41	51	152
Western Sector										
4/30	3,473	477	0	0	0	0	0	0	0	3,630
5/19	1,944	2,634	554	211	274	54	0	427	887	4,486
6/13	932	3,482	2,601	262	755	233	336	1,132	3,603	7,331
7/12	307	2,537	4,028	1,168	1,007	3,539	621	4,822	8,694	10,454
8/17	107	552	1,267	197	199	1,112	188	1,316	2,240	2,554
9/18	539	65	4,209	152	330	2,916	339	3,577	7,733	8,083
10/12	194	86	1,941	68	105	2,833	176	3,170	5,100	5,049
11/14	325	253	356	0	86	463	171	632	955	946
12/12	180	45	10	0	19	18	4	30	33	191
Eastern Sector										
4/30	7,057	909	0	0	0	0	0	0	0	7,381
5/19	14,258	7,155	831	363	917	0	0	928	1,751	22,993
6/13	1,367	4,478	730	800	751	369	316	1,504	1,878	7,265
7/12	576	1,009	2,404	1,186	831	1,735	299	3,884	6,279	7,374
8/17	239	543	995	382	215	1,364	218	1,861	2,810	2,719
9/18	424	90	981	104	110	1,332	107	1,556	2,508	2,353
10/12	366	120	687	65	67	954	99	1,111	1,611	1,407
11/14	340	42	331	7	57	279	50	352	657	781
12/12	208	55	21	0	69	16	4	76	93	253

Table 11. Percentage in different classes for *Artemia* lakewide and sector means (Table 9), April–December 2023. Adult females are separated depending on eggs present: und, undifferentiated egg mass; empty, empty ovisac; cyst, cysts in ovisac; nauplii, naupliar eggs in ovisac.Western sector refers to Stations 1-6, and eastern sector refers to Stations 7-12. Adult female "und", "cyst", and "nauplii", given as percentage of ovigerous females. Adult female "empty" given as percentage of adult females. “Instars 1-7”, “Instars 8-11”, “Adult male”, “Adult fem total”, “Adult total” given as percentage of total shrimp.

	Instars		Adult		Adult female			Adult fem	Adult	
	1-7	8-11	male	und	empty	cyst	nauplii	total	total	total
Lakewide										
4/30	97	3	0	0	0	0	0	0	0	100
5/19	57	35	5	24	74	1	0	4	9	100
6/13	14	40	26	18	58	13	12	20	46	100
7/12	2	11	41	18	24	50	8	46	87	100
8/17	1	8	42	9	4	79	8	48	90	100
9/18	12	0	49	6	9	74	10	38	88	100
10/12	16	4	41	2	2	87	9	39	80	100
11/14	37	6	25	0	10	75	15	32	57	100
12/12	74	11	5	0	73	25	3	10	15	100
Western Sector										
4/30	97	3	0	0	0	0	0	0	0	100
5/19	46	41	8	29	67	4	0	5	14	100
6/13	12	36	34	16	62	12	10	19	53	100
7/12	2	12	43	16	25	50	8	43	86	100
8/17	0	9	45	9	3	80	8	46	91	100
9/18	11	0	52	6	9	73	11	37	89	100
10/12	16	3	41	3	2	87	9	41	82	100
11/14	32	8	26	0	9	74	17	33	59	100
12/12	72	10	6	0	69	29	2	12	18	100
Eastern Sector										
4/30	97	3	0	0	0	0	0	0	0	100
5/19	61	32	3	21	79	0	0	4	7	100
6/13	16	44	19	19	54	13	13	21	41	100
7/12	3	10	37	22	20	49	8	50	87	100
8/17	3	8	38	9	5	78	8	51	89	100
9/18	14	1	44	7	9	77	8	42	86	100
10/12	17	4	42	2	2	87	9	37	78	100
11/14	43	3	24	0	11	76	13	30	54	100
12/12	76	11	4	0	78	19	3	9	13	100

Artemia lakewide abundance reached 46,680±12,588 m^{-2} by the 19 May 2023 survey as the spring hatch continued (Table 9, Table 10). The population was dominated by instars 7 and juveniles (22% and 36%, respectively) (Table 14). Naupliar abundance decreased in June 2023 with abundances ranging from 4,681 to 6,546 m^{-2} across the 12 stations and an overall lakewide mean of 5,614±837 m^{-2} (Table 9). On 12 July, naupliar

instars constituted only 2% of the total population with juveniles and adults being 11% and 87%, respectively.

Adult *Artemia* constituted only 9% of the total population on 19 May 2023 when they numbered 4,071±940. Fecund females were present during the 19 May survey, with a lakewide mean of 496±227 m^{-2} (Table 15, Table 16). Mean lakewide adult abundance peaked in July at 45,272±6,623 m^{-2}, followed by a decrease in the following months of August and September, when they numbered about the same (27,418±2,669 m^{-2} and 25,097±4,934 m^{-2}). Adult abundance further declined to 13,967±2,550 m^{-2} in October and to 4,103±574 m^{-2} on 14 November. By 12 December adult numbers were very low (377±51 m^{-2}) (Table 9).

The hatching of overwintering cysts is typically greater in the eastern half of the lake with its gradually sloping, shallow sediments. During the April and May surveys, hatching in the east was approximately double the hatch in the west. Naupliar and juvenile abundance remained higher at the eastern stations through June. This changed in July when naupliar abundance in the western sector was low but more than that observed in the east (Table 9).

Table 12. Mean *Artemia* lakewide and sector instar analysis, April–December 2023. Lakewide refers to Stations 1, 2, 5, 6, 7, 8, and 11, western sector refers to Stations 1, 2, 5, and 6, and eastern sector refers to Stations 7, 8, and 11. Instars 8-11 refers to juveniles. Note: Before making inferences from this data, it is important to review standard error associated with *Artemia* counts in Table 13.

	Instars									
	1	2	3	4	5	6	7	8-11	Adults	Total
Lakewide										
4/30	2,208	8,106	9,451	6,807	10,129	3,472	1,989	230	0	42,391
5/19	218	1,690	1,667	1,610	2,920	4,059	8,359	13,567	3,760	37,850
6/13	586	391	425	379	793	782	977	11,946	18,948	35,229
7/12	644	46	0	0	0	0	0	6,140	39,897	46,726
8/17	0	0	0	0	115	46	0	3,127	29,158	32,446
9/18	264	655	701	103	747	368	172	46	30,538	33,596
10/12	661	385	362	264	443	276	667	586	14,412	18,057
11/14	365	463	451	316	497	178	190	319	4,343	7,123
12/12	313	296	216	233	440	236	247	253	336	2,570
Western Sector										
4/30	1,046	5,010	4,789	3,380	7,907	3,179	3,159	402	0	28,873
5/19	161	1,529	1,247	1,167	1,288	1,328	5,433	12,193	3,742	28,089
6/13	584	282	382	262	624	845	946	12,455	20,684	37,062
7/12	1,046	80	0	0	0	0	0	8,290	53,280	62,696
8/17	0	0	0	0	0	0	0	3,340	36,177	39,517
9/18	322	885	885	40	1,167	483	282	80	40,201	44,346
10/12	674	332	352	161	312	282	704	423	16,328	19,567
11/14	412	352	412	231	372	201	221	412	5,161	7,777
12/12	252	267	201	221	423	277	302	277	438	2,656
Eastern Sector										
4/30	3,756	12,233	15,667	11,375	13,092	3,863	429	0	0	60,416
5/19	295	1,905	2,227	2,200	5,097	7,700	12,260	15,399	3,783	50,865
6/13	590	537	483	537	1,019	698	1,019	11,268	16,633	32,783
7/12	107	0	0	0	0	0	0	3,273	22,052	25,433
8/17	0	0	0	0	268	107	0	2,844	19,799	23,018
9/18	188	349	456	188	188	215	27	0	17,653	19,262
10/12	644	456	376	402	617	268	617	805	11,858	16,043
11/14	302	610	503	429	664	148	148	195	3,253	6,251
12/12	396	335	235	248	463	181	174	221	201	2,455

Table 13. Standard errors of *Artemia* lakewide and sector instar analysis (Table 12), April–December 2023. Lakewide refers to Stations 1, 2, 5, 6, 7, 8, and 11, western sector refers to Stations 1, 2, 5, and 6, and eastern sector refers to Stations 7, 8, and 11. Instars 8-11 refers to juveniles.

	Instars									
	1	2	3	4	5	6	7	8-11	Adults	Total
Lakewide										
4/30	577	2,116	2,874	1,785	2,061	668	930	149	0	7,417
5/19	46	365	348	457	987	1,756	2,645	3,395	970	9,762
6/13	128	140	67	76	199	229	265	2,386	2,652	5,130
7/12	272	46	0	0	0	0	0	2,272	8,111	10,124
8/17	0	0	0	0	115	46	0	544	3,953	4,098
9/18	67	172	186	67	259	120	83	46	7,727	8,338
10/12	113	66	53	60	102	43	155	91	4,241	4,121
11/14	98	90	72	68	93	51	55	61	973	1,000
12/12	90	52	17	23	34	26	35	31	65	190
Western Sector										
4/30	200	1,396	1,030	794	3,159	1,006	1,394	235	0	4,575
5/19	66	625	222	240	441	476	2,223	3,475	1,160	6,553
6/13	172	190	39	60	251	368	439	3,938	4,537	8,686
7/12	357	80	0	0	0	0	0	3,595	8,149	11,005
8/17	0	0	0	0	0	0	0	860	2,695	3,339
9/18	114	213	298	40	304	174	121	80	11,145	11,890
10/12	76	78	72	57	109	40	260	26	7,683	7,568
11/14	171	68	81	45	53	54	63	58	1,408	1,435
12/12	66	37	22	25	61	33	39	47	49	157
Eastern Sector										
4/30	387	3,541	4,678	1,666	1,444	984	215	0	0	7,678
5/19	27	336	690	1,019	1,511	3,087	5,076	7,321	1,973	20,806
6/13	234	215	161	107	326	299	326	2,903	1,834	5,298
7/12	107	0	0	0	0	0	0	1,759	7,003	8,861
8/17	0	0	0	0	268	107	0	722	4,266	4,180
9/18	27	188	117	149	97	142	27	0	4,925	4,918
10/12	279	117	97	46	149	97	176	123	1,464	872
11/14	71	169	146	132	173	107	107	76	1,272	1,491
12/12	205	122	29	47	20	0	29	35	93	437

Table 14. Lakewide and sector percentage (given as percentage of total shrimp) in different classes for *Artemia* instar analysis (Table 12), April–December 2023. Lakewide refers to Stations 1, 2, 5, 6, 7, 8, and 11, western sector refers to Stations 1, 2, 5, and 6, and eastern sector refers to Stations 7, 8, and 11. Instars 8-11 refers to juveniles.

	Instars									
	1	2	3	4	5	6	7	8-11	Adults	Total
Lakewide										
4/30	5	19	22	16	24	8	5	1	0	100
5/19	1	4	4	4	8	11	22	36	10	100
6/13	2	1	1	1	2	2	3	34	54	100
7/12	1	0	0	0	0	0	0	13	85	100
8/17	0	0	0	0	0	0	0	10	90	100
9/18	1	2	2	0	2	1	1	0	91	100
10/12	4	2	2	1	2	2	4	3	80	100
11/14	5	6	6	4	7	3	3	4	61	100
12/12	12	12	8	9	17	9	10	10	13	100
Western Sector										
4/30	4	17	17	12	27	11	11	1	0	100
5/19	1	5	4	4	5	5	19	43	13	100
6/13	2	1	1	1	2	2	3	34	56	100
7/12	2	0	0	0	0	0	0	13	85	100
8/17	0	0	0	0	0	0	0	8	92	100
9/18	1	2	2	0	3	1	1	0	91	100
10/12	3	2	2	1	2	1	4	2	83	100
11/14	5	5	5	3	5	3	3	5	66	100
12/12	9	10	8	8	16	10	11	10	16	100
Eastern Sector										
4/30	6	20	26	19	22	6	1	0	0	100
5/19	1	4	4	4	10	15	24	30	7	100
6/13	2	2	1	2	3	2	3	34	51	100
7/12	0	0	0	0	0	0	0	13	87	100
8/17	0	0	0	0	1	0	0	12	86	100
9/18	1	2	2	1	1	1	0	0	92	100
10/12	4	3	2	3	4	2	4	5	74	100
11/14	5	10	8	7	11	2	2	3	52	100
12/12	16	14	10	10	19	7	7	9	8	100

Fig. 48. Lakewide *Artemia* abundance during 2023: nauplii (instars 1-7), juveniles (instars 8-11), and adults (instars 12+).

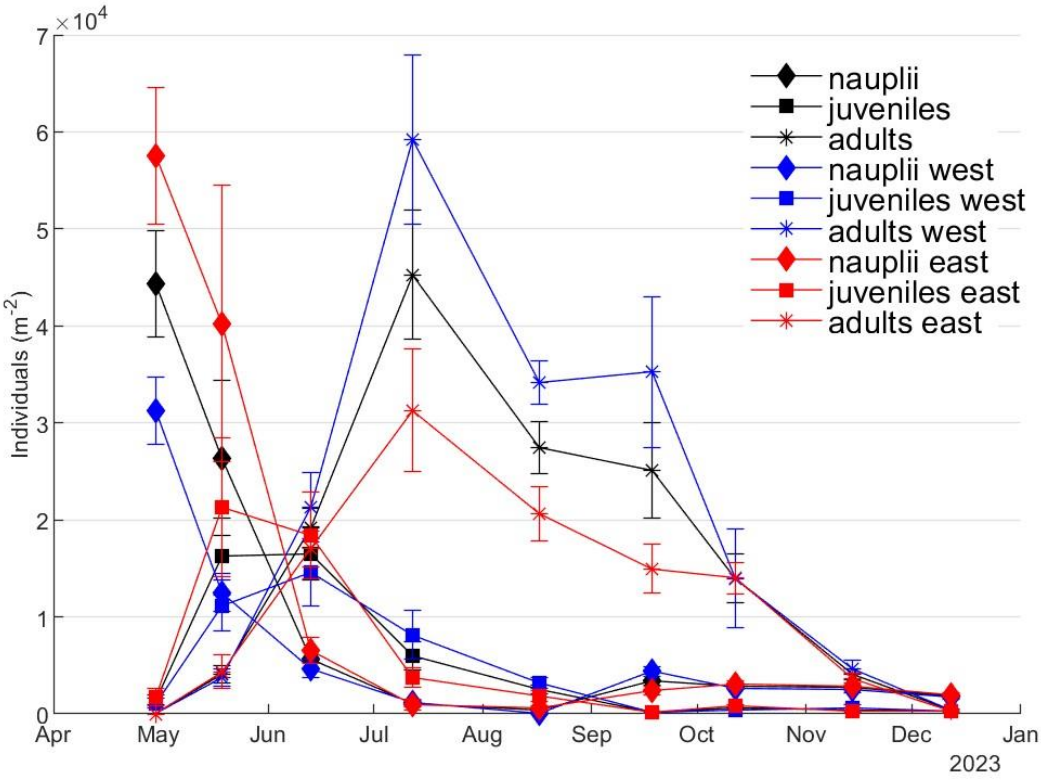

Ovoviviparous Reproduction and the Second Generation

Ovoviviparous reproduction depends on ambient food levels and age. *Artemia* produce multiple broods and ovoviviparous reproduction occurs primarily with the first brood, rarely occurring in second and subsequent broods.

On 19 May 1, 945±507 adult females comprised 4% of the total population, although the majority were non-ovigerous (74% empty), and eggs in the oviduct of 95% of ovigerous females were not sufficiently developed to discriminate between eggs and encapsulated cysts (i.e., ovoviviparous versus and oviparous reproduction) (Table 15, Table 16,

Table 17, Fig. 49). Ovigery increased to 42% of 8,270±925 individuals on 13 June, and individuals with undifferentiated egg masses decreased to 42%.

Ovigery increased throughout the summer to 76% of 23,810±3,449 females on 12 July; 96% of 14,661±1,367 on 17 August; 91% of 10,959±2,159 on 18 September and

peaking at 98% of 6,764±1,602 on 12 October, and slightly decreasing to 90% of 2,282±356 on 14 November. On 12 December only 41 fecund females were collected in all of 12 net tows. Cyst production ranged between 83% and 91% of adult females from mid-July through mid-November (Table 15, Table 16,

Table 17). The low numbers of later naupliar instars during July–September (Table 14) and the absence of a second peak in adult abundance indicate that relatively few ovoviviparously produced individuals were recruited into the adult population.

Table 15. Mean *Artemia* lakewide and sector reproductive summary, April–December 2023. Lakewide refers to Stations 1, 2, 5, 6, 7, 8, and 11, western sector refers to Stations 1, 2, 5, and 6, and eastern sector refers to Stations 7, 8, and 11. Adult female are separated depending on eggs present: und, undifferentiated egg mass; empty, empty ovisac; cyst, cysts in ovisac; nauplii, naupliar eggs in ovisac. Before making inferences from these data, review standard errors associated with *Artemia* counts in Table 16.

		Adult females				
	Total	Ovigery	empty	und	cyst	nauplii
Lakewide						
4/30	0	0	0	0	0	0
5/19	1,945	496	1,449	469	27	0
6/13	8,270	3,508	4,762	1,462	1,073	973
7/12	23,810	18,203	5,607	4,373	11,871	1,958
8/17	14,661	14,138	523	1,301	11,630	1,207
9/18	10,959	9,993	966	711	8,162	1,120
10/12	6,764	6,630	134	154	5,875	600
11/14	2,282	2,062	220	3	1,712	347
12/12	252	69	183	0	62	7
Western Sector						
4/30	0	0	0	0	0	0
5/19	1,476	483	993	429	54	0
6/13	7,525	2,884	4,641	1,180	939	765
7/12	29,725	22,160	7,565	4,775	14,970	2,414
8/17	17,411	16,928	483	1,583	13,924	1,422
9/18	14,594	13,307	1,288	939	10,704	1,663
10/12	6,942	6,821	121	188	6,036	597
11/14	2,575	2,354	221	0	1,911	443
12/12	288	91	198	0	84	7
Eastern Sector						
4/30	0	0	0	0	0	0
5/19	2,414	510	1,905	510	0	0
6/13	9,014	4,131	4,883	1,744	1,207	1,180
7/12	17,894	14,245	3,649	3,970	8,773	1,502
8/17	11,911	11,348	563	1,019	9,336	993
9/18	7,324	6,680	644	483	5,620	577
10/12	6,586	6,439	148	121	5,714	604
11/14	1,989	1,771	218	7	1,512	252
12/12	215	47	168	0	40	7

Table 16. Standard errors of *Artemia* lakewide and sector reproductive summary (Table 15), April–December 2023. Lakewide refers to Stations 1, 2, 5, 6, 7, 8, and 11, western sector refers to Stations 1, 2, 5, and 6, and eastern sector refers to Stations 7, 8, and 11. Adult females are separated depending on eggs present: und, undifferentiated egg mass; empty, empty ovisac; cyst, cysts in ovisac; nauplii, naupliar eggs in ovisac.

			Adult females			
	Total	Ovigery	empty	und	cyst	nauplii
Lakewide						
4/30	0	0	0	0	0	0
5/19	507	227	476	201	27	0
6/13	925	851	509	410	212	229
7/12	3,449	3,257	858	803	2,098	356
8/17	1,367	1,461	140	222	1,087	152
9/18	2,159	2,057	192	112	1,710	236
10/12	1,602	1,568	60	46	1,426	96
11/14	356	358	49	3	265	90
12/12	41	16	34	0	13	3
Western Sector						
4/30	0	0	0	0	0	0
5/19	427	264	274	211	54	0
6/13	1,132	831	755	262	233	336
7/12	4,822	5,328	1,007	1,168	3,539	621
8/17	1,316	1,496	199	197	1,112	188
9/18	3,577	3,408	330	152	2,916	339
10/12	3,170	3,076	105	68	2,833	176
11/14	632	634	86	0	463	171
12/12	30	22	19	0	18	4
Eastern Sector						
4/30	0	0	0	0	0	0
5/19	928	363	917	363	0	0
6/13	1,504	1,484	751	800	369	316
7/12	3,884	3,220	831	1,186	1,735	299
8/17	1,861	1,964	215	382	1,364	218
9/18	1,556	1,543	110	104	1,332	107
10/12	1,111	1,118	67	65	954	99
11/14	352	336	57	7	279	50
12/12	76	21	69	0	16	4

Table 17. *Artemia* lakewide and sector reproductive summary percentages (Table 15), April–December 2023. Lakewide refers to Stations 1, 2, 5, 6, 7, 8, and 11, western sector refers to Stations 1, 2, 5, and 6, and eastern sector refers to Stations 7, 8, and 11. Adult females are separated depending on eggs present: und, undifferentiated egg mass; empty, empty ovisac; cyst, cysts in ovisac; nauplii, naupliar eggs in ovisac. "Ovigery" and "empty" are given as percentages of total number of females. "und" is given as percentage of ovigerous females. Cyst and nauplii are given as percentage of individuals with differentiated egg masses.

	Adult females					
	Total	Ovigery	empty	und	cyst	nauplii
Lakewide						
4/30	0	0	0	0	0	0
5/19	100	26	74	95	100	0
6/13	100	42	58	42	52	48
7/12	100	76	24	24	86	14
8/17	100	96	4	9	91	9
9/18	100	91	9	7	88	12
10/12	100	98	2	2	91	9
11/14	100	90	10	0	83	17
12/12	100	27	73	0	90	10
Western Sector						
4/30	0	0	0	0	0	0
5/19	100	33	67	89	100	0
6/13	100	38	62	41	55	45
7/12	100	75	25	22	86	14
8/17	100	97	3	9	91	9
9/18	100	91	9	7	87	13
10/12	100	98	2	3	91	9
11/14	100	91	9	0	81	19
12/12	100	32	69	0	92	8
Eastern Sector						
4/30	0	0	0	0	0	0
5/19	100	21	79	100	0	0
6/13	100	46	54	42	51	49
7/12	100	80	20	28	85	15
8/17	100	95	5	9	90	10
9/18	100	91	9	7	91	9
10/12	100	98	2	2	90	10
11/14	100	89	11	0	86	14
12/12	100	22	78	0	85	15

Fig. 49. Reproductive characteristics of *Artemia* during 2023: lakewide mean abundance of total females and ovigerous females (top), brood size (middle), and percent of females ovoviviparous and ovigerous (bottom). Vertical lines are the standard errors of the estimates.

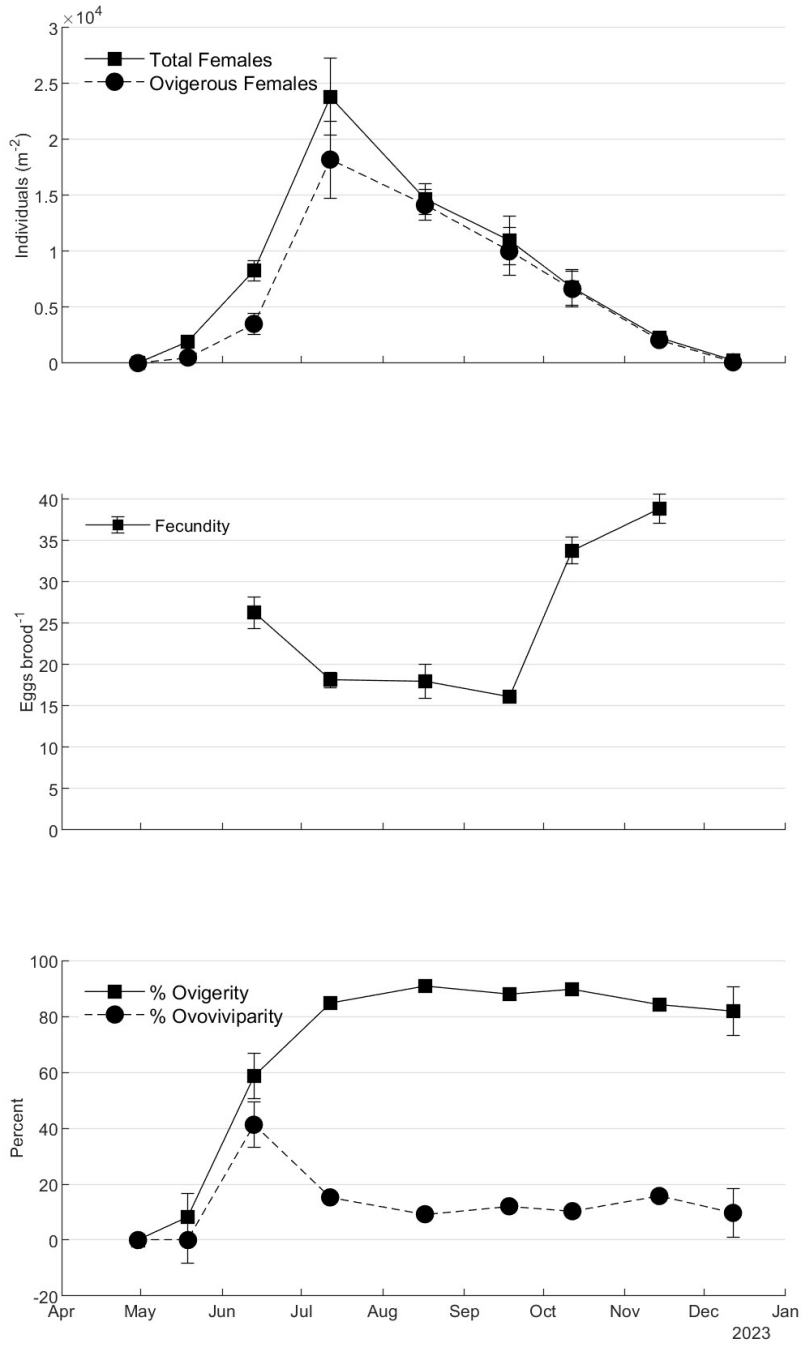

Fecundity (eggs per brood) is a function of food availability and adult female size. Lakewide mean fecundity ranged from 16 to 27 eggs brood^{-1} during June to September (Table 18, Fig. 49). Lakewide mean individual fecundity increased in October and November (34 and 39 eggs brood^{-1}, respectively) as food became abundant but total reproduction was minimal by mid-December as adult numbers were very low. The mean length of adult females varied from 8.5 to 10.1 mm (Table 18) during the year.

Table 18. *Artemia* fecundity summary, June–December 2023. "%cyst" and "%indented" refers to the percentage of the type (cyst or naupliar) and shape (indented or round) of the eggs, respectively. S.E. is standard error. 'n' refers to number of stations averaged. '#fem' refers to number of females averaged.

	#eggs/brood				Female length (mm)			
	Mean	S.E.	%cyst	%indented	Mean	S.E.	n	#fem
Lakewide								
6/13	26	1.3	76	12	9.1	0.1	7	67
7/12	18	0.9	100	60	9.3	0.1	7	70
8/17	18	1.1	87	33	8.5	0.1	7	70
9/18	16	1.0	87	62	8.7	0.1	7	69
10/12	34	1.7	81	51	9.5	0.1	7	70
11/14	39	1.9	80	43	10.1	0.1	7	70
12/12	29	5.6	75	58	9.1	0.2	4	12
Western Sector								
6/13	27	1.9	78	0	9.0	0.2	4	37
7/12	18	1.0	100	48	9.6	0.1	4	40
8/17	17	1.5	88	28	8.3	0.1	4	40
9/18	16	1.4	90	68	8.7	0.1	4	40
10/12	34	2.3	85	53	9.5	0.2	4	40
11/14	37	2.5	88	45	10.0	0.2	4	40
12/12	26	5.4	89	67	9.1	0.2	3	9
Eastern Sector								
6/13	26	1.6	73	27	9.3	0.1	3	30
7/12	19	1.5	100	77	9.0	0.2	3	30
8/17	19	1.6	87	40	8.7	0.2	3	30
9/18	16	1.3	83	55	8.8	0.1	3	29
10/12	34	2.5	77	50	9.6	0.1	3	30
11/14	41	2.9	70	40	10.2	0.2	3	30
12/12	38	17.3	33	33	9.3	0.3	1	3

Artemia Biomass

In 2023, *Artemia* biomass peaked in July at 21 g dry weight m^{-2}, followed by a decrease in the following months of August, September, and October (10, 14, and 10 g dry weight m^{-2}, respectively), before declining to 0.3 g dry weight m^{-2} in December (Table 19).

Table 19. *Artemia* biomass (g dry weight m^{-2}) summary, July–December 2023. S.E. is standard error. 'n' in last column refers to number of stations averaged.

	Date	Mean	S.E.	n
Lakewide				
	7/12	20.8	3.4	12
	8/17	9.7	0.8	12
	9/18	14.0	1.8	12
	10/12	9.7	1.7	12
	11/14	3.5	0.4	12
	12/12	0.3	0.0	12
Western Sector				
	7/12	26.2	5.1	6
	8/17	11.5	0.6	6
	9/18	17.0	2.2	6
	10/12	9.1	3.2	6
	11/14	3.8	0.7	6
	12/12	0.4	0.0	6
Eastern Sector				
	7/12	15.4	3.5	6
	8/17	8.0	1.0	6
	9/18	11.0	2.3	6
	10/12	10.2	1.3	6
	11/14	3.2	0.5	6
	12/12	0.3	0.1	6

CHAPTER 4
EVALUATION OF MONITORING METHODS, 2012–2022

Consistent methods are important for utilizing long-term data to examine changes in the plankton dynamics of Mono Lake. In reviewing data provided by LADWP from 2012 to 2022, several data processing errors and differences in how chlorophyll and ammonium analyses were conducted became apparent. Processing errors associated with profiles of temperature and salinity were identified and corrected. Ammonium and chlorophyll measurements were made by contractors on samples that had been frozen for varying periods, usually several months, and with methods different from those used by UCSB in the past and currently. Therefore, a protocol was designed to assess the impact of sample storage time and differences in analytical methods on results.

Conductivity, Temperature, and Depth Data

Conductivity, temperature, and depth data reported in LADWP annual compliance reports for years 2013–2021 used incorrect equations of state (temperature, conductivity, density relationships) for Mono Lake water, did not account for an air pressure offset for the altitude of Mono Lake, and used a seawater density correction for pressure to depth rather than Mono Lake density. These errors resulted in omitting readings from the upper 2 m of the water column and miscalculating depths up to 2 m throughout the water column, affecting analysis of seasonal and long-term changes in vertical distributions of temperature and salinity. We met and exchanged information with LADWP personnel responsible for processing these data and have resolved these issues. Subsequently, we have reprocessed all the data collected by LADWP from 2012 to 2021, and their staff developed new processing routines for their 2022 report.

Ammonium

Field and laboratory procedures performed by UCSB are described in Chapter 2. Sampling dates for comparisons with LADWP procedures were 14 July, 17 August, 18 September, 12 October, and 14 November 2023. Sampling was done at Station 6 at 0.2 m, 12 m, and 28 m using a Van Dorn water sampler. In the laboratory after each survey, UCSB samples were analyzed within 2 hours using the indophenol blue method (Strickland & Parsons 1972). A second set of field duplicates on each sample date was

frozen at -20°C for subsequent analysis at the UC Davis Analytical Lab (UCDAL), the laboratory used by LADWP for most years.

A total of 15 UCDAL samples were kept frozen until 5 December 2023 when they were shipped overnight and frozen to UCDAL for ammonium analysis. The samples were kept frozen until analysis on 20 December 2023. The storage periods of samples, from the date of collection to the analysis date, were as follows: 160 days (14 July), 125 days (17 August), 93 days (18 September), 69 days (12 October), and 36 days (14 November). UCDAL measured NH_4-N concentration by flow injection analysis based on a modified version of a method proposed by Bower & Holm-Hansen (1980). This method involves heating ammonia with salicylate and hypochlorite in an alkaline phosphate buffer. The presence of EDTA prevents the precipitation of calcium and magnesium, and sodium nitroprusside is added to enhance sensitivity. The absorbance of the reaction product is measured at 660 nm and is directly proportional to the ammonium concentration.

The variations in ammonium concentrations (µM) measured by UCSB each month for seven months are compared to the UCDAL measurements in Table 20. However, the method used by the UCDAL has a detection limit of approximately 3.6 µM, while the UCSB method has a detection limit of about 0.07 µM (Strickland & Parsons 1972, Solorzano 1969). Therefore, values below 4 µM reported by LADWP are below detection. This finding is critical to interpretation of results in the upper 9 m, where ammonium concentrations often range from 0.3 to 3.5 µM. The comparisons made below will not include results from concentrations below detection (<4 µM).

UCDAL reported ammonium data in mg L^{-1} as NH_4-N, meaning that only the nitrogen atomic mass is included. Therefore, to convert UCDAL data from mg L^{-1} to µM, the atomic mass of nitrogen (N = 14.007 g moL^{-1}) should be used. Instead, LADWP converted UCDAL data (from 2012-2022) using the molar mass of NH_4 (NH_4 = 18.038 g moL^{-1}). This mistake in the conversion can be corrected by dividing ammonium values in the LADWP reports by 0.78.

In contrast to UCDAL, UCSB uses standards prepared with Mono Lake water with very low ammonium levels attained by aging a surface sample at room temperature

in the light. Since color development is lower in Mono Lake water than deionized water, and interference with color development varies with depth, internal standards are used for water from 0.2 m, 16 m, 24 m, and 35 m (Zadorojny et al. 1973).

In general, the ammonium concentrations obtained from UCDAL measurements were higher than the results obtained by UCSB, indicating effects of analytical differences and that long storage periods can cause ammonium concentrations to be overestimated (Table 20). A linear regression explained 97% of the variation, with a standard error of 2.9 (Fig. 50). A time series plot of residuals indicated a slight systematic pattern over time with most of the residuals being positive for longer storage periods (Fig. 51, Fig. 52). These results may be associated with storage time and preservation since a storage period of more than a few days can result in losses or gains in NH_4 (Strickland & Parsons 1972).

Table 20. Comparison of ammonium (µM) profiles at Station 6, July–November, 2023, measured by the University of California Davis Analytical Lab (UCDAL) and University of California Santa Barbara (UCSB).

Sample date	Depth (m)	UCDAL (µM)	UCSB µM)
7/14	0.2	5.7	4.8
7/14	12	6.4	5.3
7/14	28	20.7	16.0
8/17	0.2	4.3	1.7
8/17	12	11.4	5.9
8/17	28	26.4	22.8
9/18	0.2	<3.6	0.9
9/18	12	20.0	14.3
9/18	28	40.7	38.9
10/12	0.2	<3.6	1.3
10/12	12	23.6	16.8
10/12	28	52.8	55.1
11/14	0.2	<3.6	0.8
11/14	12	24.3	24.3
11/14	28	58.5	67.8

Fig. 50. Regression analysis of ammonium concentrations measured by UCSB on day of collection and UCDAL after storage (Table 20).

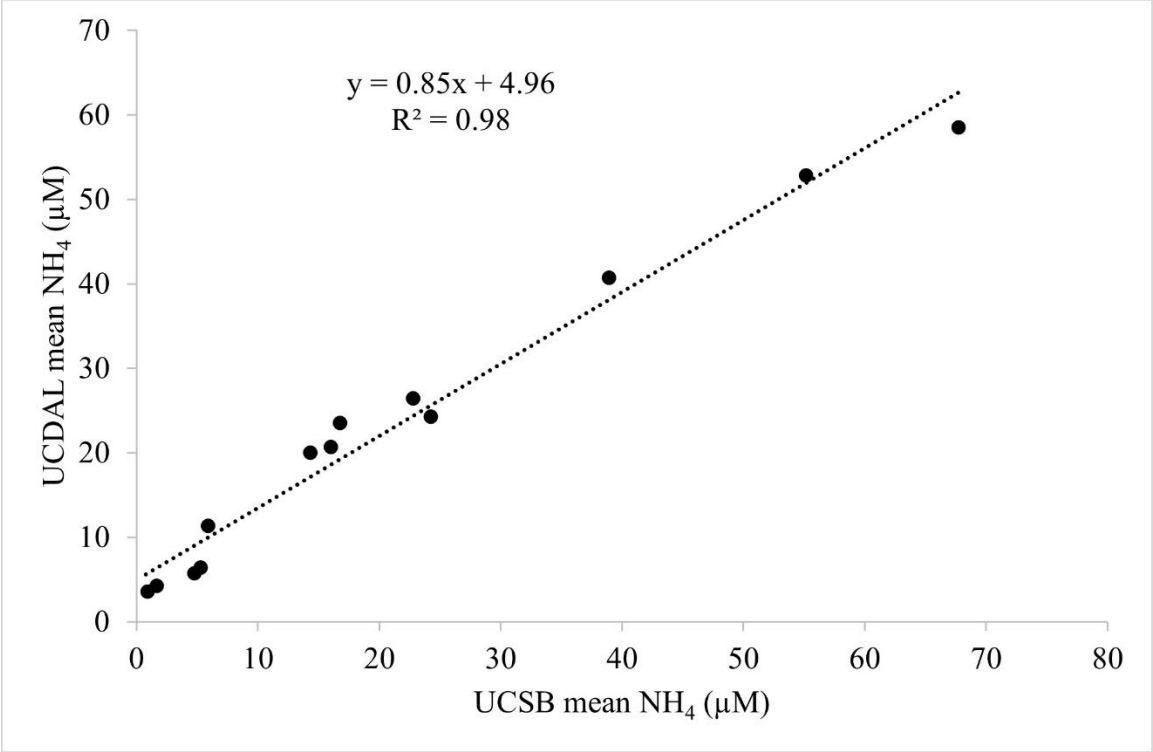

Fig. 51. Residual analysis (in µM) depicting the temporal variation in ammonium concentrations (µM) for UCDAL and UCSB.

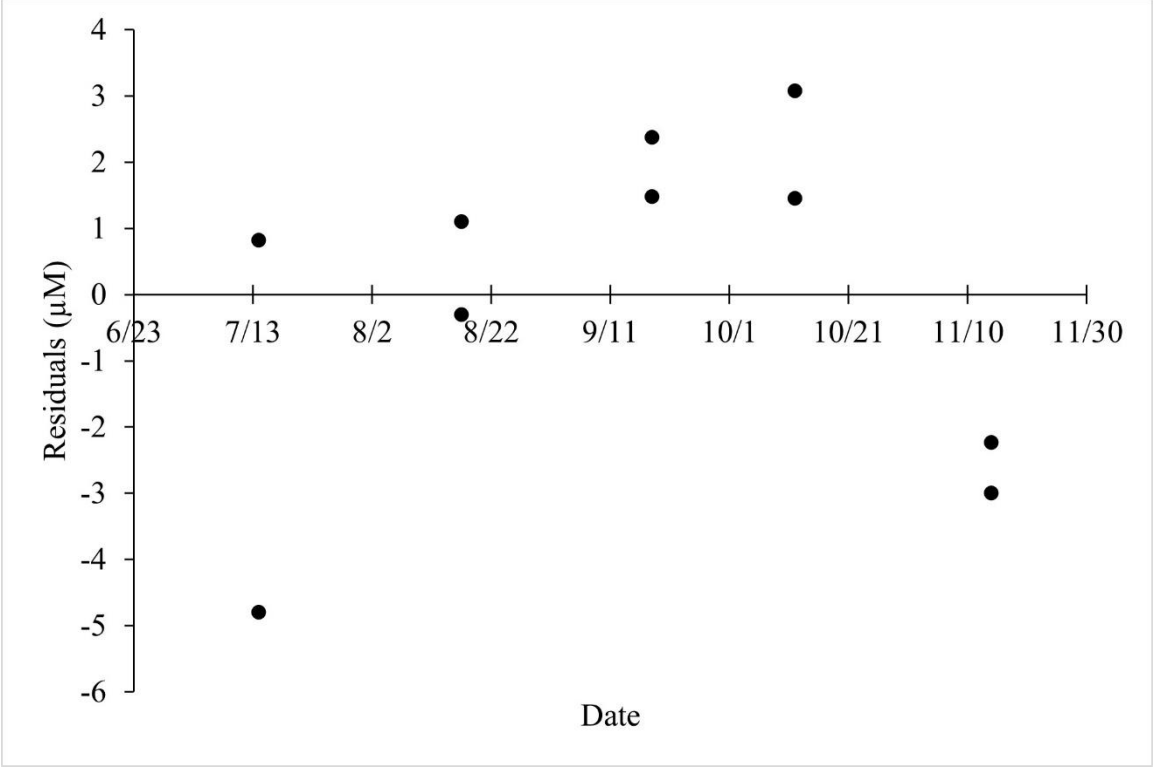

Fig. 52. Stability trends over time: Bland-Altman comparison of samples analyzed on the day of collection vs. stored ammonium samples.

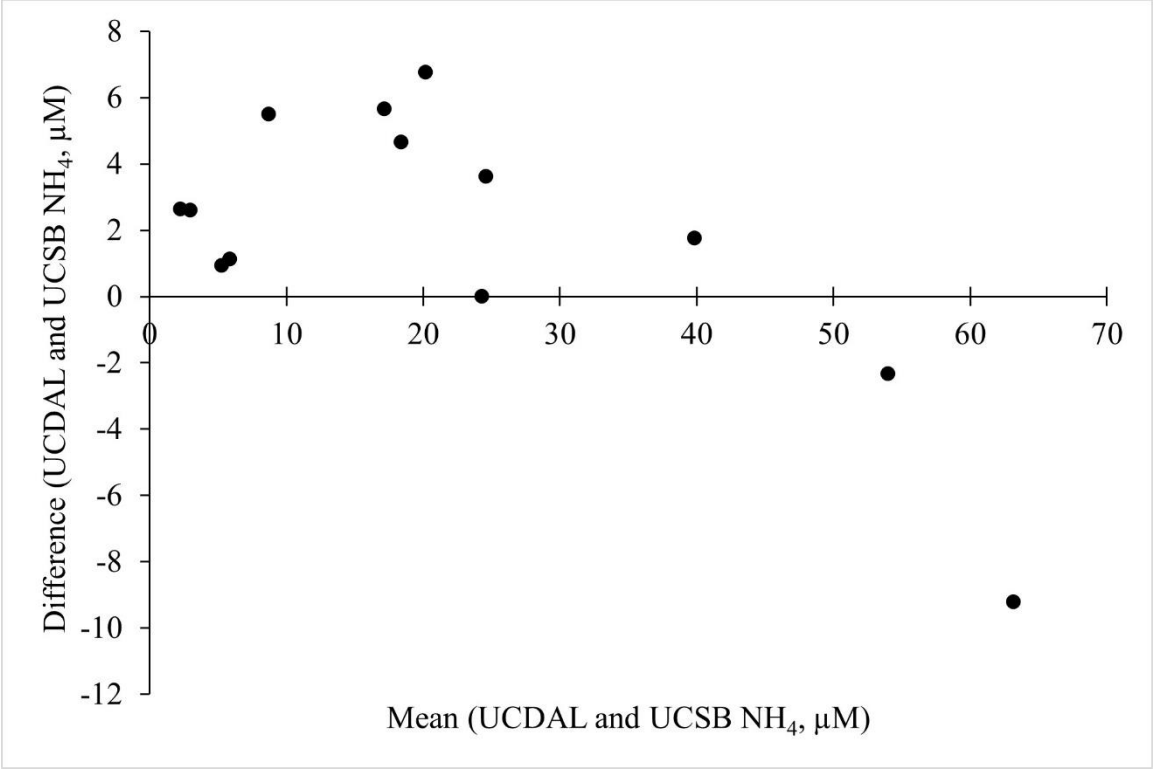

Chlorophyll

Field and laboratory procedures for analysis of chlorophyll performed by UCSB are described in Chapter 2. Sampling dates for the method and data comparison are the following: 19 May, 13 June, 14 July, 17 August, 18 September, 12 October, and 14 November 2023. Sampling was done at Station 6 with a 9-m integrated tube sampler. Upon arrival at the laboratory after each survey, subsamples were filtered within 3-4 hours onto Whatman GF/F glass microfiber filters (diameter 47 mm), and frozen at -20°C until extraction. A second set of triplicate filters of 9-m integrated samples from Station 6 on each sample date were frozen for subsequent analysis at University of Maryland Center for Environmental Science (UMCES).

A total of 21 filters were kept frozen until 4 December 2023, when they were shipped frozen and overnight to UMCES for chlorophyll *a* analysis. The samples were received on 5 December 2023 and kept frozen until analysis on 19 and 20 December 2023. The storage periods, from the date of collection to the analysis date, were as follows: 215 days (19 May), 190 days (13 June), 160 days (14 July), 125 days (17

August), 93 days (18 September), 69 days (12 October), and 36 days (14 November). The analytical method that UMCES used was based on EPA 445.0, SM10200H.3 (EPA Method 445.0). The method involves extracting chlorophyll *a* from phytoplankton cells using a 90% solution of acetone, followed by physical disruption of the cells through mechanical grinding or sonication. The samples are then refrigerated in the dark for 2 to 24 hours, centrifuged to separate the sample material from the extract, and analyzed on a fluorometer. The procedure also includes the determination of phaeophytin and active chlorophyll *a* by acidifying the extract using 5% HCl. The concentrations of chlorophyll *a* and phaeophytin are then calculated.

Concentrations of chlorophyll *a* reported by UMCES are different from data reported by UCSB (Table 21). UMCES reported chlorophyll as Chl-total, Chl-Pheophytin, and Chl-active (i.e., pheophytin-corrected chlorophyll *a*), with detection limits of 0.68, 0.46, and 0.69 µg L^{-1}, respectively. UCSB reports chlorophyll concentrations as active chlorophyll *a* (µg L^{-1}) currently and in previous reports, with detection limit of 0.2 µg L^{-1} (Golterman & Clymo 1969). In contrast, LADWP reports UMCES data (from 2012-2022) as Chl-total. This difference could be corrected by accessing each UMCES report and selecting the Chl-active values.

In general, the chlorophyll *a* concentration results obtained from UMCES measurements were significantly lower than the results obtained by UCSB, indicating that long storage periods may cause chlorophyll *a* concentrations to be underestimated (Table 21). A linear regression explained 99% of the variation, with a standard error of 1.4 (Fig. 53). A time series plot of residuals indicated a slight systematic pattern over time, with positive residuals associated with longer storage periods, and as the storage period decreases, the residuals disperse closer to zero (Fig. 54). These results may be related to preservation and storage period since it is known, including being stated in the protocol used by UMCES (EPA Method 445.0), that a storage period of more than 28 days can result in significant loss of chlorophyll *a* (Chapman 1996, Weber et al. 1986, Holm-Hansen & Riemann 1978).

Table 21. Comparison of chlorophyll *a* (µg L^{-1}) at Station 6 in upper 9 m of water column, May– November 2023. UMCES is University of Maryland Center for Environmental Science and UCSB is University of California Santa Barbara. S.E. is standard error.

	Dates						
	5/19	6/13	7/14	8/17	9/18	10/12	11/14
UCSB							
Mean	112.6	68.5	27.0	0.8	0.4	0.3	0.9
S.E.	3.2	1.3	0.8	0.01	0.00	0.01	0.01
UMCES							
Mean	47.5	31.7	15.3	2.3	1.7	1.4	5.4
S.E.	2.6	0.7	0.4	0.02	0.02	0.02	0.09

Fig. 53. Regression analysis of chlorophyll *a* concentrations (µg L^{-1}) measured by UCSB within 10 days of collection and by UMCES after long-term storage periods (Table 21).

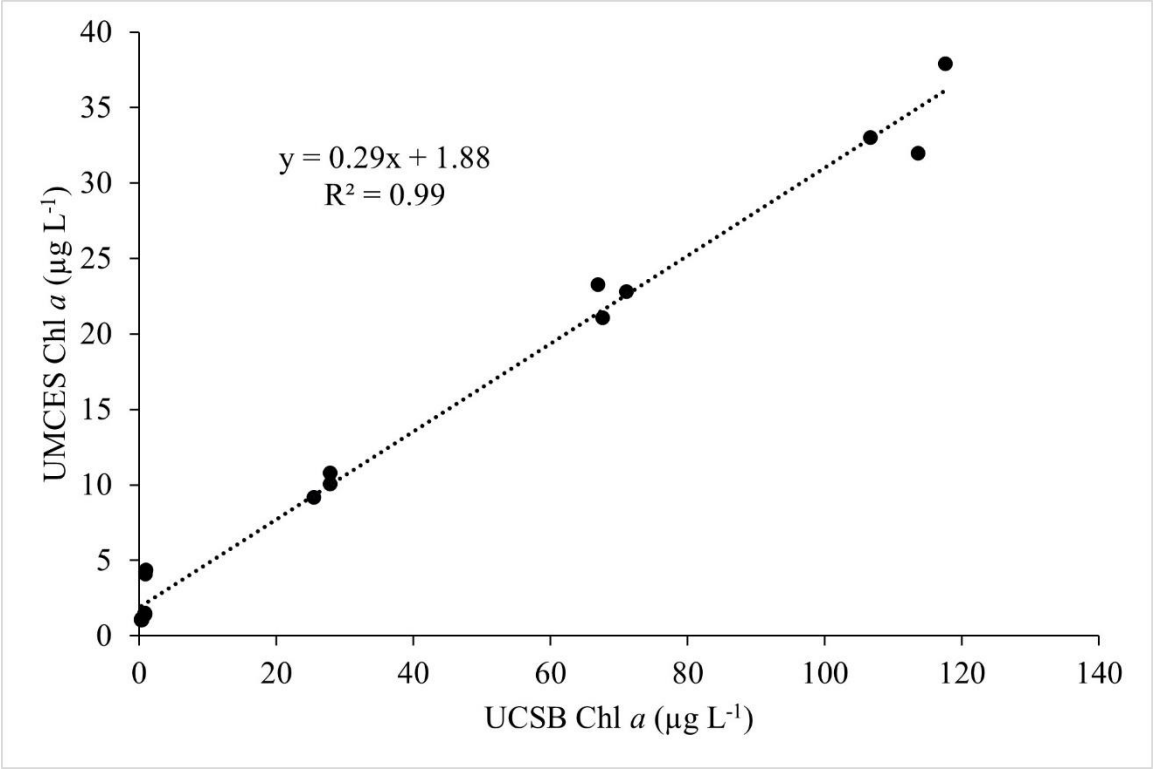

Fig. 54. Residual analysis (in µg L^{-1}) depicting the temporal variation in chlorophyll *a* concentration (µg L^{-1}) for UMCES and UCSB.

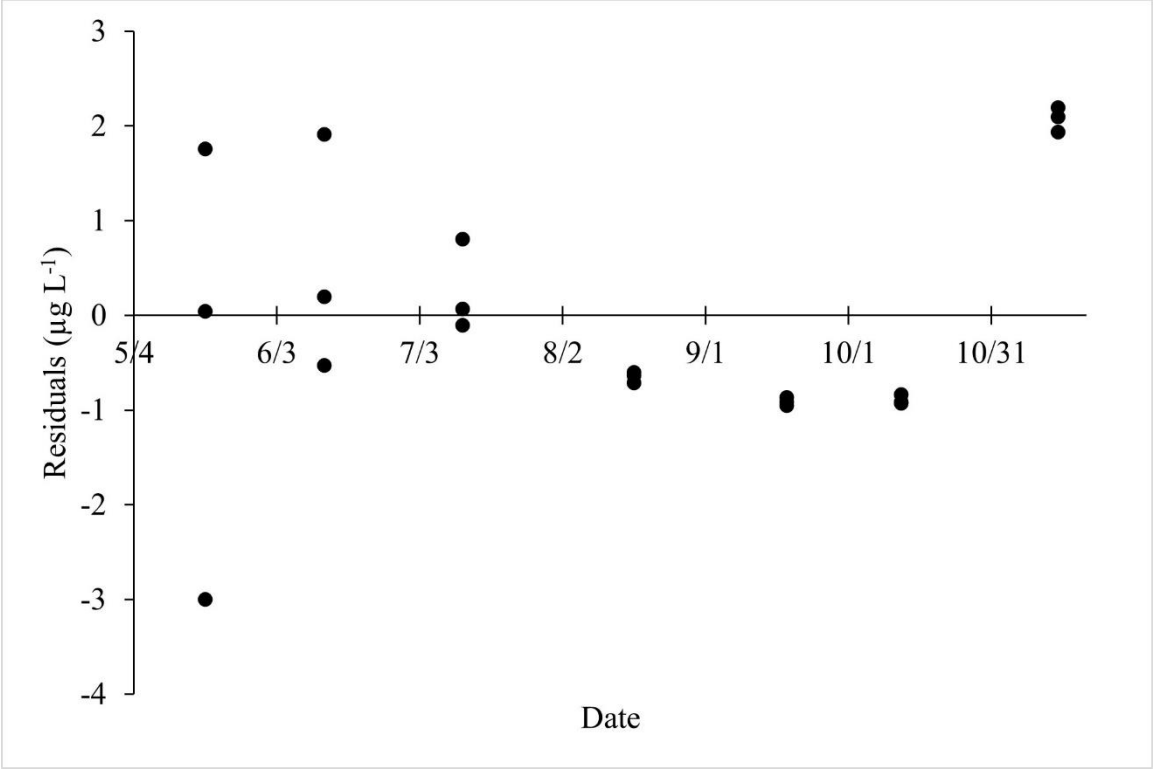

Plots of chlorophyll *a* concentrations in 9-m integrated samples vs Secchi depth show a significant regression (r^2, 0.74) using UCSB data (1982-July 2012) compared to a weaker regression (r^2, 0.43) using LADWP data (Fig. 55). LADWP chlorophyll values are only about 1/3 of what would be predicted based on Secchi depths. This is consistent with the gradual decay of chlorophyll *a* on filters held for long periods. Also, samples collected early in the year (from January to June) resulted in a lower regression coefficient than those processed later in the year (from July to December) (Fig. 56).

Information presented here indicates that LADWP chlorophyll *a* data are misleading as presented and may not be correctable without large uncertainty.

Fig. 55. Relationship between chlorophyll *a* and transparency (Secchi depth) for all 9-meter integrated samples.

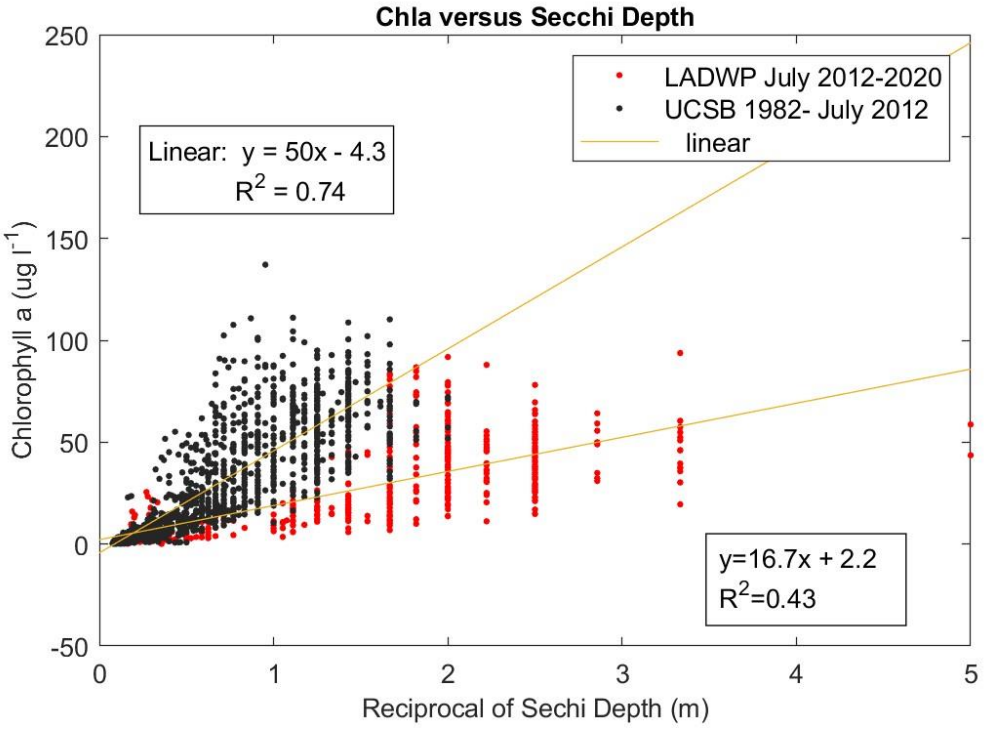

Fig. 56. Relationship between chlorophyll *a* and transparency (Secchi depth) for LADWP data sampled from January to June and from July to December. These data are from above 10 m.

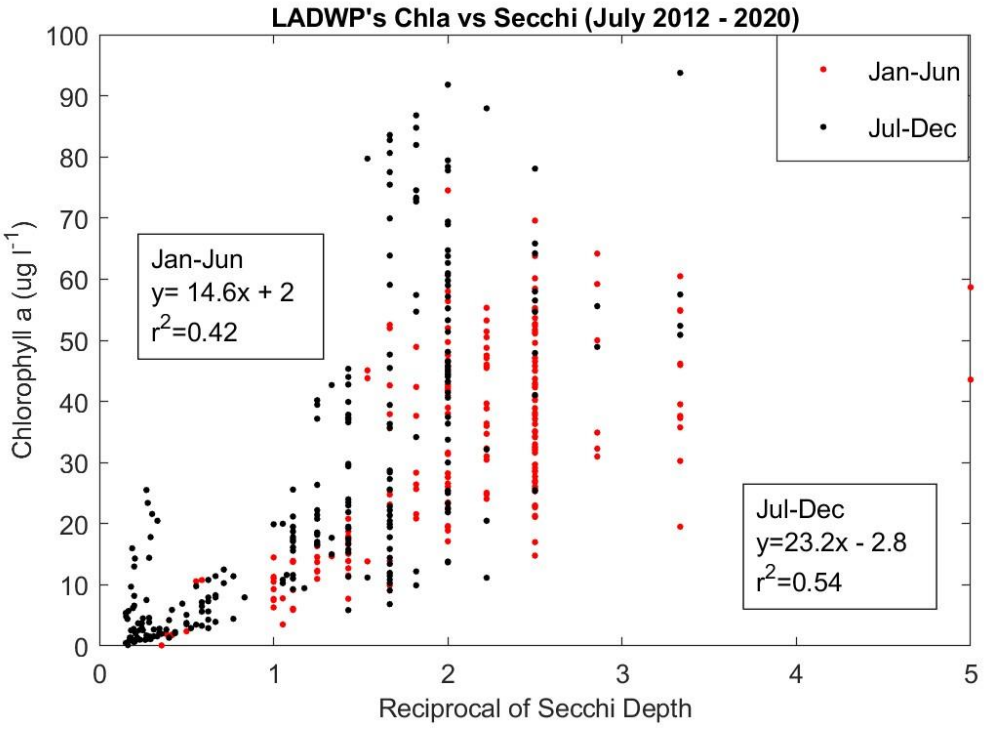

CHAPTER 5
SEASONAL, ANNUAL, AND LONG-TERM TRENDS

Introduction

Seasonal and long-term variation in the ecology of lakes is caused by a wide range of anthropogenic and climatic variables acting over various time scales. At Mono Lake, the diversion of streams out of the basin is the largest anthropogenic impact (Patten 1987, CSWRCB 1994). Climatic differences among years have led to large changes in snowmelt runoff, alterations in stratification and associated ecological effects.

Water diversions by the Los Angeles Department of Water and Power beginning in 1941, led to a 14 m drop in surface elevation and an increase in salinity from 48 g kg^{-1} in 1940 to 87 g kg^{-1} in 1980 (Blevins 1984). Based on laboratory studies (Dana & Lenz 1986; Dana et al.1993, 1995), this salinity increase influenced several life-history aspects of *Artemia*, a primary food source for large migrating and nesting bird populations. The decreased volume of the lake at the lower surface elevations resulted in another significant source of variation, recurring multiyear episodes of persistent chemical stratification (meromixis). At decreased lake volumes, above average years of snowmelt runoff during which freshwater flows into the upper layer of the lake can initiate multiyear periods of meromixis. The increased vertical density stratification reduces vertical mixing of ammonium and phytoplankton growth during summer and prevents the winter period of holomixis in which nutrients accumulated in deep anoxic waters are returned to the upper waters. These effects are well-documented (Jellison & Melack 1988, Jellison et al. 1993, Melack & Jellison 1998, Melack et al. 2017). However, the overall effects on the seasonal *Artemia* population are difficult to discern due to considerable differences in characteristics of different meromictic events and multiplicity of factors affecting the seasonal development of the *Artemia*. The increased variability due to recurring episodes of meromixis increases the difficulty of discerning and attributing causes to long-term trends in *Artemia* population dynamics.

Density Stratification and Meromictic Episodes

Most large temperate lakes undergo a regular seasonal regime of thermal stratification when upper (epilimnion) waters warm during spring and summer and then

cool through autumn and winter. In Mono Lake, the high salinity and particular chemical composition result in distinct physical properties of the lake water. In contrast to freshwater, the density of the Mono Lake water increases as a monotonic function of temperature decrease, even below 4°C. Thus, an extended period of holomixis can occur through winter until waters begin to warm in late February.

Density stratification between 2 and 32 m due to thermal stratification is quite regular and varies from -0.4 to 5.1 kg m^{-3} (Fig. 57). Overlain on the seasonal pattern of thermal stratification is that due to salinity stratification. Salinity stratification varies from year to year depending on existing salinity stratification and on the variation in timing and volume of seasonal freshwater inflows. Density stratification due to salinity has varied from -2.7 to 15.6 kg m^{-3} from 1983 to 2023. Often density stratification was sufficient to prevent the winter period of holomixis.

Fig. 57. Density stratification between 2 and 32 m at Station 6, 1983–2023.

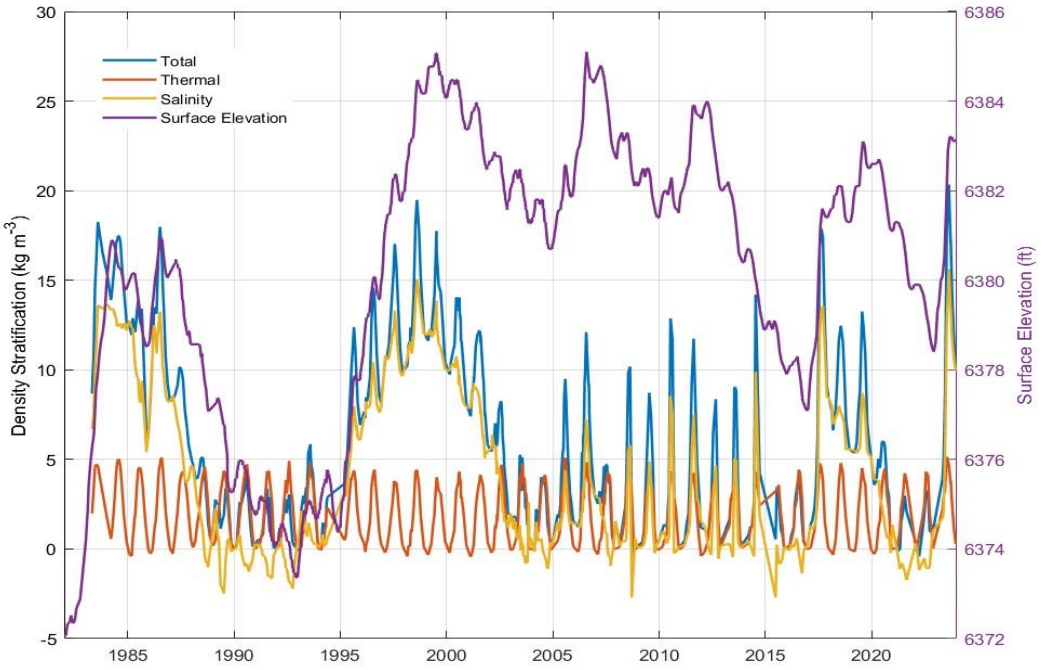

High snowmelt runoff in 2023 resulted in a 4.5 ft rise in surface elevation and initiated the 6th episode of meromixis (Fig. 58). While the end of an episode is defined by holomixis, the beginning is not well defined because Mono Lake has a summer period of

stratification due to warming of the upper water column. Here we define the beginning of a meromictic episode to be the date when the rise in surface elevation that resulted in meromixis began (Table 22). The end of an episode was calculated as the mean of the two sampling dates bracketing holomixis as indicated by temperature, conductivity, dissolved oxygen and ammonium profiles. The amount of freshwater inflow required to initiate an episode of meromixis depends on a variety of factors including the lake volume, salinity, the timing of the inflows relative to seasonal thermal stratification, and other climatic factors (e.g., precipitation, evaporation, wind speeds). Recent history would suggest at the current lake levels that an annual surface elevation rise of ~2 ft will likely initiate an episode of meromixis (Fig. 59, Table 22). In 2011, a surface elevation rise of 2.4 ft from the 1 December 2010 elevation prevented winter holomixis and initiated a 2-yr period of meromixis. Somewhat lower elevation rises in 1993 (1.7 ft) and 2005 (1.9 ft) did not initiate meromixis. Since water diversions began in 1941, the only year where the annual surface elevation change exceeded 2 ft prior to 1983 was in 1969 when surface elevation rose 2.5 ft. Whether this initiated a short period of meromixis is unknown. As the lake's salinity was lower, the density gradient formed from inflowing freshwater would have been less and a larger rise may have been required to prevent winter holomixis.

Table 22. Meromictic episodes

Meromictic Episode	Begin Date	Beginning Elevation (ft)	End Date	Ending Elevation (ft)	Initial Year Rise (ft)	Duration (years)
1	1982-06-02	6372.3	1988-11-22	6377.1	8.6	6.5
2	1994-11-21	6374.4	2003-11-30	6381.3	3.5	9.0
3	2005-12-01	6381.9	2007-11-18	6382.8	3.2	2.0
4	2010-12-01	6381.5	2012-12-02	6382.0	2.4	2.0
5	2017-01-01	6377.1	2020-12-02	6381.1	4.5	3.9
6	2022-12-01	6378.4			4.8	

Fig. 58. Surface elevation and meromictic episodes at Mono Lake. Straight lines indicate the duration of each episode (see text).

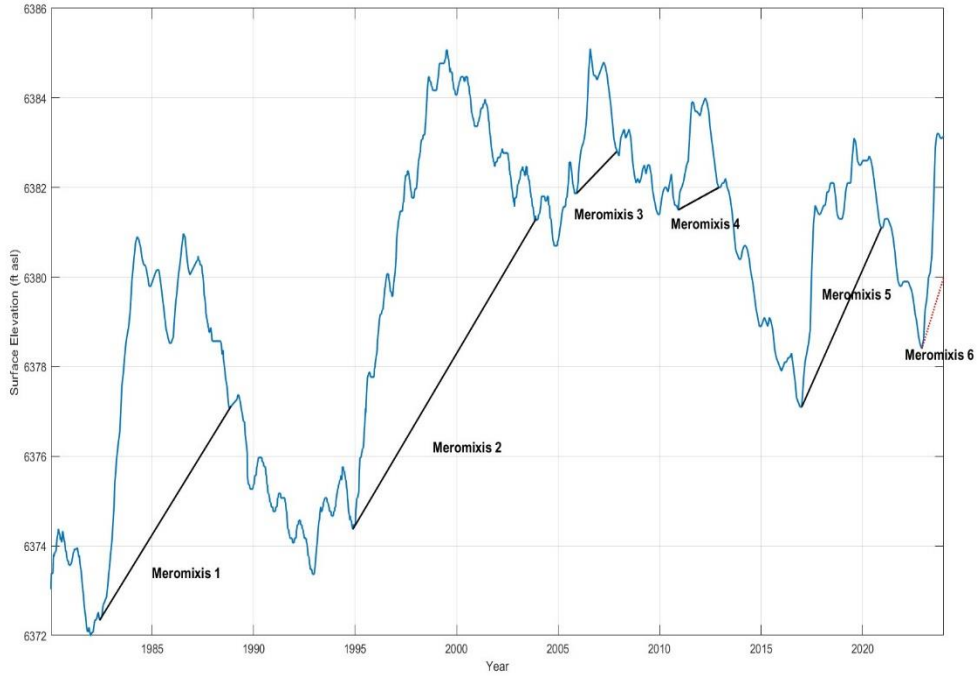

Fig. 59. Yearly change in surface elevation (ft).

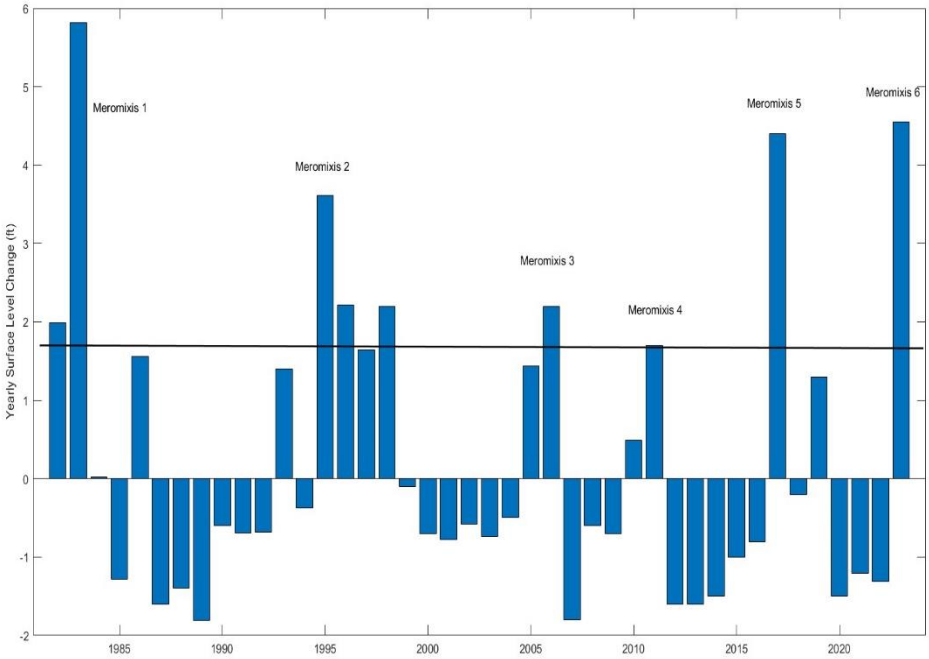

Fig. 60. Historic (1912–present) surface elevations of Mono Lake (ft asl).

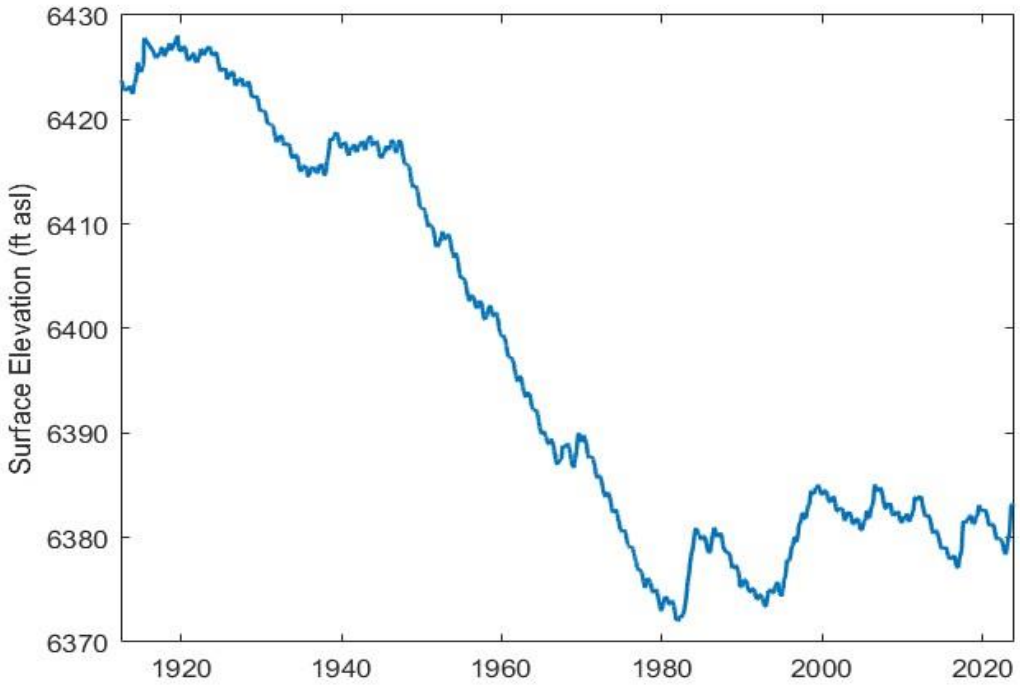

Long-term Trends in *Artemia*

Artemia Mean Annual Abundance, 1979–2023

The seasonal (1 May–30 November) mean daily abundance of the adult *Artemia* has varied 4-fold from 8,100 to 36,900 m^{-2} with an overall mean of 19,000 (Table 23, Fig. 61) over the past 45 years. The peak abundance has varied over 5-fold from 19,700 to 105,200 m^{-2} with an overall mean of 43,500.

Table 23. Mean annual adult *Artemia* abundance (1 May –30 November) and centroid of distribution, 1979–2023. The centroid of *Artemia* distribution is the average of time weighted by adult abundance.

Year	Mean (m^{-2})	Median (m^{-2})	Peak (m^{-2})	Centroid (day of year)
1979	14,100	12,300	31,700	216
1980	14,600	10,200	40,400	236
1981	32,000	21,100	101,700	238
1982	37,000	31,700	105,200	260
1983	18,100	16,500	39,900	230
1984	17,000	19,300	40,200	203
1985	18,500	20,300	33,100	220
1986	14,700	17,400	33,000	192
1987	23,800	22,700	54,300	232
1988	27,600	25,800	71,600	206
1989	36,100	29,100	92,500	256
1990	20,200	17,600	34,900	230
1991	18,100	19,500	34,600	227
1992	18,900	19,500	34,600	220
1993	15,000	16,700	26,900	215
1994	16,600	18,800	29,400	213
1995	15,600	17,200	24,400	203
1996	17,700	17,900	34,600	215
1997	14,400	16,400	27,300	203
1998	19,400	21,400	34,000	227
1999	20,200	21,500	38,400	225
2000	10,600	9,100	22,400	210
2001	20,000	20,000	38,000	209
2002	11,600	10,000	25,500	199
2003	13,100	13,800	29,500	203
2004	32,200	36,900	75,500	174
2005	20,000	19,800	45,400	192
2006	21,500	20,300	55,700	185
2007	18,800	17,500	41,800	186
2008	12,000	12,700	27,600	189
2009	26,000	17,900	72,100	179
2010	14,900	7,400	46,200	191
2011	21,300	16,900	48,900	193
2012	16,700	12,000	53,800	178
2013	27,700	33,300	57,800	195
2014	14,300	8,100	45,000	194
2015	8,200	6,200	19,900	183
2016	11,400	11,000	19,700	221
2017	16,200	16,600	27,700	223
2018	12,900	12,800	23,200	215
2019	14,400	13,400	28,200	220
2020	13,800	14,300	25,900	208
2021	22,600	23,100	50,700	198
2022	16,200	15,400	32,700	222
2023	19,800	20,000	45,300	219
Mean	18,800	17,800	42,700	210
Min	8,200	6,200	19,700	174
Max	37,000	36,900	105,200	260

Fig. 61. Summary statistics of the seasonal (1 May through 30 November) lakewide abundance of adult *Artemia*, 1979–2023. Values are based on interpolated daily abundances.

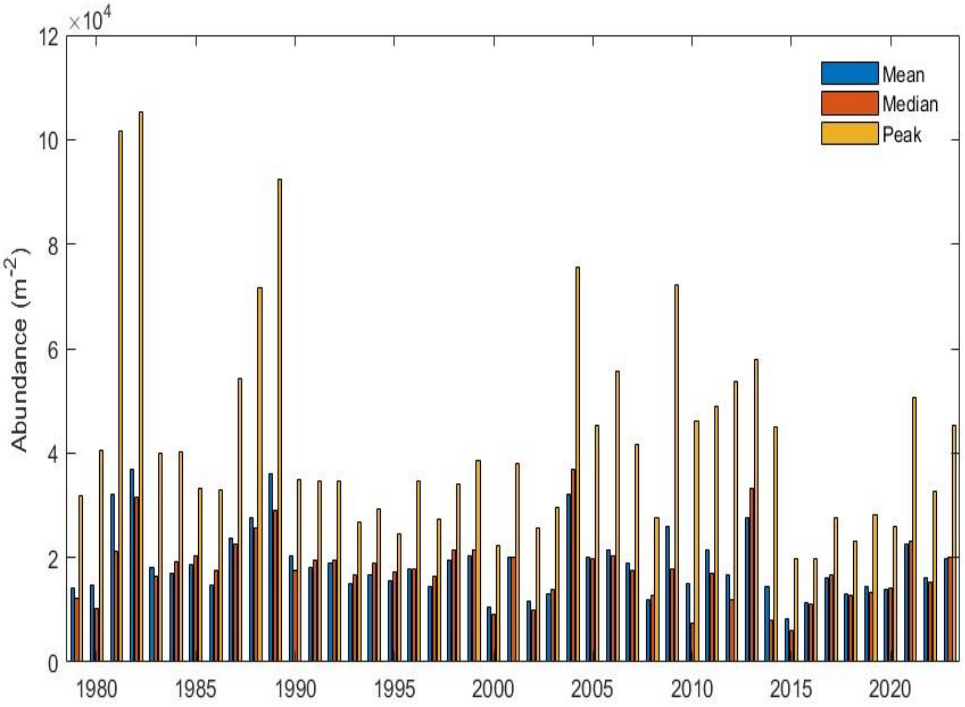

A linear regression of the mean annual abundance on year explains a small proportion (~8%) of the overall variation and is only marginally significant (p-value = 0.053). The slope of -143.6 would suggest a 29% decline of ~6,300 mean annual abundance from 1979 to 2023. However, given the low r^2, the 95% confidence bounds of the slope range are -289 to 2.3. In fact, much of negative slope of the regression is driven by 4 years of exceptionally high abundance (1981, 1982, 1988, 2004). During the period 1979–81, Lenz (1982, 1984) documented a progressive increase in the ratio of peak summer to spring abundances of adult brine shrimp. The smaller spring generations resulted in greater food availability and higher ovoviviparous production by the first generations, leading to larger second generations. The small spring generation of *Artemia* in 1982 also led to the exceptionally large 2nd generation (Melack et al. 2017). The two extended periods of meromixis that broke down in 1988 and 2003 resulted in a large pulse of ammonium accumulated in the monimolimnion into the euphotic zone, higher phytoplankton densities and increased ovoviviparous reproduction and survival resulting in large 2nd generations in 1989 and 2004 (Melack et al. 2017). If these four years are

removed as outliers, then the regression explains a trivial amount of the overall variation (r^2=0.011) and is not statistically significant (p-value=0.51).

Fig. 62. Long-term trend in mean seasonal adult *Artemia* abundance, 1979–2023. Regressions with and without the four outlier years (see explanation in text).

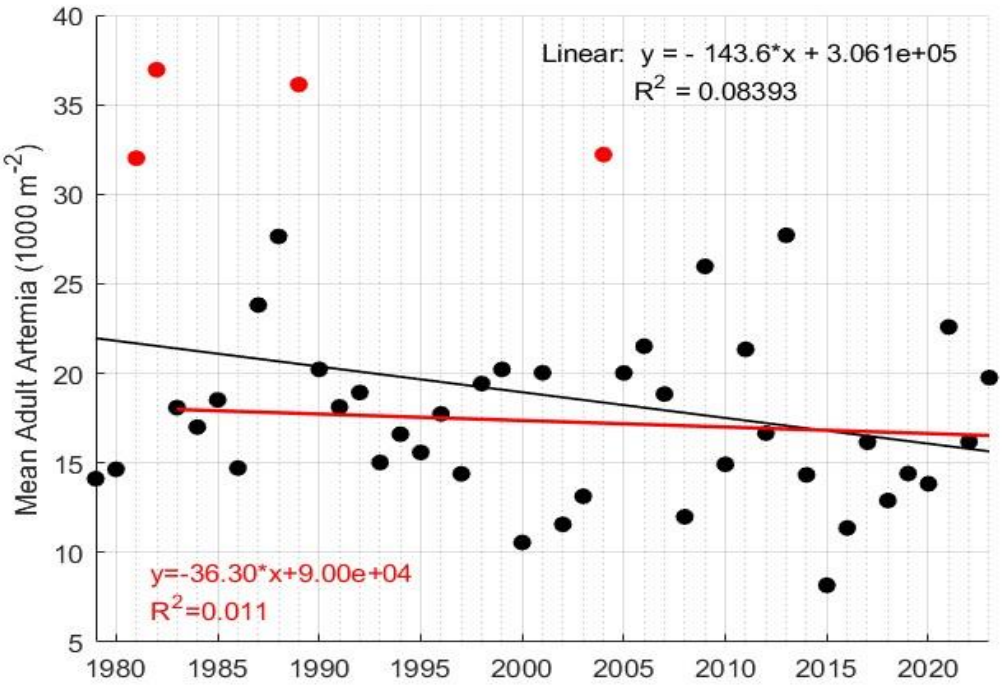

Artemia abundance has a strong seasonal component. Seasonal-trend decomposition using locally estimated scatterplot smoothing (STL) is widely used to estimate trend and seasonal components in environmental time series. Here, we use STL to decompose *Artemia* population data collected over the 41-years period from 1983 to 2023 into trend, seasonal, and noise (unexplained) components to help interpret the long-term monitoring data. The time-series decomposition of adult *Artemia* has significant annual variation in the annual trend (Fig. 63, top panel). Four of the five prominent peaks in the trend panel occur during the year after the breakdown of meromictic events in 1989, 2004, 2013, and 2020 suggesting increased nutrient availability from the upward flux of nutrients accumulated in the deep monimolimnion, subsequent increase in algal abundance, and possibly cyst hatching from recently oxygenated sediments as likely causes. Additional noise or unexplained variation mostly coincides with the peaks in trend suggesting these years are unusual and cannot be explained as part of a larger trend

or seasonal variation. The magnitude of the seasonal component appears to vary slightly over a longer ~20-yr period. The 3rd peak in 2009 is the exception in that it occurs two years after the breakdown of a 2-yr episode initiated in 2005. Regression of the 41-yr trend component yields a 27% decline from ~12,800 to 9,300 m^{-2} in the trend line of adult *Artemia*. Note the seasonal and noise components must be added to the trend line to obtain the observed data, and the line estimates the annual mean trend not abundance during the 1 May–30 November period. As with the analysis of mean annual abundance, removing the two unusual years (1989 and 2004) of high abundance following the breakdown of an extended period of meromixis results in a smaller estimate of decline (~20%) that explains a trivial portion of the overall variation (r^2=0.004) and is not statistically significant (p-value= 0.15). While a long-term decline in abundance cannot be shown to be statistically significant, the role of episodes of meromixis on the observed variability in the *Artemia* population is clear.

Fig. 63. STL decomposition of adult *Artemia* abundance, 1983–2023, into trend (top panel), seasonal variation (2nd panel), "noise" or residual (3rd panel), and the observed data (bottom panel).

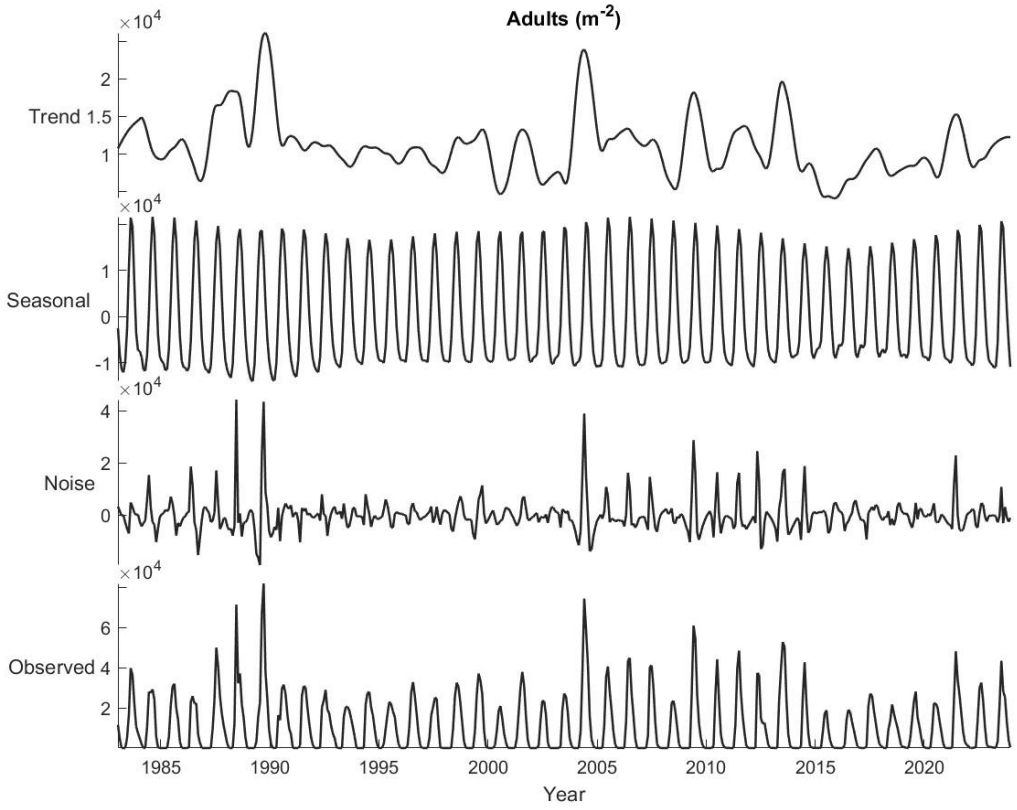

Fig. 64. Long-term trend of adult *Artemia* with seasonal component removed.

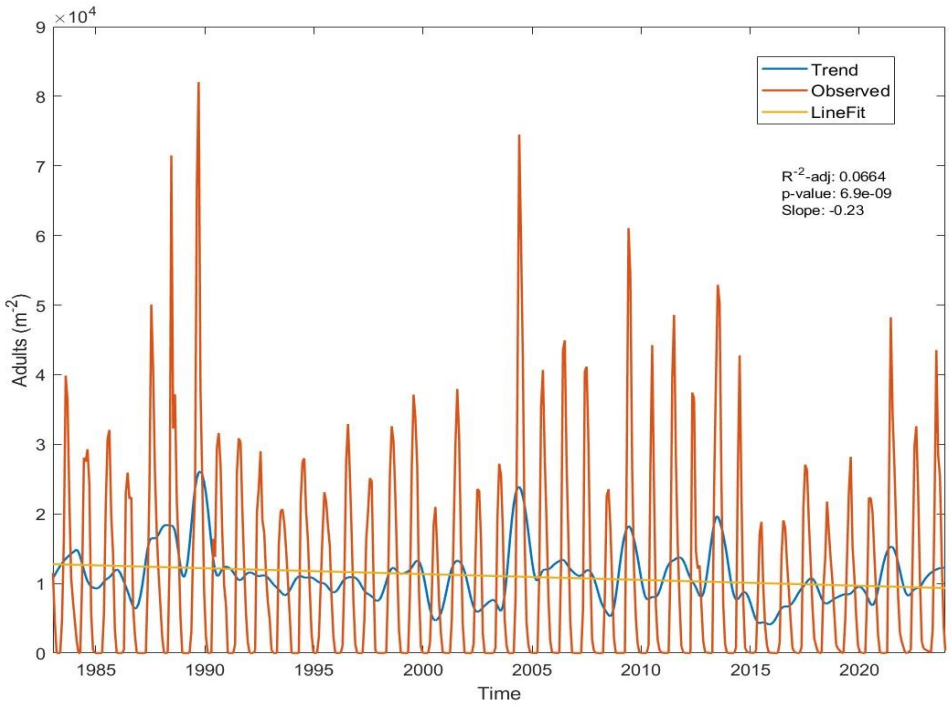

Beginning in 2000, the biomass of *Artemia* was determined by weighing of samples after enumeration and determination of reproductive characteristics. These data provide a second measure of food availability to migrating and nesting bird populations at the lake. Seasonal trend decomposition of the biomass data reveals prominent peaks following the breakdown of meromixis in 2004, 2013, and 2021. The trend line regression explains a very small portion of the observed variation (r^2=0.001) and is not statistically significant (p-value=0.59).

Fig. 65. STL decomposition of *Artemia* biomass, 2000–2023, into trend (top panel), seasonal variation (2nd panel), "noise" or residual (3rd panel), and the observed data (bottom panel).

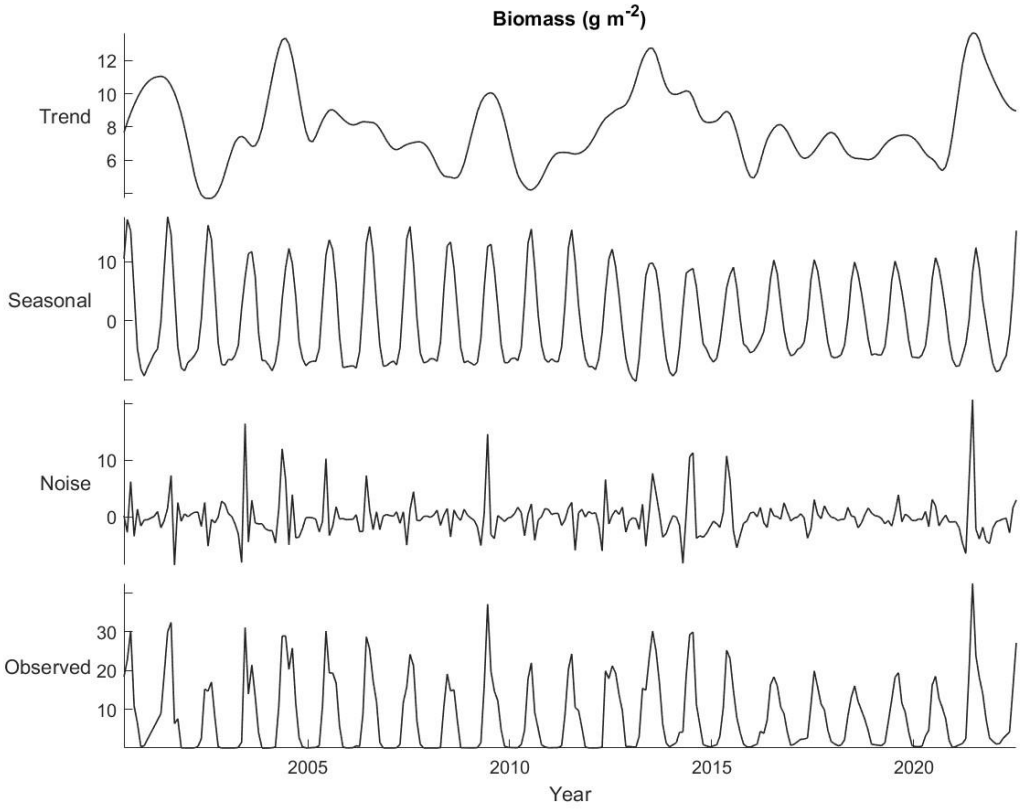

Fig. 66. Long-term trend of *Artemia* biomass with seasonal component removed.

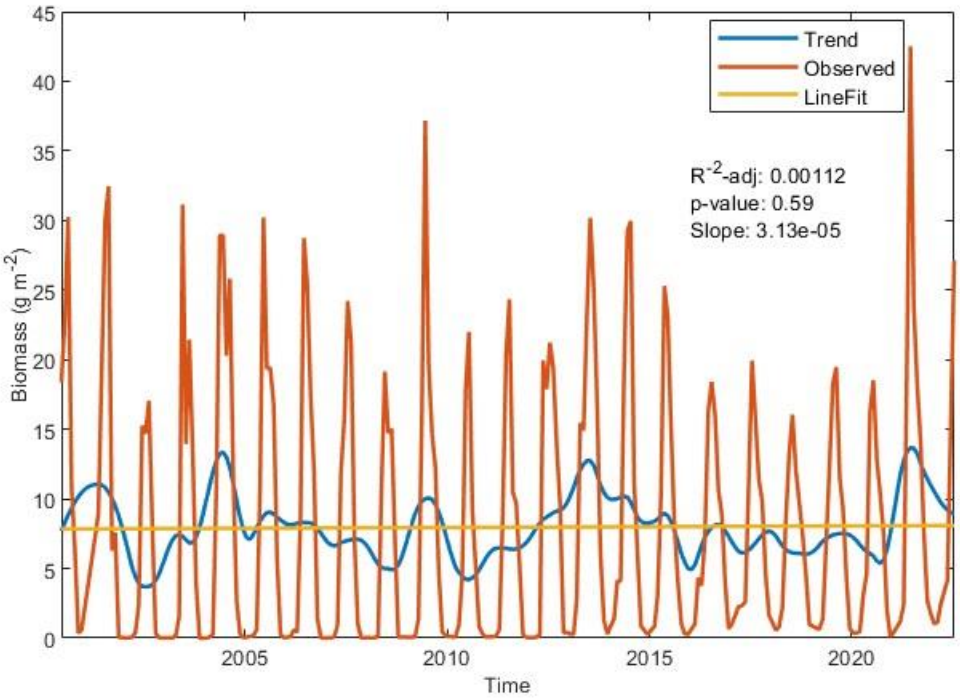

Temporal Distribution of Artemia Abundance

The temporal distribution of *Artemia* abundance may have significant effects on nesting gulls and migrating grebes. Small 1st generations have been shown to affect gull breeding and success (Wrege et al. 2006). A small 2nd generation leads to an early decline in autumn population and significantly impacts migrating grebe populations (Jehl 2007, Boyd et al. 2021). There have been large differences in the size of the 1st (May-June) and 2nd (August) generations of *Artemia* from 1979–2023 (Fig. 67). Adult abundance exceeded 40,000 m^{-2} during May–June in eleven of the 42 years, while autumn abundance approached 100,000 m^{-2} in 1982 and 1989. These two years along with 1983 had very low abundance of adults in May–June. Changes in the relative size of the two generations causes shifts in the overall temporal distribution. The centroid of the abundance distribution shifted from day 173 (23 June) to 260 (16 September) from 1982 to 2004 (Fig. 68). From 1979 to 2005 there was a general shift in the abundance centroid to earlier in the year. A linear regression explained 33% of the variation (p-value = 0.002) and indicated a shift from day 235 to 199, over a month earlier in the year. From 2006–

2015, it remained early (mean, 187) before increasing to nearly a month later (mean, 215) during 2016–2023. These temporal shifts in prey distribution may not impact avian populations if food is not limiting or alternative prey are available (e.g., alkali flies, Herbst 1990, Elphick & Rubega 1995). However, abundance ranged from ~6–34,000 m^{-2} on 1 June (a period critical for gulls) and from ~2,000–25,000 m^{-2} on 1 October (a period critical for grebes). The years in which *Artemia* abundance was at the lower end of these range would certainly impact gulls and grebes.

Fig. 67. Adult *Artemia* abundance, 1982–2023. Red lines shows years when May–June abundance exceeded 40,000 m^{-2}. Blue lines indicate years of exceptionally high autumn abundance.

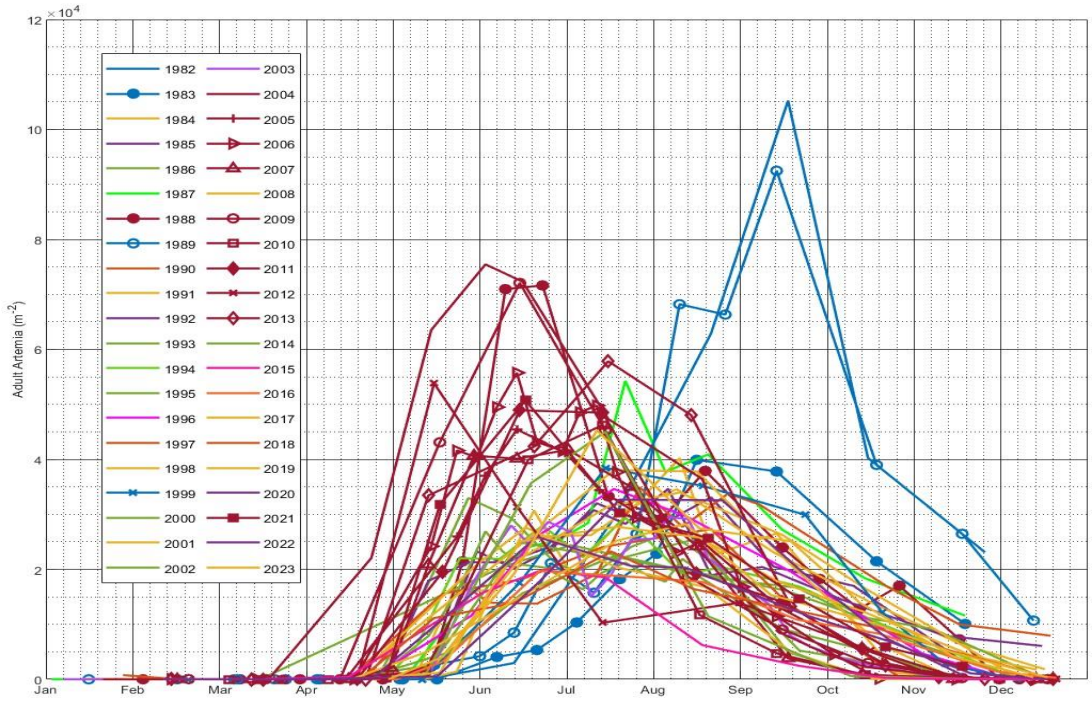

Fig. 68. Abundance-weighted centroid of adult *Artemia*, 1979–2023.

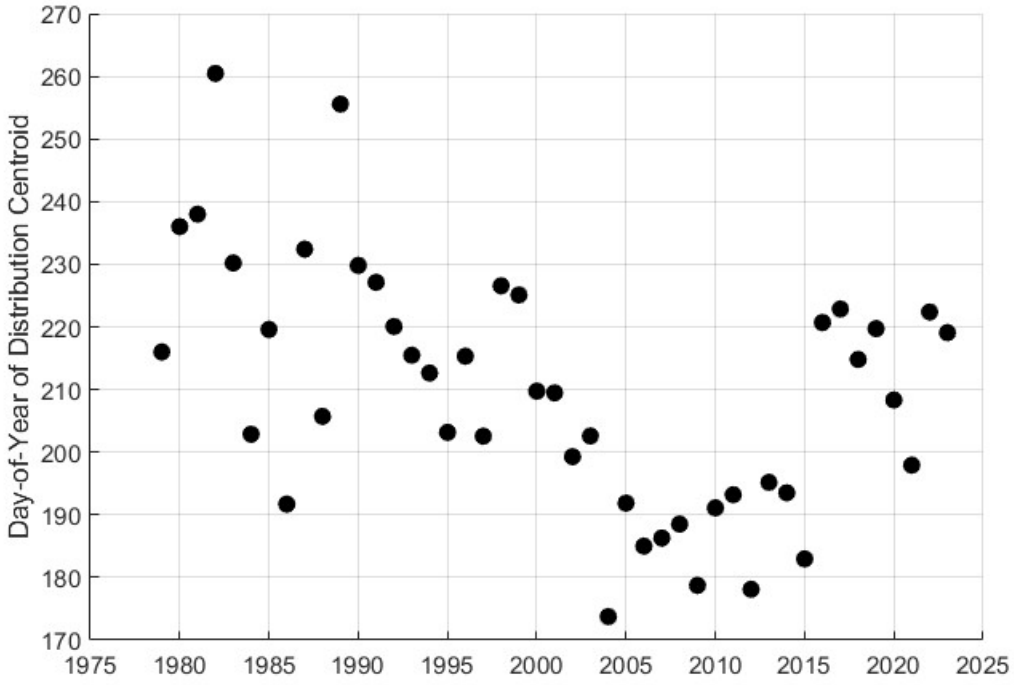

Effects of Meromixis on Seasonal Mean Adult Artemia Abundance

The effects of the onset, persistence, and breakdown of meromixis on ammonium recycling and primary productivity are well-documented (Jellison & Melack 1988, 1993, Jellison et al. 1993, Melack & Jellison 1998, 2017). However, the effects on the seasonal abundance of *Artemia* are still uncertain. Categorizing a year as meromictic or monomictic is inadequate for explaining the seasonal fluxes in nutrients and changes in primary productivity. Years of the onset, breakdown, and immediately following extended periods of meromixis are distinctly different. The spring and summer *Artemia* populations are likely to be little affected until late in the year when holomixis is prevented during the onset years. While the annual period of holomixis is absent during meromictic years and prevents the mixing of ammonium accumulated in the monimolimnion, the upward flux may be large during the last year of meromixis, when significant deepening of the mixed layer occurs. The year immediately following the breakdown of an extended period of meromixis experiences an increase in ammonium and primary productivity. The past 42 years can be divided into 5 categories: monomictic

(11), onset of meromixis (6), meromictic (i.e., persistent stratification) (15), breakdown of meromixis (5), and post breakdown years (5) (Table 24).

Table 24. Seasonal mean abundance of *Artemia* versus mixing status.

Year	Category	Spring	Summer	Autumn
1982	Onset	3,500	43,700	68,300
1983	Persist	2,900	25,400	29,000
1984	Persist	15,400	28,700	14,800
1985	Persist	14,800	30,100	17,700
1986	Persist	23,300	22,100	5,800
1987	Persist	14,600	39,300	23,000
1988	Breakdown	37,100	36,200	19,500
1989	Post Breakdown	7,100	43,100	62,800
1990	Mono	13,600	27,800	23,800
1991	Mono	11,400	30,200	18,100
1992	Mono	19,100	27,400	15,600
1993	Mono	16,300	19,100	13,600
1994	Mono	18,400	23,100	14,200
1995	Onset	18,000	21,100	13,300
1996	Persist	14,600	30,500	15,200
1997	Persist	15,800	24,800	9,400
1998	Persist	12,200	31,400	20,800
1999	Persist	10,700	35,400	22,800
2000	Persist	9,600	19,600	7,300
2001	Persist	18,200	35,900	15,200
2002	Persist	13,600	22,600	4,000
2003	Breakdown	15,800	23,300	6,500
2004	Post Breakdown	64,800	41,500	5,700
2005	Onset	31,300	29,400	8,800
2006	Persist	37,200	31,600	6,200
2007	Breakdown	31,500	30,400	3,700
2008	Post Breakdown	19,300	18,900	3,600
2009	Mono	52,300	31,800	6,200
2010	Mono	21,000	27,900	2,900
2011	Onset	31,600	33,100	9,300
2012	Breakdown	36,900	12,800	8,100
2013	Post Breakdown	35,900	49,200	10,900
2014	Mono	18,300	28,200	3,200
2015	Mono	14,100	12,400	1,900
2016	Mono	9,500	18,100	10,200
2017	Onset	12,800	26,100	14,600
2018	Persist	12,400	19,000	11,200
2019	Persist	10,500	24,600	12,700
2020	Breakdown	16,000	20,600	10,600
2021	Post Breakdown	35,500	29,800	12,100
2022	Mono	8,300	30,800	16,200
2023	Onset	13,200	34,800	18,600

One-way analysis of variance of mean adult abundance during spring (May-June), summer (July-August), and autumn (September-October) revealed only one significant

(95% confidence level) difference between the means of the five categories. Adult abundance was significantly higher during May–June of the year following the breakdown of meromixis than during meromixis (Fig. 69).

Fig. 69. Mean spring (April–May) lakewide abundance of adult *Artemia* during different mixing regimes.

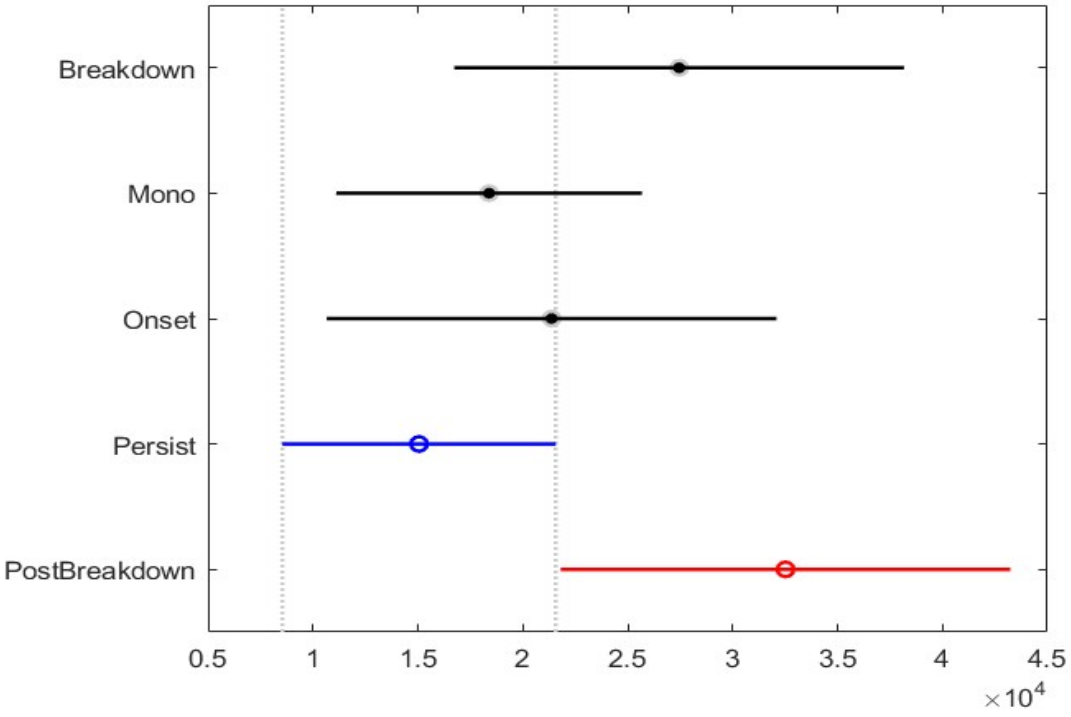

The high variability within the five categories prevents further conclusions. This variability may arise due to the different nature of the meromictic episodes or the importance of other factors on the *Artemia* population. The degree and timing of freshwater inflows during the onset of meromixis, the length of the meromictic episode, the nature of the deepening mixed layer during the meromictic episode and breakdown are all likely important and will require measures of ammonium flux, primary productivity, and hydrodynamic modeling to fully characterize. Each of these factors in addition to changing salinity and annual climatic variation likely affect cyst hatching, growth, survivorship and reproduction of *Artemia.*

Naupliar and Cyst Production

The annual production of encysted embryos (cysts) and ovoviviparously produced embryos (naupliar eggs) depends on seasonal variation in the number of ovigerous females, the mode of reproduction (cyst versus naupliar), fecundity, and brood interval. Both naupliar and cyst production are highly variable. Annual naupliar production which leads to the 2nd and sometimes a small 3rd late summer generation has varied from 5 to 634 (10^3 m^{-2}) with a 41-yr mean of 183 (10^3 m^{-2}). The total cyst production is much larger and has varied from 1.9 to 5.7 (10^6 m^{-2}) with a mean of 3.7 (10^6 m^{-2}). While there is no significant longterm trend in naupliar production, a linear regression of cyst production on year yields a significant (r^2=0.286, p-value=0.0003) decline of 47.2 (10^3 m^{-2} yr^{-1}) or a 40% decline over 40 years (Table 25, Fig. 70). The five mixing categories cannot explain a statistically significant portion of this variation (1-way Anova p-value=0.814).

Fig. 70. Long-term variation in annual cyst and nauplii production, 1983–2023.

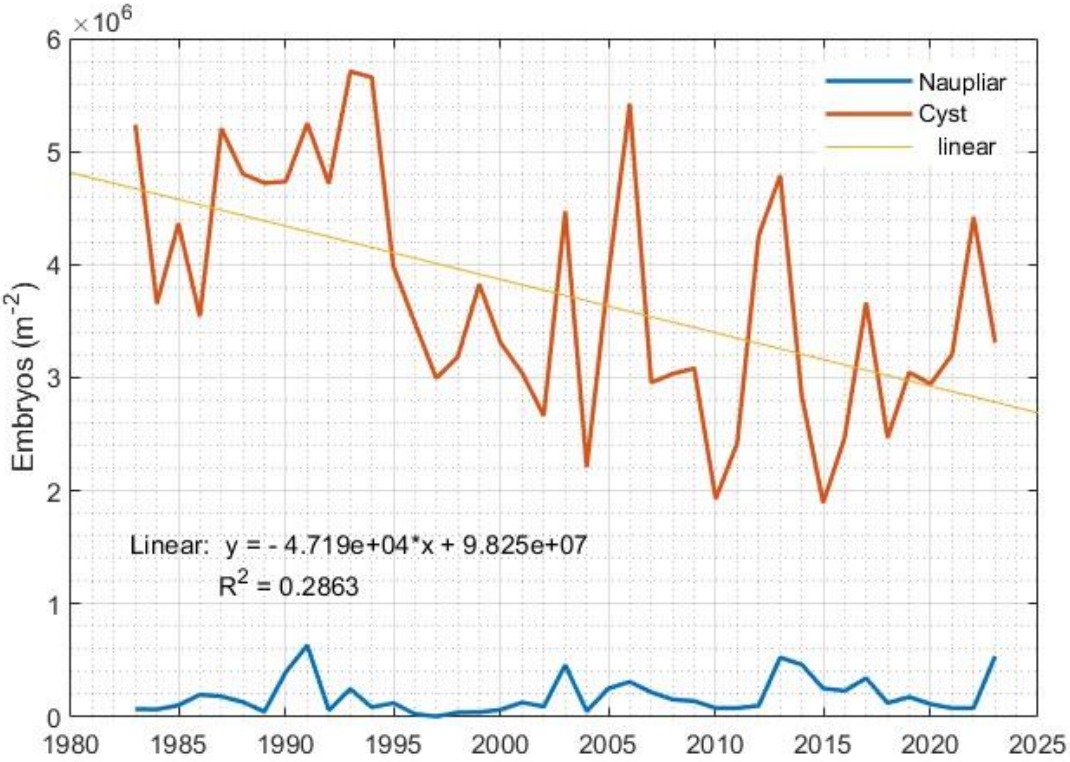

Table 25. Annual nauplii and cyst production, 1983–2023.

Year	Mixing Category	Nauplii (x 10^3 m^{-2})	Cyst (x 10^6 m^{-2})
1983	Persist	70	5.2
1984	Persist	67	3.7
1985	Persist	104	4.4
1986	Persist	197	3.5
1987	Persist	183	5.2
1988	Breakdown	132	4.8
1989	Post Breakdown	47	4.7
1990	Mono	398	4.7
1991	Mono	634	5.2
1992	Mono	60	4.7
1993	Mono	247	5.7
1994	Mono	86	5.7
1995	Onset	123	4.0
1996	Persist	27	3.5
1997	Persist	5	3.0
1998	Persist	40	3.2
1999	Persist	42	3.8
2000	Persist	64	3.3
2001	Persist	128	3.0
2002	Persist	92	2.7
2003	Breakdown	460	4.5
2004	Post Breakdown	51	2.2
2005	Onset	252	3.9
2006	Persist	311	5.4
2007	Breakdown	219	3.0
2008	Post Breakdown	155	3.0
2009	Mono	140	3.1
2010	Mono	79	1.9
2011	Onset	79	2.4
2012	Breakdown	100	4.3
2013	Post Breakdown	526	4.8
2014	Mono	464	2.8
2015	Mono	252	1.9
2016	Mono	232	2.5
2017	Onset	344	3.7
2018	Persist	124	2.5
2019	Persist	177	3.0
2020	Breakdown	114	2.9
2021	Post Breakdown	78	3.2
2022	Mono	79	4.4
2023	Onset	537	3.3

To understand the decline in cyst production further, the abundance-weighted mean of each of the factors contributing to the cyst production calculation (ovigerous females, oviparity, fecundity) was examined. A linear regression of the number of oviparous (nauplii producing) females on year shows no significant change. However, fecundity (eggs per female) declined significantly over time (r^2=0.264, p-value=0.0006

(Fig. 74). The long-term trend line ranged from 51.2 eggs brood^{-1} in 1983 to 29.5 eggs brood^{-1} in 2023, a 42% decrease, and can explain the estimated long-term decrease in cyst production of 40%. Fecundity is known to vary with adult female length. A linear regression of the abundance-weighted adult female length also showed a significant long-term decrease (r^2=0.317, p-value=0.0001) from 10.89 mm to 9.66 mm, an 11% decrease (Fig. 75). Means of abundance-weighted fecundity or female length did not vary significantly across the five mixing categories.

The mean lakewide temperature at 2 m estimated using the STL method increased from 11.5°C to 12.2°C over the 41-yr period (Fig. 71) and may contribute to slightly shorter brood intervals and higher cyst production. Neither annual abundance-weighted fecundity or female length were significantly correlated with changes in the summer (1 June - 30 September) average temperatures at 2 m.

Fig. 71. Trend line of lakewide temperature at 2 m with seasonal component removed, 1983–2023.

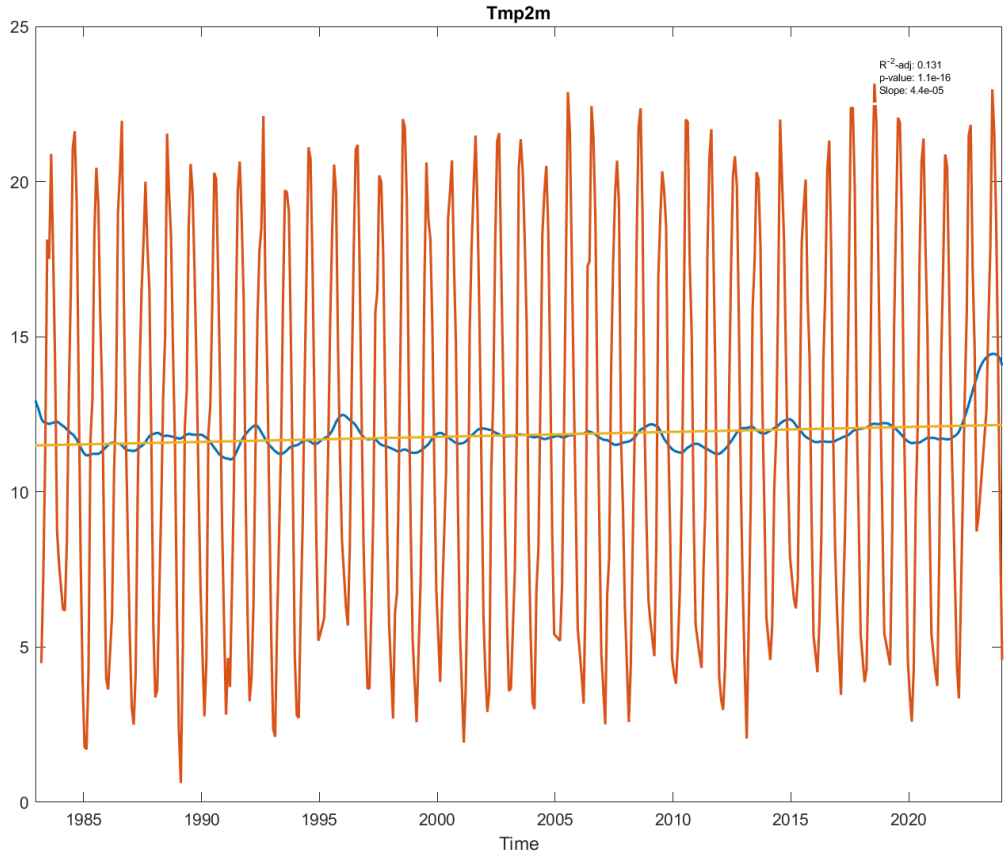

Salinity of the mixolimnion (upper mixed layer) varies due to lake level changes and seasonal changes in salinity stratification associated with the annual thermal regime during the 6 episodes of meromixis. Summer mixolimnetic salinities are more likely to affect the *Artemia* population dynamics than overall lake mean salinity. Routine conductivity measurements using high resolution conductivity-temperature-depth profilers began in 1991. For the period 1991 through 2023 there was a positive correlation of both fecundity and adult female length with the mean 1 June–30 September conductivity at 2 m. The mean conductivity at 2 m ranged from 74 to 92 mS cm^{-1} (69 to 91 g kg^{-1}). The overall best fit trend line of fecundity decreased 40% from 51 eggs ind^{-1} in 1991 to 30 eggs ind^{-1} in 2023. The best fit trend line of adult female length decreased 9% from 10.7 mm in 1991 to 9.7 mm in 2023.

This positive correlation with salinity is opposite to what is expected based on well-established osmoregulatory costs and energy constraints, and salinity bioassays using Mono Lake *Artemia* (Dana et al. 1990, 1993). This suggests that mixolimnetic salinity is inversely covarying with some other aspect of episodic meromixis that negatively effects growth and fecundity.

Fig. 72. Long-term variation in abundance-weighted fecundity, 1983–2023.

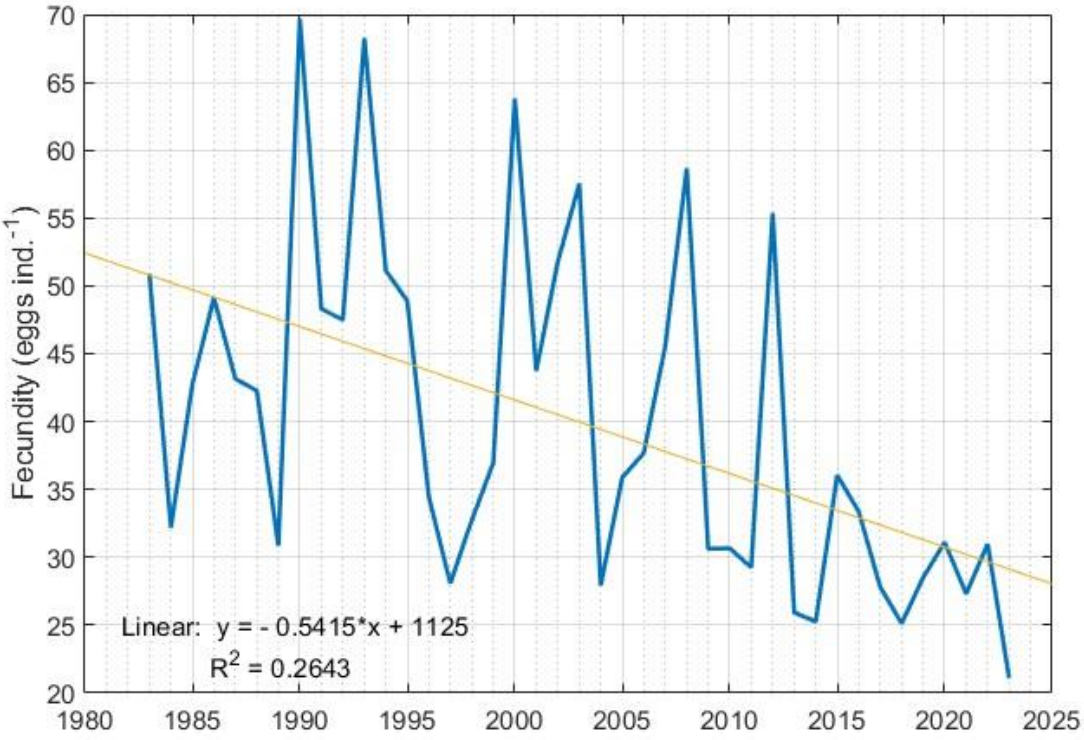

Fig. 73. Long-term variation in abundance-weighted adult female length, 1983–2023.

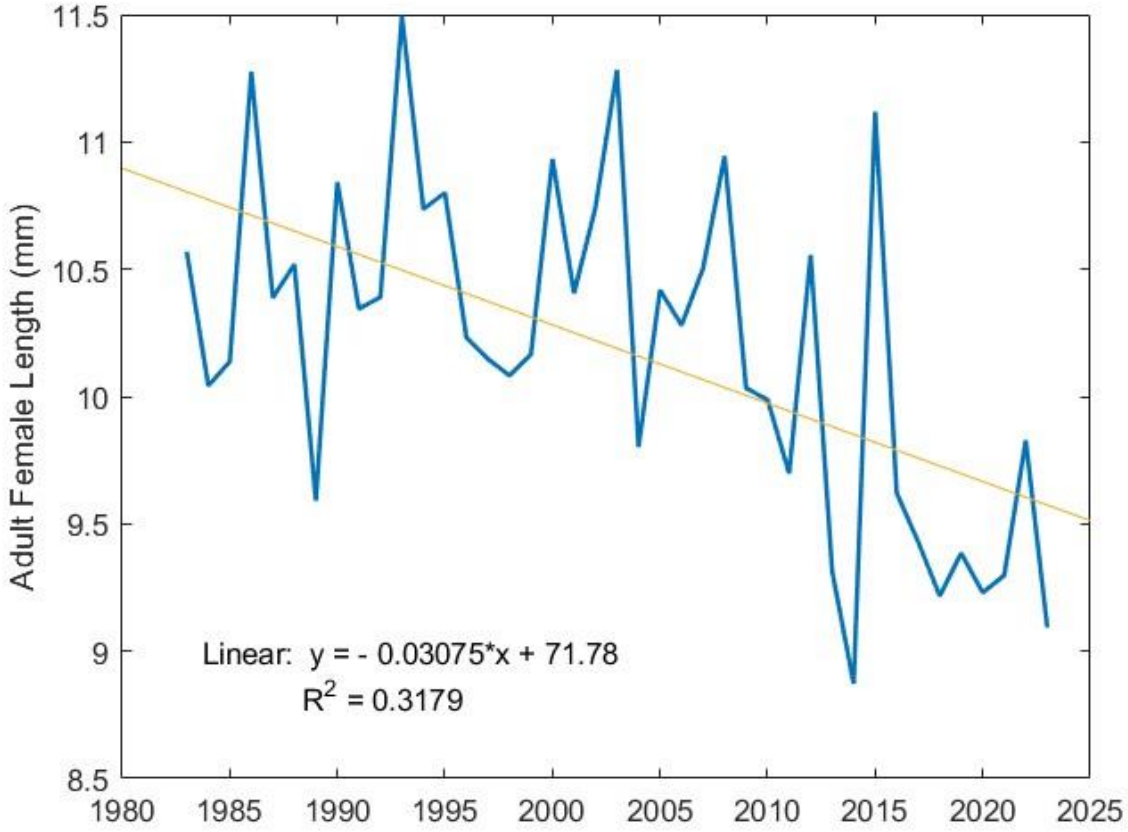

Fig. 74. Mean adult female weighted fecundity versus summer (1 June– 30 September) mean lakewide conductivity at 2 m depth.

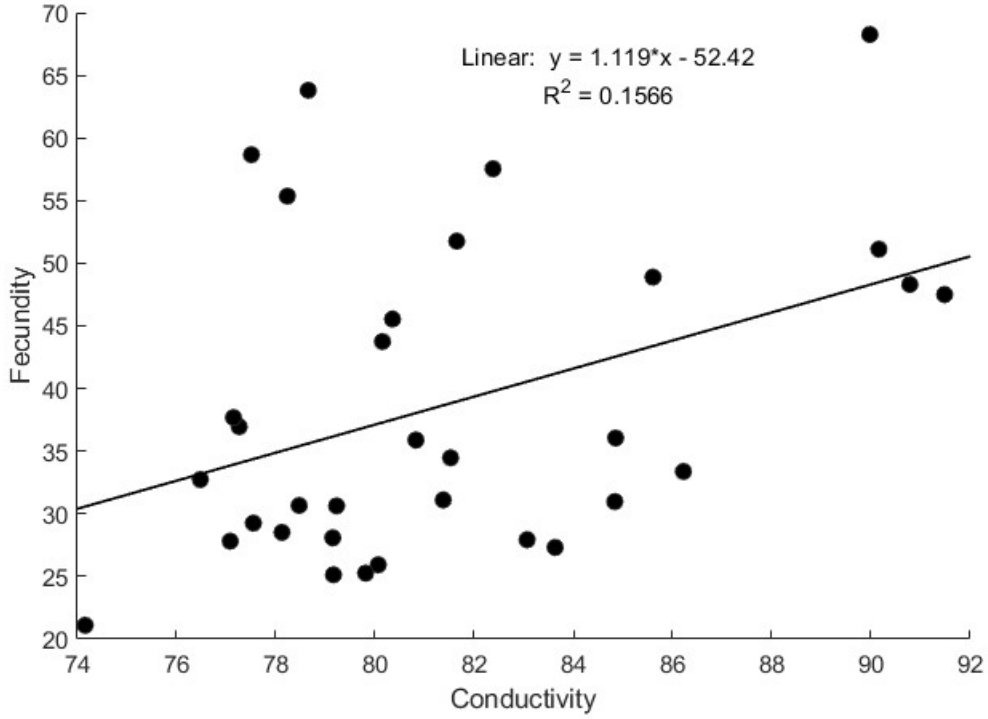

Fig. 75. Mean adult female weighted length versus summer (1 June– 30 September) mean lakewide conductivity at 2 m depth.

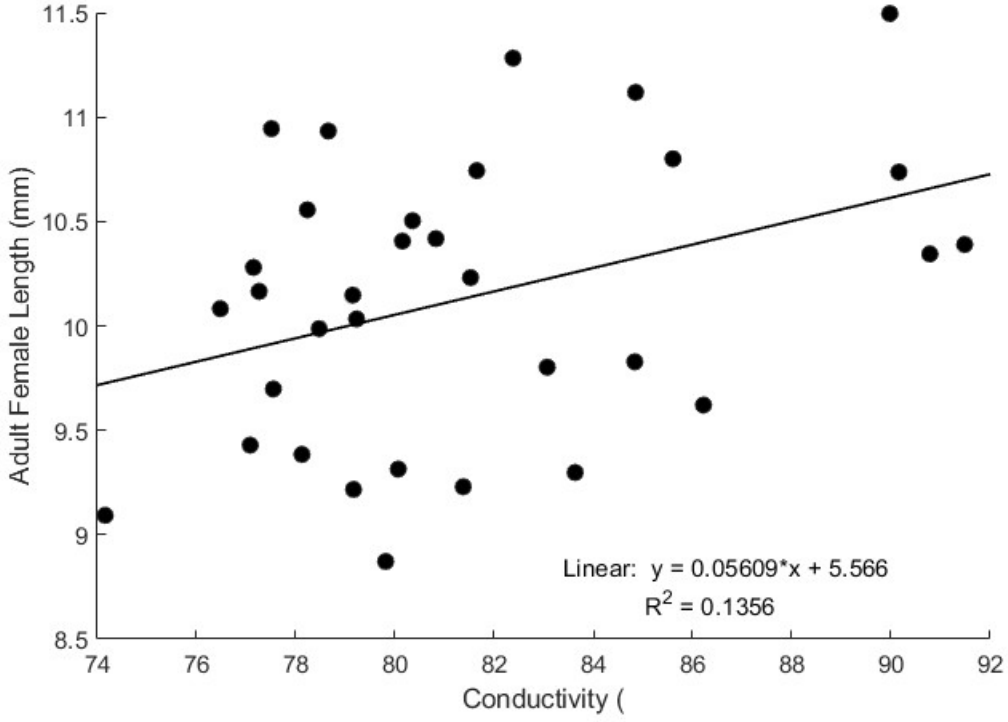

Transparency

For more than three decades (1982–2014), the plankton community of Mono Lake exhibited a regular seasonal variation of abundant phytoplankton and low transparency during winter-spring followed by decreased phytoplankton and high transparency during the summer due to grazing by abundant *Artemia*. High summer transparencies (>6 m, as measured by Secchi depth) due to *Artemia* grazing were a perennial seasonal feature. Winter transparency was generally 0.5-2 m during winter and summer values were 5-12 m (Fig. 76). During this period winter transparencies increased during periods of meromixis due to the lack of autumn turnover and mixing of nutrient-rich hypolimnetic waters throughout the water column. This increase in winter transparency was observed during three episodes of meromixis: 1983–1988, 1997–2005, and 2006–2007.

In 2014, the lake entered a state unseen during the previous thirty years as midsummer transparencies remained less than 2 m. These low transparencies continued through 2015 and 2016. Summer transparencies increased to 3–6 m during a period of meromixis, 2017–2019, but returned to the low levels during 2020–2022. Changes in transparency in Mono Lake is primarily a function of phytoplankton abundance. Unfortunately, chlorophyll measurements from 2013–2022 were improperly analyzed and have limited utility in examining the changes in transparency (see Chapter 4).

Individual filtering rates of adult *Artemia* are high (150 ml d^{-1}, Lenz 1982; 170 ml d^{-1}, Jellison, unpublished data) and, when abundant, *Artemia* can graze the standing biomass of phytoplankton daily. Thus, phytoplankton abundance in Mono Lake is a dynamic balance between growth and loss processes (grazing, sinking, senescence). This balance markedly changed in 2014–2016 and 2020–2022 due to yet undetermined causes.

Fig. 76. Long-term changes in transparency (Secchi depth) and surface elevation. Secchi depth is plotted vertically to illustrate the coincidence of adult *Artemia* and midsummer clearing of the upper water column.

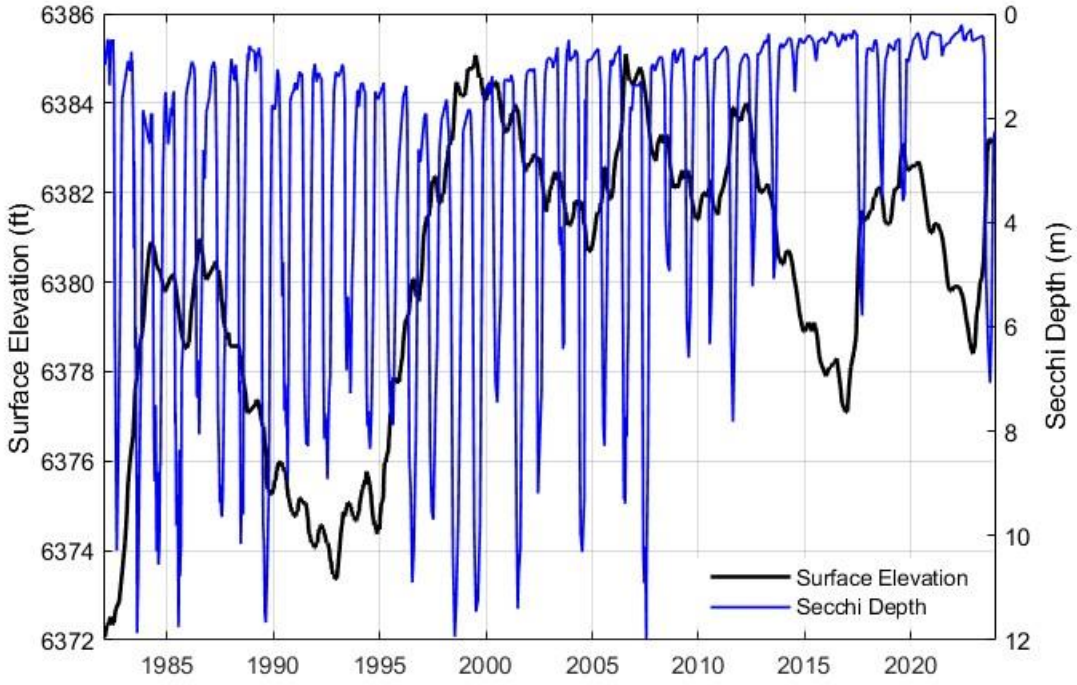

The abundant summer generation of adult *Artemia* is primarily responsible for the marked seasonal changes in transparency and phytoplankton abundance (Fig. 77). Adult *Artemia* were the lowest observed during 2015 and 2016 and coincide with the unusually low transparency and high phytoplankton abundance. However, *Artemia* were only slightly more abundant in some other years (e.g., 1996, 2001, 2008), when midsummer transparency was higher. *Artemia* were more abundant during the second period (2020–2022) of low midsummer transparency than other years of high midsummer transparency.

Fig. 77. Long-term changes in transparency (Secchi depth) and adult *Artemia* abundance. Secchi depth is plotted increasing upward to visualize the coincidence of adult *Artemia* midsummer clearing of the upper water column more easily.

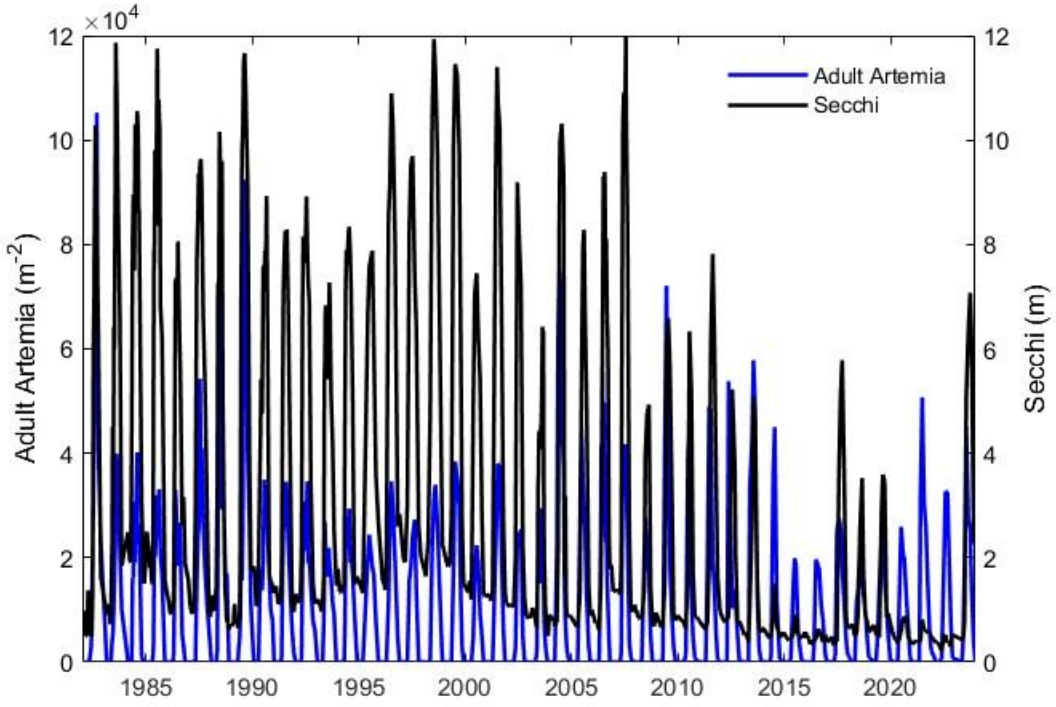

Summary

The recurring episodes of meromixis are likely to continue given the current management regime. While the short-term effects on nutrient recycling, and algal productivity have been documented, long-term effects of this change on the lake's biota and nesting and migratory bird populations, if any, are not yet known.

The five previous episodes of meromixis of varying duration and beginning of the sixth in 2023 have introduced additional components of variability to those due to climatic variation and changing management regimes. Long-term trends in the *Artemia* population and their effect on breeding and migrating bird populations are not well understood.

The long-term trend in adult *Artemia* is driven largely by two years of a large second generation associated with a very low spring hatch at the lake's highest salinity and historic low in 1981 and 1982 and a couple years of high abundance associated with the breakdown of two long periods of meromixis. Without these years, a long-term trend

in the 44-yr record is obscured by high interannual variability. *Artemia* biomass measurements, begun in 2000, show no statistically significant long-term trend.

A significant (40%) decrease in annual production of over-wintering cysts (1983–2023) did occur and is not associated with conditions during years post-breakdown of meromixis. The decrease is a result of a 42% decline in abundance-weighted fecundity. A significant, but smaller (11%), decrease in adult female length occurred. The reasons for the decline in fecundity are not known.

The changing physical, nutrient, and biotic regimes associated with episodic meromixis over the past 44 years cannot be divided into simple categories. Characterizing years as monomictic, onset of meromixis, meromictic, breakdown of meromixis, and post meromixis provided limited insight into causal explanations of observed seasonal and interannual variation. The only statistically significant difference of adult mean abundance was smaller May–June values during meromictic compared to post-meromictic years. Further understanding will require better characterization of the mixing regimes with estimates of nutrient fluxes and hydrodynamic modeling of stratification regimes.

In 2014–2016 and again in 2020–2022 summer transparencies were <2 m. These low midsummer transparencies associated with high phytoplankton abundance had not been observed from 1979 to 2013, or in earlier studies (Mason 1967, Winkler 1977). These conditions represent a significant shift from the previous balance between growth and loss of phytoplankton extending to at least 1965. The 2014–2016 period of high summer phytoplankton abundance was terminated by the onset of meromixis in 2017, and the 2020–2022 period terminated by the onset of meromixis in 2023,

The monitoring program will continue to collect a full suite of limnological data. In addition, several components have been added to address questions raised by the analysis of the long-term data. Deployment of moored arrays of temperature, salinity, chlorophyll fluorescence and dissolved oxygen sensors will provide continuous records to better characterize vertical mixing regime, nutrient fluxes and algal abundance. The design and implementation of laboratory experiments and models to examine the

dynamic balance between phytoplankton growth and loss processes in relation to *Artemia* dynamics and physical condition is recommended.

REFERENCES

Arar, E. J., and G. B. Collins. 1997. Method 445.0 In vitro determination of chlorophyll *a* and pheophytin *a* in marine and freshwater algae by fluorescence, *In* U.S. Environmental Protection Agency.

Blevins, M. 1984. Background report on Mono Basin geology and hydrology. Los Angeles Department of Water and Power, Aqueduct Division.

Bower, C. E., and T. Holm-Hansen. 1980. A salicylate–hypochlorite method for determining ammonia in seawater. Canadian Journal Fisheries Aquatic Sciences 37: 794–798.

Boyd, W., N. Clyde, A. Breault, R. Di Paolo, and M. McAdie. 2021. Abundance, distribution and migration patterns of North American Eared Grebes (*Podiceps nigricollis*). Waterbirds 44: 76–85.

California State Water Resources Control Board. 1994. Final environmental impact report for the review of Mono Basin water rights of the city of Los Angeles. California Environmental Protection Agency.

Chapman, D. V. 1996. Water quality assessments: a guide to the use of biota, sediments, and water in environmental monitoring, 2nd ed. E & FN Spon.

Dana, G., R. Jellison, and J. Melack. 1995. Effects of different natural regimes of temperature and food on survival, growth, and development of *Artemia monica* Verrill. J. Plankton Res. 17: 2117–2130.

Dana, G., R. Jellison, J. Melack, and G. Starrett. 1993. Relationships between *Artemia monica* life history characteristics and salinity. Hydrobiologia 263: 129–143.

Dana, G. L., and P. H. Lenz. 1986. Effects of increasing salinity on an *Artemia* population from Mono Lake, California. Oecologia 68: 428–436.

Elphick, C., and M. Rubega. 1995. Prey choices and foraging efficiency of recently fledged California Gulls at Mono Lake, California. Great Basin Naturalist 55: 363–367.

Golterman, H. L., and R. S. Clymo. Methods for chemical analysis of fresh waters. IBP Handbook No. 8.

Heath, H. The external development of certain phyllopods. J. Morphology 38: 453–483.

Herbst, D. 1990. Distribution and abundance of the alkali fly (*Ephydra hians*) Say at Mono Lake, California (USA) in relation to physical habitat. Hydrobiologia 197: 193–205.

Holmes, R. M., A. Aminot, R. Kerouel, B. Hooker, and B. J. Peterson. 1999. A simple and precise method for measuring ammonium in marine and freshwater ecosystems. Canadian Journal Fisheries Aquatic Sciences 56: 1801–1808.

Holm-Hansen, O., and B. Riemann. 1978. Chlorophyll *a* determination: improvements in methodology. Oikos 30: 438–447.

Jehl, J. 2007. Why do Eared Grebes leave hypersaline lakes in autumn? Waterbirds 30: 112–115.

Jellison, R., S. MacIntyre, and F. J. Millero. 1999a. Density and conductivity properties of Na-CO3-Cl-SO4 brine from Mono Lake, California, USA. Int. J. Salt Lake Research 8: 41–53.

Jellison, R., S. MacIntyre, and F. J. Millero. 1999b. Density and conductivity properties of Na-CO3-Cl-SO4 brine from Mono Lake, California, USA (erratum). Int. J. Salt Lake Research 8: 384.

Jellison, R., and J. Melack. 1988. Photosynthetic activity of phytoplankton and its relation to environmental factors in hypersaline Mono Lake, California. Hydrobiologia 158: 69–88.

Jellison, R., and J. Melack. 1993. Meromixis in hypersaline Mono Lake, California. 1. Stratification and vertical mixing during the onset, persistence, and breakdown of meromixis. Limnology and Oceanography 38: 1008–1019.

Jellison, R., L. Miller, J. Melack, and G. Dana. 1993. Meromixis in hypersaline Mono Lake, California. 1. Nitrogen fluxes. Limnology and Oceanography 38: 1020–1039.

Lenz, P. H. 1982. Population studies on *Artemia* in Mono Lake, California. PhD Dissertation. University of California, Santa Barbara.

Lenz, P. H. 1984. Life-history analysis of an *Artemia* population in a changing environment. Journal of Plankton Research 6: 967–983.

Los Angeles Department of Water and Power. 2012, 2013, …,2023. Annual Compliance Reports to State Water Resources Control Board.

Mason, D. T. 1967. Limnology of Mono Lake, California, University of California Press.

Melack, J., and R. Jellison. 1998. Limnological conditions in Mono Lake: contrasting monomixis and meromixis in the 1990s. Hydrobiologia 384: 21–39.

Melack, J., R. Jellison, S. MacIntyre, and J. Hollibaugh. 2017. Mono Lake plankton dynamics over three decades of meromixis or monomixis, p. 325–351. *In* R. Gulati, E. Zadereev, and A. Degermendzhi [eds.], Ecology of Meromictic Lakes.

Patten, D. T., F. Conte, W. E. Cooper, and others. 1987. The Mono Basin ecosystem: effects of changing lake level, National Academy Press.

Solorzano, L. 1969. Determination of ammonia in natural waters by the phenol-hypochlorite method. Limnology and Oceanography 14: 799–801.

Strickland, J. D. H., and T. R. Parsons. 1972. A practical handbook of seawater analysis. Bull. Fish. Res. Bd. Canada.

Taylor, B. W., C. F. Keep, R. O. Hall, B. J. Koch, L. M. Tronstad, A. S. Flecker, and A. J. Ulseth. 2007. Improving the fluorometric ammonium method: matrix effects, background fluorescence, and standard additions. Journal of the North American Benthological Society 26: 167–177.

Weber, C. I., L. A. Fay, G. B. Collins, D. E. Rathke, and J. Tobin. 1986. A review of methods for the analysis of chlorophyll in periphyton and plankton of marine and freshwater systems. OHSU-TB-15. OHSU-TB-15.

Winkler, D. W., ed. 1977. An ecological study of Mono lake, California, University of California, Davis.

Winkler, D. W., and S. D. Cooper. 1986. Ecology of migrant Black-necked Grebes (*Podiceps nigricollis*) at Mono Lake, California. Ibis (London, England) 128: 483–491.

Wrege, P., W. Shuford, D. Winkler, and R. Jellison. 2006. Annual variation in numbers of breeding California Gulls at Mono Lake, California: The importance of natal philopatry and local and regional conditions. CONDOR 108: 82–96.

Zadorojny, C., S. Saxton, and R. Finger. 1973. Spectrophotometric Determination of Ammonia. Journal - Water Pollution Control Federation 45: 905–912.

Section IV. Mono Basin Waterfowl Habitat Restoration Program 2023 Monitoring Report

Prepared by Deborah House, Mono Basin Waterfowl Program Director and Motoshi Honda, Watershed Resources Specialist

Mono Basin Waterfowl Habitat Restoration Program 2023 Monitoring Report

Prepared by:
Deborah House, Mono Basin Waterfowl Program Director
Los Angeles Department of Water and Power
Bishop, CA 93514

Prepared for the State Water Resources Control Board
and Los Angeles Department of Water and Power
April 2024

TABLE OF CONTENTS

EXECUTIVE SUMMARY I
1.0 INTRODUCTION 1-1
1.1 Ecological Setting 1-1
1.2 Environmental Challenges and Legal Background 1-2
2.0 WATERFOWL HABITAT RESTORATION 2-1
3.0 WATERFOWL HABITAT RESTORATION MONITORING PROGRAM 3-1
3.1 Hydrology 3-4
3.1.1 Hydrologic Monitoring Methodologies 3-5
3.1.2 Hydrology Data Summary and Analysis 3-7
3.1.3 Hydrology Results 3-8
3.1.4 Hydrology Discussion 3-13
3.2 Saltcedar Eradication 3-14
3.2.1 Overview of Saltcedar Eradication 3-14
3.2.2 Saltcedar Eradication Methodologies 3-14
3.2.3 Saltcedar Eradication Results 3-15
3.2.4 Saltcedar Eradication Discussion 3-15
3.3 Waterfowl Population Surveys and Studies 3-16
3.3.1 Waterfowl Population Surveys — Survey Areas 3-16
3.3.2 Waterfowl Population Monitoring Methodologies 3-28
3.3.3 Waterfowl Data Summary and Analysis 3-32
3.3.4 Waterfowl Population Survey Results 3-35
3.3.6 Waterfowl Survey Discussion 3-100
4.0 SUMMARY AND RECOMMENDATIONS 4-1
5.0 LITERATURE CITED 5-1

FIGURES

Figure 1. Annual Mono Basin runoff based on water year 3-9
Figure 2. Mono Lake monthly elevation, 2023 3-10
Figure 3. Mono Lake elevation between 1990 and 2023 3-11
Figure 4. Waterfowl survey areas 3-18
Figure 5. Mono Lake shoreline subareas and cross-lake transects 3-19
Figure 6. Mono Basin restoration ponds locator map 3-22
Figure 7. Bridgeport Reservoir shoreline subareas 3-25
Figure 8. Crowley Reservoir shoreline subareas 3-27
Figure 9. 2023 Breeding waterfowl population vs. long-term mean 3-37
Figure 10. Annual breeding population size vs. lake level in March 3-40
Figure 11. Total broods vs. lake level in June 3-40
Figure 12. Mean number of breeding waterfowl and total broods —restoration ponds, 2023 3-42
Figure 13. Northern Shoveler and Ruddy Duck 2023 totals vs. the long-term means 3-44
Figure 14. Other species— 2023 totals vs. the long-term means 3-44
Figure 15. 2023 Mono fall waterfowl survey totals and 2002-2022 means 3-45
Figure 16. Fall spatial distribution of waterfowl at Mono Lake 3-47
Figure 17. Trend in total fall waterfowl numbers at Mono Lake, 2002-2023 3-48
Figure 18. Mean total fall waterfowl under meromictic vs. monomictic conditions 3-48
Figure 19. Fall waterfowl totals at the restoration ponds, 2002-2023 3-50
Figure 20. Trend in total fall waterfowl at Bridgeport Reservoir, 2003-2023 3-52
Figure 21. Trend in total fall waterfowl at Crowley Reservoir, 2003-2023 3-55
Figure 22. Comparison of mean fall waterfowl at each surveys area, with 2023 totals shown 3-56
Figure 23. Proportional abundance of Northern Shovelers by survey area 3-57
Figure 24. Proportional abundance of Ruddy Ducks by survey area 3-57
Figure 25. Black Point shoreline area, western half 3-59
Figure 26. Black Point shoreline area, eastern half 3-59
Figure 27. Bridgeport Creek shoreline area, eastern portion 3-61
Figure 28. Bridgeport Creek shoreline area, western portion 3-61
Figure 29. The DeChambeau Creek area, looking west 3-63
Figure 30. DeChambeau Creek area beaver pond 3-63
Figure 31. DeChambeau Embayment, Perseverance Spring outflow area 3-65
Figure 32. DeChambeau Embayment, eastern extent 3-65
Figure 33. Lee Vining Creek delta 3-67
Figure 34. Lee Vining Creek delta, western portion (Lee Vining tufa groves) 3-67
Figure 35. Mill Creek delta, from the east 3-69
Figure 36. Mill Creek at Cemetery Road 3-69
Figure 37. Mid-summer flow in a historic Mill Creek channel. 3-70
Figure 38. Northeast Shore, Looking East 3-71
Figure 39. Ranch Cove Shoreline Area, Looking West 3-72
Figure 40. Rush Creek Delta 3-74
Figure 41. Large continuous pond at Simon's Springs in early June 3-76
Figure 42. Overview of the Simons Spring area, west of the faultline 3-77

Figure 43. Shoreline Ponds east of the faultline at Simons Springs 3-77
Figure 44. Feral horse grazing and trampling of Gurgling Mound Spring..... 3-78
Figure 45. Semipermanent pond at western edge of South Shore Lagoons..... 3-80
Figure 46. Overview of the South Shore Lagoons area..... 3-81
Figure 47. Sand Flat Spring 3-81
Figure 48. Goose Springs 3-82
Figure 49. South Tufa, near Navy Beach 3-84
Figure 50. South Tufa, eastern extent..... 3-84
Figure 51. Overview of Warm Springs..... 3-86
Figure 52. Warm Springs, north Pond, looking north. 3-86
Figure 53. Feral horse impacts along Pebble Spring channel, Warm Springs 3-87
Figure 54. Overview of the West Shore, looking north/northwest 3-88
Figure 55. Freshwater pond in Wilson Creek Bay 3-90
Figure 56. Wilson Creek, east of Tufa Mound spring..... 3-90
Figure 57. Bridgeport Reservoir, looking northwest..... 3-91
Figure 58. Chalk Cliffs..... 3-92
Figure 59. Hilton Bay 3-93
Figure 60. Layton Springs..... 3-94
Figure 61. McGee Creek shoreline area north of Pelican Point..... 3-95
Figure 62. McGee Bay shoreline south of McGee and Convict Creek outflow..... 3-95
Figure 63. North Landing 3-96
Figure 64. Sandy Point 3-97
Figure 65. Upper Owens Delta..... 3-98
Figure 66. Upper Owens Delta Shoreline Area 3-99

TABLES

Table 2.1. Mono Basin waterfowl habitat restoration activities 2-2
Table 3.1. Mono Basin habitat restoration monitoring program 3-2
Table 3.2. Runoff year types as per amended licenses 10191 and 10192 3-6
Table 3.3. Annual flow volume in acre-feet of five Mono Lake streams based on water year 3-12
Table 3.4. Total Tamarisk treatments sites by year and shoreline segment area 3-15
Table 3.5. Summer ground count survey dates, 2023 3-28
Table 3.6. Fall 2023 Mono Lake Survey Dates 3-30
Table 3.7. Fall 2023 Bridgeport Reservoir Survey Dates 3-31
Table 3.8. Fall 2023 Crowley Reservoir Survey Dates 3-31
Table 3.9. Summer Ground Count Waterfowl Detections in 2023. 3-36
Table 3.10. Waterfowl broods by shoreline area, 2023 3-38
Table 3.11. Proportional habitat use of breeding waterfowl species, 2023 3-39
Table 3.12. Total summer waterfowl by pond and species, 2023 3-41
Table 3.13. Waterfowl broods at the restoration ponds, 2023 3-42
Table 3.14. Species totals, 2023 Mono Lake fall waterfowl surveys 3-43
Table 3.15. Distribution of Ruddy Ducks on cross-lake transects, 2023 3-47
Table 3.16. Fall waterfowl totals by pond, 2023 3-49
Table 3.17. Species totals, 2023 Bridgeport Reservoir fall waterfowl surveys 3-51
Table 3.18. Bridgeport Reservoir, spatial distribution by survey, 2023 3-52
Table 3.19. Species totals, 2023 Crowley Reservoir fall waterfowl surveys 3-53
Table 3.20. Crowley Reservoir, spatial distribution by survey, 2023 3-54

EXECUTIVE SUMMARY

The Los Angeles Department of Water and Power (LADWP) conducted monitoring in the Mono Basin, Mono County, California in 2023 in support of the Mono Basin Waterfowl Habitat Restoration Plan (Plan). The Plan and State Water Resources Control Board Order WR 98-05 (SWRCB 1998) directs LADWP to conduct monitoring to assess the success of waterfowl habitat restoration efforts, evaluate the effects of changes in the Mono Lake area, and plan for future restoration activities. This report summarizes the results of hydrological monitoring, saltcedar (*Tamarix* spp.) surveillance and eradication, and waterfowl population monitoring conducted in 2023. The results of the limnology monitoring program will be in a separate report from the Mono Basin limnology director.

Runoff in the Mono Basin during the 2022 to 2023 Water Year was 224,572 acre-feet, or 187% of the long-term average, and was an “Extreme Wet” water year type. Input from the two largest creeks (Rush and Lee Vining) was 203,263 acre-feet, or 200% of the long-term mean. Given the high runoff year, Mono Lake experienced a net increase in lake level of 4.5 feet over the calendar year, peaking at 6,383.2 feet in September.

The saltcedar surveillance and eradication program at Mono Lake conducted by California State Parks has been very effective. In 2023 there were only two new plants found at previously treated locations.

Waterfowl habitat conditions at Mono Lake were dynamic, changing rapidly through summer due to high runoff and lake level rise. Conditions were generally good spring through fall due to the presence of many shoreline ponds throughout the year. The breeding waterfowl population in shoreline habitats of Mono Lake in 2023 is estimated at 193, or approximately 97 pairs, which is significantly lower than the long-term mean of 305 +/- 19 SE or 160 pairs. Breeding was confirmed for four species, and Gadwall (*Mareca strepera*) was most abundant. Although the breeding population was very low, waterfowl breeding productivity was very good, as indicated by the number of broods. The total number of waterfowl broods found in 2023 (exclusive of Canada Goose [*Branta canadensis*]) was 62, which is above the long-term average of 48.4 +/- 3.6. Breeding activity was concentrated along the northwest shore at DeChambeau and Wilson Creeks and the south shore at Simons Springs. Habitat use patterns of the breeding community suggest that freshwater ponds, brackish ponds and ria are key habitat features for waterfowl at Mono Lake. There has been no long-term trend in the size of the breeding waterfowl population at Mono Lake or the number of broods produced annually, but both indices have been positively correlated with lake level. The effect of lake level on the number of broods has been nonlinear and increases in brood

numbers have only been observed above a threshold of 6,382 feet. Below this lake level, the total number of broods has not only been significantly fewer, but the number of broods has not been influenced by further declines in lake level.

Six waterfowl surveys were conducted in 2023 at each of the three fall survey areas: Mono Lake, Bridgeport Reservoir and Crowley Reservoirs, from early September to mid-November. Eleven waterfowl species and 23,782 individuals were detected at Mono Lake which did not differ from the long-term mean of 25,462 +/-2523 SE. Northern Shoveler (*Spatula clypeata*) and Ruddy Duck (*Oxyura jamaicensis*) accounted for 90% of the fall waterfowl population. The distribution of waterfowl in fall was unusual in 2023 because of record low numbers in the Wilson Creek area. In contrast, waterfowl use of the Black Point area just east of Wilson Creek, was a record high in 2023, and the most heavily used area of shoreline this year. At Bridgeport Reservoir, 16 waterfowl species and 15,448 individuals were recorded which was significantly lower than the long-term mean of 30,188 +/-3609 SE. At Crowley Reservoir, 18 waterfowl species and 32,175 individuals were detected and this number was also significantly lower than the long-term mean of 50,204 +/-5008 SE.

Four restoration ponds were flooded throughout the summer and fall survey periods. The breeding population numbered about 18, and eight broods were produced. Thirty waterfowl were seen in total in fall which was well below the long-term mean.

Despite its much larger size, Mono Lake supports fewer waterfowl on average during fall migration than either Bridgeport or Crowley Reservoirs, accounting for 24% of all fall waterfowl at the three survey areas combined. Although Bridgeport and Crowley support larger and more diverse waterfowl populations, Mono Lake supports a significant proportion of the local Northern Shoveler and Ruddy Duck attracting 42% of Northern Shovelers, and 44% of Ruddy Duck totals for all three survey areas.

Of the measures in Order 98-05, lake level recovery remains the restoration objective that would reestablish the most waterfowl habitat. The next most viable project to improve waterfowl habitat in the Mono Basin is to enhance and restore the functioning of the restoration ponds. Projects to enhance waterfowl habitat at the restoration pond include restoring water delivery to the County Ponds and implementing a seasonal or rotational flooding regime to maintain open water and enhance forage production.

Finally, I recommend that annual Mono Basin restoration meetings be reinstated to foster communication and knowledge sharing of ongoing restoration program monitoring among the Mono Basin parties.

1.0 Introduction

1.1 *Ecological Setting*

Mono Lake is a large terminal saline lake at the western edge of the Great Basin in Mono County, California. Mono Lake is the saline and alkaline remnant of the much larger Lake Russell that filled the basin during the Pleistocene. At its highest, Lake Russell stood at 7,480 feet above sea level. Early in the Pleistocene Lake Russell was hydrologically connected to the Lahontan and Walker Lake drainage basin as it spilled to the northeast. Later in the Pleistocene Lake Russell was connected to only to the Owens-Death Valley systems through a spill point along the southeastern rim of the basin (Reheis et al. 2002). Starting in the late Pleistocene and extending through the early Holocene, climatic variation resulted in the contraction of Lake Russell, and resulting hydrologic isolation of Mono Lake. It was during this time period that the lake reached its extreme low of approximately 6,368-foot (Scholl et al. 1967 in Vorster 1985). Climate patterns in the Holocene have been warmer and drier than during the Pleistocene, leaving a smaller and more saline Mono Lake. Since 1941, lake level and salinity have been influenced by water exports by the City of Los Angeles (City), and more recently, climate change may be becoming more influential.

Mono Lake is the largest lake in Mono County and has an east-west dimension of 13 miles, a north-south dimension of over nine miles (Raumann et al. 2002), and a circumference of approximately 40 miles. With an average depth of over 60 feet and a maximum depth of approximately 150 feet (Russell 1889), Mono Lake is a large, moderately deep terminal saline lake (Jellison and Melack 1993, Melack 1983). The deepest portions of the lake are found south and east of Paoha Island in the Johnson and Putnam Basins, respectively (Raumann et al. 2002). Shallower water and a gently sloping shoreline are more typical of the north and east shores (Vorster 1985, Raumann et al. 2002).

Mono Lake is highly productive and widely known for its value to waterbirds due to the seasonal abundance of two main aquatic invertebrate taxa: Mono Lake brine shrimp (*Artemia monica*) and alkali flies (*Cirrula* spp.). The islands and numerous islets support one of the two largest nesting populations of California Gulls (*Larus californicus*) in California (Doster and Shuford 2018). The lake also functions as a fall staging area for an average of 40% of the North American population of Eared Grebes (*Podiceps nigricollis*) (Roberts et al. 2013) and a staging area and migratory stopover location for up to 140,000 Wilson's (*Phalaropus tricolor*) and Red-necked Phalaropes (*P. lobatus*) during fall migration (Jehl 1986, Jehl 1988). Waterfowl also use Mono Lake, including an established breeding population and larger numbers of migrating waterfowl in autumn.

Saline lakes such as Mono Lake are in general, highly productive ecological systems (Jellison et al. 1998), however the productivity of individual lakes is influenced by factors such as salinity, water depth, temperature, and water influx and evaporation on a seasonal, annual, and inter-annual basis. Saline lakes often respond rapidly to environmental changes and alterations to the hydrological budget (Jehl 1988, Williams 2002). As with many other saline lakes around the world (Wurtsbaugh et al. 2017), Mono Lake has been affected by water use for agricultural and municipal purposes.

1.2 *Environmental Challenges and Legal Background*

In 1940 the City of Los Angeles (City) acquired permits from the Department of Public Works, Division of Water Resources (predecessor to the SWRCB) to divert water from four Mono basin creeks for municipal use and the generation of hydroelectric power. These permits were issued under the California Water Code despite recognition of anticipated environmental impacts (SWRCB 1994), under the policy guidance that domestic use was the highest use of water. The City began diverting Lee Vining Creek, Rush Creek, Walker Creek, and Parker Creek for out-of-basin water transfers in 1941.

This initial export level resulted in a steady decline in lake level. The pre-diversion elevation of Mono Lake in April of 1941 was 6,416.9 feet. From 1941 to 1970 when the City was exporting an annual average of 56,000 acre-feet, the elevation of Mono Lake dropped over 29 vertical feet. In 1970, LADWP completed construction of the second aqueduct in Owens Valley which expanded the capacity of the Los Angeles Aqueduct system. In 1974, the SWRCB issued water rights licenses 10191 and 10192 which allowed the City to export up to 147,700 acre-feet of water from the Mono basin. Mono Basin exports were thus increased resulting in frequent full diversion of flows from Lee Vining, Walker, Parker and Rush Creek and a drying of the creek channels (SWRCB 1994). From 1970 to 1989, Mono Lake dropped another 12.6 feet as yearly exports averaged 82,000 acre-feet, with a peak export of 140,756 acre-feet in 1979. The lake level dropped to a record low of 6,371.0 feet in 1982, representing a cumulative 45-foot vertical drop in lake elevation as compared to the pre-diversion level. This rate of diversion resulted in a number of ecological consequences, and ultimately to a revision of the City's water rights licenses by the SWRCB.

The National Audubon Society filed suit with the Superior Court of California against the City (National Audubon Society v. Superior Court) in 1979 arguing that out of basin water transfers and diversions in the Mono Basin were resulting in environmental damage in violation of the Public Trust Doctrine. After a series of lawsuits and extended court hearings, the State Water Resources Control Board (SWRCB) amended the City's water rights with the Mono Lake Basin Water Right Decision 1631 (Decision 1631)

(SWRCB 1994). Decision 1631 established instream flow requirements for Rush, Lee Vining, Parker and Walker creeks for fishery protection, placed limitations on water exports, and set a target lake level of 6,392 feet. In addition, Decision 1631 required LADWP to conduct restoration and monitoring of Mono Lake ecological resources including lake level and hydrology, riparian and wetland vegetation, fisheries, lake limnology, and waterfowl populations.

Although quantitative data on waterfowl numbers was lacking, it is believed that Mono Lake was once a major stopover point for waterfowl prior to 1940 (Jones and Stokes 1993). The SWRCB concluded that water diversions and associated lake level drop had severely impacted migratory waterfowl and their habitats (SWRCB 1994). It has been suggested that waterfowl habitat was impacted by the increase in lake salinity, the loss of freshwater inflow from Rush and Lee Vining Creeks, and a loss of springs, ponds, and other shoreline wetlands (Jones and Stokes 1993). The dewatering of the creeks caused a lowering of the water tables, a loss of riparian vegetation, and led to channel incision during high runoff years. The SWRCB also concluded that waterfowl populations had been more impacted by the ecological changes associated with excessive water diversion than other common taxa at Mono Lake (such as Eared Grebe, California Gull, or phalaropes) and required LADWP to develop the Mono Basin Waterfowl Habitat Restoration Plan (LADWP 1996a) which included restoration projects and monitoring. No such monitoring plans were required for other key avian taxa at Mono Lake.

The City's water rights licenses were further revised in 2021 in order to modify the flow regimes in the creeks to comply with recommendations from the stream scientists and implement conditions of a 2013 Settlement Agreement (SWRCB 2013). The SWRCB approved Amended Water Rights Licenses 10191 and 10192 for LADWP on October 1, 2021. Pertinent to the Mono Basin Waterfowl Habitat Restoration Program were conditions 21 and 22 of these amended licenses which defined how the program would be managed in the future, including some revisions to previous orders. These amended licenses did not include any changes to the actual monitoring program; however a separate limnology director was designated to oversee and report on the limnology monitoring program. This Waterfowl Habitat Restoration report summarizes the results of monitoring conducted in 2023 pursuant to Restoration Order 98-05 and the amended licenses, exclusive of limnology.

2.0 Waterfowl Habitat Restoration

The Mono Basin Waterfowl Habitat Restoration Plan (Plan) (LADWP 1996a) identified restoration projects and associated monitoring tasks to mitigate the loss of waterfowl habitat due to water diversion and the drop in lake level. Order WR 98-05 (SWRCB 1998) directed the Los Angeles Department of Water and Power (LADWP) to implement waterfowl habitat restoration measures to mitigate the loss of waterfowl habitat in the Mono Basin from diversions. The SWRCB issued Order 98-05 in 1998, defining waterfowl habitat restoration measures and associated monitoring to be conducted in compliance with Decision 1631. The export criteria of Decision 1631 were developed to result in an eventual long-term average water elevation of Mono Lake of 6,392 feet (SWRCB 1994). In determining the most appropriate water level for the protection of public trust resources at Mono Lake, the SWRCB recognized that there was no single lake elevation that would maximize protection of, and accessibility to, all public trust resources. Decision 1631 stated that maximum restoration of waterfowl habitat would require a lake elevation of 6,405 feet. Raising the lake elevation to 6,405 feet however, would have precluded use of any water from the Mono Basin by the City for municipal needs, and limited public access to South Tufa, which is currently the most frequently visited tufa site. Furthermore, it was determined that a lower target lake elevation of 6,390 feet would accomplish some waterfowl habitat restoration, and that there were opportunities to restore additional habitat, mitigating the overall loss as a result the target being set below 6,405 feet. A target level of 6,392 feet was ultimately established as this level would restore some waterfowl habitat, allow continued access to South Tufa, and ensure compliance with federal air quality standards.

As noted in Order 98-05 and recognized in the restoration plans, the most important waterfowl habitat restoration measures were maintaining an average lake elevation of 6,392 feet and restoring perennial flow to streams tributary to Mono Lake. In addition to lake level recovery, and stream restoration, Order 98-05 included the following measures to be undertaken by LADWP:

1. reopen distributaries in the Rush Creek bottomlands,
2. provide financial assistance for the restoration of waterfowl habitat at the County Ponds and Black Point or other lake-fringing wetland area,
3. participate in a prescribed burn program subject to applicable permitting and environmental review requirements;
4. participate in exotic species control efforts if an interagency program is established in the Mono Basin; and
5. develop a comprehensive waterfowl and waterfowl habitat monitoring program.

Table 2.1 describes each restoration measure required under Order 98-05, a brief discussion on LADWP's progress to date, and the current status. Some of these

projects have been completed, some are ongoing, and others have been determined by the stakeholders to be unfeasible. More details regarding these restoration measures can be found in the *Periodic Overview Report* (LADWP 2018).

Table 2.1. Mono Basin waterfowl habitat restoration activities

Mono Basin Waterfowl Habitat Restoration Activities *(as described in SWRCB Order 98-05 and the Mono Basin Waterfowl Habitat Restoration Plan dated February 29, 1996, where relevant)*				
Activity	**Goal**	**Description**	**Progress to Date**	**Status**
Rewatering Distributary Channels to Rush Creek (below the Narrows)	To restore waterfowl and riparian habitat in the Rush Creek bottomlands.	Rewater the Channel 4bii complex	Rewatering of side channels was evaluated in 2002 by the State Appointed Stream Scientists and LADWP. At that time, rewatering of Channel 4bii was deferred because natural revegetation of riparian and wetland species was occurring. The area was reevaluated in 2007 and rewatering was completed in March 2007.	Complete
		Rewater the Channel 8 complex, unplugged lower section	In 2002, the sediment plug was removed, and the Channel 8 complex widened at the upstream end. In contrast to rewatering for constant flow, the final design called for flows overtopping the bank and flowing into Channel 8 at approximately 250 cfs and above. Woody debris was spread and willows were transplanted along new banks following excavation. Further rewatering of Rush Creek Channel 8 complex was deferred by the Stream Scientists. Final review was conducted by McBain and Trush (2010). After presentation of the final review, LADWP followed the recommendations of the Stream Scientists and SWRCB approved the plan. Channel 8 was rewatered in March 2007.	Complete
		Rewater the Channel 10 complex	Rewatering of side channels was evaluated in 2002 by the State Appointed Stream Scientists and LADWP. This evaluation concluded that rewatering the Channel 10 complex would result in detrimental impacts to reestablished fishery and riparian habitats. Therefore, there have been no further actions taken to rewater this channel. Project is complete.	Complete

Mono Basin Waterfowl Habitat Restoration Activities, cont. *(as described in SWRCB Order 98-05 and the Mono Basin Waterfowl Habitat Restoration Plan dated February 29, 1996, where relevant)*				
Activity	**Goal**	**Description**	**Progress to Date**	**Status**
Rewatering Distributary Channels to Rush Creek (below the Narrows)	To restore waterfowl and riparian habitat in the Rush Creek bottomlands.	Rewater Channel 11, unplugged lower portion	Rewatering of side channels was evaluated in 2002 by the State Appointed Stream Scientists and LADWP. At that time, it was determined that there would be little benefit to unplugging Channel 11 compared to the impacts to reestablished riparian vegetation from mechanical intrusion. Further evaluation was conducted by the Stream Scientists. After presentation of the final review, LADWP followed the recommendations of the Stream Scientists not to rewater the channel. This item is now approved by SWRCB and was therefore considered complete in 2008.	Complete
		Rewater the Channel 13 complex	Rewatering of side channels was evaluated in 2002 by the State Appointed Stream Scientists and LADWP. At that time, it was determined that Channel 13 would not be stable or persist in the long term and riparian vegetation was already rapidly regenerating in this reach. Therefore, there have been no further actions taken to rewater Channel 13. Project is considered complete.	Complete

Mono Basin Waterfowl Habitat Restoration Activities, cont. *(as described in SWRCB Order 98-05 and the Mono Basin Waterfowl Habitat Restoration Plan dated February 29, 1996, where relevant)*				
Activity	**Goal**	**Description**	**Progress to Date**	**Status**
Financial Assistance to United States Forest Service (USFS) for Waterfowl Habitat Improvement Projects at County Ponds and Black Point areas	To support repairs and improvement of infrastructure on USFS land in the County Ponds area.	Upon request of the USFS, Licensee (LADWP) shall provide financial assistance in an amount up to $250,000 for repairs and improvements to surface water diversion and distribution facilities and related work to restore or improve waterfowl habitat on USFS land in the County Ponds area.	LADWP was to make available a total of $275,000 for waterfowl restoration activities in the Mono Basin per Order 98-05. This money was to be used by the USFS if they requested the funds by December 31, 2004. Afterwards, any remaining funds are to be made available to any party wishing to do waterfowl restoration in the Mono Basin after SWRCB review. This funding allocation has been included in Section 21.a of Amended Licenses 10191 and 10192 to be administered by the Mono Basin Monitoring Administration Team (MAT).	In Progress
	To support waterfowl habitat improvement projects on USFS land in the Black Point area.	Upon request of the USFS, Licensee (LADWP) shall provide financial assistance in an amount up to $25,000 for waterfowl habitat improvements on USFS land in the Black Point area.		

Mono Basin Waterfowl Habitat Restoration Activities, cont. *(as described in SWRCB Order 98-05 and the Mono Basin Waterfowl Habitat Restoration Plan dated February 29, 1996, where relevant)*				
Activity	**Goal**	**Description**	**Progress to Date**	**Status**
Prescribed Burn Program	To enhance lake-fringing marsh and seasonal wet meadow habitats for waterfowl	The licensee shall proceed with obtaining the necessary permits and approval for the prescribed burning program described in the Mono Basin Waterfowl Habitat Restoration Plan dated February 29, 1996 and provide the SWRCB a copy of any environmental documentation for the program. Following review of the environmental documentation, the SWRCB may direct Los Angeles to proceed with implementation of the prescribed burning program pursuant to D1631 and Order 98-05, or modify the program.	LADWP began a prescribed burn program with limited success. LADWP requested to remove this item from the requirements in 2002 and the SWRCB instead ruled that the prescribed burn program will be deferred until Mono Lake reaches the target elevation. Per Condition 21.b in Amended Licenses 10191 and 10192, when Mono Lake reaches an elevation of 6,391 feet, the SWRCB will consider the options and benefits of Licensee reactivating the prescribed waterfowl habitat burn program. If the program is reactivated, Licensee shall proceed with obtaining the necessary permits and approvals for the prescribed burning program.	Deferred
Saltcedar Eradication Program	To control non-native vegetation in the Mono Basin	In the event that an interagency program is established for the control or elimination of saltcedar or other non-native vegetation deemed harmful to waterfowl habitat in the Mono Basin, Licensee (LADWP) shall participate in that program and report any work it undertakes to control saltcedar or other non-native vegetation.	LADWP continues treatment of saltcedar as needed. Progress of the salt cedar eradication efforts is reported in the annual reports following the vegetation monitoring efforts. This item is carried over to Condition 21.c in Amended licenses 10191 and 10192.	Ongoing

3.0 Waterfowl Habitat Restoration Monitoring Program

The Plan and SWRCB Order WR 98-05 directed LADWP to conduct monitoring to assess the success of waterfowl habitat restoration efforts, evaluate the effects of changes in the Mono Lake area, and plan for future restoration activities. Components of the Mono Basin Waterfowl Habitat Monitoring Program (Program) include hydrology, limnology, the vegetation status of riparian and lake-fringing wetlands, and waterfowl population surveys. Table 3.1 provides a brief description of the monitoring components, their required frequency under the Plan and Order 98-05, and the dates that each monitoring task has been performed.

In 2023, monitoring conducted under the Program included lake elevation, stream flows, lake limnology and secondary producers, saltcedar eradication, waterfowl population surveys and aerial photography of waterfowl habitats. In 2023, U.C. Santa Barbara resumed control of the limnology monitoring program. The remainder of this report provides a summary and discussion on the 2023 data collected under the Program, apart from lake limnology and secondary producers.

Table 3.1. Mono Basin habitat restoration monitoring program

Mono Basin Habitat Restoration Monitoring Program *(as described in SWRCB Order 98-05 and the Waterfowl Habitat Restoration Plan dated February 29, 1996)*			
Monitoring Component	**Description**	**Required Frequency**	**Dates Monitoring Performed**
Hydrology	Lake Elevation	Weekly through one complete wet/dry cycle after the lake level has stabilized.	Monthly data collected 1936-present; ongoing
	Stream Flows	Daily through one complete wet/dry cycle after the lake level has stabilized.	Daily data collected 1935-present; ongoing
	Spring Surveys	Five-year intervals (August) through one complete wet/dry cycle after the lake level has stabilized.	1999, 2004, 2009, 2014, 2019; ongoing
Lake Limnology and Secondary Producers	Meteorological data, data on physical and chemical environment of the lake, phytoplankton, and brine shrimp population levels	Annually (monthly February-December) until the lake reaches a relatively stable level. LADWP will evaluate monitoring at that time and make a recommendation to the SWRCB whether to continue.	1987-present; ongoing
Vegetation Status in Riparian and Lake Fringing Wetland Habitats	Establishment and monitoring of vegetation transects and permanent photopoints in lake fringing wetlands	Five-year intervals or after extremely wet year events (whichever comes first) until 2014. Due to heavy feral horse in some areas, reinstate the program and monitor all sites again in 2026. Reevaluate the need to continue monitoring after 2026 data are evaluated.	2000, 2005, 2010, 2015; 2021, ongoing
	Aerial photographs of lake fringing wetlands and Mono Lake tributaries	Five-year intervals until target lake elevation of 6,392 feet is achieved.	1999, 2005, 2009, 2014; 2017, 2022, ongoing

Table 3.1 continued

Mono Basin Habitat Restoration Monitoring Program *(as described in SWRCB Order 98-05 and the Waterfowl Habitat Restoration Plan dated February 29, 1996)*			
Monitoring Component	**Description**	**Required Frequency**	**Dates Monitoring Performed**
Waterfowl Population Surveys and Studies	Fall aerial counts	Two counts conducted every other year October 15-November 15. All waterfowl population survey work will continue until 2014, through one complete wet/dry cycle after the target lake elevation of 6,392 feet is achieved. Since 2002, six fall counts have been conducted annually at Mono Lake, Bridgeport Reservoir and Crowley Reservoir between September and mid-November. In 2023, surveys were conducted using a combination of helicopter, boat and ground counts.	Annual; ongoing
	Aerial photography of waterfowl habitats	Conducted during or following one fall aerial count.	Annual; ongoing
	Ground counts	Total of eight ground counts annually (two in summer, six in fall). All waterfowl population survey work will continue until 2014, or through one complete wet/dry cycle after the target lake elevation of 6,392 feet is achieved. Since 2002, three summer ground counts have been conducted. Fall ground counts were replaced with six aerial counts.	Annual; ongoing
	Waterfowl time activity budget study	To be conducted during each of the first two fall migration periods after restoration plans are approved, and then again when the lake is at or near the target elevation.	Conducted one of two fall migration periods (in 2000); completion of second study is recommended

3.1 *Hydrology*

Mono Lake lies in the hydrologically closed Mono Basin, and as such, all surface and groundwater drains towards Mono Lake. Water inflow into Mono Lake includes runoff from streams and groundwater discharge to the lake (approximately 82% of inputs), and precipitation (~18% of inflow) (Ficklin et al. 2012).

All perennial streams flowing into Mono Lake originate on the east slope of the Sierra Nevada, entering the lake along the west or northwest shore. The largest stream is Rush Creek, accounting for approximately 50% of stream-flow contributions to Mono Lake. Lee Vining Creek is the second largest, and Mill Creek the third largest stream. Parker and Walker Creeks are small creeks tributary to Rush Creek. Rush Creek was permanently re-watered in 1982, however Parker Creek and Walker Creek, were not re-watered until 1990. Lee Vining Creek was re-watered in 1986. Creeks and streams providing minor contributions include Log Cabin Creek, DeChambeau Creek, and Wilson Creek. Log Cabin Creek is monitored as part of the spring monitoring program, but not included in annual runoff totals. DeChambeau Creek is a gaged creek whose flows are included in runoff, although flows are intermittent, and do not consistently reach the lakeshore. Wilson Creek discharges to Mono Lake just west of Black Point. Although formerly perennial, in recent years this creek has experienced periodic drying of its lower reaches due to upstream diversion.

There are several other intermittent creeks that drain the surrounding hills north and south of Mono Lake that are not measured, but likely contribute to groundwater inputs to some extent. Examples of intermittent drainages are Bridgeport Creek and Cottonwood Creek out of the Bodie Hills to the north and Dry Creek draining the Glass Mountains to the south.

Streams and creeks in the Mono Basin are primarily snowmelt fed systems and around 89% of all runoff originates from the Sierran snowpack. Stream flow is highly seasonal, and peak flows typically occur in June or July, especially in normal-to-wet years, although they may occur in April or May in dry years or on the smaller creeks (Beschta 1994).

Since it is a terminal lake, lake level is a function of the interplay between inflow (surface runoff, groundwater inflow and precipitation), and evaporation. The level of Mono Lake is one of the key components of ecological restoration in the Mono Basin. Lake level influences nearshore groundwater processes, vegetation growth, the development of onshore ponds, the connectivity of spring flow and wetland vegetation to the shoreline, and lake salinity.

3.1.1 Hydrologic Monitoring Methodologies

Annual Runoff

Runoff year is the period from April 1 to March 31 of each year. Each year, a modeled runoff prediction is made using rainfall, snow survey, and creek flow data from various locations in Mono County. LADWP produces an April 1 Mono Basin runoff forecast based on modeled prediction, although adjustments may be made on May 1. The Mono Basin forecast represents the combined forecasted runoff of Lee Vining, Rush, Parker and Walker creeks. The measured flows from these creeks represent approximately 75 to 85% of the surface and subsurface inflow into the basin (National Research Council, 1987). The runoff prediction is used to set instream base and channel maintenance flows in the creeks for the runoff period. The prescribed flows in any one year are based on runoff year type. Runoff year type is determined by comparing the total acre-feet of predicted runoff to the 1941 to 1990 average runoff of 122,124 acre-feet (Table 3.2).

Stream Flow

LADWP is required to monitor stream flow in the four Mono Lake creeks from which the City diverts water for export - Rush, Lee Vining, Parker and Walker creeks. Stream flow data are used to manage releases and ensure compliance with the prescribed base and channel maintenance flows. Instream and channel maintenance flows for other Mono Lake creeks were not specified by the Orders. Stream flow data are used to determine compliance with the Mono Basin Stream and Stream Channel Restoration Plan (LADWP 1996b) and amended licenses, and to provide environmental data to evaluate the response of biological indicators under the Mono Basin Waterfowl Habitat Restoration Plan (LADWP 1996a). Instream base and channel maintenance flows, initially dictated by Decision 1631 and Order 98-05, were superseded by Amended licenses 10191 and 10192, approved on October 1, 2021 (SWRCB 2021). The flows released to these creeks on any one year are driven by the “runoff year type”. Runoff year type is used to determine the required annual restoration flows for Rush and Lee Vining Creeks.

Table 3.2. Runoff year types as per amended licenses 10191 and 10192

Water Year- Type	Runoff	Percent Exceedance
Dry	Less than or equal to 68.5% of average runoff	80 - 100 %
Dry/Normal	Between 68.5% and 82.5% of average runoff	60 - 80%
Dry/Normal I	Greater than 68.5% and less than or equal to 75%	60 - 70%
Dry/Normal II	Greater than 75% and less than or equal to 82.5%	70 - 80%
Normal	Greater than 82.5% and less than or equal to 107% of average runoff	40 - 60%
Wet/Normal	Greater than 107% and less than or equal to 136.5% of average runoff	20 - 40%
Wet	Greater than 136.5% of average runoff	0 - 20%
Extreme Wet	Greater than 160% of average runoff	0 - 8%

The year-type classifications are based on 1941-1990 average runoff of 122,124 AF

LADWP hydrographers collect flow data using continuous instream data recorders that measure flow at 15-minute intervals. The measuring stations used to determine Rush Creek flows are Mono Gate One Return Ditch (STAID 5007) and Grant Lake Spill (STAID5078). The flow in Lee Vining Creek is measured at Lee Vining Creek below Conduit (STAID5009). The stations for Parker (Parker Creek below Conduit—STAID5003) and Walker Creek (Walker Creek below Conduit—STAID5002) are located just downstream of the diversion point into the Mono Craters Tunnel.

In order to provide a more complete record of annual stream flow contributions to Mono Lake, we also report on flows for DeChambeau Creek, and the estimated inputs of Mill Creek and Wilson Creek, when available. LADWP maintains a continuous instream data recorder station on DeChambeau Creek west of Highway 395 (Dechambeau Creek above Diversion—STAID5049). LADWP does not maintain flow measuring stations on Mill or Wilson Creeks, however flow data was obtained from USGS National Water Information System (waterdata.usgs.gov) for Mill Creek below Lundy Lake (10287069) and Lundy Power Plant Tailrace (10287195). Mill Creek below Lundy Lake measures flow in Mill Creek downstream of the diversion to the Lundy Powerhouse. The Lundy

Power Plant Tailrace measures flows downstream of the Lundy Powerhouse. Water downstream of the Lundy Powerhouse is split between return flows to Mill Creek, a diversion to Conway Ranch, and a diversion to Wilson Creek. Further downstream on Wilson Creek, water is diverted off Wilson Creek for use in the Restoration Ponds.

Mono Lake Elevation
LADWP hydrographers record the elevation of Mono Lake monthly using a staff gauge installed at the boat dock on the west shore. The staff gauge is demarcated in tenths and hundredths of a foot. These data were standardized to the USGS datum by adding 0.37 feet. Lake elevation is used to evaluate progress in meeting the target lake level, and for determining the annual allowable export. Lake elevation data is also used to evaluate the response of biological indicators including secondary producers, vegetation, and waterfowl.

3.1.2 Hydrology Data Summary and Analysis

Annual Runoff
Although "Runoff Year" type is used for determining the yearly prescribed stream flows, total runoff and stream flow were summarized by "Water Year", or the period from October 1 to September 30 of each year for this report. This is the preferred approach for biological analysis as the "Water Year" will encompass winter precipitation contributing to ecological conditions and processes the following year. Mono Basin runoff was calculated using the combined stream flow data for Rush, Lee Vining, Parker, and Walker Creeks. The water year was compared to the annual data back to 1935.

Stream Flow
The real-time station flow data were converted into daily flow, which was used to calculate monthly and annual inflow into Mono Lake. Inflow from Rush Creek is estimated by summing Mono Gate One Return Ditch (MGORD) (STAID 5007), Grant Lake Spill (STAID5078), Parker Creek below Conduit (STAID5003) and Walker Creek below Conduit (STAID5002). Lee Vining Creek below Conduit (STAID5009) and Dechambeau Creek above Diversion (STAID5049) are used to estimate inflow from Lee Vining and Dechambeau Creeks, respectively.

The contribution of Mill and Wilson Creek into Mono Lake cannot be precisely determined due to a lack of direct measure, and therefore the input amounts we report should be considered estimates. The estimated combined contribution of Mill Creek and Wilson Creek was calculated by summing USGS Stations Mill Creek below Lundy Lake (10287069) and Lundy Power Plant Tailrace (10287195). This calculation will

overestimate flows to Mono Lake as diversions to Conway Ranch and the Restoration Ponds have not been subtracted.

Lake Elevation
Monthly LADWP Mono Lake elevation data were summarized for 2023, and for the time period 1990 to 2023. The 1990 to 2023 time series represents the period during which a preliminary injunction was in place that halted exports until the lake level recovered to 6,377 feet, followed by the implementation of Decision 1631, beginning in September 1994. Patterns of lake elevation change were evaluated on a yearly and long-term basis.

3.1.3 Hydrology Results

Annual Runoff
Runoff during the 2022 to 2023 Water Year was 224,572 acre-feet, or 187% of the long-term average, and was an “Extreme Wet” water year-type. The 2022 to 2023 Water Year was the third wettest since 1935 (Figure 1). The 2022 to 2023 Water Year was exceeded only by 2016 to 2017 (248,359 acre-feet), and 1982 to 1983 (245,096 acre-feet).

Since Decision 1631, there have been five distinct wet periods or years, however the duration of the most recent wet periods has shorter than previous wet periods. The first wet period lasted from 1995 to 1998 and averaged 147% of normal based on the 50-year average between 1971 and 2020; the second wet period only lasted two years (2005 to 2006) and averaged 156% of normal; the third wet period also lasted two years (2010 to 2011) and averaged 131% of Normal. Following this third wet period was an extended drought that resulted in the driest 5-year period on record. This extended dry period year ended in 2017 with what was the second wettest on record of 207% of normal, or an “Extreme Wet” year. The fifth wet period observed in the 2022 to 2023 Water Year is to date, just a single year.

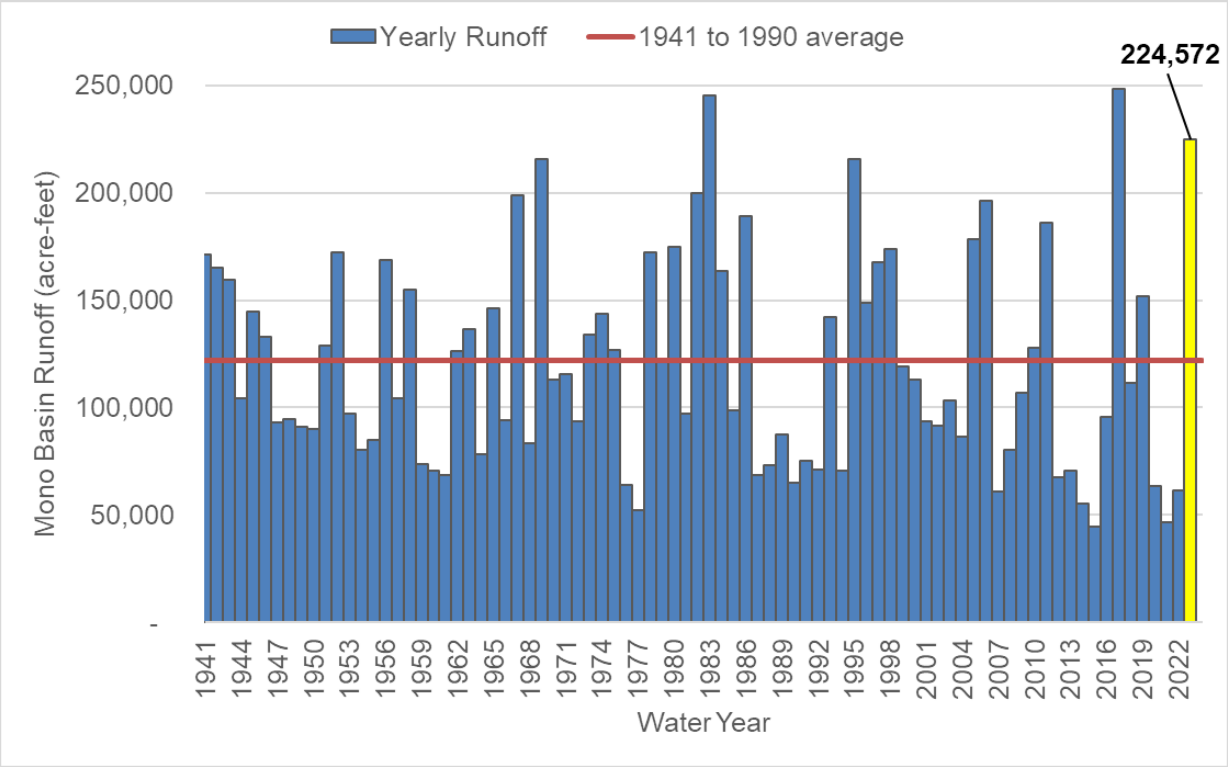

Figure 1. Annual Mono Basin runoff based on water year
Water year is from October 1 to September 30 of each year.

Stream Flows

In water year 2022 to 2023, the input from Rush Creek was 124,027 acre-feet or approximately 198% of the long-term average since 1990 (Table 3.3). Since 1990, Rush Creek has provided the largest inputs to Mono Lake averaging 62,631 acre-foot of discharge, and an average contribution of 50% of total inputs since 1990. The peak input over this time period of 145,349 acre-feet occurred in 2017. The input from Lee Vining Creek in 2023 was 79,237 acre-feet, or approximately 203% of the long-term average of 38,960 acre-foot. As was the case with Rush Creek, the highest input in this time period was 91,132 acre-feet in 2017. Input from the two major streams (Rush and Lee Vining Creeks) in 2023 was 203,263 acre-feet, or 200% of the long-term average since 1990. The input from Dechambeau Creek in 2023 was 1,421 acre-feet, 186% of its long-term mean. DeChambeau Creek has averaged 766 acre-feet since 1982 and has contributed less than 1% of total annual input since 1990. We were unable to get the 2023 flow data from Southern California Edison for Mill and Wilson Creek.

Lake Elevation

In 2023, Mono Lake experienced a period of increasing lake level and a net increase of 4.5 feet (Figure 2). Lake level was at its minimum for the year in January at 6,378.6 feet. Small but steady increases in lake level were seen each month thereafter until June. Lake level rose most steeply from June to August, leveling off after that. The

lake was at its highest level in 2023 of 6,383.2 feet in September. Lake level remained fairly stable in late fall, only declining 0.1 feet by December, and ending the year at 6,383.1 feet.

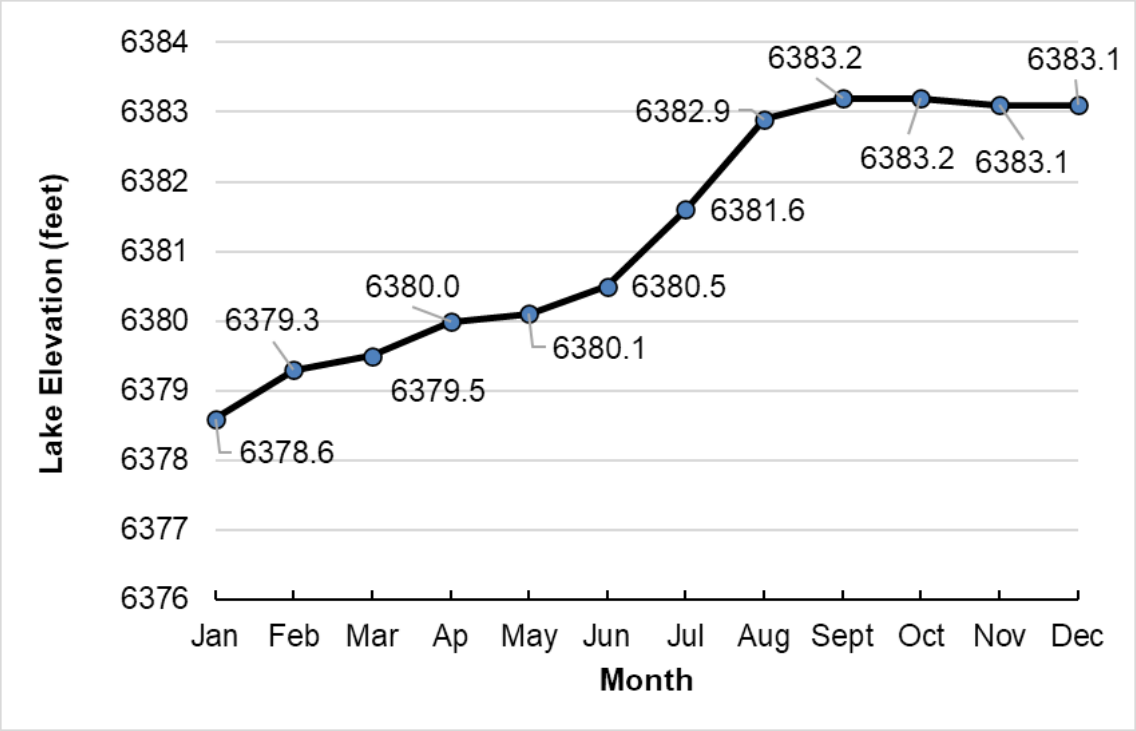

Figure 2. Mono Lake monthly elevation, 2023

From 1994 to 2023, Mono Lake has experienced five periods of increasing elevation in response to the five wet periods or years, and four subsequent decreases, through a total elevation range of almost 8.0 feet (Figure 3). The highest elevation the lake achieved since 1994 was 6,384.7 feet, which occurred in July 1999. During a period of extended drought from 2012 to 2016, the lake elevation dropped almost 7 feet to a low of 6,376.8 feet in October 2016, the lowest level since implementation of the Order. Following the “Extreme Wet” runoff year of 2016-2017, followed by a “Normal” and then “Wet Normal” year, lake level showed some recovery from the extreme low point of 2016, but declining again with two consecutive very dry years. The Extreme Wet year of 2022 to 2023 resulted in the fifth increase in lake level since 1994 (Figure 3).

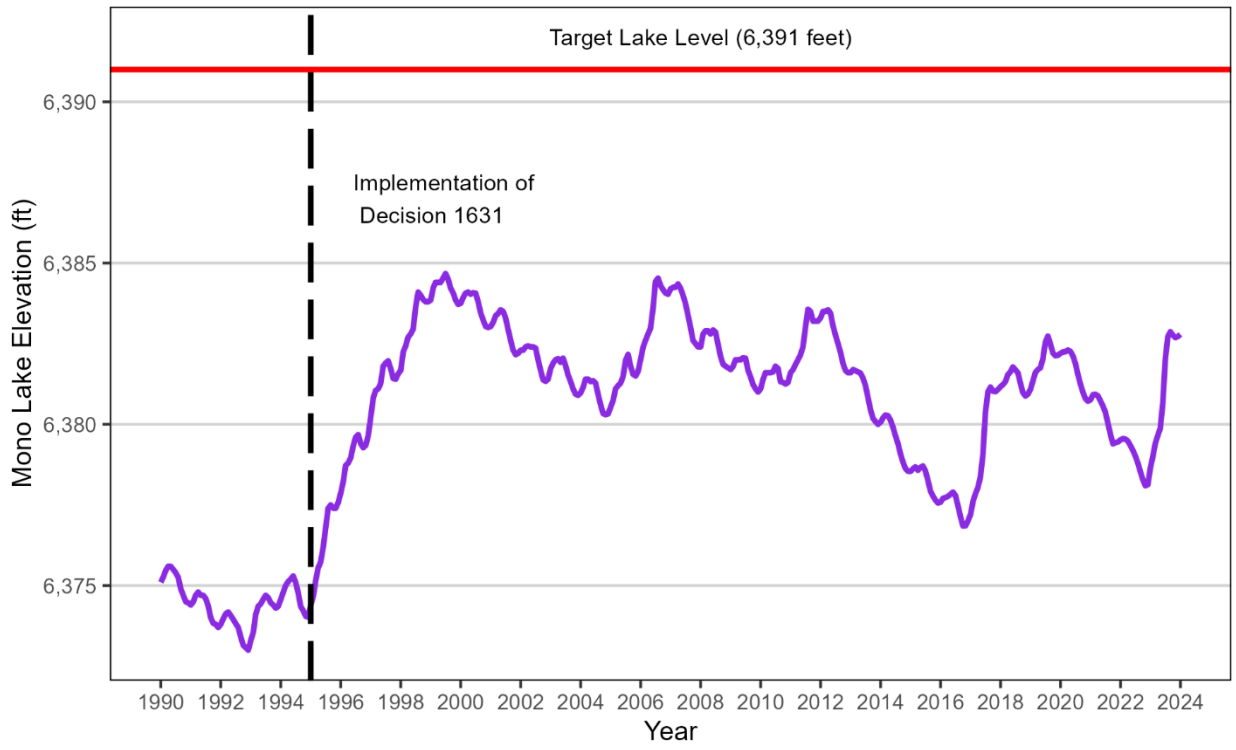

Figure 3. Mono Lake elevation between 1990 and 2023
Since Decision 1631, there have been five periods of lake level increase associated with above-average runoff.

Table 3.3. Annual flow volume in acre-feet of five Mono Lake streams based on water year

Year	Rush	Lee Vining	Dechambeau	Mill/Wilson
1990	71,046	18,643	325	9,115
1991	35,713	20,561	264	8,725
1992	44,632	20,798	178	10,590
1993	77,460	42,279	439	18,710
1994	56,776	29,376	450	11,118
1995	94,595	66,443	910	31,899
1996	91,841	56,284	1,243	25,557
1997	82,423	66,317	1,485	30,912
1998	93,177	62,335	1,325	27,113
1999	58,047	46,204	1,150	19,472
2000	50,497	40,432	749	16,370
2001	49,357	31,033	575	13,272
2002	45,900	36,599	405	12,708
2003	49,028	30,777	529	15,199
2004	47,644	31,871	549	15,115
2005	72,765	55,367	994	26,640
2006	108,899	75,860	1,459	32,149
2007	38,428	24,090	997	10,173
2008	45,159	25,631	587	13,265
2009	36,569	30,653	585	15,769
2010	57,622	34,775	671	19,343
2011	96,432	65,454	1,150	29,997
2012	46,890	19,486	926	11,272
2013	35,084	18,319	475	10,416
2014	31,893	20,047	340	8,539
2015	32,753	16,525	272	8,485
2016	44,242	28,748	275	15,232
2017	145,349	91,132	1,433	45,410
2018	63,397	33,624	1,211	21,720
2019	89,858	48,687	1,095	27,762
2020	41,437	20,149	747	11,344
2021	35,435	16,752	425	9,190
2022	35,073	20,130	368	12,612
2023	124,026	79,236	1,421	-

3.1.4 Hydrology Discussion

Annual Runoff

Runoff in the Mono Basin has been typified by dry periods interrupted by short wet periods, except in the late 1930s to early 1940s, the late 1970s to 1980s, and the late 1990s when wet periods were found to last longer than the more recent wet periods (LADWP 2018). As mentioned previously, five of the ten lowest runoff years have occurred since the 2011 to 2012 runoff year, including 2014 to 2015 and 2020 to 2021, the driest and the second driest on record, respectively. Recent dry years appear to be much drier.

Stream Flows

The 2023 runoff resulted in above-average total stream discharge into Mono Lake from the primary tributaries. The increased stream discharge contributed to the increase in lake level observed in 2023.

Lake Elevation

The extreme runoff of 2022 to 2023 reversed the trend of declining lake level occurring since 2019. At the final lake level read in December of 2023 (6383.1 feet), Mono Lake was 4.5 feet higher than in December 2022. As is typical of wet years (LADWP 2018), the maximum lake level occurred late in summer, and after a delayed runoff due to cool spring temperatures and high snowpack level.

The implementation of Decision 1631 has resulted in a stabilization of Mono Lake level changes. Since export amounts are now regulated, and greatly reduced as compared to historic export amount prior to Decision 1631, variations in lake level are mainly driven by climate and runoff patterns. An updated lake level model would help determine the influence of various factors currently influencing Mono Lake elevation, including climate change.

3.2 *Saltcedar Eradication*

3.2.1 Overview of Saltcedar Eradication

Saltcedar (*Tamarix* spp.) is a fast-growing, highly prolific invasive, widely distributed nonnative large shrub to shrubby tree that can be found in the Mono Basin. The California Invasive Plant Council (Cal-IPC) considers saltcedar as a plant with the potential to have severe impacts to ecological systems including physical processes and biological communities (Cal-IPC 2006). Saltcedar can influence native plant communities by increasing soil salinities, displacing native vegetation, or increasing fire frequency and intensity (University of California 2010).

The control of saltcedar and other invasive weeds in the Mono Basin has been a cooperative effort conducted largely by California State Parks and the Mono Lake Committee. LADWP staff have informed State Parks personnel of new noxious weed populations found while conducting fieldwork in the Mono Basin and have on occasion removed tamarisk. Although multiple entities have contributed to weed control, these efforts have largely remained undocumented in the annual Mono Basin reports.

A recommendation put forth in the 2018 Periodic Overview Report was to improve the sharing of information between LADWP and California State Parks regarding tamarisk locations and treatment efforts so that efforts are not duplicated, and to assist in assessing the progress toward eradication efforts (LADWP 2018). In 2020, we began reporting on the Saltcedar Eradication Program.

3.2.2 Saltcedar Eradication Methodologies

Since 2016, a tamarisk surveillance and treatment program has been implemented by California State Parks, with the work conducted primarily by a contractor. In 2021, the Waterfowl Director contacted California State Parks regarding their tamarisk control program in order to provide documentation to the California State Water Resources Control Board regarding the status of tamarisk control efforts and increase coordination between agencies. California State Parks provided a brief overview of their program, and a Calflora website link of their observations (https://www.calflora.org/entry/observ.html#srch=t&taxon=Tamarix&cols=b&inma=t&y=38.0065&x=-118.9794&z=11). Locations of all tamarisk on the Calflora website since 2016 were downloaded and displayed in ArcGIS. Tamarisk locations were associated with a shoreline location using the waterfowl survey lakeshore segment boundaries. Tamarisk treatment sites were summed by year and shoreline segment.

3.2.3 Saltcedar Eradication Results

Total tamarisk treatment sites represent the number of sites treated per year and may include plants found previous years. Since 2016, most of the tamarisk has been found in the western basin, including Mill Creek, Ranch Cove, and Rush Creek. The total number of saltcedar treatment sites was highest in 2016 (151), when the level of Mono Lake was at its most recent low point. Since 2016, the number of sites decreased dramatically, and only two sites were treated in 2023. The two sites treated in 2023 were new plants that were found at previously treated locations (Joe Woods, pers. comm.).

Table 3.4. Total Tamarisk treatments sites by year and shoreline segment area

	Year								Total Treated per
Shoreline Area	2016	2017	2018	2019	2020*	2021	2022	2023	Shoreline Area
Bridgeport Creek	2		1	1					4
Lee Vining Creek	8	2	2	1					13
Mill Creek	62	7	8	6		2	2	1	88
Ranch Cove	30	9	6	5			1		51
Rush Creek	23	8	10	6		1		1	49
South Shore Lagoons	6	5	4	4					19
South Tufa	2			8		1			11
West Shore	8	4	4	5	1	1	1		24
Wilson Creek	10					1	1		12
Yearly Total Treated	151	35	35	36	1	6	5	2	271

*Surveys were not conducted in the southern portion of the Mono Basin due to a wildfire closure.

3.2.4 Saltcedar Eradication Discussion

The saltcedar eradication program conducted by California State Parks over the past six years has been very effective. The high number of treatment sites in 2016 occurred during a time of reduced lake level, and a high level of recruitment was observed (D. House, pers. obs.) This flush of new recruitment was effectively controlled as only 35 sites were located in 2017. Although two new plants were found in 2023, this number is small compared to previous years.

3.3 *Waterfowl Population Surveys and Studies*

Population surveys are conducted to evaluate the response of waterfowl to the reestablishment of waterfowl habitat at Mono Lake. There is limited historic data for waterfowl use of Mono Lake, however, based on the information available, the SWRCB concluded that Mono Lake was at one time a major concentration area for migratory waterfowl, and supported a much larger waterfowl population prior to out-of-basin diversions (SWRCB 1994). The SWRCB determined that diversion-induced impacts to waterfowl were more significant than for other waterbird species.

Waterfowl population monitoring in 2023 included summer ground counts at Mono Lake and fall surveys at Mono Lake, Bridgeport Reservoir, and Crowley Reservoir (Figure 85). Deborah House, Mono Basin Waterfowl Director, along with assistance from LADWP Watershed Resources staff, has conducted waterfowl population monitoring annually at these three sites since 2002. Mono Lake, Bridgeport Reservoir, and Crowley Reservoir are the main areas of waterfowl concentration in Mono County, and combined, support the largest number of waterfowl in the county (D. House, pers. obs.). These data not only provide local site data, but data from the three sites combined can serve as an index to waterfowl population numbers and trends in Mono County.

3.3.1 Waterfowl Population Surveys — Survey Areas

Mono Lake

Mono Lake is almost centrally located in Mono County and lies just east of the town of Lee Vining (Figure 4). Mono Lake is a highly productive, deep-water saline lake. Invertebrate foods predominate, and Mono Lake brine shrimp and alkali flies are virtually the only aquatic invertebrates in the open water. Although the highly saline water, overall depth, and low diversity of food items may limit habitat quality for waterfowl - nearshore and onshore resources for waterfowl include several perennial creeks and their deltas along the west shore, numerous fresh and brackish springs scattered around the perimeter, and small, temporary and semi-permanent fresh and brackish ponds. The fall migratory waterfowl community at Mono Lake is dominated by species able to exploit these invertebrate resources, and Northern Shoveler and Ruddy Duck, together constitute approximately 90% of all waterfowl between September and mid-November (LADWP 2018).

Shoreline subareas and Cross-lake Transects

The shoreline and open water areas were divided into shoreline subareas and cross-lake transect zones for determining the spatial distribution of waterfowl (Figure 5). The entire Mono Lake shoreline was divided into 15 shoreline subareas, generally following

those established by Jehl (2002). A sampling grid established in 2002 to survey open-water areas of Mono Lake consists of eight parallel transects spaced at one-minute (1/60th of a degree, approximately one nautical mile) intervals that were further divided into a total of 25 sub-segments of approximately equal length.

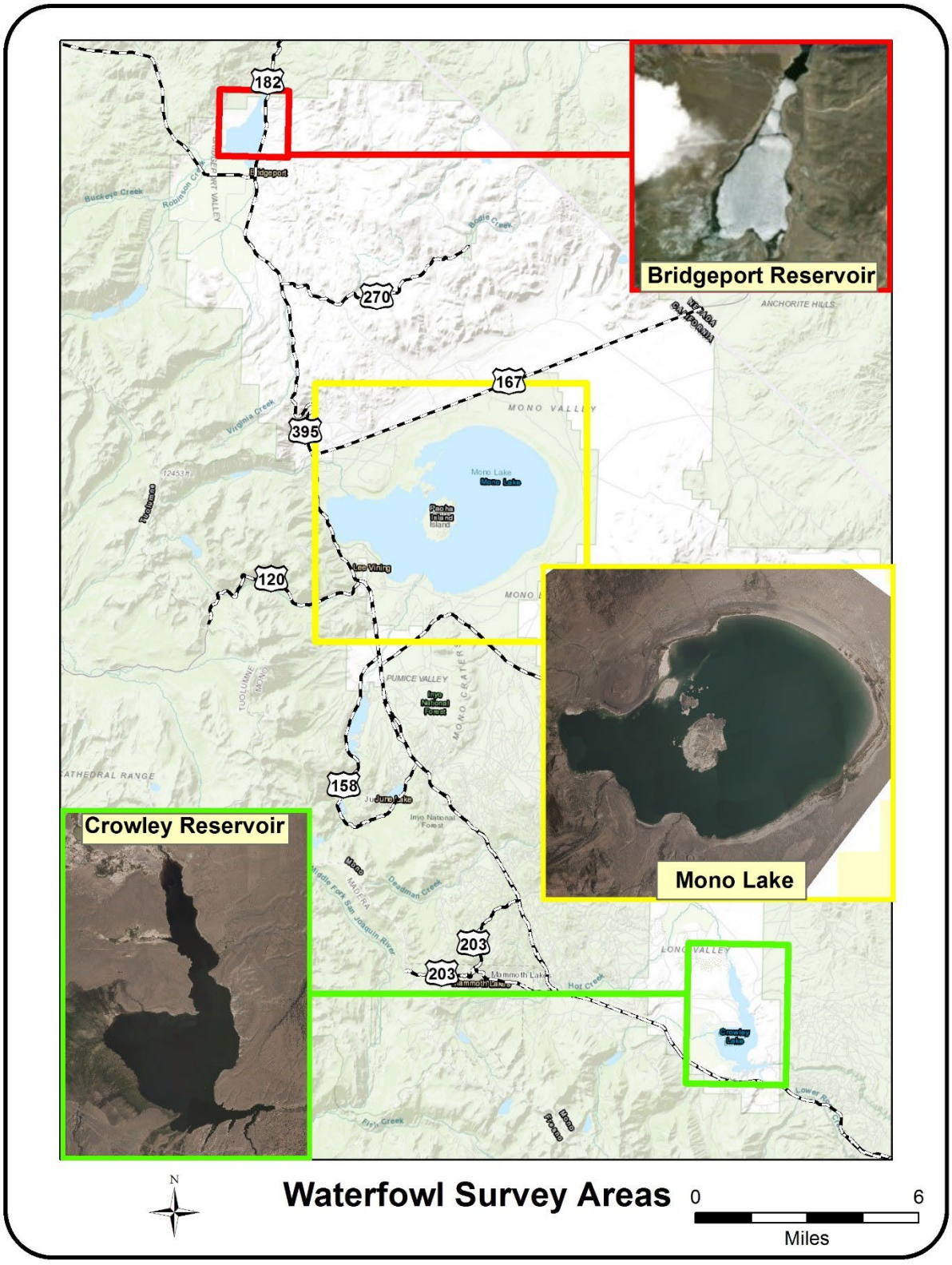

Figure 4. Waterfowl survey areas

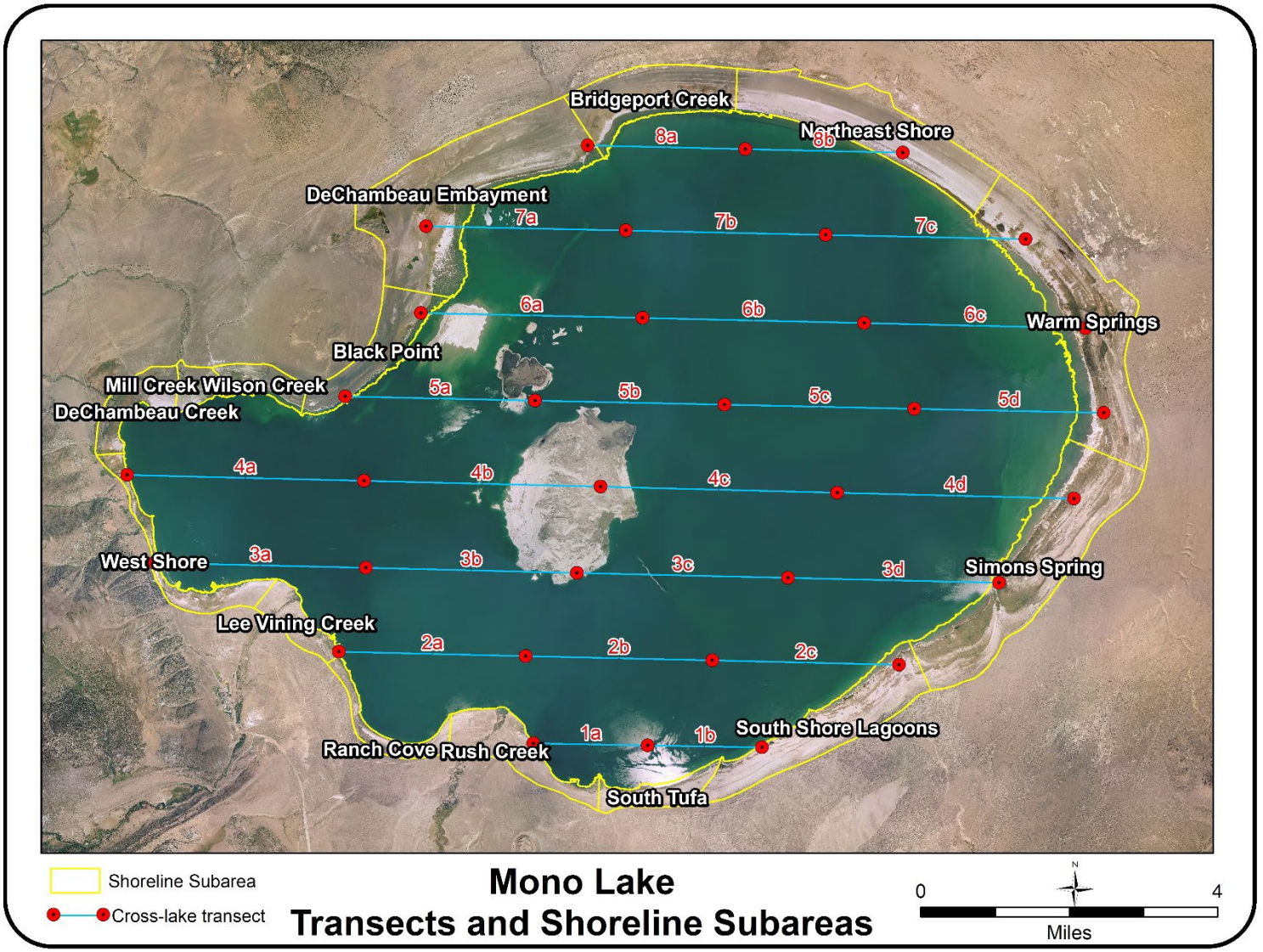

Figure 5. Mono Lake shoreline subareas and cross-lake transects

Mono Basin Restoration Ponds

The Mono Basin Restoration Ponds are located on the north side of Mono Lake, near the historic DeChambeau Ranch, and upgradient of the DeChambeau Embayment shoreline area (Figure 6). The Restoration Pond complex consists of the five DeChambeau Ponds and two County Ponds.

The DeChambeau Ponds are a complex of five small artificial ponds of varying size ranging from about 0.7 to 4.0 acres when flooded. The DeChambeau Ponds were initially created at the onset of trans-basin diversions in the 1940s (LADWP 1996a) and restored in the mid-1990's (LADWP 2018). Project goals for the restoration in the 1990's included the creation of seasonal waterfowl habitat consisting of semi-permanent ponds (DEPO1 and DEPO2), and seasonal impoundments (DEPO3, DEPO4 and DEPO5), as well as adjacent seasonal wet meadow and willow habitat (LADWP 1996a, USDA Forest Service 2005). Management has seemingly differed from these original goals, as some ponds (DEPE2 and DEPO4) have been continuously inundated and DEPO1 and DEPO5 infrequently flooded. Failing infrastructure has also altered management.

There are two water sources currently supplying water to the DeChambeau Ponds. Most of the water for the DeChambeau Ponds is from Wilson Creek and delivered via an underground pipe averaging 1-2 cfs recently (N. Carle, pers. com.). The underground piping flows water from DEPO1 to DEPO5. The second source is water from a hot artesian source adjacent to DEPO4. Hot spring water is delivered to each of the five ponds through piping. A leak developed around 2008 or 2009 in the pipe supplying the ponds (N. Carle, pers. com.), and for several years, hot spring water was only delivered to DEPO4. In 2021, repairs to the piping had restored the ability to deliver artesian water to additional ponds in the DeChambeau Pond complex.

The County Pond complex consists of two ponds – County Pond East (COPOE) and County Pond West (COPOW). The two County Ponds lie in a natural basin and former lagoon that dried as the lake level dropped below 6,405 feet in the 1950s. The County Ponds were temporarily re-flooded on an occasional basis after that time with water diverted from Wilson Creek, until an underground pipeline was installed to deliver water from DEPO4 to the County Ponds (USDA Forest Service 2005) in the late 1990s. A clay sealant was also applied to COPOE to reduce water use. A diverter box at the County Ponds allows some control over water releases to the individual ponds. COPOW has had little open water and poor habitat since 2010 and appearing dry since 2018. In early June of 2023, there was a small amount of shallow ponded water present as a result of the high runoff year. COPOE had been the most productive of the

restoration ponds for waterfowl until 2018 when infrastructure failure left both County Ponds dry. In late fall of 2023, water was once again being released to these ponds.

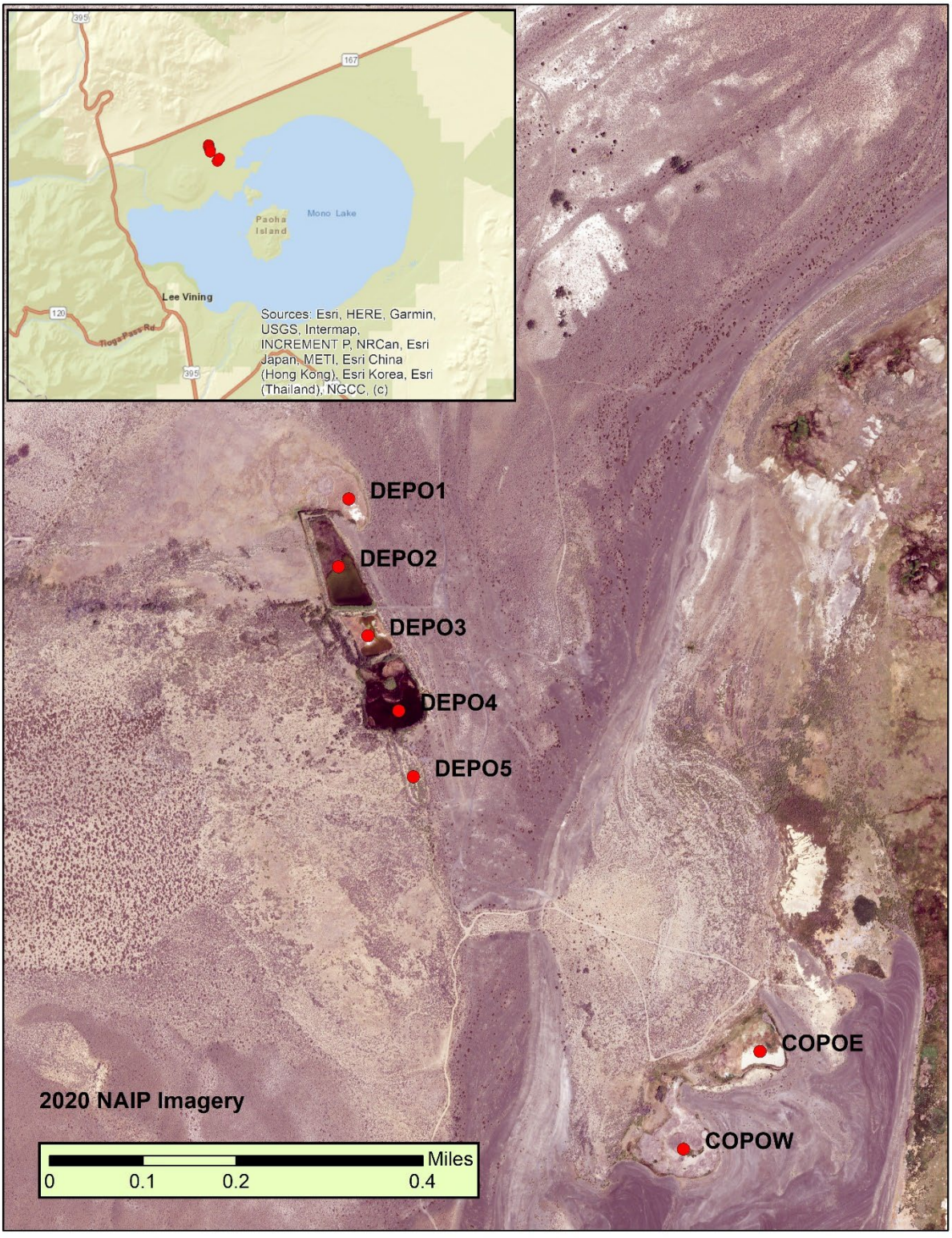

Figure 6. Mono Basin restoration ponds locator map

Bridgeport Reservoir

Bridgeport Reservoir is approximately 22 miles northwest of Mono Lake near the town of Bridgeport (Figure 4). Bridgeport Reservoir is located in Bridgeport Valley in northern Mono County, California, at an elevation of 6,460 feet. Bridgeport Valley has an arid continental climate (Zellmer 1977) and experiences relatively cool, mild summers and cold, snowy winters. The average July temperate is 63°F, and the maximum July temperature is in the low 90s. Winters are cold as the average minimum January temperature is 9.1°F, and the average maximum is 42.5°F. Precipitation averages 10 inches, mostly in the form of snow, and Bridgeport averages only 65 frost-free days a year. Bridgeport Reservoir typically freezes over in the winter for varying lengths of time. The mid-November surveys are generally ice-free, however in some years, a thin layer of ice is present in some areas of the reservoir.

Bridgeport is part of the hydrologically closed Walker River Basin, which spans the California/Nevada border. Bridgeport Reservoir, completed in 1923, provides irrigation water to Smith and Mason Valleys in Nevada (Sharpe et al. 2007). Numerous creeks originating from the east slope of the Sierra Nevada drain toward Bridgeport Reservoir. These tributaries are used for upslope irrigation of Bridgeport Valley to support the primary land use of cattle grazing. The creeks directly tributary to the reservoir are the East Walker River, Robinson Creek and Buckeye Creek. Downstream of Bridgeport Reservoir Dam, the East Walker River continues flowing into Nevada, joining the West Walker River, ultimately discharging into the terminal Walker Lake, Nevada (House 2021). In Nevada, the Walker River system supports extensive agricultural operations.

Bridgeport Reservoir is a small to moderately sized reservoir with a surface area of approximately 7.4 square miles and a storage capacity of 42,600 acre-feet. In September 2023, Bridgeport Reservoir held 28,880 acre-feet (https://cdec.water.ca.gov/dynamicapp/QueryMonthly?s=BDP), which is approximately 250% above the long-term 2002 to 2022 average of 11,312 acre-feet. The September 2023 storage level was 3.5 higher than that the September of 2022 storage level of 8,079 acre-feet.

The reservoir is rather shallow with a mean depth of 15 feet and a maximum depth of 43 feet (Horne 2003). Due to the shallow-sloping topography of the southwestern portion of the valley, reservoir level greatly influences surface area (House 2021).

Flood-irrigated pastures border the gently sloping south and southwestern portion of Bridgeport Reservoir, while Great Basin scrub is dominant along the more steeply-sloped north arm and east shore. In shallow areas and creek deltas, submergent aquatic vegetation is abundant, including broad beds of water smartweed (*Persicaria*

amphibia stipulacea). Marsh, dense wetlands, or woody riparian vegetation are lacking in the immediate vicinity of the reservoir and Bridgeport Valley proper. The reservoir is eutrophic due to high nutrient loading and experiences summer blooms of colonial forms of cyanobacteria that form dense floating scum (Horne 2003). Algal blooms in fall frequently result in the issuance of temporary recreational advisories due to the presence of cyanobacteria and associated toxins.

The shoreline of Bridgeport Reservoir was subdivided three shoreline survey areas (Figure 7).

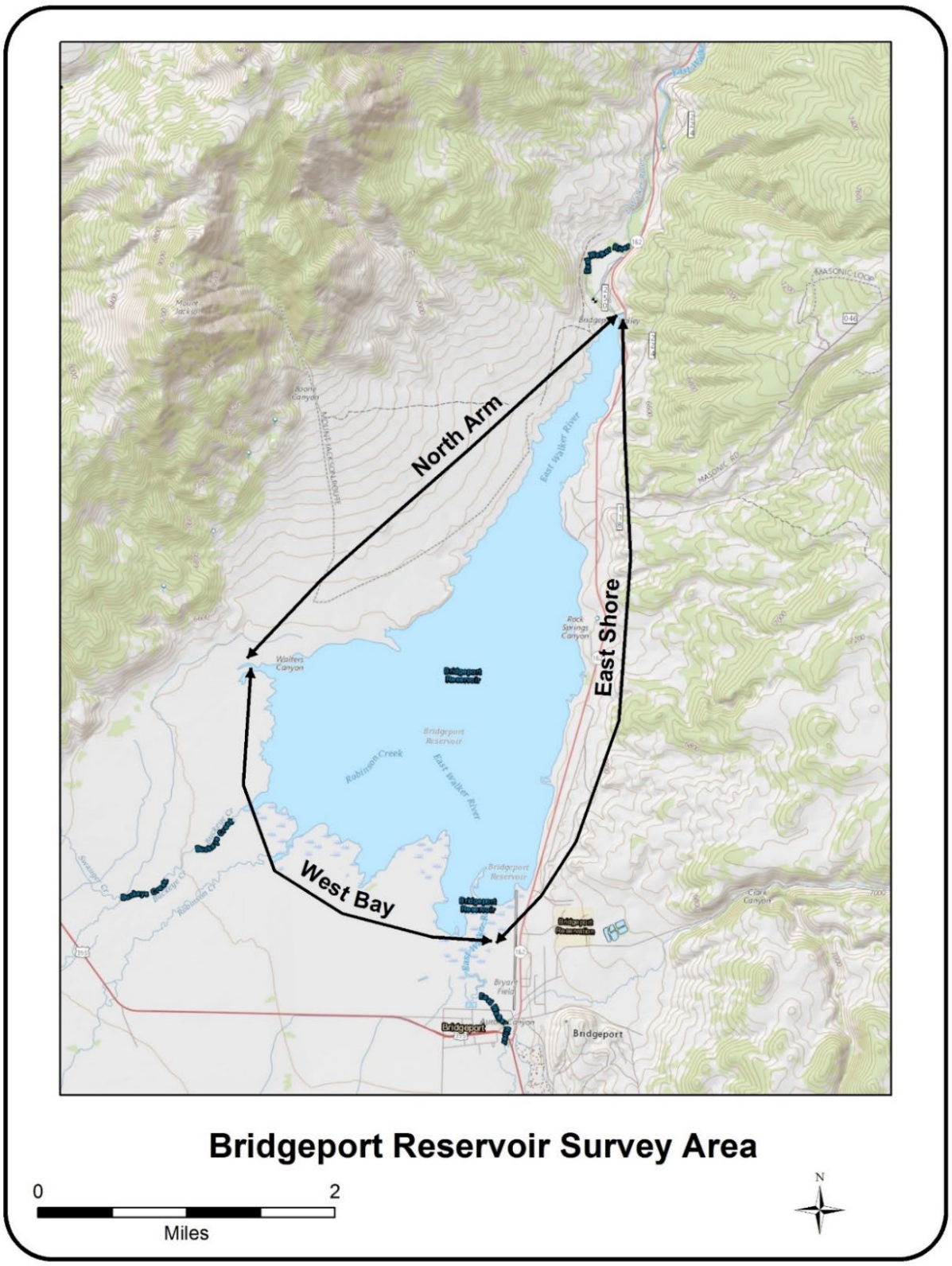

Figure 7. Bridgeport Reservoir shoreline subareas

Crowley Reservoir

Crowley Reservoir is approximately 31 miles southeast of Mono Lake, and 12 miles southeast of the town of Mammoth Lakes (Figure 4). Crowley Reservoir is located in Long Valley, at an elevation of 6,780 feet. Created by the construction of the Long Valley Dam in 1941, Crowley Reservoir is the second largest lake in Mono County, and the largest reservoir in the county, averaging 13.2 square miles. The primary source of freshwater input to Crowley Reservoir is the Owens River. Other freshwater input includes flows from McGee Creek, Convict Creek, Hilton Creek, and Crooked Creek. Crowley Reservoir also receives spring flow from Layton Springs along the northeast shoreline, and unnamed springs and subsurface flow along the west shore. Crowley is much deeper than Bridgeport Reservoir, with a mean depth of 35 feet and a maximum depth of 125 feet (Corvallis Environmental Research Laboratory and Environmental Monitoring Support Laboratory 1978).

Crowley Reservoir is moderately sized with a storage capacity of 183,465 acre-feet. In September 2023, Crowley Reservoir held 170,844 acre-feet (https://cdec.water.ca.gov/dynamicapp/QueryMonthly?s=CRW), which is 60% higher than the long-term 2002 to 2022 average of 105,166 acre-feet. The September 2023 storage level was at a record high for month since regular waterfowl surveys were initiated in 2002. The level was almost 60% greater than the September of 2022 level of 102,223.

Crowley Reservoir is eutrophic and experiences summer blooms of the nitrogen-fixing cyanobacteria *Gloeotrichia* in summer, and late-summer and fall season blooms of the cynaobacteria *Aphanizomenon* (Jellison et al. 2003). An algal bloom in August 2023 resulted in the issuance of a temporary recreational advisory due to the presence of cyanobacteria and associated toxins. In shallow areas near the deltas, submergent aquatic vegetation is generally abundant, but there was little growth this year as compared to the past several years. Crowley Reservoir is known for supporting a healthy population of midges (Chironomidae).

The shoreline of Crowley Reservoir was subdivided into seven shoreline survey areas (Figure 8).

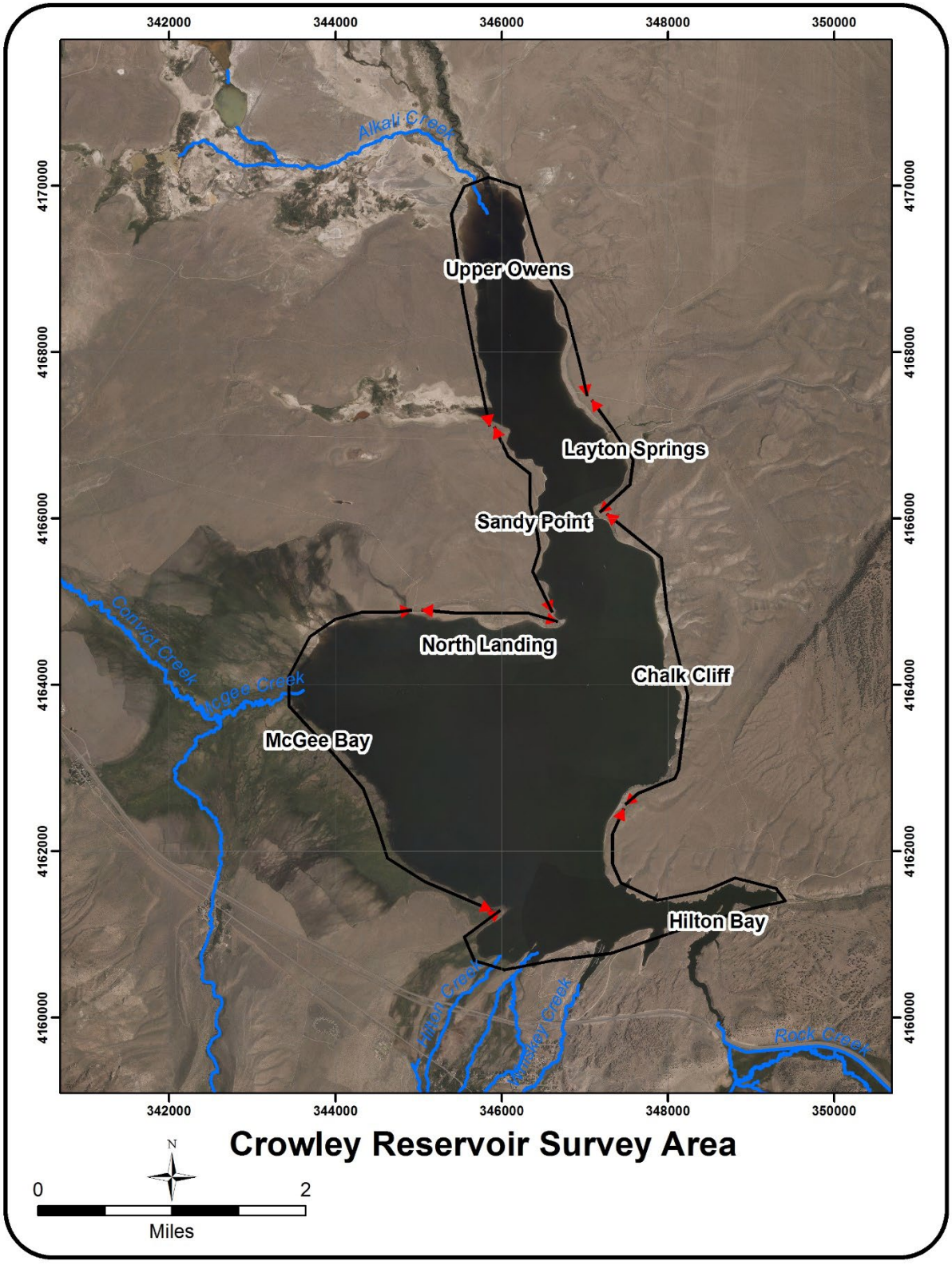

Figure 8. Crowley Reservoir shoreline subareas

3.3.2 Waterfowl Population Monitoring Methodologies

Mono Lake Waterfowl Surveys

Summer Surveys

Summer ground surveys were conducted in the Mono Basin along the shoreline of Mono Lake and at the DeChambeau and County Pond complexes. Nine of the 15 shoreline subareas were surveyed in summer: South Tufa (SOTU), South Shore Lagoons (SSLA), Simons Spring (SASP), Warm Springs (WASP), Wilson Creek (WICR), Mill Creek (MICR), DeChambeau Creek Delta (DECR), lower Rush Creek and Rush Creek Delta (RUCR), and lower Lee Vining Creek and delta (LVCR).

Three summer ground-count surveys were conducted at each of these nine shoreline subareas and all seven restoration ponds in 2023. The only exception to this in 2023 is that survey 1 in early June was not completed at Warm Springs because of access issues due to road flooding.

Surveys were conducted at three-week intervals beginning in early June (Table 3.5). Surveys of the shoreline subareas were conducted by walking at an average rate of approximately 1 mile/hr, depending on conditions, and recording waterfowl species as they were encountered. Surveys started within one hour of sunrise, and all shoreline areas were surveyed over a 4 to 5-day period. The order in which subareas were visited was varied in order to minimize the effect of time-of-day on survey results. The restoration ponds were surveyed on foot, spending a minimum of 5 minutes at each pond to record any waterfowl and broods present.

For each waterfowl observation, the following was recorded: time of the observation; the habitat type being used; and an activity code indicating how the bird, or birds were using the habitat. Examples of activities recorded include resting, foraging, flying over, nesting, brooding, sleeping, swimming, or calling.

Table 3.5. Summer ground count survey dates, 2023

	2023 Survey Number and Date		
Subarea	**Survey 1**	**Survey 2**	**Survey 3**
DECR	9-Jun	28-Jun	18-Jul
LVCR	6-Jun	27-Jun	19-Jul
MICR	8-Jun	27-Jun	18-Jul
RUCR	6-Jun	28-Jun	19-Jul
SASP	7-Jun	29-Jun	20-Jul
SOTU	5-Jun	28-Jun	18-Jul

SSLA	5-Jun	26-Jun	17-Jul
WASP	No survey	30-Jun	21-Jul
WICR	8-Jun	27-Jun	18-Jul
COPO	6-Jun	27-Jun	19-Jul
DEPO	6-Jun	27-Jun	19-Jul

When conducting summer ground counts at Mono Lake, emphasis was placed on finding and recording all waterfowl broods. Because waterfowl are easily flushed, and females with broods are especially wary, the shoreline was scanned frequently well ahead of the observer in order to increase the probability of detecting broods. Information recorded for broods included species, size, GPS coordinates (UTM, NAD 83, Zone 11, CONUS), habitat use, and age. Broods were aged based on plumage and body size (Gollop and Marshall 1954).

Since summer surveys were conducted at three-week intervals, any brood assigned to Class I, using the Gollop and Marshall age classification scheme (which includes subclasses Ia, Ib, and Ic), would be a brood that had hatched since the previous visit. Assigning an age class to broods allowed for a determination of the minimum number of "unique broods" using the Mono Lake wetland and shoreline habitats.

Habitat use was recorded to document habitat use by waterfowl at Mono Lake. Habitat use was recorded using the mapped landtype categories (LADWP 2018). Two additional habitat types: open water near shore (within 50 meters of shore), and open water offshore (>50 meters offshore), were added to the existing classification system to more completely represent areas used by waterfowl.

Salinity measurements of lake-fringing ponds were taken using an Extech EC400 Conductivity/TDS/Salinity probe to aid in the classification of fresh versus brackish ponds when recording habitat use. Ponds with a salinity of less than 500 ppm were classified as fresh. Ponds with vegetation present and a salinity of greater than 500 ppm were classified as brackish. Ponds with a measured salinity greater than 10 ppt (the maximum range of the probe) lacking vegetation and subsurface or surface freshwater inflow were classified as hypersaline.

Fall Surveys

The fall 2023 surveys included the entire shoreline of Mono Lake, a subset of the eight established cross-lake transects, and all seven restoration ponds. Six fall surveys were completed at two-week intervals between September 5 and November 15 (Table 3.6).

Helicopter-based shoreline surveys were completed by flying the perimeter of Mono Lake, maintaining a distance of approximately 500 to 800 feet from the shoreline. The

beginning and ending points for each shoreline area were determined using both landscape features and the mobile mapping program Avenza®. Waterfowl not identifiable to species were recorded as the next identifiable taxa higher (e.g. *Aythya* spp.).

The open-water cross-lake transects were surveyed by boat using a 17-foot Boston Whaler. The areas surveyed in 2023 were: 4b, 5a, 5b, 6a, 7a, 7b, 7c, 8a, and 8b. These nine subsections of the cross-lake transects were sampled as they have been highly predictive of both total lakewide Ruddy Ducks (r^2=0.990, p<0.001) and offshore Ruddy Duck detections (r^2=0.831, p<0.001). Boat surveys of the cross-lake transects were conducted by cruising slowly at a speed of 8-10 knots along each transect subsection. The beginning and ending points for each shoreline or cross-lake transect area were determined using both landscape features and the mobile mapping program Avenza®. Slower speeds were used when waterfowl flocks were encountered, or when shallow conditions and/or the presence of submerged objects required reduced speeds for safety. On occasion, we stopped on the open water to prevent flushing, or to allow observers improved viewing of waterfowl. In some areas we could not follow the transect for the entire length due to low water depths or the presence of submerged objects including tufa or pumice blocks.

In 2023 fall waterfowl surveys were conducted by the Mono Basin Waterfowl Program Director, Deborah House, and LADWP Watershed Resources Specialists, Bill Deane and Erin Nordin.

Table 3.6. Fall 2023 Mono Lake Survey Dates

Survey Period	Shoreline	Cross-lake	Restoration Ponds
Survey 1	5-Sep	5-Sep	No Survey
Survey 2	19-Sep	22-Sep	19-Sep
Survey 3	3-Oct	4-Oct	5-Oct
Survey 4	17-Oct	18-Oct	18-Oct
Survey 5	31-Oct	1-Nov	31-Oct
Survey 6	14-Nov	15-Nov	14-Nov

Bridgeport Reservoir Fall Waterfowl Surveys

The fall 2023 surveys included the entire shoreline and open water areas of Bridgeport Reservoir. Six fall surveys were completed at two-week intervals between 6 September and 14 November (Table 3.7). The primary survey method was aerial surveys from a helicopter; however Survey 1 and Survey 3 were conducted from a boat as the helicopter was not available.

Table 3.7. Fall 2023 Bridgeport Reservoir Survey Dates

Survey Period	Survey Date	Method
Survey 1	6-Sep	Boat
Survey 2	19-Sep	Helicopter
Survey 3	5-Oct	Boat
Survey 4	17-Oct	Helicopter
Survey 5	31-Oct	Helicopter
Survey 6	14-Nov	Helicopter

Crowley Reservoir Fall Waterfowl Surveys

The fall 2023 surveys included the entire shoreline and open water areas of Crowley Reservoir. Six fall surveys were completed at two-week intervals between 7 September and 14 November (Table 3.8). The primary survey method was aerial surveys from a helicopter; however Survey 1 and Survey 3 were conducted from a boat as the helicopter was not available.

Boat surveys were conducted from by paralleling the shoreline at low speeds, stopping when lighting and viewing conditions were most favorable to count waterfowl in the different shoreline areas. Unlike the previous three years, there was little growth of aquatic vegetation including widgeongrass (*Ruppia* sp.) and boat travel into shallow shoreline areas was not impeded. Because of good visibility and access from the shoreline, boat and ground survey are comparable in terms of providing good coverage of the lake.

Table 3.8. Fall 2023 Crowley Reservoir Survey Dates

Survey Period	Survey Date	Method
Survey 1	7-Sep	Boat
Survey 2	19-Sep	Helicopter
Survey 3	10-Oct	Boat
Survey 4	17-Oct	Helicopter
Survey 5	31-Oct	Helicopter
Survey 6	14-Nov	Helicopter

Aerial Photography of Waterfowl Habitats

The shoreline configuration of Mono Lake is dynamic, as seasonal and annual changes in lake level influence the development and presence of ponds, the amount of shoreline exposed, and other features important to waterfowl. Due to the dynamic nature of the Mono Lake shoreline, the aerial or satellite imagery studies and subsequent mapping performed at five-year intervals do not adequately capture annual changes that may influence waterfowl use. These still aerial photographs are taken yearly in fall to assess shoreline changes at Mono Lake, particularly in years when aerial imagery is not available.

In 2023, digital photographs were taken from a helicopter to document shoreline conditions. Photos of all three waterfowl survey areas were taken 18 September 2023. At each waterfowl survey area, representative photos were taken of each shoreline subarea established for use in evaluating the spatial distribution of waterfowl. For reference, the elevation of Mono Lake in September 2023 was 6,383.2 feet. This work was conducted by Deborah House, Mono Basin Waterfowl Program Director.

3.3.3 Waterfowl Data Summary and Analysis

Mono Lake Summer Surveys

Summer Waterfowl Community

The summer waterfowl community data summary includes all breeding, migrant, and non-breeding/oversummering species observed in 2023. Waterfowl species were classified as breeding or nonbreeding based on whether a territorial pair, nest, or brood has been observed over the entire length of the study. The 2023 summer waterfowl survey data were summarized by species and summer survey number.

Breeding Population Size and Composition

The size of the Mono Lake breeding waterfowl population was estimated by averaging the sum of all breeding waterfowl species and individuals over the three surveys. Waterfowl totals for the Restoration Ponds will be reported separately and not included when estimating population size. The 2023 breeding waterfowl population total was compared to the long-term 2002 to 2022 mean. The population size of each species was evaluated by comparing 2023 values to the 2002 to 2023 mean plus standard error for each breeding species. The 2020 data were not included as only two summer surveys were completed in that year.

The total number of broods observed during shoreline surveys will be used as an index of waterfowl breeding productivity at Mono Lake. The total number of broods raised at

Mono Lake in a year was estimated by removing broods potentially double-counted over the season from all broods recorded. The species, age, size and location of each brood were used to determine which broods to eliminate from the total. For example, all Class I broods observed on a survey would be included in the total, but older broods (e.g. Class II) would be removed, unless there was justification to include it (e.g. no broods of that species had been observed yet).

The calculation of brood parameters included all nesting species except Canada Goose. Canada Goose initiates nesting earlier than the other waterfowl species and family groups can be difficult to approach closely on foot except in areas where they have become habituated to humans. These factors combined with the tendency of this species to be highly mobile has made ageing broods accurately and determining the minimum number of Canada Goose broods less reliable. Waterfowl brood totals were compared to the long-term 2002 to 2022 means +/-SE. Brood totals for the Restoration Ponds will be reported separately and not included in the shoreline counts.

The spatial distribution of breeding waterfowl was evaluated by calculating the total number of broods observed for each shoreline area in 2023. The total broods observed per shoreline subarea was compared with the long-term averages by shoreline subarea.

Habitat Use

Habitat use data were summarized on breeding species for which there was sufficient sample size: Canada Goose, Cinnamon Teal, Gadwall, Green-winged Teal and Mallard. The proportional use of modeled and mapped vegetation types was calculated for each of these five breeding species.

Long-term Trend in Breeding Waterfowl Population

Linear regression was used to evaluate long-term trends in the size of the breeding waterfowl population and the number of broods produced. This analysis was done for shoreline waterfowl only. The relationship between monthly lake level and the breeding waterfowl indices were evaluated using simple linear regression. Welch's t-test was used to further investigate the presence of a potential threshold lake elevation and brood production.

Restoration Ponds

The size of the breeding waterfowl population at the ponds was estimated by averaging the sum of all breeding waterfowl species and individuals over the three surveys. Waterfowl and brood totals from 2023 were compared to the long-term 2002 to 2022 means +/-SE.

Fall Waterfowl Surveys

Fall Waterfowl Population Size and Species Composition

Waterfowl community composition was described by classifying species into three groups: geese and swans, dabbling ducks, and diving ducks, and then determining the proportional abundance of each group.

For Mono Lake data, waterfowl species totals were summed by survey area and survey period. Survey totals for 2023 were compared to the long-term 2002 to 2022 mean for each of the six surveys by site. Fall waterfowl totals from 2023 were compared to the long-term 2002 to 2022 means +/-SE. The 2023 species totals of the most abundant fall migrants were compared to their respective long-term means.

At Bridgeport and Crowley Reservoirs, long-term means were calculated for the 2003 to 2022 time period. Fall waterfowl totals from 2023 were compared to the long-term 2002 or 2003 to 2022 means +/-SE.

Spatial distribution

The spatial distribution of waterfowl at each of the surveys areas was evaluated by summing the total waterfowl found in each shoreline area over the six fall surveys. For Mono Lake, the 2023 distribution was compared to the long-term 2002 to 2022 trend of proportional distribution of waterfowl at Mono Lake (both offshore on the cross-lake transects and the shoreline areas). The distribution of Ruddy Ducks by survey and cross-lake transect is also presented for Mono Lake.

Long-term Trend of Fall Waterfowl Populations

For each survey area, the long-term trend in total fall waterfowl was evaluated using totals for all six surveys at each site. The count data was log transformed in order to satisfy test assumptions of normality. Over the length of the study, there were two missing surveys (mid-September of 2020 and 2022). Missing data for these two points at each survey site were estimated using cubic spline interpolation (SRS1 Software, LLC).

For the Mono Lake data, two environmental variables were tested for their relationship to fall waterfowl totals – Mono Lake level in September of each survey year and the mixing state. The relationship between lake level in September and the annual total fall waterfowl were evaluated using simple linear regression. The waterfowl count data was log transformed to satisfy test assumptions of normality. Mixing state was classified as either meromictic or monomictic based on whether the lake was chemically or thermally

stratified during the fall of each year. Under meromictic conditions, the lake is stratified, and monomixis is when the lake has undergone mixing and little to no stratification exists. Annual limnology reports were reviewed in order to classify each year. The following years were considered monomictic: 2003 to 2004; 2008 to 2010; 2012 to 2016; 2020 to 2022. These years were meromictic: 2002, 2005 to 2007; 2011; 2017 to 2019; 2023. A one-way Welch's ANOVA was used to determine if the mean number of total fall waterfowl at Mono Lake differed between years classified as monomictic and meromictic.

Restoration Ponds

The number of waterfowl seen at the restoration ponds over the five fall surveys in 2023 were summed by species, pond and across ponds and surveys. Waterfowl totals from 2023 were compared to the long-term 2002 to 2022 means +/-SE. Linear regression was used to evaluate long-term trends in the total number of fall waterfowl observed at all restoration ponds combined.

Comparison of Fall Waterfowl Among Survey Areas

Fall waterfowl data from Mono Lake was compared to Bridgeport and Crowley Reservoirs by first calculating the annual means for each site +/- SE. Annual means for Mono Lake included all years (2002 to 2022) but excluded 2002 for the other two sites since only three of the annual six surveys were conducted in 2002. The long-term means and the 2023 results were compared were compared across sites. The distribution of Northern Shoveler and Ruddy Duck among the three survey areas was assessed by comparing the proportions of these species that occurred at each site.

Aerial Photography of Waterfowl Habitats

The annual photographs of waterfowl habitats at Mono Lake, Bridgeport Reservoir and Crowley Reservoir were reviewed and compiled. Representative photos from each shoreline subarea are included in this report. The annual photos, combined with field notes taken over the summer and fall survey periods, were used to evaluate and subjectively describe shoreline conditions in 2023.

3.3.4 Waterfowl Population Survey Results

Mono Lake Summer Surveys

Summer Waterfowl Community

In 2023, 585 waterfowl and eight waterfowl species were observed over the three summer shoreline surveys (Table 3.9) including seven breeding and one non-breeding

species. Breeding waterfowl comprised most waterfowl present in summer (580 of 585). Waterfowl numbers were highest on Survey 2 and essentially the same on Survey 1 and 3. Of the breeding species, Gadwall was most abundant, comprising 50% of breeding waterfowl at Mono Lake in 2023.

Table 3.9. Summer Ground Count Waterfowl Detections in 2023.
Mono Lake breeding waterfowl species are in bold type.

Species	Survey 1 June 5-9	Survey 2 June 26-30	Survey 3 July 17-21	Total Detections
Canada Goose	64	70	58	192
Cinnamon Teal			1	1
Gadwall	87	109	98	294
Mallard	25	12	10	47
Northern Pintail	1		6	7
Green-winged Teal	12	10	15	37
Bufflehead	1	2	2	5
Ruddy Duck		1	1	2
Total waterfowl by survey	**190**	**204**	**191**	**585**

Breeding Population Size and Composition

The breeding waterfowl population at Mono Lake in 2023 is estimated at 193, or approximately 97 pairs. The 2023 breeding population was significantly lower as compared to the long-term mean of 305 +/- 19 SE or 160 pairs. Breeding was confirmed for Canada Goose, Cinnamon Teal (*Spatula cyanoptera*), Gadwall, Green-winged Teal (*Anas crecca*), and Mallard (*Anas platyrhynchos*). Canada Goose numbers were slightly above average in 2023 (Figure 9), and Green-winged Teal was about average. The numbers of all other breeding species were below their respective long-term means.

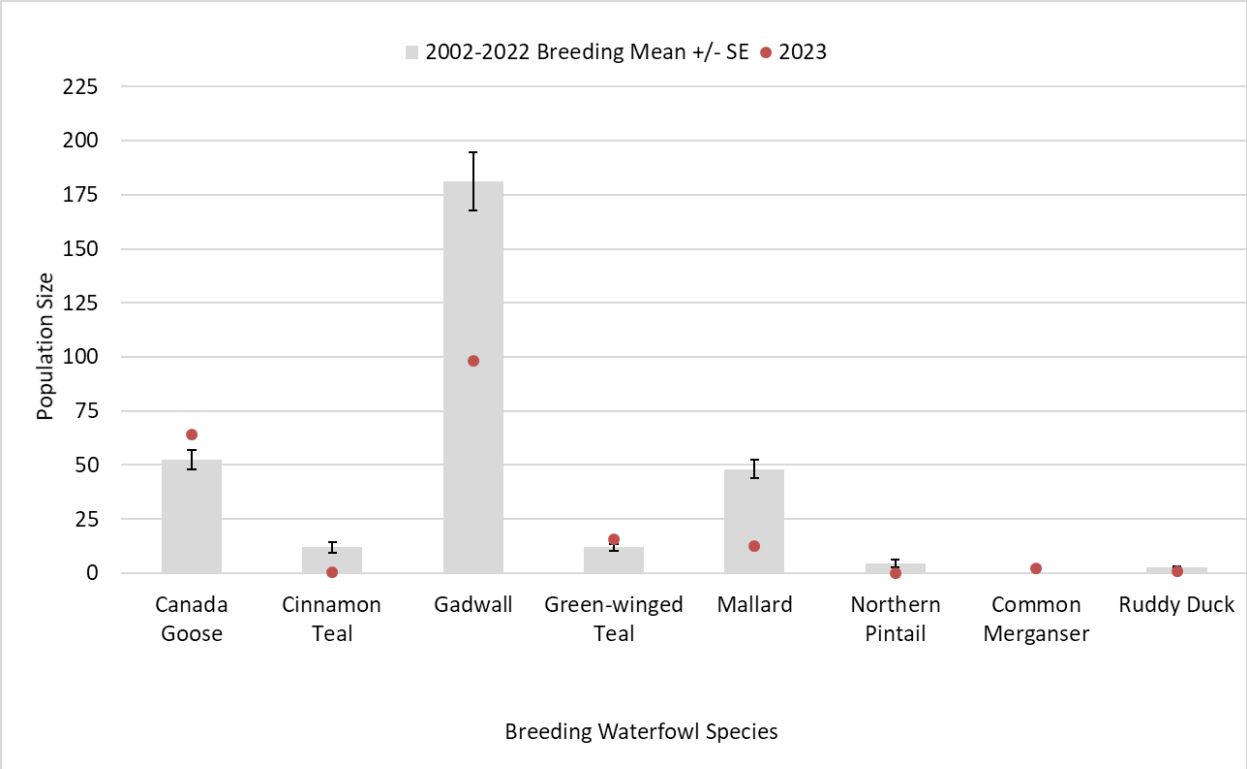

Figure 9. 2023 Breeding waterfowl population vs. long-term mean

A total of 69 waterfowl broods were found on the three surveys conducted in 2023, including seven Canada Goose and 62 dabbling duck broods. Breeding was confirmed for four species, with brood numbers highest for Gadwall (Table 3.10). In 2023, dabbling duck broods were found at all shoreline areas, except South Tufa and Warm Springs, but one Canada Goose brood was seen at South Tufa. Most broods (42; 61%) were found along the northwest shore areas of DeChambeau Creek and Wilson Creek shoreline areas. Other areas supporting a large proportion of the broods were Simons Spring, and South Shore Lagoons.

The total number of waterfowl broods found (exclusive of Canada Goose) in 2023 (62) was above the long-term average of 48.4 +/- 3.6 of all three surveys combined. While conducting Survey 3, three additional Gadwall hens and a Green-winged Teal were highly agitated, but no broods were seen at the time. Based on their behavior, there birds may have had broods and thus the total brood count could be higher. No other pairs or females without broods were observed. Interestingly, during ground visits to the shoreline in late August and early September, several young Gadwall broods were encountered, which is not typical for that late in the year. I also saw evidence of an extended breeding season at Bridgeport and Crowley Reservoirs as young broods incapable of flight were present into September.

Table 3.10. Waterfowl broods by shoreline area, 2023

Breeding Waterfowl Species	DECR	LVCR	MICR	RUCR	SASP	SOTU	SSLA	WASP	WICR	Total 2023 Broods
Canada Goose	2		2			1	1		1	**7**
Gadwall	15	1		2	13		5		16	**52**
Green-winged Teal	1		2	1	1				1	**6**
Mallard							2		2	**4**
Total broods per shoreline area	**18**	**1**	**4**	**3**	**14**	**1**	**8**	**0**	**20**	**69**

Habitat Use

The Canada Geese at Mono Lake were primarily observed foraging and brooding in alkaline wet meadow, barren lake bed, and open water areas >50 m from shore (Table 3.11). Dabbling duck activity (Cinnamon Teal, Gadwall, Green-winged Teal and Mallard) was concentrated in and around nearshore water features (on shore or <50 m from shore) and ria. Cinnamon Teal were only seen in freshwater ponds. Gadwall were observed most frequently feeding and with broods in ria, but also in fresh and brackish ponds, and occasionally on the open water >50 m from shore. Green-winged Teal were most associated with ria and freshwater ponds. Mallard used freshwater ponds most frequently and were the species most associated with freshwater streams and mudflat.

Table 3.11. Proportional habitat use of breeding waterfowl species, 2023

Landtypes		Breeding Waterfowl Species				
Modeled	Mapped	Canada Goose	Cinnamon Teal	Gadwall	Green-winged Teal	Mallard
Meadow Marsh		27%	0%	2%	0%	4%
	Marsh	*0%*	*0%*	*0%*	*0%*	*4%*
	Wet Meadow	*0%*	*0%*	*1%*	*0%*	*0%*
	Alkaline Wet Meadow	*27%*	*0%*	*1%*	*0%*	*0%*
	Dry Meadow/Forb	*0%*	*0%*	*0%*	*0%*	*0%*
Water		21%	100%	32%	43%	79%
	Freshwater Stream	*2%*	*0%*	*2%*	*3%*	*13%*
	Streambar	*7%*	*0%*	*2%*	*0%*	*4%*
	Freshwater Pond	*0%*	*100%*	*10%*	*41%*	*36%*
	Brackish Pond	*1%*	*0%*	*16%*	*0%*	*4%*
	Hypersaline Pond	*0%*	*0%*	*0%*	*0%*	*0%*
	Mudflat	*11%*	*0%*	*1%*	*0%*	*21%*
Ria		14%	0%	56%	51%	9%
Open Water		26%	0%	8%	3%	9%
Riparian		0%	0%	0%	0%	0%
Barren Lake Bed		12%	0%	0%	0%	0%
Upland		0%	0%	1%	3%	0%
Tufa		1%	0%	0%	0%	0%

Long-term Trend in Breeding Waterfowl Population

The breeding waterfowl population has ranged from a low of 145 in 2017 to a high of 555 in 2007. There has been no long-term trend in the size of the breeding waterfowl population from 2002 to 2023 (r^2=0.138, p=0.098), but there has been a positive correlation with lake level. Higher lake levels in spring through early summer were correlated with larger breeding population size. The month with the highest correlation coefficient was March (r = 0.762, p=<0.001, (Figure 10).

The number of broods produced at Mono Lake has ranged from a low of 26 in 2016 to a high of 74 in 2021. The total number of broods was most strongly correlated with the lake elevation in June. An examination of the scatter plot showed a different response to lake level above and below a threshold of about 6,382 feet. The total number of broods produced at Mono Lake when the lake is below 6,382 feet has been significantly fewer than when the lake elevation is at or above 6,382 feet (Figure 11) (Welch's t-statistic = 3.69, df=17.0, effect size = 1.59, p=0.002).

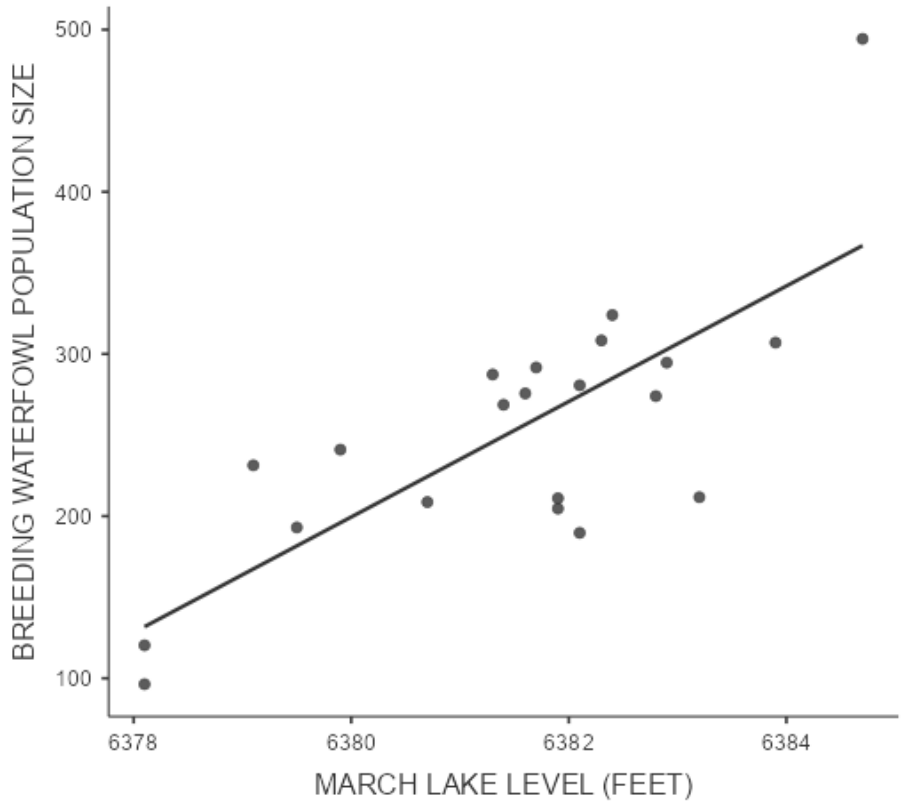

Figure 10. Annual breeding population size vs. lake level in March

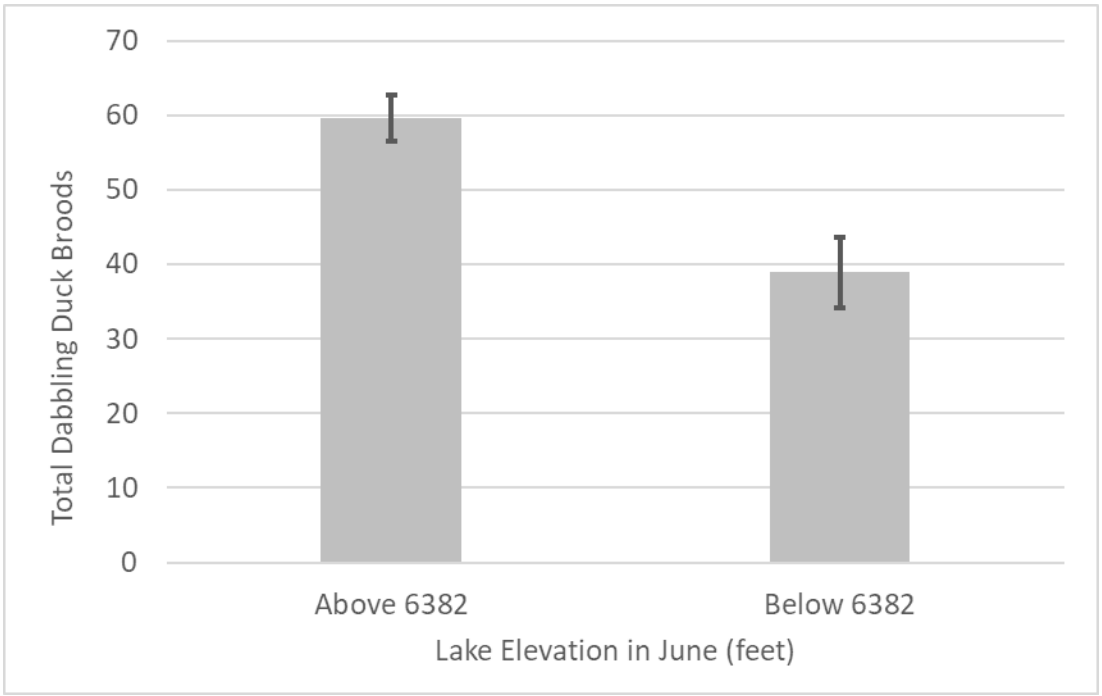

Figure 11. Total broods vs. lake level in June

Restoration Ponds

Summer Surveys

Four ponds were flooded all summer in 2023 (DEPO1, DEPO2, DEPO3 and DEPO4). COPOW had a very small amount of water in June due to an elevated water table from the heavy runoff year but appeared dry by July. COPOE and DEPO5 were dry all summer. The habitat in DEPO1 was good on survey 1 in early June as the pond was very flooded and there was much open water and flooded meadow. By the third week of June, the pond had retracted significantly, and was small and algae filled. By July, there had been noticeable expansion of emergent vegetation, little open water, and heavy algal growth. The other three DEPO ponds with water were very full when surveyed in early June as well, but no significant changes in condition were observed through the summer, with the exception of the development of surface algae on DEPO3.

The breeding waterfowl population at the Restoration Ponds is estimated at 18 or approximately 9 pairs. Six species were seen over the three summer surveys (Table 3.12). Most of the ducks were seen in DEPO4. Fewer than 10 individuals were seen at the other ponds with water. At DEPO1, waterfowl were seen only on survey 1. Most of the waterfowl at COPOW were seen on survey 1, when the most water was present at the bottom of the basin.

Eight waterfowl broods were observed at the Restoration Ponds including one at DEPO3 and seven at DEPO4 (Table 3.13). Gadwall and Ruddy Duck were the only species that bred at the Restoration Ponds in 2023, and as was the case for the shoreline areas, Gadwall broods were most abundant. The number of waterfowl and broods at the Restoration Ponds in 2023 did not differ from the long-term 2002-2022 mean (Figure 12).

Table 3.12. Total summer waterfowl by pond and species, 2023

Species	DEPO1	DEPO2	DEPO3	DEPO4	DEPO5	COPOW	COPOE	Species Total
Cinnamon Teal	1							1
Gadwall			2	19		3		24
Green-winged Teal					D	3	D	3
Mallard	4				r	3	r	7
Northern Pintail				2	y		y	2
Ruddy Duck		4	7	7				18
Pond Totals	5	4	9	28				55

Table 3.13. Waterfowl broods at the restoration ponds, 2023

Species	DEPO3	DEPO4	Species Total
Gadwall	1	5	6
Ruddy Duck		2	2
Total Broods	1	7	8

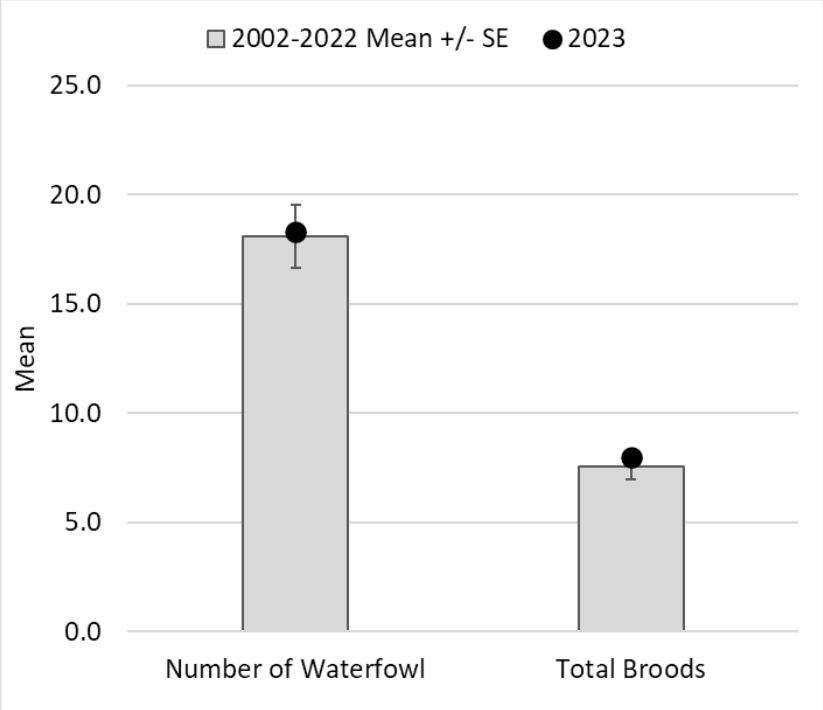

Figure 12. Mean number of breeding waterfowl and total broods —restoration ponds, 2023

Fall Waterfowl Surveys

Mono Lake

Fall Waterfowl Population Size and Species Composition

A total of 11 identifiable waterfowl species and 23,782 individuals were detected during the six 2023 Mono Lake fall surveys (Table 3.14). The total number of waterfowl observed in 2023 did not differ from the long-term mean of 25,462 +/-2523 SE. Northern Shoveler and Ruddy Duck were the most abundant species, and each accounted for approximately 45% of all waterfowl in 2023. The next three most common species of Mallard, Green-winged Teal and Gadwall totaled around 7% of all fall waterfowl. Northern Shoveler totals were slightly below, and Ruddy Duck totals were slightly above their respective long-term means (Figure 13). Notable findings in 2023 among other regularly occurring species were significantly higher numbers of Gadwall and very low numbers of Northern Pintail (*Anas acuta*) (Figure 14).

Northern Shoveler have typically shown a seasonal peak in numbers on the early- or mid-September survey, followed by a steep decline through the remainder of the season (House and Honda 2018). In 2023, Northern Shoveler numbers followed this this general pattern and totals were highest in early September (Table 3.14). Shovelers numbers remained steady through the remainder of September, and then exhibited a gradual decline through mid-November. Northern Shoveler numbers were below average through mid-September, and above average on the end of October and mid-November counts. In contrast to shovelers, Ruddy Duck numbers generally increase though early fall, peak at the end of September, then gradually decline. In 2023, Ruddy Duck numbers were below average through the end of September, but above average mid-October through mid-November.

Table 3.14. Species totals, 2023 Mono Lake fall waterfowl surveys

Species	Early Sept	Mid-Sept	End Sept	Mid-Oct	End Oct	Mid-Nov	Species Totals
Snow Goose						9	9
Canada Goose	2		67	13	27	59	168
Blue-winged/Cinnamon Teal				1			1
Cinnamon Teal		33	3				36
Northern Shoveler	3099	2364	2335	1345	993	633	10769
Gadwall	260	73	76	38			447
Mallard	27	20	88	192	97	206	630
Northern Pintail	2	2	10	86	2	6	108
Green-winged Teal	1	20	72	111	165	124	493
Unidentified Dabbling Duck	37	41	218	23	10		329
Redhead	1		1				2
Ring-necked Duck						6	6
Ruddy Duck	64	337	1828	2829	2646	3080	10784
Totals	3493	2890	4698	4638	3940	4123	23782

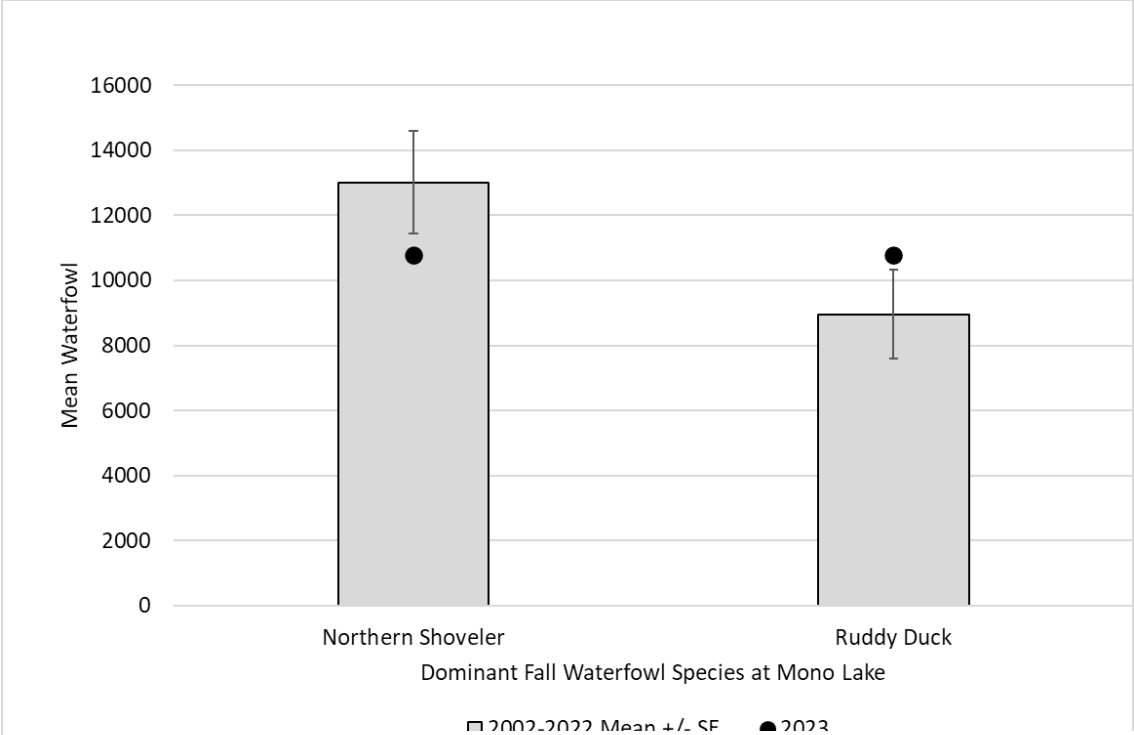

Figure 13. Northern Shoveler and Ruddy Duck 2023 totals vs. the long-term means

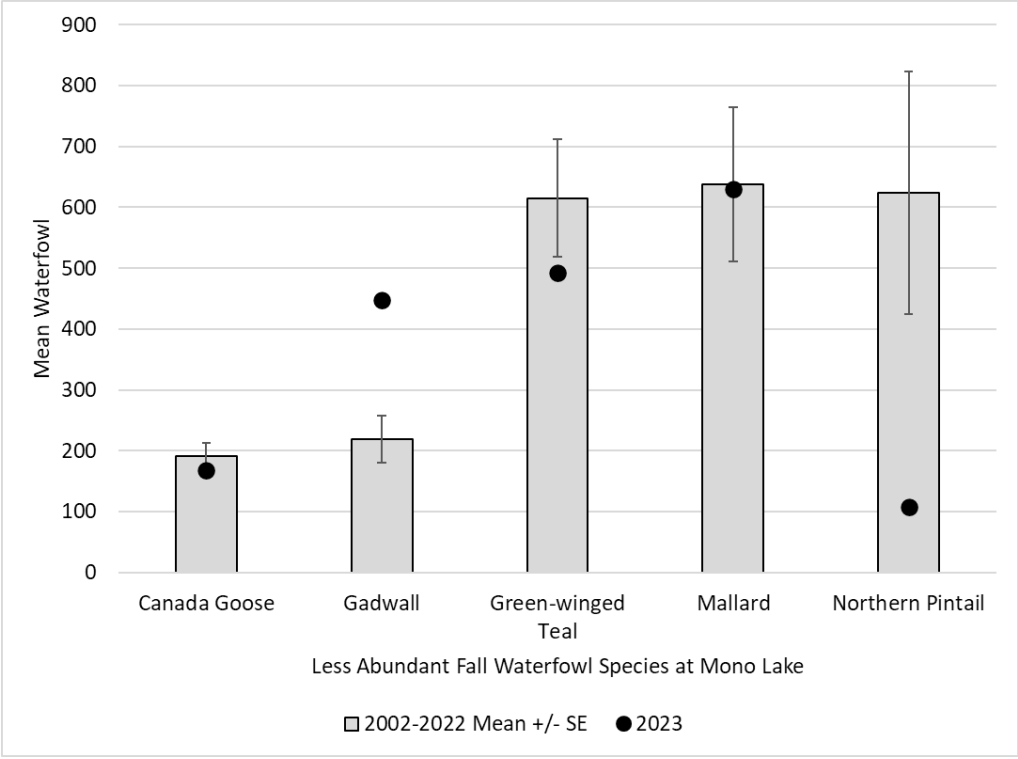

Figure 14. Other species— 2023 totals vs. the long-term means

Total waterfowl numbers have typically demonstrated a clear seasonal pattern at Mono Lake as numbers have been highest in early fall (Survey 1 through 3, early September through the end of September) and lower in late fall (October to mid-November (Figure 15). This early season peak has been largely due to the abundance of Northern Shovelers, an early season migrant in the region. In 2023, the total waterfowl numbers differed from this general pattern. Totals were lowest in early and mid-September due to below average shoveler numbers. The peak overall waterfowl count occurred at the end of September as is typical but remained elevated and above average through mid-November (Figure 15) due to higher than average numbers of Ruddy Duck and Northern Shoveler in this same time period.

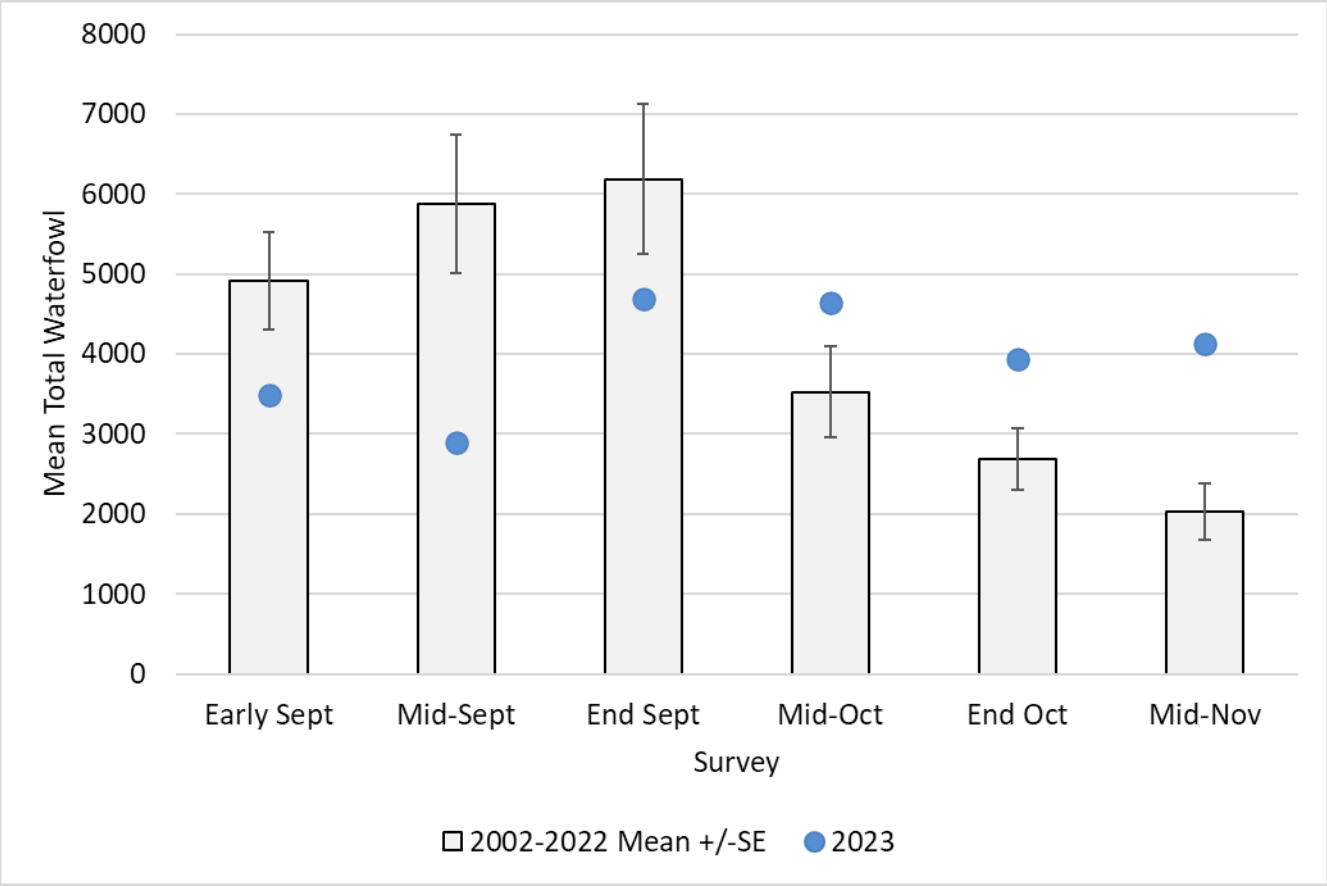

Figure 15. 2023 Mono fall waterfowl survey totals and 2002-2022 means

Spatial Distribution

Since 2002, on average, approximately 78% of all fall waterfowl have been recorded on the shoreline surveys (onshore or <250 m from shore), and 23% in offshore areas along the cross-lake transect surveys. The single area of the lake that has supported

significantly more waterfowl than any other has been Wilson Creek, accounting for 28% of all waterfowl in fall.

In 2023, offshore use was comparable to the long-term mean. Wilson Creek is typically the main staging area in fall for Northern Shoveler, and frequently the only shoreline location where large numbers of this species are seen (typically several 1,000). Since Northern Shoveler are the dominant species at Mono Lake in fall, their frequent use of Wilson Creek results in this shoreline area supporting a large proportion of all waterfowl. Ruddy Duck, the other dominant species at Mono Lake occurs primarily off-shore, thus driving the trend of off-shore areas contributing to the other main area of use.

The fall distribution of waterfowl was unusual in 2023 because the total number and proportional abundance of waterfowl seen at Wilson Creek were record lows for the entire 2002 to 2023 time period (Figure 16). Waterfowl at Mill Creek and Samman's Spring were also well below average. In contrast, waterfowl use of the Black Point area, just east of Wilson Creek, was a record high in 2023, representing the most heavily used area of shoreline this year. The waterfowl at Black Point consisted of a large flock of Northern Shoveler concentrated at the east end of the shoreline area. Waterfowl numbers at Rush Creek, South Tufa and Ranch Cove were also above average.

In 2023, Ruddy Ducks were most numerous in the DeChambeau Embayment area, covered by cross-lake transects 7A and 6A (Table 3.15).

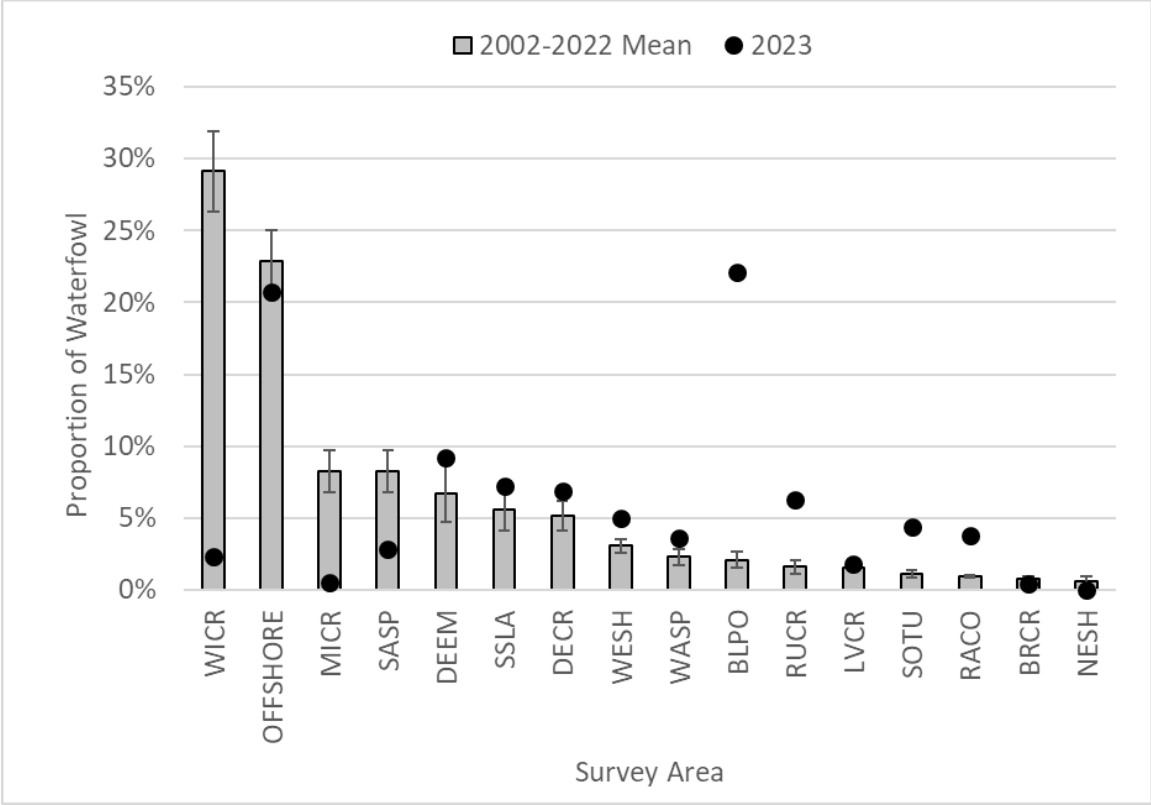

Figure 16. Fall spatial distribution of waterfowl at Mono Lake

Table 3.15. Distribution of Ruddy Ducks on cross-lake transects, 2023

Cross-lake subsection	Early Sept	Mid-Sept	End Sept	Mid-Oct	End Oct	Mid-Nov	Total
4B				17	10	17	**44**
5A		2	7	105	169	90	**373**
5B				43	40	25	**108**
6A		34	197	196	70	356	**853**
7A	13	59	366	1173	458	809	**2878**
7B		4	45	6	12	3	**70**
7C			9	57	29	33	**128**
8A		9	148	34	38	16	**245**
8B		4	102	48	25	13	**192**
Total Offshore	**13**	**112**	**874**	**1679**	**851**	**1362**	**4891**

Long-term Trend in Mono Lake Fall Waterfowl Population

The total number of waterfowl observed at Mono Lake in fall has varied from a low of 8,755 in 2018 to a high of 51,494 in 2004. Total fall waterfowl counts have been trending downward, but the 2002 to 2023 trend is not statistically significant (r^2= 0.1662, p=0.060, Figure 17). Unlike the breeding waterfowl population at Mono Lake, lake level has had no direct effect on the size of the fall migratory waterfowl population within the

range of lake levels observed since 2002 (r^2=0.0105, p=0.650); however, waterfowl numbers in years when the lake is monomictic have been higher on average than when the lake is meromictic (F=5.03, df=18.3, p=0.37, Figure 18).

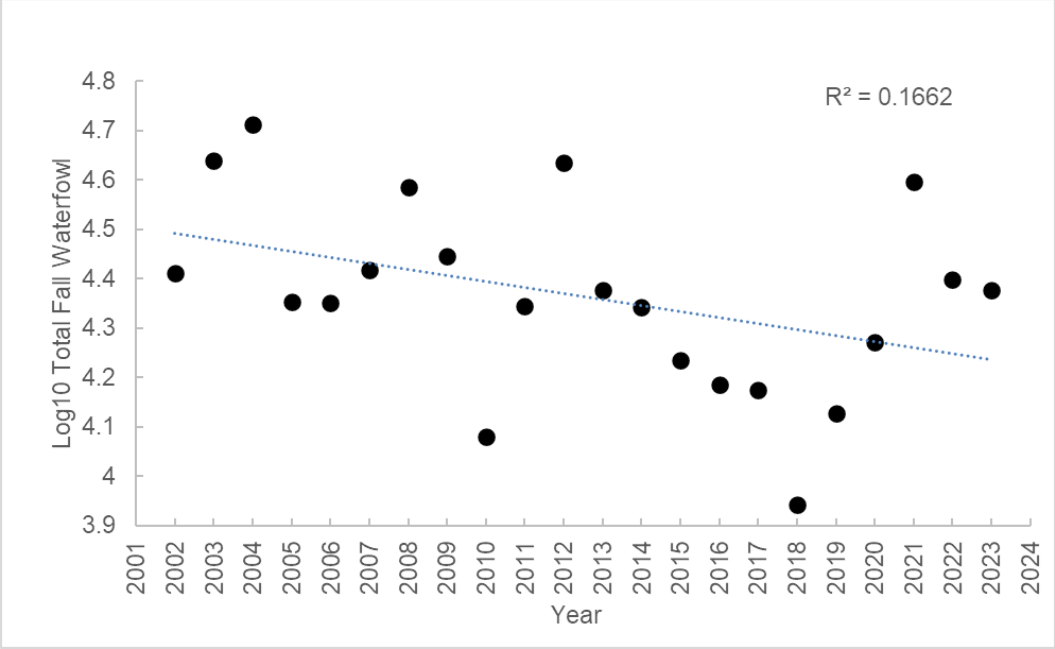

Figure 17. Trend in total fall waterfowl numbers at Mono Lake, 2002-2023

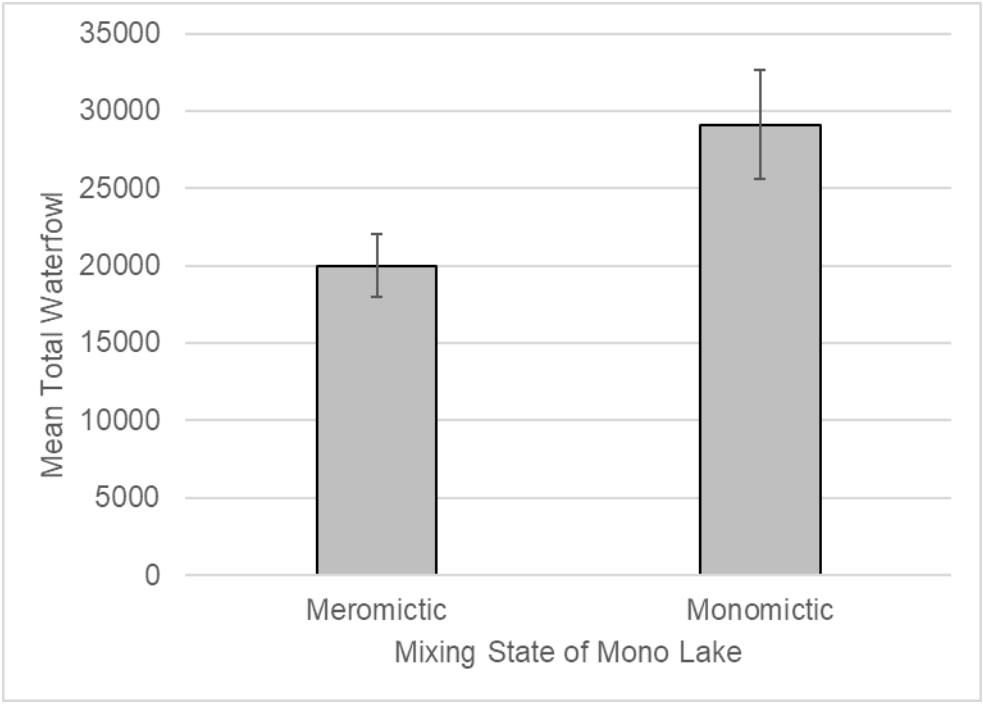

Figure 18. Mean total fall waterfowl under meromictic vs. monomictic conditions

Restoration Ponds

Pond conditions were the same in fall as in the summer in that DEPO5, COPOW, and COPOE remained dry, and DEPO1 algae covered. Late in fall, water delivery was restored to COPOW and COPOE but during the fall survey period, there was little standing water and no open water was visible. A total of 30 waterfowl of six species were seen over the six fall surveys (Table 3.16). As was the case in the summer, DEPO4 attracted the most waterfowl. The 2023 total of 30 waterfowl over the six surveys was significantly below the 2002-2022 mean of 179 +/-26.3.

The total number of waterfowl seen at the restoration ponds in fall has shown a significant downward trend (r^2=0.667, p<0.001, Figure 19). Apart from low counts in 2004, waterfowl totals at the ponds remained high from 2002 to 2008. Since 2016, totals have been consistently low.

Table 3.16. Fall waterfowl totals by pond, 2023

Species	DEPO1	DEPO2	DEPO3	DEPO4	DEPO5	COPOW	COPOE	Species Total
Tundra Swan		2						2
Gadwall			4	4				8
Mallard		2			D	D	D	2
Unidentified dabbling duck				2	r	r	r	2
Ring-necked Duck			1		y	y	y	1
Lesser Scaup				1				1
Ruddy Duck		1	6	7				14
Pond Totals	0	5	11	14	0	0	0	30

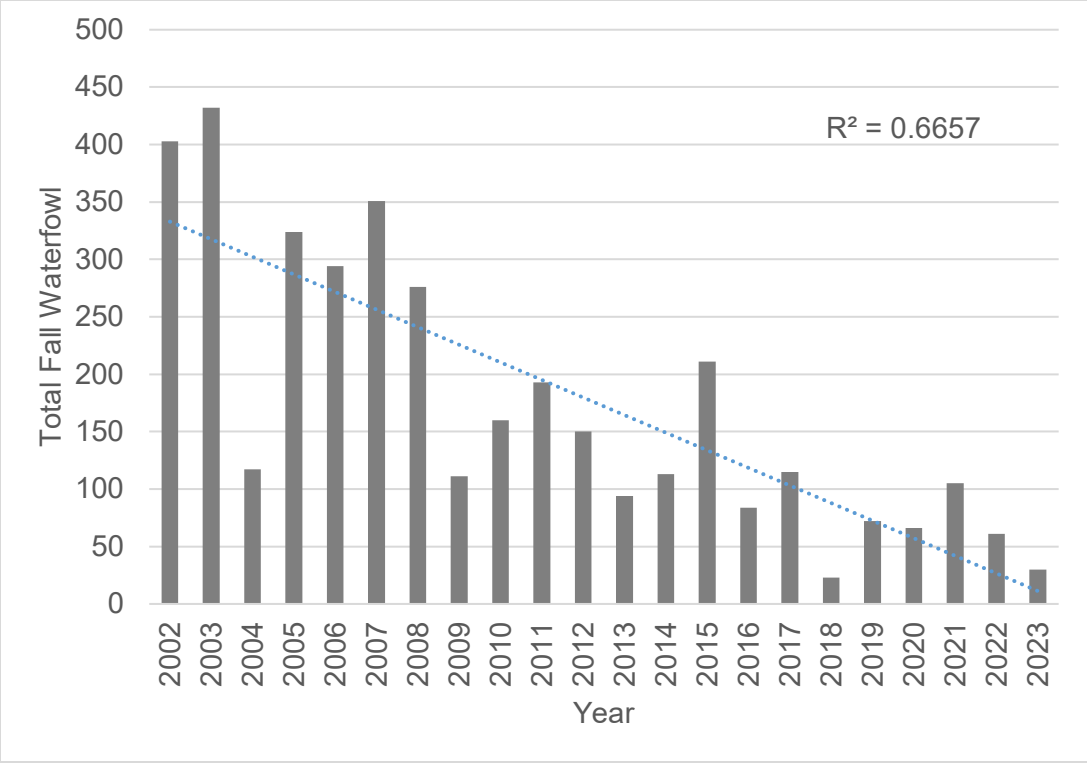

Figure 19. Fall waterfowl totals at the restoration ponds, 2002-2023

Bridgeport Reservoir

Fall Waterfowl Totals and Species Composition

A total of 16 waterfowl species were identified, and 15,448 individuals recorded at Bridgeport Reservoir over the six fall surveys in 2023 (Table 3.17). The total number of waterfowl observed in 2023 was significantly lower than the long-term mean of 30,188 +/-3609 SE. Geese and swans comprised approximately 5% of all waterfowl, and of this group, only Canada Goose was seen. Dabbling ducks totaled 85% of all waterfowl, and of the seven dabbling duck species identified, Northern Shoveler and Gadwall were most abundant. The eight species of divers as a whole comprised approximately 10% of all waterfowl.

Table 3.17. Species totals, 2023 Bridgeport Reservoir fall waterfowl surveys

Species	Early Sept	Mid-Sept	End Sept	Mid-Oct	End Oct	Mid-Nov	Species Totals
Canada Goose	128	32	111	288	200		759
Cinnamon Teal		1	2				3
Northern Shoveler	151	971	1,038	751	1,017	187	4,115
Gadwall	738	956	519	499	308	28	3,048
American Wigeon	5	6	20				31
Mallard	22	10	18	220	354	274	898
Northern Pintail	10	10	10	21	2	40	93
Green-winged Teal	26	420	35	209	135	415	1,240
Unidentified Dabbling Duck		990	118	2,102	155	320	3,685
Canvasback		3			8		11
Redhead		20		30		2	52
Ring-necked Duck			2			19	21
Lesser Scaup					15	3	18
Bufflehead			13		16	10	39
Common Merganser	93	114	16	10		6	239
Red-breasted Merganser	1						1
Ruddy Duck	18		82		425	670	1,195
Totals	1,192	3,533	1,984	4,130	2,635	1,974	15,448

Spatial distribution

Of the three subareas at Bridgeport Reservoir, waterfowl numbers were highest in the West Bay throughout the season (Table 3.18). Waterfowl were found throughout the West Bay, particularly among the deltas and inlets of Buckeye Creek and Robinson Creek. Geese were most often found out on the irrigated pastures and meadows south of the reservoir, away from the water's edge. Waterfowl use in the East Shore subarea occurred primarily in the southern half of this segment area, in proximity to inflow from the East Walker River, where shallow water feeding areas and mudflats occur. In the North Arm, waterfowl were few in number and scattered along the immediate shoreline area.

Table 3.18. Bridgeport Reservoir, spatial distribution by survey, 2023

Survey	EASH	NOAR	WEBA
Early September	249	36	907
Mid-September	903	113	2,517
End of September	381	66	1,537
Mid-October	1,423	7	2,700
End of October	430	52	2,153
Mid-November	787	92	1,095
Total waterfowl by shoreline segment	**4,173**	**366**	**10,909**

Long-term Trend in Bridgeport Reservoir Fall Waterfowl Population

The total number of waterfowl observed at Bridgeport Reservoir in fall has varied from a low of 13,119 in 2014 to a high of 83,186 in 2005. Total fall waterfowl counts have shown a significant downward trend from 2003 to 2023 trend (r^2= 0.339, p=0.006, Figure 20).

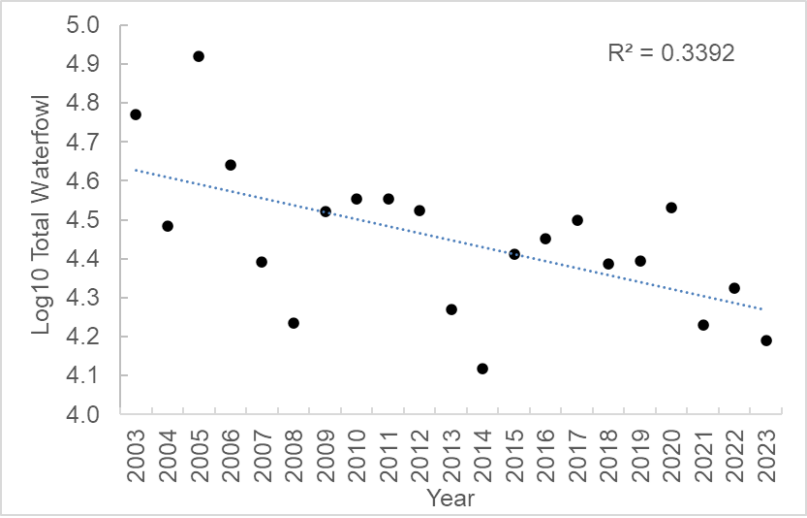

Figure 20. Trend in total fall waterfowl at Bridgeport Reservoir, 2003-2023

Crowley Reservoir

Fall Waterfowl Totals and Species Composition

At Crowley Reservoir a total of 18 waterfowl species were identified, and 32,175 individuals were recorded over the six fall surveys in 2023 (Table 3.19). The total number of waterfowl observed at Crowley Reservoir in 2023 was significantly lower than the long-term mean of 50,204 +/-5008 SE. Geese and swans comprised only 1.3% of all waterfowl and only Canada Goose was present on all surveys. Dabbling ducks totaled 61% of all waterfowl, and of the eight dabbling duck species identified, Northern Shoveler, Gadwall and Mallard were most abundant. Seven species of diving ducks were observed, and divers as a whole comprised approximately 38% of all waterfowl. Ruddy Duck was overwhelmingly the most abundant of the divers.

Table 3.19. Species totals, 2023 Crowley Reservoir fall waterfowl surveys

Species	Early Sept	Mid-Sept	End Sept	Mid-Oct	End Oct	Mid-Nov	Species Totals
Snow Goose					1		1
Canada Goose	132	105	57	63	15	30	402
Tundra Swan					1	6	7
Blue-winged Teal			25				25
Blue-winged/Cinnamon Teal			11	3			14
Cinnamon Teal	169	435	7				611
Northern Shoveler	859	1,749	1,957	50	1,025	46	5,686
Gadwall	792	2,441	364	36	80	171	3,884
American Wigeon	12	2	70		20	6	110
Mallard	135	247	78	204	590	1,841	3,095
Northern Pintail	15	26	139	55	70	94	399
Green-winged Teal	3	65	302	130	321	382	1,203
Unidentified Dabbling Duck	60	1,346	85	1,477	276	1,310	4,554
Canvasback					4	6	10
Redhead	5		163	29	3	24	224
Ring-necked Duck	32	4	296	60	178	86	656
Lesser Scaup			66	20	60	150	296
Bufflehead	9	1	22	14	409	280	735
Common Merganser					6		6
Ruddy Duck	190	186	2,914	1,171	2,734	2,722	9,917
Unidentified Diving Duck			90		110	140	340
Totals	2,413	6,607	6,646	3,312	5,903	7,294	32,175

Spatial Distribution

During the 2023 surveys, the largest waterfowl concentrations at Crowley Reservoir were in the McGee Bay area, where almost 55% of all waterfowl were tallied. The delta of the Owens River (Table 3.20), was the second most used area of Crowley Reservoir, supporting 32% of all waterfowl. Waterfowl in McGee Bay used the entire shoreline area, although higher densities were observed in the area of the shoreline where open cattail marsh existed due to flooding of the shoreline marsh system from the extremely high water level of the reservoir. The other area of waterfowl concentration was the Upper Owens River delta where flows from the Owens River enter the reservoir. Due to the very high reservoir levels, mudflats for loafing were absent and waterfowl were more dispersed than is typical. Many flocks were found among flooded shrubs in the small, flooded bays that formed in 2023 in the Upper Owens River delta and Layton Springs shoreline areas due to high reservoir levels. During early season surveys, waterfowl generally avoid the Chalk Cliffs area as there are limited feeding opportunities due the deep water and lack of freshwater inflow. However, waterfowl continued to show a pattern of late-season use of the Chalk Cliffs area when increased numbers of dabbling ducks are seen offshore or loafing along the narrow, dry beach. Yearly, this late season increase in use of the Chalk Cliffs area has coincided with the opening of waterfowl hunting season, and waterfowl may be seeking refuge in this area, which is difficult for hunters to access. Hilton Bay has good waterfowl habitat with adjacent meadows, some freshwater inflow, and shallow waters, but supports fewer numbers of waterfowl than areas of comparable quality, likely because of its smaller size. Waterfowl use of the Layton Spring subarea is usually concentrated near the spring inflow. Birds may also be scattered in smaller numbers along the mudflats or nearshore throughout the remainder of the subarea, which is primarily sandy beach. North Landing is another shoreline area with no direct freshwater inflow, and limited shallow water areas near shore and typically supports lower waterfowl use. The Sandy Point subarea is also an area of limited use by waterfowl due to a lack of freshwater input and limited shallow feeding areas.

Table 3.20. Crowley Reservoir, spatial distribution by survey, 2023

Survey	CHCL	HIBA	LASP	MCBA	NOLA	SAPO	UPOW
Early September	3	101	44	1,344	19	84	818
Mid-September		153	139	4,516	359	153	1,287
End of September	5	168	485	3,686	282	52	1,968
Mid-October	8	92	140	1,566	15	14	1,477
End of October	292	308	156	3,186	71	128	1,762
Mid-November	401	207	190	3,485	256	140	2,615
Total waterfowl by shoreline segment	**709**	**1,029**	**1,154**	**17,783**	**1,002**	**571**	**9,927**

CHCL=Chalk Cliffs HIBA=Hilton Bay LASP= Layton Springs MCBA= McGee Bay
NOLA=North Landing SAPO=Sandy Point UPOW=Upper Owens Delta

Long-term Trend in Crowley Reservoir Fall Waterfowl Population

The total number of waterfowl observed at Crowley Reservoir in fall has varied from a low of 17,955 in 2007 to a high of 119,280 in 2022. Waterfowl totals at Crowley Reservoir may be trending upwards over the 2003 to 2023 period, but this trend is not statistically significant (r^2= 0.054, p=0.309,Figure 21).

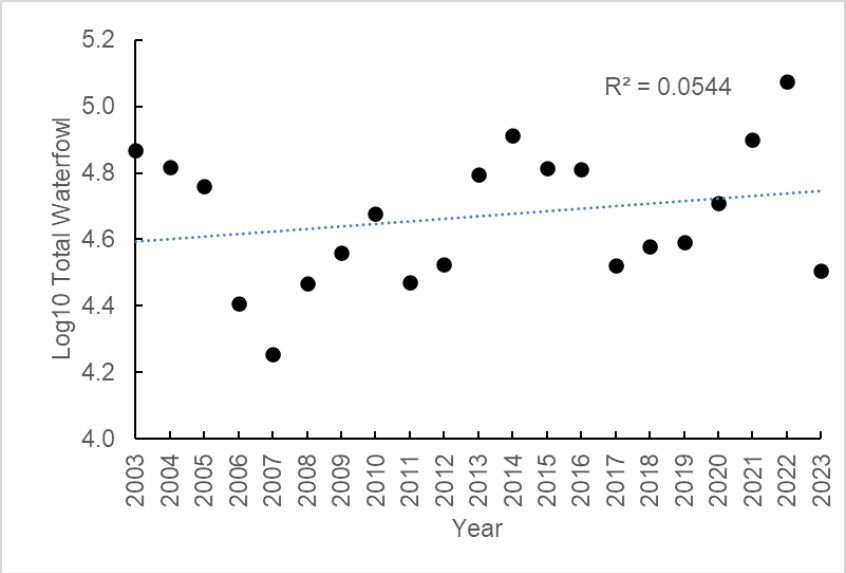

Figure 21. Trend in total fall waterfowl at Crowley Reservoir, 2003-2023

Comparison of Fall Waterfowl Among Survey Areas

The long-term mean waterfowl totals have differed among sites (Figure 22). Despite its much larger size, on average, Mono Lake supports fewer total waterfowl than either Bridgeport or Crowley Reservoirs. Crowley Reservoir has accounted for 47% of all waterfowl and waterfowl numbers have been significantly higher at Crowley Reservoir than the other two sites. Bridgeport Reservoir has supported 29% of all waterfowl, and waterfowl totals have also been significantly higher than Mono Lake. Waterfowl totals at Mono Lake have accounted for 24% of all survey areas. In 2023, waterfowl totals at Mono Lake did not differ from the long-term mean. Waterfowl totals at Bridgeport and Crowley Reservoirs however were well below the long-term means.

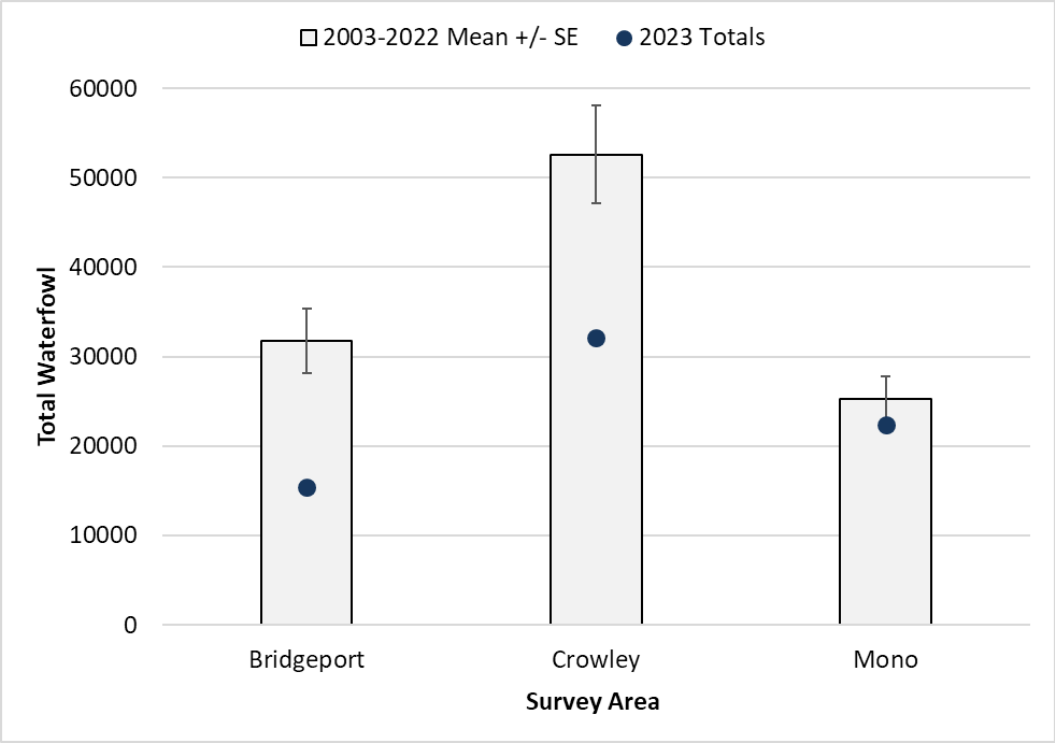

Figure 22. Comparison of mean fall waterfowl at each surveys area, with 2023 totals shown

The species composition of the waterfowl community at Mono Lake also differs notably from the other two survey areas in that it is dominated primarily by two species typically associated with saline lakes – Northern Shoveler and Ruddy Duck. In contrast, the waterfowl communities of Bridgeport and Crowley Reservoirs are more diverse, and have numerous codominant species as is typical of freshwater systems.

Although Bridgeport and Crowley support larger and more diverse waterfowl populations, Mono Lake has supported a significant proportion of the Northern Shoveler and Ruddy Duck fall migratory populations. Mono Lake has on average attracted the largest proportion of Northern Shoveler of the three waterbodies (42%) (Figure 23), and in 2023, supported a significantly higher proportion of shovelers than average (52%). Ruddy Duck totals at Mono Lake have accounted for approximately 44% of the total for all three survey areas, roughly equal to that observed at Crowley Reservoir (Figure 24). The proportional abundance of Ruddy Ducks at the three waterbodies did not differ from the long-term mean at Crowley and Mono but was slightly reduced at Bridgeport Reservoir in 2023.

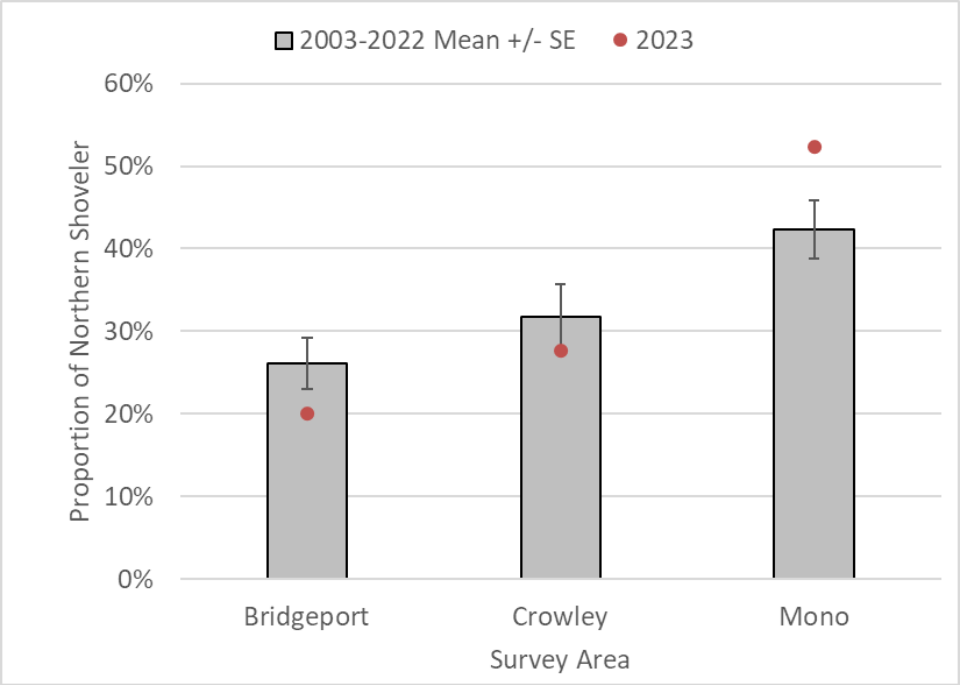

Figure 23. Proportional abundance of Northern Shovelers by survey area

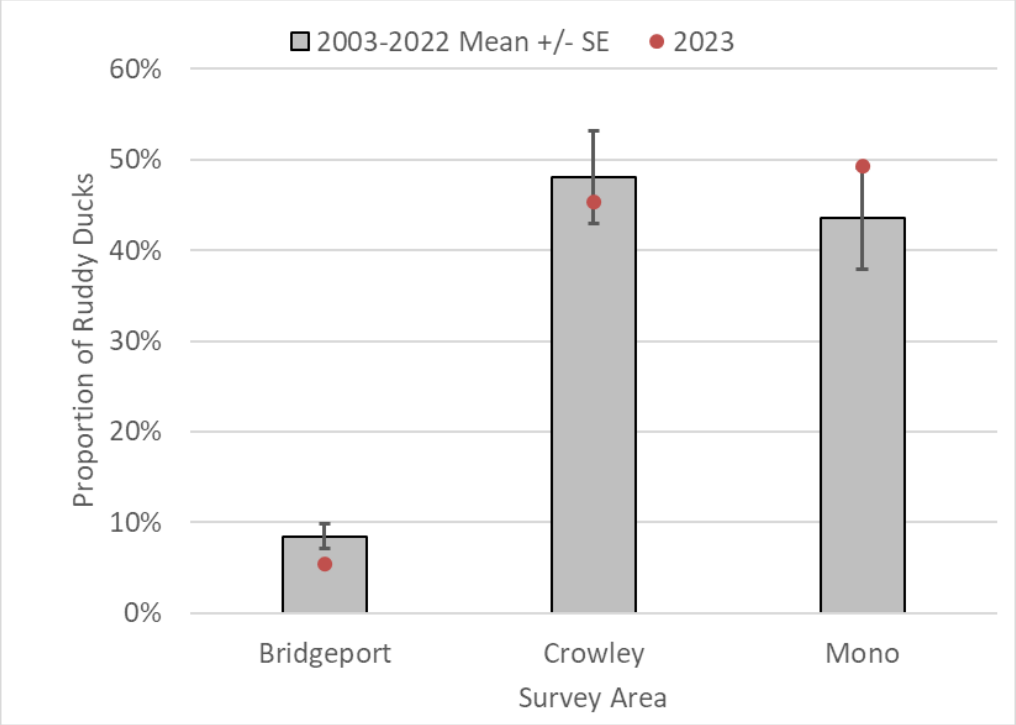

Figure 24. Proportional abundance of Ruddy Ducks by survey area

Aerial Photography of Waterfowl Habitats

Please refer to Figure 5 for the location of each of the following shoreline subareas at Mono Lake.

Mono Lake Shoreline Subareas

Black Point (BLPO)

The Black Point (BLPO) shoreline area lies at the base of a volcanic hill on the northwest shore of Mono Lake. The shoreline in this area is composed of loose volcanic soils. At lower lake elevations, barren shoreline and alkali meadow predominate. In the western portion of BLPO, dry alkali meadow exists as a linear strip paralleling the shoreline. In the eastern portion of the shoreline area are unmapped springs and seepage that support small shallow brackish bays and wet alkali meadow at higher lake levels. Based on a review of annual photos, brackish ponds become more numerous in the BLPO area at lake elevations above 6,382 feet, but relatively absent at lake elevations below this level. In 2023, at a lake level of 6383.2 feet, numerous small ponds were present along the Black Point shoreline area (Figure 25, Figure 26). The main Northern Shoveler flock at Mono Lake in fall of 2023 was found in the eastern portion of Black Point, remaining through the end of September.

Figure 25. Black Point shoreline area, western half
Small shoreline ponds developed in response to the lake level rise.

Figure 26. Black Point shoreline area, eastern half
The brackish ponds and small bays present in 2023 attracted the main Northern Shoveler flock in fall.

Bridgeport Creek (BRCR)

This shoreline area is at the terminus of the Bridgeport Creek drainage, however there is typically no surface flow of water in the creek near the lakeshore. In 2023 however, Bridgeport Creek was flowing down to the shoreline at least through early June due to the extremely wet winter of 2022 to 2023. There are several springs in this area, most of which are slightly brackish and support small brackish ponds. The other wetland resources in the Bridgeport Creek shoreline area include alkaline wet meadow and small amounts of wet meadow and marsh. Waterbird use is often most concentrated at the western end of this area, where spring flow has consistently reached the shoreline at all elevations observed. At higher lake elevations, brackish ponds develop along much of the length of this shoreline area. With decreasing lake elevations, barren lakebed increases substantially without a subsequent expansion of vegetation, and brackish ponds disappear.

In 2023, the eastern portion supported primarily meadow vegetation and barren playa, and standing water was present in the Bridgeport Creek channel near shore (Figure 27). Good waterfowl habitat existed in the western portion of this shoreline area in fall of 2023. In the “Seeping Springs” area, there was spring discharge to the lake, and small onshore brackish ponds present (Figure 28) attracting shorebirds and small numbers of waterfowl.

Figure 27. Bridgeport Creek shoreline area, eastern portion
Water was present in the Bridgeport Creek drainage near shore in fall.

Figure 28. Bridgeport Creek shoreline area, western portion
The "Seeping Springs" area supported marsh, brackish ponds and spring flow reaching the lake in 2023.

DeChambeau Creek (DECR)

The DeChambeau Creek shoreline area is along the northwest shore of Mono Lake (see Figure 5). Flow in DeChambeau Creek proper is intermittent and does not consistently reach the lakeshore. The DECR shoreline area has abundant year-round freshwater resources however, due to the presence of numerous springs that discharge directly to the lake.

The freshwater springs at DeChambeau Creek support lush wet meadow and riparian scrub habitats. During periods of declining lake level, freshwater mudflats develop due to the extensive spring flow. Wet meadow vegetation will encroach onto exposed mudflats in this area of the shoreline due to the abundance of freshwater spring flow. Increases in barren playa with declining lake elevation have been much less apparent in the DECR area as compared to other shoreline subareas due to the slope of the shoreline and the expansion of vegetation onto the mudflats that occurs. However, downcutting of the spring channels and subsequent drying of the shore has occurred at the lowest lake levels observed. During periods of subsequent increasing lake elevations, this wet meadow vegetation, mudflats, and playa has become inundated, leaving little exposed shoreline.

Due to the extreme runoff year, DeChambeau Creek flowed to the shore of Mono Lake throughout summer and fall. The rise in lake level throughout the spring and summer of 2023 resulted in inundation of shoreline vegetation and very little exposed mudflats (Figure 29, Figure 30). Spring flow continued to reach the lake shore in numerous places. A small beaver dam near shore, first noted in this area in 2014, was still active. (Figure 30). During summer ground surveys, extremely high concentrations of *Artemia monica* were seen in the spring channels.

Figure 29. The DeChambeau Creek area, looking west

Figure 30. DeChambeau Creek area beaver pond
There is a small beaver pond in the center of the image.

DeChambeau Embayment (DEEM)

The DeChambeau Embayment area lies just east of the DeChambeau Ranch, and the DeChambeau and County restoration ponds (see Figure 5). Historically, Wilson Creek discharged to the lake in the DeChambeau Embayment area, although there was extensive upstream diversion for irrigation of the DeChambeau Ranch. Past diversions altered the discharge point of Wilson Creek to almost 5 miles west along the shoreline, on the west side of Black Point and at the current "Wilson Creek" shoreline area.

The wetland resources in DeChambeau Embayment include alkaline wet meadow, small amounts of marsh, and several small brackish ponds. There are fresh, slightly brackish and moderately brackish springs in this area, the largest of which — Perseverance Spring (Figure 31) — is slightly brackish. Perseverance Spring has discharged directly to the lake at all elevations observed.

The bathymetry of the shoreline and offshore area is more complex than other subareas. Very shallow sloping topography exists nearshore in the southern portion of the subarea, with a deeper bay just offshore. Pumice blocks litter the entire subarea and are most often visible in the southern portion of this area due to the topography and shallow nearshore waters. At the higher lake elevations observed, the pumice blocks become partially to completely submerged and the shallow nearshore areas expand. As the lake level drops, this shoreline area experiences rapid increases in the acreage of barren lakebed and a land bridge forms with Gaines Island. At more extreme low lake levels, such as those observed in 2016, the geographic extent of the pumice blocks in the eastern portion of the subarea are revealed (LADWP 2018). In 2023, the increased lake level submerged a large area of pumice blocks (Figure 31). The eastern portion of the shoreline in this subarea has a gradually sloping shoreline which extends offshore. In 2023, the eastern extent of this shoreline subarea supported numerous, small, brackish shoreline ponds (Figure 32). The DeChambeau Embayment area has typically supported most of the Ruddy Ducks in fall.

Figure 31. DeChambeau Embayment, Perseverance Spring outflow area
In 2023, the increased lake level resulted in the submergence of a large proportion of the pumice blocks in this shoreline area.

Figure 32. DeChambeau Embayment, eastern extent
Numerous small brackish ponds were present in 2023.

Lee Vining Creek (LVCR)

Lee Vining Creek is the second largest stream in the Mono Basin. Lee Vining Creek is a woody riparian system that supplies abundant freshwater to its delta year-round. The lower reaches of Lee Vining Creek and its delta support small patches of wet meadow vegetation along with riparian trees and shrubs. The creek remains confined to the main channel under low flow conditions but inundates the lower floodplain under high flow conditions. Discharge to the lake is "split" by a berm nearshore, and most of the creek flow discharges on the south side of this berm. The north part typically receives a low flow that supports freshwater ponds at some lake levels. At higher lake levels, the delta becomes flooded with lake water, inundating the willows and wet meadow close to shore, resulting in some dieback of willows and freshwater emergent vegetation due to salt water stress. During periods of descending lake elevations, freshwater ponds may form behind littoral bars. At the most recent extreme low lake elevation observed in 2016, extensive drying of the delta meadows occurred. Ria extends offshore beyond the mapping boundary of Lee Vining Creek subarea due to flows from Lee Vining Creek, however this waterfowl resource is not captured by landtype mapping (LADWP 2018).

Bathymetry of the area indicates limited shallow water areas near shore. Shallow sloping areas of water are limited to the delta and areas around the Lee Vining tufa grove to the south, but depths rapidly increase offshore in this area of the lake (LADWP 2018).

In 2023 creek flows were very high all summer due to the very high runoff conditions. On the north side, the high flows cut through the existing littoral bar creating multiple exit points to the lake. Small freshwater ponds were present in the lower reaches of the delta. The delta was very flooded, there were high flows in both the north and south sides of the delta, there was bare ground, and by fall, some dieoff of wetland vegetation was evident along the immediate shoreline (Figure 33). The Lee Vining tufa grove has numerous small bays, shallow areas along the immediate shoreline (Figure 34). Ruddy Ducks are common in fall in the tufa grove area.

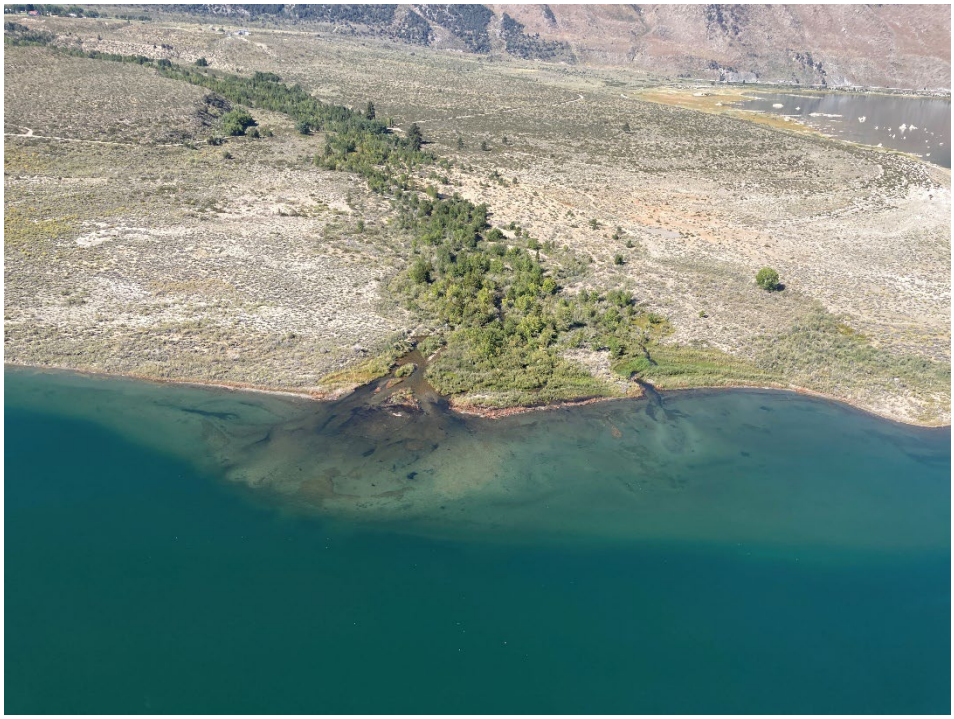

Figure 33. Lee Vining Creek delta

Figure 34. Lee Vining Creek delta, western portion (Lee Vining tufa groves)

Mill Creek (MICR)

Mill Creek is Mono Lake's third largest stream and originates in Lundy Canyon. The Lundy Powerhouse along Mill Creek is operated by Southern California Edison and historically diverted most of the flow off of Mill Creek and impacting the lower reaches of Mill Creek. LADWP does not export any water from the Mill Creek system but does hold some water rights.

Much of the Mill Creek riparian system is tree-dominated, but the delta has dense stands of shrub willow, small amounts of wet meadow, and a series of beaver ponds. Freshwater often enters the lake at several points in the delta due to seepage through the loose volcanic soils. Previous bathymetry studies have indicated the creek mouth constitutes the only shallow areas in the Mill Creek delta area, and water depths increase rapidly offshore.

The Mill Creek shoreline area was wild and wet in 2023 because of the extreme wet runoff year. During peak runoff, the high flows breached all of the beaver dams in the delta. By fall, the water levels dropped, the beavers had made some repairs, and the ponds had reformed (Figure 35).

During the peak runoff, debris washed down from upstream blocked the culvert along Mill Creek at Cemetery Road, redirecting most of the creek flow into a former channel to the west (Figure 36). In other recent high runoff years (i.e. 2017), some water has reached this former channel, but this is the first time since 2002 that I have seen it capture most of the flow. The high flow in this former channel resulted in significant downcutting due to a lack of riparian vegetation to stabilize the channel, and a large amount of sediment and some dislodged shrubs flowing into Mono Lake through the summer months (Figure 37) until repairs were made to the culvert and road.

Figure 35. Mill Creek delta, from the east

Figure 36. Mill Creek at Cemetery Road

During peak runoff, debris blocked a culvert, temporarily diverting most of the flow in the main channel to the historic channel in the foreground. Photo taken July 20, 2023.

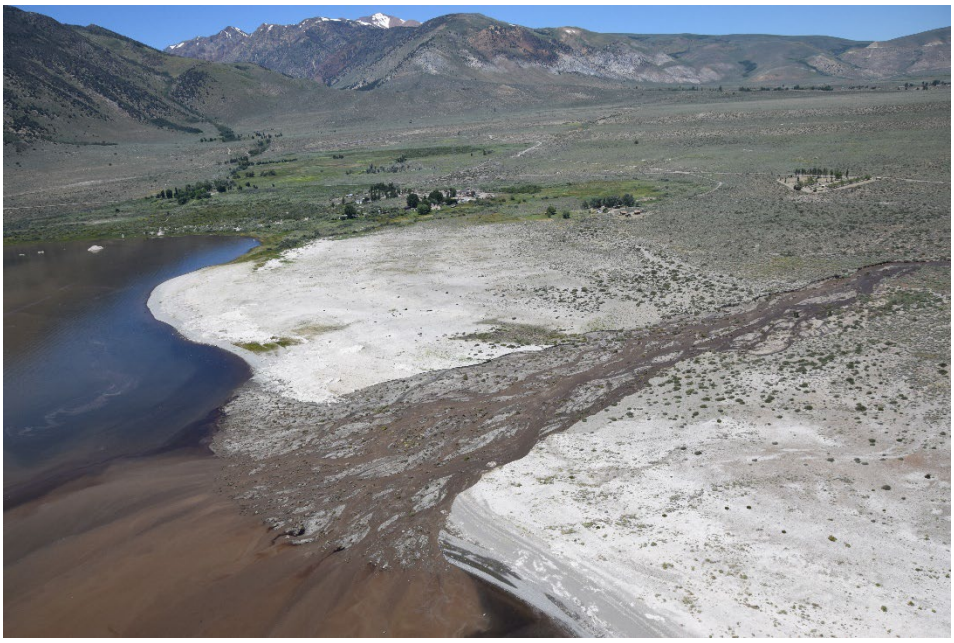

Figure 37. Mid-summer flow in a historic Mill Creek channel.

Large amounts of sediment were discharged to Mono Lake during the summer months as high flows caused downcutting and the uprooting of shrubs in this historic channel. Photo taken July 20, 2023.

Northeast Shore (NESH)

In the Northeast Shore area, extensive areas of barren playa predominate at most lake elevations as the saline groundwater in this part of the basin prevents the growth of vegetation. Barren playa comprises 99% of the Northeast Shore area, and only small amounts of alkali meadow are present.

Historically, large perennial brackish ponds were present along the northeast shore. These historic ponds persisted in depressional areas above the high-water mark and above the target lake level set for Mono Lake. Since 2002, temporary ponds have developed along the length of the shoreline segment, but downslope of the historic ponds. These ephemeral ponds are presumed to be brackish due to the saline nature of the groundwater in the eastern basin. Although there are no known mapped springs in this reach, some are evident (D. House, pers. obs.). Bathymetry studies indicates a very gradual sloped shoreline in this subarea. In 2023, the Northeast Shore area consisted primarily of dry playa, however narrow brackish ponds were present along a portion of the shoreline area (Figure 38).

Figure 38. Northeast Shore, Looking East
Narrow brackish ponds were present in some parts of this shoreline area in 2023.

Ranch Cove (RACO)

The Ranch Cove shoreline area is a relatively small area located between Rush Creek and Lee Vining Creek. The shoreline area is narrow and generally dry, supporting primarily coyote willow (*Salix exigua*), rabbitbrush, upland scrub, and barren playa. The bathymetry data shows a steeply sloped shoreline offshore. This shoreline area has not shown significant changes with lake elevation. Waterfowl resources are limited in this area, and there is no direct spring flow to the lake.

As is typical, in 2022 Ranch Cove showed a dry beach lacking onshore ponds or direct spring input (Figure 39).

Figure 39. Ranch Cove Shoreline Area, Looking West

Rush Creek (RUCR)

Rush Creek (RUCR) is the largest stream in the Mono Basin. There is a long history dating back to the 1860s of diversion of Rush Creek flows for irrigation, followed by out of basin water export by LADWP starting in 1941 and resulting in a dry channel in the lower reaches of the creek in some years. Notable large runoff events occurring in 1967, 1969, and the early 1980s, caused substantial incision and scouring due to an absence of riparian vegetation to protect the banks and stabilize the soils. Floodplain incision then drained the shallow groundwater table and left former side channels stranded above the newly incised mainstem channel (SWRCB 1994). Under Decision 1631, LADWP developed a stream restoration plan and has undertaken projects to rehabilitate Rush Creek (LADWP 1996b). Channel maintenance and flushing flows, referred to as “stream restoration flows” were established to mimic seasonal snowmelt runoff, with the magnitude based on the hydrological conditions for the year (SWRCB 1994).

The wetland resources available at Rush Creek are primarily meadow and woody riparian vegetation (*Salix* spp.) and the creek supplies abundant freshwater outflow to Mono Lake year-round. Immediately upstream of the delta, the floodplain is a broad meadow supporting scattered shrub willows. At higher lake levels or high creek flows, flooding has extended across the delta mouth. During periods of lake elevation recession, much channel braiding exists in the delta. From 2002 through 2014, side channels distributed water throughout the lower floodplain meadow, creating saturated conditions, freshwater channels, and a stable freshwater pond along the eastern edge. In 2014, headcutting occurred along the mainstem resulting in channel erosion, and side channel abandonment. By the following summer of 2015, pond and channels formerly used by breeding waterfowl in the delta area disappeared as the lower floodplain experienced significant drying.

Runoff into Rush Creek in 2023 was very high all summer and continued to be elevated above the average base flows into fall. The high flows deposited sediments in the delta, dislodged trees and shrubs in the channel, and flooded the delta creating a large freshwater pond (Figure 40). The freshwater ponds in the delta continued to receive inflow from the mainstem all summer and were present into fall as well.

Figure 40. Rush Creek Delta
In 2023, high flows in Rush Creek resulted in the development of a large freshwater pond in the delta.

Simons Spring (SASP)

The Simons Spring shoreline area is in along the southeastern portion of the lakeshore (see Figure 5). Located centrally in the subarea is the Simons Spring fault line, a conspicuous feature on the landscape. Several large springs arise from the fault, conducting groundwater to the surface (Rogers et al. 1992). The bathymetry map of this area indicates a gradual offshore slope in the western half of the subarea, a steep offshore slope where the tufa towers of the fault line reach shore, and an increasing shallow slope to the east (LADWP 2018). Due to the shoreline gradient in this area, small changes in lake elevation result in large changes in the degree of shoreline flooding or the extent of exposed mudflats or playa.

The combination of high spring flow, shallow shoreline gradient, and the action of longshore currents, makes the Simons Spring shoreline area particularly dynamic, particularly west of Simons Spring fault line. Fresh water ponds are a prominent feature of the Simons Spring area due to the abundant spring flow in the area, however their presence and condition tends to be ephemeral, especially west of Simons Spring fault. Over the years, longshore currents have resulted in the development of several parallel littoral bars west of the Simons Springs fault line. These littoral bars retain upgradient spring flow and support the creation of ponds, wet meadow, and marsh behind the sandbars. During periods of increasing lake level, lake water inundates areas supporting wetland vegetation upgradient of littoral bars. The vegetation dies back due to salt stress, opening up areas previously grown over with marsh or meadow. During subsequent decreases in lake level, open freshwater ponds develop, supported by inflow from up gradient springs. If the lake level stabilizes, then wetland vegetation will recolonize the open water ponds, decreasing the amount of open water. Many of the freshwater springs in this area reach the lakeshore through breaks in littoral bars, creating extensive mudflats on exposed playa at certain lake levels. Although there may be a physical connection between the mudflats and lake water, the very shallow ponds that form on shore are typically fresh due to the high spring flow and are colonized within 1 to 2 years by wetland vegetation.

Just east of the Simons Spring fault line, permanent to semi-permanent brackish water ponds are generally present year-round. The remainder of the subarea to the east lacks spring flow to the lake and supports alkali wet meadow up gradient and barren playa on shore.

Waterfowl habitat conditions continued to be good at Simons Springs in 2023, but variable throughout the year, changing rapidly particularly through summer due to the rising lake level. On summer survey 1 in early June, there was a large continuous fresh to brackish shoreline pond behind a sandbar that extended from the Simon’s Spring faultline west to the Goose Springs (Figure 41). By June 29, the lake level had risen

enough to overtop the sandbar, and the discrete pond was no longer present. The shoreline habitat at this time consisted of broad flooded flats covered in short-statured wetland vegetation, primarily Nevada sedge (*Scirpus nevadensis*). Due to the extensive spring flow in the Simon's Spring shoreline area, this created a shallow flooded wetland habitat with fresh and brackish water areas due to mixing with Mono Lake waters. The rise in lake level flooded alkali meadow vegetation and this flooded vegetation was covered with large numbers of adult alkali flies in July.

Figure 41. Large continuous pond at Simon's Springs in early June

During the fall survey period, shoreline ponds were present but discontinuous along the Simon's Spring shoreline area. West of the faultline, ponds were present only in the far western portion of the shoreline area, and there were no ponds or exposed shoreline east to the faultline (Figure 42). East of the faultline however, was an expansive brackish shoreline pond system present throughout the fall waterfowl survey period (Figure 43).

Impacts from feral horse grazing continued, particularly east of the Faultline, as shown in Figure 44 taken at Gurgling Mound spring.

Figure 42. Overview of the Simons Spring area, west of the faultline

Figure 43. Shoreline Ponds east of the faultline at Simons Springs

Figure 44. Feral horse grazing and trampling of Gurgling Mound Spring
This spring is east of the Simon's Spring Faultline.

South Shore Lagoons (SSLA)

The South Shore Lagoons is a broad stretch of shoreline with scattered waterfowl habitat features. Waterfowl habitat features include permanent freshwater ponds supported by springs, seasonal to semi-permanent ponds supported by groundwater, and ephemeral brackish ponds. Like Simons Spring, the shoreline configuration in the South Shore Lagoons subarea is influenced by longshore currents.

At the western border of the subarea, a semi-permanent pond exists along a southwest-northeast trending fault line. The presence of this semi-permanent pond has been a function of lake elevation. At the higher lake elevations observed (approximately 6,383 feet), the pond has been full. Below approximately 6282.5 feet, the pond experiences notable contraction in size and, at elevations below 6,381.9 feet, has been absent.

Sandflat Spring is an isolated freshwater spring supporting two small freshwater ponds- an upper pond, and a lower pond, both partly surrounded by coyote willow. These were open water ponds until 2014, when water speedwell (*Veronica anagallis-aquatica*) and cattails (*Typha* sp.) encroached and enclosed the open water.

At the east end of the subarea is the Goose Springs complex. Goose Springs is a large spring complex that forms a series of interconnected freshwater ponds surrounded by wet meadow and marsh. In some years, the development of a littoral bar downgradient has captured spring flow, creating large onshore ponds that can be either fresh or brackish.

Away from the immediate shoreline in this subarea, the terrain is sandy hummocks with numerous small, depressions supporting alkali meadow in most years. Groundwater levels in this area have been found to be responsive to lake elevation changes (Rodgers et al. 1992) due to the high topographic gradient and very permeable soils. In 2006 and 2007 when the lake elevation was at its highest observed (above 6,385 feet), these nearshore depressions filled with groundwater, creating a series of scattered freshwater ponds in the South Shore Lagoons subarea that were quite attractive to waterfowl.

Waterfowl habitat conditions in the South Shore Lagoons area were good in 2023. Large brackish ponds were present on shore along the length of this shoreline area in early June, but the upgradient depressions were not yet flooded. The semi-permanent pond at the west end of the shoreline area was dry in early June, flooded by mid-July, and by September (lake level 6383.2 feet), this pond was at least half full (Figure 45). Shoreline ponds continued to be well-developed through the fall waterfowl survey period, and waterfowl were seen regularly in these ponds (Figure 46). At Sand Flat

Spring, there was no direct connection between spring flow and the open water of Mono Lake, however small freshwater ponds formed behind a sandbar (Figure 47).

The Goose Springs area was excellent waterfowl habitat for many years, before showing signs of degrading as the ponds around the springs filled in with vegetation. Conditions were better in 2023 than 2022 as the freshwater ponds around the springs had more open water, and there were numerous shoreline ponds (Figure 48). The rise in lake level flooded alkali meadow vegetation and this flooded vegetation was covered with large numbers of adult alkali flies in July.

Figure 45. Semipermanent pond at western edge of South Shore Lagoons

Figure 46. Overview of the South Shore Lagoons area

Figure 47. Sand Flat Spring
In 2023, small fresh onshore ponds were present much of the year.

Figure 48. Goose Springs
In fall of 2023, shoreline ponds were most numerous around Goose Springs in the South Shore Lagoons shoreline area.

South Tufa (SOTU)

The South Tufa area is the primary visitor access point to the Mono Lake shoreline, notable for its large display of tufa towers. The western portion of the survey area, just east of the main tufa tower stand differs notably in terms of waterbird habitat from the eastern portion, just east of a small tufa prominence onshore between the South Tufa access point and Navy Beach. In the western portion, the shoreline is narrow, the offshore topography steep, and the brackish springs create wet mudflat conditions under most lake levels observed. East of the prominence, the shoreline is very gradually sloped onshore as well as offshore. The eastern portion supports an ephemeral brackish pond whose presence has varied as a function of lake elevation and season. At somewhat intermediate lake elevations, the shoreline pond in the eastern section has persisted from summer through fall. In periods of lower lake elevation, the brackish pond has been present in summer, but generally dried by fall.

In 2023, the rise in lake level resulted in inundation of alkali meadow vegetation in the western portion of this shoreline area leaving little exposed shoreline (Figure 49). In July the flooded meadow vegetation was covered with adult brine flies. In the eastern portion from Navy Beach to the tufa grove had a fairly dry beach, but small shoreline ponds were present into fall (Figure 50).

Figure 49. South Tufa, near Navy Beach

Figure 50. South Tufa, eastern extent

Warm Springs (WASP)

The Warm Springs area is located on the eastern shore of Mono Lake. The main feature of the Warm Springs area is a permanent brackish pond fed by the outflow of Pebble and Twin Warm Springs (referred to as “north pond”). These and other springs in the area support extensive wet alkali meadow and marsh vegetation, primarily around the pond and springheads. The springs in the Warm Springs area are slightly to moderately brackish.

The north pond has been present at all lake elevations observed. Some expansion and contraction have occurred, with the pond at its largest extent in 2006. This pond has been the most reliable place in the Warm Springs subarea to find waterfowl.

Due to the very gradual sloping shoreline in this area, small changes in lake elevation result in large differences in the amount of exposed playa on shore. Longshore action also shapes this shoreline area as evidenced by the prominent littoral bars creating the north pond and ponds downgradient. During periods of declining lake elevation, seepage of water from the north pond through the loose sandy soil results in the development of ephemeral brackish ponds downgradient of the north pond as was noted in 2010 (LADWP 2018).

When the lake level was rising in the summer of 2023, ephemeral onshore ponds were not present. By fall, however, as the lake level stabilized, an extensive shoreline pond system had developed along the length of the Warm Springs shoreline area (Figure 53). Waterfowl were observed in the brackish ponds immediately downgradient of spring flow (Figure 52), but few were seen elsewhere along the length of the Warm Springs area.

Feral horse activity at Mono Lake continues to be high in the Warm Springs area. Warm Springs was severely grazed again this year, and virtually all wetland vegetation along spring channels and ponds had been consumed. The meadows were grazed down to almost zero stubble, and bare patches of compacted soil were present in areas formerly supporting wetland vegetation (Figure 53). Marsh-dwelling bird species formerly common at Warm Springs such as Marsh Wren (*Cistothorus palustris*), Red-winged Blackbird (*Agelaius phoeniceus*) and Yellow-headed Blackbird (*Xanthocephalus xanthocephalus*) were absent or few in number due to the loss of emergent vegetation from excessive feral horse grazing.

Figure 51. Overview of Warm Springs
Large brackish ponds extended much of the length of the Warm Springs area in 2023.

Figure 52. Warm Springs, north Pond, looking north.
Large brackish ponds extended the length of the Warm Spring shoreline area.

Figure 53. Feral horse impacts along Pebble Spring channel, Warm Springs

Prior to feral horse use of the area, the Pebble Spring Channel was filled with sedges. Heavy grazing has denuded the spring channels and ponds in the Warm Springs Area.

West Shore (WESH)

Much of the West Shore subarea is located immediately east of Highway 395, along a steep fault scarp. Although some shallow gradient areas exist along the southern boundary, most of this shoreline area is steeply sloping lakeward. Several fractured rock gravity springs (LADWP 1987) and two small drainages, Log Cabin Creek and Andy Thom Creek provide freshwater resources along the length of this shoreline subarea, although ponds are lacking. A very narrow beach exists along much of the length and becomes inundated at higher lake elevations. Significant changes have not been noted in the configuration of this shoreline subarea with lake elevation changes. The area supports lush wetland resources, but waterfowl use is limited (Figure 54).

Figure 54. Overview of the West Shore, looking north/northwest

Wilson Creek (WICR)

Wilson Creek, along the northwest shore, is one of the best and most important waterfowl habitat areas at Mono Lake. Wilson Creek supports a large expanse of wet meadow, multiple freshwater springs, and mudflats. The Wilson Creek subarea has the second highest median spring flow of the monitored springs (LADWP 2018). Due to the shoreline configuration and presence of large tufa towers, this subarea also has two protected bays. Submerged pumice blocks are present throughout the shallows of the eastern portion of the subarea. The bathymetry indicates a very gentle sloping topography throughout the protected bays and all along the shoreline (LADWP 2018). Due to the sheltered nature of the bay, the spring flow, and shallow waters near shore, the hypopycnal layer may be extensive in this area. The spring flow and shallow waters also lend toward the formation of mudflats, which have been present at most lake elevations observed. At the lowest elevation observed (2016), the retreat of shoreline resulted in some loss of the protection of the bays, however, mudflats were still prominent due to the high spring flow. The extreme low lake elevation observed in 2016 allowed an opportunity to visualize the near shore topography and the significance of spring flow to Wilson Creek bay (LADWP 2018). The topography is very gently sloping throughout the entire bay, extending out beyond the mouth of the bay and east of Tufa Mound spring. The high spring flow in this area combined with the sheltered nature of the bay is conducive to creating hypopycnal conditions. Even at higher lake elevations, such as in 2012, hypopycnal conditions would likely occur across the bay except under windy conditions, due to the high spring flow and contribution from Wilson Creek to the west in 2012. The shallow, protected areas in the bay would make food more accessible to waterfowl. The high spring flow conditions combined with the sheltering of the bay and shallow waters support ideal feeding and loafing conditions for waterfowl at Mono Lake.

In 2023, the Wilson Creek area continued to support a freshwater pond along the west side of the bay (Figure 55). In early June, the extreme runoff conditions were depositing sediment into the ponds, and sheet flow conditions were occurring. The pond continued to receive input through late June and this pond was the focal point of waterfowl activity and broods. By the third summer survey in mid-July, this pond was no longer receiving direct input, appeared stagnant, and lacked waterfowl activity. As lake level increased through summer, the wetland vegetation in the bay became inundated. Large numbers of alkali flies were noted on the shoreline vegetation and on the surface of Mono Lake in mid-July.

Figure 55. Freshwater pond in Wilson Creek Bay
The freshwater pond on the west side of the bay attracted waterfowl when receiving inflow, but little use when inflow ceased by mid-July.

Figure 56. Wilson Creek, east of Tufa Mound spring
Tufa Mound spring is the circular tufa tower on the left side of the photo.

Bridgeport Reservoir Shoreline

Please refer to Figure 7 for the location of each shoreline subareas at Bridgeport Reservoir. All three shoreline segments at Bridgeport Reservoir: North Arm, West Bay, and East Shore are shown in Figure 57. The North Arm seen at the far end of the photo is in the narrowest part of the reservoir and includes primarily sandy beaches bordered by upland vegetation. The West Bay receives freshwater inflows from Buckeye and Robinson Creeks and the East Walker River, creating extensive mudflat areas adjacent to these creek inflow areas, especially when the water level in the reservoir is higher. The West Bay also receives seepage and runoff from the adjacent irrigated pastures. The East Shore includes some mudflat and meadow areas in the vicinity of the East Walker River, but most of the East Shore area is bordered by Great Basin scrub or exposed reservoir bottom.

Due to the extreme runoff conditions in 2023, the level of Bridgeport Reservoir was very high summer through fall. The high reservoir level inundated meadow vegetation in the West Bay and reduced the amount of mudflat area typically available. The West Bay supported abundant aquatic vegetation, flooded smartweed (*Polygonum*), and algae. Waterfowl breeding activity was very high at Bridgeport Reservoir in 2023 (D. House, pers. obs.), however fall numbers were below average.

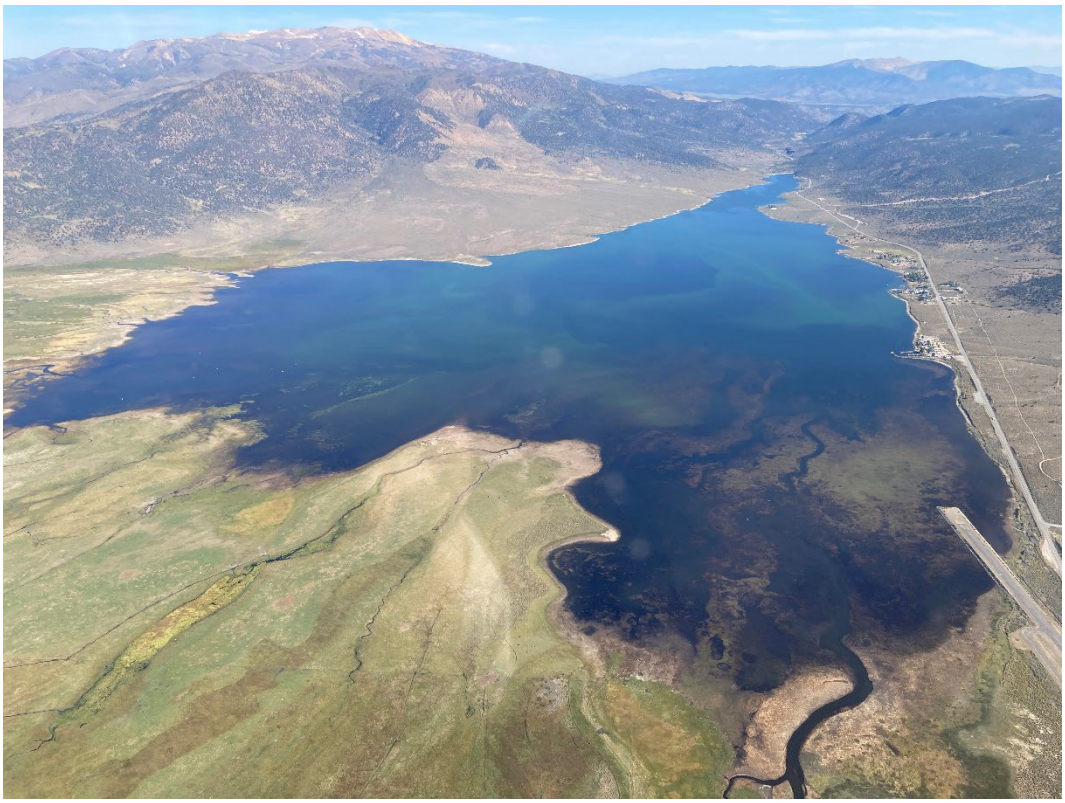

Figure 57. Bridgeport Reservoir, looking northwest

Crowley Reservoir Shoreline Subareas

Please refer to Figure 8 for the location of each of the following shoreline subareas at Crowley Reservoir. The major source of freshwater input to Crowley Reservoir is the Owens River. Other freshwater input includes flows from McGee and Convict Creeks, Layton Springs, and subsurface flow from other springs along the west shore. Vegetation communities immediately surrounding Crowley Reservoir include irrigated pasture, wet meadow, Great Basin scrub, alkali meadow, and mudflats.

Chalk Cliffs (CHCL)

The Chalk Cliffs subarea lacks freshwater inflow areas and wetland habitats, and is dominated by sandy beaches adjacent to steep, sagebrush-covered slopes. The high water level of Crowley in fall 2023 inundated some of the favored waterfowl loafing beaches and rocks, but created a few shallow protected areas onshore that attracted some ducks (Figure 58).

Figure 58. Chalk Cliffs

Hilton Bay (HIBA)

The Hilton Bay shoreline area includes Big Hilton Bay to the north and Little Hilton Bay to the south (Figure 59). The Hilton Bay area, surrounded by meadow and sagebrush habitat, receives small amounts of freshwater input from Hilton Creek, Whiskey Creek, and area springs. In 2023, the high water level of the reservoir inundated shoreline vegetation, eliminated mudflats in the bays, and also flooded most of Pelican Point, a favored sleeping and loafing area for waterbirds including waterfowl.

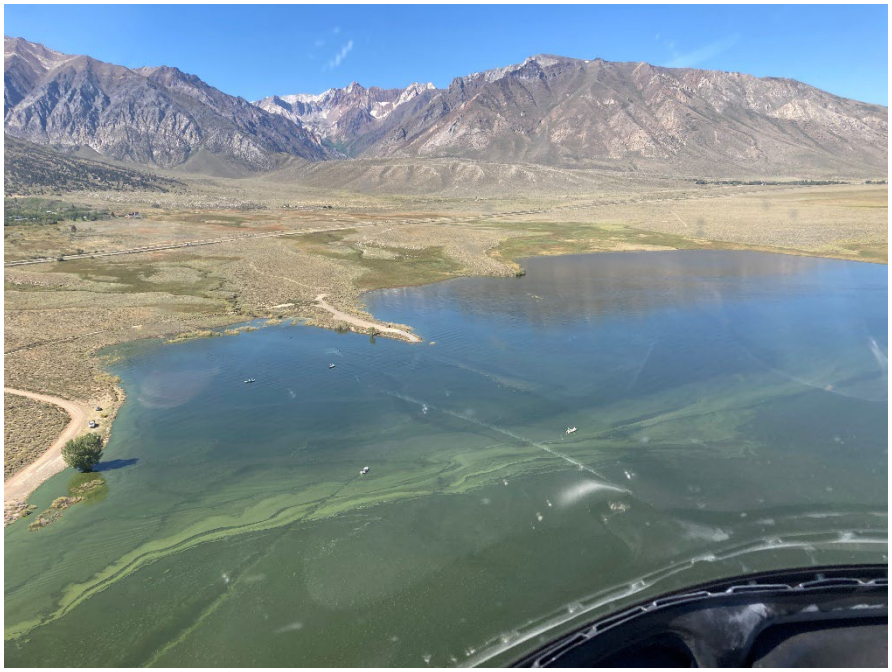

Figure 59. Hilton Bay

Layton Springs (LASP)

The Layton Springs shoreline area is bordered by upland vegetation and a sandy beach. Layton Springs provides freshwater input at the southern border of this lakeshore segment. The high reservoir level resulted in flooding of rabbitbrush, sagebrush and meadow along much of the length of this shoreline area (Figure 60). These flooded stands of shrubs seemed particularly attractive to waterfowl in fall.

Figure 60. Layton Springs

McGee Bay (MCBA)

The McGee Bay shoreline area supports the best waterfowl habitat at Crowley Reservoir. McGee Creek and Convict Creek supply perennial freshwater flow to this area of Crowley. At most reservoir levels, vast mudflats and wetlands occur along the west shore due to the low gradient slope of the shoreline and input from springs and subsurface flow from up-gradient irrigation.

In 2023, the reservoir level was very high, eliminating most of the mudflats in this shoreline area (Figure 61). The high water levels also inundated cattail marsh and shrub willows on shore. This area of flooded cattails was particularly attractive to waterfowl in fall, providing cover and some protection from wave action (Figure 61). The growth of the aquatic plant widgeonweed (*Ruppia* sp.) appeared reduced as compared to the previous few years.

Figure 61. McGee Creek shoreline area north of Pelican Point
Mudflats were absent in this area in fall of 2023 due to the high reservoir level.

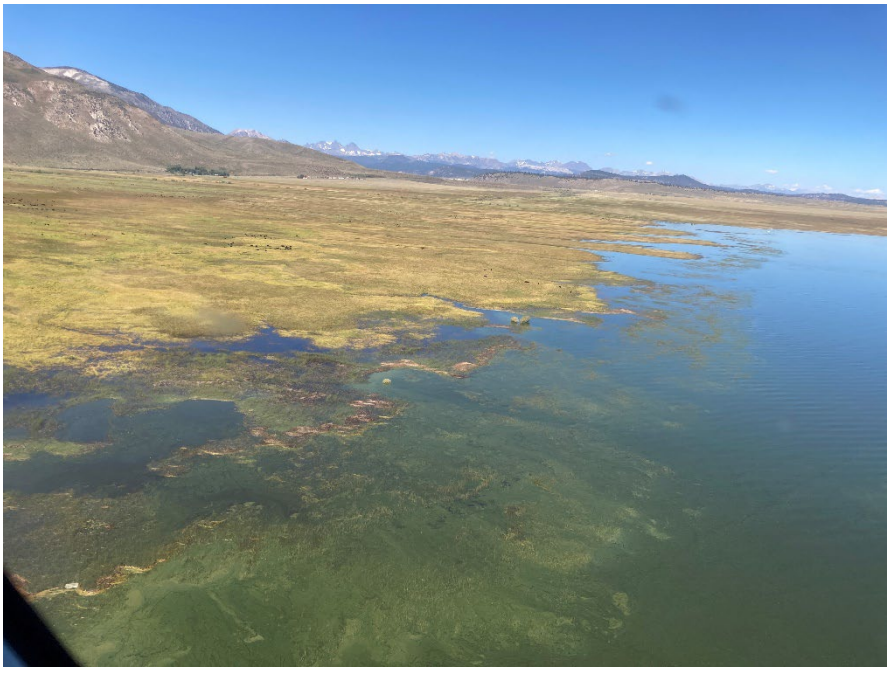

Figure 62. McGee Bay shoreline south of McGee and Convict Creek outflow
The high reservoir level eliminated mudflats but created flooded tall marsh habitat that attracted many waterfowl.

North Landing (NOLA)

The North Landing area is influenced by subsurface flows and supports meadow, wet meadow and mudflat habitats. In 2023 the very high reservoir level essentially eliminated existing mudflats and flooded shoreline meadow and shrub habitats (Figure 63). These flooded stands of shrubs seemed particularly attractive to waterfowl in fall. The depression at Sandy Point was filled all year, but only attracted low numbers of waterfowl.

Figure 63. North Landing

Sandy Point (SAPO)

Most of the length of Sandy Point area is bordered by short cliffs or upland vegetation. Small areas of meadow habitat occur in this area, and limited freshwater seepage occurs at Green Banks Bay. In fall of 2023, the high reservoir level resulted in the flooding of nearshore shrubs and meadow vegetation, and the elimination of mudflat habitats (Figure 64).

Figure 64. Sandy Point

Upper Owens River (UPOW)

The Upper Owens River receives direct flow from the Owens River, the largest source of freshwater input to Crowley Reservoir. Except at high reservoir levels, this subarea includes a large area of exposed reservoir bottom, and variable amounts of mudflats.

The very high reservoir level in 2023 eliminated most all mudflats in the delta (Figure 65). The high reservoir level also flooded rabbitbrush, sagebrush and meadow along much of the length of this shoreline area, forming small bays supporting flooded shrubs (Figure 66). These flooded stands of shrubs seemed particularly attractive to waterfowl in fall.

Figure 65. Upper Owens Delta

Figure 66. Upper Owens Delta Shoreline Area

In 2023, high water levels flooded shoreline shrubs and meadows.

3.3.6 Waterfowl Survey Discussion

Summary of Waterfowl Habitat Conditions

The extreme wet runoff year of 2022 to 2023 resulted in a rapid change in the level of Mono Lake from late spring through summer. In general, shoreline ponds were abundant spring through fall, although the extent and location of shoreline ponds changed throughout the year. In early June for example, shoreline ponds were essentially continuous along the southern shoreline. The rise in lake level inundated many of these ponds along the southern shoreline, other ponds developed elsewhere around the perimeter of the lake and shoreline vegetation was flooded. Waterfowl habitat conditions were good due to the presence of many shoreline ponds and qualitatively high numbers of *Artemia* and alkali flies in nearshore areas.

Breeding Waterfowl

The breeding population of waterfowl at Mono Lake has responded positively to lake level increases. Over the years, higher lake levels have increased the size of the breeding population and the number of broods. The spring of 2023 started with a low lake level of 6379.5 feet in March, and the breeding population was well below the long-term average. The extreme wet year and delayed, but high runoff conditions led to a steady rise in lake level throughout summer, and above average brood production, despite the low number of the breeding birds.

These observations suggest that breeding and/or brooding conditions at Mono Lake ended up being good for the year. Of note also was my observation of an extended breeding season for waterfowl at Mono Lake, and Bridgeport and Crowley Reservoir as well, suggesting waterfowl breeding conditions in the local area were favorable and remained so late into the season, perhaps supporting double-brooding by some individuals.

Habitat Use and Spatial Distribution

Breeding waterfowl habitat at Mono Lake occurs in localized areas of the shoreline where freshwater resources exist for young ducklings. Young ducklings require fresh water in order to survive and gain weight (Swanson et al. 1984), and thus freshwater is a necessary component of the habitat of the breeding waterfowl community at Mono Lake. Freshwater resources at Mono Lake include freshwater ponds, streams and deltas, and spring outflow areas.

In 2023, breeding conditions were good along the northwest shore (DeChambeau Creek and Wilson Creek) and Simons Spring. The northwest shore supports an abundance of fresh water from springs and inflow from Mill Creek, and some of the most extensive wet meadow habitat at Mono Lake. Beaver activity in the northwest shoreline area has also led to the development of additional freshwater ponds, although the beaver dams along Mill Creek were breached in summer due to the high runoff. Invertebrate foods appeared to be abundant at least in the DeChambeau Creek area as very high concentrations of *Artemia* were observed in the spring channels, and at Wilson Creek where high numbers of adult alkali flies were seen on the flooded shoreline vegetation as lake level rose through the summer.

Conditions at Simons Spring remained good for waterfowl as was the case in 2022, but changed rapidly through the year, particularly in summer due to the rising lake level. Fresh and brackish shoreline ponds were present summer and fall, however the rising lake level overtopped berms and eliminated most of the extensive pond system initially present in early June. Invertebrate food resources appeared high by late summer as clouds of adult alkali flies blanketed the shoreline vegetation inundated by rising lake water, and large numbers of *Artemia* were seen at the interface of spring outflow areas.

Rush Creek and Lee Vining Creek experienced high flows much of the summer, and the deltas were very flooded. These conditions did not attract more breeding waterfowl, possibly due to the continuous high flows. Lower Rush Creek below the County Road continues to show an increase in sinuosity and the presence of backwater ponds, thus improving conditions for waterfowl foraging.

In 2023, breeding dabbling duck activity was concentrated in and around freshwater sources including ponds, spring and creek outflow areas of ria although the species use these resources in slightly different manners. Freshwater ponds were used more by Cinnamon Teal, Green-winged Teal and Mallard, and less so by Gadwall. Gadwall and Green-winged Teal were seen in ria more than half of all observations, but Mallard less than 10% of the time. These different habitat types will support differing food resources for waterfowl, and the habitat use differences observed.

Many studies have shown that waterfowl breeding productivity is linked to the abundance and quality of open water wetlands and ponds supporting high densities of aquatic invertebrates (Kaminski and Prince 1981, Krapu et al. 1983, Cox et al. 1998, Pietz et al. 2003). In addition, the abundance and availability of aquatic invertebrates limits the number of breeding waterfowl and waterfowl brood survival (Sjoberg et al. 2000). Habitat use patterns of the breeding community suggest that freshwater ponds, brackish ponds and ria are key habitat features for waterfowl at Mono Lake.

Factors Influencing Waterfowl Breeding Populations

Lake level has strongly influenced the breeding waterfowl population at Mono Lake. Spring lake levels, particularly March and April, have had the largest influence on the size of the breeding population. Habitat conditions in spring when the birds arrive will influence whether waterfowl pairs chose to settle and breed at Mono Lake. Higher lake levels, at least within the range of lake levels observed, improve waterfowl habitat in general by increasing shoreline ponds, and decreasing the distance between nesting habitat, brooding ponds, and shoreline feeding areas.

Annual brood numbers are also strongly influenced by lake level, particularly in the month of June, but the effect of lake level is nonlinear. Increases in brood numbers as a function of lake level have been observed above a threshold of 6,382 feet. Below this lake level, the total number of broods has not only been significantly fewer, but the number of broods has not been influenced by further declines in lake level. In June 2023, the lake level was 6380.7 feet, thus below the 6,382-foot threshold, however brood numbers were higher than average. Based on field observations and a qualitative assessment, food resources in nearshore areas appeared to be high in the summer of 2023, possibly supporting good waterfowl production.

Lake level-related changes to breeding habitat quality and quantity are believed to be an important factor influencing breeding waterfowl populations at Mono Lake. As lake level decreases, the number and size of the ponds— particularly along the south shore from South Shoreline to Simons Springs—decreases. Decreases in lake level also result in increased barren playa at most places around the lake, resulting in increased physical distance between nesting and brooding cover, and high productivity feeding areas near shore. This apparent 6,382-foot threshold effect on brood numbers is being further investigated to determine critical habitat components that may be influencing this response. Other factors such as access to food, which are influenced by lake level and bathymetry, could potentially influence waterfowl breeding, and are also being further investigated.

Fall Waterfowl Counts

The fall 2023 waterfowl totals at Mono Lake did not differ from the long-term mean, and therefore no immediate response to the rise in lake level in 2023 was observed. Notable findings in 2023 were significantly higher numbers of Gadwall in fall, which were likely lingering breeding birds and their broods as a result of the extended breeding season, and very low numbers of Northern Pintail. The spatial distribution of waterfowl in fall differed from what is typically observed with much higher use of the

Black Point and Rush Creek shoreline areas, and surprisingly low use of Wilson Creek. The largest Northern Shoveler flock typically stages at Wilson Creek but this flock appeared to have shifted to a shoreline area of Black Point with brackish springs, shallow shoreline water, and pumice blocks that created loafing and perhaps good foraging habitat (see Figure 26). Above average numbers of Northern Shoveler were also seen at Rush Creek and were observed to be feeding in the plume of the creek outflow well offshore. This was notable because dabbling ducks such as Northern Shoveler are more typically seen close to shore except when flushed.

Fall waterfowl numbers have averaged higher in years when Mono Lake is monomictic as opposed to meromictic. One potential reason for this is the effect of lake mixing and nutrient cycling on *Artemia* populations at Mono Lake (Melack et al. 2017). *Artemia* feed on phytoplankton, and these algal populations are dependent for growth on inorganic nitrogen, which is a limited substance in Mono Lake. The main sources of nitrogen are brine shrimp excretion and vertical mixing of ammonium-rich deep water (Melack et al. 2017). Following high freshwater input occurring in wet years, a persistent chemocline develops, preventing vertical mixing ("meromixis"). When a chemocline persists for multiple years, nitrogen accumulates on the bottom. When dry conditions return and lake level declines, the chemocline breaks down, the lake completely mixes in late fall or early winter ("monomixis"), and nitrogen is released to the system. This release of nutrients can result in an algal bloom, and a population boom for *Artemia*. A similar relationship to lake productivity in terms of the *Artemia* population has been seen in the nesting population of California Gulls at Mono Lake. Gull productivity has shown increases under monomictic conditions associated with declining lake levels and decreases under meromictic conditions associated with rising lake levels (Burnett et al. 2021).

Variability in the abundance or distribution of other food resources may also influence yearly waterfowl use. Other foods available for waterfowl at Mono Lake are alkali fly larvae and pupae, various aquatic invertebrate species in lake-fringing ponds, algae, and the seeds and vegetative parts of wetland plants. The only waterfowl food resource for which monitoring data exists is *Artemia*, so the influence of these other foods on waterfowl use patterns cannot be assessed.

In contrast to Mono Lake, fall waterfowl totals at both Bridgeport and Crowley Reservoirs were significantly below their respective long-term means in 2023. There are many factors that could contribute to this result including breeding ground conditions or factors along the migration corridor. For example, wet conditions in the winter of 2022 to 2023 in California, Oregon and Washington may have increased habitat

availability, resulting in more dispersed populations. Very warm conditions in autumn in western Canada (September thru November) https://www.canada.ca/en/environment-climate-change/services/climate-change/science-research-data/climate-trends-variability/trends-variations/autumn-2023-bulletin.html) and a lack of cold fronts may have delayed migration. A local observation suggestive of delayed migration is the presence of a very large flock of Northern Shoveler at Crowley Reservoir in mid-December of 2023 (D. House, pers. obs.). Northern Shoveler are typically in very low numbers or absent at Crowley in mid-December, and the flock of over 3,500 birds was quite unusual. This flock was also larger than any seen at Crowley during the fall surveys from September to mid-November.

Waterfowl populations at Mono Lake are relatively small compared to Bridgeport and Crowley, likely due to a combination of salinity and water depth which limits feeding opportunities. Salinity and water depth influence not only the types and abundance of food items, but also accessibility. Mono Lake is deep, highly saline, with limited shallow shoreline areas. Despite the productivity of Mono Lake, access of these food resources to dabbling duck species is somewhat limited due to its depth, as foods must not only be available, but accessible. The topography and bathymetry are such that shallow water feeding areas, especially those near springs, are widely spaced and not extensive. The range of water depths for optimal foraging by dabbling ducks is 2 to10 inches (Fredrickson 1982). Prey will generally be less accessible in water depths greater than about 10 inches, and thus foraging efficiency will decrease. At Mono Lake, dabbling ducks have been observed to feed almost exclusively near shore, and more specifically, where the bathymetry data suggests a greater extent of shallow water than areas where waterfowl use is lower or absent. The highly saline water of Mono Lake currently only support *Artemia* and *Cirrula*, however, other species may have occurred historically when the lake was no more than 50 gm/L salinity. The highly saline water also limits the availability of vegetable food sources favored by many dabbling duck species in fall, to isolated fresh water and brackish ponds since the salinity of the lake is above the tolerance of wetland plants.

Mono Lake is deep, highly saline, with limited shallow shoreline areas. These features limit the habitat quality for waterfowl and may ultimately limit recovery of waterfowl populations. In order for waterfowl to meet their energetic demands, food resources need to be accessible, abundant, and of sufficient quality.

Restoration Ponds

The waterfowl habitat at the Restoration Ponds continues to be impacted by ageing infrastructure and water delivery problems as the County Ponds remained essentially

dry through summer and fall of 2023, although releases were resumed in mid-November. Waterfowl use of the restoration pond complex as a whole continued to be below the long-term average since the County Ponds remained inactive throughout the summer and fall waterfowl survey periods. Repair work to the infrastructure of the DeChambeau ponds continues, with a goal of further improvements in habitat conditions.

4.0 Summary and recommendations

The extreme wet year of 2022 to 2023 allowed Mono Lake to achieve a 4.5-foot vertical gain in lake level. This is the fifth such increase in lake level observed since export restrictions of D1631 were implemented in 1994. Waterfowl habitat conditions seemed very good summer through fall. Shoreline ponds were numerous, there was good habitat connectivity between nearshore shoreline wetland habitats, the shoreline and freshwater outflow areas, and abundant invertebrate resources.

The breeding waterfowl population responded favorably to these conditions and had a productive year. As has been typical since 2002, however, higher lake levels did not translate into more ducks in fall.

The level of Mono Lake has seen increases of several feet in response to wet years, followed by decreases of several feet in dry years. The protection afforded by D1631 has stabilized the lake level and at its high point in 2023 of 6383.2 feet, the lake was almost 9 vertical feet below the target lake level set in 1994. Since 2002, lake level has gone up and down within a relatively narrow range of about 8 feet (6377.1 to 6385.1 feet). There has not been a steady rise in lake level with which to evaluate the response of waterfowl populations to restoration among the backdrop of annual variation in other factors influencing migratory populations. Higher lake levels within this range have supported higher breeding populations and production. This trend may or may not hold with further increases in lake level above the highest observed over the 2002 to 2023 time period. Unlike the breeding birds, the fall migrating waterfowl has not demonstrated a correlation with lake level, nor has there been a significant trend in total numbers, thus no conclusions can be drawn so far regarding the response to restoration and whether higher lake levels above which has been observed since 1994, would attract higher numbers of fall migrating waterfowl.

The following are my recommendations for the Program:

1) **Continue to implement measures to support lake level recovery.** Of the restoration measure outlined in Order 98-05, lake level recovery remains the restoration objective that would reestablish the most potential waterfowl habitat.

2) **Enhance and restore the functioning of the Restoration Ponds.** Although the total number of waterfowl that could be supported by the Restoration Ponds is just a fraction of that occurring on Mono Lake, there are management strategies, repairs, and improvements that would enhance waterfowl habitat. The most basic of improvements would be to restore water

delivery to the County Ponds, which have been dry for several years. The second would be to implement seasonal or rotational flooding regime to enhance forage production for waterfowl, while continuing to provide waterfowl habitat year-round at the ponds. In addition, I recommend the Mono Basin Waterfowl Director continue to work with partners to help restore the functioning of the DeChambeau Ponds.

3) **Conduct a second waterfowl time budget study.** Order 98-05 required a time budget study to be conducted during each of the first two fall migration periods after the plan was approved, and again when Mono Lake reaches its target lake elevation. A single time budget study of Ruddy Ducks was completed in fall of 2000 by Joe Jehl. A time budget study allows for the determination of the relative importance of different shoreline sites and habitats for feeding, resting, or drinking.

4) **Reinstate the vegetation monitoring programs in lake-fringing wetlands and riparian areas.** The vegetation monitoring conducted at the lake-fringing wetland sites in 2021 (LADWP 2022) documented impacts from feral horse grazing at Warm Springs. Horses are also impacting ponds and wetland habitats at Simons Springs. In early 2022, horses were first observed in the Rush Creek delta area, although no significant impacts have been seen to date. I recommend at a minimum, reinstating the wetland vegetation monitoring transects at Warm Springs and Simons Springs to provide data on either continued impacts from horses, or how these areas respond if the feral horse herds are removed.

5) **Reinstate annual restoration meetings.** In prior years, the Mono Basin Parties met to hear the reports from the scientists and their findings during their annual monitoring. These meetings are an excellent way to foster communication and knowledge sharing among the parties, and I recommend reinstating an annual meeting, perhaps separate from the Annual Operations Plan meeting so that more time is available for the discussion of scientific findings. The advent of the “virtual meeting” makes it easier for all to participate, especially if travel is an issue.

5.0 Literature Cited

Beschta, R. L. 1994. Rush Creek – Flows, channels, and riparian conditions: Pre-1941 and Today. Report for the Rush Creek Restoration Technical Committee.

Burnett, R.D., K. Nelson, and A.E. Schmidt. 2021. Population size and reproductive success of California Gulls at Mono Lake. Contribution No. 2347, Point Blue Conservation Science, Petaluma, CA.

California Invasive Plant Council (Cal-IPC). 2006. California Invasive Plant Inventory. Published February 2006.

Corvallis Environmental Research Laboratory and Environmental Monitoring and Support Laboratory. 1978. U.S. Environmental Protection Agency National eutrophication survey. Working Paper Series. No. 743. Report on Lake Crowley, Mono County, California, EPA Region IX.

Cox, R.R., M.A. Hanson, C.C. Roy, D.H. Johnson, and M.G. Butler. 1998. Mallard duckling growth and survival in relation to aquatic invertebrate. The Journal of Wildlife Management, Vol. 62(1): 124–133.

Doster, R.H., and W.D. Shuford. 2018. Recent trends in population size and distribution of Ring-billed and California gulls in the western United States, *in* Trends and traditions: Avifaunal change in western North America (W.D. Shuford, R.E. Gill Jr., and C.M Handel, eds.), pp. 161–179. Studies of Western Birds 3. Western Field Ornithologists, Camarillo, CA.

Ficklin, D.L, I.T. Stewart, and E.P. Maurer. 2012. Effects of projected climate change on the hydrology in the Mono Lake Basin, California. Climate Change. 116: 111–131. DOI 10.1007/s10584-012-0566-6.

Fredrickson, L.H. 1982. Strategies for water manipulations in moist-soil systems. Waterfowl Management Handbook. 26.

Gollop, J. B, and W. H. Marshall. 1954. A guide for aging duck broods in the field. Mississippi Flyway Council. Tech. Sect. Report.

Horne, A. J. 2003. Report on Bridgeport Reservoir beneficial use impairment: limnology in the summer-fall 2000 and comparisons with 1989. Report prepared for Lahontan Regional Water Quality Control Board. South Lake Tahoe.

House, D. 2021. Fall waterfowl use of Bridgeport Reservoir, Mono County, California. Western Birds 52(4): 278–295.

Jehl, J. R. 1986. Biology of the Red-necked Phalarope (*Phalaropus lobatus*) at the western edge of the Great Basin in fall migration. Great Basin Naturalist Vol. 46(2): Article 1.

Jehl, J. R. 1988. Biology of the Eared Grebe and Wilson's Phalarope in the nonbreeding season: a study of adaptations to saline lakes. Studies in Avian Biology No. 12. Cooper Ornithological Society.

Jehl, J. R. 2002. Waterfowl populations at Mono Lake, California 2001. Hubbs Sea World Institute. Technical Report 2002-330. Prepared for Los Angeles Department of Water and Power.

Jellison, R. and J.M. Melack. 1993. Meromixis in hypersaline Mono Lake, California. 1 Stratification and vertical mixing during the onset, persistence, and breakdown of meromixis. Limnol. Oceanogr. 38(5): 1008–1019.

Jellison, R., J. Romero, and J.M. Melack. 1998. The onset of meromixis during restoration of Mono Lake, California: Unintended consequences of reducing water diversions. Limnol. Oceanogr. 43(4): 706–711.

Jellison, R., K. Rose and J. M. Melack. 2003. Assessment of internal nutrient loading to Crowley Lake, Mono County. Final Report to the State Water Resources Control Board.

Jones and Stokes Associates, Inc. 1993. Draft environmental impact report for the review of Mono Basin water rights of the city of Los Angeles. Prepared for California State Water Resources Control Board. May 1993.

Kaminski, R. M., and H. H. Prince. 1981. Dabbling duck activity and foraging responses to aquatic macroinvertebrates. The Auk 98(1): 115–126.

Krapu, G., and A. Klett, and D. Jorde. 1983. The effect of variable spring water conditions on Mallard reproduction. The Auk 100: 689–698.

Los Angeles Department of Water and Power (LADWP). 1987. Mono Basin geology and hydrology. Prepared by Aqueduct Division Hydrology Section. March 1987.

Los Angeles Department of Water and Power (LADWP). 1996a. Mono Basin waterfowl habitat restoration plan. Prepared for the State Water Resources Control Board. In response to Mono Lake Basin Water Right Decision 1631.

Los Angeles Department of Water and Power (LADWP). 1996b. Mono Basin stream and stream channel restoration plan. Prepared for the State Water Resources Control Board. In response to Mono Lake Basin Water Right Decision 1631.

Los Angeles Department of Water and Power (LADWP). 2018. Mono Basin Waterfowl Habitat Restoration Program Periodic Overview Report. Prepared by Deborah House and Motoshi Honda for the State Water Resources Control Board. May 2018.

Los Angeles Department of Water and Power (LADWP). 2022. Mono Basin waterfowl habitat restoration compliance report. Prepared for the State Water Resources Control Board. In response to State Water Resources Control Board Order Nos. 98-05 and 98-07.

McBain and Trush, Inc, and R. Taylor and Associates. 2010. Mono Basin stream restoration and monitoring program: synthesis of instream flow recommendations to the State Water Resources Control Board and the Los Angeles Department of Water and Power. Final Report. April 30, 2010.

Melack, J. M. 1983. Large, deep salt lakes: a comparative limnological analysis. Hydrobiologia 105: 223–230.

Melack, J.M., R. Jellison, S. MacIntyre, and J.T. Hollibaugh. Mono Lake: Plankton dynamics over three decades of meromixis or monomixis. Ch. 11 in Ecology of Meromictic Lakes, Ecological Studies 228. DOI 10.1007/978-3-319-49143-1_11.

National Research Council. 1987. The Mono Basin ecosystem: effects of changing lake level. Washington, DC: The National Academies Press. https://doi.org/10.17226/1007.

Pietz, P., G. Krapu, D. Brandt, and R. Cox, Jr. 2003. Factors affecting Gadwall brood and duckling survival in prairie pothole landscapes. The Journal of Wildlife Management. Vol 67(3): 564–575.

Raumann, C. G., S. Stine, A. Evans, and J. Wilson. 2002. Digital bathymetric model of Mono Lake, California. Miscellaneous Field Studies Map MF 2393.

Reheis, M. C., S. Stine, and A. M. Sarna-Wojcicki. 2002. Drainage reversals in Mono Basin during the late Pliocene and Pleistocene. Geological Society of America Bulletin. V:114(8): 991–1006. August 2002.

Roberts, A.J., M.R. Conover, J. Luft, and J. Neill. 2013. Population fluctuations and distribution of staging Eared Grebes (*Podiceps nigricollis*) in North America. Can. J. Zool. 91:906–913. Doi.org/10.1139/cjz-2013-0181.

Rogers, D.B., S.J. Dreiss and D.P. Groeneveld. 1992. Near-Shore Groundwater and Salt-Flat Processes at Mono Lake, White Mountain Research Station Symposium, 4, 367–395.

Russell, I.C. 1889. Quaternary history of Mono Valley, California. University of Michigan Library.

Sharpe, S. E., M. E. Cablk, and J. M. Thomas. 2007. The Walker Basin, Nevada and California: physical environment, hydrology, and biology. Desert Research Institute Publication No. 41231. May 2007. Revision 01 May 2008.

Sjoberg, K., H. Poysa, J. Elmberg, and P. Nummi. 2000. Response of Mallard ducklings to variation in habitat quality: an experiment of food limitation. Ecology 81(2): 329–335.

State Water Resources Control Board (SWRCB). 1994. Mono Lake Basin water right decision 1631.

State Water Resources Control Board (SWRCB). 1998. Order WR 98-05. Order requiring stream and waterfowl habitat restoration measures. September 2, 1998.

State Water Resources Control Board (SWRCB). 2013. Settlement agreement regarding continuing implementation of water rights orders 98-05 and 98-07. September 2013.

State Water Resources Control Board (SWRCB). 2021. Order WR 2021-0086 EXEC. In the matter of licenses 10191 and 10192 (applications 8042 and 8043) held by the City of Los Angeles, Department of Water and Power. October 1, 2021.

Swanson, G. A., V.A. Adomaitis, F.B. Lee, J.R. Serie, and J.A. Shoesmith. 1984. Limnological conditions influencing duckling use of saline lake in South-Central North Dakota. The Journal of Wildlife Management. Vol. 48(2): 340–349.

University of California. 2010. Saltcedar. A nonnative invasive plant in the western U.S. WRIC leaflet #02-2.

U.S.D.A. Forest Service. 2005. Decision Memo. Pond 3-Barrow Pit Pond Wildlife Habitat Improvement. Inyo National Forest. Mono County, CA. July 18, 2005.

Vorster, P. 1985. A water balance forecast model for Mono Lake, California. Monograph 10. USDA Forest Service Region 5.

Williams, W. D. 2002. Environmental threats to salt lakes and the likely status of inland saline ecosystems in 2025. Environmental Conservation 29(2): 154–167.

Wurtsbaugh, W.A., C. Miller, S. Null, R. Justin DeRose, P. Wilcock, M. Hahenberger, F. Howe, and J. Moore. 2017. Decline of the worlds saline lakes. Nature Geoscience 10: 816–821.

Zellmer, J. T. 1977. Environmental and engineering geology of Bridgeport Valley, Mono County California. Thesis. University of Nevada, Reno.